ODYSSEY OF SURFACTANT PROTEINS SP-A AND SP-D: INNATE IMMUNE SURVEILLANCE MOLECULES

EDITED BY: Uday Kishore, Roberta Bulla and Taruna Madan
PUBLISHED IN: Frontiers in Immunology

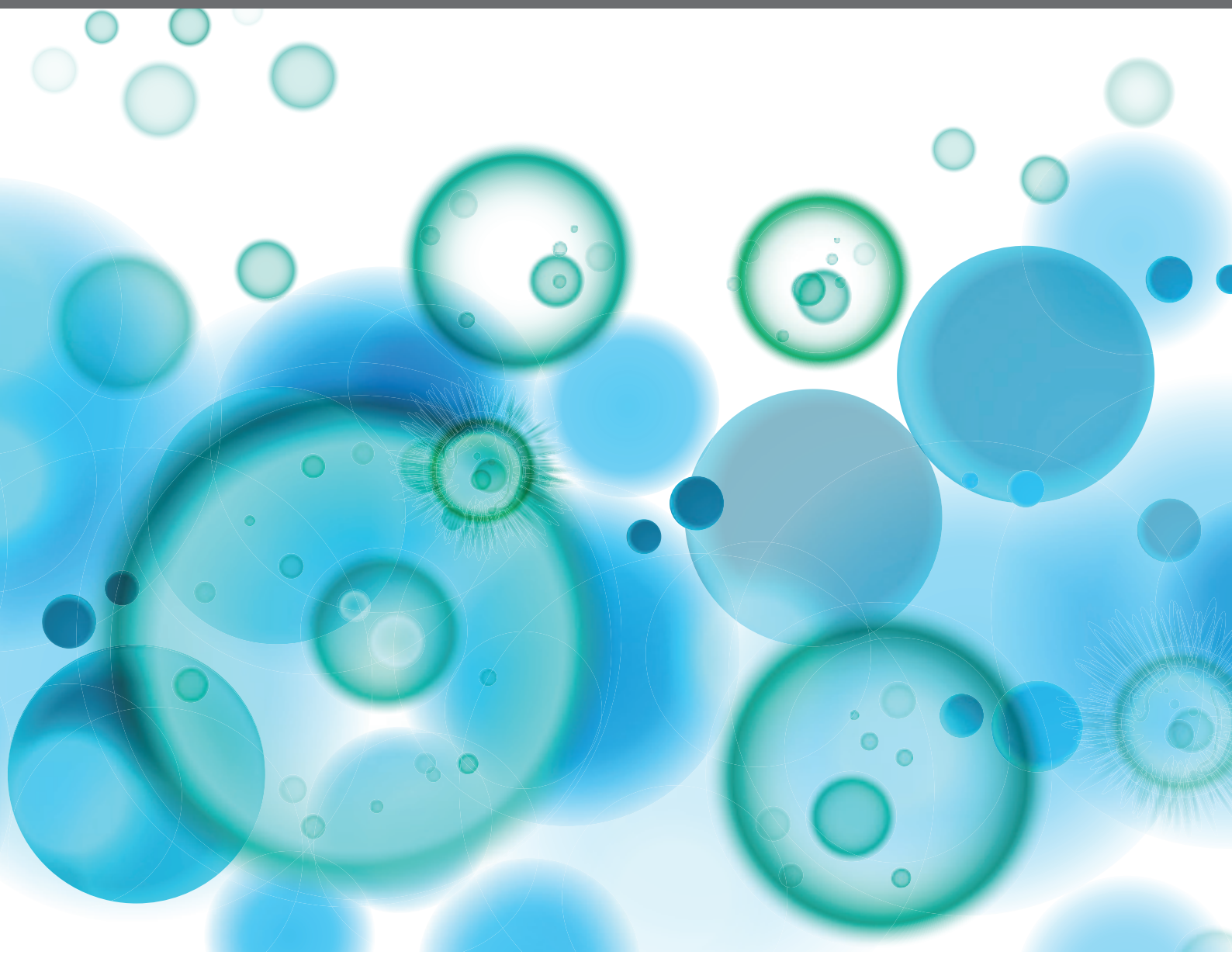

frontiers Research Topics

frontiers

ISSN 1664-8714
ISBN 978-2-88963-680-8
DOI 10.3389/978-2-88963-680-8

About Frontiers

Frontiers is more than just an open-access publisher of scholarly articles: it is a pioneering approach to the world of academia, radically improving the way scholarly research is managed. The grand vision of Frontiers is a world where all people have an equal opportunity to seek, share and generate knowledge. Frontiers provides immediate and permanent online open access to all its publications, but this alone is not enough to realize our grand goals.

Frontiers Journal Series

The Frontiers Journal Series is a multi-tier and interdisciplinary set of open-access, online journals, promising a paradigm shift from the current review, selection and dissemination processes in academic publishing. All Frontiers journals are driven by researchers for researchers; therefore, they constitute a service to the scholarly community. At the same time, the Frontiers Journal Series operates on a revolutionary invention, the tiered publishing system, initially addressing specific communities of scholars, and gradually climbing up to broader public understanding, thus serving the interests of the lay society, too.

Dedication to Quality

Each Frontiers article is a landmark of the highest quality, thanks to genuinely collaborative interactions between authors and review editors, who include some of the world's best academicians. Research must be certified by peers before entering a stream of knowledge that may eventually reach the public - and shape society; therefore, Frontiers only applies the most rigorous and unbiased reviews.
Frontiers revolutionizes research publishing by freely delivering the most outstanding research, evaluated with no bias from both the academic and social point of view. By applying the most advanced information technologies, Frontiers is catapulting scholarly publishing into a new generation.

What are Frontiers Research Topics?

Frontiers Research Topics are very popular trademarks of the Frontiers Journals Series: they are collections of at least ten articles, all centered on a particular subject. With their unique mix of varied contributions from Original Research to Review Articles, Frontiers Research Topics unify the most influential researchers, the latest key findings and historical advances in a hot research area! Find out more on how to host your own Frontiers Research Topic or contribute to one as an author by contacting the Frontiers Editorial Office: researchtopics@frontiersin.org

ODYSSEY OF SURFACTANT PROTEINS SP-A AND SP-D: INNATE IMMUNE SURVEILLANCE MOLECULES

Topic Editors:
Uday Kishore, Brunel University London, United Kingdom
Roberta Bulla, University of Trieste, Italy
Taruna Madan, National Institute for Research in Reproductive Health (ICMR), India

Citation: Kishore, U., Bulla, R., Madan, T., eds. (2020). Odyssey of Surfactant Proteins SP-A and SP-D: Innate Immune Surveillance Molecules. Lausanne: Frontiers Media SA. doi: 10.3389/978-2-88963-680-8

Table of Contents

frontiers in Immunology

EDITORIAL
published: 11 March 2020
doi: 10.3389/fimmu.2020.00394

Editorial: Odyssey of Surfactant Proteins SP-A and SP-D: Innate Immune Surveillance Molecules

Uday Kishore[1]*, *Roberta Bulla*[2]* and *Taruna Madan*[3]*

[1] Biosciences, College of Health and Life Sciences, Brunel University London, Uxbridge, United Kingdom, [2] Department of Life Sciences, University of Trieste, Trieste, Italy, [3] Department of Innate Immunity, ICMR—National Institute for Research in Reproductive Health, Mumbai, India

Keywords: SP-A, SP-D, inflammation, cancer, innate immunity, infection, polymorphisms

Editorial on the Research Topic

Odyssey of Surfactant Proteins SP-A and SP-D: Innate Immune Surveillance Molecules

Surfactant protein A (SP-A) and D (SP-D) are hydrophilic collagenous C-type lectins, which were originally discovered in the lungs associated with surfactant phospholipids. It was later shown that the two proteins, unlike hydrophobic surfactant proteins, SP-B and SP-C, are keenly involved in protecting lungs against insults from pathogens, allergens, apoptotic, and necrotic cells (1). Two aspects became clear in subsequent years that (i). SP-A and SP-D have extra-pulmonary existence; and (ii). They can manipulate immune cells, and thus, regulate inflammatory responses (2). Although there have been a constant debate about their candidate receptor(s)—there are several reported so far (1). Much of the immunological studies, beyond interaction with surfactant system and pathogens, have been followed up toward SP-D. It has become apparent that SP-D is an innate immune surveillance molecule at the mucosal surfaces, which can act as a bridge between innate and adaptive immunity. The role of SP-D in modulating antigen presentation, helper T cell polarization and B cell differentiation and class switching (3) are few neat examples. This volume comprises 14 papers that extend our knowledge on SP-A and SP-D, and their roles in infection, inflammation and cancer.

A consistent theme discussed by several contributors is the differential role of two forms of SP-A in oxidative stress and lung innate immunity (Thorenoor, Umstead et al.; Nalian et al.; Thorenoor, Kawasawa et al.; Wang et al.). In humans, there are two SP-A variants differing in the collagen region, SP-A1 and SP-A2, encoded by SFTPA1 and SFTPA2, respectively, and produced by the alveolar type II cells in the lung. Importantly, SP-A1 and SP-A2 seem to differentially bind to phagocytic, but not to non-phagocytic cells (Thorenoor, Umstead et al.). SP-A1 and SP-A2 differentially bind and regulate neonatal and adult human alveolar macrophages (AMs) (Thorenoor, Umstead et al.). AMs from transgenic mice expressing human SP-A1 and SP-A2 exhibit differential expression of cell surface proteins (Thorenoor, Kawasawa et al.) Rodents express only one SP-A variant; thus, Nalian et al. have compared the rodent and human SP-A with respect to structural determinants of the function. The data infers that mouse SP-A is a functional hybrid of human SP-A1 and SP-A2. Particularly striking in this regard is the differential response in the two sexes. Humanized transgenic (hTG) male and female mice, carrying both SP-A1/SP-A2 (6A2/1A0, co-expressed) and SP-A-gene deficient mice were exposed to filtered air (FA) or ozone (O_3), and miRNA levels were measured in isolated AMs (Thorenoor, Kawasawa et al.). The AM miRNome of co-expressed females was significantly downregulated in response to ozone induced oxidative stress. Several of the validated miRNA targets were involved in pro-inflammatory response, anti-apoptosis, cell cycle, cellular growth, and proliferation (Thorenoor, Kawasawa et al.). Continuing with this

OPEN ACCESS

Edited and reviewed by:
Francesca Granucci,
University of Milano Bicocca, Italy

***Correspondence:**
Uday Kishore
ukishore@hotmail.com
Roberta Bulla
rbulla@units.it
Taruna Madan
taruna_madan@hotmail.com

Specialty section:
This article was submitted to Molecular Innate Immunity, a section of the journal Frontiers in Immunology

Received: *07 February 2020*
Accepted: *19 February 2020*
Published: *11 March 2020*

Citation:
Kishore U, Bulla R and Madan T (2020) Editorial: Odyssey of Surfactant Proteins SP-A and SP-D: Innate Immune Surveillance Molecules. Front. Immunol. 11:394. doi: 10.3389/fimmu.2020.00394

theme, Wang et al. have analyzed bronchoalveolar lavage (BAL) proteomic profile and associated signaling pathways in hTG SP-A1 and SP-A2 mice, as well as in SP-A knock-out mice exposed to O_3 or *Klebsiella pneumoniae*. The hTG-SP-A2 mice showed significantly higher number of differentially expressed proteins, with the majority being increased in male mice while decreased in female mice. Survival of hTG mice (expressing SP-A1 alleles/ SP-A2 alleles/ Co-ex) challenged with *Klebsiella pneumoniae* was observed to be gene specific (co-ex and SP-A2 showing higher survival), variant-specific [co-expressed hTG (6A2/1A0) and hTG (1A0)] showing higher survival and sex specific (females showing higher survival). Cystic Fibrosis (CF) is characterized by altered SP levels. Lin et al. demonstrated that complex single nucleotide polymorphisms (SNPs)-SNP interactions of the surfactant genes may contribute to the pulmonary disease in CF patients. Wang Group have looked into SP-D gene polymorphisms and susceptibility to tuberculosis, by identifying/cloning two major SP-D exonic polymorphisms and examining their interaction with *Mycobacterium bovis* bacillus Calmette–Guérin (*M. bovis*) BCG. The authors seem to suggest that C92T (rs721917; amino acid rSP-D 92T variant) may increase susceptibility to TB (Hsieh et al.).

Hartshorn group have elegantly reviewed the molecular mechanisms used by SP-D to neutralize influenza A Virus (IAV) (Hsieh et al.). The group has been a pioneer in the field and the review summarizes the highlights of their credible work over a couple of decades. Al-Ahdal et al. have shown that a recombinant form of truncated human SP-D (rfhSP-D), composed of homotrimeric neck and C-type lectin domains, was able to restrict H1N1 and H3N2 subtypes of IAV (as well as their pseudotyped viral counterparts) from infecting A549 cells, a lung epithelial cell line, thus acting as an entry inhibitor. This is in contrast to the recombinant fragment of human SP-A that seems to promote IAV infectivity; however, full-length SP-A inhibits viral entry (4). These results seem to suggest that the two molecules i.e., SP-A and SP-D, especially their C-type lectin domains, can be very distinct in their functional properties; this point has been emphasized by other papers in this volume. One important point that needs mentioning is that rfhSP-D is also able to dampen the pro-inflammatory cytokine storm induced by IAV, which could minimize the lung injury caused by the virus. Next two papers are focused on how SP-D (rather rfhSP-D) can offer protection against HIV-1 at the mucosal surface. Dodagatta-Marri et al. show, for the first time, that DC-SIGN is a putative receptor for SP-D; the binding takes place via the C-type lectin domains of both proteins. This interaction is interestingly poised since both SP-D and DC-SIGN can interact with HIV-1. The authors show that opsonizing HIV-1 with rfhSP-D prior to viral exposure to DC-SIGN bearing cells reduced viral ability to get transferred to $CD4^+$ T cells *in trans*. Thus, this is another layer of protection that rfhSP-D works at against HIV-1, and follows up earlier studies (5, 6). A seminal study by Pandit et al. in this volume reports use of vaginal explants and inhibition of HIV-1 transfer in an *ex vivo* context. The authors have also carried out a transcriptomics analysis revealing how rfhSP-D modulates a wide range of target cells and pathways in order to act as a mucosal barrier to HIV-1. In addition, the study has utilised a rabbit model of vaginal irritation in order to demonstrate that rfhSP-D is a safe prophylactic molecule for vaginal use.

Madan et al. showed nearly 20 years ago that rfhSP-D could offer therapeutic protection in a murine model of pulmonary hypersensitivity induced by *Aspergillus fumigatus* allergens/antigens (7). Subsequently, SP-D knock-out mice were found to be hyper-eosinophilic that could be ameliorated by rfhSP-D intranasal treatment (8). The mechanism of eosinophil clearance remained unclear until Mahajan et al. showed that eosinophils derived from allergic patients were susceptible to apoptosis induction by rfhSP-D (9) via p53 pathway, as revealed by proteomics analysis of a eosinophilic leukemic cell line, AML14.3D10 (10). This opened the area of SP-D mediated immune surveillance in cancer. It was subsequently shown that SP-D binds to EGF receptor on A549 cells and had an anti-proliferative and anti-invasive effect (11). In this volume, Kaur, Riaz, Murugaiah et al. reported the ability of rfhSP-D to induce apoptosis *via* TNF-α/Fas-mediated pathway regardless of the p53 status in human pancreatic adenocarcinoma (PDAC) using Panc-1 ($p53^{mt}$), MiaPaCa-2 ($p53^{mt}$), and Capan-2 ($p53^{wt}$) cell lines. Treatment of these cell lines with rfhSP-D caused growth arrest in G1 cell cycle phase, triggered transcriptional upregulation of pro-apoptotic factors such as TNF-α, and induced apoptosis *via* Fas-mediated pathway in a p53-independent manner. In another paper, Kaur, Riaz, Singh et al. demonstrate that rfhSP-D is also capable of inhibiting TGF-β expression in the PDAC cell lines, and thus, suppressing their invasive-mesenchymal properties. The rfhSP-D-treated pancreatic cancer cell lines showed reduced expression in the cytoplasm of Smad2/3, suggesting that an interrupted signal transduction negatively affected the transcription of key mesenchymal genes. Thus, expressions of Vimentin, Zeb1, and Snail were found to be downregulated upon rfhSP-D treatment. Both these studies suggest that rfhSP-D can potentially be used to therapeutically target pancreatic cancer cells. A bioinformatics analysis using Oncomine dataset and the survival analysis platforms Kaplan–Meier plotter has been performed by Mangogna et al., which showed that in the lung, gastric, and breast cancers, there is a lower expression of SP-D than normal tissues. On the contrary, a higher expression than normal tissue was observed in ovarian cancer. In lung cancer, the presence of SP-D could be associated with a favorable prognosis. On the contrary, at non-pulmonary sites such as gastric, breast, and ovarian cancers, the presence of SP-D could be associated with unfavorable prognosis. All these data indicate that SP-D could also be used as a potential diagnostic marker.

In a critical assessment, Colmorten et al. have reviewed the role of SP-D in the vascular inflammation, inferring a dual role of SP-D in the development of atherosclerosis. A pro-atherogenic role of SP-D is evident from *in vivo* studies in SP-D knock-out mice. Clinical studies have shown a positive association between circulatory SP-D levels, carotid intima-media thickness, coronary artery calcification and risk of both total and cardiovascular disease mortality.

It is clear from the studies being reported in this volume that the field of SP-A and SP-D continues to grow and is

now throwing a number of pleasant surprises. The therapeutic potential of rfhSP-D needs to be realized via planned clinical trials. This decade is going to be an exciting one for surfactant protein research.

AUTHOR CONTRIBUTIONS

All authors listed have made an equal, direct and intellectual contribution to the work, and approved it for publication.

REFERENCES

1. Kishore U, Greenhough TJ, Waters P, Shrive AK, Ghai R, Kamran MF, et al. Surfactant proteins SP-A and SP-D: structure, function and receptors. *Mol Immunol*. (2006) 43:1293–315. doi: 10.1016/j.molimm.2005.08.004
2. Wright JR. Immunomodulatory functions of surfactant. *Physiol Rev*. (1997) 77:931–62. doi: 10.1152/physrev.1997.77.4.931
3. Qaseem AS, Singh I, Pathan AA, Layhadi JA, Parkin R, Alexandra F, et al. A recombinant fragment of human surfactant protein d suppresses basophil activation and T-helper type 2 and B-cell responses in grass pollen-induced allergic inflammation. *Am J Respir Crit Care Med*. (2017) 196:1526–34. doi: 10.1164/rccm.201701-0225OC
4. Al-Qahtani AA, Murugaiah V, Bashir HA, Pathan AA, Abozaid SM, Makarov E, et al. Full-length human surfactant protein A inhibits influenza A virus infection of A549 lung epithelial cells: a recombinant form containing neck and lectin domains promotes infectivity. *Immunobiology*. (2019) 224:408–18. doi: 10.1016/j.imbio.2019.02.006
5. Gaiha GD, Dong T, Palaniyar N, Mitchell DA, Reid KB, Clark HW. Surfactant protein A binds to HIV and inhibits direct infection of $CD4^+$ cells, but enhances dendritic cell-mediated viral transfer. *J Immunol*. (2008) 181:601–9. doi: 10.4049/jimmunol.181.1.601
6. Pandit H, Gopal S, Sonawani A, Yadav AK, Qaseem AS, Warke H, et al. Surfactant protein D inhibits HIV-1 infection of target cells via interference with gp120-CD4 interaction and modulates pro-inflammatory cytokine production. *PLoS ONE*. (2014) 9:e102395. doi: 10.1371/journal.pone.0102395
7. Madan T, Kishore U, Singh M, Strong P, Clark H, Hussain EM, et al. Surfactant proteins A and D protect mice against pulmonary hypersensitivity induced by *Aspergillus fumigatus* antigens and allergens. *J Clin Invest*. (2001) 107:467–75. doi: 10.1172/JCI10124
8. Madan T, Reid KB, Singh M, Sarma PU, Kishore U. Susceptibility of mice genetically deficient in the surfactant protein (SP)-A or SP-D gene to pulmonary hypersensitivity induced by antigens and allergens of *Aspergillus fumigatus*. *J Immunol*. (2005) 174:6943–54. doi: 10.4049/jimmunol.174.11.6943
9. Mahajan L, Madan T, Kamal N, Singh VK, Sim RB, Telang SD, et al. Recombinant surfactant protein-D selectively increases apoptosis in eosinophils of allergic asthmatics and enhances uptake of apoptotic eosinophils by macrophages. *Int Immunol*. (2008) 20:993–1007. doi: 10.1093/intimm/dxn058
10. Mahajan L, Pandit H, Madan T, Gautam P, Yadav AK, Warke H, et al. Human surfactant protein D alters oxidative stress and HMGA1 expression to induce p53 apoptotic pathway in eosinophil leukemic cell line. *PLoS ONE*. (2013) 8:e85046. doi: 10.1371/journal.pone.0085046
11. Hasegawa Y, Takahashi M, Ariki S, Asakawa D, Tajiri M, Wada Y, et al. Surfactant protein D suppresses lung cancer progression by downregulation of epidermal growth factor signaling. *Oncogene*. (2015) 34:838–45. doi: 10.1038/onc.2014.20

Conflict of Interest: The authors declare that the research was conducted in the absence of any commercial or financial relationships that could be construed as a potential conflict of interest.

frontiers in Immunology

ORIGINAL RESEARCH
published: 16 October 2018
doi: 10.3389/fimmu.2018.02404

Survival of Surfactant Protein-A1 and SP-A2 Transgenic Mice After *Klebsiella pneumoniae* Infection, Exhibits Sex-, Gene-, and Variant Specific Differences; Treatment With Surfactant Protein Improves Survival

Nithyananda Thorenoor[1], *Todd M. Umstead*[1], *Xuesheng Zhang*[1], *David S. Phelps*[1] *and Joanna Floros*[1,2]*

[1] Center for Host defense, Inflammation, and Lung Disease (CHILD) Research, Department of Pediatrics, The Pennsylvania State University College of Medicine, Hershey, PA, United States, [2] Department of Obstetrics & Gynecology, The Pennsylvania State University College of Medicine, Hershey, PA, United States

OPEN ACCESS

Edited by:
Uday Kishore,
Brunel University London,
United Kingdom

Reviewed by:
Hrishikesh Pandit,
National Cancer Institute at Frederick,
United States
Thomas Vorup-Jensen,
Aarhus University, Denmark

***Correspondence:**
Joanna Floros
jxf19@psu.edu;
jfloros@pennstatehealth.psu.edu

Specialty section:
This article was submitted to Molecular Innate Immunity, a section of the journal Frontiers in Immunology

Received: 02 July 2018
Accepted: 28 September 2018
Published: 16 October 2018

Citation:
Thorenoor N, Umstead TM, Zhang X, Phelps DS and Floros J (2018) Survival of Surfactant Protein-A1 and SP-A2 Transgenic Mice After Klebsiella pneumoniae Infection, Exhibits Sex-, Gene-, and Variant Specific Differences; Treatment With Surfactant Protein Improves Survival. Front. Immunol. 9:2404. doi: 10.3389/fimmu.2018.02404

Surfactant protein A (SP-A) is involved in lung innate host defense and surfactant-related functions. The human SFTPA1 and SFTPA2 genes encode SP-A1 and SP-2 proteins, and each gene has been identified with numerous genetic variants. SP-A1 and SP-A2 differentially enhance bacterial phagocytosis. Sex differences have been observed in pulmonary disease and in survival of wild type and SP-A knockout (KO) mice. The impact of human SP-A variants on survival after infection is unknown. In this study, we determined whether SP-A variants differentially affect survival of male and female mice infected with *Klebsiella pneumoniae*. Transgenic (TG) mice, where each carries a different human (h) SP-A1 ($6A^2$, $6A^4$), SP-A2 ($1A^0$, $1A^3$) variant or both variants SP-A1/SP-A2 ($6A^2/1A^0$, co-ex), and SP-A- KO, were utilized. The hTG and KO mice were infected intratracheally with *K. pneumoniae* bacteria, and groups of KO mice were treated with SP-A1 or SP-A2 either prior to and/or at the time of infection and survival for both experimental groups was monitored over 14 days. The binding of purified SP-A1 and SP-A2 proteins to phagocytic and non-phagocytic cells and expression of cell surface proteins in alveolar macrophages (AM) from SP-A1 and SP-A2 mice was examined. We observed gene-, variant-, and sex-specific (except for co-ex) differences with females showing better survival: (a) Gene-specific differences: co-ex = SP-A2 > SP-A1 > KO (both sexes); (b) Variant-specific survival co-ex ($6A^2/1A^0$) = $1A^0$ > $1A^3$ = $6A^2$ > $6A^4$ (both sexes); (c) KO mice treated with SPs (SP-A1 or SP-A2) proteins exhibit significantly ($p < 0.05$) better survival; (d) SP-A1 and SP-A2 differentially bind to phagocytic, but not to non-phagocytic cells, and AM from SP-A1 and SP-A2 hTG mice exhibit differential expression of cell surface proteins. Our results indicate that sex and SP-A genetics differentially affect survival after infection and that exogenous SP-A1/SP-A2 treatment significantly improves survival. We postulate that the differential SP-A1/SP-A2 binding to

the phagocytic cells and the differential expression of cell surface proteins that bind SP-A by AM from SP-A1 and SP-A2 mice play a role in this process. These findings provide insight into the importance of sex and innate immunity genetics in survival following infection.

Keywords: pulmonary surfactant protein A, pneumonia infection, surfactant protein A1 and A2, sex differences, innate host defense

INTRODUCTION

Cells and molecules of innate immunity in the lung provide the first line of host defense against a number of harmful pathogens, allergens, and air pollutants. The major outcomes of lung infection depend on several factors, such as effective clearance of pathogens and extra-pulmonary dissemination of infection into other internal organs. Pneumonia is a major health problem and a significant cause of infectious disease-related illness and death (1, 2). It has been observed previously in animal studies that, during pneumonia infection, pulmonary clearance, and the ability to limit bacterial dissemination, play an important role in differential outcome in survival between males and females in the presence or absence of oxidative stress (3, 4).

The Gram-negative bacteria *Klebsiella pneumoniae* (*K. pneumoniae*) are the most common hospital-acquired pathogens of the respiratory tract (5, 6). *K. pneumoniae* causes a wide range of infections, including pneumonia, urinary tract infections, bacteremias, and liver abscesses. Although immunocompromised individuals are more affected by *K. pneumoniae* infection, the development of new hypervirulent strains has affected a number of people including those who are healthy and immunosufficient or immunocompetent (7). The spread of *K. pneumoniae* infection to the blood stream is a critical step in disease pathogenesis, which leads to multiple organ failure (8).

Surfactant protein A (SP-A) is an important innate immune defense molecule. The human SP-A genetic locus consists of two functional genes, SFTPA1 and SFTPA2, encoding human SP-A1 and SP-A2, respectively. Each has been identified with a number of variants (9, 10). The SP-A1 and SP-A2 variants have been identified with both qualitative (i.e., functional, biochemical and/or structural) (11–23), and quantitative (regulatory) differences (24–28). The SP-A1 and SP-A2 variants have been shown to differ in their ability to modulate the proteomic expression profile of AM and the AM actin cytoskeleton (29–31), the AM miRNome (32), and the biophysical function of surfactant, where SP-A1 exhibits a higher efficiency in pulmonary surfactant reorganization (33). However, no differences have been observed between SP-A1 ($6A^2$) and SP-A2 ($1A^0$) in the inhibition of hemagglutination activity of influenza virus when *in vitro* expressed SP-A1 and SP-A2 was used (34).

SP-A has been found to enhance phagocytosis of microspheres, by exerting a direct effect on the phagocytic cell itself (35). Previously, we have also shown that SP-A2 variants enhance bacterial cell association and phagocytosis more effectively than SP-A1 variants (18, 19), and this activity is differentially compromised in response to oxidative stress (22). Furthermore, sex-dependent survival was observed in wild type and SP-A KO mice in response to *K. pneumoniae* infection, with females exhibiting higher survival compared to males, and the reverse was observed after oxidative stress (4, 36, 37), with females exhibiting lower survival compared to males. Sex hormones were implicated in the differential survival (38). Recent findings indicated that the SP-A1 and SP-A2 variants play a crucial role in the differential outcome of airway function in males and females with significant sex- and gene-specific differences in airway function mechanics in response to *K. pneumoniae* infection and methacholine challenge (23).

In the present study building on our previous findings we investigated the role of two SP-A1 ($6A^2$, $6A^4$) and two SP-A2 ($1A^0$, $1A^3$) variants, which are frequently observed in the general population (10), on survival in response to *K. pneumoniae*. We also studied whether treatment with SP-A1 or SP-A2 prior to and/or at the time of infection improves survival. In an attempt to gain insight into potential mechanisms, we studied SP-A1 and SP-A2 binding to phagocytic cells and differential expression AM cell surface proteins in SP-A1 and SP-A2 mice. The findings indicated a differential outcome in survival that is sex-, gene-, and variant- specific, and differential binding and differential expression of cell surface proteins may contribute to the observed differences.

METHODS

Animals

We used humanized transgenic (hTG) mice that each carried SP-A1 ($6A^2$, $6A^4$), SP-A2 ($1A^0$, $1A^3$), or both variants SP-A1/SP-A2 ($6A^2/1A^0$, co-ex), as well as SP-A knockout (KO) mice. hTG mice were generated on the C57BL6/J SP-A (KO) background (39). The animals used in this study were maintained as described previously (23). Briefly, the animals were raised and maintained in a pathogen-free environment, at the Penn State College of Medicine animal facility. Both males and females were used in this study. The females were synchronized with regard to the estrous cycle by placing female (group housed) mice in a dirty bedding from male cages 7 days prior to infection to stimulate estrus. All mice used in the present study were ∼12 weeks of age. A total of 490 mice (484 for infection and survival, 6 for Flow cytometry analysis) and 3 Sprague Dawley male rats (Harlan,

Abbreviations: AM, Alveolar macrophages; ANOVA, Analysis of variance; SP-A, surfactant protein A; hSP-A, human SP-A; hTG, humanized transgenic; HBSS, Hank's Balanced Salt solution; K. pneumoniae, Klebsiella pneumoniae; KO, knockout; PBS, Phosphate Buffered Saline; SFTPA1, gene encoding SP-A1; SFTPA2, gene encoding SP-A2; TSB, Tryptic soy broth.

Indianapolis, IN) for binding assay were used in the present study. All the procedures involving animal studies were approved by The Penn State Hershey Medical Center Institutional Animal Care and Use Committee (IACUC).

Preparation of Bacteria

K. pneumoniae bacteria (ATCC 43816) were obtained from American Tissue Culture Collection (Rockville, MD) and prepared as described previously (23, 37). Fifty μl of a suspension containing ∼ 450 CFU was used to infect each mouse. CFU/ml values were calculated based on the standard curve obtained at OD_{660} of the bacterial suspension.

Infection of Mice With *K. pneumoniae*

Mice were infected and monitored as described previously (23, 37). Briefly, hTG mice, SP-A1 ($6A^2$, $6A^4$), SP-A2 ($1A^0$, $1A^3$), SP-A1/SP-A2 ($6A^2/1A^0$, co-ex), and SP-A KO male and female mice were anesthetized, and infected intratracheally with *K. pneumoniae*, and monitored for survival twice a day for 14 days. Mice fallen sick and unable to recover, were euthanized immediately according to Penn State University IACUC protocol.

Treatment of Mice With SP-A Protein

SP-A KO male and female mice were anesthetized and pretreated with vehicle (0.9% NaCl, and 1 mM $CaCl_2$) and/or 10 μg of SP-A1 ($6A^2$), SP-A2 ($1A^0$) protein in 50 μl of 0.9% NaCl, and 1 mM $CaCl_2$ intratracheally for 18 h prior to infection. The mice were infected with *K. pneumoniae* (∼450 CFU/mouse) as described above, in combination with vehicle or with 10 μg of purified SP-A1 or SP-A2 protein expressed by stably transfected CHO cells as described (13, 17) in 50 μl of PBS intratracheally (23, 37), and monitored for survival for 14 days.

SP-A1 and SP-A2 Variant Binding Assay

Bronchoalveolar lavage was performed using PBS containing 1mM EDTA. AMs were then washed two times with PBS, 1mM EDTA and re-suspended in HBSS and adhered to 96-well, flat-bottom tissue culture plates. Adherent cells were washed with HBSS and blocked with HBSS containing 1 mg/mL human serum albumin. Plates were washed with binding buffer (10 mM HEPES/NaOH (pH 7.4), 0.14 M sodium chloride, 2.5 mM calcium chloride) and then incubated with 2.5 μg/mL of SP-A2 or SP-A1 in binding buffer. After binding, plates were washed four times with binding buffer and AM were extracted with extraction buffer (Tris-buffered saline, 6% SDS, 1% β-mercaptoethanol, 1mM EDTA). The extracted AMs were then diluted in TBS, and filtered using a Pall AcroPrep 96 filter plate to remove particulates. The samples were analyzed by dot blot method using nitrocellulose membrane and SP-A protein binding was detected using rabbit polyclonal antibody against hSP-A (1:25,000) and a goat anti–rabbit (IgG) HRP-conjugated (1:25,000, Bio-rad) and quantified by densitometry. For binding assays with THP-1(human monocyte derived, a macrophage-like and phagocytic) cell line, and CHO (non-phagocytic), cells were cultured as previously described (11, 13, 17), and assays were performed as mentioned above for AM cells.

Measurement of AM Cell Surface Proteins by Flow Cytometry

Staining for flow cytometry was performed on mouse alveolar macrophages (AMs) obtained from bronchoalveolar lavage of SP-A1 ($6A^2$) and SP-A2 ($1A^0$) hTG mice. Cells were washed with FACS buffer (PBS, 0.1 mM EDTA, 1% BSA, 0.02% sodium azide) and then blocked for 20 min at 4°C in FACS buffer containing 2 μg/mL Mouse BD Fc Block (BD Biosciences, Franklin Lakes, NJ) and 5% normal mouse serum. Fluorescently-conjugated mouse antibodies (PE-labeled) to specific cell surface markers (CD14 and TLR2, eBioscience, NY) were then added (1 μL/reaction) directly to the blocking solution and incubated for 30 min at room temperature. Cells were next washed 2 times with FACS buffer and fixed for 30 min at 4°C with 1% paraformaldehyde in FACS buffer. AMs were washed and re-suspended in FACS buffer and analyzed using a Special Order BD LSR II flow cytometer (BD). AMs were gated on the basis of forward scatter and side scatter and data for the expression of fluorescently-labeled cell surface proteins were collected from a population of 1×10^4 gated AMs using FACS Diva (BD) and analyzed using Cyflogic (CyFlo Ltd., Turku, Finland).

Statistical Analysis

Survival was analyzed by Chi-Square test (daily survival). The surviving animals were compared with a one-way analysis of variance (ANOVA) followed by Bonferroni multiple comparisons correction for each experimental group. Two-tailed *t*-tests were used to compare the SP-A variant binding assay results, and cell surface protein measurements. Data were presented as ± standard deviation. *P*-value <0.05 was considered to be significant (GraphPad Prism version 5; GraphPad Software, San Diego, USA).

RESULTS

hTG mice, SP-A1 ($6A^2$, $6A^4$), SP-A2 ($1A^0$, $1A^3$), SP-A1/SP-A2 ($6A^2/1A^0$, co-ex), and SP-A KO male and female mice were infected with *K. pneumoniae*, and monitored for 14 days for survival.

When we compared the overall survival of SP-A1, SP-A2, and mice carrying both SP-A variants (co-ex) we found that all mice had a better survival than the KO indicating that SP-A protects them from *K.pneumoniae* infection. SP-A2 and co-ex mice exhibited similar survival rates and better than mice carrying SP-A1 variants (**Figure 1A**). Thus the survival is genotype specific in the following order, co-ex = SP-A2 > SP-A1 > KO.

Next, we investigated whether survival differences exist between variants of a given gene or among variants. The survival (males and females combined) of SP-A variants ($1A^0$, $1A^3$, $6A^2$, $6A^4$), co-ex, and KO, is shown in **Figure 1B**. Mice carrying either an SP-A single gene variant or both gene variants (co-ex) had significantly higher survival compared to KO. Co-ex and SP-A2 ($1A^0$) had a similar survival rate over a 14 day period and this was significantly ($p < 0.05$) higher than that observed for mice carrying SP-A1 ($6A^2$, $6A^4$) and SP-A2 ($1A^3$) variants, indicating a gene and variant specific survival (**Figure 1B**). The mice carrying

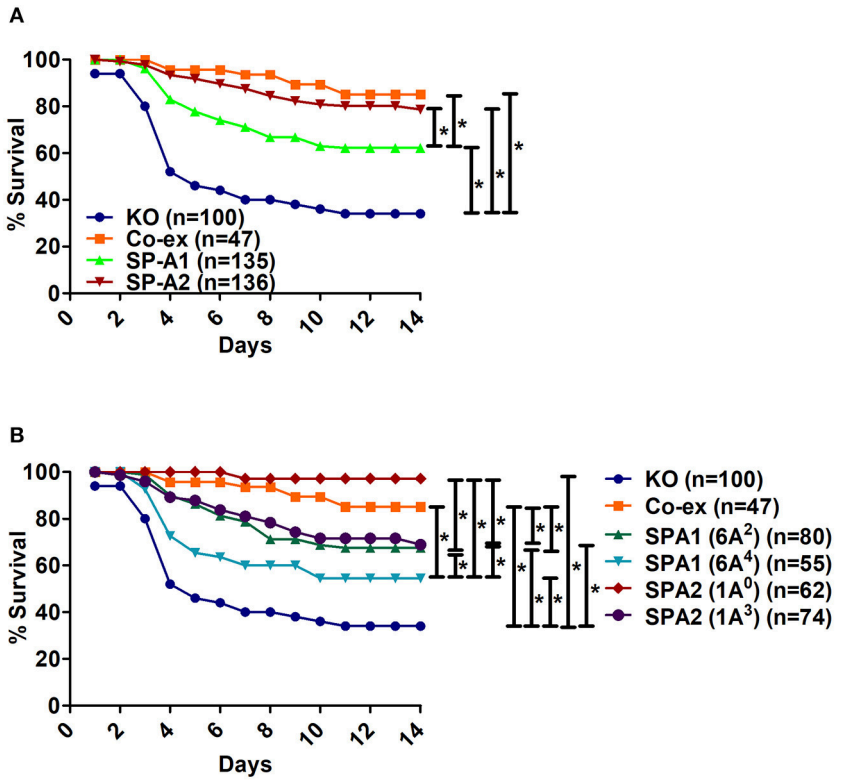

FIGURE 1 | Comparison of survival after *K. pneumoniae* infection. **(A)** Depicts differences in survival of male and female mice carrying a single SP-A1 or SP-A2 variant or both SP-A1 and SP-A2 (co-ex) variants and lacking SP-A (KO). **(B)** Depicts differences in survival of KO, SP-A2 ($1A^0$, $1A^3$), SP-A1 ($6A^2$, $6A^4$) and co-ex (males and females combined). Significant differences are indicated for survival $^*p < 0.05$.

the SP-A2 ($1A^3$) variant had similar survival rate with those carrying the SP-A1 ($6A^2$), and both exhibited significantly better survival compared to $6A^4$ variant (**Figure 1B**). The order of survival is, coex = SP-A2 ($1A^0$) > SP-A2 ($1A^3$) = SP-A1 ($6A^2$) > SP-A1 ($6A^4$) > KO.

Effect of Sex and SP-A Variants on the Course of Pneumonia

Sex Differences in Survival of Between SP-A1, SP-A2, KO, and SP-A1/SP-A2 ($6A^2/1A^0$, co-ex) Mice

Infection with *K.pneumoniae* resulted in significant sex differences over a period of time. In the SP-A1 ($6A^2$, $6A^4$), SP-A2 ($1A^0$, $1A^3$), and KO groups, all males compared to females showed a significant decrease in survival after infection (**Figures 2A–E**). The difference seemed to be considerably larger between males and females for $6A^2$ and $1A^3$ mice and to a lesser degree for $6A^4$ mice (**Figures 2A,B,D**), whereas, $1A^0$ and KO showed small but significant difference between males and females (**Figures 2C,E**). However, in mice carrying both SP-A1/SP-A2 variants ($6A^2/1A^0$, co-ex), no significant sex differences in survival were observed (**Figure 2F**).

Sex Differences Between Gene-Specific Variants

SP-A1

Bacterial infection resulted in significant differences in survival between males and females of $6A^2$ and $6A^4$ variants (**Figure 3A**). The $6A^2$ and $6A^4$ females had significantly higher survival compared to their respective $6A^2$ and $6A^4$ males, whereas, no significant differences were observed in males or females between each genotype (**Figure 3A**).

SP-A2

The $1A^0$ and $1A^3$ females had higher survival compared to their respective males (**Figure 3B**). $1A^0$ male had significantly higher survival compared to $1A^3$ males but similar to $1A^3$ females. Whereas, the $1A^0$ female had significantly higher survival compared to $1A^3$ male (**Figure 3B**).

Differences Among SP-A1 and SP-A2 Variants

The SP-A2 ($1A^0$) males exhibited significantly higher survival compared to SP-A1 ($6A^2$, $6A^4$) and SP-A2 ($1A^3$) males (**Figure 4A**). The $1A^0$ females exhibited a significant increase in survival compared to $6A^4$ females, but similar to $1A^3$ and $6A^2$ females (**Figure 4B**).

The SP-A2 ($1A^3$) males exhibited similar survival compared to $6A^2$, $6A^4$ males but lower than $1A^0$ (**Figure 4A**), whereas $1A^3$ females had significantly higher survival compared to $6A^4$ females, and similar to $6A^2$ and $1A^0$ females (**Figure 4B**).

In summary, Males: SP-A2 ($1A^0$) > SP-A2 ($1A^3$) = SP-A1 ($6A^2$, $6A^4$); Females: SP-A2 ($1A^0$) = SP-A2 ($1A^3$) = SP-A1 ($6A^2$) > ($6A^4$).

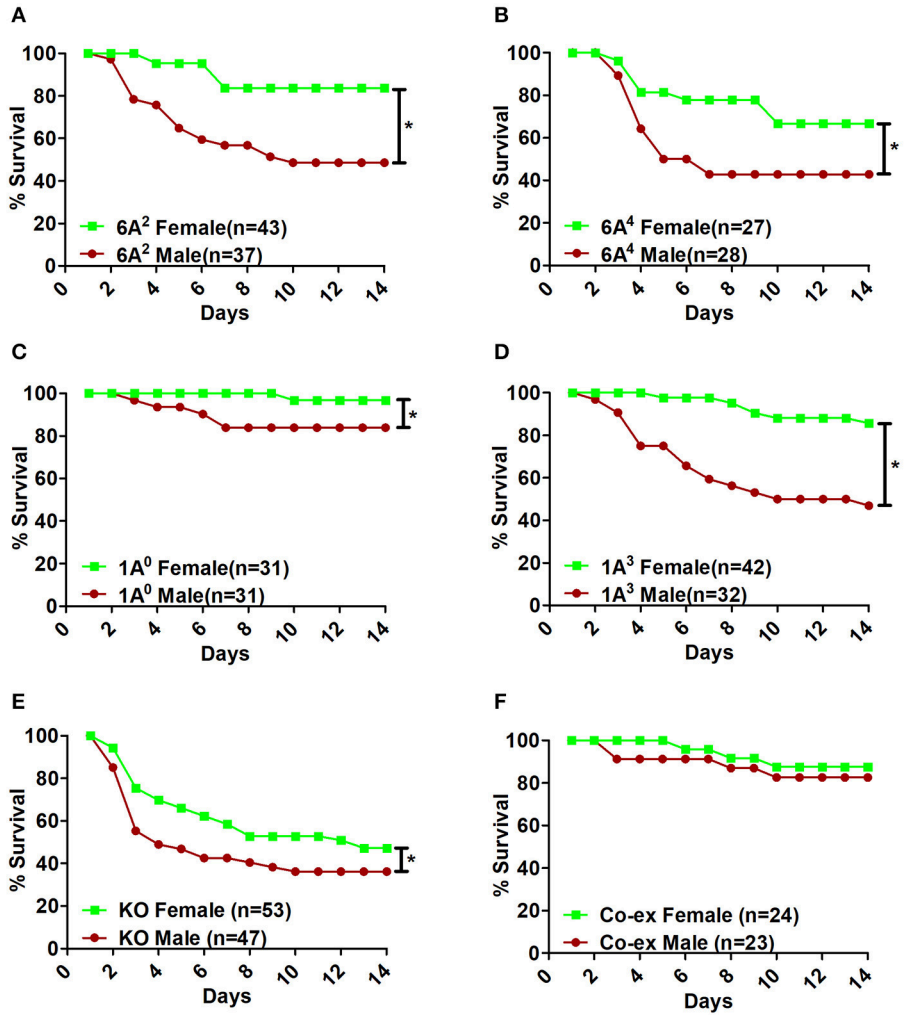

FIGURE 2 | Effect of sex on survival after *K. pneumoniae* infection. The survival rate was measured in SP-A1 ($6A^2$, $6A^4$) **(A,B)**, SP-A2 ($1A^0$, $1A^3$) **(C,D)**, SP-A KO **(E)**, and SP-A1/SP-A2 [$6A2/1A^0$, (co-ex)] **(F)** male and female mice over a period of 14 days after infection. Significant differences for survival are indicated $^*p < 0.05$. The number of mice used in each group is shown in Figure panels in parenthesis (n =).

Differences Between SP-A1/SP-A2 (co-ex) or KO and SP-A1 or SP-A2 Variants:

i The SP-A1/SP-A2 (co-ex) exhibited significant differences in survival compared to SP-A single gene variants in both males and females, as shown in **Figures 5A,B**. The co-ex males and females exhibited significantly higher survival compared to $1A^3$ (**Figure 5A**) and $6A^2$, and $6A^4$ males (**Figure 5B**) males. Of interest, the survival rate of co-ex males and females was similar to $1A^0$ males and females, and $1A^3$ females (**Figure 5A**), and $6A^2$ and $6A^4$ females (**Figure 5B**).

ii The KO exhibited significant differences in survival compared to SP-A variants and co-ex for both males and females, as shown in **Figures 6A,B**. The KO males and females had significantly lower survival compared to $1A^0$ males and females, $1A^3$ females (**Figure 6A**), $6A^2$ and $6A^4$ females (**Figure 6B**). However, the survival rate of KO males and females was similar to $1A^3$ males (**Figure 6A**), and $6A^2$ and $6A^4$ males (**Figure 6B**).

iii The SP-A1/SP-A2 (co-ex) exhibited significant differences in survival compared to KO in both males and females, as shown in **Figure 6C**.

Effect of Exogenous SP-A1 and SP-A2 Treatment on Survival

The overall survival of KO mice (male and female combined) that were treated prior to infection and/or at the time of infection with 10 μg of SP-A1 ($6A^2$), or SP-A2 ($1A^0$) purified proteins (indicated as SPs in **Figure 7A**) is shown in **Figure 7A**. SP-A treatment prior to infection, at the time of infection or prior to and at the time of infection resulted in a significantly better survival than mice treated with vehicle alone. However, no significant difference was observed among SP-treated groups

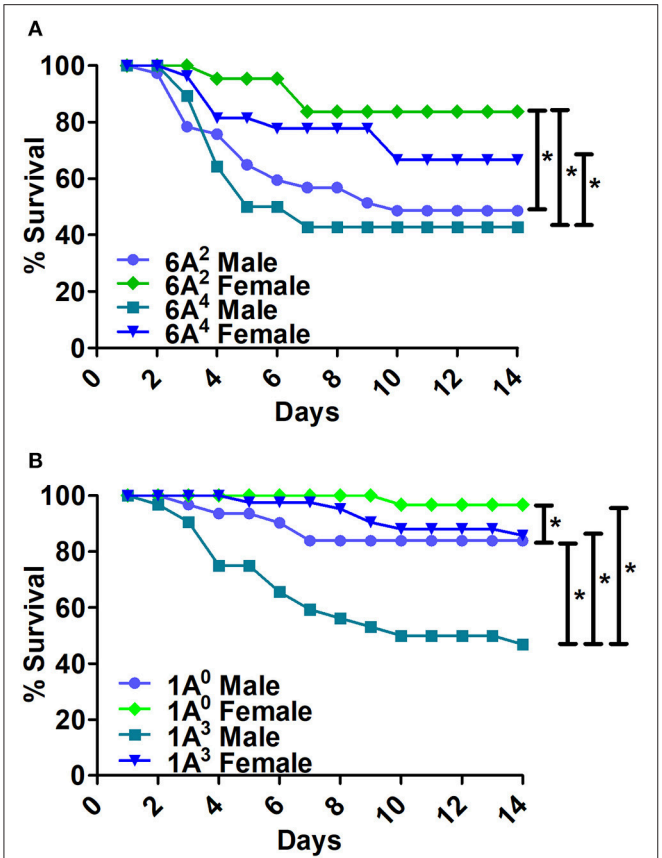

FIGURE 3 | Comparison of survival as a function of SP-A gene-specific variant after *K. pneumoniae* infection**. (A)** Depicts differences in survival between male and female mice of SP-A1 ($6A^2$, $6A^4$) and **(B)** depicts differences of SP-A2 ($1A^0$, $1A^3$) variants. Mouse survival was monitored for 14 days after infection. Significant differences for survival are indicated $^*p < 0.05$. The number of mice used for each group is shown in **Figure 2**.

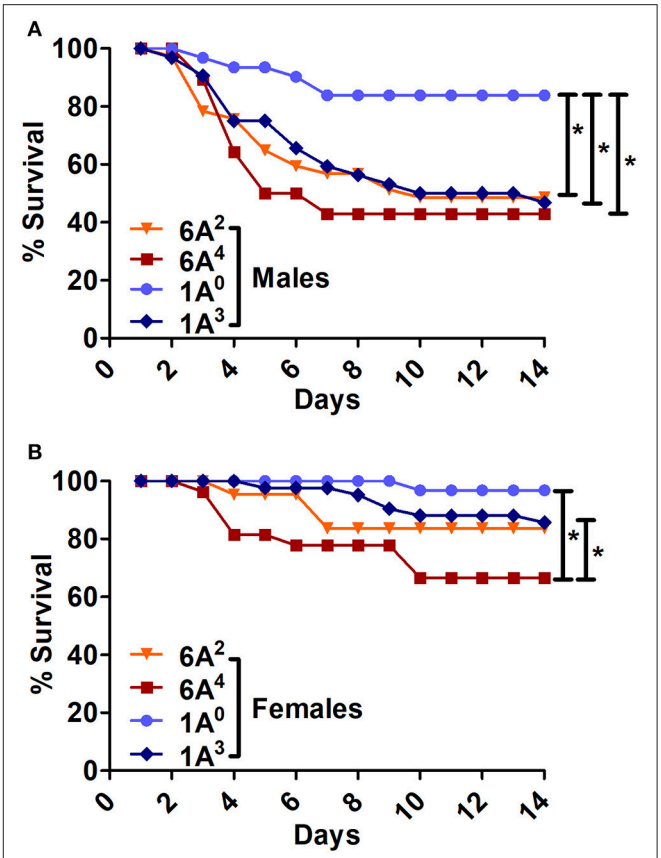

FIGURE 4 | Comparison of survival among SP-A1 and SP-A2 variants after *K. pneumoniae* infection. **(A)** Depicts differences in survival among males and **(B)** Depicts differences among females of SP-A1 ($6A^2$, $6A^4$) and SP-A2 ($1A^0$, $1A^3$). Mouse survival was monitored for 14 days after infection. Significant differences for survival are indicated $^*p < 0.05$. The number of mice used for each group is shown in **Figure 2**.

(**Figure 7A**). No significant difference was observed (a) between vehicle and SP-A1 or SP-A2 treatment prior to infection (**Figure 7B**), (b) between vehicle and SP-A1 or SP-A2 treatment at the time of infection (**Figure 7C**), or (c) between vehicle and SP-A1 or SP-A2 treatment prior to infection and at the time of infection (**Figure 7D**).

Binding of SP-A Variants to Phagocytic and non-phagocytic Cells and Cell Surface Protein Expression by AM From SP-A1 and SP-A2 Mice

Incubation of rat AMs with 2.5 μg/mL purified proteins SP-A1 ($6A^2$), or SP-A2 ($1A^0$) resulted in significant differences in binding between SP-A variants. SP-A2 ($1A^0$) bound significantly more to AMs than SP-A1 ($6A^2$) (**Figure 8A**). Similarly SP-A2 bound THP-1, a phagocytic cell line, significantly more than SP-A1 but no differences were observed when CHO cells, a non-phagocytic cell line was used (**Figure 8A**).

Next we investigated whether the AM differentially expresses cell surface proteins shown previously to bind SP-A. Expression of SP-A binding proteins such as CD14 and TLR2 on the cell surface of the AMs isolated from SP-A1 ($6A^2$), or SP-A2 ($1A^0$) mice were measured by flow cytometry. **Figure 8B** shows that the expression of these proteins differed significantly between the two variants. The SP-A2 ($1A^0$) variant showed significantly higher expression of CD14 and TLR2 than SP-A1 ($6A^2$). This differential expression of SP-A binding proteins on the cell surface of AM may play a role in the differential SP-A1 and SP-A2 binding.

DISCUSSION

Differences have been observed between SP-A1 and SP-A2 variants in their ability to enhance association of bacteria with the alveolar macrophage (AM), and SP-A2 variants were more effective than SP-A1 (18, 19, 40). A recent study indicated that the SP-A1 and SP-A2 variants differentially affect airway function in response to *K. pneumoniae* infection and methacholine challenge (23). In the current study, we wished to investigate whether SP-A variants differentially affect survival and whether rescue of SP-A KO mice with exogenous SP-A1 or SP-A2 improves survival. Toward this: we (a) Infected hTG mice carrying a

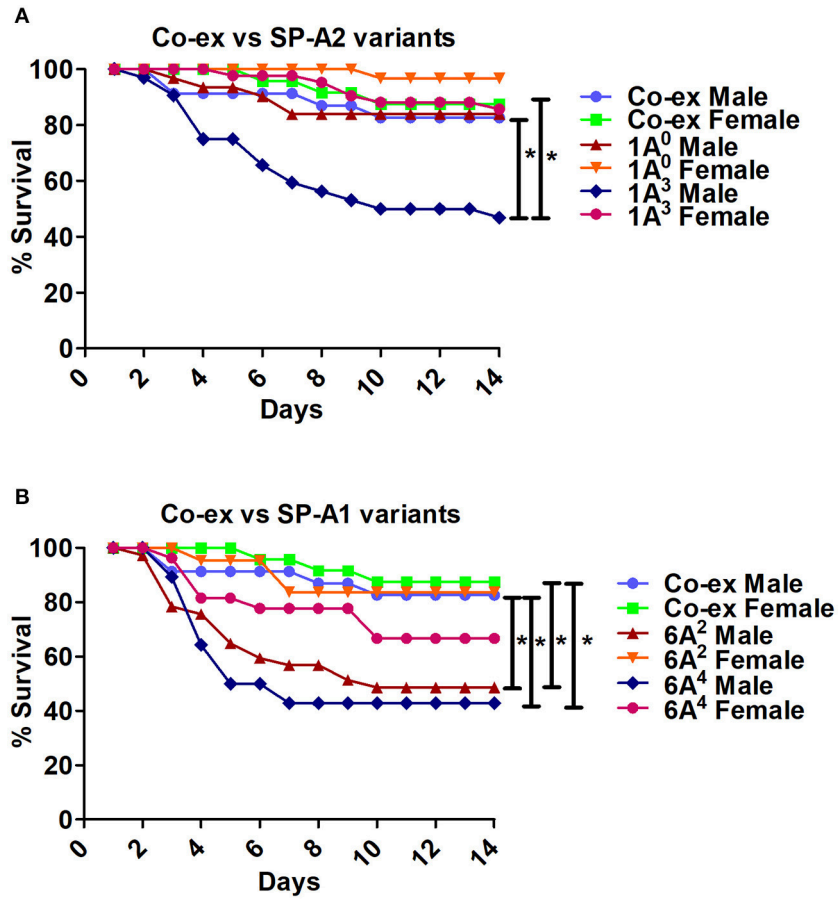

FIGURE 5 | Comparison of survival between co-ex and single gene SP-A variants after *K. pneumoniae* infection**. (A)** Depicts differences in survival between males and females of co-ex vs. SP-A2 ($1A^0$, $1A^3$) and **(B)** depicts differences of co-ex vs. SP-A1 ($6A^2$, $6A^4$). Mouse survival was monitored for 14 days after infection. Significant differences for survival are indicated $^*p < 0.05$. The number of mice used for each group is shown in **Figure 2**.

different SP-A1 or SP-A2 variant or both SP-A1/SP-A2 (co-ex) as well as mice lacking SP-A (i.e., KO) with *K. pneumoniae* and studied their daily survival over a 14 day period; (b) Rescued *K. pneumoniae* infected KO mice with exogenous SP-A1 or SP-A2 treatment prior to and/or at the time infection; (c) Carried out pilot binding studies of SP-A1 ($6A^2$) and SP-A2 ($1A^0$) to the AM as well as expression of cell surface proteins from AMs of SP-A1 ($6A^2$) and SP-A2 ($1A^0$) mice. The results showed, (a) Gene-specific survival: co-ex = SP-A2 > SP-A1 > KO (male and female together); (b) Variant-specific survival co-ex ($6A^2/1A^0$) = $1A^0$ > $1A^3$ = $6A^2$ > $6A^4$ (male and female together); (c) Sex differences in survival in SP-A variants and KO mice, with females showing better survival than males; (d) The co-ex ($6A^2/1A^0$) did not exhibit sex differences; (e) exogenous treatment of KO mice with SPs (SP-A1 or SP-A2) proteins significantly improved the overall survival; (f) Differential gene-specific SP-A1 and SP-A2 binding was observed with phagocytic but not with non-phagocytic cells, as well as differential expression of cell surface proteins in AM from SP-A1 and SP-A2 mice. The latter may in part contribute to the observed differences.

The SP-A protein is a major component of innate immune system. It has been previously observed that SP-A KO mice are more susceptible to pneumonia and show poor survival compared to the wild type mice (4), and display enhanced susceptibility to pulmonary infections (41, 42). In the present study we observed significant SP-A1 and SP-A2 specific differences, with SP-A2 or co-ex having a better survival than SP-A1. The observed gene- specific differences in survival may be due to structural differences between SP-A1 and SP-A2. The sequence of human SP-A1 and SP-A2 genes differs within the coding region (10, 43). Four amino acid differences located within the collagen-like domain distinguish between SP-A1 and SP-A2 variants. These are Met66, Asp73, Ile81 and Cys85 for SP-A1, and Thr66, Asn73, Val81, and Arg85 for SP-A2. The amino acid at position 85 of the precursor molecule, where SP-A1 has a cysteine and SP-A2 has an arginine (10) is a key difference between SP-A1 and SP-A2. This single amino acid change has a major impact on SP-A oligomerization, lipopolysaccharide (LPS) aggregation, and phagocytosis (20). It was proposed that a cysteine in the collagen-like domain as it is in SP-A1 may cause micro instability resulting in a less stable protein (12).

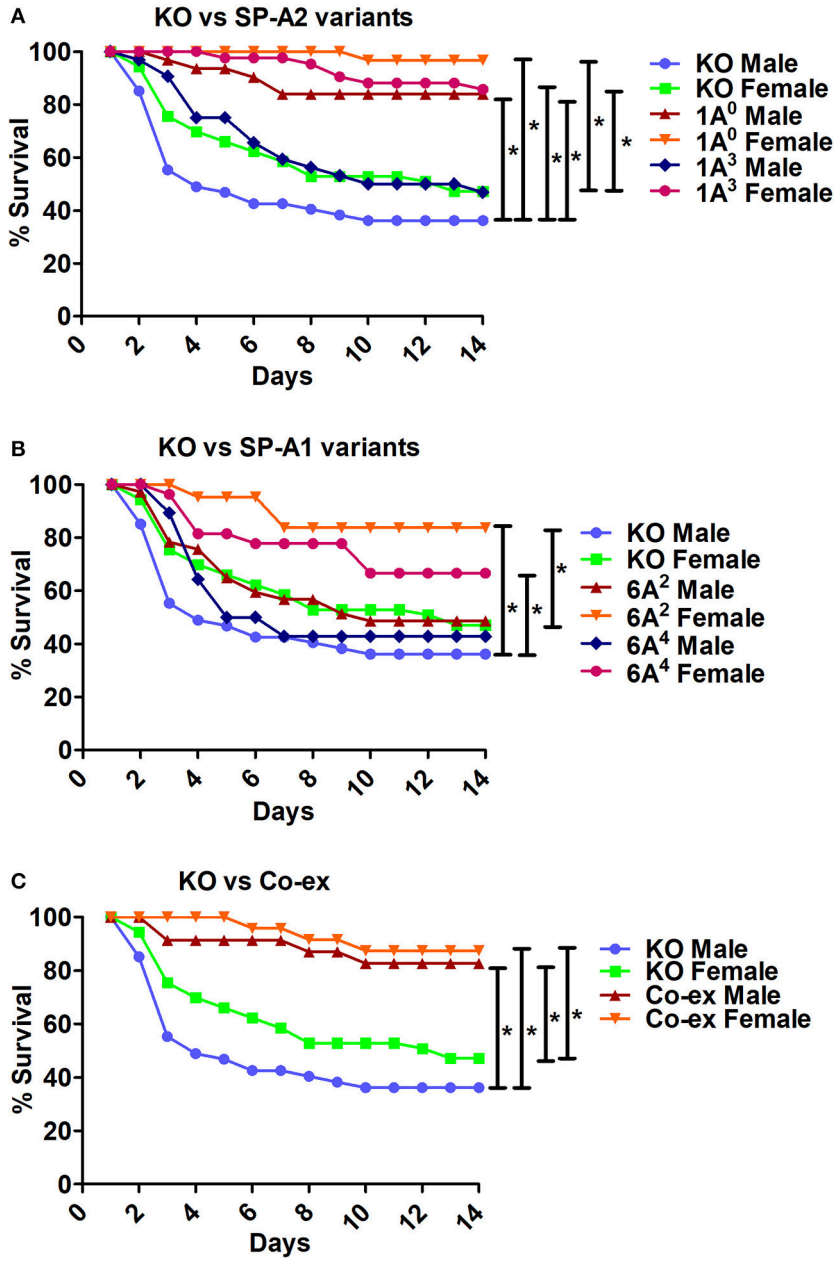

FIGURE 6 | Comparison of survival between KO and SP-A variants, and between KO and co-ex after *K. pneumoniae* infection**. (A)** Depicts differences in survival between males and females of KO vs. SP-A2 ($1A^0$, $1A^3$), **(B)** depicts differences between KO vs. SP-A1 ($6A^2$, $6A^4$), and **(C)** depicts differences between KO vs. co-ex. Mouse survival was monitored for 14 days after infection. Significant differences for survival are indicated $^*p < 0.05$. The number of mice used for each group is shown in **Figure 2**.

This change may play a key role in the gene-specific differences observed and may modulate functional capabilities mediated by the carbohydrate recognition domain (CRD) region. Thus, structural differences due to Cys85 and other amino acids may underlie the differences in function observed between SP-A1 and SP-A2.

Recently, SP-A1 and SP-A2 variants have been shown to play an important role in the differential outcome of airway function, with significant sex-, gene-, and variant-specific differences in lung function mechanics (23). In the current study, SP-A1 and SP-A2 variants also exhibited sex-, gene-, and variant- specific differences in survival. The $1A^3$ variant exhibited higher airway hyperreactivity compared to $1A^0$ for either sex, and the $6A^2$ and $6A^4$ variants exhibited diverse changes in both sexes in the lung function parameters studied (23). However, the $1A^3$ variant in the present study exhibited a decrease in survival than $1A^0$ in both sexes, and $6A^2$ and $6A^4$ variants did not differ in survival in either sex. The apparent discrepancies between SP-A2 variants

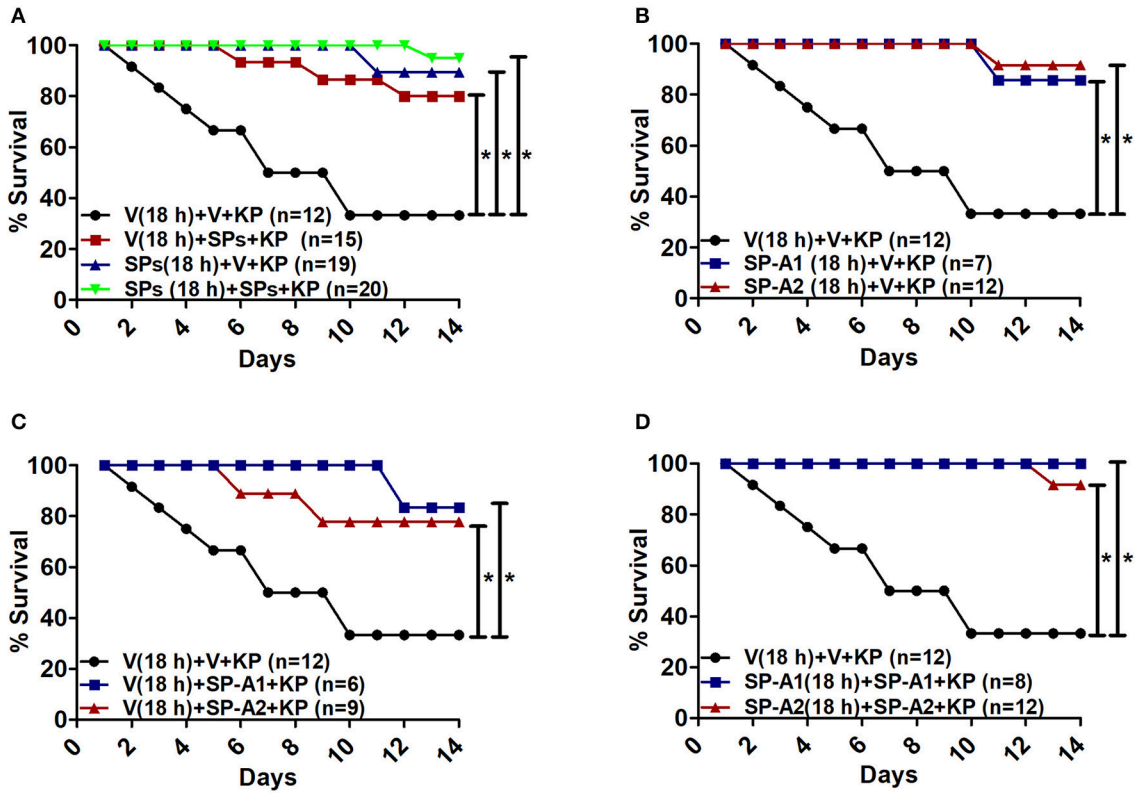

FIGURE 7 | Rescue by exogenous SP-A1 or SP-A2 treatment**. (A)** Depicts overall survival of infected KO mice after surfactant protein (SPs) treatment. **(B)** Depicts KO mouse survival after pretreatment with SP-A1 or SP-A2 prior to infection, **(C)** depicts KO survival after pretreatment with vehicle (Vp) and rescue at the time of infection with SP-A1 or SP-A2, **(D)** depicts KO survival after pretreatment with SP-A1 or SP-A2 and rescue with SP-A1 or SP-A2 at the time of infection. Mouse survival was monitored for 14 days after infection and treatment. Significant differences are indicated for survival $^*p < 0.05$.

in survival and lung function may be due to differences in the amount of time mice were exposed to *K. pneumoniae*, as lung functions were analyzed after 18 h of infection, whereas, the survival was monitored for a period of 14 days. We also speculate that the differences in amino acids at the collagen-like domain (as mentioned above) and in the CRD region of SP-A1 and SP-A2 at amino acid position 219 (Arg for $6A^2$ and Trp for $6A^4$) and at position 223 (Gln for $1A^0$ and Lys for $1A^3$) (10), may along with the lung microenvironment at the different time intervals further contribute to the apparent discrepancies in survival and lung function.

Sex Differences

In animal models, males exhibit a higher level of susceptibility to infection (*Candida albicans* and Mycobacterium marinum) (44, 45) and respiratory disease (Mycoplasma pulmonis) (46). Moreover, in clinical studies, sex influences significantly lung disease susceptibility, and males in general are more susceptible than females to lung disease, as observed in neonatal respiratory distress syndrome (RDS) after premature birth (47, 48), IPF, and COPD (49, 50), as well as different types of pneumonia (49, 51–53). This indicates that the relationship between sex and lung disease may be a complex one (50) and requires further investigation.

All SP-A1 and SP-A2 variants studied showed sex differences in survival with females showing a better rate of survival than males. This is consistent with our previous observations with animal models where wild type and SP-A KO mice showed similar sex differences after exposure to pneumonia and/or environmental stress (4, 36, 37). Sex hormones were shown to play a key role in the survival differences between males and females after infection and ozone-induced oxidative stress (38). In line with the sex differences observed in survival in the present study, are our recent findings where hTG SP-A1 and SP-A2 mice showed differences in their respiratory mechanics, with females exhibiting a significantly higher airway hyperreactivity in response to infection compared to males and the pattern was reversed after methacholine challenge (23). However, the SP-A1/SP-A2 (co-ex) mice showed no sex differences in survival, but did show sex differences in lung function mechanics with females to have higher airway hyperreactivity compared to males in response to infection. Interestingly, similar to survival, no sex differences were found in co-ex in response to infection and methacholine challenge (23). These differences (as mentioned above) may be due to (i) experimental differences in terms of the time interval of *K. pneumoniae* exposure, and (ii) the lung microenvironment at different time intervals after infection. In humans differences in the relative levels of SP-A1 and SP-A2 may

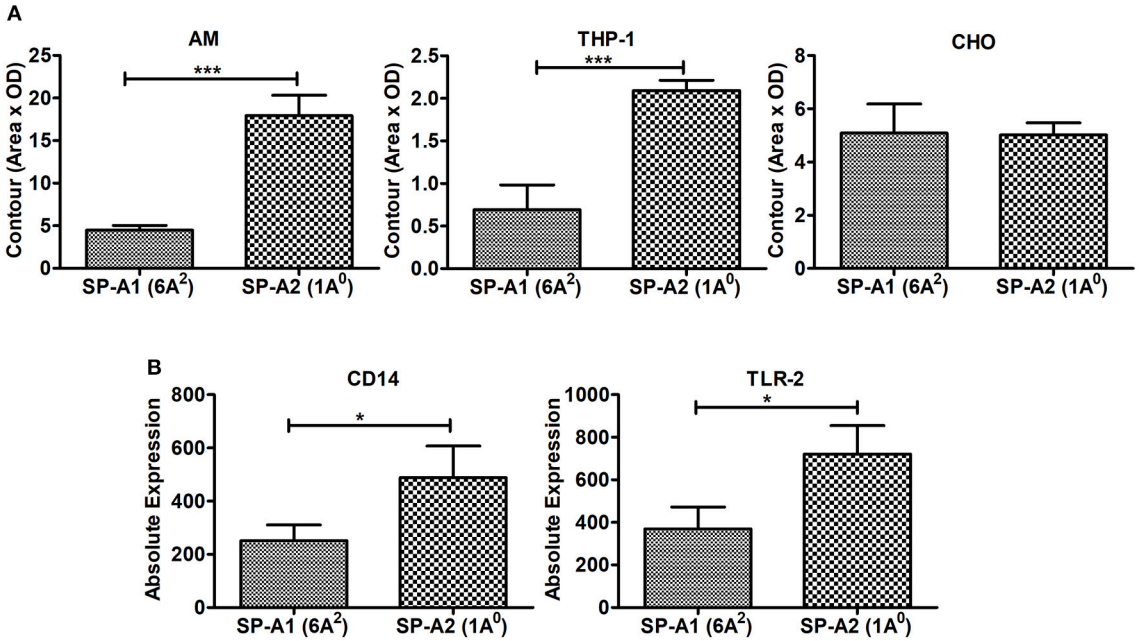

FIGURE 8 | Binding of SP-A1 ($6A^2$) and SP-A2 ($1A^0$) variants to phagocytic and non-phagocytic cells and expression of cell surface proteins in AMs of SP-A1 ($6A^2$) and SP-A2 ($1A^0$) mice. **(A)** depicts binding of rat AM and two cell lines (THP-1, a macrophage-like and phagocytic and the other CHO, non-phagocytic) to SP-A variants expressed by stably transfected mammalian cell lines. Cells (AM, THP-1, and CHO) were adhered to 96-well tissue culture plates and incubated with purified SP-A2 ($1A^0$) and SP-A1 ($6A^2$). Cells were then washed and lysed and the SP-A content of the lysates determined by Western dot blot and densitometry. A significant increase in binding of SP-A2 vs. SP-A1 ($p = 0.0007$) to AM was seen as was for the phagocytic THP-1 cells ($p = 0.0015$), but no differences were observed with the non-phagocytic CHO cells. **(B)** Depicts expression of SP-A binding proteins from AMs of hTG SP-A1 ($6A^2$) and SP-A2 ($1A^0$) mice. Bronchoalveolar lavage was performed on hTG SP-A2 ($1A^0$) and SP-A1 ($6A^2$) mice. AM were stained for SP-A binding proteins CD14 and TLR2 and analyzed by flow cytometry. A significant increase in expression of CD14 ($p = 0.036$) and TLR2 ($p = 0.022$) was seen in SP-A2 ($1A^0$) AM vs. SP-A1 ($6A^2$) AM. $^*p < 0.05$, $^{***}p < 0.001$.

further contribute to the observed differences in lung function mechanics and/or survival.

The hormonal mechanism as to how sex hormones regulate SP-A1 and SP-A2 are not known. However, other groups have reported that, SP-A gene expression in fetal lung tissues of various species to be regulated by a variety of hormones and factors, including retinoids, insulin, growth factors and cytokines, glucocorticoids and cAMP (54), estrogen related receptor –α, which is an important mediator of SP-A gene expression and its induction by cAMP (55), and testosterone to positively regulate the expression of SP-A (56). Moreover, human SP-A1 and SP-A2 genes are differentially regulated during development by cAMP and glucocorticoids (24, 25, 57).

E2 has been implicated in the immune response against infection, and involves the transcriptional activation of genes encoding TLR2 (58). SP-A modulates the lung inflammatory response by regulating macrophage TLR activity and specifically by enhancing the expression of TLR2 (59). It was observed that treatment of THP-1 cells (macrophage-like cell line) with E2 resulted in increased TLR2 mRNA and protein levels, indicating that the TLR2 is an estrogen-regulated gene whose expression is upregulated by interaction with ER-α (60). In our previous study, gonadectomy of FA-exposed females resulted in decreased survival, indicating that the female gonadal hormones (E2 and progesterone) are important for protection. Treatment of gonadectomized males with E2 increased the survival similar to intact females and survival of gonadectomized females treated with DHT was similar to that of intact males (38). Thus the available literature not only supports a role of sex hormones in animal survival but also sex hormones may affect expression of SP-A and TLR2 via which SP-A modulates lung inflammatory response.

We and others have shown that SP-A KO mice are more susceptible to pneumonia and show poor survival compared to the wild type mice (4), as well as display enhanced susceptibility to pulmonary infections (41, 42), with females being better than males indicating a role of SP-A in host defense. We have also shown that SP-A2 variants enhance bacterial cell association and phagocytosis more effectively than SP-A1 variants (18, 19), and these SP-A2 variants exhibited a better outcome of airway function (23). These together indicate a role of SP-A in infection and hat SP-A1 and SP-A2 differ in their activities in several lung processes/function and these may in part explain differences observed in the survival of SP-A1 and SP-A2 hTG mice.

Rescue

A single or a double SP-A1 or SP-A2 treatment before and/or at the time of infection significantly improved survival. Also, a single SP-A treatment has been shown previously to nearly

restore the AM proteomics profile of SP-A KO mice to that of wild type mice (61). Moreover, a single treatment with exogenous SP-A1 or SP-A2 differentially affected the AM proteome of SP-A KO mice (30). Further, the proteomic expression profile of the AM and the actin cytoskeleton of the AM from SP-A1 and SP-A2 mice are shown to differ (29, 31) as well as the AM miRNome is shown to differ in these mice (32). Together these indicate that the SP-A (SP-A1 and SP-A2) variants not only protect against common pathogens but point to future possibilities of use of SP-A proteins or perhaps peptides of SPs as a modulatory contributor to innate immune function.

Binding and Cell Surface Proteins

Phagocytosis of microspheres by a macrophage-like cell line, indicated that SP-A has a direct effect on the phagocytic cell (35). In the present study we observed that SP-A1 and SP-A2 differentially bind to AM, with SP-A2 binding being more than SP-A1. Similar differential binding was observed for a phagocytic cell line but not for a non-phagocytic cell line suggesting that cell surface molecules present on phagocytic cells mediate differential binding of SP-A1 and SP-A2. In fact in our pilot studies we observed in AMs from SP-A1 and SP-A2 hTG mice, a differential expression of cell surface proteins, CD14 and TLR2, previously shown to bind SP-A (62–64). In line with the above general possibility are our observations, where SP-A2 variants enhanced bacterial cell association and phagocytosis more effectively than SP-A1 variants (18, 19), and this activity was differentially compromised in response to oxidative stress (22). Also higher levels of pro-inflammatory cytokines have been observed in a macrophage-like cell line in response to SP-A2 treatment compared to SP-A1 treatment (13). Collectively these differential functional effects of SP-A1 and SP-A2 on the AM may, in part, contribute to the survival differences observed between SP-A1 and SP-A2 mice.

In summary, the genetics of the innate immunity and specifically the variants of human SP-A1 and SP-A2 affect survival after *K. pneumoniae* infection in a sex-, gene-, and variant-specific manner with females showing a better survival than males: (a) Gene-specific survival: co-ex = SP-A2 > SP-A1 > KO (male and female together); (b) Variant-specific survival co-ex $(6A^2/1A^0) = 1A^0 > 1A^3 = 6A^2 > 6A^4$ (male and female together); (c) Treatment with exogenous SP-A1 or SP-A2 before and/or at the time of infection improves survival significantly. We speculate that the differential binding of SP-A1 and SP-A2 to the AM mediated by differentially expressed cell surface proteins on the AM contributes to the observed differences. This study identifies a potential contributor (i.e., SP-A genetics) to differences in individual variability to lung disease susceptibility. Moreover, treatment with exogenous SP-A or SP-A mimics is likely to improve disease outcome in bacterial pneumonia or other types irritant-induced lung disorders.

ETHICS STATEMENT

All protocols used in this study were evaluated and approved by the Pennsylvania State University College of Medicine Institutional Animal Care and Use Committee and conformed to the guidelines of the National Institute of Health on the care and use of laboratory animals.

AUTHOR CONTRIBUTIONS

NT: Performed experiments, ran statistics, analyzed and synthesized the data, contributed to the manuscript writing; TU: Performed binding assay, flow cytometry, mouse line maintenance, breeding, and infection; XZ: Performed mouse line maintenance, breeding, and infection; DP: Contributed to manuscript writing; JF: Designed the study and provided oversight to the entire project, involved in data analysis, integration, and writing of the manuscript. All authors read and approved the final manuscript.

FUNDING

This work was supported by CHILD fund, Department of Pediatrics, College of Medicine at Pennsylvania State University.

REFERENCES

1. Black RE, Morris SS, Bryce J. Where and why are 10 million children dying every year? *Lancet* (2003) 361:2226–34. doi: 10.1016/S0140-6736(03)13779-8
2. Waterer G, Wunderink R. Respiratory infections: a current and future threat. *Respirology* (2009) 14:651–5. doi: 10.1111/j.1440-1843.2009.01554.x
3. Mikerov AN, Cooper TK, Wang G, Hu S, Umstead TM, Phelps DS, et al. Histopathologic evaluation of lung and extrapulmonary tissues show sex differences in *Klebsiella pneumoniae* - infected mice under different exposure conditions. *Int J Physiol Pathophysiol Pharmacol.* (2011) 3:176–90.
4. Mikerov AN, Hu S, Durrani F, Gan X, Wang G, Umstead TM, et al. Impact of sex and ozone exposure on the course of pneumonia in wild type and SP-A (-/-) mice. *Microb Pathog.* (2012) 52:239–49. doi: 10.1016/j.micpath.2012.01.005
5. Podschun R, Ullmann U. Klebsiella spp. as nosocomial pathogens: epidemiology, taxonomy, typing methods, and pathogenicity factors. *Clin Microbiol Rev.* (1998) 11:589–603.
6. Kofteridis DP, Papadakis JA, Bouros D, Nikolaides P, Kioumis G, Levidiotou S, et al. Nosocomial lower respiratory tract infections: prevalence and risk factors in 14 Greek hospitals. *Eur J Clin Microbiol Infect Dis.* (2004) 23:888–91. doi: 10.1007/s10096-004-1245-y
7. Paczosa MK, Mecsas J. *Klebsiella pneumoniae*: going on the offense with a strong defense. *Microbiol Mol Biol Rev.* (2016) 80:629–61. doi: 10.1128/MMBR.00078-15
8. Yinnon AM, Butnaru A, Raveh D, Jerassy Z, Rudensky B. *Klebsiella bacteraemia*: community versus nosocomial infection. *Qjm* (1996) 89:933–41. doi: 10.1093/qjmed/89.12.933
9. Karinch AM, Floros J. 5' splicing and allelic variants of the human pulmonary surfactant protein A genes. *Am J Respir Cell Mol Biol.* (1995) 12:77–88. doi: 10.1165/ajrcmb.12.1.7811473
10. DiAngelo S, Lin Z, Wang G, Phillips S, Ramet M, Luo J, et al. Novel, non-radioactive, simple and multiplex PCR-cRFLP methods for genotyping human SP-A and SP-D marker alleles. *Dis Markers* (1999) 15:269–81. doi: 10.1155/1999/961430
11. Wang G, Phelps DS, Umstead TM, Floros J. Human SP-A protein variants derived from one or both genes stimulate TNF-alpha production in the THP-1 cell line. *Am J Physiol Lung Cell Mol Physiol.* (2000) 278:L946–54. doi: 10.1152/ajplung.2000.278.5.L946

12. Garcia-Verdugo I, Wang G, Floros J, Casals C. Structural analysis and lipid-binding properties of recombinant human surfactant protein a derived from one or both genes. *Biochemistry* (2002) 41:14041–53. doi: 10.1021/bi026540l
13. Wang G, Umstead TM, Phelps DS, Al-Mondhiry H, Floros J. The effect of ozone exposure on the ability of human surfactant protein a variants to stimulate cytokine production. *Environ Health Perspect.* (2002) 110:79–84. doi: 10.1289/ehp.0211079
14. Oberley RE, Snyder JM. Recombinant human SP-A1 and SP-A2 proteins have different carbohydrate-binding characteristics. *Am J Physiol Lung Cell Mol Physiol.* (2003) 284:L871–81. doi: 10.1152/ajplung.00241.2002
15. Selman M, Lin HM, Montano M, Jenkins AL, Estrada A, Lin Z, et al. Surfactant protein A and B genetic variants predispose to idiopathic pulmonary fibrosis. *Hum Genet.* (2003) 113:542–50. doi: 10.1007/s00439-003-1015-4
16. Huang W, Wang G, Phelps DS, Al-Mondhiry H, Floros J. Human SP-A genetic variants and bleomycin-induced cytokine production by THP-1 cells: effect of ozone-induced SP-A oxidation. *Am J Physiol Lung Cell Mol Physiol.* (2004) 286:L546–53. doi: 10.1152/ajplung.00267.2003
17. Wang G, Bates-Kenney SR, Tao JQ, Phelps DS, Floros J. Differences in biochemical properties and in biological function between human SP-A1 and SP-A2 variants, and the impact of ozone-induced oxidation. *Biochemistry* (2004) 43:4227–39. doi: 10.1021/bi036023i
18. Mikerov AN, Umstead TM, Huang W, Liu W, Phelps DS, Floros J. SP-A1 and SP-A2 variants differentially enhance association of *Pseudomonas aeruginosa* with rat alveolar macrophages. *Am J Physiol Lung Cell Mol Physiol.* (2005) 288:L150–8. doi: 10.1152/ajplung.00135.2004
19. Mikerov AN, Wang G, Umstead TM, Zacharatos M, Thomas NJ, Phelps DS, et al. Surfactant protein A2 (SP-A2) variants expressed in CHO cells stimulate phagocytosis of *Pseudomonas aeruginosa* more than do SP-A1 variants. *Infect Immun.* (2007) 75:1403–12. doi: 10.1128/IAI.01341-06
20. Wang G, Myers C, Mikerov A, Floros J. Effect of cysteine 85 on biochemical properties and biological function of human surfactant protein A variants. *Biochemistry* (2007a) 46:8425–35. doi: 10.1021/bi7004569
21. Wang G, Taneva S, Keough KM, Floros J. Differential effects of human SP-A1 and SP-A2 variants on phospholipid monolayers containing surfactant protein B. *Biochim Biophys Acta* (2007b) 1768:2060–9. doi: 10.1016/j.bbamem.2007.06.025
22. Mikerov AN, Umstead TM, Gan X, Huang W, Guo X, Wang G, et al. Impact of ozone exposure on the phagocytic activity of human surfactant protein A (SP-A) and SP-A variants. *Am J Physiol Lung Cell Mol Physiol.* (2008c) 294:L121–30. doi: 10.1152/ajplung.00288.2007
23. Thorenoor N, Zhang X, Umstead TM, Scott Halstead E, Phelps DS, Floros J. Differential effects of innate immune variants of surfactant protein-A1 (SFTPA1) and SP-A2 (SFTPA2) in airway function after *Klebsiella pneumoniae* infection and sex differences. *Respir Res.* (2018) 19:23. doi: 10.1186/s12931-018-0723-1
24. Karinch AM, Deiter G, Ballard PL, Floros J. Regulation of expression of human SP-A1 and SP-A2 genes in fetal lung explant culture. *Biochim Biophys Acta* (1998) 1398:192–202. doi: 10.1016/S0167-4781(98)00047-5
25. Kumar AR, and Snyder JM. Differential regulation of SP-A1 and SP-A2 genes by cAMP, glucocorticoids, and insulin. *Am J Physiol.* (1998) 274(2 Pt 1):L177–85.
26. Scavo LM, Ertsey R, and Gao BQ. Human surfactant proteins A1 and A2 are differentially regulated during development and by soluble factors. *Am J Physiol.* (1998) 275(4 Pt 1):L653–69.
27. Wang G, Guo X, Floros J. Human SP-A 3'-UTR variants mediate differential gene expression in basal levels and in response to dexamethasone. *Am J Physiol Lung Cell Mol Physiol.* (2003) 284:L738–48. doi: 10.1152/ajplung.00375.2002
28. Tagaram HR, Wang G, Umstead TM, Mikerov AN, Thomas NJ, Graff GR, et al. Characterization of a human surfactant protein A1 (SP-A1) gene-specific antibody; SP-A1 content variation among individuals of varying age and pulmonary health. *Am J Physiol Lung Cell Mol Physiol.* (2007) 292:L1052–63. doi: 10.1152/ajplung.00249.2006
29. Phelps DS, Umstead TM, Silveyra P, Hu S, Wang G, Floros J. Differences in the alveolar macrophage proteome in transgenic mice expressing human SP-A1 and SP-A2. *J Proteom Genom Res.* (2013) 1:2–26. doi: 10.14302/issn.2326-0793.jpgr-12-207
30. Phelps DS, Umstead TM, Floros J. Sex differences in the acute *in vivo* effects of different human SP-A variants on the mouse alveolar macrophage proteome. *J Proteomics* (2014) 108:427–44. doi: 10.1016/j.jprot.2014.06.007
31. Tsotakos N, Phelps DS, Yengo CM, Chinchilli VM, Floros J. Single-cell analysis reveals differential regulation of the alveolar macrophage actin cytoskeleton by surfactant proteins A1 and A2: implications of sex and aging. *Biol Sex Differ.* (2016) 7:18. doi: 10.1186/s13293-016-0071-0
32. Noutsios GT, Thorenoor N, Zhang X, Phelps DS, Umstead TM, Durrani F, et al. SP-A2 contributes to miRNA-mediated sex differences in response to oxidative stress: pro-inflammatory, anti-apoptotic, and anti-oxidant pathways are involved. *Biol Sex Differ.* (2017) 8:37. doi: 10.1186/s13293-017-0158-2
33. Lopez-Rodriguez E, Pascual A, Arroyo R, Floros J, Perez-Gil J. Human pulmonary surfactant protein SP-A1 provides maximal efficiency of lung interfacial films. *Biophys J.* (2016) 111:524–36. doi: 10.1016/j.bpj.2016.06.025
34. Mikerov AN, White M, Hartshorn K, Wang G, Floros J. Inhibition of hemagglutination activity of influenza A viruses by SP-A1 and SP-A2 variants expressed in CHO cells. *Med Microbiol Immunol.* (2008d) 197:9–12. doi: 10.1007/s00430-007-0051-4
35. Ding J, Umstead TM, Floros J, Phelps DS. Factors affecting SP-A-mediated phagocytosis in human monocytic cell lines. *Respir Med.* (2004) 98:637–50. doi: 10.1016/j.rmed.2003.12.018
36. Mikerov AN, Gan X, Umstead TM, Miller L, Chinchilli VM, Phelps DS, et al. Sex differences in the impact of ozone on survival and alveolar macrophage function of mice after Klebsiella pneumoniae infection. *Respir Res.* (2008a) 9:24. doi: 10.1186/1465-9921-9-24
37. Mikerov AN, Haque R, Gan X, Guo X, Phelps DS, Floros J. Ablation of SP-A has a negative impact on the susceptibility of mice to *Klebsiella pneumoniae* infection after ozone exposure: sex differences. *Respir Res.* (2008b) 9:77. doi: 10.1186/1465-9921-9-77
38. Durrani F, Phelps DS, Weisz J, Silveyra P, Hu S, Mikerov AN, et al. Gonadal hormones and oxidative stress interaction differentially affects survival of male and female mice after lung *Klebsiella pneumoniae* infection. *Exp Lung Res.* (2012) 38:165–72. doi: 10.3109/01902148.2011.654045
39. Wang G, Guo X, Diangelo S, Thomas NJ, Floros J. Humanized SFTPA1 and SFTPA2 transgenic mice reveal functional divergence of SP-A1 and SP-A2: formation of tubular myelin *in vivo* requires both gene products. *J Biol Chem.* (2010) 285:11998–2010. doi: 10.1074/jbc.M109.046243
40. Floros J, Wang G, Mikerov AN. Genetic complexity of the human innate host defense molecules, surfactant protein A1 (SP-A1) and SP-A2–impact on function. *Crit Rev Eukaryot Gene Expr.* (2009) 19:125–37. doi: 10.1615/CritRevEukarGeneExpr.v19.i2.30
41. Korfhagen TR, Bruno MD, Ross GF, Huelsman KM, Ikegami M, Jobe AH, et al. Altered surfactant function and structure in SP-A gene targeted mice. *Proc Natl Acad Sci USA.* (1996) 93:9594–9. doi: 10.1073/pnas.93.18.9594
42. LeVine AM, Whitsett JA. Pulmonary collectins and innate host defense of the lung. *Microbes Infect.* (2001) 3:161–6. doi: 10.1016/S1286-4579(00)01363-0
43. Floros J, Hoover RR. Genetics of the hydrophilic surfactant proteins A and D. *Biochim Biophys Acta* (1998) 1408:312–22. doi: 10.1016/S0925-4439(98)00077-5
44. Ashman RB, Kay PH, Lynch DM, Papadimitriou JM. Murine candidiasis: sex differences in the severity of tissue lesions are not associated with levels of serum C3 and C5. *Immunol Cell Biol.* (1991) 69:7–10. doi: 10.1038/icb.1991.2
45. Yamamoto Y, Saito H, Setogawa T, Tomioka H. Sex differences in host resistance to *Mycobacterium marinum* infection in mice. *Infect Immun.* (1991) 59:4089–96.
46. Yancey AL, Watson HL, Cartner SC, Simecka JW. Gender is a major factor in determining the severity of mycoplasma respiratory disease in mice. *Infect Immun.* (2001) 69:2865–71. doi: 10.1128/IAI.69.5.2865-2871.2001
47. Perelman RH, Palta M, Kirby R, Farrell PM. Discordance between male and female deaths due to the respiratory distress syndrome. *Pediatrics* (1986) 78:238–44.
48. Nielsen HC. Testosterone regulation of sex differences in fetal lung development. *Proc Soc Exp Biol Med.* (1992) 199:446–52. doi: 10.3181/00379727-199-43379

49. Gordon HS, Rosenthal GE. The relationship of gender and in-hospital death: increased risk of death in men. *Med Care* (1999) 37:318–24. doi: 10.1097/00005650-199903000-00011
50. Caracta CF. Gender differences in pulmonary disease. *Mt Sinai J Med.* (2003) 70:215–24.
51. Loeb M, McGeer A, McArthur M, Walter S, Simor AE. Risk factors for pneumonia and other lower respiratory tract infections in elderly residents of long-term care facilities. *Arch Intern Med.* (1999) 159:2058–64. doi: 10.1001/archinte.159.17.2058
52. Gannon CJ, Pasquale M, Tracy JK, McCarter RJ, Napolitano LM. Male gender is associated with increased risk for postinjury pneumonia. *Shock* (2004) 21:410–4. doi: 10.1097/00024382-200405000-00003
53. Gutierrez F, Masia M, Mirete C, Soldan B, Rodriguez JC, Padilla S, et al. The influence of age and gender on the population-based incidence of community-acquired pneumonia caused by different microbial pathogens. *J Infect.* (2006) 53:166–74. doi: 10.1016/j.jinf.2005.11.006
54. Mendelson CR. Role of transcription factors in fetal lung development and surfactant protein gene expression. *Annu Rev Physiol.* (2000) 62:875–915. doi: 10.1146/annurev.physiol.62.1.875
55. Liu D, Hinshelwood MM, Giguere V, Mendelson CR. Estrogen related receptor-alpha enhances surfactant protein-A gene expression in fetal lung type II cells. *Endocrinology* (2006) 147:5187–95. doi: 10.1210/en.2006-0664
56. Rokade S, Madan T. Testicular expression of SP-A, SP-D and MBL-A is positively regulated by testosterone and modulated by lipopolysaccharide. *Immunobiology* (2016) 221:975–85. doi: 10.1016/j.imbio.2016.05.005
57. McCormick, S. M., Boggaram, V., and Mendelson, C. R. Characterization of mRNA transcripts and organization of human SP-A1 and SP-A2 genes. *Am J Physiol.* (1994) 266(4 Pt 1):L354–66.
58. Soucy G, Boivin G, Labrie F, Rivest S. Estradiol is required for a proper immune response to bacterial and viral pathogens in the female brain. *J Immunol.* (2005) 174:6391–8. doi: 10.4049/jimmunol.174.10.6391
59. Henning LN, Azad AK, Parsa KV, Crowther JE, Tridandapani S, Schlesinger LS. Pulmonary surfactant protein A regulates TLR expression and activity in human macrophages. *J Immunol.* (2008) 180:7847–58. doi: 10.4049/jimmunol.180.12.7847
60. Li X, Li M, Bai X. Upregulation of TLR2 expression is induced by estrogen via an estrogen-response element (ERE). *Arch Biochem Biophys.* (2014) 549:26–31. doi: 10.1016/j.abb.2014.01.028
61. Phelps DS, Umstead TM, Quintero OA, Yengo CM, Floros J. *In vivo* rescue of alveolar macrophages from SP-A knockout mice with exogenous SP-A nearly restores a wild type intracellular proteome; actin involvement. *Proteome Sci.* (2011) 9:67. doi: 10.1186/1477-5956-9-67
62. Sano H, Sohma H, Muta T, Nomura S, Voelker DR, Kuroki Y. Pulmonary surfactant protein A modulates the cellular response to smooth and rough lipopolysaccharides by interaction with CD14. *J Immunol.* (1999) 163:387–95.
63. Sano H, Chiba H, Iwaki D, Sohma H, Voelker DR, Kuroki Y. Surfactant proteins A and D bind CD14 by different mechanisms. *J Biol Chem.* (2000) 275:22442–51. doi: 10.1074/jbc.M001107200
64. Sato M, Sano H, Iwaki D, Kudo K, Konishi M, Takahashi H, et al. Direct binding of Toll-like receptor 2 to zymosan, and zymosan-induced NF-kappa B activation and TNF-alpha secretion are down-regulated by lung collectin surfactant protein A. *J Immunol.* (2003) 171:417–25. doi: 10.4049/jimmunol.171.1.417

Conflict of Interest Statement: The authors declare that the research was conducted in the absence of any commercial or financial relationships that could be construed as a potential conflict of interest.

frontiers in Immunology

ORIGINAL RESEARCH
published: 07 November 2019
doi: 10.3389/fimmu.2019.02613

Structural and Functional Determinants of Rodent and Human Surfactant Protein A: A Synthesis of Binding and Computational Data

Armen Nalian[1,2], *Todd M. Umstead*[3,4], *Ching-Hui Yang*[2†], *Patricia Silveyra*[3,4†], *Neal J. Thomas*[3,5], *Joanna Floros*[3,6,7], *Francis X. McCormack*[8] *and Zissis C. Chroneos*[2,3,4,9*]

[1] *Department of Biology, Stephen F. Austin State University, Nacogdoches, TX, United States,* [2] *The Center of Biomedical Research, University of Texas Health Science Center at Tyler, Tyler, TX, United States,* [3] *Department of Pediatrics, Pennsylvania State University College of Medicine and PennState Health Children's Hospital, Hershey, PA, United States,* [4] *Pulmonary Immunology and Physiology Laboratory, Pennsylvania State University College of Medicine and PennState Health Children's Hospital, Hershey, PA, United States,* [5] *Department of Public Health Sciences, Pennsylvania State University College of Medicine and PennState Health Children's Hospital, Hershey, PA, United States,* [6] *Center of Host Defense and Inflammatory Disease Research, Pennsylvania State University College of Medicine and PennState Health Children's Hospital, Hershey, PA, United States,* [7] *Department of Obstetrics and Gynecology, Pennsylvania State University College of Medicine and PennState Health Children's Hospital, Hershey, PA, United States,* [8] *Division of Pulmonary, Critical Care, and Sleep Medicine, Department of Internal Medicine, University of Cincinnati College of Medicine, Cincinnati, OH, United States,* [9] *Department of Microbiology and Immunology, Pennsylvania State University College of Medicine and PennState Health Children's Hospital, Hershey, PA, United States*

OPEN ACCESS

Edited by:
Uday Kishore, Brunel University London, United Kingdom

Reviewed by:
Thomas Vorup-Jensen, Aarhus University, Denmark
Anthony George Tsolaki, Brunel University London, United Kingdom

***Correspondence:**
Zissis C. Chroneos
zchroneos@pennstatehealth.psu.edu

†Present address:
Ching-Hui Yang, Corteva AgriScience, Johnston, IA, United States
Patricia Silveyra, Behavioral Laboratory, University of North Carolina at Chapel Hill, Chapel Hill, NC, United States

Specialty section:
This article was submitted to Molecular Innate Immunity, a section of the journal Frontiers in Immunology

Received: *17 July 2019*
Accepted: *21 October 2019*
Published: *07 November 2019*

Citation:
Nalian A, Umstead TM, Yang C-H, Silveyra P, Thomas NJ, Floros J, McCormack FX and Chroneos ZC (2019) Structural and Functional Determinants of Rodent and Human Surfactant Protein A: A Synthesis of Binding and Computational Data. Front. Immunol. 10:2613. doi: 10.3389/fimmu.2019.02613

Surfactant protein A (SP-A) provides surfactant stability, first line host defense, and lung homeostasis by binding surfactant phospholipids, pathogens, alveolar macrophages (AMs), and epithelial cells. Non-primates express one SP-A protein whereas humans express two: SP-A1 and SP-A2 with core intra- and inter-species differences in the collagen-like domain. Here, we used macrophages and solid phase binding assays to discern structural correlates of rat (r) and human (h) SP-A function. Binding assays using recombinant rSP-A expressed in insect cells showed that lack of proline hydroxylation, truncations of amino-terminal oligomerization domains, and site-directed serine (S) or alanine (A) mutagenesis of cysteine 6 (C6S), glutamate 195 (E195A), and glutamate 171 (E171A) in the carbohydrate recognition domain (CRD) all impaired SP-A binding. Replacement of arginine 197 with alanine found in hSP-A (R197A), however, restored the binding of hydroxyproline-deficient rSP-A to the SP-A receptor SP-R210 similar to native rat and human SP-A. *In silico* calculation of Ca^{++} coordination bond length and solvent accessibility surface area revealed that the "humanized" R197A substitution alters topology and solvent accessibility of the Ca^{++} coordination residues of the CRD domain. Binding assays in mouse AMs that were exposed to either endogenous SP-A or hSP-A1 ($6A^2$) and hSP-A2 ($1A^0$) isoforms *in vivo* revealed that mouse SP-A is a functional hybrid of hSP-A1 and hSP-A2 in regulating SP-A receptor occupancy and binding affinity. Binding assays using neonatal and adult human AMs indicates that the interaction of SP-A1 and SP-A2 with AMs is developmentally regulated. Furthermore, our data indicate that the auxiliary ion coordination loop encompassing the conserved E171 residue may comprise a conserved site of interaction with macrophages, and SP-R210

specifically, that merits further investigation to discern conserved and divergent SP-A functions between species. In summary, our findings support the notion that complex structural adaptation of SP-A regulate conserved and species specific AM functions in vertebrates.

Keywords: alveolar macrophages, binding, lung, surfactant protein A, receptor

INTRODUCTION

Surfactant protein A (SP-A) is the most abundant lipid binding and immune-surveillance component of pulmonary surfactant. SP-A belongs to the collectin family of proteins consisting of four structural domains that include an amino-terminal tail, a collagen-like domain (CDM) with Gly-X-Y repeats, an α-helical coiled-coil neck domain with heptad repeats, and a Ca^{++}-dependent carbohydrate recognition domain (CRD) (1–3). The neck and collagen-like domains of SP-A trimerize and assemble into higher order deca-octamers via inter-chain disulfide bonds in the amino-terminal tail and non-covalent interactions between trimers. Binding to extracellular ligands depends on the neck-CRD trimer and high avidity multivalent binding of the SP-A deca-octamer. Crystallographic and molecular modeling studies of the rat SP-A CRD revealed that conformational flexibility of the Ca^{++} coordination site and CRD surface loops impart versatility in the ability of SP-A to bind structurally diverse endogenous and pathogen-derived ligands (2, 4–7). The interaction of SP-A with AMs and epithelial cells is receptor-mediated (8–10). Deletion, site-directed mutagenesis, and ligand competition studies showed that the amino-terminal and collagen-like domains influence receptor occupancy and functional responses in alveolar type II epithelial cells and macrophages, and interaction of the CRD domain with surfactant phospholipids (10–16). SP-A binds dipalmitoyl phosphatidylcholine, the major surfactant phospholipid, that is required for the formation of tubular myelin from secreted lamellar bodies, contributes to the adsorption of surface active phospholipids at the air-liquid interface, and facilitates turnover of spent surfactant vesicles by alveolar type II epithelial cells through the p63 receptor (7, 17–21). In host defense, SP-A binds different pathogen ligands such as the lipid A portion of lipopolysaccharide on Gram-negative bacteria (7), surface proteins and glycolipids on gram positive bacteria (22), mycobacteria (23, 24), and fungi (25, 26). These interactions facilitate pathogen clearance through agglutination, opsonization, and direct killing (22, 26–29). SP-A enhances opsonic and non-opsonic phagocytosis (22, 30–32), and shapes pathogen-dependent polarization of inflammatory responses through the SP-R210 SP-A receptor (aka Myo18A or CD245) (22, 27, 33) in macrophages.

Unlike non-primate amniotes (34), humans express two SP-A protein isoforms, SP-A1 and SP-A2 encoded by different genes *SFTPA1* and *SFTPA2* (35), and each gene has been identified with several variants. The hSP-A1 and hSP-A2 proteins and their respective variants differ at four core amino acids in the collagen-like domain and the variants of each gene are distinguished among themselves by additional amino acid differences present in domains other than the collagen-like domain (36–38). SP-A1 and SP-A2 differentially modulate macrophage function (39–41) and in suppressing development of idiopathic interstitial pneumonia, fibrosis, and cancer (42–45). Moreover, significant differences have been observed among SP-A1 and SP-A2 variants in survival after infection and lung function (46, 47). The presence of both proteins is required for tubular myelin formation, supra-trimeric assembly of SP-A oligomers, and optimal function of surfactant (21, 48, 49) and one SP-A gene is sufficient to exert these functions in lower vertebrates (19, 50, 51). Both human and rodent SP-As have a discrete kink peptide in the middle of the CDM that confers conformational flexibility, contributes to the quaternary organization of higher order SP-A oligomers, and spatial separation of CRD domains (52–54). The kink sequence is conserved between SP-A1 and SP-A2 but different from rodent SP-A; PCPP in human SP-As and MGLP in rodents (34, 54). The kink peptide and a unique GEC collagen triplet in SP-A1 (GER in SP-A2) result in 2 cysteine residues in the CDM of SP-A1 compared to 1 in SP-A2 and none in rodent SP-A. The GEC triplet contributes to distinct oligomeric structures in SP-A1 and the two proteins distribute differently in interfacial surfactant films (48, 49, 55). Compared to SP-A2, SP-A1 improved the biophysical activity of surfactant in lowering surface tension and resistance to inhibition by serum (56). Recombinant SP-A1 lacking the ability to form oligomers, however, retains anti-inflammatory effects on macrophages (57, 58), whereas SP-A2 variants compared to SP-A1 have been shown to exhibit higher activity in bacterial phagocytosis by AMs (59) and cytokine production in a macrophage-like cell line (39, 60).To better understand SP-A function we used binding assays and molecular modeling to define molecular and functional attributes in rodent and human SP-A.

Abbreviations: AMs, alveolar macrophages; BAL, bronchoalveolar lavage; CDM, collagen-like domain; CLL, carbohydrate, lipids, LPS binding site; CRD, carbohydrate recognition domain; GEC, Glycine Glutamate Cysteine; GER, Glycine Glutamate Arginine; MDLG, Methionine Aspartate Leucine Glycine; NCRD, coiled-coil neck and CRD domain; PCPP, Proline Cysteine Proline Proline; SP-A, surfactant protein A; rSP-A, native rat SP-A; hSP-A, native human SP-A; hSP-A1 6A2, human SP-A isoform 1 variant 6A2; hSP-A2 1A0, human SP-A isoform 2 variant 1A0; rSP-Ahyp, hydroxyproline-deficient recombinant rat SP-A; SP-R210, SP-A receptor 210; Myo18A, Myosin 18A.

MATERIALS AND METHODS

Animals

Wild type ($SP\text{-}A^{+/+}$) C57BL/6J mice were purchased from JAX labs and bred locally. Transgenic $SP\text{-}A^{-/-}$ and humanized $mSftpa^{-/-,hSFTPA1(6A2)}$ and $mSftpa^{-/-,hSFTPA2(1A0)}$ mice were generated as described previously (21). Sprague-Dawley rats were

obtained from Harlan. All animal procedures were performed under IACUC approved protocols.

Production and Purification of Recombinant Proteins

Recombinant rat SP-A proteins were synthesized in insect Sf9 cells via baculovirus expression of rat SP-A WT cDNA or mutant cDNAs generated by nested deletion or site directed mutagenesis as described in detail previously (25, 61). The present studies utilized rat SP-A with C6S, E171A, E195A, R197A, and D215A point mutations and deletion mutants lacking both amino terminal and collagen-like domains (ΔN1-G80), the collagen-like domain (ΔG8-G80), kink (ΔG8-G40) and proximal (ΔG40-G80) halves of the collagen-like domain. Recombinant rat SP-A proteins were isolated by affinity chromatography over mannose-Sepharose. Native rat SP-A was isolated from the bronchoalveolar lavage (BAL) of Sprague-Dawley rats 4 weeks after instillation of 40 mg/Kg of silica-induced alveolar proteinosis Rat BAL surfactant was separated by NaBr-density gradient centrifugation followed by delipidation, affinity and gel exclusion chromatography (12, 19, 25, 61–64). Native human SP-A was isolated from discarded alveolar proteinosis BAL by sequential isobutanol/β-octylglucoside extraction, repeated precipitation/solubilization in 20 mM $CaCl_2$/EDTA, and extensive dialysis in 5 mM HEPES, pH 7.4 (32). Recombinant human SP-A1 (variant $6A^2$) and SP-A2 (variant $1A^0$) were expressed in CHO-K1 cells via the pEE14 expression vectors (39). SP-A1 and SP-A2 secreted in media were purified by affinity chromatography over mannose-Sepharose and gel filtration chromatography over Superose 6 (39). The purity of rat and human proteinosis SP-A was >95% and recombinant human SP-A1 and SP-A2 was >95% pure as assessed by 1 and/or 2-dimensional SDS-PAGE (39, 65), respectively. All SP-A preparations contained negligible amounts of bacterial endotoxin lipopolysaccharide below 0.1 pg/mg of protein as assessed by the Limulus Amoebocyte Lysate assay.

Isolation of Alveolar Macrophages From Transgenic Mice and Human Lung

Mouse AMs were isolated by BAL using five sequential intratracheal instillation of 0.5 mL PBS/1 mM EDTA for a total of 2.5 mL. The BAL was centrifuged at 250 × g for 10 min to pellet the macrophages. The macrophages were washed once in PBS, counted, and then suspended in iodination blocking buffer. Human AMs were isolated from donated human lungs which were rejected for transplant *ex vivo* as described previously (66, 67). All procedures were approved by the Penn State College of Medicine Institutional Review Board. Cell purity was assessed microscopically after cytospin centrifugation and HEMA-3 differential staining (29).

Molecular Dynamics Simulation

The starting coordinates for molecular dynamics (MD) simulations were obtained from the recombinant rat SP-A crystal structure 1R13 (4) (http://www.rcsb.org/pdb/explore.do?structureId=1r13) consisting of the neck and CRD domain with a mutation at the glycosylation site consensus asparagine 187 (N187S) and lacking the amino-terminal and collagen-like domains (ΔN1-80) using Swiss-Pdb Viewer (68). Molecular dynamics simulations were carried out as described previously (69). We tested the impact of alanine point mutations in the primary Ca^{++} coordination residues of the CRD carbohydrate-lipid-LPS (CLL) binding pocket, E195A, R197A, N214A, and D215A, and E171A in the auxiliary metal ion coordination loop on Ca^{++}- coordination bond length and solvent accessibility surface area. All residues tested are conserved between rodent and human SP-A, except for R197 which is naturally substituted by an alanine in both human SP-A1 and SPA2.

Sequence Alignment and Numbering of Rodent and Human SP-A

Sequence alignments were performed using ClustalW (70, 71) (**Figure 1**). The amino acid alignment and location of Ca^{++}-coordination residues of rat SP-A and human SP-A2 (variant $1A^0$) are shown on **Figure 1A** and part of the CDM on **Figure 1B**. The numbering of amino acid residues on **Figure 1A** is based on the mature rat SP-A after cleavage of the respective signal peptide between residues C20-N21 or as stated otherwise (Uniprot Accession No: P08427) (72, 73). In humans, although the signal peptide cleavage has been shown to affect a few amino acids (74), here we based the numbering on one of the cleaved variants in C20-E21 of the SP-A2 variant $1A^0$ (Uniprot Accession No: Q8IWL1). For the CDM alignments numbering is from the start of respective signal sequences (**Figure 1B**) to avoid confusion with differences in amino-acid numbering for rat and human SP-A1 and SP-A2 in the literature. The numbering of all rat SP-A point and deletion mutants is based on the mature rat peptide.

Macrophage and Solid Phase Binding Assays

Macrophage binding assays were performed using mouse or human AMs, or the RAW264.7 macrophage cell line and ^{125}I-labeled SP-A as described in detail previously (10, 32). The purified His-tagged SP-A binding neck domain of SP-R210 (32, 75) was used in solid phase binding assays with SP-A. Flat bottomed 96 well ELISA plates were treated with 0.1 M Na_2CO_3, pH9.3, and coated with 10 μg/mL of purified nSP-R210, and blocked in 0.1% BSA. Recombinant rat SP-A, native rat, or human SP-A1 or SP-A2 were added at increasing concentration in SP-A binding buffer (HBSS not containing phenol red, 20 mM HEPES (pH 7.4), 1 mM $CaCl_2$, 0.2 mM $MgCl_2$, 1% bovine serum albumin) and incubated at 37°C in a humidified chamber. Plates were washed in binding buffer, incubated with HRP-conjugated anti-rat affinity purified polyclonal rabbit anti-SP-A antibody for 1 hr. at room temperature, and then washed. Bound antibody was visualized using 3, 3′, 5, 5′-tetramethylbenzidine (TMB) HRP substrate at 450 nM.

Data Analysis

Graphical analyses of binding data were performed with GraphPad Prism software (GraphPad Software, San Diego, CA). Binding data were analyzed by non-linear regression of saturation curves fitted to a single site equilibrium binding equation using Prism software to calculate the number of SP-A binding sites/cell (B_{max}) and binding affinities (K_d). The hill equation embedded in Prizm software was used to calculate

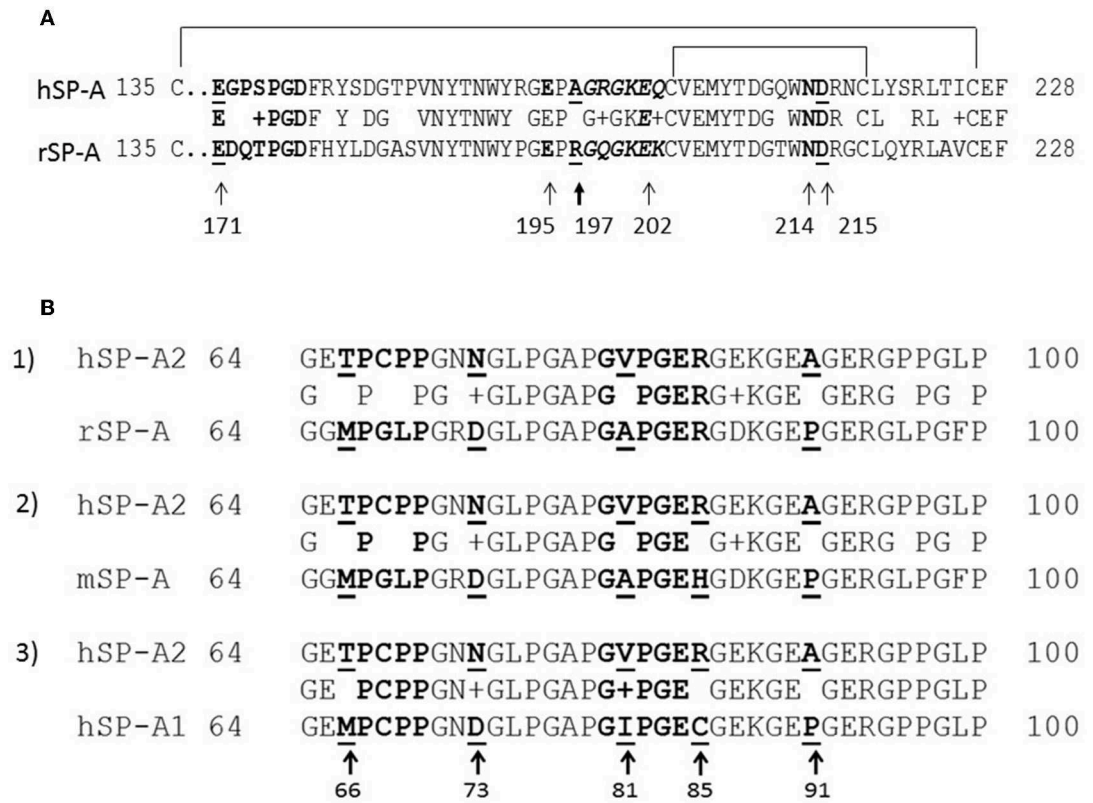

FIGURE 1 | Partial sequence alignment of the CRD **(A)** and CDM **(B)** domains of rodent and human SP-A. **(A)** Alignment of the CRD domains of human SP-A2 $1A^0$ variant (hSP-A2) and rat SP-A carbohydrate recognition domain. Amino acid numbering is based on the mature peptide of rat SP-A. Arrows point to Ca^{++}-coordination residues. **(B)** Alignment of the collagen-like domains of human SP-A1 ($6A^2$) (hSP-A1) and hSP-A2 $1A^0$ variant, mouse SP-A (mSP-A), and rat SP-A (rSP-A). All alignments are made to hSP-A2 ($1A^0$). The aligned sequences shown encompass the kink peptide (bolded residues 66–50) to the end of the CDM. Arrows point to core amino acids in the CDM that distinguish SP-A1 and SP-A2; the numbering is based on the precursor molecule. Residues shown in italicized red font show the sequence of embedded integrin binding motifs in the CDM. Sequence alignments were performed using ClustalW.

the Hill coefficient of cooperativity for human SP-A binding to murine and human alveolar macrophages.

RESULTS

Spatial Interaction of Oligomerization and CRD Domains of SP-A

We used deletion and point mutants of insect cell expressed rat SP-A to map SP-A binding to macrophages and recombinant SP-R210 compared to native human or rat SP-A isolated from BAL. Insect cell expressed SP-A lacks proline hydroxylation of Gly-X-Pro repeats in the CDM of SP-A (rSP-A^{hyp}) and also exhibits an altered pattern of glycosylation (61). Hydroxyproline imparts thermal stability that influences the degree of oligomerization of the collagen-like domain of SP-A (61). Saturation binding assays demonstrated that lack of hydroxyproline reduced SP-A binding potential to both macrophages (**Figures 2A,C,E,F**, **Table 1**) and recombinant SP-R210 (**Figures 3A–D**, **Table 2**) as demonstrated by 3–9 fold decreases in both maximal binding (Bmax) and binding affinity (Kd) compared to native SP-A.

Deletion and site-directed mutagenesis were then used to assess the effect of the amino-terminal and CDM oligomerization domains on the binding of rSP-A^{hyp} (**Figures 1A,B**, **2A**, **Tables 1**, **2**). Complete CDM deletion (rSP-$A^{hyp,\Delta G8-G80}$) impaired binding to both macrophages and SP-R210 compared to rSP-A^{hyp}. Point mutation of cysteine 6 to serine in the amino terminal peptide (rSP-$A^{hyp,C6S}$) diminished Bmax with similar binding affinity to both macrophages and SP-R210 compared to rSP-A^{hyp}. The partial CDM deletion rSP-$A^{hyp,\Delta G8-G40}$ and rSP-$A^{hyp,\Delta G40-G80}$ mutants had increased high affinity binding at reduced Bmax in macrophages compared to rSP-A^{hyp}. The rSP-$A^{hyp,\Delta G40-G80}$ mutant, however, exhibited reduced affinity to SP-R210, whereas rSP-$A^{hyp,\Delta N1-G80}$ bound SP-R210 with increased affinity compared to rSP-A^{hyp}. The Hughes-Klotz double reciprocal plots (**Figures 2B,F**, **3B**) indicated negative cooperativity for rSP-A^{hyp}, native SP-A (**Figure 2F**), and the partial CDM deletion mutants rSP-$A^{hyp,\Delta G8-G40}$ and rSP-$A^{hyp,\Delta G40-G80}$ compared to non-interacting binding sites for rSP-$A^{hyp,C6S}$, rSP-$A^{hyp,\Delta G8-G80}$ and rSP-$A^{hyp,\Delta N1-G80}$, indicating that oligomerization modulates the binding behavior of SP-A. Mutants to examine the role of the neck coiled-coil domain are not available. Molecular dynamics simulations with and without the coiled-coil domain showed as the CRD alone did not equilibrate *in silico* as

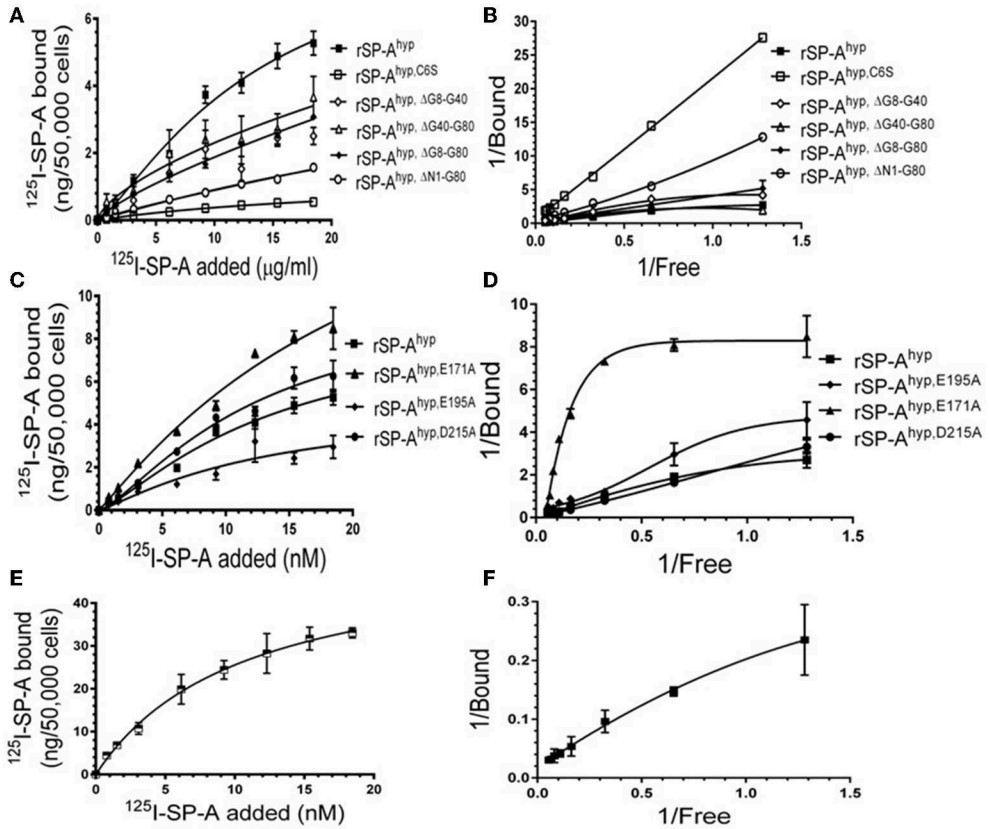

FIGURE 2 | Impact of domain deletion and site directed mutagenesis on SP-A binding to macrophages. Binding assays used Raw264.7 macrophages in suspension. Cells were incubated with increasing concentrations of either radiolabeled recombinant rat SP-A proteins **(A–D)** or human SP-A **(E,F)** purified from alveolar proteinosis lavage. Binding data were fitted by non-linear regression to generate binding isotherms **(A,C,E)** or transformed into double reciprocal plots to evaluate SP-A binding behavior **(B,D,F)**. Assays were carried out at 4°C for 1.5 h. at the 50,0000 cells/assay. Bound SP-A was separated by centrifugation over a silicon oil mixture to separate bound from free SP-A. Assays were performed in triplicate and data pooled from 2 independent experiments. Data shown are Means ± SE.

TABLE 1 | Parameters of SP-A binding to macrophages.

Protein	Bmax (ng/50,000 cells)	Kd (nM)
hSP-A	52.83 ± 0.01	6.94 ± 0.002
rSP-A^{hyp}	8.94 ± 2.71	13.60 ± 6.60
rSP-A$^{hyp,\Delta N1-G80}$	7.12 ± 1.80	68.57 ± 20.59
rSP-A$^{hyp,\Delta G8-G40}$	4.68 ± 1.14	16.10 ± 6.90
rSP-A$^{hyp,\Delta G40-G80}$	3.21 ± 0.93	7.84 ± 4.04
rSP-A$^{hyp,\Delta G8-G80}$	8.58 ± 7.10	34.42 ± 39.81
rSP-A^{hyp,E171A}	24.96 ± 6.00	33.56 ± 11.35
rSP-A^{hyp,E195A}	5.05 ± 4.64	13.22 ± 21.16
rSP-A^{hyp,D215A}	19.38 ± 5.82	36.29 ± 19.56
rSP-A^{hyp,C6S}	1.01 ± 0.25	15.62 ± 6.52

indicated by the increasing root mean square deviation (RMSD) of the CRD α-carbon atoms compared to the NCRD (**Figure 4**).

We then examined the effect of alanine (A) mutagenesis of residues that influence geometry and Ca^{++} coordination in the CRD domain (4, 5) using binding assays and MD simulations (**Table 1**). Compared to the crystal structure, the MD simulations indicate that the side chain carbonyl for asparagine (N) 214 and backbone carbonyl of aspartate (D) 215 occupy spaces further away from Ca^{++} in the WT CRD. The side chain hydroxyl of D215 and both oxygens in the E202 side chain are oriented closer to the Ca^{++} ion (**Table 3**). The invariant glutamate 171 (E171) influences Ca^{++} coordination of the E202 residue side chain, conformation of the double-loop structure surrounding the CRD carbohydrate binding pocket via a side-chain salt bridge with lysine K203, and coordination of an auxiliary ion (4, 5). The E171A substitution mutant (rSP-A^{hyp,E171A}) exhibited increased binding at high concentrations to macrophages compared to rSP-A^{hyp} (**Figure 2C**). The double-reciprocal Hughes-Klotz plot (76) of rSP-A^{hyp,E171A} showed strongly increased negative cooperativity compared to rSP-A^{hyp} (**Figure 2D**), suggesting abortive interaction with macrophages at low concentration. Binding to SP-R210 was not be determined. The E202 side chain of rSP-A^{hyp,E171A} did not coordinate Ca^{++}, consistent with crystallographic data (4). The average surface area solvent accessibility (SASA) of the Ca^{++} ion and Ca^{++} coordination amino acids, however, was not altered by the E171A substitution compared to WT (**Tables 4**, **5**). In previous studies, mutation

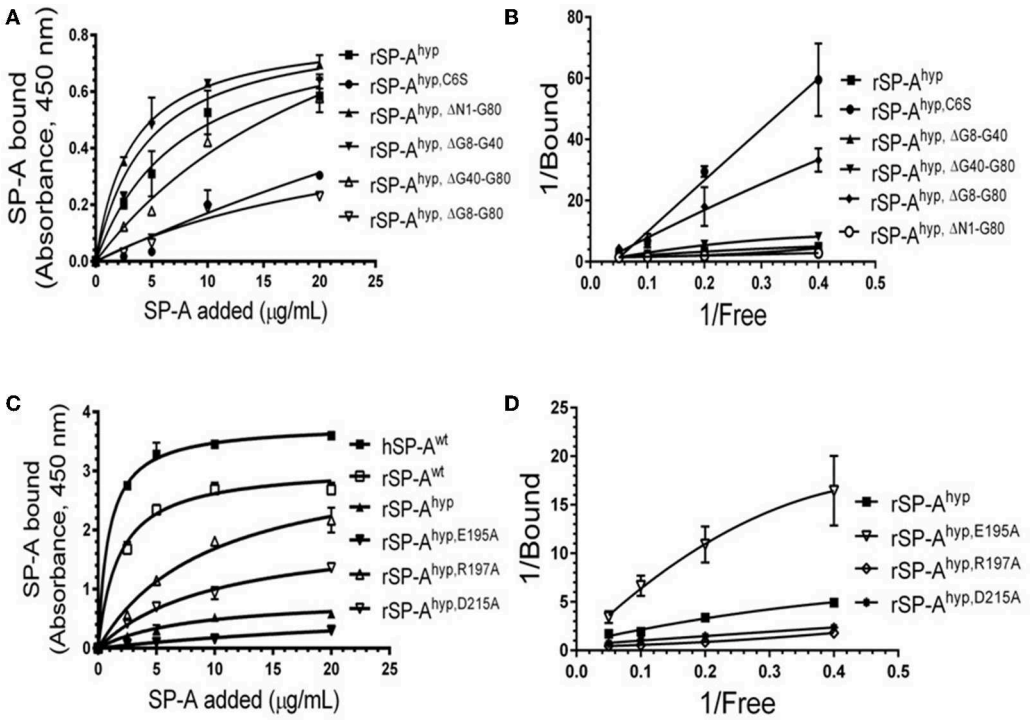

FIGURE 3 | Impact of domain deletion and site-directed mutagenesis on SP-A binding to SP-R210. The recombinant SP-A binding domain of SP-R210 was coated onto microtiter well plates, and incubated with increasing concentration of indicated recombinant rat SP-A proteins **(A–D)**, or native human or rat SP-A proteins **(C,D)**. Bound protein was detected using an HRP-conjugated SP-A antibody. Binding data were fitted by non-linear regression to generate binding isotherms **(A,C)** or transformed into double reciprocal plots to evaluate SP-A binding behavior **(B,D)**. Assays were performed in duplicate or triplicate and data pooled from 2 independent experiments. Data shown are Means ± SE.

TABLE 2 | Parameters of SP-A binding to SP-R210.

Protein	Bmax (A405)	Kd (nM)
hSP-A	3.78 ± 0.08	0.90 ± 0.12
rSP-A	3.08 ± 0.11	1.76 ± 0.28
rSP-A^{hyp}	0.86 ± 0.13	7.81 ± 2.60
rSP-A$^{hyp,\Delta N1-G80}$	0.82 ± 0.02	3.19 ± 0.27
rSP-A$^{hyp,\Delta G8-G40}$	0.92 ± 0.20	4.54 ± 2.60
rSP-A$^{hyp,\Delta G40-G80}$	1.32 ± 0.40	24.77 ± 11.70
rSP-A$^{hyp,\Delta G8-G80}$	0.57 ± 0.31	27.80 ± 22.75
rSP-A^{hyp,E195A}	0.82 ± 0.43	36.27 ± 26.02
rSP-A^{hyp,R197A}	3.31 ± 0.08	9.64 ± 2.03
rSP-A^{hyp,D215A}	2.01 ± 0.18	10.10 ± 1.88
rSP-A^{hyp,C6S}	0.32 ± 0.07	8.66 ± 1.77

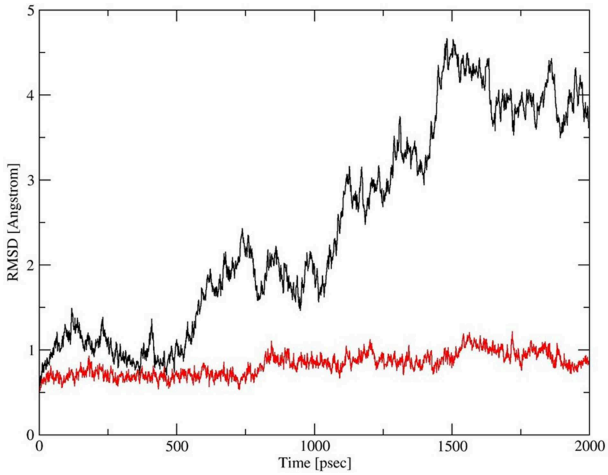

FIGURE 4 | Dynamics of CRD and neck-CRD domains. Plot of root mean square deviation (RMSD) of α-Carbon atoms over time for CRD (red trace) and neck-CRD (black trace).

of residues E195 (rSP-A^{hyp,E195A}) and D215 (rSP-A^{hyp,D215A}), two invariant residues that coordinate Ca^{++}, demonstrated critical roles in Ca^{++}-dependent binding and aggregation of DPPC, and binding to alveolar type II epithelial cells (13). E195 coordinates Ca^{++} via its side chain oxygens. Here, the binding affinity of the rSP-A^{hyp,E195A} mutant could not be accurately determined from the binding curves (**Table 1**). The double-reciprocal plot of rSP-A^{hyp,E195A} binding data, however, revealed atypical sigmoidal behavior suggesting interaction with low and high affinity binding sites in macrophages (**Figure 2D**), whereas this mutant exhibits negative cooperativity with recombinant SP-R210 (**Figure 3D**). In the E195A substitution, the R197

TABLE 3 | Calcium coordination bond length in WT and mutant rat SP-A NCRD.

	X-ray (ΔN1-G80)	WT NCRD (ΔN1-G80)	E171A	E195A	R197A	N214A	D215A
E195:OE1	2.43	2.14 ± 0.05	2.15 ± 0.06		2.73 ± 0.71	2.17 ± 0.07	2.19 ± 0.07
E195:OE2	3.73	3.77 ± 0.2	3.63 ± 0.36		2.64 ± 0.7	3.32 ± 0.53	2.31 ± 0.13
R197:O	2.87	2.3 ± 0.09	2.27 ± 0.07	6.93 ± 0.32	2.25 ± 0.08	2.28 ± 0.09	5.82 ± 1.03
N214:ON1	2.46	4.61 ± 0.58	4.62 ± 0.39	5.12 ± 0.50	2.25 ± 0.08		4.15 ± 0.41
D215:O	2.34	3.75 ± 0.22	4.2 ± 0.28	3.63 ± 0.70	2.77 ± 0.52	4.54 ± 0.26	2.42 ± 0.26
D215:OD1	2.27	2.22 ± 0.08	2.19 ± 0.07	2.11 ± 0.05	2.13 ± 0.05	2.19 ± 0.07	
D215:OD2	4.03	2.25 ± 0.1	2.29 ± 0.13	3.95 ± 0.17	4.09 ± 0.17	2.27 ± 0.12	
E202:OE1	5.91	3.91 ± 0.2		2.22 ± 0.09	5.11 ± 1.07	4.25 ± 0.12	2.23 ± 0.12
E202:OE2	4.25	2.13 ± 0.05		2.23 ± 0.09	6.28 ± 0.51	2.14 ± 0.06	2.35 ± 0.42

TABLE 4 | Effect of CRD mutation on binding pocket water occupancy.

Protein	% of time within 3Å				SASA of Ca^{++}
	1	2	3	4	
WT	100%	100%			4.92 ± 1.89
E171A	100%	98%			5.07 ± 2.32
E195A	100%	73%	73%	67%	27.74 ± 5.03
R197A	100%	100%			7.02 ± 1.62
N214A	10%	98%			6.12 ± 2.38
D215A	100%	100%	87%		11.10 ± 2.57
X-Ray	+	+			

TABLE 5 | Effect of mutation on SASA of Ca^{++} coordination residues.

Protein	
WT	227.38 ± 23.94
E171A	192.57 ± 20.65
E195A	220.28 ± 16.24
R197A	106.33 ± 11.50
N214A	194.83 ± 15.71
D215A	231.82 ± 28.77
X-Ray	265.76

backbone carbonyl moved 4.63 Å away from Ca^{++}, and also altered the orientation of asparagine (N) 214, D215, and E202 side chains relative to the Ca^{++} ion (**Table 3** and **Figures 5A,B**). These changes were accompanied by increased H_2O occupancy and average SASA of the Ca^{++} coordination site residues (**Tables 4**, **5**), suggesting that H_2O modifies the ligand binding properties of this mutant. The rSP-$A^{hyp,D215A}$ mutant, on the other hand, displayed increased Bmax and low affinity non-cooperative binding compared to rSP-A^{hyp} (**Figures 2C**, **3C** and **Tables 1**, **2**). The D215 residue contributes both its side chain and peptide bond carbonyl to Ca^{++}-coordination. The *in silico* calculations showed that the D215 backbone carbonyl moves closer to Ca^{++} by 1.33 Å when the side chain is replaced by Alanine (**Table 3**). The D215A substitution also influenced the orientation of E195 and E202 side chains, Ca^{++} proximity of the R197 carbonyl, and increased Ca^{++}-H_2O occupancy (**Tables 3**–**5**). The arginine (R) 197 residue, which coordinates Ca^{++}-H_2O occupancy via its peptide bond carbonyl, is naturally switched with alanine in human SP-A. Interestingly, the R197A substitution increased the binding of rSP-$A^{hyp,R197A}$ to SP-R210 similar to the level of native rat and human SP-A, neutralizing the negative impact of proline hydroxylation deficiency in the CDM (**Figure 3C** and **Table 2**). The computational analysis revealed that the R197A switch brings the hydroxyl oxygens of E195 and N214 side chains and peptide chain carbonyl oxygen of D215 closer to Ca^{++} by 1-2.5 Å while the hydroxyl oxygen of D215 and both side chain oxygens of E202 orient away from Ca^{++} (**Table 3**). The hydroxyl oxygen of the D215 side chain rotated the farthest, 4.15 Å away from Ca^{++} compared to WT. These adjustments in Ca^{++} coordination are accompanied by >50% decrease in hydrophilic SASA of the Ca^{++} coordination shell from 227.38 ± 23.94 to 106 ± 11.50 $Å^2$ of WT and rSP-$A^{hyp,R197A}$, respectively, suggesting a more compact structure of the "humanized" CRD (**Tables 4**, **5**).

Cross-Species Paracrine Effects of Mouse and Human SP-A on AMs

We took advantage of previously developed "humanized" SP-A transgenic mice to determine the impact of SP-A isoforms on AM binding phenotype. The hSP-A1 and hSP-A2 isoforms were expressed in the lungs of SP-$A^{-/-}$ mice. Binding assays were carried out in AMs from WT (SP-$A^{+/+}$), SP-A-deficient (SP-$A^{-/-}$), or SP-$A^{-/-}$ mice carrying either expression of human SP-A genes *SFTPA1 (6A²) or SFTPA2 (1A⁰)* via the alveolar epithelial *Sftpc* promoter (21). The coding sequences of $6A^2$ and $1A^0$ hSP-A1 and hSP-A2 variants, respectively, differ in four core amino acids in their collagen-like domain plus amino acids 19 and 91 (77), based on the numbering of the precursor molecule. The binding assays in **Figures 6A–D** and **Table 6** show that *in vivo* expression of hSP-A2 resulted in ligand-induced upregulation of hSPA2 binding to AMs compared to SP-$A^{-/-}$ and hSP-A1 exposed AMs as demonstrated by the 2-2.5 increase in Bmax (**Table 6**). hSP-A2 also improved the binding potential of hSP-A1 by increasing binding affinity. hSPA1 did not bind SP-$A^{-/-}$ AMs and its expression alone induced only low affinity

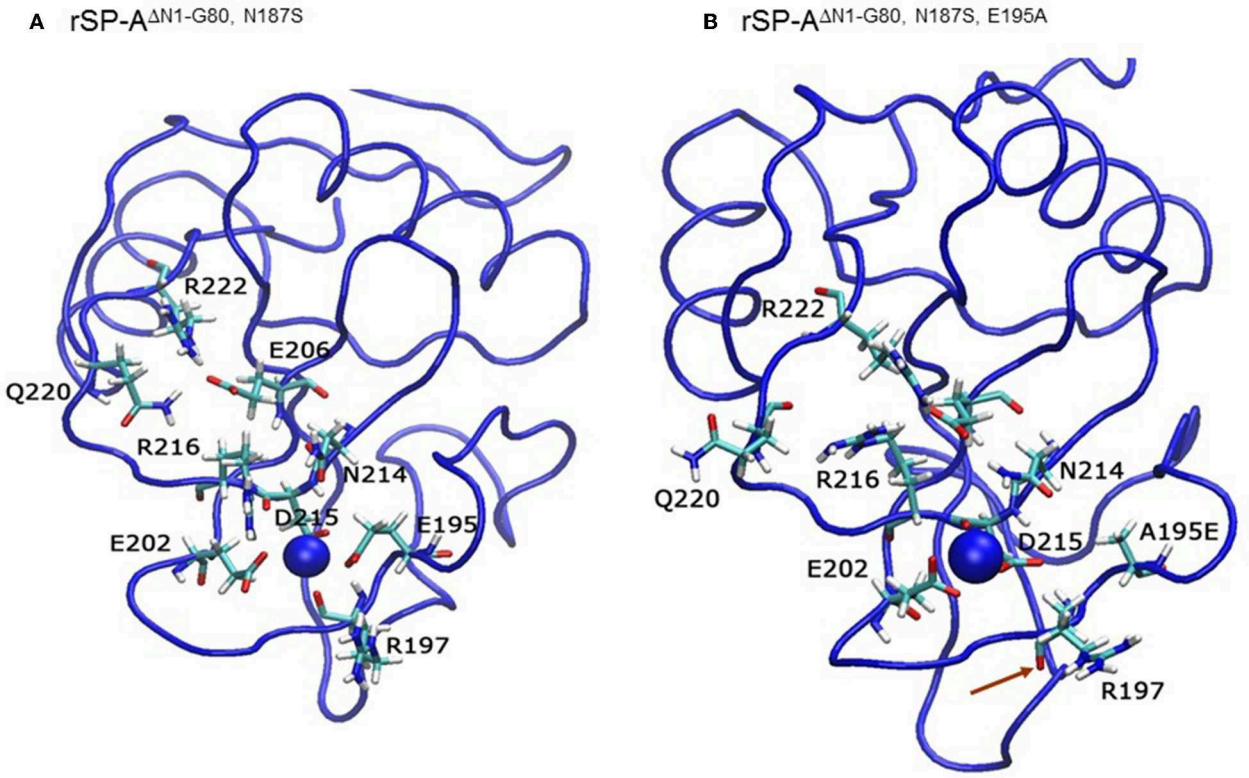

FIGURE 5 | The E195A substitution alters the Ca^{++}-coordination mode in the CLL binding pocket. Ribbon diagrams depicting the geometry of Ca^{++}-coordination site of the native **(A)** and mutant E195A NCRD **(B)**. Red arrows point to the carbonyl oxygen in the R197 residue.

binding of hSPA1 compared to high affinity binding for hSP-A2, although at lower Bmax compared to the hSPA2 expression. High affinity binding of hSP-A1 was observed only in AMs from hSP-A2 or WT mice. The endogenous SP-A, however, had a hybrid effect enhancing both binding affinity and Bmax with positive cooperativity. Compared to one another, the Bmax of hSP-A1 binding was 2–3-fold lower than that of hSP-A2 binding to murine AMs, indicating that the CDM is responsible for differences in receptor binding capacity of hSP-A isoforms with identical CRD.

To address differences in receptor binding properties between mouse and human AMs, we performed binding assays with human AMs obtained from donated non-transplanted lung from a 6 month old newborn and a 20 year old adult individual. **Figure 6E** and **Table 7** demonstrate that the Bmax for hSP-A2 was 3-fold higher in adult AMs than newborn AMs compared to a 1.6-fold increase for hSP-A1. The binding affinities were similar. Non-linear regression analysis of saturation data (**Figure 6E**, **Table 7**) revealed a change from non-cooperative to cooperative binding in newborn vs. adult AMs, respectively. The binding assays in mouse AMs exposed to endogenous or human SP-As *in vivo* indicate that hSP-A2 and endogenous mouse SP-A shaped the positive cooperativity binding phenotype of AMs (**Figures 6A,B**, and **Table 6**), whereas hSP-A1 did not. Additional assays in the presence of EDTA revealed that 30–50% of Bmax for hSP-A1 and hSP-A2 represent Ca^{++}-independent binding sites (**Figure 6F**). The cooperative binding behavior in the absence of Ca^{++} was not altered. The binding affinities for both hSP-A isoforms were higher in newborn AMs compared to adult AMs, suggesting developmental regulation of SP-A binding in postnatal life.

DISCUSSION

The present studies refine our understanding of structural features that modulate rodent and human SP-A binding properties to macrophages. To our knowledge, the present study is the first direct comparison of rodent and human SP-A variants. Nested deletion mutagenesis, point mutations, and *in silico* simulations of rat SP-A indicated that high affinity binding to macrophages or SP-R210 depends on inter-domain interactions and binding sites in the CDM and CRD domains. Previous studies reported that the CDM of rat and human SP-A mediates binding to macrophages (10, 14). Here, deletion of the entire CDM abolished high affinity binding to both macrophages and SP-R210, whereas the rSP-$A^{hyp,\Delta N1-80}$ mutant lacking both domains displayed low affinity binding relative to SP-A^{hyp}, suggesting that the amino-terminal peptide plays a conformational role in modulating binding distally. Partial

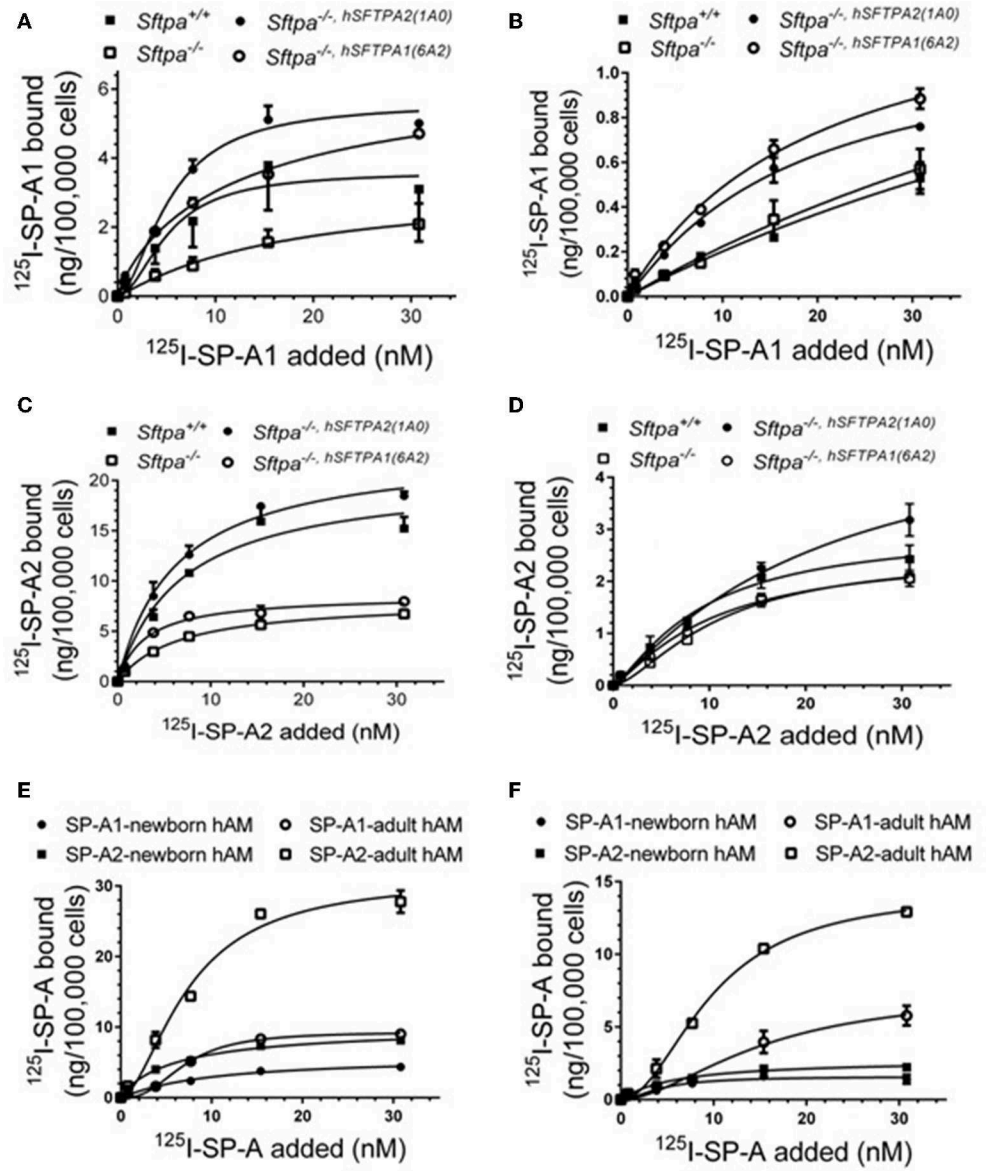

FIGURE 6 | Murine and human SP-A variants are paracrine regulators of SP-A binding to alveolar macrophages in postnatal lung. Binding assays were carried out with alveolar macrophages obtained from either murine lung **(A–D)** or human lung **(E,F)** using radiolabeled human SP-A1 or SP-A2 in the presence **(A,C,E)** or absence of calcium **(B,D,F)**. Alveolar macrophages from murine lungs **(A–D)** were obtained from WT (SP-A$^{+/+}$), SP-A-deficient (SP-A$^{-/-}$), or humanized mice expressing either SP-A1 variant 1A^{0} (SP-A$^{-/-,hSFTPA2(1A0)}$), or SP-A2 variant 6A^{2} (SP-A$^{-/-,hSFTPA2(6A2)}$) in the absence of endogenous murine SP-A (*Sftpa*). Human alveolar macrophages were obtained from 6 month **(E)** and 20 years old **(F)** rejected transplant lungs. Assays were carried out at 4°C for 1.5 h at 50,0000 cells/assay. Bound SP-A was separated by centrifugation over a silicon oil mixture. Assays were performed in duplicate and data pooled from 2 independent experiments. Alveolar macrophages from mouse lungs were pooled from 10 mice per genotype to obtain sufficient number of cells per experiment. Binding isotherms were generated using Prizm software by non-linear regression analysis using the Hill equation. Data shown are Means ± SE.

CDM deletion, however, indicated that the amino-terminal half of the CDM that follows the kink peptide binds macrophages and SP-R210. On the other hand, site directed mutagenesis in the CRD domain showed that the E171A, D215A, and E195A point mutants altered binding behavior. All three mutations altered the conformation of Ca^{++} coordination and, furthermore, D215A and E195A increased accessibility to solvent. The E171 residue stabilizes the conformation of the CRD surface loops, while D215 and E195 are critical for binding to carbohydrates, lipids, and LPS (4–7). The present findings support the notion that the SP-R210 binding site on the CRD domain lies outside the CLL binding pocket.

Species adaptation in the CDM domain produced two alternate SP-A isoforms, SP-A1 and SP-A2, and changes in the

TABLE 6 | Parameters of human SP-A binding to murine alveolar macrophages.

	SP-A1			SP-A2		
Genotype	**Bmax**	**Kd (nM)**	**h**	**Bmax**	**Kd (nM)**	**h**
SP-A$^{+/+}$	3.60 ± 1.32	5.14 ± 3.13	1.88 ± 2.3	16.57 ± 1.30	5.00 ± 0.70	1.88 ± 0.49
SP-A$^{-/-}$	No binding	–	–	8.43 ± 1.40	7.04 ± 3.00	0.93 ± 0.20
SP-A$^{-/-,Sftpa2(1A0)}$	5.60 ± 0.54	5.29 ± 0.17	1.76 ± 0.47	20.37 ± 1.31	5.00 ± 0.67	1.36 ± 0.22
SP-A$^{-/-,Sftpa1(6A2)}$	6.84 ± 1.45	12.96 ± 7.01	0.89 ± 0.17	8.10 ± 0.45	2.80 ± 0.47	1.25 ± 0.21
	SP-A1+EDTA			**SP-A2+EDTA**		
SP-A$^{+/+}$	No binding	–	–	3.00 ± 0.42	9.20 ± 2.52	1.29 ± 0.27
SP-A$^{-/-}$	No binding	–	–	2.50 ± 0.28	10.82 ± 2.04	1.53 ± 0.26
SP-A$^{-/-,Sftpa2(1A0)}$	1.19 ± 0.33	17.63 ± 9.85	1.07 ± 0.23	5.32 ± 1.60	21.40 ± 11.95	1.14 ± 0.23
SP-A$^{-/-,Sftpa1(6A2)}$	1.66 ± 0.62	26.20 ± 21.13	0.92 ± 0.19	2.60 ± 0.28	10.26 ± 2.16	1.24 ± 0.17

TABLE 7 | Parameters of human SP-A binding to human alveolar macrophages.

AM source	SP-A1			SP-A2		
	Bmax	**Kd (nM)**	**h**	**Bmax**	**Kd (nM)**	**h**
Newborn AM	5.74 ± 0.75	9.55 ± 2.84	1.06 ± 0.17	10.23 ± 1.30	6.42 ± 0.70	0.91 ± 0.49
Adult AM	9.30 ± 0.34	7.02 ± 0.40	2.61 ± 0.34	31.12 ± 2.62	7.46 ± 1.10	1.73 ± 0.34
	SP-A1+EDTA			**SP-A2+EDTA**		
Newborn AM	1.60 ± 0.24	4.43 ± 1.25	1.72 ± 0.90	2.74 ± 0.27	5.94 ± 1.42	1.02 ± 0.16
Adult AM	7.49 ± 2.22	15.23 ± 6.46	1.78 ± 0.65	14.36 ± 0.71	9.80 ± 0.73	1.97 ± 0.20

CRD produced four variants, two for SP-A1 and two for SP-A2. These demarcate differences in ligand-induced modulation of receptor occupancy on AMs *in vivo*. In the present study we studied two of the CRD variants, one for SP-A1 ($6A^2$) and one for SP-A2 ($1A^0$). The amino-terminal half of the CDM of rat SP-A (**Figure 1B**) contains contiguous ^{85}RGDKGE^{90} integrin binding motifs that are partially conserved in mouse SP-A with a corresponding ^{85}HGDKGE^{90} but diverged in human SP-A with ^{85}CGEKGE^{90} in SP-A1 and ^{85}RGEKGE^{90} in SP-A2 (**Figure 1B**). Although RGD, HGD, and KGE motifs are well-known for binding to integrins (78, 79), other studies have reported interactions with the C2 membrane binding domain of phospholipases and other proteins (80–82). The interaction of this motif with SP-R210 remains to be determined. Evolutionary adaptation in the CRD domain of both isoforms introduced a natural R197A substitution between rodent and human SP-A2 ($1A^0$) (**Figure 1A**). This substitution appears to isolate the impact of post-translational hydroxylation of proline on receptor occupancy by altering the interaction of the CRD domain with solvent and topology of Ca^{++} coordination residues in the CLL. These CDM and CRD adaptations may compensate for differences in dietary requirements for ascorbic acid and proline hydroxylation between rodents and humans (83). The present findings, however, indicate that single amino acid changes can profoundly affect CRD conformation, domain-domain interaction, and binding to macrophage receptors via CDM and CRD domains. In this regard, the CRD domain of human SP-A1 and SP-A2 is polymorphic resulting in diverse allelic combinations of SP-A1 and SP-A2 variants. Both coding and non-coding polymorphisms have been associated with increased or decreased risk to lung disease in numerous studies (77, 84). Understanding the structure-function relationship on human SP-A isoforms will require better understanding of copy number variation and biochemical characterization of polymorphic chain composition of SP-A1 and SP-A2 isoforms.

SP-A plays versatile roles in host defense through concomitant interactions with pathogens, surfactant lipids, and immune cells (1). SP-A controls the direction of macrophage activation, suppressing or inducing macrophage inflammatory responses as well as polarization toward either M1 or M2 types of differentiation and intrinsic regulation of innate immune receptor expression and function through the coordination of two SP-R210 isoforms (14, 27, 29, 33, 85, 86). Given present evidence that the SP-A CLL interacts with pattern recognition receptors (87), a distinct receptor binding site could be used to facilitate transfer of diverse SP-A cargo to innate immune receptors on macrophages. The SP-A structural determinants that differentially modulate receptor occupancy and signaling in AMs in the face of diverse immune challenges in the local lung microenvironment are subject to extensive investigation at the molecular level.

CONCLUSIONS

Human SP-A isolated from alveolar proteinosis fluid has been utilized extensively to discern function utilizing rodent alveolar macrophages without knowledge of the donor SP-A genotype. These studies generated invaluable information but also produced controversial as well as disparate results on SP-A immune functions and identity of SP-A receptors. The present findings in mouse AMs exposed to human SP-A isoforms not only support cross-species conservation and validity of *ex vivo* studies but also indicate genetic origin of SP-A preparations as an important variable in understanding versatility of SP-A function in humans. In this regard, the presence of SP-A1 may attenuate receptor occupancy, which likely regulates functional interactions with AMs at physiologically high levels of SP-A at homeostasis. Furthermore, although the present studies are limited by the small numbers of samples, the findings in newborn and adult AMs suggest increased receptor complexity that is developmentally regulated in humans.

Finally, our simulation and binding data indicate that the auxiliary ion coordination loop encompassing the conserved E171 residue may comprise a conserved site of interaction with macrophages, and SP-R210 specifically, that merits further investigation to discern conserved and divergent SP-A functions between species. In this context, we recognize that there are limitations inherent to MD simulations that impact the behavior of ions. MD simulations, however, have the potential to unveil how structural differences alter dynamic properties that are crucial for understanding the interplay of structure and function as well as providing guidelines for experiments. The purpose of the simulations, however, was not to reproduce the exact theoretical or experimental ion interactions but instead, to carry out a comparative study of wild type and mutated structures and specifically investigate the distances and their stability. This comparative *in silico* analysis of the R197A mutant in combination with our binding results showing that this species adapted residue modulates binding to the receptor opens exciting questions on future structure-function studies to understand the basis of molecular adaptation of the human SP-A molecules.

DATA AVAILABILITY STATEMENT

The raw datasets supporting the conclusions of this manuscript will be made available by the authors upon request.

ETHICS STATEMENT

The animal study was reviewed and approved by Institutional Animal Care and Use Committee, Pennsylvania State University College of Medicine. All procedures with isolation of human alveolar macrophages were approved by the Penn State College of Medicine Institutional Review Board.

AUTHOR CONTRIBUTIONS

AN acquired and generated figures and tables for all the molecular dynamics simulation data. TU performed all binding assays with hSP-A1 and hSP-A2, isolated macrophages from mouse and lung BAL, and purified human SP-A proteins. C-HY performed all binding assays with recombinant rat SP-A, purified recombinant SP-R210, and cultured cells. PS and NT coordinated the procurement and logistics of donated human lung and contributed to the isolation of human alveolar macrophages. JF provided humanized SP-A1 and SP-A2 mice for the isolation of alveolar macrophages, and edited the manuscript critically. FM produced all recombinant rat SP-A proteins. ZC conceptualized, designed, led the study, and wrote the manuscript.

FUNDING

This work was supported by the National Institutes of Health [grant numbers HL068127 and EHS009882]; The Department of Pediatrics, Penn State College of Medicine, and The Children's Miracle Network.

REFERENCES

1. Chroneos ZC, Sever-Chroneos Z, Shepherd VL. Pulmonary surfactant: an immunological perspective. *Cell Physiol Biochem.* (2010) 25:13–26. doi: 10.1159/000272047
2. Seaton BA, Crouch EC, McCormack FX, Head JF, Hartshorn KL, Mendelsohn R. Review: structural determinants of pattern recognition by lung collectins. *Innate Immun.* (2010) 16:143–50. doi: 10.1177/1753425910368716
3. Nathan N, Taytard J, Duquesnoy P, Thouvenin G, Corvol H, Amselem S, et al. Surfactant protein A: a key player in lung homeostasis. *Int J Biochem Cell Biol.* (2016) 81:151–5. doi: 10.1016/j.biocel.2016.11.003
4. Head JF, Mealy TR, McCormack FX, Seaton BA. Crystal structure of trimeric carbohydrate recognition and neck domains of surfactant protein A. *J Biol Chem.* (2003) 278:43254–60. doi: 10.1074/jbc.M305628200
5. Shang F, Rynkiewicz MJ, McCormack FX, Wu H, Cafarella TM, Head JF, et al. Crystallographic complexes of surfactant protein A and carbohydrates reveal ligand-induced conformational change. *J Biol Chem.* (2011) 286:757–65. doi: 10.1074/jbc.M110.175265
6. Goh BC, Wu H, Rynkiewicz MJ, Schulten K, Seaton BA, McCormack FX. Elucidation of Lipid binding sites on lung surfactant protein A using X-ray crystallography, mutagenesis, and molecular dynamics simulations. *Biochemistry.* (2016) 55:3692–701. doi: 10.1021/acs.biochem.6b00048
7. Rynkiewicz MJ, Wu H, Cafarella TR, Nikolaidis NM, Head JF, Seaton BA, et al. Differential ligand binding specificities of the pulmonary collectins are determined by the conformational freedom of a surface loop. *Biochemistry.* (2017) 56:4095–105. doi: 10.1021/acs.biochem.6b01313
8. Kuroki Y, Mason RJ, Voelker DR. Alveolar type II cells express a high-affinity receptor for pulmonary surfactant protein A. *Proc Natl Acad Sci USA.* (1988) 85:5566–70. doi: 10.1073/pnas.85.15.5566
9. Wright JR, Borchelt JD, Hawgood S. Lung surfactant apoprotein SP-A (26-36 kDa) binds with high affinity to isolated alveolar type II cells. *Proc Natl Acad Sci USA.* (1989) 86:5410–4. doi: 10.1073/pnas.86.14.5410
10. Chroneos ZC, Abdolrasulnia R, Whitsett JA, Rice WR, Shepherd VL. Purification of a cell-surface receptor for surfactant protein A. *J Biol Chem.* (1996) 271:16375–83. doi: 10.1074/jbc.271.27.16375
11. Pison U, Wright JR, Hawgood S. Specific binding of surfactant apoprotein SP-A to rat alveolar macrophages. *Am J Physiol.* (1992) 262:L412–L417. doi: 10.1152/ajplung.1992.262.4.L412

12. McCormack FX, Kuroki Y, Stewart JJ, Mason RJ, Voelker DR. Surfactant protein A amino acids Glu195 and Arg197 are essential for receptor binding, phospholipid aggregation, regulation of secretion, and the facilitated uptake of phospholipid by type II cells. *J Biol Chem.* (1994) 269:29801–7.
13. McCormack FX, Stewart J, Voelker DR, Damodarasamy M. Alanine mutagenesis of surfactant protein A reveals that lipid binding and pH-dependent liposome aggregation are mediated by the carbohydrate recognition domain. *Biochemistry.* (1997) 36:13963–71. doi: 10.1021/bi970745q
14. Borron P, McCormack FX, Elhalwagi BM, Chroneos ZC, Lewis JF, Zhu S, et al. Surfactant protein A inhibits T cell proliferation via its collagen-like tail and a 210-kDa receptor. *Am J Physiol.* (1998) 275:L679–686. doi: 10.1152/ajplung.1998.275.4.L679
15. Chiba H, Sano H, Saitoh M, Sohma H, Voelker DR, Akino T, et al. Introduction of mannose binding protein-type phosphatidylinositol recognition into pulmonary surfactant protein A. *Biochemistry.* (1999) 38:7321–31. doi: 10.1021/bi990353e
16. Yu SH, McCormack FX, Voelker DR, Possmayer F. Interactions of pulmonary surfactant protein SP-A with monolayers of dipalmitoylphosphatidylcholine and cholesterol: roles of SP-A domains. *J Lipid Res.* (1999) 40:920–9.
17. Korfhagen TR, Levine AM, Whitsett JA. Surfactant protein A (SP-A) gene targeted mice. *Biochim Biophys Acta.* (1998) 1408:296–302. doi: 10.1016/S0925-4439(98)00075-1
18. Ikegami M, Elhalwagi BM, Palaniyar N, Dienger K, Korfhagen T, Whitsett JA, et al. The collagen-like region of surfactant protein A (SP-A) is required for correction of surfactant structural and functional defects in the SP-A null mouse. *J Biol Chem.* (2001) 276:38542–8. doi: 10.1074/jbc.M102054200
19. Palaniyar N, Ikegami M, Korfhagen T, Whitsett J, McCormack FX. Domains of surfactant protein A that affect protein oligomerization, lipid structure and surface tension. *Comp Biochem Physiol A Mol Integr Physiol.* (2001) 129:109–27. doi: 10.1016/S1095-6433(01)00309-9
20. Bates SR. P63 (CKAP4) as an SP-A receptor: implications for surfactant turnover. *Cell Physiol Biochem.* (2010) 25:41–54. doi: 10.1159/000272062
21. Wang G, Guo X, DiAngelo S, Thomas NJ, Floros J. Humanized SFTPA1 and SFTPA2 transgenic mice reveal functional divergence of SP-A1 and SP-A2: formation of tubular myelin *in vivo* requires both gene products. *J Biol Chem.* (2010) 285:11998–2010. doi: 10.1074/jbc.M109.046243
22. Sever-Chroneos Z, Krupa A, Davis J, Hasan M, Yang CH, Szeliga J, et al. Surfactant protein A (SP-A)-mediated clearance of Staphylococcus aureus involves binding of SP-A to the staphylococcal adhesin eap and the macrophage receptors SP-A receptor 210 and scavenger receptor class A. *J Biol Chem.* (2011) 286:4854–70. doi: 10.1074/jbc.M110.125567
23. Sidobre S, Nigou J, Puzo G, Riviere M. Lipoglycans are putative ligands for the human pulmonary surfactant protein A attachment to mycobacteria. Critical role of the lipids for lectin-carbohydrate recognition. *J Biol Chem.* (2000) 275:2415–22. doi: 10.1074/jbc.275.4.2415
24. Ragas A, Roussel L, Puzo G, Riviere M. The *Mycobacterium tuberculosis* cell-surface glycoprotein apa as a potential adhesin to colonize target cells via the innate immune system pulmonary C-type lectin surfactant protein A. *J Biol Chem.* (2007) 282:5133–42. doi: 10.1074/jbc.M610183200
25. McCormack FX, Festa AL, Andrews RP, Linke M, Walzer PD. The carbohydrate recognition domain of surfactant protein A mediates binding to the major surface glycoprotein of *Pneumocystis carinii*. *Biochemistry.* (1997) 36:8092–9. doi: 10.1021/bi970313f
26. McCormack FX, Gibbons R, Ward SR, Kuzmenko A, Wu H, Deepe GS Jr. Macrophage-independent fungicidal action of the pulmonary collectins. *J Biol Chem.* (2003) 278:36250–6. doi: 10.1074/jbc.M303086200
27. Weikert LF, Lopez JP, Abdolrasulnia R, Chroneos ZC, Shepherd VL. Surfactant protein A enhances mycobacterial killing by rat macrophages through a nitric oxide-dependent pathway. *Am J Physiol Lung Cell Mol Physiol.* (2000) 279:L216–223. doi: 10.1152/ajplung.2000.279.2.L216
28. Wu H, Kuzmenko A, Wan S, Schaffer L, Weiss A, Fisher JH, et al. Surfactant proteins A and D inhibit the growth of Gram-negative bacteria by increasing membrane permeability. *J Clin Invest.* (2003) 111:1589–602. doi: 10.1172/JCI16889
29. Yang L, Carrillo M, Wu YM, DiAngelo SL, Silveyra P, Umstead TM, et al. SP-R210 (Myo18A) isoforms as intrinsic modulators of macrophage priming and activation. *PLoS ONE.* (2015) 10:e0126576. doi: 10.1371/journal.pone.0126576
30. Tenner AJ, Robinson SL, Borchelt J, Wright JR. Human pulmonary surfactant protein (SP-A), a protein structurally homologous to C1q, can enhance FcR- and CR1-mediated phagocytosis. *J Biol Chem.* (1989) 264:13923–8.
31. Crowther JE, Kutala VK, Kuppusamy P, Ferguson JS, Beharka AA, Zweier JL, et al. Pulmonary surfactant protein a inhibits macrophage reactive oxygen intermediate production in response to stimuli by reducing NADPH oxidase activity. *J Immunol.* (2004) 172:6866–74. doi: 10.4049/jimmunol.172.11.6866
32. Yang CH, Szeliga J, Jordan J, Faske S, Sever-Chroneos Z, Dorsett B, et al. Identification of the surfactant protein A receptor 210 as the unconventional myosin 18A. *J Biol Chem.* (2005) 280:34447–57. doi: 10.1074/jbc.M505229200
33. Minutti CM, Jackson-Jones LH, Garcia-Fojeda B, Knipper JA, Sutherland TE, Logan N, et al. Local amplifiers of IL-4Ralpha-mediated macrophage activation promote repair in lung and liver. *Science.* (2017) 356:1076–80. doi: 10.1126/science.aaj2067
34. Floros J, Wang G, Mikerov AN. Genetic complexity of the human innate host defense molecules, surfactant protein A1 (SP-A1) and SP-A2–impact on function. *Crit Rev Eukaryot Gene Expr.* (2009) 19:125–37. doi: 10.1615/CritRevEukarGeneExpr.v19.i2.30
35. Floros J, Steinbrink R, Jacobs K, Phelps D, Kriz R, Recny M, et al. Isolation and characterization of cDNA clones for the 35-kDa pulmonary surfactant-associated protein. *J Biol Chem.* (1986) 261:9029–33.
36. Karinch AM, Floros J. 5' splicing and allelic variants of the human pulmonary surfactant protein A genes. *Am J Respir Cell Mol Biol.* (1995) 12:77–88. doi: 10.1165/ajrcmb.12.1.7811473
37. Floros J, Hoover RR. Genetics of the hydrophilic surfactant proteins A and D. *Biochim Biophys Acta.* (1998) 1408:312–22. doi: 10.1016/S0925-4439(98)00077-5
38. DiAngelo S, Lin Z, Wang G, Phillips S, Ramet M, Luo J, et al. Novel, non-radioactive, simple and multiplex PCR-cRFLP methods for genotyping human SP-A and SP-D marker alleles. *Dis Markers.* (1999) 15:269–81. doi: 10.1155/1999/961430
39. Wang G, Umstead TM, Phelps DS, Al-Mondhiry H, Floros J. The effect of ozone exposure on the ability of human surfactant protein a variants to stimulate cytokine production. *Environ Health Perspect.* (2002) 110:79–84. doi: 10.1289/ehp.0211079
40. Mikerov AN, Wang G, Umstead TM, Zacharatos M, Thomas NJ, Phelps DS, et al. Surfactant protein A2 (SP-A2) variants expressed in CHO cells stimulate phagocytosis of Pseudomonas aeruginosa more than do SP-A1 variants. *Infect Immun.* (2007) 75:1403–12. doi: 10.1128/IAI.01341-06
41. Phelps DS, Umstead TM, Floros J. Sex differences in the acute *in vivo* effects of different human SP-A variants on the mouse alveolar macrophage proteome. *J Proteomics.* (2014) 108:427–44. doi: 10.1016/j.jprot.2014.06.007
42. Wang Y, Kuan PJ, Xing C, Cronkhite JT, Torres F, Rosenblatt RL, et al. Genetic defects in surfactant protein A2 are associated with pulmonary fibrosis and lung cancer. *Am J Hum Genet.* (2009) 84:52–9. doi: 10.1016/j.ajhg.2008.11.010
43. Mitsuhashi A, Goto H, Kuramoto T, Tabata S, Yukishige S, Abe S, et al. Surfactant protein A suppresses lung cancer progression by regulating the polarization of tumor-associated macrophages. *Am J Pathol.* (2013) 182:1843–53. doi: 10.1016/j.ajpath.2013.01.030
44. Phelps DS, Umstead TM, Silveyra P, Hu S, Wang G, Floros J. Differences in the alveolar macrophage proteome in transgenic mice expressing human SP-A1 and SP-A2. *J Proteom Genom Res.* (2013) 1:2–26. doi: 10.14302/issn.2326-0793.jpgr-12-207
45. Nathan N, Giraud V, Picard C, Nunes H, Dastot-Le Moal F, Copin B, et al. Germline SFTPA1 mutation in familial idiopathic interstitial pneumonia and lung cancer. *Hum Mol Genet.* (2016) 25:1457–67. doi: 10.1093/hmg/ddw014
46. Thorenoor N, Umstead TM, Zhang X, Phelps DS, Floros J. Survival of surfactant protein-A1 and SP-A2 transgenic mice after *Klebsiella pneumoniae* infection, exhibits sex-, gene-, and variant specific differences; treatment with surfactant protein improves survival. *Front Immunol.* (2018) 9:2404. doi: 10.3389/fimmu.2018.02404

47. Thorenoor N, Zhang X, Umstead TM, Scott Halstead E, Phelps DS, Floros J. Differential effects of innate immune variants of surfactant protein-A1 (SFTPA1) and SP-A2 (SFTPA2) in airway function after *Klebsiella pneumoniae* infection and sex differences. *Respir Res.* (2018) 19:23. doi: 10.1186/s12931-018-0723-1
48. Sanchez-Barbero F, Rivas G, Steinhilber W, Casals C. Structural and functional differences among human surfactant proteins SP-A1, SP-A2 and co-expressed SP-A1/SP-A2: role of supratrimeric oligomerization. *Biochem J.* (2007) 406:479–89. doi: 10.1042/BJ20070275
49. Wang G, Myers C, Mikerov A, Floros J. Effect of cysteine 85 on biochemical properties and biological function of human surfactant protein A variants. *Biochemistry.* (2007) 46:8425–35. doi: 10.1021/bi7004569
50. Korfhagen TR, Bruno MD, Ross GF, Huelsman KM, Ikegami M, Jobe AH, et al. Altered surfactant function and structure in SP-A gene targeted mice. *Proc Natl Acad Sci USA.* (1996) 93:9594–9. doi: 10.1073/pnas.93.18.9594
51. Veldhuizen RA, Yao LJ, Hearn SA, Possmayer F, Lewis JF. Surfactant-associated protein A is important for maintaining surfactant large-aggregate forms during surface-area cycling. *Biochem J.* (1996) 313 (Pt 3):835–40. doi: 10.1042/bj3130835
52. Voss T, Schafer KP, Nielsen PF, Schafer A, Maier C, Hannappel E, et al. Primary structure differences of human surfactant-associated proteins isolated from normal and proteinosis lung. *Biochim Biophys Acta.* (1992) 1138:261–7. doi: 10.1016/0925-4439(92)90002-5
53. Ridsdale RA, Palaniyar N, Holterman CE, Inchley K, Possmayer F, Harauz G. Cation-mediated conformational variants of surfactant protein A. *Biochim Biophys Acta.* (1999) 1453:23–34. doi: 10.1016/S0925-4439(98)00057-X
54. Uemura T, Sano H, Katoh T, Nishitani C, Mitsuzawa H, Shimizu T, et al. Surfactant protein A without the interruption of Gly-X-Y repeats loses a kink of oligomeric structure and exhibits impaired phospholipid liposome aggregation ability. *Biochemistry.* (2006) 45:14543–51. doi: 10.1021/bi061338u
55. Wang G, Taneva S, Keough KM, Floros J. Differential effects of human SP-A1 and SP-A2 variants on phospholipid monolayers containing surfactant protein B. *Biochim Biophys Acta.* (2007) 1768:2060–9. doi: 10.1016/j.bbamem.2007.06.025
56. Lopez-Rodriguez E, Pascual A, Arroyo R, Floros J, Perez-Gil J. Human pulmonary surfactant protein SP-A1 provides maximal efficiency of lung interfacial films. *Biophys J.* (2016) 111:524–36. doi: 10.1016/j.bpj.2016.06.025
57. Sanchez-Barbero F, Strassner J, Garcia-Canero R, Steinhilber W, Casals C. Role of the degree of oligomerization in the structure and function of human surfactant protein A. *J Biol Chem.* (2005) 280:7659–70. doi: 10.1074/jbc.M410266200
58. Watson A, Kronqvist N, Spalluto CM, Griffiths M, Staples KJ, Wilkinson T, et al. Novel expression of a functional trimeric fragment of human SP-A with efficacy in neutralisation of RSV. *Immunobiology.* (2017) 222:111–8. doi: 10.1016/j.imbio.2016.10.015
59. Mikerov AN, Umstead TM, Gan X, Huang W, Guo X, Wang G, et al. Impact of ozone exposure on the phagocytic activity of human surfactant protein A (SP-A) and SP-A variants. *Am J Physiol Lung Cell Mol Physiol.* (2008) 294:L121–L130. doi: 10.1152/ajplung.00288.2007
60. Huang W, Wang G, Phelps DS, Al-Mondhiry H, Floros J. Human SP-A genetic variants and bleomycin-induced cytokine production by THP-1 cells: effect of ozone-induced SP-A oxidation. *Am J Physiol Lung Cell Mol Physiol.* (2004) 286:L546–553. doi: 10.1152/ajplung.00267.2003
61. McCormack FX, Calvert HM, Watson PA, Smith DL, Mason RJ, Voelker DR. The structure and function of surfactant protein A. *Hydroxyproline- and carbohydrate-deficient mutant proteins J Biol Chem.* (1994) 269:5833–41.
62. Pattanajitvilai S, Kuroki Y, Tsunezawa W, McCormack FX, Voelker DR. Mutational analysis of Arg197 of rat surfactant protein A. His197 creates specific lipid uptake defects. *J Biol Chem.* (1998) 273:5702–7. doi: 10.1074/jbc.273.10.5702
63. Tsunezawa W, Sano H, Sohma H, McCormack FX, Voelker DR, Kuroki Y. Site-directed mutagenesis of surfactant protein A reveals dissociation of lipid aggregation and lipid uptake by alveolar type II cells. *Biochim Biophys Acta.* (1998) 1387:433–46. doi: 10.1016/S0167-4838(98)00159-9
64. McCormack FX, Damodarasamy M, Elhalwagi BM. Deletion mapping of N-terminal domains of surfactant protein A. The N-terminal segment is required for phospholipid aggregation and specific inhibition of surfactant secretion. *J Biol Chem.* (1999) 274:3173–81. doi: 10.1074/jbc.274.5.3173
65. Wang G, Phelps DS, Umstead TM, Floros J. Human SP-A protein variants derived from one or both genes stimulate TNF-alpha production in the THP-1 cell line. *Am J Physiol Lung Cell Mol Physiol.* (2000) 278:L946–L954. doi: 10.1152/ajplung.2000.278.5.L946
66. Yu WC, Chan RW, Wang J, Travanty EA, Nicholls JM, Peiris JS, et al. Viral replication and innate host responses in primary human alveolar epithelial cells and alveolar macrophages infected with influenza H5N1 and H1N1 viruses. *J Virol.* (2011) 85:6844–55. doi: 10.1128/JVI.02200-10
67. Silveyra P, Chroneos ZC, DiAngelo SL, Thomas NJ, Noutsios GT, Tsotakos N, et al. Knockdown of Drosha in human alveolar type II cells alters expression of SP-A in culture: a pilot study. *Exp Lung Res.* (2014) 40:354–66. doi: 10.3109/01902148.2014.929757
68. Guex N, Peitsch MC. SWISS-MODEL and the Swiss-PdbViewer: an environment for comparative protein modeling. *Electrophoresis.* (1997) 18:2714–23. doi: 10.1002/elps.1150181505
69. Iakhiaev AV, Nalian A, Koenig K, Idell S. Thrombin-thrombomodulin inhibits prourokinase-mediated pleural mesothelial cell-dependent fibrinolysis. *Thromb Res.* (2007) 120:715–25. doi: 10.1016/j.thromres.2006.12.001
70. Thompson JD, Higgins DG, Gibson TJ. CLUSTAL W: improving the sensitivity of progressive multiple sequence alignment through sequence weighting, position-specific gap penalties and weight matrix choice. *Nucleic Acids Res.* (1994) 22:4673–80. doi: 10.1093/nar/22.22.4673
71. Larkin MA, Blackshields G, Brown NP, Chenna R, Mcgettigan PA, Mcwilliam H, et al. Clustal W and clustal X version 2.0. *Bioinformatics.* (2007) 23:2947–8. doi: 10.1093/bioinformatics/btm404
72. McCormack FX. Structure, processing and properties of surfactant protein A. *Biochim Biophys Acta.* (1998) 1408:109–31. doi: 10.1016/S0925-4439(98)00062-3
73. Lin Z, Wang Y, Zhu K, Floros J. Differential allele expression of host defense genes, pulmonary surfactant protein-A and osteopontin, in rat. *Mol Immunol.* (2004) 41:1155–65. doi: 10.1016/j.molimm.2004.06.006
74. Wang G, Bates-Kenney SR, Tao JQ, Phelps DS, Floros J. Differences in biochemical properties and in biological function between human SP-A1 and SP-A2 variants, and the impact of ozone-induced oxidation. *Biochemistry.* (2004) 43:4227–39. doi: 10.1021/bi036023i
75. Szeliga J, Jordan J, Yang CH, Sever-Chroneos Z, Chroneos ZC. Bacterial expression of recombinant MyoXVIIIA domains. *Anal Biochem.* (2005) 346:179–81. doi: 10.1016/j.ab.2005.07.021
76. Yoshida M, Ikegami M, Reed JA, Chroneos ZC, Whitsett JA. GM-CSF regulates protein and lipid catabolism by alveolar macrophages. *Am J Physiol Lung Cell Mol Physiol.* (2001) 280:L379–386. doi: 10.1152/ajplung.2001.280.3.L379
77. Silveyra P, Floros J. *Gene*tic complexity of the human surfactant-associated proteins SP-A1 and SP-A2. *Gene.* (2013) 531:126–32. doi: 10.1016/j.gene.2012.09.111
78. Xu J, Rodriguez D, Petitclerc E, Kim JJ, Hangai M, Moon YS, et al. Proteolytic exposure of a cryptic site within collagen type IV is required for angiogenesis and tumor growth *in vivo*. *J Cell Biol.* (2001) 154:1069–79. doi: 10.1083/jcb.200103111
79. Lu X, Lu D, Scully MF, Kakkar VV. Integrins in drug targeting-RGD templates in toxins. *Curr Pharm Des.* (2006) 12:2749–69. doi: 10.2174/138161206777947713
80. Andersen MH, Graversen H, Fedosov SN, Petersen TE, Rasmussen JT. Functional analyses of two cellular binding domains of bovine lactadherin. *Biochemistry.* (2000) 39:6200–6. doi: 10.1021/bi992221r
81. Simoes I, Mueller EC, Otto A, Bur D, Cheung AY, Faro C, et al. Molecular analysis of the interaction between cardosin A and phospholipase D(alpha). Identification of RGD/KGE sequences as binding motifs for C2 domains. *FEBS J.* (2005) 272:5786–98. doi: 10.1111/j.1742-4658.2005.04967.x
82. Rothwangl KB, Rong L. Analysis of a conserved RGE/RGD motif in HCV E2 in mediating entry. *Virol J.* (2009) 6:12. doi: 10.1186/1743-422X-6-12
83. Parsons KK, Maeda N, Yamauchi M, Banes AJ, Koller BH. Ascorbic acid-independent synthesis of collagen in mice. *Am J Physiol Endocrinol Metab.* (2006) 290:E1131–E1139. doi: 10.1152/ajpendo.00339.2005
84. Noutsios GT, Floros J. Childhood asthma: causes, risks, and protective factors; a role of innate immunity. *Swiss Med Wkly.* (2014) 144:w14036. doi: 10.4414/smw.2014.14036

85. Weikert LF, Edwards K, Chroneos ZC, Hager C, Hoffman L, Shepherd VL. SP-A enhances uptake of bacillus Calmette-Guerin by macrophages through a specific SP-A receptor. *Am J Physiol.* (1997) 272:L989–995. doi: 10.1152/ajplung.1997.272.5.L989
86. Samten B, Townsend JC, Sever-Chroneos Z, Pasquinelli V, Barnes PF, Chroneos ZC. An antibody against the surfactant protein A (SP-A)-binding domain of the SP-A receptor inhibits T cell-mediated immune responses to *Mycobacterium tuberculosis*. *J Leukoc Biol.* (2008) 84:115–23. doi: 10.1189/jlb.1207835
87. Vieira F, Kung JW, Bhatti F. Structure, genetics and function of the pulmonary associated surfactant proteins A and D: the extra-pulmonary role of these C type lectins. *Ann Anat.* (2017) 211:184–201. doi: 10.1016/j.aanat.2017.03.002

Conflict of Interest: The authors declare that the research was conducted in the absence of any commercial or financial relationships that could be construed as a potential conflict of interest.

frontiers in Immunology

ORIGINAL RESEARCH
published: 16 August 2019
doi: 10.3389/fimmu.2019.01960

Differential Impact of Co-expressed SP-A1/SP-A2 Protein on AM miRNome; Sex Differences

*Nithyananda Thorenoor[1], Yuka Imamura Kawasawa[2], Chintan K. Gandhi[1], Xuesheng Zhang[1] and Joanna Floros[1,3]**

[1] Department of Pediatrics, Center for Host Defense, Inflammation, and Lung Disease Research, The Pennsylvania State University College of Medicine, Hershey, PA, United States, [2] Departments of Pharmacology and Biochemistry and Molecular Biology, Institute for Personalized Medicine, The Pennsylvania State University College of Medicine, Hershey, PA, United States, [3] Department of Obstetrics and Gynecology, The Pennsylvania State University College of Medicine, Hershey, PA, United States

OPEN ACCESS

Edited by:
Francesca Granucci, University of Milano-Bicocca, Italy

Reviewed by:
Eswari Dodagatta-Marri, University of California, San Francisco, United States
Taruna Madan, National Institute for Research in Reproductive Health (ICMR), India

***Correspondence:**
Joanna Floros
jxf19@psu.edu; jfloros@pennstatehealth.psu.edu

Specialty section:
This article was submitted to Molecular Innate Immunity, a section of the journal Frontiers in Immunology

Received: *01 May 2019*
Accepted: *02 August 2019*
Published: *16 August 2019*

Citation:
Thorenoor N, Kawasawa YI, Gandhi CK, Zhang X and Floros J (2019) Differential Impact of Co-expressed SP-A1/SP-A2 Protein on AM miRNome; Sex Differences. Front. Immunol. 10:1960. doi: 10.3389/fimmu.2019.01960

In humans there are two surfactant protein A (SP-A) functional genes *SFTPA1* and *SFTPA2* encoding innate immune molecules, SP-A1 and SP-A2, respectively, with numerous genetic variants each. SP-A interacts and regulates many of the functions of alveolar macrophages (AM). It is shown that SP-A variants differ in their ability to regulate the AM miRNome in response to oxidative stress (OxS). Because humans have both SP-A gene products, we were interested to determine the combined effect of co-expressed SP-A1/SP-A2 (co-ex) in response to ozone (O_3) induced OxS on AM miRNome. Human transgenic (hTG) mice, carrying both SP-A1/SP-A2 ($6A^2/1A^0$, co-ex) and SP-A- KO were utilized. The hTG and KO mice were exposed to filtered air (FA) or O_3 and miRNA levels were measured after AM isolation with or without normalization to KO. We found: (i) The AM miRNome of co-ex males and females in response to OxS to be largely downregulated after normalization to KO, but after Bonferroni multiple comparison analysis only in females the AM miRNome remained significantly different compared to control (FA); (ii) The targets of the significantly changed miRNAs were downregulated in females and upregulated in males; (iii) Several of the validated mRNA targets were involved in pro-inflammatory response, anti-apoptosis, cell cycle, cellular growth and proliferation; (iv) The AM of SP-A2 male, shown, previously to have major effect on the male AM miRNome in response to OxS, shared similarities with the co-ex, namely in pathways involved in the pro-inflammatory response and anti-apoptosis but also exhibited differences with the cell-cycle, growth, and proliferation pathway being involved in co-ex and ROS homeostasis in SP-A2 male. We speculate that the presence of both gene products vs. single gene products differentially impact the AM responses in males and females in response to OxS.

Keywords: surfactant protein A, alveolar macrophages, miRNA, surfactant protein A1/A2, sex differences, oxidative stress

INTRODUCTION

Surfactant protein A (SP-A) plays important role in lung innate immunity and surfactant-related functions under basal conditions (1–5) and in response to various insults such as infection and oxidative stress (6–10). The human SP-A locus consists of two functional genes, *SFTPA1* and *SFTPA2*, and one pseudogene (11, 12). The functional genes encode human SP-A1 and SP-A2 proteins, respectively, and each gene has been shown to have several genetic and splice variants (13, 14).

Human SP-A is expressed in alveolar epithelial type II cells (15) and in other tissues (16–19). It has been reported that human SP-A exists as octadecamer with six trimers (20), and that SP-A trimers have two SP-A1 molecules, and one SP-A2 molecule in the ratio of 2:1 (21). Previous studies from our group and others have shown that the ratio of the proposed model at mRNA and protein levels varies (22, 23). In bronchoalveolar lavage (BAL) fluid the ratio between SP-A1 to total SP-A varies as a function of age and health status (23, 24). The SP-A1 and SP-A2 mRNA content was found to vary in explant cultures under different conditions (25–27). Moreover, more SP-A2 mRNA than SP-A1 was observed in lung tissues of adults, whereas more SP-A1 mRNA transcripts were detected in neonates (28).

Several studies demonstrated that single gene products, SP-A1 and SP-A2, exhibit both qualitative (i.e., functional, biochemical and/or structural) (29–43), and quantitative (regulatory) differences (23, 25–27, 44–46). For example, SP-A1 and SP-A2 variants have been shown to differ in their ability to modulate the proteomic expression profile of AM and the AM actin cytoskeleton (47–49). The proteome profile of AM from KO mice, after treatment with exogenous SP-A1 or SP-A2 resulted in significant changes in proteins involved in the oxidative stress response pathway, with females being more responsive to SP-A1 and males to SP-A2 (48), as well as the single cell analysis revealed sex- and age-related differences in alveolar macrophage phenotypes from KO mice in response to SP-A1 and SP-A2 proteins (49). Moreover, sex differences have been observed between SP-A1 and SP-A2 and among variants in survival and lung function mechanics in response to bacterial infection (42, 43), and SP-A1 compared to SP-A2 exhibits a higher efficiency in pulmonary surfactant reorganization (50). The major contributor for at least some of these differences appears to be amino acid 85 of the precursor molecule; where SP-A1 has a cysteine and SP-A2 has an arginine (14). This Cys/Arg is a key difference between SP-A1 and SP-A2. This single amino acid change has a major impact on SP-A oligomerization, lipopolysaccharide (LPS) aggregation, and phagocytosis (38). The replacement of cysteine of SP-A1 with arginine or the arginine of SP-A2 with cysteine resulted in a reversal pattern of SP-A oligomerization and functional activity of both mutants of SP-A1 and SP-A2 (38). Thus, structural differences due to Cys85 and other amino acids may underlie differences in function observed between SP-A1 and SP-A2.

Ozone (O_3), a major component of air pollution and a strong oxidizing agent known to cause toxicity in the lower airways, has significant effects on innate host defense and lung function (51). The O_3 exposure can cause, edema, contributing to lung injury, and pulmonary surfactant derangement (52). A significant difference in survival has been observed with females being more affected than males in several lung diseases (53–56). In our animal studies, we observed significant differences in survival after infection and O_3 exposure, with females being more susceptible to oxidative stress than males (7, 9) and sex hormones have been implicated in the observed differences in survival (57) but the mechanism underlying these differences is unknown. Moreover, during pneumonie infection and bacterial clearance, the ability to limit bacterial dissemination, and the phagocytic activity of alveolar macrophages may play an important role in the differential outcome in survival between males and females in the presence or absence of oxidative stress (7, 9, 58). Previously, we observed significant changes in AM miRNome of SP-A2 males but not in SP-A2 females or in SP-A1 males and females in response to OxS (41).

In the present study, we investigated the hypothesis that male and female mice expressing both SP-A1/SP-A2 gene products (co-ex) differentially regulate the AM miRNome in response to ozone-induced oxidative stress and that this differs from that previously observed in SP-A single gene variants (41). Toward this co-ex male and female mice were exposed to filtered air (FA) or O_3 and the expression levels of 307 miRNAs was measured with or without normalizing to miRNAs identified from KO under the same conditions. We found significant differences in the AM miRNome of co-ex in terms of sex, exposure, with or without normalization to KO. Comparison of the co-ex miRNome to that of hTG mice carrying SP-A2 variant showed that the pathways involved in AM SP-A2 share some similarities to that of co-ex, but also exhibit differences.

Abbreviations: AKT1, AKT Serine/Threonine Kinase 1; ARG1, Arginase 1; AM, Alveolar macrophages; ANOVA, analysis of variance; BAL, bronchoalveolar lavage; BCL2, B-cell lymphoma 2; CCND1, Cyclin D1; CCND2, Cyclin D2; CCNE1, Cyclin E1; CDK2, Cyclin-dependent kinase 2; CDK7, Cyclin-dependent kinase 7; E2F3, E2F transcription factor 3; EGR2, Early growth response 2; FA, Filtered air; GAPDH, Glyceraldehyde 3-phosphate dehydrogenase; hTG, Humanized transgenic; IkBa, NFKB Inhibitor Alpha; IL4, Interleukin 4; IL6, Interleukin 6; IL10, Interleukin 10; IL2RG, Interleukin 2 receptor subunit gamma; IPA, Ingenuity Pathway Analysis; JUN, Jun proto-oncogene; KO, knock-out; LPS, lipopolysaccharide; MAPK, Mitogen-activated protein kinases; MDTH, Metadherin; miRNAs, microRNAs; MMP2, Matrix metallopeptidase 2; MYC, MYC proto-oncogene; MYD88, Myeloid differentiation primary response 88; NF-kB, Nuclear factor kappa-light-chain-enhancer of activated B cells; O_3, ozone; OxS, oxidative stress; PPARA, Peroxisome proliferator activated receptor alpha; PTEN, Phosphatase and tensin homolog; ROS, reactive oxygen species; *SFTPA1*, gene encoding SP-A1; *SFTPA2*, gene encoding SP-A2; SMAD2, SMAD family member 2; SP-A, surfactant protein A; STAT3, Signal transducer and activator of transcription 2; TLR2, Toll-like receptor 2; TLR3, Toll-like receptor 3; TNF, Tumor necrosis factor; TNFSF12, TNF super family member 12; TRIF, TIR-domain containing adaptor protein.

METHODS

Animals

Humanized transgenic (hTG) mice carrying both gene variants, SP-A1/SP-A2 ($6A^2/1A^0$, co-ex), as well as SP-A knockout (KO) mice were used in this study. They were 12 weeks old. hTG mice were generated on the C57BL/6J SP-A (KO) background (59). The animals used in this study were raised and maintained

in a pathogen-free environment, at the Penn State College of Medicine animal facility as described previously (43). Both males and females were used. The females were synchronized with regard to the estrous cycle as described previously (43). A total of 44 mice (32 for miRNA analysis and 12 for qRT-PCR analysis) were used in the present study. All the procedures were approved by The Penn State Hershey Medical Center Institutional Animal Care and Use Committee (IACUC).

Filtered Air (FA) and Ozone (O_3) Exposure

The animals were exposed to FA or O_3 in parallel as described previously (60). A group of 4 animals (males, females) were exposed to FA or O_3 for 3 h, and alveolar macrophages (AM) were isolated after 4 h of recovery as described (61).

RNA Preparation, Library Construction, and Sequencing

Total RNA was extracted from AMs using mirVana kit (#AM1560, Ambion, Waltham, MA). The extracted RNAs were quantified and quality checked using a BioAnalyzer RNA 6000 Nano Kit (Agilent Technologies, Santa Clara, CA). Small RNA-seq libraries were generated by NEXTflex Small RNA Library Prep Kit v3 for Illumina (BioO Scientific, Austin, TX), followed by deep sequencing on an Illumina HiSeq 2500 as per the manufacturer's instructions. Briefly, 1-2 ng of total RNA was ligated with chemically modified 3′- and 5′- adapters that can specifically bind to mature micro RNAs, followed by reverse transcription and PCR amplification. Unique index sequence tags were introduced during PCR to enable multiplexed sequencing. Each library was assessed for the presence of desired micro RNA population and approximate library quantity by Bioanalyzer High Sensitivity DNA Kit (Agilent Technologies). Pooled libraries were denatured and loaded onto a TruSeq Rapid flow cell on an Illumina HiSeq 2500 and run for 50 cycles using a single-read recipe according to the manufacturer's instructions. De-multiplexed sequencing reads passed the default purify filtering of Illumina CASAVA pipeline (released version 1.8) and were quality trimmed/filtered using The FASTX-Toolkit (http://hannonlab.cshl.edu/fastx_toolkit). The filtered reads were further trimmed with both 5′ and 3′ adapter sequences and subjected to Chimira suite to align and count miRNA expression (62). The differentially expressed miRNAs (DEG) between FA to O_3, males and females were identified by using the edgeR (63) and the TCC v1.14.0 R package (64) with false discovery rate (FDR) adjusted p-value of 0.1 as a significance cutoff.

miRNA Data Analysis

We successfully identified 307 miRNAs with good correlation between mice (3 out of 4, **Supplementary Table 1**). We used two different parameters (methods) to analyze the identified miRNA expression (fold change). (a) The expression levels (fold change) of miRNAs from co-ex (FA to O_3 for males and females) and KO (FA to O_3 for males and females) were analyzed and differentially expressed miRNAs in co-ex and KO males and females were identified in response to FA or O_3. (b) The changes in miRNA expression in co-ex were calculated by normalizing to KO, i.e., the level of expression of each individual experimental miRNA in co-ex males and females exposed to FA or O_3 was divided by the corresponding miRNA in the KO. Next, the differentially expressed miRNAs between co-ex males and females were determined by dividing a specific individual male miRNA by the corresponding female miRNA (**Supplementary Table 1**).

Gene Expression Analysis

The expression levels of CCND1, CCND2, CCNE1, CDK7, IL-6, IL-10, TLR2, TLR3, STAT3, MYD88, IL-4, IL2RG, EGR2, PTEN, TNFSF12, MDTH, JUN, E2F3, BCL2, TNF, CDK2, SMAD2, MMP2, ARG1, AKT1, PPARA, and MYC genes at mRNA level in the female and male co-ex and KO AM, were validated by qRT-PCR as described previously (41). The RT2 qPCR Primer assays were purchased from Qiagen. The AM cell samples [3 animals/treatment (FA or O_3)] were analyzed in triplicates/animal and quantified relative to GAPDH mRNA.

Statistical Analysis

Statistical differences between miRNA expression levels (fold change) in FA vs. O_3 and male vs. female were evaluated by two-tailed t-test and nonparametric Mann-Whitney test. For multiple comparison analysis one-way analysis of variance (ANOVA) was employed followed by Bonferroni multiple comparisons. The p-values < 0.05 were considered to be significant. All the data points are means $\pm$ standard deviation, and analyses were performed using Graph-Pad Prism software version 5.0 (Graph-Pad Software, San Diego, USA).

RESULTS

We have previously studied the AM miRNome in hTG mice carrying either SP-A1 or SP-A2 variants using the qRT-PCR method (41). In this study, because humans have both SP-A gene products, we were interested to a) determine the combined effect of SP-A1/SP-A2 ($6A^2/1A^0$, co-ex) on the AM miRNome in response to oxidative stress with or without normalization to KO in males and females; b) identify sex, treatment, and gene (co-ex) impact on the AM miRNome; c) use differentially expressed miRNAs of $\geq$2 fold in co-ex in response to O_3 exposure in Ingenuity Pathway Analysis (IPA) to identify biological functions and regulatory network targets of the identified and differentially expressed miRNAs after normalized to KO and Bonferroni multiple corrections; d) compare the co-ex miRNome (present study) and its targets to that of hTG mice carrying SP-A2 (41) variant under the same condition.

Effect of SP-A1/SP-A2 ($6A^2/1A^0$, co-ex) on AM miRNome Regulation

Without Normalization to KO

A total of 307 miRNAs from AMs of co-ex and KO in response to FA or O_3 were identified from males and females (**Supplementary Table 1**). We observed significant differences ($p < 0.05$) in the expression of AM miRNAs in response to FA or O_3 in co-ex females and KO males and females (**Figures 1A,C,D**). No significant differences were observed in co-ex males, after exposure to FA or O_3 (**Figure 1B**). One-way ANOVA and Bonferroni multiple comparison analysis was

performed to find the effect of treatment (FA, and O_3) and sex (males, and females) as well as the interaction between the two parameters (sex and treatment). In co-ex, there was a significant difference between FA-exposed males and females (**Figure 1E**) but no significant difference was observed after O_3 exposure between males and females (**Figure 1E**). However, females (but not males) showed a significant difference between FA or O_3 exposure (**Figure 1E**). Whereas, in KO (i.e., in the absence of SP-A altogether), there was a significant difference between male and female after O_3 exposure, no significant difference was observed after FA exposure (**Figure 1F**), indicating a role of SP-A in O_3 exposure between sexes. However, similar to what was shown for the co-ex (**Figure 1E**), the KO females (but not the males) showed a significant difference after FA or O_3 exposures (**Figure 1F**). Moreover, the miRNAs identified from KO females exposed to O_3, showed a significant difference compared to KO males exposed to FA (**Figure 1F**).

Normalization to KO

By normalizing the expression of miRNAs in co-ex to KO, i.e., the level of expression of each individual experimental miRNA (i.e., in SP-A1/SP-A2, co-ex) was divided by the level of the corresponding miRNA in the KO (**Supplementary Table 1**), we found significant differences in the differential expression of miRNAs in both males and females after FA or O_3 exposure (**Figures 2A,B**). The one-way ANOVA and Bonferroni multiple comparison analysis resulted in similar observations as those observed in **Figure 1E** in the absence of KO normalization. Significant differences in miRNAs differentially expressed were observed in females between FA to O_3 exposure and FA-exposed females to FA-exposed males, with no significant difference observed of differentially expressed miRNAs after O_3 exposure between males and females (**Figure 2C**). Unlike in **Figure 1E**, FA-exposed females differed significantly from O_3-exposed males (**Figure 2C**).

The observations made with or without normalization to KO indicate that the AM miRNome of hTG mice carrying both SP-A1/SP-A2 ($6A^2/1A^0$, co-ex), exhibit no differences in miRNA expression between sexes in response to oxidative stress (O_3 exposure), but sex differences are observed in controls (i.e., after FA exposure; **Figures 1E**, **2C**). Female co-ex exhibited significant differences between FA or O_3 exposure. The presence of the two genes may play a protective role in the outcome of miRNA expression in response to oxidative stress, especially in males.

Regulation of miRNAs That Changed ≥2 Fold in Response to FA, O_3, and Sex

We further looked into the AM miRNAs, whose expression compared to control miRNAs is altered ≥2 fold in response to FA or O_3 from co-ex and KO males and females, and compared them between males and females.

Without Normalization to KO

First we compared AM miRNAs of FA vs. O_3 exposed animals. We found that in co-ex females, 49 miRNAs were changed after FA and 36 miRNAs after O_3 exposure, whereas in males, 31 miRNAs were changed in FA and 45 in O_3 exposure. The same comparison in KO AM miRNome showed that in females 45 miRNAs were changed ≥2 fold in FA and 94 miRNAs in O_3, while in males 34 miRNAs were changed ≥2 fold in FA and 41 miRNAs in O_3 (**Figure 3A**, **Supplementary Table 1**). In both co-ex and KO, all the miRNAs that had ≥2 fold are specific either to FA or O_3 exposure, with no miRNAs in common between FA or O_3 in either males or females.

Next, we compared males vs. females (co-ex, KO) in response to oxidative stress. In co-ex females, 36 miRNAs were differentially expressed (≥2 fold) compared to 45 miRNAs in males, with 7 miRNAs (≥2 fold) being in common in both males and females. Of these, 29 miRNAs are unique to females and 38 are unique to males (**Figure 3A**). In KO females after O_3 exposure, 94 miRNAs had ≥2 fold expression compared to 41 miRNAs in males. Of these 32 miRNAs were found in common in both sexes (**Figure 3A**), and 62 miRNAs are unique to females and 9 to males (**Figure 3A**). Of the seven miRNAs found to be in common between co-ex male and females after O_3 exposure only one miRNA is included in the 32 miRNAs found in common between KO males and females (**Supplementary Table 1**). Of interest the co-ex had a significantly lower number of shared miRNAs between the sexes compared to KO (7 vs. 32), indicating the major effect of sex on co-ex (**Supplementary Table 1**).

With Normalization to KO

By normalizing the miRNAs identified in co-ex to KO, we found 102 miRNAs to be differentially expressed ≥2 fold in females after FA exposure compared to 50 miRNAs after O_3 exposure (**Figure 3B**). In the case of males, 36 miRNAs are differentially expressed after FA exposure and 59 miRNAs had ≥2 fold after O_3 exposure. In both co-ex males and females, all the miRNAs with ≥2 fold are specific to either FA or O_3. A comparison of miRNAs from males and females after O_3 exposure showed 50 miRNAs ≥2 fold in females vs. 59 miRNAs in males (**Figure 3B**). Of these, 41 are unique to females and 50 to males, with 9 being found in common. These data indicate that when the expression of the AM miRNome in co-ex, after normalization to KO is compared in males and females, following exposure to FA or O_3, the observed changes in miRNA levels are either specific to males or females. However, when the miRNome between males and females co-ex normalized KO is compared after oxidative stress there are few miRNAs that are found in common in co-ex males and females (**Supplementary Table 1**).

Ingenuity Pathway Analysis (IPA)

We performed IPA to further understand the role of significantly changed miRNAs in co-ex males and females under the studied conditions. After Bonferroni correction, expression of miRNAs in co-ex females exhibited significant differences in response to OxS, but not in males (**Figure 2C**). However, the IPA analyses before and after the Bonferroni correction were identical because the miRNA data input in IPA was same. We were able to identify biological functions and regulatory network targets of these differentially expressed miRNAs. The targets shown in **Figure 4** are involved in anti-apoptosis, cell cycle, cellular growth and proliferation, as well as pro-inflammatory response are affected by differential expression of miRNAs in response to

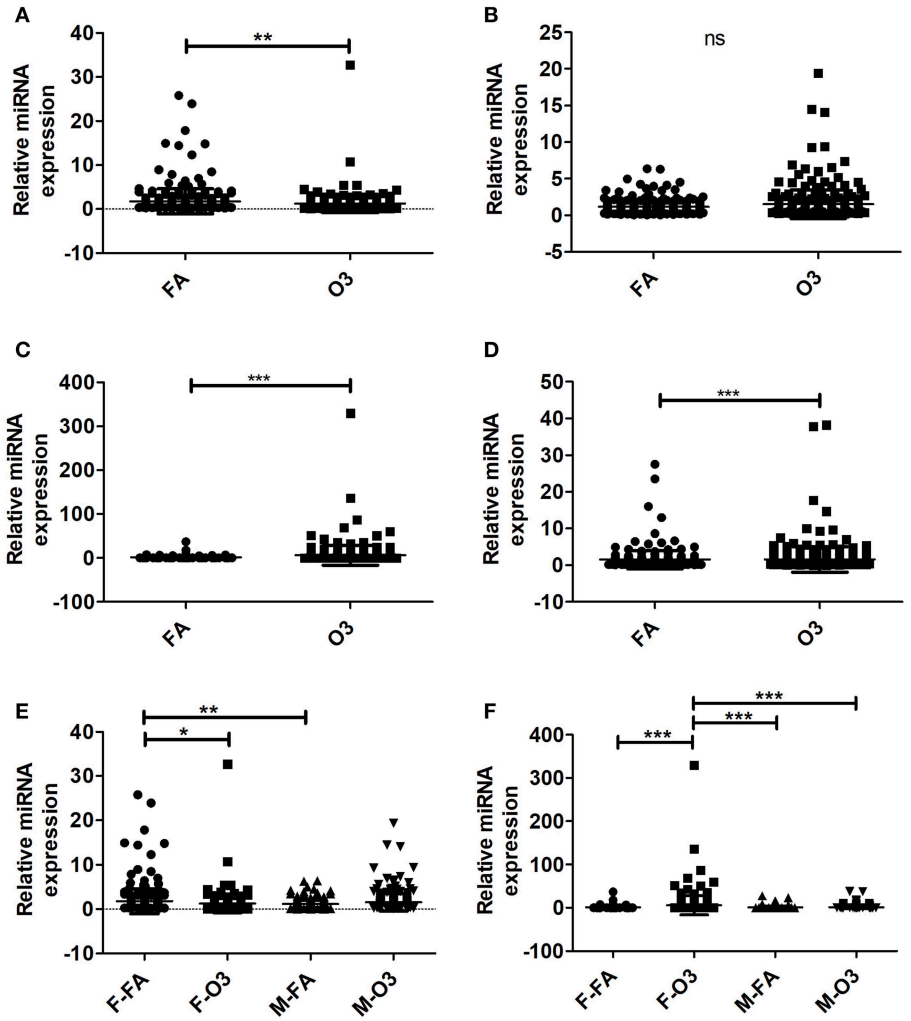

FIGURE 1 | Regulation of the AM miRNome in co-ex and KO males (M) and females (F) after Filter air (FA) and Ozone (O_3) exposure. Comparisons between miRNAs identified after FA or O_3 exposure in co-ex females **(A)**, males **(B)**, and KO females **(C)**, males **(D)**. Significant differences observed between treatment in co-ex females, KO males and females (**A,C,D**; $P < 0.05$). **(E,F)** Depict the Bonferroni multiple comparisons of the miRNAs identified after FA or O_3 exposure in co-ex and KO, respectively. A significant difference is observed in co-ex and KO females as a function of treatment **(E,F)**. Significant differences ($P < 0.05$) in miRNA regulation were observed between sexes in co-ex (F-FA vs. M-FA, **E**), and in KO (F-O_3 vs. M-O_3, F-O_3 vs. M-FA, **F**). ns, not significant. *$p < 0.05$, **$p < 0.001$, **$p < 0.0001$.

O_3 exposure (**Supplementary Table 1**). These targets include CCND1, CCND2, CCNE1, CDK7, IL-6, IL-10, TLR2, TLR3, STAT3, TNFSF12, MYD88, IL-4, IL2RG, EGR2, PTEN, MDTH, JUN, E2F3, BCL2, TNF, CDK2, MYC, SMAD2, MMP2, ARG1, AKT1, and PPARA mRNAs. The miRNAs that were changed significantly in co-ex females and males in response to O_3 exposure and their targets are listed in **Table 1**.

In general, we observed largely a downregulation of miRNAs in both males and females and upregulation of their targets in co-ex males but not in females (**Figures 4A,B**). For example, a significant downregulation of miR-191-5p, miR-155-5p, and miR-92a-3p expression was observed in response to O_3 in both co-ex males and females but their target IL-6 mRNA is upregulated in males but downregulated in females. Though most of the miRNAs are downregulated in both males and females, the expression of miR-340-5p, miR455-3p, miR-143-3p, and miR-503-5p in females, and miR1195 and miR101b-3p in males is upregulated (**Figures 4A,B**).

Validation of miRNA Target Genes

To measure the expression levels of target genes by differentially expressed miRNA in response to FA or O_3, we performed qRT-PCR analysis on AM cell samples isolated from co-ex and KO males and females after FA or O_3 exposure (**Figure 5**).

In response to OxS, the expression level of all target genes studied, with the exception of SMAD2 that remained similar in both sexes under OxS, was significantly upregulated in co-ex males compared to females (**Figure 5A**, **Supplementary Table 2**). These included CCND1, CCND2, CCNE1, CDK7, IL-6, IL-10, TLR2, TLR3, STAT3, MYD88, IL-4, IL2RG, EGR2, PTEN,

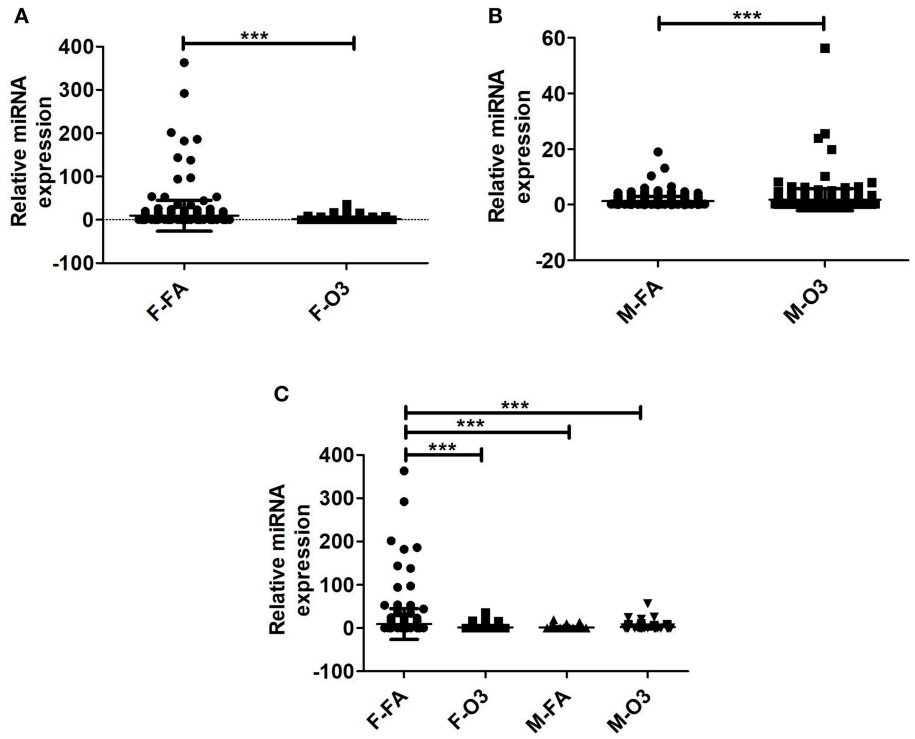

FIGURE 2 | Effect of normalization on the regulation of miRNAs. The miRNAs identified from co-ex were normalized to same miRNAs identified in KO males and females after FA or O_3 exposure. **(A,B)** Depict the differences in miRNA regulation in females and males after FA or O_3. Significant differences ($P < 0.05$) were observed in both sexes after FA or O_3 exposure **(A,B)**. **(C)** Depicts the Bonferroni multiple comparisons of the miRNAs identified after FA or O_3 exposure in co-ex. A significant difference ($P < 0.05$) was observed between co-ex FA or O_3 exposed females and between sexes in co-ex (F-FA vs. M-FA, and F-FA vs. M-O_3) **(C)**. ***$p < 0.0001$.

TNFSF12, MTDH, JUN, E2F3, BCL2, TNF, CDK2, MMP2, ARG1, AKT1, PPARA, and MYC. A similar analysis in KO males and females resulted in significant upregulation of CCND1, CCND2, CCNE1, CDK7, IL-6, TLR2, TLR3, STAT3, MYD88, PTEN, TN*F*SF12, MTDH, JUN, E2F3, TNF, CDK2, SMAD2, and AKT1 in KO males (**Figure 5B**, **Supplementary Table 2**), whereas the expression level of IL-10, MMP2, ARG1, and PPARA was significantly upregulated in KO females (**Figure 5B**). The levels of IL-4, IL2RG, EGR2, BCL2, and MYC remained similar in both sexes under OxS (**Figure 5B**).

In Summary the collective information of the significantly changed miRNAs and their targets indicate sex specific differences. Females (unlike males) largely failed to upregulate the target genes as expected when regulatory miRNAs are downregulated.

DISCUSSION

Surfactant protein-A (SP-A), is a key molecule in the lung innate immunity and surfactant related functions. The human SP-A locus consists of two functional genes, *SFTPA1* and *SFTPA2* (11, 12) and encodes two functional proteins, SP-A1 and SP-A2, respectively, and each is identified with several genetics variants (13, 14). Recently, it has been shown that SP-A1 and SP-A2 variants differ in their ability to regulate the AM miRNome in response to ozone (O_3)-induced oxidative stress (OxS) (41) as well as in lung function mechanics and survival in response to bacterial infection (42, 43). Because humans express both SP-A gene products, we wished to investigate the combined effect of co-expressed SP-A1/SP-A2 (co-ex) in response to O_3 induced OxS on AM miRNome. Toward this, human transgenic (hTG) mice, carrying both SP-A1/SP-A2 ($6A^2/1A^0$, co-ex) and SP-A-KO were exposed to filtered air (FA) and O_3 and miRNA levels were measured after AM isolation with or without normalization to KO. The observation made include, (i) Significant differences in AM miRNome of co-ex in terms of sex, exposure, with or without normalization to KO, and after Bonferroni multiple comparison analysis; (ii) After normalization with KO, both males and females showed significant differences in response to OxS; (iii) The AM miRNome of females was largely down regulated significantly in response to OxS compared to control (FA) in all comparisons made including the multiple comparison analysis; (iv) The miRNA targets were largely downregulated in females and upregulated in males; (v) Several of the mRNA targets identified of the significantly altered miRNAs in females were involved in pro-inflammatory response, anti-apoptosis, cell cycle, cellular growth and proliferation; (vi) The AM of the SP-A2 male (41) shares similarities with the co-ex, as well as differences.

We studied the AM miRNome in co-ex male and female mice that express human SP-A1/SP-A2 ($6A^2/1A^0$, co-ex)

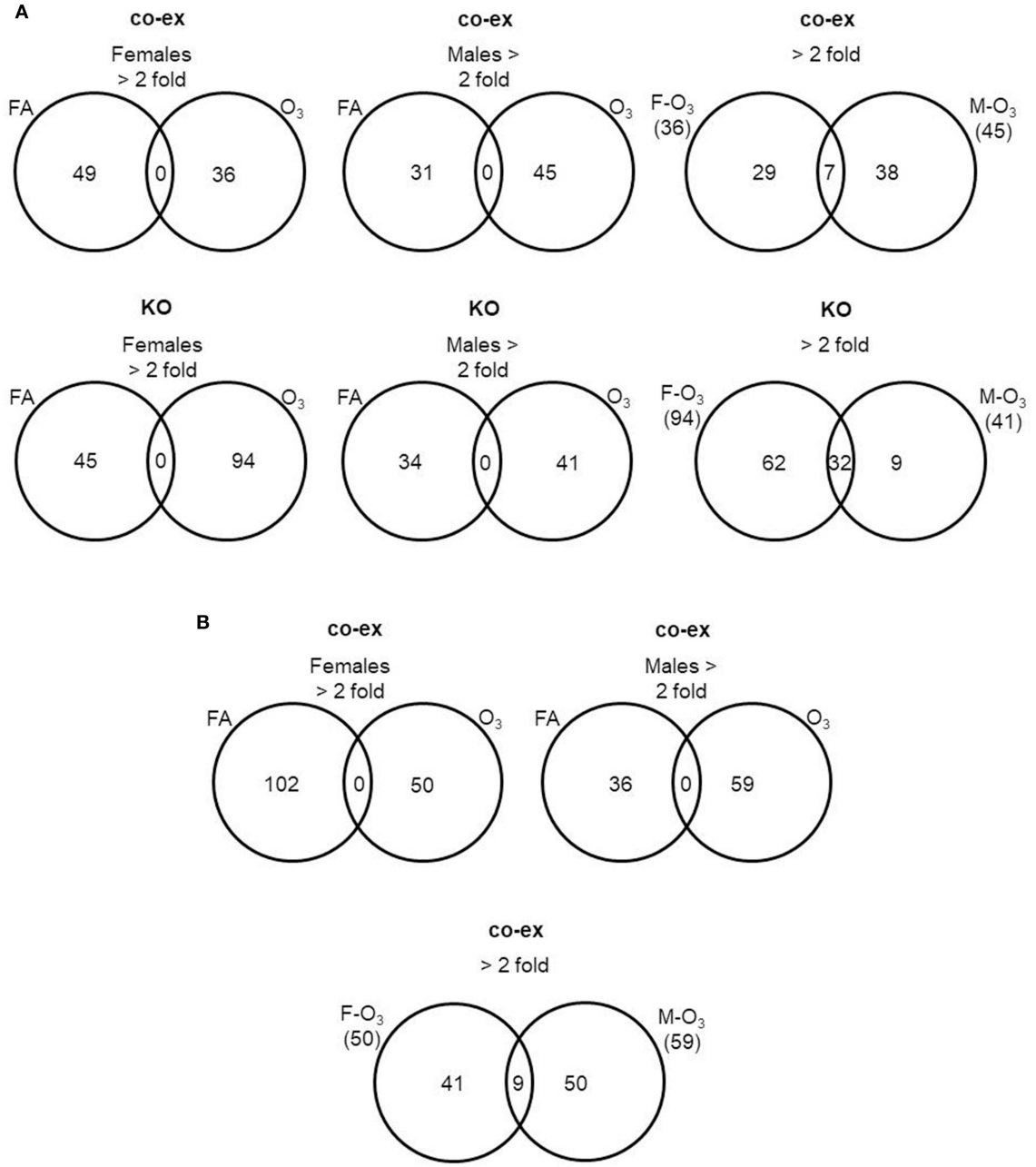

FIGURE 3 | Comparison of miRNAs affected by FA or O_3 in co-ex females and males. A. The Venn diagrams show miRNAs with significant changes ≥2 fold in response to FA or O_3 in AM of males and female co-ex and KO. Out of the 307 miRNAs identified after FA or O_3, 49 miRNAs had ≥2 fold and 36 miRNAs were ≥2 fold after FA or O_3 exposure respectively, in co-ex females and in co-ex males 31 miRNAs had ≥2 fold and 45 miRNAs were ≥2 fold after FA or O_3 exposure **(A)**. A similar comparison in KO resulted in 45 miRNAs with ≥2 fold and 94 miRNAs with ≥2 fold after FA or O_3 exposure, respectively, in KO females, and in KO males 34 miRNAs and 41 miRNAs with ≥2 fold after FA or O_3 exposure, respectively. In both co-ex and KO there were no differentially regulated miRNAs found in common after FA or O_3 exposure **(A)**. A comparison of differentially regulated miRNAs after O_3 exposure in co-ex between females and males, identified 36 miRNAs ≥2 fold in females and of these 29 were specific to females. In males 45 miRNAs ≥2 fold were identified and of these 38 were specific to males. Seven miRNAs were identified to be in common between females and males after O_3 exposure **(A)**. Whereas, in KO of the 94 miRNAs ≥2 fold in females, 62 were specific to females, and of the 41 miRNAs ≥2 fold in males, 9 were specific to males. Thirty-two miRNAs were identified to be in common between females and males after O_3 exposure **(A)**. **(B)** The Venn diagrams show the number of miRNAs identified from co-ex after normalization to the same miRNAs identified in KO males and females after FA or O_3 exposure. Out of the 307 miRNAs identified after FA or O_3, 102 miRNAs ≥2 fold and 50 miRNAs ≥2 fold were observed after FA or O_3 exposure, respectively, in co-ex females. In co-ex males, 36 miRNAs ≥2 fold and 59 miRNAs ≥2 fold were identified after FA or O_3 exposure, respectively. In both co-ex females and males, there were no differentially regulated miRNAs found in common after FA or O_3 exposure. A comparison of differentially regulated miRNAs after O_3 exposure in co-ex between females and males, identified 50 miRNAs ≥2 fold in females and of these, 41 were specific to females. In males of the 59 miRNAs ≥2 fold, 50 were specific to males and 9 miRNAs were identified to be in common between females and males after O_3 exposure.

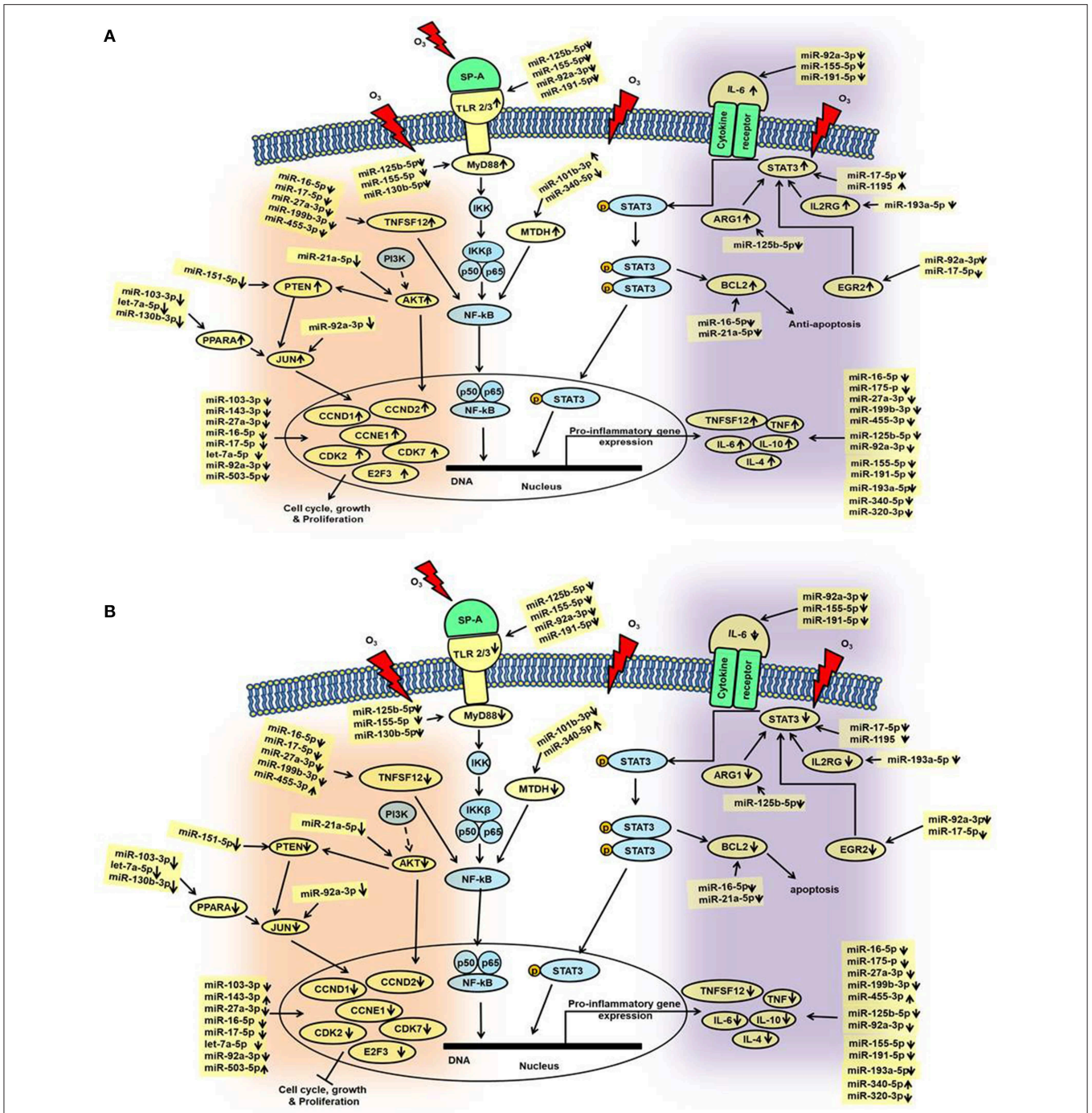

FIGURE 4 | Schematic representation of the identified miRNAs in co-ex AM and their targets in response to OxS. This diagram depicts the significantly changed miRNAs and their targets in the various pathways. These include pathways of cell cycle, and cellular growth and proliferation as well as, pathways of pro-inflammatory response and anti-apoptosis, **(A)** males and **(B)** females. The miRNAs and genes studied in the present study are highlighted with yellow. Up (↑) and down (↓) arrows indicate increase or decrease.

after O_3 exposure and compared it to that of KO mice lacking SP-A. In response to OxS, AM miRNome changes were observed in both males and females (with or without normalization to KO), although after multiple comparison analysis, AM miRNAs significantly changed only in females. Furthermore, IPA of the differentially expressed co-ex AM miRNome data identified several miRNA targets involved in the pro-inflammatory response, anti-apoptosis, cell cycle, and

TABLE 1 | Expression levels of co-ex AM miRNAs (males and females) in response to OxS and its mRNA targets identified by IPA analysis.

miRNA ID	Fold change in females	Fold change in males	Target molecule
let-7a-5p	1.089*	1.327*	CCND1, CCND2, E2F3, PPARA
miR-101b-3p	1.152*	2.338	MTDH
miR-103-3p	0.819*	0.845*	E2F3, PPARA
miR-125b-5p	1.269*	0.834*	TLR2, TNF, ARG1, MYD88
miR-143-3p	2.370	0.835*	E2F3
miR-151-5p	1.127*	1.452*	PTEN
miR-155-5p	1.248*	1.316*	IL-6, TLR2, MYD88
miR-16-5p	1.148*	1.012*	CCND1, CCNE1, CDK7, TNFSF12, E2F3, BCL2
miR-17-5p	0.959*	0.952*	CCND1, CCND2, CCNE1, CDK7, STAT3, EGR2, E2F3, MYC, TNFSF12
miR-181a-5p	0.577*	1.053*	SMAD2
miR-191-5p	1.032*	0.455*	IL-6, TLR3
miR-193a-5p	0.252*	0.856*	IL-10, IL2RG
miR-199b-3p	1.829*	0.542*	PTEN, TNFSF12
miR-21a-5p	1.739*	1.447*	BCL2, AKT
miR-27a-3p	1.053*	1.482*	E2F3
miR-340-5p	2.572	1.051*	MTDH, MYD88
miR-455-3p	2.776	0.491*	TNFSF12
miR-503-5p	2.332	0.918*	CDK2
miR-92a-3p	0.773*	0.795*	CCND1, CCNE1, CDK7, IL-6, TLR2, TLR3, EGR2, JUN, E2F3, TNF, SMAD2
miR-1195	0.797*	4.739	STAT3
miR-320-3p	0.700*	0.876*	MYD88
miR-130b-3p	0.127*	0.505*	PPARA
miR-130b-5p	0.581*	0.445*	MYD88

**Indicates downregulation.*

cellular growth and proliferation, as shown in **Figure 4** and discussed below.

Pro-inflammatory Responses

The expression of miR-191-5p, miR-155-5p and miR-92a-3p were decreased significantly in response to O_3 in both co-ex males and females (**Figures 4A,B**). These miRNAs target pro- and anti-inflammatory IL-6 cytokine (41, 65–67). The IL-6 level decreased significantly in co-ex females, whereas this increased significantly in co-ex males (**Figures 4A,B**) compared to the control mRNA (GAPDH). The latter is consistent with our previous observation with SP-A2 males in response to OxS (41).

IL-6 plays a crucial role in the activation of STAT3 (68–70). In response to OxS, STAT3 gets phosphorylated which results in the activation of genes involved in inflammation and injury (71). miR-17-5p, and miR-1195 that were significantly altered in response to OxS, are known to interact with STAT3 (**Figures 4A,B**). In co-ex females and males miR-17-5p is downregulated whereas miR-1195 is downregulated in co-ex females but upregulated in co-ex males. Although, the downregulation of these miRNAs in females should have resulted in an increase in the expression of STAT3, the opposite was observed, indicating that either the regulation of STAT3 by these (and perhaps other) miRNAs is dysfunctional or mechanisms other than miRNAs are involved. The downregulation of STAT3 in females was associated with decreased levels of TNF, TNFSF12, IL-6, IL-10, and IL-4 (**Figure 4B**). In contrast, in male co-ex, although miR-17-5p is decreased, and miR-1195 is increased, STAT3, which is target for both, is increased, as well as the levels of the pro-inflammatory cytokines were increased as one may expect. Also in males the levels of a number of target genes (ARG1, EGR2, and IL2RG) that contribute, via STAT3, to the upregulation of pro-inflammatory cytokines were upregulated. Although, the details of the underlying mechanisms are unknown currently, these data show a disconnect between miRNA expression and target gene expression in females. The emerging picture is that pro-inflammatory cytokines are downregulated in females and upregulated in males (**Figure 4A**).

Toll like receptors (TLRs) are a family of membrane bound proteins that recognize pathogen-associated molecular patterns and mediate innate immune response (72). SP-A differentially regulates TLR expression (73). We found four co-ex regulated miRNAs (miR-92a-3p, miR-125b-5p, miR-155-5p, and miR-191-5p) that target TLR2, and TLR3. The expression of these miRNAs is significantly downregulated in our study in both males and females, and this is associated with increased mRNA levels of TLR2 and TLR3 in co-ex males but a decrease in co-ex females. Both miR-125b-5p and miR-155-5p are shown in several studies to regulate TLRs (74–77). TLR2 engages the ubiquitous intracellular adaptor MyD88 (myeloid differentiation primary response 88) and TLR3 engages TRIF (TIR-domain containing adaptor protein). In the current study, the level of miR-125b-5p,

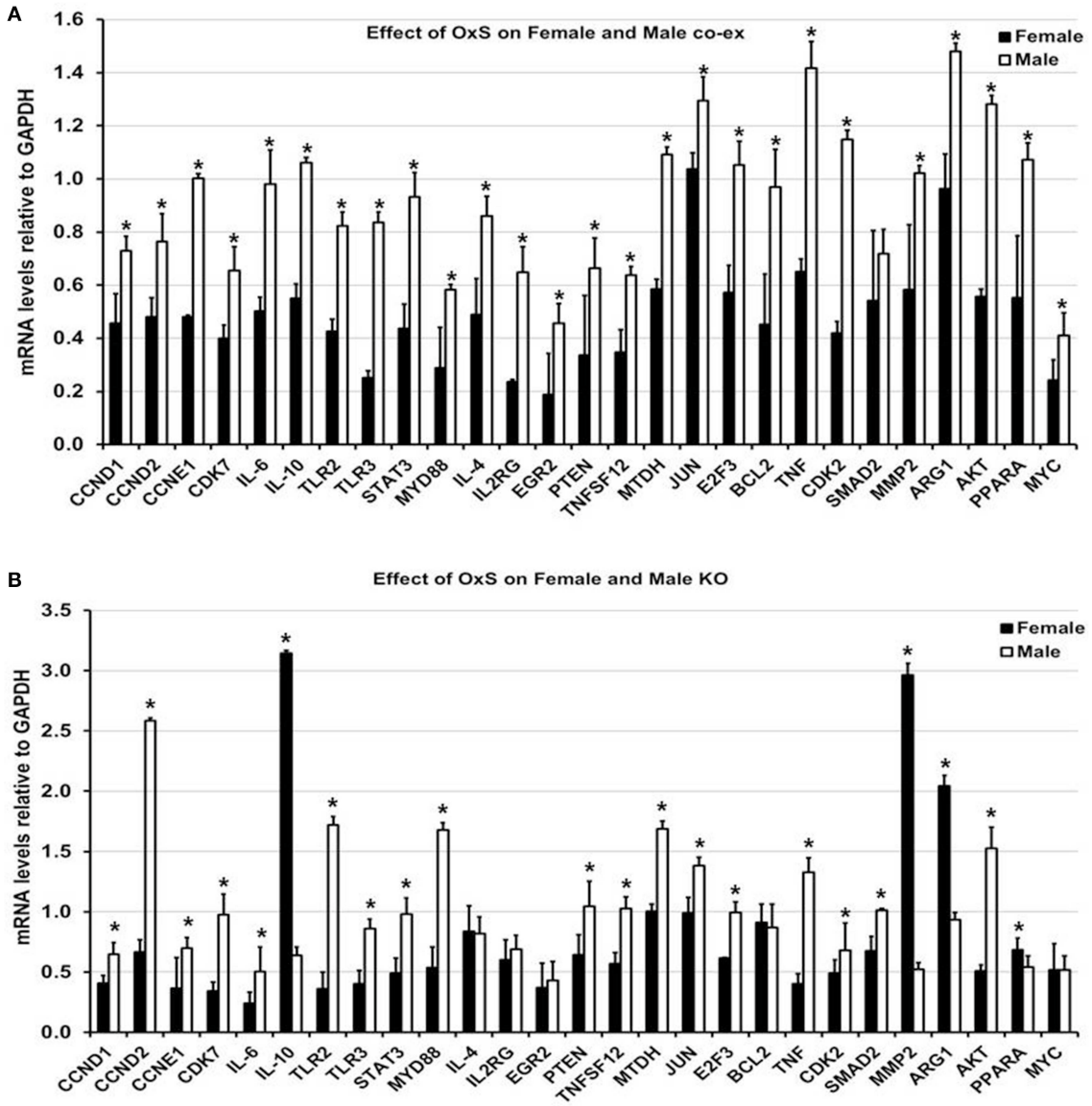

FIGURE 5 | Effect of OxS on mRNA targets of co-ex and KO. **(A)** The expression of level of CCND1, CCND2, CCNE1, CDK7, IL-6, IL-10, TLR2, TLR3, STAT3, MYD88, IL-4, IL2RG, EGR2, PTEN, TNFSF12, MTDH, JUN, E2F3, BCL2, TNF, CDK2, MMP2, ARG1, AKT1, PPARA, and MYC, were significantly upregulated in co-ex males compared to females. The level of SMAD2 did not change between males and females. The expression levels were normalized to GAPDH and significant differences ($P < 0.05$) between sexes in co-ex are noted by an asterisk (*). **(B)** Similar analysis of the above genes was performed in KO males and females. Significant upregulation was observed for CCND1, CCND2, CCNE1, CDK7, IL-6, TLR2, TLR3, STAT3, MYD88, PTEN, TNFSF12, MTDH, JUN, E2F3, TNF, CDK2, SMAD2, and AKT1 in KO males, whereas the expression levels of IL-10, MMP2, ARG1, and PPARA were significantly upregulated in KO females. The expression levels were normalized to GAPDH and the significant differences ($P < 0.05$) between sexes in KO are noted by an asterisk (*).

miR155-5p and miR130b-5 targeting MyD88 are downregulated and the mRNA level of MyD88 is upregulated in co-ex males but decreased in co-ex females. The involvement of TLR2, TLR3, and activation of MyD88 in co-ex males may result in the recruitment of other genes involved in the activation of NF-kB (78, 79), and this may result in the transcription of pro-inflammatory genes, such as TNF, TNFSF12, IL-10, and IL-4, as observed in the present study (**Figures 4A,B**). Previous studies have provided evidence that SP-A activates NF-kB (80) either through accumulation of inhibitory IkBa (81, 82) or via direct interaction with TLR2 and TLR4 (73, 80, 83–85) or SIRPα and CD91 (86). It has also been shown that, SP-A is unable to activate NF-kB in response to O_3 as assessed by the lack of changes in the nuclear p65 subunit and the cytoplasmic IkBa levels as it would have been expected in the classical NF-kB pathway (87). Moreover, it has been shown that decreased levels of MTDH expression attenuate NF-kB signaling (88) and that TNFSF12 regulates NF-kB activity (89). Upregulation of TNFSF12 and

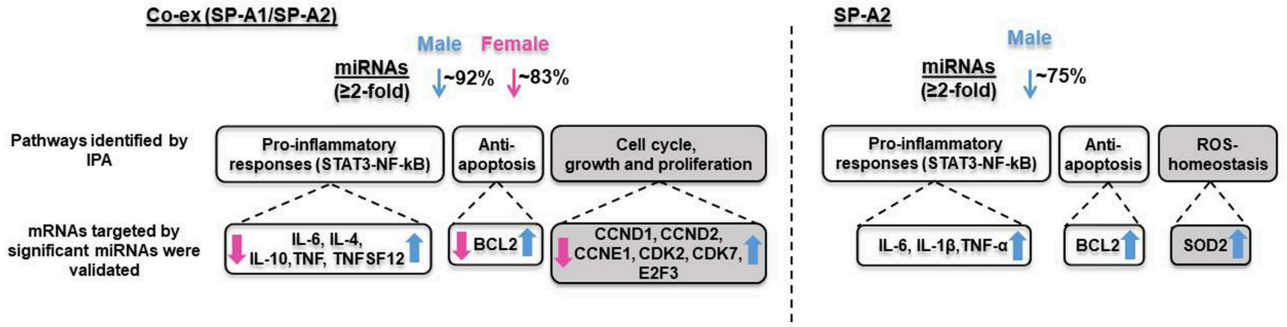

FIGURE 6 | Overview of the effect of both gene (SP-A1/SP-A2) product and of single gene product (SP-A2) on the regulation AM miRNome on both males and females, and males respectively. The diagram depicts comparison of miRNAs, target genes, and pathways after OxS in AM from mice carrying both (co-ex) SP-A1/SP-A2 variants (male and female, left, current study) and from mice carrying a single SP-A2 (male) gene variant (right) (41). The SP-A2 work has been published (41) and is used here for comparison reasons only. The significantly regulated miRNAs (23 and 11) in co-ex male and female and in SP-A2 male, respectively, in response to OxS were largely decreased (∼92% in co-ex male, ∼83% in co-ex female, and ∼75% in SP-A2 male) with the exception of few miRNAs that were increased (see **Figure 4**). All the mRNA targets were upregulated in co-ex male and in SP-A2 and are shown in blue arrow (on the right). The mRNA targets in co-ex females were downregulated and are shown in pink arrow (on the left). The pathways that differ in SP-A2 and co-ex in response to OxS are shown in gray background and those that are similar between co-ex males and SP-A2 male are shown in white background.

MTDH as it occurs in co-ex males in the current study may alter NF-kB signaling, enhance its translocation to the nucleus to facilitate the transcription of pro-inflammatory genes in co-ex males but not in females. The present data support the idea that NF-kB and STAT3-mediated pathways play a role in the pro-inflammatory gene expression in co-ex males, and that these pathways in females are compromised in response to OxS.

Anti-apoptosis, Cell Cycle, Growth, and Proliferation

The expression of two miRNAs miR-16-5p and miR-21a-5p (TargetScan) that bind BCL2 (90–93) was significantly downregulated in both males and females in response to OxS and the BCL2 mRNA levels were increased in co-ex males but decreased in females. An increase in BCL2 is likely to result in the inhibition of apoptosis and cell proliferation in males, but not in co-ex females (**Figures 4A,B**). These findings together indicate that OxS differentially affects anti-apoptotic pathways in co-ex males and females, and that females seem to have a disconnect between miRNA expression and target gene expression.

A number of miRNAs whose expression was for the most part downregulated significantly in response to OxS were predicted to target CCND1, CCND2, CCNE1, CDK2, CDK7, and E2F3 (**Figures 4A,B**). miR-16-5p and miR-17-5p, predicted to bind CCND1, CCND2, CCNE1, and E2F3 mRNAs (TargetScan), have been shown in several studies that these genes are regulated by these two miRNAs (94–97). The expression of all the target genes followed a similar pattern as described above, there was an increase in males and decrease in females. These genes are involved in cell cycle, and growth and proliferation, indicating that ozone differentially affects expression of molecules involved in cell cycle and proliferation pathways in co-ex male and female mice. Of interest significant differences in survival have been observed with females being more affected than males in several lung diseases (53–56). In our animal studies, we observed a significant difference in survival after infection and O_3 exposure. Females were more susceptible to oxidative stress than males and exhibited lower survival (7, 9). Sex hormones were shown to play a role in the observed survival differences (57).

AKT, PPARA, PTEN, and JUN involved in the MAPK pathway were significantly upregulated in co-ex males but not in females in response to OxS. The miRNAs that targeted these genes, miR-21-5p, miR-103-3p, let-7a-5p, miR-130b-3p, miR-151-5p, and miR-92-3p, were significantly downregulated in co-ex males and females (**Figures 4A,B**). The upregulation of MAPK pathway genes has the potential to regulate the genes involved in cell cycle, growth and proliferation (as shown in **Figure 4**), as well as pro-inflammatory and anti-apoptotic genes (not shown) in co-ex males but not in co-ex females in response to OxS.

We have previously studied the effect of a single, SP-A1 or SP-A2 gene, on the AM miRNome after OxS, and found that SP-A2 (but not SP-A1) had a significant impact on AM in males (41). To gain further insight into the contributions of SP-A2 vs. the co-ex on AM miRNome, we compared the data from two studies. This comparison is shown diagrammatical in **Figure 6**. A number of observations are readily evident. Broadly these show (1) the miRNAs that changed (≥2 fold) significantly in response to OxS were decreased in male SP-A2 and co-ex male and female after normalization to KO. (2) In males (SP-A2 & co-ex) the expression of all validated target genes (except SMAD2), of the significant miRNAs, identified by IPA, is increased but decreased in co-ex females. (3) The common pathways include pro-inflammatory response, and anti-apoptosis. However the SP-A2 males include ROS-homeostasis processes and the co-ex include cell cycle, growth, and proliferation processes. These data show that SP-A2 alone or in combination with SP-A1 may regulate the expression of pro-inflammatory genes via the STAT3-NF-kB pathway and anti-apoptotic genes in response

to OxS (**Figure 4A**). Furthermore, this indicated that these pathways may in part (if not in their entirety) be regulated or driven by SP-A2 and that the presence of SP-A1 does not negatively affect this. However, although SP-A1 by itself did not have any significant effect on AM, in presence of SP-A2 is shown to regulate genes involved in cell cycle, growth and proliferation, whereas SP-A2 alone regulates genes involved in homeostasis of ROS (41).

Although the data of this study are largely in line with our previous observations, the current study has a few limitations: (a) the study is carried out at single time point, (b) validation analysis was performed only for genes which are targeted by significantly changed miRNAs in co-ex males and females after normalizing to KO, and we did not look at the protein levels of the targeted mRNAs, (c) we did not study the molecular mechanisms of the identified pathways, (d) we did not differentiate the impact of varying amount SP-A1 and SP-A2 on miRNA expression in response to OxS. It has been shown that the ratio of SP-A1 to SP-A differs in lung diseases (23, 24), and this may have functional consequences given the varying activities of SP-A1 and SP-A2, (e) we did not study the impact of gonadectomy on the expression of AM miRNAs from co-ex and KO males and females. However, we have previously studied the effect of a single, SP-A1, or SP-A2 gene, on the AM miRNome after OxS, and found that SP-A2 (but not SP-A1) had a significant impact on AM in males (41). In this study, we observed that the regulation of the miRNome of the SP-A2 male mice compared to that of female mice in response to OxS is significantly altered after gonadectomy (41). It has also been shown that different stages of the estrous cycle have significant impact on the lung miRNA expression (98). In addition, a role of sex hormones on survival after *Klebsiella pneumoniae* infected wildtype (SP-A) mice with or without exposure to ozone has been observed (57). This study indicated that (1) after removal of gonadal hormones, differences in survival in animals after infection, and oxidative stress are minimized in males, and eliminated in females. (2) Treatment of gonadectomized females with DHT and males with E2 resulted in a similar kind of survival compared to the intact male and female animals, respectively. This further supports a role of DHT and E2 in survival after infection and oxidative stress. Based on these observations, we speculate that in co-ex males and females sex hormones play a significant role in the regulation of AM miRNome. However, the result of this study advances our knowledge of the differential impact of co-expressed SP-A1/SP-A2 and sex on the AM miRNome.

We postulate that in males in response to OxS, SP-A2 via its activity in ROS-homeostasis provides some protection from the injurious ROS in its microenvironment. Whereas, the co-ex males via cell cycle, growth, and proliferation process may promote cellular recovery, perhaps a more sustained recovery. We further postulate that in co-ex females the disconnect between the downregulation of miRNAs and the expression of their target genes is responsible or contributes to the reduced ability in females to enhance phagocytosis by AM as well as to the poorer survival we observed in females after OxS and infection (9). Although the details of the underlying mechanisms are unknown, the AM miRNome appears to play a significant role in OxS.

In summary, SP-A1/SP-A2 ($6A^2/1A^0$, co-ex) regulate miRNAs that play a role in pathways involved in inflammatory responses, anti-apoptosis, cell cycle, growth, and proliferation. Both gene products are needed to alleviate the deleterious effects of OxS in males and promote cellular recovery. However, in females even in the presence of both SP-A1 and SP-A2 genes, expression of target genes to mitigate the OxS injury is lacking, indicating that other hormone dependent mechanisms are involved. Because the innate immune molecules, SP-A1 and SP-A2 appear to play a differential role in the outcome of males and females after OxS, the potential impact on health of innate immune genetics should be considered separately in males and females.

DATA AVAILABILITY

The datasets generated for this study are included in the manuscript and the **Supplementary Files**, and has been deposited in the Gene Expression Omnibus repository GSE135233 (https://www.ncbi.nlm.nih.gov/geo/query/acc.cgi?&acc=GSE135233).

ETHICS STATEMENT

All protocols used in this study was evaluated and approved by the Pennsylvania State University College of Medicine Institutional Animal Care and Use Committee and Confirmed to the guidelines of the National Institute of Health on the care and use of laboratory animals.

AUTHOR CONTRIBUTIONS

NT performed experiments, run statistics, analyzed and synthesized the data, contributed to the manuscript writing. YK performed RNA sequencing analysis. CG contributed to the manuscript writing. XZ performed mouse line maintenance, breeding. JF designed the study and provided oversight to the entire project, involved in data analysis, integration, and writing of the manuscript. All authors read and approved the final manuscript.

FUNDING

This work was supported by CHILD fund, Department of Pediatrics, College of Medicine at Pennsylvania State University.

SUPPLEMENTARY MATERIAL

The Supplementary Material for this article can be found online at: https://www.frontiersin.org/articles/10.3389/fimmu.2019.01960/full#supplementary-material

Supplementary Table 1 | Identification of miRNAs from SP-A1/SP-A2 (co-ex), KO males and females in response to Filtered air or Ozone.

Supplementary Table 2 | Expression levels of target genes by differentially expressed miRNAs in response to FA or Ozone by qRT-PCR.

REFERENCES

1. Johansson J, Curstedt T. Molecular structures and interactions of pulmonary surfactant components. *Eur J Biochem*. (1997) 244:675–93. doi: 10.1111/j.1432-1033.1997.00675.x
2. Batenburg JJ, Haagsman HP. The lipids of pulmonary surfactant: dynamics and interactions with proteins. *Prog Lipid Res*. (1998) 37:235–76. doi: 10.1016/S0163-7827(98)00011-3
3. Phelps DS. Surfactant regulation of host defense function in the lung: a question of balance. *Pediatr Pathol Mol Med*. (2001) 20:269–92. doi: 10.1080/15513810109168822
4. Wright JR. Immunoregulatory functions of surfactant proteins. *Nat Rev Immunol*. (2005) 5:58–68. doi: 10.1038/nri1528
5. Bates SR, Dodia C, Tao JQ, Fisher AB. Surfactant protein-A plays an important role in lung surfactant clearance: evidence using the surfactant protein-A gene-targeted mouse. *Am J Physiol Lung Cell Mol Physiol*. (2008) 294:L325–33. doi: 10.1152/ajplung.00341.2007
6. Mason RJ, Greene K, Voelker DR. Surfactant protein A and surfactant protein D in health and disease. *Am J Physiol*. (1998) 275(1 Pt 1):L1–13. doi: 10.1152/ajplung.1998.275.1.L1
7. Mikerov AN, Gan X, Umstead TM, Miller L, Chinchilli VM, Phelps DS, et al. Sex differences in the impact of ozone on survival and alveolar macrophage function of mice after *Klebsiella pneumoniae* infection. *Respir Res*. (2008) 9:24. doi: 10.1186/1465-9921-9-24
8. Mikerov AN, Haque R, Gan X, Guo X, Phelps DS, Floros J. Ablation of SP-A has a negative impact on the susceptibility of mice to *Klebsiella pneumoniae* infection after ozone exposure: sex differences. *Respir Res*. (2008) 9:77. doi: 10.1186/1465-9921-9-77
9. Mikerov AN, Hu S, Durrani F, Gan X, Wang G, Umstead TM, et al. Impact of sex and ozone exposure on the course of pneumonia in wild type and SP-A (-/-) mice. *Microb Pathog*. (2012) 52:239–49. doi: 10.1016/j.micpath.2012.01.005
10. Mikerov AN, Phelps DS, Gan X, Umstead TM, Haque R, Wang G, et al. Effect of ozone exposure and infection on bronchoalveolar lavage: sex differences in response patterns. *Toxicol Lett*. (2014) 230:333–44. doi: 10.1016/j.toxlet.2014.04.008
11. Floros J, Hoover RR. Genetics of the hydrophilic surfactant proteins A and D. *Biochim Biophys Acta*. (1998) 1408:312–22. doi: 10.1016/S0925-4439(98)00077-5
12. Hoover RR, Floros J. Organization of the human SP-A and SP-D loci at 10q22-q23. Physical and radiation hybrid mapping reveal gene order and orientation. *Am J Respir Cell Mol Biol*. (1998) 18:353–62. doi: 10.1165/ajrcmb.18.3.3035
13. Karinch AM, Floros J. 5' splicing and allelic variants of the human pulmonary surfactant protein A genes. *Am J Respir Cell Mol Biol*. (1995) 12:77–88. doi: 10.1165/ajrcmb.12.1.7811473
14. DiAngelo S, Lin Z, Wang G, Phillips S, Ramet M, Luo J, et al. Novel, non-radioactive, simple and multiplex PCR-cRFLP methods for genotyping human SP-A and SP-D marker alleles. *Dis Markers*. (1999) 15:269–81. doi: 10.1155/1999/961430
15. Phelps DS, Floros J. Localization of surfactant protein synthesis in human lung by *in situ* hybridization. *Am Rev Respir Dis*. (1988) 137:939–42. doi: 10.1164/ajrccm/137.4.939
16. Goss KL, Kumar AR, Snyder JM. SP-A2 gene expression in human fetal lung airways. *Am J Respir Cell Mol Biol*. (1998) 19:613–21. doi: 10.1165/ajrcmb.19.4.3155
17. Saitoh H, Okayama H, Shimura S, Fushimi T, Masuda T, Shirato K. Surfactant protein A2 gene expression by human airway submucosal gland cells. *Am J Respir Cell Mol Biol*. (1998) 19:202–9. doi: 10.1165/ajrcmb.19.2.3239
18. Lin Z, deMello D, Phelps DS, Koltun WA, Page M, Floros J. Both human SP-A1 and Sp-A2 genes are expressed in small and large intestine. *Pediatr Pathol Mol Med*. (2001) 20:367–86. doi: 10.1080/15513810109168621
19. MacNeill C, Umstead TM, Phelps DS, Lin Z, Floros J, Shearer DA, et al. Surfactant protein A, an innate immune factor, is expressed in the vaginal mucosa and is present in vaginal lavage fluid. *Immunology*. (2004) 111:91–9. doi: 10.1111/j.1365-2567.2004.01782.x
20. Voss T, Eistetter H, Schafer KP, Engel J. Macromolecular organization of natural and recombinant lung surfactant protein SP 28-36. Structural homology with the complement factor C1q. *J Mol Biol*. (1988) 201:219–27. doi: 10.1016/0022-2836(88)90448-2
21. Voss T, Melchers K, Scheirle G, Schafer KP. Structural comparison of recombinant pulmonary surfactant protein SP-A derived from two human coding sequences: implications for the chain composition of natural human SP-A. *Am J Respir Cell Mol Biol*. (1991) 4:88–94. doi: 10.1165/ajrcmb/4.1.88
22. Karinch AM, deMello DE, Floros J. Effect of genotype on the levels of surfactant protein A mRNA and on the SP-A2 splice variants in adult humans. *Biochem J*. (1997) 321(Pt 1):39–47. doi: 10.1042/bj3210039
23. Tagaram HR, Wang G, Umstead TM, Mikerov AN, Thomas NJ, Graff GR, et al. Characterization of a human surfactant protein A1 (SP-A1) gene-specific antibody; SP-A1 content variation among individuals of varying age and pulmonary health. *Am J Physiol Lung Cell Mol Physiol*. (2007) 292:L1052–63. doi: 10.1152/ajplung.00249.2006
24. Wang Y, Voelker DR, Lugogo NL, Wang G, Floros J, Ingram JL, et al. Surfactant protein A is defective in abrogating inflammation in asthma. *Am J Physiol Lung Cell Mol Physiol*. (2011) 301:L598–606. doi: 10.1152/ajplung.00381.2010
25. Karinch AM, Deiter G, Ballard PL, Floros J. Regulation of expression of human SP-A1 and SP-A2 genes in fetal lung explant culture. *Biochim Biophys Acta*. (1998) 1398:192–202. doi: 10.1016/S0167-4781(98)00047-5
26. Kumar AR, Snyder JM. Differential regulation of SP-A1 and SP-A2 genes by cAMP, glucocorticoids, and insulin. *Am J Physiol*. (1998) 274(2 Pt 1):L177–185. doi: 10.1152/ajplung.1998.274.2.L177
27. Scavo LM, Ertsey R, Gao BQ. Human surfactant proteins A1 and A2 are differentially regulated during development and by soluble factors. *Am J Physiol*. (1998) 275(4 Pt 1):L653–69. doi: 10.1152/ajplung.1998.275.4.L653
28. McCormick SM, Mendelson CR. Human SP-A1 and SP-A2 genes are differentially regulated during development and by cAMP and glucocorticoids. *Am J Physiol*. (1994) 266(4 Pt 1):L367–74. doi: 10.1152/ajplung.1994.266.4.L367
29. Wang G, Phelps DS, Umstead TM, Floros J. Human SP-A protein variants derived from one or both genes stimulate TNF-alpha production in the THP-1 cell line. *Am J Physiol Lung Cell Mol Physiol*. (2000) 278:L946–54. doi: 10.1152/ajplung.2000.278.5.L946
30. Garcia-Verdugo I, Wang G, Floros J, Casals C. Structural analysis and lipid-binding properties of recombinant human surfactant protein a derived from one or both genes. *Biochemistry*. (2002) 41:14041–53. doi: 10.1021/bi026540l
31. Wang G, Umstead TM, Phelps DS, Al-Mondhiry H, Floros J. The effect of ozone exposure on the ability of human surfactant protein a variants to stimulate cytokine production. *Environ Health Perspect*. (2002) 110:79–84. doi: 10.1289/ehp.0211079
32. Oberley RE, Snyder JM. Recombinant human SP-A1 and SP-A2 proteins have different carbohydrate-binding characteristics. *Am J Physiol Lung Cell Mol Physiol*. (2003) 284:L871–881. doi: 10.1152/ajplung.00241.2002
33. Selman M, Lin HM, Montano M, Jenkins AL, Estrada A, Lin Z, et al. Surfactant protein A and B genetic variants predispose to idiopathic pulmonary fibrosis. *Hum Genet*. (2003) 113:542–50. doi: 10.1007/s00439-003-1015-4
34. Huang W, Wang G, Phelps DS, Al-Mondhiry H, Floros J. Human SP-A genetic variants and bleomycin-induced cytokine production by THP-1 cells: effect of ozone-induced SP-A oxidation. *Am J Physiol Lung Cell Mol Physiol*. (2004) 286:L546–53. doi: 10.1152/ajplung.00267.2003
35. Wang G, Bates-Kenney SR, Tao JQ, Phelps DS, Floros J. Differences in biochemical properties and in biological function between human SP-A1 and SP-A2 variants, and the impact of ozone-induced oxidation. *Biochemistry*. (2004) 43:4227–39. doi: 10.1021/bi036023i
36. Mikerov AN, Umstead TM, Huang W, Liu W, Phelps DS, Floros J. SP-A1 and SP-A2 variants differentially enhance association of *Pseudomonas aeruginosa* with rat alveolar macrophages. *Am J Physiol Lung Cell Mol Physiol*. (2005) 288:L150–158. doi: 10.1152/ajplung.00135.2004
37. Mikerov AN, Wang G, Umstead TM, Zacharatos M, Thomas NJ, Phelps DS, et al. Surfactant protein A2 (SP-A2) variants expressed in CHO cells stimulate phagocytosis of *Pseudomonas aeruginosa* more than do SP-A1 variants. *Infect Immun*. (2007) 75:1403–12. doi: 10.1128/IAI.01341-06
38. Wang G, Myers C, Mikerov A, Floros J. Effect of cysteine 85 on biochemical properties and biological function of human surfactant protein A variants. *Biochemistry*. (2007) 46:8425–35. doi: 10.1021/bi7004569
39. Wang G, Taneva S, Keough KM, Floros J. Differential effects of human SP-A1 and SP-A2 variants on phospholipid monolayers containing

surfactant protein B. *Biochim Biophys Acta.* (2007) 1768:2060–9. doi: 10.1016/j.bbamem.2007.06.025
40. Mikerov AN, Umstead TM, Gan X, Huang W, Guo X, Wang G, et al. Impact of ozone exposure on the phagocytic activity of human surfactant protein A (SP-A) and SP-A variants. *Am J Physiol Lung Cell Mol Physiol*. (2008) 294:L121–30. doi: 10.1152/ajplung.00288.2007
41. Noutsios GT, Thorenoor N, Zhang X, Phelps DS, Umstead TM, Durrani F, et al. SP-A2 contributes to miRNA-mediated sex differences in response to oxidative stress: pro-inflammatory, anti-apoptotic, and anti-oxidant pathways are involved. *Biol Sex Differ*. (2017) 8:37. doi: 10.1186/s13293-017-0158-2
42. Thorenoor N, Umstead TM, Zhang X, Phelps DS, Floros J. Survival of surfactant protein-A1 and SP-A2 transgenic mice after *Klebsiella pneumoniae* infection, exhibits sex-, gene-, and variant specific differences; treatment with surfactant protein improves survival. *Front Immunol.* (2018) 9:2404. doi: 10.3389/fimmu.2018.02404
43. Thorenoor N, Zhang X, Umstead TM, Scott Halstead E, Phelps DS, Floros J. Differential effects of innate immune variants of surfactant protein-A1 (SFTPA1) and SP-A2 (SFTPA2) in airway function after *Klebsiella pneumoniae* infection and sex differences. *Respir Res*. (2018) 19:23. doi: 10.1186/s12931-018-0723-1
44. Wang G, Guo X, Floros J. Human SP-A 3'-UTR variants mediate differential gene expression in basal levels and in response to dexamethasone. *Am J Physiol Lung Cell Mol Physiol*. (2003) 284:L738–748. doi: 10.1152/ajplung.00375.2002
45. Silveyra P, Raval M, Simmons B, Diangelo S, Wang G, Floros J. The untranslated exon B of human surfactant protein A2 mRNAs is an enhancer for transcription and translation. *Am J Physiol Lung Cell Mol Physiol.* (2011) 301:L795–803. doi: 10.1152/ajplung.00439.2010
46. Silveyra P, DiAngelo SL, Floros J. An 11-nt sequence polymorphism at the 3'UTR of human SFTPA1 and SFTPA2 gene variants differentially affect gene expression levels and miRNA regulation in cell culture. *Am J Physiol Lung Cell Mol Physiol*. (2014) 307:L106–19. doi: 10.1152/ajplung.00313.2013
47. Phelps DS, Umstead TM, Silveyra P, Hu S, Wang G, Floros J. Differences in the alveolar macrophage proteome in transgenic mice expressing human SP-A1 and SP-A2. *J Proteom Genom Res*. (2013) 1:2–26. doi: 10.14302/issn.2326-0793.jpgr-12-207
48. Phelps DS, Umstead TM, Floros J. Sex differences in the acute *in vivo* effects of different human SP-A variants on the mouse alveolar macrophage proteome. *J Proteomics*. (2014) 108:427–44. doi: 10.1016/j.jprot.2014.06.007
49. Tsotakos N, Phelps DS, Yengo CM, Chinchilli VM, Floros J. Single-cell analysis reveals differential regulation of the alveolar macrophage actin cytoskeleton by surfactant proteins A1 and A2: implications of sex and aging. *Biol Sex Differ*. (2016) 7:18. doi: 10.1186/s13293-016-0071-0
50. Lopez-Rodriguez E, Pascual A, Arroyo R, Floros J, Perez-Gil J. Human pulmonary surfactant protein SP-A1 provides maximal efficiency of lung interfacial films. *Biophys J*. (2016) 111:524–36. doi: 10.1016/j.bpj.2016.06.025
51. Al-Hegelan M, Tighe RM, Castillo C, Hollingsworth JW. Ambient ozone and pulmonary innate immunity. *Immunol Res*. (2011) 49:173–91. doi: 10.1007/s12026-010-8180-z
52. Putman E, van Golde LM, Haagsman HP. Toxic oxidant species and their impact on the pulmonary surfactant system. *Lung*. (1997) 175:75–103. doi: 10.1007/PL00007561
53. Caracta CF. Gender differences in pulmonary disease. *Mt Sinai J Med*. (2003) 70:215–24.
54. Mudway IS, Kelly FJ. An investigation of inhaled ozone dose and the magnitude of airway inflammation in healthy adults. *Am J Respir Crit Care Med*. (2004) 169:1089–95. doi: 10.1164/rccm.200309-1325PP
55. Wong CM, Thach TQ, Chau PY, Chan EK, Chung RY, Ou CQ, et al. Part 4. Interaction between air pollution and respiratory viruses: time-series study of daily mortality and hospital admissions in Hong Kong. *Res Rep Health Eff Inst*. (2010) 283–62.
56. Tam A, Churg A, Wright JL, Zhou S, Kirby M, Coxson HO, et al. Sex differences in airway remodeling in a mouse model of chronic obstructive pulmonary disease. *Am J Respir Crit Care Med*. (2016) 193:825–34. doi: 10.1164/rccm.201503-0487OC
57. Durrani F, Phelps DS, Weisz J, Silveyra P, Hu S, Mikerov AN, et al. Gonadal hormones and oxidative stress interaction differentially affects survival of male and female mice after lung *Klebsiella pneumoniae* infection. *Exp Lung Res*. (2012) 38:165–72. doi: 10.3109/01902148.2011.654045
58. Mikerov AN, Cooper TK, Wang G, Hu S, Umstead TM, Phelps DS, et al. Histopathologic evaluation of lung and extrapulmonary tissues show sex differences in *Klebsiella pneumoniae* - infected mice under different exposure conditions. *Int J Physiol Pathophysiol Pharmacol*. (2011) 3:176–90.
59. Wang G, Guo X, Diangelo S, Thomas NJ, Floros J. Humanized SFTPA1 and SFTPA2 transgenic mice reveal functional divergence of SP-A1 and SP-A2: formation of tubular myelin *in vivo* requires both gene products. *J Biol Chem*. (2010) 285:11998–2010. doi: 10.1074/jbc.M109.046243
60. Haque R, Umstead TM, Ponnuru P, Guo X, Hawgood S, Phelps DS, et al. Role of surfactant protein-A (SP-A) in lung injury in response to acute ozone exposure of SP-A deficient mice. *Toxicol Appl Pharmacol.* (2007) 220:72–82. doi: 10.1016/j.taap.2006.12.017
61. Phelps DS, Umstead TM, Floros J. Sex differences in the response of the alveolar macrophage proteome to treatment with exogenous surfactant protein-A. *Proteome Sci*. (2012) 10:44. doi: 10.1186/1477-5956-10-44
62. Vitsios DM, Enright AJ. Chimira: analysis of small RNA sequencing data and microRNA modifications. *Bioinformatics*. (2015) 31:3365–7. doi: 10.1093/bioinformatics/btv380
63. Robinson MD, McCarthy DJ, Smyth GK. edgeR: a Bioconductor package for differential expression analysis of digital gene expression data. *Bioinformatics.* (2010) 26:139–40. doi: 10.1093/bioinformatics/btp616
64. Sun J, Nishiyama T, Shimizu K, Kadota K. TCC: an R package for comparing tag count data with robust normalization strategies. *BMC Bioinformatics.* (2013) 14:219. doi: 10.1186/1471-2105-14-219
65. Scheller J, Chalaris A, Schmidt-Arras D, Rose-John S. The pro- and anti-inflammatory properties of the cytokine interleukin-6. *Biochim Biophys Acta*. (2011) 1813:878–88. doi: 10.1016/j.bbamcr.2011.01.034
66. Tufekci KU, Oner MG, Genc S, Genc K. MicroRNAs and multiple sclerosis. *Autoimmune Dis*. (2010) 2011:807426. doi: 10.4061/2011/807426
67. Migita K, Iwanaga N, Izumi Y, Kawahara C, Kumagai K, Nakamura T, et al. TNF-α-induced miR-155 regulates IL-6 signaling in rheumatoid synovial fibroblasts. *BMC Res Notes.* (2017) 10:403. doi: 10.1186/s13104-017-2715-5
68. Zhang Z, Jones S, Hagood JS, Fuentes NL, Fuller GM. STAT3 acts as a co-activator of glucocorticoid receptor signaling. *J Biol Chem*. (1997) 272:30607–10. doi: 10.1074/jbc.272.49.30607
69. Nguyen VA, Gao B. Cross-talk between alpha(1B)-adrenergic receptor (alpha(1B)AR) and interleukin-6 (IL-6) signaling pathways. Activation of alpha(1b)AR inhibits il-6-activated STAT3 in hepatic cells by a p42/44 mitogen-activated protein kinase-dependent mechanism. *J Biol Chem*. (1999) 274:35492–8. doi: 10.1074/jbc.274.50.35492
70. Miller AM, Wang H, Park O, Horiguchi N, Lafdil F, Mukhopadhyay P, et al. Anti-inflammatory and anti-apoptotic roles of endothelial cell STAT3 in alcoholic liver injury. *Alcohol Clin Exp Res*. (2010) 34:719–25. doi: 10.1111/j.1530-0277.2009.01141.x
71. Carballo M, Conde M, El Bekay R, Martin-Nieto J, Camacho MJ, Monteseirin J, et al. Oxidative stress triggers STAT3 tyrosine phosphorylation and nuclear translocation in human lymphocytes. *J Biol Chem*. (1999) 274:17580–6. doi: 10.1074/jbc.274.25.17580
72. Akira S, Takeda K. Toll-like receptor signalling. *Nat Rev Immunol*. (2004) 4:499–511. doi: 10.1038/nri1391
73. Henning LN, Azad AK, Parsa KV, Crowther JE, Tridandapani S, Schlesinger LS. Pulmonary surfactant protein A regulates TLR expression and activity in human macrophages. *J Immunol.* (2008) 180:7847–58. doi: 10.4049/jimmunol.180.12.7847
74. Ruckerl D, Jenkins SJ, Laqtom NN, Gallagher IJ, Sutherland TE, Duncan S, et al. Induction of IL-4Rα-dependent microRNAs identifies PI3K/Akt signaling as essential for IL-4-driven murine macrophage proliferation *in vivo*. *Blood.* (2012) 120:2307–16. doi: 10.1182/blood-2012-02-408252
75. Elton TS, Selemon H, Elton SM, Parinandi NL. Regulation of the MIR155 host gene in physiological and pathological processes. *Gene*. (2013) 532:1–12. doi: 10.1016/j.gene.2012.12.009
76. Hu X, Ye J, Qin A, Zou H, Shao H, Qian K. Both microRNA-155 and virus-encoded MiR-155 ortholog regulate TLR3 expression. *PLoS ONE.* (2015) 10:e0126012. doi: 10.1371/journal.pone.0126012
77. Arboleda JF, Fernandez GJ, Urcuqui-Inchima S. Vitamin D-mediated attenuation of miR-155 in human macrophages infected with dengue virus: implications for the cytokine response. *Infect Genet Evol*. (2019) 69:12–21. doi: 10.1016/j.meegid.2018.12.033

78. Tak PP, Firestein GS. NF-κB: a key role in inflammatory diseases. *J Clin Invest*. (2001) 107:7–11. doi: 10.1172/JCI11830
79. Lim R, Barker G, Lappas M. TLR2, TLR3 and TLR5 regulation of pro-inflammatory and pro-labour mediators in human primary myometrial cells. *J Reprod Immunol*. (2017) 122:28–36. doi: 10.1016/j.jri.2017.08.004
80. Koptides M, Umstead TM, Floros J, Phelps DS. Surfactant protein A activates NF-kappa B in the THP-1 monocytic cell line. *Am J Physiol.* (1997) 273(2 Pt 1):L382–8. doi: 10.1152/ajplung.1997.273.2.L382
81. Wu Y, Adam S, Hamann L, Heine H, Ulmer AJ, Buwitt-Beckmann U, et al. Accumulation of inhibitory κB-α as a mechanism contributing to the anti-inflammatory effects of surfactant protein-A. *Am J Respir Cell Mol Biol*. (2004) 31:587–94. doi: 10.1165/rcmb.2004-0003OC
82. Moulakakis C, Adam S, Seitzer U, Schromm AB, Leitges M, Stamme C. Surfactant protein A activation of atypical protein kinase C zeta in IκB-α-dependent anti-inflammatory immune regulation. *J Immunol*. (2007) 179:4480–91. doi: 10.4049/jimmunol.179.7.4480
83. Guillot L, Balloy V, McCormack FX, Golenbock DT, Chignard M, Si-Tahar M. Cutting edge: the immunostimulatory activity of the lung surfactant protein-A involves Toll-like receptor 4. *J Immunol*. (2002) 168:5989–92. doi: 10.4049/jimmunol.168.12.5989
84. Konishi M, Nishitani C, Mitsuzawa H, Shimizu T, Sano H, Harimaya A, et al. Alloiococcus otitidis is a ligand for collectins and Toll-like receptor 2, and its phagocytosis is enhanced by collectins. *Eur J Immunol*. (2006) 36:1527–36. doi: 10.1002/eji.200535542
85. Yamada C, Sano H, Shimizu T, Mitsuzawa H, Nishitani C, Himi T, et al. Surfactant protein A directly interacts with TLR4 and MD-2 and regulates inflammatory cellular response. Importance of supratrimeric oligomerization. *J Biol Chem*. (2006) 281:21771–80. doi: 10.1074/jbc.M513041200
86. Gardai SJ, Xiao YQ, Dickinson M, Nick JA, Voelker DR, Greene KE, et al. By binding SIRPalpha or calreticulin/CD91, lung collectins act as dual function surveillance molecules to suppress or enhance inflammation. *Cell*. (2003) 115:13–23. doi: 10.1016/S0092-8674(03)00758-X
87. Janic B, Umstead TM, Phelps DS, Floros J. Modulatory effects of ozone on THP-1 cells in response to SP-A stimulation. *Am J Physiol Lung Cell Mol Physiol*. (2005) 288:L317–325. doi: 10.1152/ajplung.00125.2004
88. Jiao Y, Yang H, Qian J, Gong Y, Liu H, Wu S, et al. miR36645P suppresses the proliferation and metastasis of gastric cancer by attenuating the NFκB signaling pathway through targeting MTDH. *Int J Oncol*. (2019) 54:845–58. doi: 10.3892/ijo.2019.4680
89. Zhu C, Zhang L, Liu Z, Li C, Bai Y. TWEAK/Fn14 interaction induces proliferation and migration in human airway smooth muscle cells via activating the NF-κB pathway. *J Cell Biochem*. (2018) 119:3528–36. doi: 10.1002/jcb.26525
90. Cimmino A, Calin GA, Fabbri M, Iorio MV, Ferracin M, Shimizu M, et al. miR-15 and miR-16 induce apoptosis by targeting BCL2. *Proc Natl Acad Sci USA*. (2005) 102:13944–9. doi: 10.1073/pnas.0506654102
91. Shen J, Wan R, Hu G, Yang L, Xiong J, Wang F, et al. miR-15b and miR-16 induce the apoptosis of rat activated pancreatic stellate cells by targeting Bcl-2 *in vitro*. *Pancreatology*. (2012) 12:91–9. doi: 10.1016/j.pan.2012.02.008
92. Jia X, Ouyang H, Abdalla BA, Xu H, Nie Q, Zhang X. miR-16 controls myoblast proliferation and apoptosis through directly suppressing Bcl2 and FOXO1 activities. *Biochim Biophys Acta Gene Regul Mech*. (2017) 1860:674–84. doi: 10.1016/j.bbagrm.2017.02.010
93. Yang Y, Hu Z, Du X, Davies H, Huo X, Fang M. miR-16 and fluoxetine both reverse autophagic and apoptotic change in chronic unpredictable mild stress model rats. *Front Neurosci*. (2017) 11:428. doi: 10.3389/fnins.2017.00428
94. Yu Z, Wang C, Wang M, Li Z, Casimiro MC, Liu M, et al. A cyclin D1/microRNA 17/20 regulatory feedback loop in control of breast cancer cell proliferation. *J Cell Biol*. (2008) 182:509–17. doi: 10.1083/jcb.200801079
95. Attar M, Arefian E, Nabiuni M, Adegani FJ, Bakhtiari SH, Karimi Z, et al. MicroRNA 17-92 expressed by a transposone-based vector changes expression level of cell-cycle-related genes. *Cell Biol Int*. (2012) 36:1005–12. doi: 10.1042/CBI20110089
96. Shu J, Xia Z, Li L, Liang ET, Slipek N, Shen D, et al. Dose-dependent differential mRNA target selection and regulation by let-7a-7f and miR-17-92 cluster microRNAs. *RNA Biol*. (2012) 9:1275–87. doi: 10.4161/rna.21998
97. Wang F, Mao A, Tang J, Zhang Q, Yan J, Wang Y, et al. microRNA-16-5p enhances radiosensitivity through modulating Cyclin D1/E1-pRb-E2F1 pathway in prostate cancer cells. *J Cell Physiol*. (2018) 234:13182–90. doi: 10.1002/jcp.27989
98. Fuentes N, Roy A, Mishra V, Cabello N, Silveyra P. Sex-specific microRNA expression networks in an acute mouse model of ozone-induced lung inflammation. *Biol Sex Differ*. (2018) 9:18. doi: 10.1186/s13293-018-0177-7

Conflict of Interest Statement: The authors declare that the research was conducted in the absence of any commercial or financial relationships that could be construed as a potential conflict of interest.

frontiers in Immunology

ORIGINAL RESEARCH
published: 26 March 2019
doi: 10.3389/fimmu.2019.00561

Differential Effects of Human SP-A1 and SP-A2 on the BAL Proteome and Signaling Pathways in Response to *Klebsiella pneumoniae* and Ozone Exposure

Guirong Wang[1,2]*, *Todd M. Umstead*[1], *Sanmei Hu*[1], *Anatoly N. Mikerov*[1], *David S. Phelps*[1] *and Joanna Floros*[1,3]*

[1] Department of Pediatrics, Center for Host defense, Inflammation, and Lung Disease (CHILD) Research, The Pennsylvania State University College of Medicine, Hershey, PA, United States, [2] Department of Surgery, SUNY Upstate Medical University, Syracuse, NY, United States, [3] Department of Obstetrics and Gynecology, The Pennsylvania State University College of Medicine, Hershey, PA, United States

Surfactant protein A (SP-A) plays critical roles in host defense, regulation of inflammation and surfactant metabolism in the lung. The human SP-A locus consists of two functional genes, *SFTPA1* and *SFTPA2* encoding surfactant proteins SP-A1 and SP-A2, respectively. Structural and functional differences exist between SP-A1 and SP-A2 *in vitro* and *in vivo*. Ozone is a major air pollutant with a negative impact on many biological processes. In this study we used humanized transgenic (hTG) SP-A1 and SP-A2 mice, and SP-A KO mice to study *in vivo* effects of SP-A1 and SP-A2 on the bronchoalveolar lavage (BAL) proteomic profile and associated signaling pathways in response to ozone or filtered air (FA) exposure and *Klebsiella pneumoniae* infection. The BAL samples were harvested 24 h after ozone (2 ppm for 3 h) or FA exposure and infection and analyzed by two-dimensional difference gel electrophoresis (2D-DIGE) and MALDI-ToF/ToF. We found: that (1) Ozone exposure, but not infection, is a major factor for increases in total BAL protein content. (2) A total of 36 proteins were identified, accounting for 89.62% of the BAL proteins resolved by the 2D-DIGE system. (3) The number of proteins in which levels were altered more than 25% following infection and FA exposure was: SP-A2 > SP-A1 > KO for male mice, and SP-A2 ≈ SP-A1 > KO for female mice. (4) The number of proteins with more than 25% increase/decrease after ozone exposure and infection was: SP-A2 > SP-A1 ≈ KO, with the majority being increases in male mice and decreases in female mice. (5) Eleven out of the 36 proteins, including annexin A5, glutathione S-transferase A4, SP-A1/SP-A2, and 14-3-3 zeta protein, exhibited significant differences among SP-A genotypes. The acute phase response (APR) that includes the NF-kB signaling pathway plays a critical role, followed by Nrf2-mediated oxidative response, and others. These associated with SP-A genotype, sex, and ozone-induced oxidative stress in response to infection. We concluded that human SP-A2 and SP-A1 exhibit differential genotype-and sex-dependent innate immune responses to microbial pathogens and/or ozone-induced oxidative stress by modulating proteomic patterns and signaling pathways in the lung.

Keywords: humanized transgenic mice, innate immunity, oxidative stress, proteomic profile, surfactant protein A (SP-A), signaling pathway

OPEN ACCESS

Edited by:
Taruna Madan,
National Institute for Research in Reproductive Health (ICMR), India

Reviewed by:
Kenneth Reid,
University of Oxford, United Kingdom
Poonam Gautam,
National Institute of Pathology (ICMR), India

***Correspondence:**
Guirong Wang
wangg@upstate.edu
Joanna Floros
jfloros@pennstatehealth.psu.edu

Specialty section:
This article was submitted to Molecular Innate Immunity, a section of the journal Frontiers in Immunology

Received: *29 December 2018*
Accepted: *04 March 2019*
Published: *26 March 2019*

Citation:
Wang G, Umstead TM, Hu S, Mikerov AN, Phelps DS and Floros J (2019) Differential Effects of Human SP-A1 and SP-A2 on the BAL Proteome and Signaling Pathways in Response to Klebsiella pneumoniae and Ozone Exposure. Front. Immunol. 10:561. doi: 10.3389/fimmu.2019.00561

INTRODUCTION

Surfactant protein A (SP-A) is a surfactant-associated protein that plays an important role in innate host defense, regulation of inflammation, and surfactant-related physiology in lung (1, 2). SP-A is a member of the C-type lectin (collectin) protein family. Each monomer consists of four domains, N-terminal region, collagen-like domain, neck domain, and carbohydrate-recognition domain (CRD). Native SP-A from bronchoalveolar lavage (BAL) is thought to consist primarily of octadecamers with six SP-A trimers. The literature from SP-A knockout (KO) mouse research revealed that SP-A is a critical factor for host defense (3–7), surfactant metabolism (8, 9), surfactant large-aggregate structure and tubular myelin formation (10–12) in the lung, and survival after infection (13, 14).

The human SP-A locus consists of two functional genes, *SFTPA1* and *SFTPA2* encoding SP-A1 and SP-A2, respectively, plus a pseudogene and is located on chromosome 10q22-23 (15, 16). Each of the functional genes has been characterized and several genetic variants for each gene have been identified. The SP-A1 variants (6A, $6A^2$, $6A^3$, $6A^4$) and the SP-A2 variants (1A, $1A^0$, $1A^1$, $1A^2$, $1A^3$, $1A^5$) are the most frequently found variants in the population (17, 18). Human SP-A is expressed in alveolar epithelial type II cells (19), as well as in other tissues (20–22). SP-A2 expression has been observed in tracheal and bronchial submucosal gland cells in the lung (23, 24). SP-A1 or SP-A2 genetic variants have been associated with several human pulmonary diseases (25). Structural and functional differences between SP-A1 and SP-A2 and among *in vitro* expressed SP-A genetic variants have been observed using several different approaches (26–37). SP-A2 for the most part appeared to exhibit higher activity in terms of its ability to enhance phagocytosis by alveolar macrophages (29, 31–33), enhance cytokine production by a macrophage-like cell line (27, 30, 38), and inhibit surfactant secretion by alveolar epithelial type II cells (28). Moreover, SP-A1 and SP-A2 differentially enhance aggregation of LPS and phospholipid monolayer formation (26, 35). In a study of humanized transgenic (hTG) mice the function of SP-A1 and SP-A2 was shown to have diverged in terms of tubular myelin (TM) formation, an extracellular form of pulmonary surfactant (39). Recently, *in vivo* functional differences between SP-A1 and SP-A2 genetic variants were observed in the regulation of alveolar macrophage actin cytoskeleton (40), the alveolar macrophage proteome (37, 41), the alveolar macrophage microRNAome (42), pulmonary mechanics (43) and bacterial-induced mortality (44). However, in a recent study SP-A1 was found to more efficiently affect surfactant structural organization compared to SP-A2 (36).

Ozone is one of the major air pollutants that can have a negative impact on a variety of biological processes including inflammation, increased airway reactivity, and an increased susceptibility to lung infection in humans (45–49). Ozone exposure can affect innate immunity, epithelial integrity, impair phagocytosis, and compromise mucociliary clearance (45, 50), and therefore can modulate risk for many respiratory diseases including asthma (47). Furthermore, a large population study demonstrated a significant increase in the risk of death from respiratory causes, with an increase of ozone concentration (51). Differences among individuals in ozone-induced symptoms have also been observed and polymorphisms in genes related to oxidative stress may underlie these differences Ozone-exposure has shown to have a negative impact on SP-A function (52). Differential effects on the function of SP-A1 and SP-A2 *in vitro* (28, 30, 33, 38) and *in vivo* (42, 52) have been observed.

In the present study we used gel-based proteomic analysis as a discovery tool to study potential molecular mechanisms, Specifically we used the 2D-DIGE proteomic approach along with MALDI-ToF/ToF to analyze global changes of proteins in lung BAL fluid to study the BAL proteome in hTG mice, each carrying an SP-A1 or SP-A2 variant, in response to *K. pneumoniae* infection and in the presence or absence of ozone.

MATERIALS AND METHODS

Animals

We have generated and characterized hTG SP-A1 ($6A^4$) and SP-A2 ($1A^3$) mice on the SP-A −/− (KO) C57BL/6 genetic background (39). These mice express human SP-A1 or SP-A2 and secrete it into BAL fluid. In this study, we used these hTG SP-A1 and SP-A2 mice, as well as SP-A KO C57BL/6 mice from the same litters as controls. The mice used in these experiments were 10–12 weeks old and ∼25 g in body weight. The mice were bred and maintained under pathogen-free conditions and fed rodent chow and tap water *ad libitum* in the animal core facility. This study was approved by the Institutional Animal Care and Use Committee at the Pennsylvania State University College of Medicine.

Bacterial Strain

Klebsiella pneumoniae bacteria (ATCC 43816) were purchased from the American Tissue Culture Collection (Rockville, MD). Bacteria were cultured in 250 ml flasks with 50 ml of 3% tryptic soy broth (TSB) for 18 h at 37°C with shaking at 100 rpm. The bacterial culture was diluted in TSB to obtain an OD_{660} of 0.4 and then 200 μl of the diluted bacterial suspension was added to 50 ml of TSB medium and shaken for 3 h to reach mid-log phase of growth (OD_{660} ∼0.4, corresponding to $\sim 2 \times 10^8$ CFU/ml). Bacteria were placed on ice to stop their growth and then serially diluted in PBS to obtain $\sim 9 \times 10^3$ CFU/ml. Mice were infected by the intratracheal instillation of 50 μl of the suspension with ∼450 CFU/mouse.

Experimental Design and Mouse Model

A total of forty-eight 10–12 week old mice (8 male and 8 female hTG SP-A1mice, 8 male and 8 female hTG SP-A2 mice, and 8 male and 8 female SP-A KO mice) were divided into 12 groups with 4 animals per group (**Table 1**).

Mice were exposed to either 2 parts/million (ppm) ozone or to filtered air (FA) for 3 h as described previously (13, 53). In brief, four mice were put into a glass exposure vessel with stainless steel wire mesh lids and then placed in a closed glass exposure chamber. Exposures to FA were conducted in parallel at room temperature and 50% humidity using the ozone exposure system as described previously (50, 53, 54). After FA

TABLE 1 | Experimental design.

Mouse genotype	Male		Female	
	FA + infection	O_3 + infection	FA + infection	O_3 + infection
SP-A1 ($6A^4$)	SP-A1M_FA	SP-A1M_O_3	SP-A1F_FA	SP-A1F_O_3
SP-A2 ($1A^3$)	SP-A2M_FA	SP-A2M_O_3	SP-A2F_FA	SP-A2F_O_3
SP-A KO	KOM_FA	KOM_O_3	KOF_FA	KOF_O_3

Four mice were used in each of the 12 groups.

or ozone exposure, the mice were immediately infected with *K. pneumoniae* bacteria. This was done by anesthetizing the mice, surgically exposing the trachea, and instilling 50 μl of bacterial suspension. The mice were sacrificed 24 h after infection by anesthetizing them with an intramuscular injection of a 40 μl mixture of Ketamine/HCl a (Ketaset, Fort Dodge Animal Health, IO) and Xylazine (XYLA-JECT, Phoenix Pharmaceuticals Inc., St. Joseph, MO) and exsanguination. The lungs were lavaged with normal saline.

Cell Counts and Total Protein Assessment in BAL

BAL was obtained by instilling 0.6 ml of saline into the lungs three times through a tracheal cannula using a volume equal to 80% of lung vital capacity (for a total of 1.5 ml). Total BAL fluid recovery was ∼90% of the instilled volume and did not differ significantly between experimental groups. The BAL was centrifuged (150 × g, 10 min, 4°C) and the cell pellet was resuspended in saline (0.9% sodium chloride). Total cell counts were performed using a hemocytometer and cytocentrifuge (Cytospin) preparations were used to obtain differential cell counts. The cell-free BAL supernatant was frozen at −80°C for subsequent proteomic studies. Total protein concentrations in BAL were determined using the Bio-Rad protein assay (Bio-Rad, Hercules, CA).

TCA/Acetone Precipitation

One volume of ice cold 100% trichloroacetic acid (TCA) was added to four volumes of BAL, mixed and incubated overnight at 4°C. Following overnight incubation, samples were centrifuged (15,000 × g, 15 min, 4°C) and the protein pellets washed with 250 μl of chilled acetone, centrifuged again, and resuspended in a minimum volume of standard cell lysis buffer (30 mM Tris-HCl, 2 M thiourea, 7 M urea, 4% CHAPS, pH 8.5). The concentration of protein was adjusted to 2 mg/ml for CyDye labeling.

2D-DIGE Labeling (Minimal Labeling) and Electrophoresis for 2D-DIGE

Information about the 2D-DIGE is provided in a form that complies with the most recent version <http://www.psidev.info/sites/default/files/MIAPE_GE_1_4.pdf> of Minimum Information About a Proteomics Experiment—Gel Electrophoresis (MIAPE-GE) standards developed by the Human Proteome Organization Proteomics Standards Initiative (55) (**Supplemental File 1**). 2D-DIGE has been widely used to study the proteomic profiles (37, 41, 50, 54, 56–59). The methods of 2D-DIGE labeling and electrophoresis for 2D-DIGE used in this study have been described in previous publications (37, 41, 50, 54, 56, 59, 60).

For preparative (picking) gels an aliquot of 500 μg of sample was diluted with an equal volume of 2X sample buffer (2 M thiourea, 7 M urea, 2% IPG buffer (pH 4–7) and 1.2% DeStreak reagent) and then brought up to a volume of 450 μl with rehydration buffer (DeStreak™ Rehydration Solution and 0.5% IPG buffer (pH 4–7). Proteins were focused using the following voltages and times: 14 h at 0 V (passive rehydration); 6 h at 30 V (active rehydration); 3 h at 300 V (step and hold); 3 h at 600 V (gradient); 3 h at 1,000 V (gradient); 3 h at 8,000 V (gradient); 4 h at 8,000 V (step and hold). Each of the strips was equilibrated as described above and applied to a 10% polyacrylamide preparative picking gel (26 cm-w × 20 cm-h × 1 mm thick). After the completion of electrophoresis the preparative picking gels were stained with Deep Purple Total Protein Stain (GE, Healthcare) as described (50, 56, 60).

Gel Scanning and Image Analysis

Information about the acquisition and processing of data from the 2D-DIGE studies are provided in the form that complies with the most recent version of the guidelines established for Minimum Information about a Proteomics Experiment—Gel Informatics (MIAPE-GI) developed by the Human Proteome Organization Proteomics Standards Initiative http://www.psidev.info/sites/default/files/MIAPE_GE_1_4.pdf (**Supplemental File 2**). 2D-gels were scanned as described previously (50, 56, 60).

Gel images were imported into the Progenesis SameSpots v3.0 (Nonlinear Dynamics, Durham, NC) for analysis as described previously (50, 60). Gel alignment was conducted automatically and then checked manually to ensure correct alignment. A reference gel with minimum distortion and streaks was then selected from the Cy2 gels. Detection and matching of protein spots across all the gels was conducted automatically, then manually checked and edited to ensure correct matching, merging, and splitting of spots. All the included spots were transported to Progenesis PG240 module of the Progenesis SameSpots v3.0 software. Quantization of spots was accomplished by comparing the ratio of each Cy3 and Cy5 value to the values obtained from the normalization pool/Cy2 channel present on each gel.

Protein Identification by Mass Spectrometry

To identify specific proteins we collected spots from the preparative picking gel. We digested the gel pieces with trypsin and then eluted the digested peptides from the gel and analyzed them by MALDI-ToF/ToF as described previously (50, 56, 60). Peptides were analyzed by MALDI-ToF/ToF in the Mass Spectrometry Core at the Penn State University College of Medicine. A total of 5 μl of ZipTip cleaned samples (1 μl at a time) was applied onto a 384-well MALDI plate (Opti-TOF™ 384 Well Insert, Applied Biosystems, Foster City, CA) and then 0.7 μl of 2 mg/ml ACH cinnamic acid in 73:27 (acetonitrile:water) was then spotted on each well containing peptide. All 13 calibration

wells on the MALDI plate were spotted with (1:12 diluted) 4700 calibrant. Autolytic trypsin peptides were also used to internally calibrate the spectra to an accuracy of 20 ppm. Peptides were then analyzed by MALDI-ToF/ToF mass spectrometry using a 4800 Proteomics Analyzer (Applied Biosystems), calibrated with Applied Biosystems 4700 Proteomics Calibration Mix. Using GPS Explorer 3.0 software (Applied Biosystems), the MS and MS/MS data were submitted to a MASCOT (v2.0.00) search engine for identification. The NCBI nonredundant database with the *Mus musculus* taxonomy and a concatenated, reversed "decoy" version were used for the searches with a mass accuracy of 50 ppm, 1 missed trypsin cleavage, fixed carbamidomethylation of cysteine residues and variable oxidation of methionine residues. A protein was considered identified if the MASCOT confidence interval was >95th percentile and those proteins with a MASCOT confidence interval <95% were excluded from the subsequent analyses.

The PANTHER database and the scientific literature were used to assign molecular function and biological process to each identified protein. As in our previous publications (37, 41, 50, 56, 59–61), we assigned the identified proteins to three broad functional groups in this study: (1) host defense proteins (DEF); (2) proteins involved in redox metabolism and balance (RED); (3) proteins involved in protein metabolism and modification (PMM). It should be noted that some proteins are involved in multiple functional groups in this study. In addition, the Ingenuity Pathway Analysis program (Ingenuity Systems, Redwood City, CA) was used to analyze the identified proteins and their changes between different types of mice in order to gain additional insight into the functional significance and the signaling pathway(s) involved.

Determination of NRF2 Levels in the Lungs of Ozone-Exposed Mice

In a separate study, C57BL/6J mice were exposed to 2 PPM of ozone for either 1, 2, or 3 h with 0, 1, 2, or 3 h of recovery time after ozone. Lungs were then harvested and nuclear and cytoplasmic extracts were prepared using Thermo Scientific NE-PER Nuclear and Cytoplasmic Extraction Reagents and following the manufacturer's instructions. Ten micrograms of each extract were then separated by SDS-PAGE and the proteins transferred to nitrocellulose for detection and quantitation of NRF2 levels by Western ECL and densitometry.

Statistical Analysis

Initial statistical analysis was performed in Progenesis SameSpots v3.0 by Student's *t*-test to confirm the level of significance among various groups. For identified proteins having multiple isoforms, the normalized volumes of all isoforms of a given protein were added together and statistical analysis was repeated on the totals. In the following analysis, all the data were expressed as mean ± SEM and analyzed by one-way analysis of variance or student's *t* test using the standard program software SigmaStat (version 3.5, SPSS). Differences were considered statistically significant at $p < 0.05$.

RESULTS

As stated in the section of Materials and Methods (**Table 1**), all mice in this study were infected with *K. pneumoniae*. Three types of mice used are: (1) hTG SP-A2 ($1A^3$); (2) hTG SP-A1 ($6A^4$) mice; (3) SP-A KO mice. Equal numbers of males and females were used in this study. Mice were sacrificed 24 h after bacterial infection.

Cell Counts and Total Protein Concentrations in the BAL

Total cell and differential cell counts in the BAL of each group with varying genotypes, sex, and exposure conditions are listed in **Table 2**. The data indicate significant differences between FA-exposed and ozone-exposed KO or hTG SP-A2 mice of both sexes. Typically there was a two- to three-fold increase in the ozone-exposed mice. Differences were less pronounced and not significantly different between FA- and ozone-exposed hTG SP-A1 mice of both sexes. Much of the increase in all markers was likely due to an influx of neutrophils, ranging from 14.4 to 37.8% in FA-exposed mice, and from 63.8 to 79.3% in ozone-exposed animals (**Table 2**). While some of this increase is due to the effect of ozone (53), most of it is probably due to the *K. pneumoniae* infection (56). There were no significant differences in the percentages of neutrophils or macrophages between male and female mice of each genotype and under both exposure conditions.

We also determined the total protein concentration in the BAL of each group. The data from male and female mice of each genotype showed no remarkable differences, therefore, the data from male and female mice of each group were combined in this analysis. The results (**Figure 1**) indicated that total protein concentration of each ozone-exposed group was significantly higher (approximately three times) than that of the corresponding FA-exposed group ($p < 0.01$). These levels, and the ozone-induced increases, are consistent with observations we have published previously (53) indicating that these are largely a consequence of the ozone exposure rather

TABLE 2 | Total cells and its composition from mouse BAL.

Mouse genotype/sex/ treatment	Cell counts (x10^4)	% of Macrophage		% of Neutraphil	
	Mean ± *SD*	Mean	*SD*	Mean	*SD*
SP-A1_M_FA	14.62 ± 6.65	62.2	29.1	37.8	29.1
SP-A1_M_O3	23.31 ± 5.5	36.2	30.9	63.8	30.9
SP-A1_F_FA	15.43 ± 15.5	75.1	26.2	24.5	26.5
SP-A1_F_O3	18.75 ± 5.3	31.8	11.4	67.8	11.3
SP-A2_M_FA	6.81 ± 2.9	57.0	45.6	14.4	15.0
SP-A2_M_O3	21.43 ± 9.8	25.3	19.0	74.7	19.0
SP-A2_F_FA	8.18 ± 3.1	69.8	21.7	30.2	21.7
SP-A2_F_O3	21.43 ± 5.1	26.1	11.2	73.8	11.2
KO_M_FA	10.87 ± 4.6	77.3	30.6	22.7	30.6
KO_M_O3	31.87 ± 7.1	26.5	5.6	73.5	5.6
KO_F_FA	9.31 ± 3.4	80.1	10.3	19.9	10.3
KO_F_O3	31.56 ± 15.6	20.8	16.8	79.3	16.8

than the infection. There were no significant differences among the three types of mice of FA-exposed groups, or among the ozone-exposed groups. To better understand the effect of ozone-induced increase of total proteins in BAL, three additional groups, which were not used for other analyses of this study, were used as controls. These were hTG SP-A1 mice with exposure to either ozone (SP-A1_O_3_Saline) or FA (SP-A1_FA_Saline), in which 50 μl of saline were instilled instead of the bacterial suspension, as well as SP-A KO mice without any treatment. These results demonstrate that ozone exposure of mice was the major factor influencing the total protein concentration of the BAL under the present experimental conditions.

Protein Identification of BAL by 2D-DIGE Analysis of hTG and KO Mice

BAL samples of the 12 experimental groups were subjected to 2D-DIGE and analyzed with Progenesis SameSpots. For 2D-DIGE analysis, BAL samples were labeled with Cy3 or Cy5 dye. A normalization pool consisting of equal aliquots of all samples was labeled with Cy2. Samples were separated by isoelectric focusing (pH 4–7) and then 10% PAGE-gel electrophoresis (2-D) as described in the Materials and Methods. A total of 36 proteins from 201 spots were identified by MALDI-ToF/ToF in this study (**Table 3**). The 36 identified proteins accounted for 89.62% of BAL proteins resolved in our gel system. **Figure 2** shows a reference gel in which the 36 identified proteins are circled and numbered. In the case of proteins consisting of multiple isoforms, positive identification by MALDI-ToF/TOF was made on each isoform and statistical analysis was done on the sum of all isoforms. All identified proteins are shown in **Table 3**.

To gain insight into the changes in protein levels, the identified proteins ($n = 36$) were assigned into three broad functional groups as described previously (37, 41, 50, 54, 56, 59–61). One group contained proteins ($n = 24$) involved in defense and immunity functions (DEF), including proteins playing roles in host defense, regulation of inflammatory processes, and other immune processes. The second group consisted of proteins ($n = 15$) playing a role in the regulation of redox balance in the lung (RED). These proteins are involved in the generation of reactive oxygen and nitrogen species (RONS), neutralization of RONS, or are proteins that bind molecules such as iron, copper, and heme. The third group consisted of proteins ($n = 20$) that we broadly categorized as being involved in protein metabolism and modification (PMM), including a number of proteases and antiproteases, several chaperones, proteins involved in molecular signal, and transportation processes (**Table 3**). It should be noted that many of the proteins studied have been assigned into more than one of the three groups because these proteins play roles in multiple biological processes. To perform 2D-DIGE, the same amount of protein from each sample was loaded

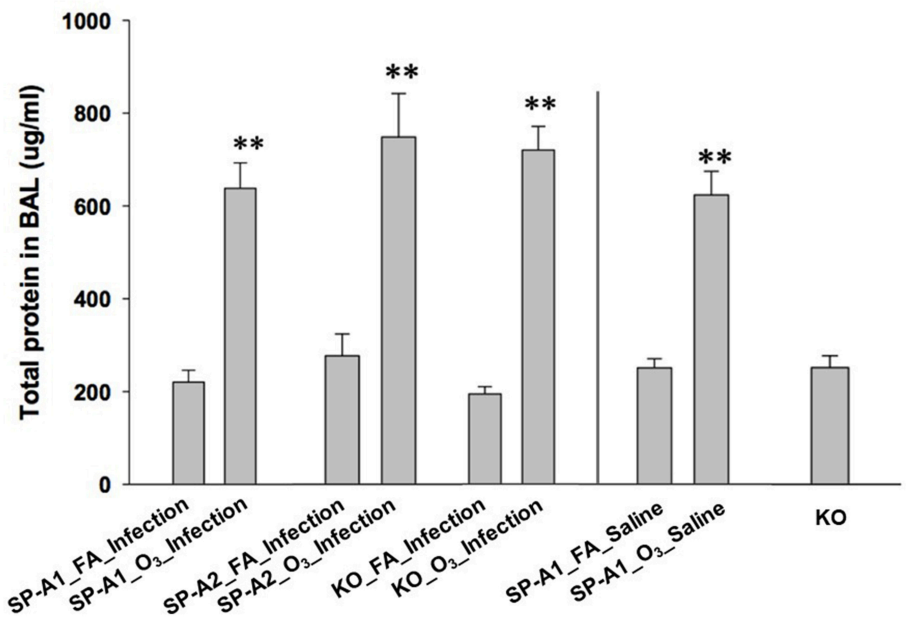

FIGURE 1 | Comparison of total protein concentration in the BAL fluid from exposed and infected mice. Three genotypes of mice (hTG SP-A1 and SP-A2 mice and SP-A KO mice) were exposed to ozone (3 ppm) or filtered air for 3 h and then intratracheally infected with 50 μl of bacterial solution (containing about 450 CFU of *K. pneumoniae*, control with 50 μl of saline). After 24 h of infection the mice were sacrificed and the lungs were subjected to BAL. Total protein concentration was determined in the supernatant of BAL. The results indicate that the total protein level of ozone-exposed mice, regardless of bacterial infection or saline control was significantly higher than that of FA-exposed mice (**$p < 0.01$). No significant difference is found among FA-exposed mouse groups regardless of infection or saline control, or among ozone-exposed mouse groups regardless of infection or saline control. In addition, no significant differences in total protein level in the BAL fluid are observed between KO background control and FA-exposed mice regardless of infection or saline control (The experimental groups and controls were separated by a vertical line).

TABLE 3 | List of identified proteins.

No.	Protein ID	Gene symbol	Accession No.	Functional group
1	(Similar to) Glutathione S-transferase A1	Gsta1	P13745	RED, DEF
2	14-3-3 zeta protein	Ywhaz	P63101	DEF, RED, PMM
3	Albumin	Alb1	P07724	RED
4	Annexin A3	Anxa3	Q3UCL0	DEF
5	Annexin A5	Anxa5	P48036	DEF
6	Ceruloplasmin	Cp	Q61147	RED
7	Complement C5	C5	P06684	DEF
8	Complement component 3	C3	Q80XP1	DEF
9	Cytosolic malate dehydrogenase	Mdh1	P14152	RED
10	Esterase 1	Es1	P23953	DEF
11	Gamma-actin	Actg1	P63260	PMM
12	Gelsolin	Gsn	P13020	DEF, RED, PMM
13	Glutathione S transferase, omega 1	Gsto1	O09131	DEF, RED
14	Glutathione S-transferase A4	Gsta4	P24472	DEF, RED
15	Haptoglobin	Hp	Q60574	DEF, RED
16	Heat shock protein 5	Hspa5	P20029	DEF, PMM
17	Heat shock protein, 1A	Hsp90aa1	Q80Y52	DEF, PMM
18	Hemopexin	Hpxn	Q8K1U6	RED
19	Kininogen 1	Kng1	O08677	DEF, PMM
20	Kpnb1 protein	Kpnb1	Q99KM9	PMM
21	Lactate dehydrogenase 2	Ldhb	P16125	RED, DEF
22	Murinoglobulin-1	Mug1	P28665	PMM, DEF
23	Peroxiredoxin 6	Prdx6	Q6GT24	RED, DEF
24	Pregnancy zone protein	Pzp	Q61838	PMM, DEF
25	Pulmonary surfactant-associated protein A (SP-A)	sftpa1	P35242	DEF, RED
26	Rho GDP dissociation inhibitor (GDI) alpha	Arhgdia	Q99PT1	PMM
27	SEC 14-like 3	Sec14l3	Q5SQ27	PMM
28	Selenium binding protein	Selenbp1	P17563	DEF, RED
29	Serine protease inhibitor, A1a	Serpina1a	P07758	DEF, PMM
30	Serine protease inhibitor, A1c	Serpina1c	Q00896	PMM
31	Serine protease inhibitor, A3k	Serpina3k	P07759	PMM
32	Serine protease inhibitor, A1e	Serpina1e	Q00898	PMM
33	Serine protease inhibitor, A1	Serpina1	P26595	DEF, PMM
34	Serine protease inhibitor (antithrombin III), C1	Serpinc1	P32261	PMM
35	Serum amyloid P-component	Apcs	P12246	DEF, PMM
36	Transferrin	Trf	Q921I1	PMM, RED, DEF

on gels. However, because total BAL protein concentration was about 3 times higher in ozone-exposed mice than in FA-exposed mice, in order to have the same amount of protein from both FA- and ozone-exposed samples on gels we loaded a much smaller fraction of the total amount of BAL from the ozone-exposed samples on each gel. To compensate for this we corrected all values for normalized volumes of all spots so that they represented the quantity of each protein spot in the total amount of BAL. These corrected normalized volumes, representing a constant proportion of the total BAL in both ozone-exposed and FA-exposed mice, were used for all subsequent analyses.

Comparisons of BAL Proteomic Profiles of SP-A Genotypes in Response to FA or Ozone

This study included three experimental variables, e.g., SP-A genotype (SP-A1 or SP-A2), sex (male or female), and exposure (FA or ozone). To compare the influence of each genotype on the BAL proteomic profile 12 group comparisons were studied (**Table 1S**). The effect of each genotype in these comparisons was studied by examining the 6 male (first set) and 6 female (second set) comparisons separately. The percent change of each of the 36 identified proteins between two samples was calculated with the following formula. For example, to compare sample A to sample B, the % change $= 100 \times$ (the average content of A—the average content of B)/the average content of B. The % change of each of the 36 identified proteins, as well as significant difference between groups ($p < 0.05$) are shown in **Table 1S**. In addition, according to suggestions from previous publications (62, 63), a 25% protein content change (increase or decrease) was used as a threshold, because this is one of the criteria used for defining acute-phase response proteins. Therefore, the 25% change (increase or decrease) was used as a threshold in the subsequent analysis.

Infected Male Mice After Exposure to FA or Ozone

Comparison of FA-exposed and infected SP-A1 or SP-A2 vs. KO male mice

Based on **Tables 1S**, **2S**, when compared to KO male mice, out of the 36 identified proteins, 15 proteins (42%) in SP-A1 male mice and 30 proteins (83%) in SP-A2 male mice, exhibited marked increases (% change >25%; pink highlighting). In addition, three proteins (i.e., Annexin A5, Glutathione S-transferase A4, and serum amyloid p-component) in SP-A1 male mice and complement component 3 in SP-A2 male mice were markedly decreased (% change > −25%; green highlighting) compared to KO male mice.

Comparison of ozone-exposed and infected SP-A1 or SP-A2 vs. KO male mice

In the comparison between infected SP-A1 and KO male mice and in response to ozone, only haptoglobin (no comparison of SP-A was done due to a lack of SP-A expression in KO mice) showed a pronounced increase of 33.6%, but the 14-3-3 zeta protein and the pregnancy zone protein exhibited a decrease by 31 and 26.1%, respectively (**Table 1S**). However, with ozone

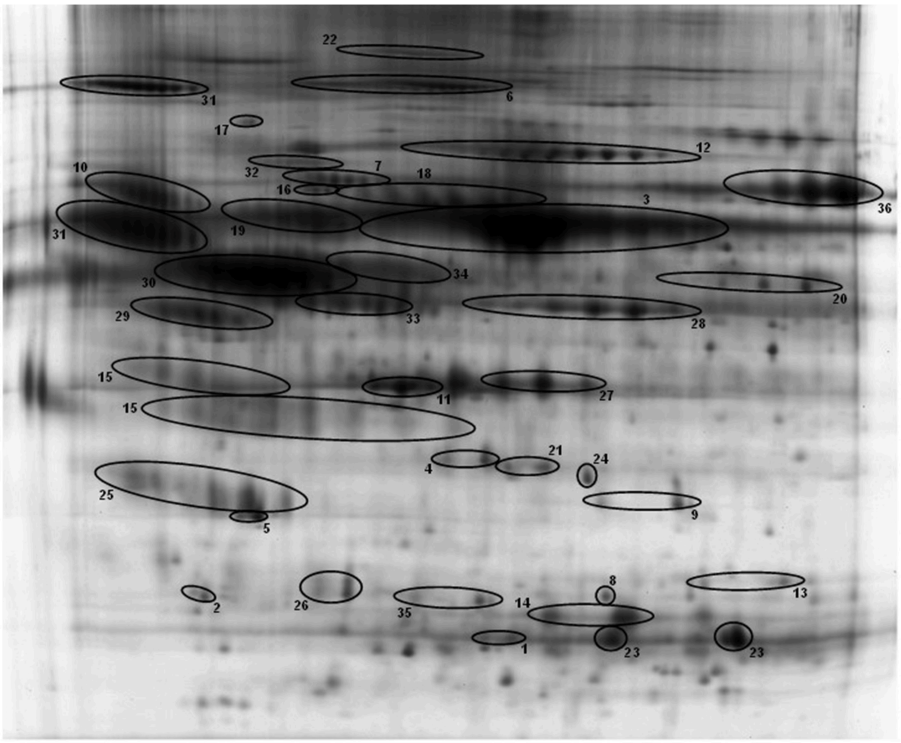

FIGURE 2 | A representative reference gel with identified proteins. Protein spots identified by MALDI-ToF/ToF are circled and numbered, and the names of all the proteins and the corresponding numbers are given in **Table 3**. Many proteins have multiple isoforms in the 2-D gel and all isoforms of these proteins are identified and confirmed by MALDI-ToF/ToF.

exposure, infected SP-A2 male mice exhibited marked increases in 16 (44%) of the 36 proteins compared with infected KO male mice, with 13 of the 16 proteins being in the host defense and immunity category (DEF) (**Tables 1S–3S**).

Comparison between FA- and ozone-exposed and infected SP-A2 and SP-A1 male mice

The results showed that 18 out of the 36 proteins exhibited increases between infected SP-A2M_FA vs. SP-A1M_FA mice (**Table 1S**), of which 12 of the 18 proteins were involved in host defense and immunity (**Table 2S**). With ozone exposure, more than half of the proteins (19 of the 36 proteins) showed increases, but one protein (hemopexin) showed a decrease by 27.7% between infected SP-A2M_O_3 vs. SP-A1M_ O_3 mice. Thirteen of the increased proteins were also found in the 18 increased proteins in FA exposure and in the 19 increased proteins in ozone exposure, indicating that the observed changes are primarily due to infection and not to ozone exposure. These findings indicate that the SP-A2 (compared to SP-A1) male mice directly or indirectly regulate levels of many proteins in response to FA and ozone.

Infected Female Mice After Exposure to FA or Ozone

Fewer differences in the BAL proteomic profile among SP-A genotypes in infected female mice were observed in response to FA or ozone.

Comparison of FA- and ozone-exposed and infected SP-A1 or SP-A2 vs. KO female mice

Of the 35 proteins (excluding SP-A due to its absence in KO mice), 14 (40%) proteins and 13 (37%) proteins in FA-exposed and infected SP-A1 and SP-A2 female mice, respectively, showed profound increases compared to KO female mice (data shown in the second set of **Table 1S**). However, if exposed to ozone, of the 35 proteins, 4 and 12 proteins in infected SP-A1 and SP-A2 mice, respectively, showed marked decreases, and only two proteins (annexin A5 with increase of 145.3% and glutathione S-transferase A4 with increase of 55.3%) in infected SP-A2 female mice were expressed at higher levels than infected KO female mice. These indicate that the infected SP-A2 female mice are profoundly affected and more responsive to ozone exposure than the infected SP-A1 female mice.

Comparison of FA- or ozone exposed and infected SP-A2 and SP-A1 female mice

The results demonstrated that out of the total 36 proteins, 4 (11%) proteins (annexin A5, heat shock protein 1A, Kpnb1 protein, and SP-A) with marked increase and 4 (11%) proteins (glutathione S-transferase A1, 14-3-3 zeta protein, glutathione S-transferase A4, and Sec14-like 3) with marked decrease in infected SP-A2 female mice compared to infected SP-A1 female mice exposed to FA (**Tables 1S**, **2S**). If exposed to ozone, infected SP-A2 female mice showed increases in 3 proteins (annexin

A5, glutathione S-transferase A4, and SP-A), and decreases in 5 proteins (complement component 3, heat shock protein 1A, Kpnb1 protein, murinoglobulin-1, and Serpin A1 compared to infected SP-A1 female mice (**Tables 1S**, **2S**).

Specific Proteins With Significant Differences in SP-A Genotypes

Several of the 36 identified proteins exhibited statistically significant differences in the level of protein expression in several comparisons in SP-A genotypes. It should be noted that comparisons between ozone-exposed to FA-exposed infected mice were excluded because of about two thirds of the 36 proteins were found to be significantly different between ozone-exposed and FA-exposed mice. Below we focus on comparisons of infected males and females, exposed to FA or to ozone.

Statistically significant differences were observed primarily in males with only two protein changes in female mice (i.e., SP-A level between SP-A1F_FA and SP-A2F_FA, and haptoglobin level between SP-A1F_O_3 and KOF_O_3) (**Figure 3**). In male mice, three specific proteins exhibited significant differences in at least two of the 6 comparisons (**Figure 4**). These proteins include annexin A5, 14-3-3 zeta protein, and glutathione S-transferase A4. These are involved in host defense (annexin A5, 14-3-3 zeta protein, and glutathione S-transferase A4), redox balance (glutathione S-transferase A4), and protein metabolism (14-3-3 zeta protein) in lung physiology and pathophysiology (64).

Proteins with significant differences in male mice after ozone exposure that are found only in one comparison out of 6 comparisons made are shown in **Figure 5**, and include SP-A, (similar to) glutathione S-transferase A1, glutathione S-transferase, omega 1, and Rho GDP dissociation inhibitor, alpha. As stated in the introduction, SP-A plays a critical role in host defense, regulation of inflammation, homeostasis, and anti-oxidative damage in lung (1, 65). Ozone-exposed SP-A2 mice had higher level of glutathione S-transferase A1 than ozone-exposed KO mice and had higher levels of glutathione S-transferase, omega 1, and Rho GDP dissociation inhibitor, alpha, than ozone-exposed SP-A1 male mice. Thus, the SP-A2 mice in response to ozone not only express a higher level of SP-A protein compared to SP-A1 mice (**Figure 5A**), but they appear to directly or indirectly regulate/influence the expression of other proteins (also see **Figure 4**). Of interest, SP-A content in SP-A1 and SP-A2 male mice in response to a single insult (infection) is the same, but in response to a double insult (infection and ozone exposure) the SP-A content in the SP-A2 mice is significantly higher ($p < 0.05$) than that in SP-A1 mice (**Figure 5A**). On the other hand, in female FA infected SP-A2 mice the SP-A content is significantly increased ($p < 0.05$) by 137.3% compared to SP-A1 female mice, but no differences were observed in SP-A levels between SP-A1 and SP-A2 female mice after ozone exposure (**Figure 3B**). In addition, four proteins (complement C5, haptoglobin, hemopexin, and lactate dehydrogenase 2) exhibited small but significant changes in FA-exposed SP-A1 mice compared to FA-exposed KO male mice (**Figure 6**).

Signaling Pathways Associated With Ozone Exposure and Infection

To explore signaling pathways involved in this experimental model the 36 identified proteins were analyzed with the Ingenuity Pathway Analysis program. The results indicate that 11 proteins (albumin, ceruloplasmin, complement C5, complement component 3, haptoglobin, hemopexin, Serine protease inhibitor A1, Serine protease inhibitor A1c, Serine protease inhibitor A1e, serum amyloid P-component, transferrin) of the 36 proteins are related to the acute phase response (APR) signaling pathway (p-value = 4.17E-11), in which most of them were associated with the ERK1/2 and NF-IL6 signaling pathways (**Figure 7**). Most of the 11 proteins found with a marked change in the present study were members of the NF-IL6 pathway. For example, the comparison between SP-A2M_FA and KOM_FA (shown in **Figure 7**), revealed that 8 (ceruloplasmin, haptoglobin, hemopexin, serine protease inhibitor A1, serine protease inhibitor A1c, serine protease inhibitor A1e, serum amyloid P-component, transferrin) of the 11 proteins increased more than 25% (marked in red) and one (complement component 3) decreased more than 25% (marked in green); the other two (marked in gray) exhibited <25% change. As shown in **Figure 7** the three proteins encoded by serine protease inhibitor A1, serine protease inhibitor A1c, serine protease inhibitor A1e are shown together as "SERPINA1." The differences in the levels of protein expression of the 11 proteins between SP-A2 and KO male mice provide evidence that the SP-A2 protein could regulate/influence the expression of other proteins that are involved in the APR signaling pathway, specifically in the ERK1/2 and NF-IL6 pathways in this experimental model.

The SP-A1M_FA vs. KOM_FA comparison revealed a similar number of proteins with changed levels (>25%) (8 in the SP-A1 comparison vs. 9 in the SP-A2 comparison described above). Six of the changing proteins; ceruloplasmin, haptoglobin, hemopexin, serine protease inhibitor A1c, serine protease inhibitor A1e, and transferrin were the same between the SP-A1M_FA and SP-A2M_FA, when each of them was compared to KOM_FA. All showed a similar trend (either increase or decrease) with the exception of serum amyloid P-component which was decreased in the SP-A1M_FA and increased in the SP-A2_FA. However, in FA-exposed females of either genotype or in response to ozone a considerably fewer number of proteins in the APR pathway exhibited changes (>25%) for FA: SP-A1 $n = 1$ (albumin with increase); SP-A2 $n = 1$ (haptoglobin with decrease); for ozone: SP-A1 $n = 1$ (complement C5 with decrease); SP-A2 $n = 3$ (all decreases of complement component 3, haptoglobin, and serine protease inhibitor A1c). The results indicate that the role of SP-A genotype in response to bacterial infection and FA or ozone exposure may be through the APR (ERK1/2 and NF-IL6) signaling pathway, especially for males in response to infection and FA exposure.

Furthermore, four additional pathways were identified to be related to the BAL protein changes although only a few proteins were associated with these pathways. These include the Nrf2-mediated oxidative stress response pathway (p-value = 3.98E-4) with 4 changed proteins (gamma-actin, glutathione S-transferase A1, glutathione S transferase, omega 1, and glutathione

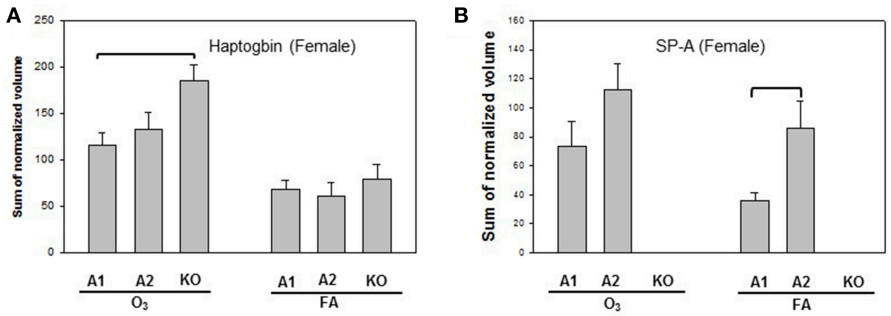

FIGURE 3 | Representative graphs of significant protein changes among genotypes in female mice. Two proteins (haptoglobin and SP-A) exhibit significant differences in comparisons among SP-A genotypes of female mice after exposure to ozone (O_3) or filtered air (FA). Histograms depicting levels of each specific protein are shown in **(A)** (Haptoglobin) and **(B)** (SP-A). Comparisons between groups that were statistically significant ($p < 0.05$) are indicated with a bracket.

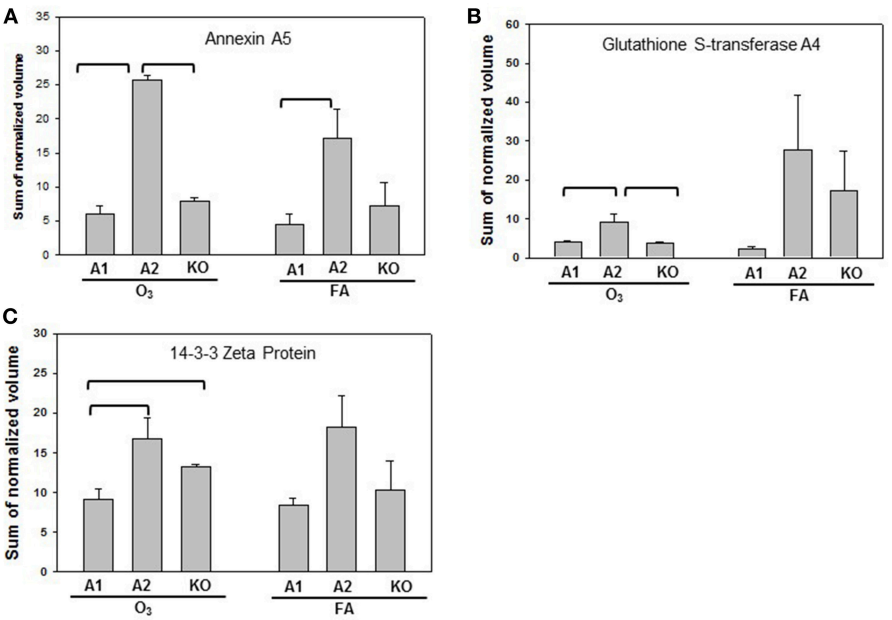

FIGURE 4 | Representative graphs of significant protein changes among genotypes in male mice. The proteins shown exhibit significant differences in at least 2 group comparisons among genotypes of male mice [SP-A1 (A1), SP-A2(A2), KO] after exposure to O_3 or filtered air (FA) following bacterial infection. Histograms depicting levels of each specific protein includes: **(A)** annexin A5; **(B)** glutathione S-transferase A4; **(C)** 14-3-3 zeta protein. Comparisons between groups that were statistically significant ($p < 0.05$) are indicated with a bracket.

S-transferase A4), the glutathione metabolism pathway (p-value = 2.2E-5) with 3 changed proteins (glutathione S-transferase A1, glutathione S transferase, omega 1, and glutathione S-transferase A4), the aryl hydrocarbon receptor signaling pathway (p-value = 1.81E-4) with 4 proteins (heat shock protein 1A, glutathione S-transferase A1, glutathione S transferase, omega 1, and glutathione S-transferase A4), and the xenobiotic metabolism signaling pathway (p-value = 2.47E-4) with 5 proteins (heat shock protein 5, glutathione S-transferase A1, glutathione S transferase, omega 1, and glutathione S-transferase A4, esterase 1). The three members (glutathione S-transferase A1, glutathione S transferase, omega 1, and glutathione S-transferase A4) of the glutathione S-transferase family were determined to be associated with all the identified pathways. We observed differences in the levels of expression of several members of glutathione S-transferase family in several comparisons among SP-A genotypes, indicating that there may be an important effect of the SP-A genotype on the activation of these in response to bacterial infection and FA/ozone exposure.

Experimental Confirmation of Nrf2 Signaling Activation

Nrf2 has been identified as an important pathway in proteomics studies of this study, as well as previous studies (41, 59, 61), where the alveolar macrophage proteome in hTG SP-A1 and SP-A2 mice was studied in response to ozone-induced oxidative

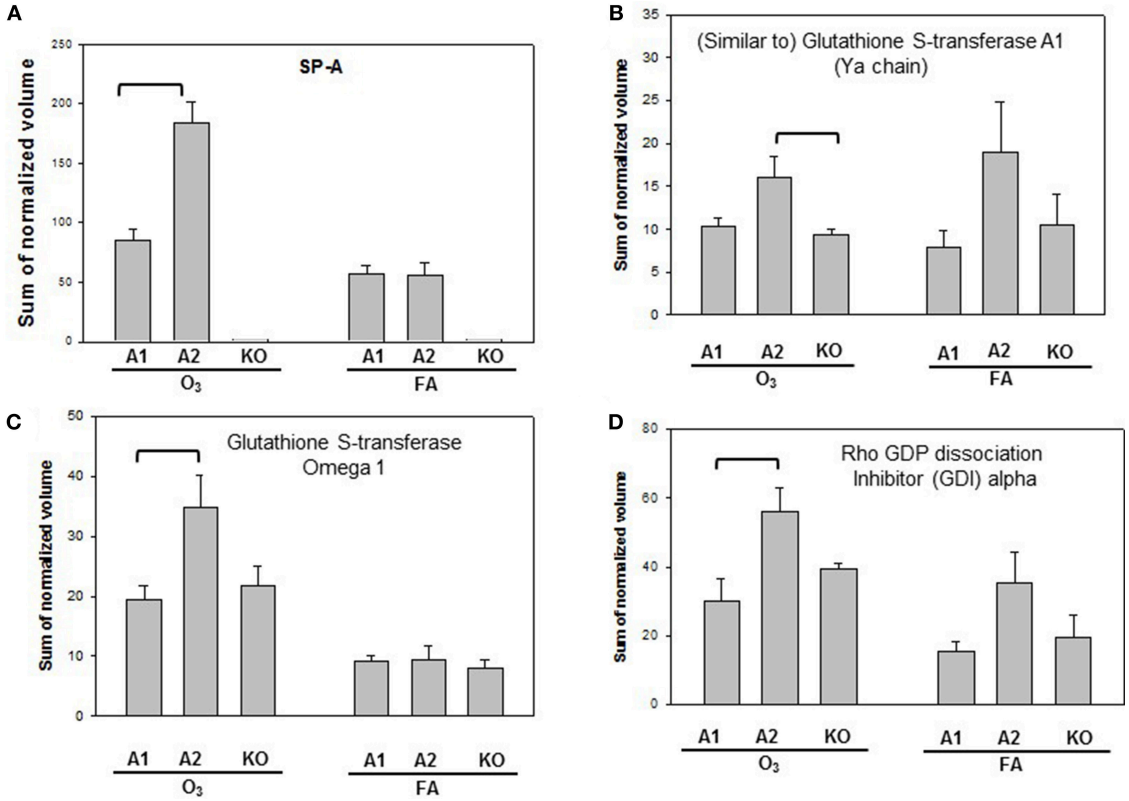

FIGURE 5 | Representative graphs of specific protein changes among genotypes of ozone-exposed male mice. Histograms depict levels of each specific protein, **(A)** SP-A; **(B)** (Similar to) glutathione S-transferase A1; **(C)** glutathione S transferase, omega 1; **(D)** Rho GDP dissociation inhibitor (GDI) alpha. These proteins exhibit significant differences in one group of comparisons of male mice with different genotypes (A1, A2, KO) after exposure to O_3 and bacterial infection. Comparisons between groups that are statistically significant ($p < 0.05$) are indicated with a bracket.

stress and/or infection. Here we performed a pilot experiment to confirm its involvement in ozone-induced oxidative stress. Nuclear and cytoplasmic extracts of the lung tissue from treated mice, exposed to ozone (2 ppm) for 1, 2, and 3 h with a post-exposure recovery period of 0, 1, 2, and 4 h were used to study the change of Nrf2 level. **Figure 8** shows a time-dependent translocation of Nrf2 to the nucleus following ozone-induced oxidative stress, indicating that Nrf2 does play a role in the system.

DISCUSSION

SP-A plays critical roles in host defense, regulation of inflammation, and surfactant-related physiology in the lung. Structural and functional differences have been observed between human SP-A1 and SP-A2 proteins expressed *in vitro* by insect or mammalian cells (26–34) and *in vivo, ex vivo,* or *in vitro* (36, 37, 39–44). In the present study we have used hTG SP-A1 and SP-A2 and SP-A KO mice, and studied *in vivo* the effect of human SP-A1 and SP-A2 genotypes on BAL proteomic profile and associated signaling pathways in response to bacterial infection in the presence or absence of ozone.

All the data from this study are summarized in **Figure 9**. This Figure shows that after FA exposure and infection, when compared to KO, the number of proteins with increased level (>25%) are SP-A2 > SP-A1 > KO in male mice, and SP-A2 ≈ SP-A1 > KO in female mice, and after ozone exposure and infection, SP-A2 > SP-A1 ≈ KO in male mice, and SP-A2 > SP-A1 ≈ KO (decrease) in female mice. These observations indicate genotype and sex differences in the BAL proteome under the studied conditions. A greater number of proteins were found with altered levels in SP-A2 male mice compared to SP-A1 and this was independent of the presence or absence of ozone exposure. This is consistent with *in vitro* observations, where SP-A2 variants had a higher ability than SP-A1 variants to stimulate cytokine production by macrophage-like THP-1 cells (27, 30, 38), to enhance phagocytosis of bacteria by macrophages (29, 31–33), and to interact with LPS and phospholipids (26, 35). Female mice, on the other hand, showed no differences between SP-A2 and SP-A1 mice under the same conditions. However, if in addition to infection, these were exposed to ozone, the SP-A2 mice had a higher number of proteins with altered levels compared to SP-A1 or KO mice, with no major differences observed between SP-A1 and KO mice in either males or females. This general observation is in line with recent findings showing that the alveolar macrophage miRNome from male SP-A2 mice in response to ozone-induced oxidative stress, differs significantly from that of the SP-A1 (42).

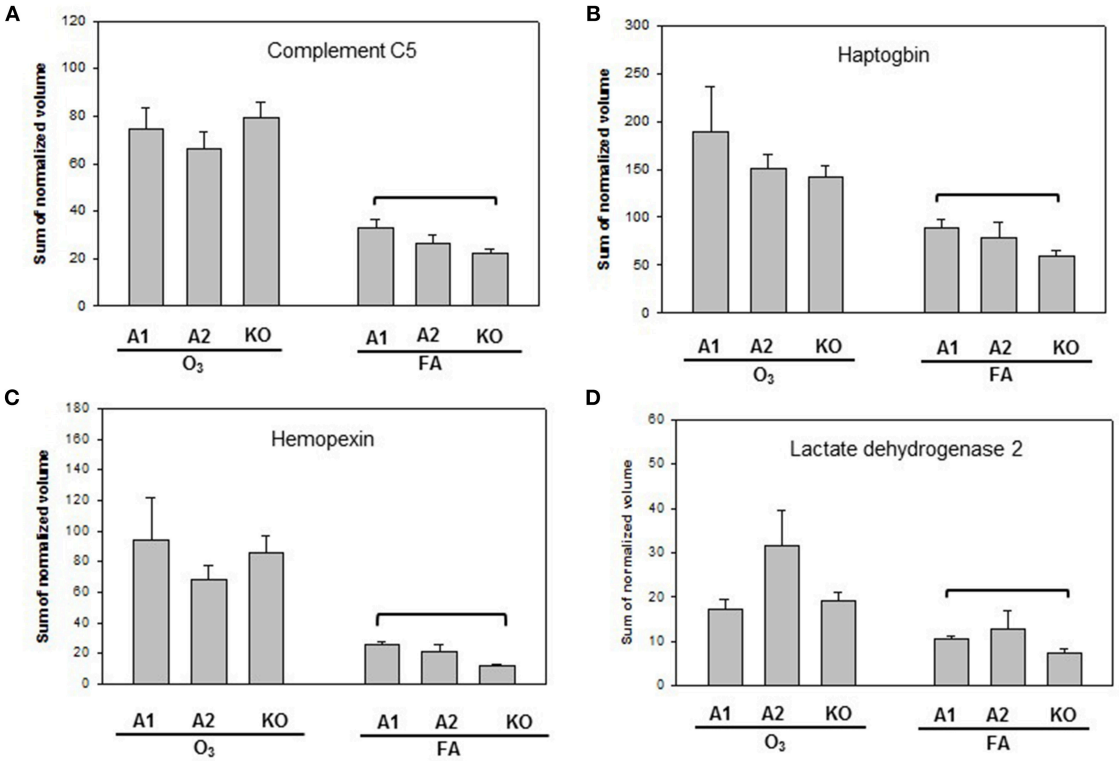

FIGURE 6 | Representative graphs of specific protein changes among genotypes of FA-exposed mice. Histograms depicting levels of each specific protein are included in **(A)** complement C5; **(B)** haptoglobin; **(C)** hemopexin; and **(D)** Lactate dehydrogenase 2. These proteins exhibit significant differences in one of the comparisons of male mice with different genotypes (A1, A2, KO) after exposure to filtered air (FA) and bacterial infection. Comparisons between groups that were statistically significant ($p < 0.05$) are indicated with a bracket.

In vitro ozone exposure of SP-A variants has been shown previously to decrease the functional activity of SP-A1 and SP-A2 variants (28, 30, 33, 38). Although ozone exposure has been shown to affect the functional activity of SP-A2 relatively more compared to SP-A1, at low physiological concentrations no difference was observed in SP-A2 and SP-A1function after ozone exposure (33) indicating a concentration-dependent effect of ozone-induced oxidation. Whether the differences in the proteomic profiles between hTG SP-A1 and SP-A2 mice may reflect regulatory differences in the translation between SP-A1 and SP-A2 (66) and/or qualitative functional differences between SP-A1 and SP-A2 remains to be determined. For example, there are 15 DEF proteins with marked increase in ozone-exposed hTG SP-A2 male mice compared to ozone-exposed SP-A1 male mice (**Table 1S**). These proteins could play a critical role in the host defense and inflammatory regulation in the lung in the presence of pneumonia and/or oxidative stress.

Increased levels of proteins related to APR signaling pathway were found in the FA-exposed SP-A1 and SP-A2 mice (except for SP-A2 female where it may decrease) compared to the FA-exposed KO mice; SP-A2 males showed an increase compared to SP-A1 males with no differences between SP-A1 and SP-A2 females. After ozone exposure, SP-A1 and SP-A2 male mice exhibited increased levels of APR related proteins compared to KO male mice, and SP-A2 male mice showed increased APR protein level compared to SP-A1 male mice. Recently as noted above, ozone exposure was shown to differentially affect the microRNAome of the alveolar macrophage in SP-A1 and SP-A2 mice, with SP-A2 mice exhibiting a more robust response (42). However, after ozone exposure, SP-A1 and SP-A2 female mice showed decreased levels of proteins related to the APR signal pathways compared to KO female mice; SP-A2 females showed decreased levels when compared to SP-A1 female mice. Together, these indicate that the BAL proteome is SP-A genotype- and sex-dependent in response to environmental insults.

The APR (ERK1/2 and NF-IL6) signal pathway has been shown to play a critical role in host defense against various infections and in the regulation of inflammation, as well as in oxidative stress (67). The ERK1/2 signaling pathway was involved in an SP-A-enhanced response of macrophages to mycobacteria (68). In the present study SP-A2 and SP-A1 mice compared with SP-A KO mice showed a regulatory effect on BAL protein expression that are associated with the activation of APR (ERK1/2 and NF-IL6) signaling pathways. After ozone exposure, however, only SP-A1 and SP-A2 male mice, but not females, could maintain this regulatory ability (**Figure 9**). This is of interest and

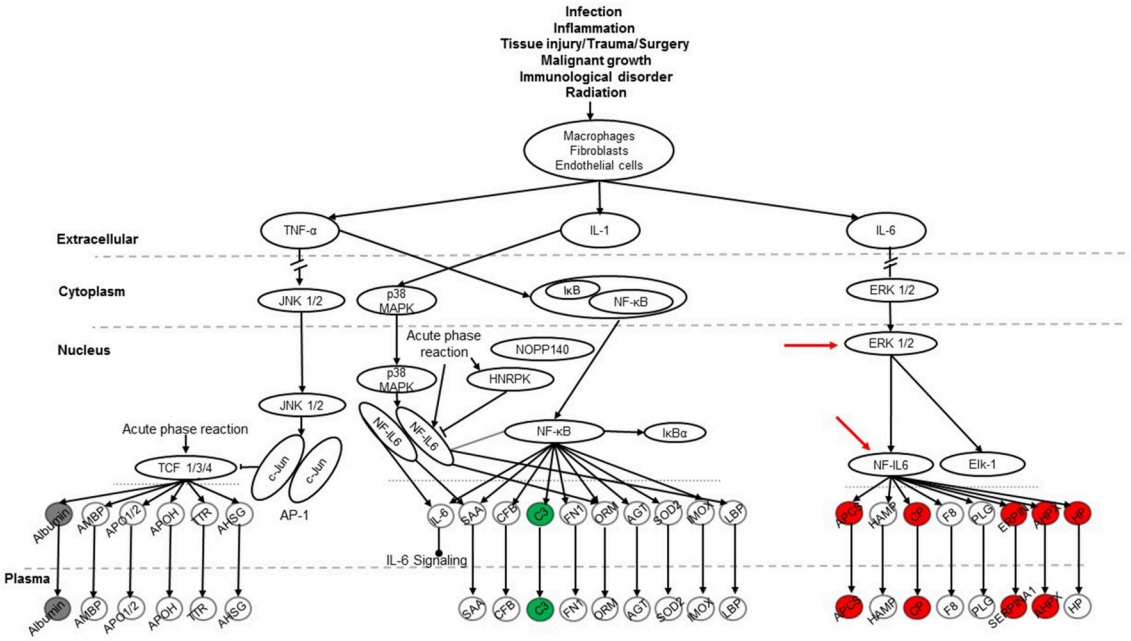

FIGURE 7 | The APR signaling pathway is associated with ozone exposure and bacterial infection. A total of 36 proteins were identified in this study and were used for Ingenuity Pathway Analysis. The canonical "APR signaling" pathway was found to be associated with these proteins ($p < 4.17E-11$). An example of the comparison among SP-A genotypes is shown for the SP-A2M_FA vs. KOM_FA comparison where proteins with increases in (>25%) expression are shown in red, proteins with decreases (>-25%) are shown in green, and proteins with changes <25% are shown in gray. ERK1/2 and NF-IL6 in the pathway are indicated with red arrows.

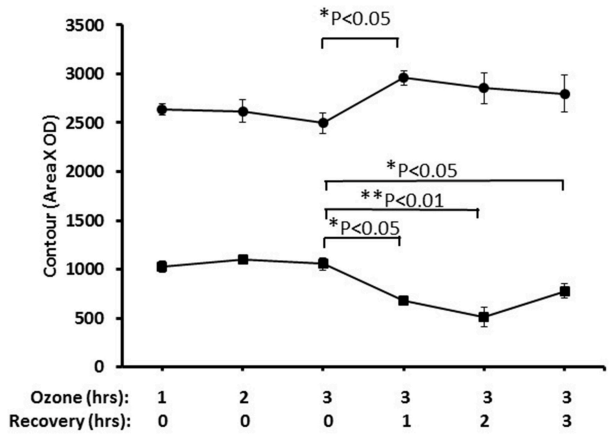

FIGURE 8 | Nuclear and cytoplasmic levels of NRF2 in lung tissue after ozone exposure. Mice were exposed to 2 PPM ozone for 1, 2, or 3 h and then allowed to recover for either 0, 1, 2, or 3 h after exposure. Lungs were then removed, and nuclear and cytoplasmic extracts prepared and run on SDS-PAGE gels. NRF2 levels were quantitated by Western blot ECL and densitometry (• nuclear, ■ cytoplasmic). The results indicated the time-dependent translocation of Nrf2 from cytoplasm to nucleus after ozone exposure (*$P < 0.05$; **$P < 0.01$).

consistent with survival studies where females showed decreased survival after O_3 exposure of infected mice (13, 14, 69, 70), allowing us to speculate that the regulatory changes observed in males are positive with regards to survival. The present findings indicate that male mice may have a dominant effect or greater ability to regulate the APR (ERK1/2 and NF-IL6) signaling pathway that does not occur in female mice. It is likely that other sex-related factors such as sex hormones are involved in the regulation of the APR (ERK1/2 and NF-IL6) signaling pathway in the response to infection and ozone-induced oxidative stress (14, 42, 43, 71). NF-kB signaling is a critical part of the APR pathway and a few proteins were associated with the NF-kB pathway from the 36 proteins identified in this study. NF-kB signaling is essential for bacterial infection and inflammatory regulation. Previous studies have provided evidence that SP-A activates NF-kB (72) through accumulation of inhibitory IkB-a (73, 74) or direct interaction with cell receptors like TLR-2 and TLR-4 (72, 75–77) or SIRP alpha and CD91 (78). In response to ozone the ability of SP-A to activate NF-kB is decreased as assessed by the lack of changes in the nuclear p65 and cytoplasmic IkB-a levels (79). Furthermore, the data from this *in vivo* study are consistent with the results in WT mice exposed to ozone (14, 50, 56), as well as *in vitro* findings (33, 38), where ozone-exposed SP-A1 and SP-A2 mice reduced (for male) or abrogated (for female) the ability to enhance APR (ERK1/2 and NF-IL6) signaling pathway activation.

Four other signaling pathways including the Nrf2 signaling pathway appeared significant but had fewer proteins than the APR. The Nrf2 signaling pathway has been shown to be a cellular defense mechanism against oxidative stress and inflammation (80, 81). Under normal conditions, Nrf2 is sequestered in the

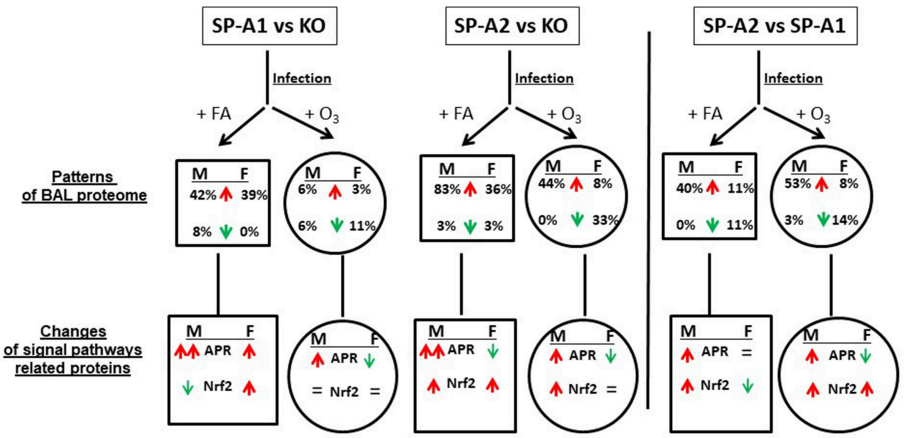

FIGURE 9 | A summary of the BAL proteome and signaling pathways in this study. This figure, following synthesis of all the data, depicts patterns of male (M) and female (F) mice of SP-A1 vs. KO, SP-A2 vs. KO, and SP-A2 vs. SP-A1 after FA or ozone exposure and bacterial infection. An up (↑) arrow (red) and down (↓) arrow (green) indicate increases (>25%) and decreases (>-25%), respectively. The percentage of changed proteins (>25% increase or >-25% decrease) is shown under M and F. In the signaling pathway of related proteins, up (↑) arrows (red) indicate that the number of proteins involved in the signaling pathways with increases (>25%) is more than that of the proteins showing decreases (>-25%). The number in double up (↑↑) arrows (red) is more than in single up (↑) arrows (red). Down (↓) arrows (green) indicates that the number of decreased proteins (>-25%) is more than the number of increased proteins. "=" means no marked changes of proteins (<25%). Based on this model, we found differential effects of SP-A genotypes and sex on the patterns of BAL proteomes and signaling pathways in response to ozone exposure and bacterial infection.

cytoplasm via binding to its repressor molecule Keap1, but under oxidative ER stress, the Nrf2 is released from its repressor and translocated into nucleus to regulate antioxidant molecules. Experimental evidence has shown that the Nrf2 signaling pathway is important for oxidative stress and inflammation (80–82), and Nrf2 signal is a critical regulator of innate immune response and survival during sepsis (83, 84). Nrf2-deficient mice exhibit enhanced susceptibility to severe airway inflammation and asthma (85) and to cigarette smoke-induced emphysema (86). Nrf2 has been shown to be an important pathway in a rescue experiment where SP-A KO mice were treated with exogenous SP-A and the proteomes of the alveolar macrophages from the KO and rescue mice were studied (59, 61). The findings from this study indicate that SP-A1 and SP-A2 infected mice exhibit higher levels of Nrf2-related protein expression than KO mice, suggesting that SP-A plays protective roles against infection and oxidative stress. SP-A1 mice exhibit sex differences in this regard. After ozone exposure the effect of SP-A1 was eliminated, but SP-A2 males (but not females) still showed increased level of proteins associated with the Nrf2 pathway (**Figure 9**). This is consistent with recent findings where the SP-A2 male miRNome of the alveolar macrophage exhibited a robust response after ozone exposure compared to SP-A1 males and females and SP-A2 females (42). Furthermore, male mice after ozone exposure and infection had been shown to have a better survival compared to females (13, 14, 52) and these sex differences were minimized or eliminated after gonadectomy (71) implicating sex hormones. Therefore, it is possible that sex hormones play a role in this SP-A1/SP-A2 genotype-sex interaction.

Of interest, the Nrf2 pathway is part of the xenobiotic metabolism signaling pathway, which was also associated with protein changes in this study. In addition, the glutathione metabolism pathway and the aryl hydrocarbon receptor signaling pathway are associated with the protein changes in this model. These pathways share three proteins, i.e., glutathione S-transferase A1, glutathione S transferase, omega 1, and glutathione S-transferase A4, which are present in the Nrf2 and the xenobiotic metabolism signaling pathways. The major function of the glutathinone S-transferase superfamily is to detoxify xenobiotics by catalyzing the nucleophilic attack by GSH on electrophilic carbon, sulfur, or nitrogen atoms of nonpolar xenobiotic substrates, thus preventing the damage of crucial cellular proteins and nucleic acids in cells (87).

Eleven proteins were observed to be statistically significant different among mice with different SP-A genotype and with or without ozone exposure. SP-A2 mice showed higher levels of annexin A5, SP-A, 14-3-3 zeta protein, and glutathione S-transferase A4 than SP-A1 and KO mice in response to ozone and infection (**Figure 4**). These proteins are involved in host defense, immunity functions, and redox balance. Therefore, higher levels of defense and immunity proteins are likely to enhance the ability of SP-A2 mice to protect the lung from bacterial infection and ozone-induced oxidative stress. Annexin A5 regulates the permeability of the channel pore to ions and plays a central role in the machinery of membrane repair (88, 89). In addition, 14-3-3 zeta protein is an important regulator for a wide range of regulatory processes, such as mitogenic signal transduction, and apoptotic cell death (64). Although members of the 14-3-3 family regulate SP-A2 expression by

directly binding at the 5′UTR, the 14-3-3 zeta isoform did not appear to be involved (66). In infected SP-A2 mice the 14-3-3 zeta protein level was higher than in infected SP-A1 and KO mice (**Figure 4C**). Whether this higher level could improve neutrophil cell apoptosis and benefit apoptotic cell clearance in the alveolar space remains to be determined. Moreover, as mentioned above, infected SP-A2 mice could increase the expression levels of the Nrf2 signaling pathway-related proteins, such as members of glutathione S-transferase family. The higher levels of these Nrf2-related proteins may enhance the defense ability in hTG SP-A2 mice against various infection and environmental insults such as oxidative stress and LPS exposure (80, 85, 90). Although SP-A1 mice have a lower level in host defense-related protein expression compared to SP-A2 mice, about one half of the 36 identified proteins in SP-A1 mice increased when compared to KO mice after infection. However, these increases were abrogated after ozone exposure. This indicates that the biological function mediated by these proteins in hTG mice could be significantly impaired *in vivo* by ozone-induced oxidation. In fact, SP-A oxidation in WT mice after ozone exposure has been observed (52, 53) and this may result in a reduction of function (52).

In summary, the findings of the present study, where the *in vivo* differential effects of SP-A genotypes were investigated on the BAL proteomic patterns and associated signaling pathways in response to ozone or FA exposure and bacterial infection, revealed: (a) ozone exposure significantly increases the level of total BAL proteins compared to bacterial infection alone; (b) of the 36 proteins identified in BAL fluid, 11 were found with significant differences in one or more comparisons of the study groups; (c) APR and Nrf2 related signaling pathways were identified as important pathways in response to SP-A genotype, sex and ozone/FA exposure in this bacterial infection. The NF-kB signaling, a critical part of the APR pathway may also play an important role. These findings may provide new insight into molecular mechanisms of human SP-A1 and SP-A2 genetic variants in response to environmental insults.

AUTHOR CONTRIBUTIONS

GW, SH, and AM performed animal experiments. GW and TU carried out data analysis and result interpretation. DP guided proteomic analysis and result interpretation. GW and JF designed the experiments and wrote the manuscript. JF provided oversight throughout this project.

ACKNOWLEDGMENTS

We thank Susan DiAngelo for her excellent technical support of mouse genotyping analysis, and Dr. Freeman for the use of the Ingenuity Pathway Analysis software. We acknowledge the core facility of The Penn State Hershey College of Medicine for MALDI-ToF/ToF analysis. This study was supported by 1R01 NIH ES09882 and in part by HL136706.

SUPPLEMENTARY MATERIAL

The Supplementary Material for this article can be found online at: https://www.frontiersin.org/articles/10.3389/fimmu.2019.00561/full#supplementary-material

REFERENCES

1. Wright JR. Immunoregulatory functions of surfactant proteins. *Nat Rev Immunol.* (2005) 5:58–68. doi: 10.1038/nri1528
2. Floros J, Wang G, Mikerov AN. Genetic complexity of the human innate host defense molecules, surfactant protein A1 (SP-A1) and SP-A2–impact on function. *Crit Rev Eukaryot Gene Exp.* (2009) 19:125–37. doi: 10.1615/CritRevEukarGeneExpr.v19.i2.30
3. LeVine AM, Bruno MD, Huelsman KM, Ross GF, Whitsett JA, Korfhagen TR. Surfactant protein A-deficient mice are susceptible to group B streptococcal infection. *J Immunol.* (1997) 158:4336–40.
4. LeVine AM, Gwozdz J, Stark J, Bruno M, Whitsett J, Korfhagen T. Surfactant protein-A enhances respiratory syncytial virus clearance *in vivo*. *J Clin Invest.* (1999) 103:1015–21. doi: 10.1172/JCI5849
5. LeVine AM, Kurak KE, Bruno MD, Stark JM, Whitsett JA, Korfhagen TR. Surfactant protein-A-deficient mice are susceptible to *Pseudomonas aeruginosa* infection. *Am J Respir Cell Mol Biol.* (1998) 19:700–8. doi: 10.1165/ajrcmb.19.4.3254
6. Li G, Siddiqui J, Hendry M, Akiyama J, Edmondson J, Brown C, et al. Surfactant protein-A–deficient mice display an exaggerated early inflammatory response to a beta-resistant strain of influenza A virus. *Am J Respir Cell Mol Biol.* (2002) 26:277–82. doi: 10.1165/ajrcmb.26.3.4584
7. Giannoni E, Sawa T, Allen L, Wiener-Kronish J, Hawgood S. Surfactant proteins A and D enhance pulmonary clearance of Pseudomonas aeruginosa. *Am J Respir Cell Mol Biol.* (2006) 34:704–10. doi: 10.1165/rcmb.2005-0461OC
8. Ikegami M, Korfhagen TR, Bruno MD, Whitsett JA, Jobe AH. Surfactant metabolism in surfactant protein A-deficient mice. *Am J Physiol.* (1997) 272:L479–85.
9. Bates SR, Dodia C, Tao JQ, Fisher AB. Surfactant protein-A plays an important role in lung surfactant clearance: evidence using the surfactant protein-A gene-targeted mouse. *Am J Physiol.* (2008) 294:L325–33. doi: 10.1152/ajplung.00341.2007
10. Korfhagen TR, Bruno MD, Ross GF, Huelsman KM, Ikegami M, Jobe AH, et al. Altered surfactant function and structure in SP-A gene targeted mice. *Proc Natl Acad Sci USA.* (1996) 93:9594–9. doi: 10.1073/pnas.93.18.9594
11. Ikegami M, Elhalwagi BM, Palaniyar N, Dienger K, Korfhagen T, Whitsett JA, et al. The collagen-like region of surfactant protein A (SP-A) is required for correction of surfactant structural and functional defects in the SP-A null mouse. *J Biol Chem.* (2001) 276:38542–8. doi: 10.1074/jbc.M102054200
12. Ikegami M, Korfhagen TR, Whitsett JA, Bruno MD, Wert SE, Wada K, et al. Characteristics of surfactant from SP-A-deficient mice. *Am J Physiol.* (1998) 275:L247–54.
13. Mikerov AN, Gan X, Umstead TM, Miller L, Chinchilli VM, Phelps DS, et al. Sex differences in the impact of ozone on survival and alveolar macrophage function of mice after *Klebsiella pneumoniae* infection. *Respir Res.* (2008) 9:24. doi: 10.1186/1465-9921-9-24
14. Mikerov AN, Hu S, Durrani F, Gan X, Wang G, Umstead TM, et al. Impact of sex and ozone exposure on the course of pneumonia in wild type and SP-A (-/-) mice. *Microb Pathog.* (2012) 52:239–49. doi: 10.1016/j.micpath.2012.01.005

15. Hoover RR, Floros J. Organization of the human SP-A and SP-D loci at 10q22-q23. Physical and radiation hybrid mapping reveal gene order and orientation. *Am J Respir Cell Mol Biol.* (1998) 18:353–62. doi: 10.1165/ajrcmb.18.3.3035
16. Bruns G, Stroh H, Veldman GM, Latt SA, Floros J. The 35 kd pulmonary surfactant-associated protein is encoded on chromosome 10. *Hum Genet.* (1987) 76:58–62. doi: 10.1007/BF00283051
17. Floros J, Hoover RR. Genetics of the hydrophilic surfactant proteins A and D. *Biochim Biophys Acta.* (1998) 1408:312–22. doi: 10.1016/S0925-4439(98)00077-5
18. DiAngelo S, Lin Z, Wang G, Phillips S, Ramet M, Luo J, et al. Novel, non-radioactive, simple and multiplex PCR-cRFLP methods for genotyping human SP-A and SP-D marker alleles. *Dis Markers.* (1999) 15:269–81. doi: 10.1155/1999/961430
19. Phelps DS, Floros J. Localization of surfactant protein synthesis in human lung by *in situ* hybridization. *Am Rev Respir Dis.* (1988) 137:939–42. doi: 10.1164/ajrccm/137.4.939
20. Hu F, Ding G, Zhang Z, Gatto LA, Hawgood S, Poulain FR, et al. Innate immunity of surfactant proteins A and D in urinary tract infection with uropathogenic *Escherichia coli*. *Innate Immun.* (2016) 22:9–20. doi: 10.1177/1753425915609973
21. MacNeill C, Umstead TM, Phelps DS, Lin Z, Floros J, Shearer DA, et al. Surfactant protein A, an innate immune factor, is expressed in the vaginal mucosa and is present in vaginal lavage fluid. *Immunology.* (2004) 111:91–9. doi: 10.1111/j.1365-2567.2004.01782.x
22. Liu J, Abdel-Razek O, Liu Z, Hu F, Zhou Q, Cooney RN, et al. Role of surfactant proteins a and d in sepsis-induced acute kidney injury. *Shock.* (2015) 43:31–8. doi: 10.1097/SHK.0000000000000270
23. Goss KL, Kumar AR, Snyder JM. SP-A2 gene expression in human fetal lung airways. *Am J Respir Cell Mol Biol.* (1998) 19:613–21. doi: 10.1165/ajrcmb.19.4.3155
24. Saitoh H, Okayama H, Shimura S, Fushimi T, Masuda T, Shirato K. Surfactant protein A2 gene expression by human airway submucosal gland cells. *Am J Respir Cell Mol Biol.* (1998) 19:202–9. doi: 10.1165/ajrcmb.19.2.3239
25. Silveyra P, Floros J. Genetic variant associations of human SP-A and SP-D with acute and chronic lung injury. *Front Biosci.* (2012) 17:407–29. doi: 10.2741/3935
26. Garcia-Verdugo I, Wang G, Floros J, Casals C. Structural analysis and lipid-binding properties of recombinant human surfactant protein a derived from one or both genes. *Biochemistry.* (2002) 41:14041–53. doi: 10.1021/bi026540l
27. Wang G, Phelps DS, Umstead TM, Floros J. Human SP-A protein variants derived from one or both genes stimulate TNF-α production in the THP-1 cell line. *Am J Physiol.* (2000) 278:L946–54. doi: 10.1152/ajplung.2000.278.5.L946
28. Wang G, Bates-Kenney SR, Tao JQ, Phelps DS, Floros J. Differences in biochemical properties and in biological function between human SP-A1 and SP-A2 variants, and the impact of ozone-induced oxidation. *Biochemistry.* (2004) 43:4227–39. doi: 10.1021/bi036023i
29. Wang G, Myers C, Mikerov A, Floros J. Effect of cysteine 85 on biochemical properties and biological function of human surfactant protein A variants. *Biochemistry.* (2007) 46:8425–35. doi: 10.1021/bi7004569
30. Huang W, Wang G, Phelps DS, Al-Mondhiry H, Floros J. Human SP-A genetic variants and bleomycin-induced cytokine production by THP-1 cells: effect of ozone-induced SP-A oxidation. *Am J Physiol.* (2004) 286:L546–53. doi: 10.1152/ajplung.00267.2003
31. Mikerov AN, Umstead TM, Huang W, Liu W, Phelps DS, Floros J. SP-A1 and SP-A2 variants differentially enhance association of Pseudomonas aeruginosa with rat alveolar macrophages. *Am J Physiol Lung Cell Mol Physiol.* (2005) 288:L150–8. doi: 10.1152/ajplung.00135.2004
32. Mikerov AN, Wang G, Umstead TM, Zacharatos M, Thomas NJ, Phelps DS, et al. Surfactant protein A2 (SP-A2) variants expressed in CHO cells stimulate phagocytosis of Pseudomonas aeruginosa more than do SP-A1 variants. *Infect Immun.* (2007) 75:1403–12. doi: 10.1128/IAI.01341-06
33. Mikerov AN, Umstead TM, Gan X, Huang W, Guo X, Wang G, et al. Impact of ozone exposure on the phagocytic activity of human surfactant protein A (SP-A) and SP-A variants. *Am J Physiol Lung Cell Mol Physiol.* (2008) 294:L121–30. doi: 10.1152/ajplung.00288.2007
34. Oberley RE, Snyder JM. Recombinant human SP-A1 and SP-A2 proteins have different carbohydrate-binding characteristics. *Am J Physiol.* (2003) 284:L871–81. doi: 10.1152/ajplung.00241.2002
35. Wang G, Taneva S, Keough KM, Floros J. Differential effects of human SP-A1 and SP-A2 variants on phospholipid monolayers containing surfactant protein B. *Biochim Biophys Acta.* (2007) 1768:2060–9. doi: 10.1016/j.bbamem.2007.06.025
36. Lopez-Rodriguez E, Pascual A, Arroyo R, Floros J, Perez-Gil J. Human pulmonary surfactant protein SP-A1 provides maximal efficiency of lung interfacial films. *Biophys J.* (2016) 111:524–36. doi: 10.1016/j.bpj.2016.06.025
37. Phelps DS, Umstead TM, Floros J. Sex differences in the acute *in vivo* effects of different human SP-A variants on the mouse alveolar macrophage proteome. *J Proteomics.* (2014) 108:427–44. doi: 10.1016/j.jprot.2014.06.007
38. Wang G, Umstead TM, Phelps DS, Al-Mondhiry H, Floros J. The effect of ozone exposure on the ability of human surfactant protein a variants to stimulate cytokine production. *Environ Health Perspect.* (2002) 110:79–84. doi: 10.1289/ehp.0211079
39. Wang G, Guo X, Diangelo S, Thomas NJ, Floros J. Humanized SFTPA1 and SFTPA2 transgenic mice reveal functional divergence of SP-A1 and SP-A2: formation of tubular myelin *in vivo* requires both gene products. *J Biol Chem.* (2010) 285:11998–2010. doi: 10.1074/jbc.M109.046243
40. Tsotakos N, Phelps DS, Yengo CM, Chinchilli VM, Floros J. Single-cell analysis reveals differential regulation of the alveolar macrophage actin cytoskeleton by surfactant proteins A1 and A2: implications of sex and aging. *Biol Sex Differ.* (2016) 7:18. doi: 10.1186/s13293-016-0071-0
41. Phelps DS, Umstead TM, Silveyra P, Hu S, Wang G, Floros J. Differences in the alveolar macrophage proteome in transgenic mice expressing human SP-A1 and SP-A2. *J Proteom Genom Res.* (2013) 1:2–26. doi: 10.14302/issn.2326-0793.jpgr-12-207
42. Noutsios GT, Thorenoor N, Zhang X, Phelps DS, Umstead TM, Durrani F, et al. SP-A2 contributes to miRNA-mediated sex differences in response to oxidative stress: pro-inflammatory, anti-apoptotic, and anti-oxidant pathways are involved. *Biol Sex Differ.* (2017) 8:37. doi: 10.1186/s13293-017-0158-2
43. Thorenoor N, Zhang X, Umstead TM, Scott Halstead E, Phelps DS, Floros J. Differential effects of innate immune variants of surfactant protein-A1 (SFTPA1) and SP-A2 (SFTPA2) in airway function after *Klebsiella pneumoniae* infection and sex differences. *Respir Res.* (2018) 19:23. doi: 10.1186/s12931-018-0723-1
44. Thorenoor N, Umstead TM, Zhang X, Phelps DS, Floros J. Survival of surfactant protein-A1 and SP-A2 transgenic mice after *Klebsiella pneumoniae* infection, exhibits sex-, gene-, and variant specific differences; treatment with surfactant protein improves survival. *Front Immunol.* (2018) 9:2404. doi: 10.3389/fimmu.2018.02404
45. Hollingsworth JW, Kleeberger SR, Foster WM. Ozone and pulmonary innate immunity. *Proc Am Thorac Soc.* (2007) 4:240–6. doi: 10.1513/pats.200701-023AW
46. Holz O, Jorres RA, Timm P, Mucke M, Richter K, Koschyk S, et al. Ozone-induced airway inflammatory changes differ between individuals and are reproducible. *Am J Respir Crit Care Med.* (1999) 159:776–84. doi: 10.1164/ajrccm.159.3.9806098
47. Kim JJ. Ambient air pollution: health hazards to children. *Pediatrics.* (2004) 114:1699–707. doi: 10.1542/peds.2004-2166
48. Morrison D, Rahman I, MacNee W. Permeability, inflammation and oxidant status in airspace epithelium exposed to ozone. *Respir Med.* (2006) 100:2227–34. doi: 10.1016/j.rmed.2005.10.005
49. Holz O, Heusser K, Muller M, Windt H, Schwarz K, Schindler C, et al. Airway and systemic inflammatory responses to ultrafine carbon black particles and ozone in older healthy subjects. *J Toxicol Environ Health A.* (2018) 81:576–88. doi: 10.1080/15287394.2018.1463331
50. Haque R, Umstead TM, Freeman WM, Floros J, Phelps DS. The impact of surfactant protein-A on ozone-induced changes in the mouse bronchoalveolar

lavage proteome. *Proteome Sci.* (2009) 7:12. doi: 10.1186/1477-5956-7-12
51. Jerrett M, Burnett RT, Pope CA III, Ito K, Thurston G, Krewski D, et al. Long-term ozone exposure and mortality. *N Engl J Med.* (2009) 360:1085–95. doi: 10.1056/NEJMoa0803894
52. Mikerov AN, Haque R, Gan X, Guo X, Phelps DS, Floros J. Ablation of SP-A has a negative impact on the susceptibility of mice to *Klebsiella pneumoniae* infection after ozone exposure: sex differences. *Respir Res.* (2008) 9:77. doi: 10.1186/1465-9921-9-77
53. Haque R, Umstead TM, Ponnuru P, Guo X, Hawgood S, Phelps DS, et al. Role of surfactant protein-A (SP-A) in lung injury in response to acute ozone exposure of SP-A deficient mice. *Toxicol Appl Pharmacol.* (2007) 220:72–82. doi: 10.1016/j.taap.2006.12.017
54. Umstead TM, Freeman WM, Chinchilli VM, Phelps DS. Age-related changes in the expression and oxidation of bronchoalveolar lavage proteins in the rat. *Am J Physiol Lung Cell Mol Physiol.* (2009) 296:L14–29. doi: 10.1152/ajplung.90366.2008
55. Gibson F, Anderson L, Babnigg G, Baker M, Berth M, Binz PA, et al. Guidelines for reporting the use of gel electrophoresis in proteomics. *Nat Biotechnol.* (2008) 26:863–4. doi: 10.1038/nbt0808-863
56. Ali M, Umstead TM, Haque R, Mikerov AN, Freeman WM, Floros J, et al. Differences in the BAL proteome after *Klebsiella pneumoniae* infection in wild type and SP-A-/- mice. *Proteome Sci.* (2010) 8:34. doi: 10.1186/1477-5956-8-34
57. Freeman WM, Hemby SE. Proteomics for protein expression profiling in neuroscience. *Neurochem Res.* (2004) 29:1065–81. doi: 10.1023/B:NERE.0000023594.21352.17
58. Bortner JD Jr, Das A, Umstead TM, Freeman WM, Somiari R, Aliaga C, et al. Down-regulation of 14-3-3 isoforms and annexin A5 proteins in lung adenocarcinoma induced by the tobacco-specific nitrosamine NNK in the A/J mouse revealed by proteomic analysis. *J Proteome Res.* (2009) 8:4050–61. doi: 10.1021/pr900406g
59. Phelps DS, Umstead TM, Quintero OA, Yengo CM, Floros J. *In vivo* rescue of alveolar macrophages from SP-A knockout mice with exogenous SP-A nearly restores a wild type intracellular proteome; actin involvement. *Proteome Sci.* (2011) 9:67. doi: 10.1186/1477-5956-9-67
60. Umstead TM, Lu CJ, Freeman WM, Myers JL, Clark JB, Thomas NJ, et al. Dual-platform proteomics study of plasma biomarkers in pediatric patients undergoing cardiopulmonary bypass. *Pediatr Res.* (2010) 67:641–9. doi: 10.1203/PDR.0b013e3181dceef5
61. Phelps DS, Umstead TM, Floros J. Sex differences in the response of the alveolar macrophage proteome to treatment with exogenous surfactant protein-A. *Proteome Sci.* (2012) 10:44. doi: 10.1186/1477-5956-10-44
62. Huang YC, Bassett MA, Levin D, Montilla T, Ghio AJ. Acute phase reaction in healthy volunteers after bronchoscopy with lavage. *Chest.* (2006) 129:1565–9. doi: 10.1378/chest.129.6.1565
63. Gabay C, Kushner I. Acute-phase proteins and other systemic responses to inflammation. *N Engl J Med.* (1999) 340:448–54. doi: 10.1056/NEJM199902113400607
64. Fu H, Subramanian RR, Masters SC. 14-3-3 proteins: structure, function, and regulation. *Ann Rev Pharmacol Toxicol.* (2000) 40:617–47. doi: 10.1146/annurev.pharmtox.40.1.617
65. Phelps DS. Surfactant regulation of host defense function in the lung: a question of balance. *Pediatr Pathol Mol Med.* (2001) 20:269–92. doi: 10.1080/15513810109168822
66. Noutsios GT, Ghattas P, Bennett S, Floros J. 14-3-3 isoforms bind directly exon B of the 5′-UTR of human surfactant protein A2 mRNA. *Am J Physiol Lung Cell Mol Physiol.* (2015) 309:L147–57. doi: 10.1152/ajplung.00088.2015
67. Rahman I, MacNee W. Oxidative stress and regulation of glutathione in lung inflammation. *Eur Respir J.* (2000) 16:534–54. doi: 10.1034/j.1399-3003.2000.016003534.x
68. Lopez JP, Vigerust DJ, Shepherd VL. Mitogen-activated protein kinases and NFκB are involved in SP-A-enhanced responses of macrophages to mycobacteria. *Respir Res.* (2009) 10:60. doi: 10.1186/1465-9921-10-60
69. Mikerov AN, Phelps DS, Gan X, Umstead TM, Haque R, Wang G, et al. Effect of ozone exposure and infection on bronchoalveolar lavage: Sex differences in response patterns. *Toxicol Lett.* (2014) 230:333–44. doi: 10.1016/j.toxlet.2014.04.008
70. Mikerov AN, Cooper TK, Wang G, Hu S, Umstead TM, Phelps DS, et al. Histopathologic evaluation of lung and extrapulmonary tissues show sex differences in *Klebsiella pneumoniae* - infected mice under different exposure conditions. *Int J Physiol Pathophysiol Pharmacol.* (2011) 3:176–90.
71. Durrani F, Phelps DS, Weisz J, Silveyra P, Hu S, Mikerov AN, et al. Gonadal hormones and oxidative stress interaction differentially affects survival of male and female mice after lung *Klebsiella pneumoniae* infection. *Exp Lung Res.* (2012) 38:165–72. doi: 10.3109/01902148.2011.654045
72. Koptides M, Umstead TM, Floros J, Phelps DS. Surfactant protein A activates NF-κ B in the THP-1 monocytic cell line. *Am J Physiol.* (1997) 273:L382–8.
73. Wu Y, Adam S, Hamann L, Heine H, Ulmer AJ, Buwitt-Beckmann U, et al. Accumulation of inhibitory κB-α as a mechanism contributing to the anti-inflammatory effects of surfactant protein-A. *Am J Respir Cell Mol Biol.* (2004) 31:587–94. doi: 10.1165/rcmb.2004-0003OC
74. Moulakakis C, Adam S, Seitzer U, Schromm AB, Leitges M, Stamme C. Surfactant protein A activation of atypical protein kinase C ζ in IκB-α-dependent anti-inflammatory immune regulation. *J Immunol.* (2007) 179:4480–91. doi: 10.4049/jimmunol.179.7.4480
75. Yamada C, Sano H, Shimizu T, Mitsuzawa H, Nishitani C, Himi T, et al. Surfactant protein A directly interacts with TLR4 and MD-2 and regulates inflammatory cellular response. Importance of supratrimeric oligomerization. *J Biol Chem.* (2006) 281:21771–80. doi: 10.1074/jbc.M513041200
76. Konishi M, Nishitani C, Mitsuzawa H, Shimizu T, Sano H, Harimaya A, et al. Alloiococcus otitidis is a ligand for collectins and Toll-like receptor 2, and its phagocytosis is enhanced by collectins. *Eur J Immunol.* (2006) 36:1527–36. doi: 10.1002/eji.200535542
77. Guillot L, Balloy V, McCormack FX, Golenbock DT, Chignard M, Si-Tahar M. Cutting edge: the immunostimulatory activity of the lung surfactant protein-A involves Toll-like receptor 4. *J Immunol.* (2002) 168:5989–92. doi: 10.4049/jimmunol.168.12.5989
78. Gardai SJ, Xiao YQ, Dickinson M, Nick JA, Voelker DR, Greene KE, et al. By binding SIRPα or calreticulin/CD91, lung collectins act as dual function surveillance molecules to suppress or enhance inflammation. *Cell.* (2003) 115:13–23. doi: 10.1016/S0092-8674(03)00758-X
79. Janic B, Umstead TM, Phelps DS, Floros J. Modulatory effects of ozone on THP-1 cells in response to SP-A stimulation. *Am J Physiol Lung Cell Mol Physiol.* (2005) 288:L317–25. doi: 10.1152/ajplung.00125.2004
80. Kim HJ, Vaziri ND. Contribution of impaired Nrf2-Keap1 pathway to oxidative stress and inflammation in chronic renal failure. *Am J Physiol Renal Physiol.* (2010) 298:F662–71. doi: 10.1152/ajprenal.00421.2009
81. Singh A, Rangasamy T, Thimmulappa RK, Lee H, Osburn WO, Brigelius-Flohe R, et al. Glutathione peroxidase 2, the major cigarette smoke-inducible isoform of GPX in lungs, is regulated by Nrf2. *Am J Respir Cell Mol Biol.* (2006) 35:639–50. doi: 10.1165/rcmb.2005-0325OC
82. Vomund S, Schafer A, Parnham MJ, Brune B, von Knethen A. Nrf2, the master regulator of anti-oxidative responses. *Int J Mol Sci.* (2017) 18:2772. doi: 10.3390/ijms18122772
83. Thimmulappa RK, Lee H, Rangasamy T, Reddy SP, Yamamoto M, Kensler TW, et al. Nrf2 is a critical regulator of the innate immune response and survival during experimental sepsis. *J Clin Invest.* (2006) 116:984–95. doi: 10.1172/JCI25790
84. Battino M, Giampieri F, Pistollato F, Sureda A, de Oliveira MR, Pittala V, et al. Nrf2 as regulator of innate immunity: a molecular Swiss army knife! *Biotechnol Adv.* (2018) 36:358–70. doi: 10.1016/j.biotechadv.2017.12.012
85. Rangasamy T, Guo J, Mitzner WA, Roman J, Singh A, Fryer AD, et al. Disruption of Nrf2 enhances susceptibility to severe airway inflammation and asthma in mice. *J Exp Med.* (2005) 202:47–59. doi: 10.1084/jem.200;50538
86. Rangasamy T, Cho CY, Thimmulappa RK, Zhen L, Srisuma SS, Kensler TW, et al. Genetic ablation of Nrf2 enhances susceptibility to cigarette

smoke-induced emphysema in mice. *J Clin Invest.* (2004) 114:1248–59. doi: 10.1172/JCI200421146

87. Josephy PD. Genetic variations in human glutathione transferase enzymes: significance for pharmacology and toxicology. *Hum Genomics Proteomics.* (2010) 2010:876940. doi: 10.4061/2010/876940
88. Grundmann U, Abel KJ, Bohn H, Lobermann H, Lottspeich F, Kupper H. Characterization of cDNA encoding human placental anticoagulant protein (PP4): homology with the lipocortin family. *Proc Natl Acad Sci USA.* (1988) 85:3708–12. doi: 10.1073/pnas.85.11.3708
89. Bouter A, Carmeille R, Gounou C, Bouvet F, Degrelle SA, Evain-Brion D, et al. Review: annexin-A5 and cell membrane repair. *Placenta.* (2015) 36(Suppl. 1):S43–9. doi: 10.1016/j.placenta.2015.01.193
90. Thimmulappa RK, Scollick C, Traore K, Yates M, Trush MA, Liby KT, et al. Nrf2-dependent protection from LPS induced inflammatory response and mortality by CDDO-Imidazolide. *Biochem Biophys Res Commun.* (2006) 351:883–9. doi: 10.1016/j.bbrc.2006.10.102

Conflict of Interest Statement: The authors declare that the research was conducted in the absence of any commercial or financial relationships that could be construed as a potential conflict of interest.

frontiers in Immunology

ORIGINAL RESEARCH
published: 02 October 2018
doi: 10.3389/fimmu.2018.02256

Genetic Association of Pulmonary Surfactant Protein Genes, SFTPA1, SFTPA2, SFTPB, SFTPC, and SFTPD With Cystic Fibrosis

Zhenwu Lin[1†], Nithyananda Thorenoor[2†], Rongling Wu[3†], Susan L. DiAngelo[2], Meixia Ye[3,4], Neal J. Thomas[2], Xiaojie Liao[2], Tony R. Lin[2], Stuart Warren[2] and Joanna Floros[2,5]*

[1] Department of Radiology, University of Pennsylvania Perelman School of Medicine, Philadelphia, PA, United States, [2] Department of Pediatrics, Center for Host Defense, Inflammation, and Lung Disease (CHILD) Research, Pennsylvania State University, Hershey, PA, United States, [3] Public Health Science, College of Medicine, Pennsylvania State University, Hershey, PA, United States, [4] Center for Computational Biology, College of Biological Sciences and Technology, Beijing Forestry University, Beijing, China, [5] Obstetrics and Gynecology, Pennsylvania State University College of Medicine, Hershey, PA, United States

Surfactant proteins (SP) are involved in surfactant function and innate immunity in the human lung. Both lung function and innate immunity are altered in CF, and altered SP levels and genetic association are observed in Cystic Fibrosis (CF). We hypothesized that single nucleotide polymorphisms (SNPs) within the SP genes associate with CF or severity subgroups, either through single SNP or via SNP-SNP interactions between two SNPs of a given gene (intragenic) and/or between two genes (intergenic). We genotyped a total of 17 SP SNPs from 72 case-trio pedigree (SFTPA1 (5), SFTPA2 (4), SFTPB (4), SFTPC (2), and SFTPD (2)), and identified SP SNP associations by applying quantitative genetic principles. The results showed (a) Two SNPs, SFTPB rs7316 ($p = 0.0083$) and SFTPC rs1124 ($p = 0.0154$), each associated with CF. (b) Three intragenic SNP-SNP interactions, SFTPB (rs2077079, rs3024798), and SFTPA1 (rs1136451, rs1059057 and rs4253527), associated with CF. (c) A total of 34 intergenic SNP-SNP interactions among the 4 SP genes to be associated with CF. (d) No SNP-SNP interaction was observed between SFTPA1 or SFTPA2 and SFTPD. (e) Equal number of SNP-SNP interactions were observed between SFTPB and SFTPA1/SFTPA2 ($n = 7$) and SP-B and SFTPD ($n = 7$). (f) SFTPC exhibited significant SNP-SNP interactions with SFTPA1/SFTPA2 ($n = 11$), SFTPB ($n = 4$) and SFTPD ($n = 3$). (g) A single SFTPB SNP was associated with mild CF after Bonferroni correction, and several intergenic interactions that are associated ($p < 0.01$) with either mild or moderate/severe CF were observed. These collectively indicate that complex SNP-SNP interactions of the SP genes may contribute to the pulmonary disease in CF patients. We speculate that SPs may serve as modifiers for the varied progression of pulmonary disease in CF and/or its severity.

Keywords: surfactant protein, SP-A, SP-B, SP-C, SP-D, cystic fibrosis

OPEN ACCESS

Edited by:
Uday Kishore,
Brunel University London,
United Kingdom

Reviewed by:
Anthony George Tsolaki,
Brunel University London,
United Kingdom
Taruna Madan,
National Institute for Research in Reproductive Health (ICMR), India
Grith Lykke Sorensen,
University of Southern Denmark
Odense, Denmark

***Correspondence:**
Joanna Floros
jxf19@psu.edu;
jfloros@pennstatehealth.psu.edu

† These authors have contributed equally to this work

Specialty section:
This article was submitted to Molecular Innate Immunity, a section of the journal Frontiers in Immunology

Received: *01 June 2018*
Accepted: *11 September 2018*
Published: *02 October 2018*

Citation:
Lin Z, Thorenoor N, Wu R, DiAngelo SL, Ye M, Thomas NJ, Liao X, Lin TR, Warren S and Floros J (2018) Genetic Association of Pulmonary Surfactant Protein Genes, SFTPA1, SFTPA2, SFTPB, SFTPC, and SFTPD With Cystic Fibrosis. Front. Immunol. 9:2256. doi: 10.3389/fimmu.2018.02256

INTRODUCTION

Cystic fibrosis (CF) is an autosomal multi-organ recessive inherited disease. Mutations in the cystic fibrosis transmembrane conductance regulator (CFTR) protein are key in CF pathogenesis (1). CFTR is activated via cAMP through β_2 adrenoceptor stimulation; coding sequence polymorphisms in the CFTR result in CF (2). CFTR functions as a chloride channel on the surface of airway epithelial cells. In patients with CF, loss of CFTR channel function at the cell surface results in impermeability and increased sodium absorption (3, 4). Depletion of the airway surface liquid causes reduced mucus clearance resulting in bacterial colonization, recurrent infections, chronic inflammation, and irreversible damage to the airway epithelium.

Pulmonary function deterioration is one of the primary complications of CF and pulmonary surfactant is essential for normal lung function. Pulmonary surfactant, a surface-active lipoprotein complex, is composed of 90% lipids and 10% surfactant proteins. The latter includes plasma proteins and surfactant proteins SP-A1, SP-A2, SP-B, and SP-C. The surfactant proteins comprise a hydrophobic group of proteins (SP-B and SP-C) and a hydrophilic group of proteins (SP-A1 and SP-A2). The SP-D, although co-isolates with surfactant, is not an integral part of the surfactant complex, but it is grouped with SP-A1/A2 based on its structural similarity and function (5, 6). Pulmonary surfactant is synthesized and secreted by the alveolar epithelial Type II cells of the lung and maintains the stability of the pulmonary tissue by reducing the surface tension of fluids that coat the lung. Broadly speaking the hydrophobic surfactant proteins (SP-B and SP-C) are primarily involved in surface properties of surfactant and are important for normal lung function (7); the hydrophilic proteins (SP-A1, SP-A2, and SP-D) are primarily involved in host defense (6, 8, 9), although SP-A1 and SP-A2 exhibit differential effects on the surfactant structural reorganization (10), on the organization of phospholipid monolayers containing SP-B (11), and lung mechanics (12). Moreover, lipid-mediated interactions of SP-A/SP-B may contribute to normal lung surfactant function (13).

Unlike in rodents that have a single gene encoding surfactant protein A (SP-A), in humans SP-A consists of SP-A1 and SP-A2 encoded by SFTPA1 and SFTPA2, respectively; each gene has been identified with several genetic variants (14), and these have been shown to associate with several pulmonary diseases (15, 16). The human SP-D locus is linked to the SP-A locus and is located proximal to the centromere at approximately 80–100 kb from the SFTPA2 gene (14). Genetic associations between SFTPD SNPs and lung disease have also been identified (17, 18). Although SP-A1, SP-A2, and SP-D are molecules of the innate immunity of the lung, there may be differences in the mechanisms via which host defense is achieved (19, 20). Surfactant proteins SP-B and SP-C play a key role in lung function in normal lung. SP-B is essential for life (21), and both SP-B and SP-C via their role in surfactant function may contribute to CF.

Lung surfactant proteins may contribute to the outcome in CF (22). Bronchoalveolar lavage levels of SP-A have been shown to be increased early in the course of the CF (23), but decrease as disease progresses. Lower levels are correlated with more inflammation and diminished lung function (22, 24–27). Although, the level of SP-B (encoded by SFTPB) was unchanged in BAL from CF patients (24, 28, 29), in CF patients with mild lung disease (30) SP-B was found to be increased, but SP-A did not change. No changes were observed in the levels of SP-C and SP-D, encoded by the SFTPC and SFTPD genes, respectively. However, increased levels of SP-D were observed in serum of CF patients (31).

Moreover, in CF patients with well-conserved lung function (26), SP-C was increased, SP-A was decreased but SP-B and SP-D were not changed. Recently, it was reported that in CF patients, complex forms of SP-A were associated with better lung function. This indicates that the structural organization of SP-A affects its functional activity and this is linked to disease severity (32). SP-A1, shown previously to form higher size oligomers compared to SP-A2 (33), was shown recently to affect more efficiently (than SP-A2) the structural organization of surfactant, which in turn may affect lung function (10). Furthermore, genetic associations of SFTPA1 and SFTPA2 with CF have been observed (34). Moreover, different size SP-D oligomers have been associated with functional differences in patients with chronic lung disease such as CF (35).

Because individuals with identical CFTR mutations may differ in their pulmonary disease, it has been postulated that other genetic factors (i.e. gene modifiers) as well as the microenvironment may contribute to the variable outcome of pulmonary disease (36–41). Surfactant proteins play an important role in surfactant function (7, 34, 42), pulmonary mechanics (12), and innate immunity (6, 8, 9). Furthermore, disruption of these functions can compromise normal lung health. Therefore, we postulated that the surfactant proteins contribute to the progression of the pulmonary disease in CF. We hypothesized that multiple genetic variants of the surfactant protein genes, SFTPA1, SFTPA2, SFTPB, SFTPC, and/or SFTPD, are associated with CF or disease severity subgroups (mild and moderate/severe) through single genetic variations within a gene, and through intragenic or intergenic interactions between variants of a single gene or variants of two different genes. Allele frequencies and linkage disequilibrium of these loci in races and ethnic groups has been previously studied (43). We further hypothesized that some of the associations are unique to patients with mild CF and moderate/severe CF. The observations made indicate that complex SNP-SNP interactions of the surfactant protein genes may contribute to the pulmonary disease in CF patients, and the SPs could serve as modifier genes in lung CF.

MATERIALS AND METHODS

Study Samples

The patient samples were collected with informed and written consent from patients and/or parents under an approved protocol by the institutional review board from the Human

Abbreviations: CF, Cystic fibrosis; CFTR, cystic fibrosis transmembrane conductance regulator; FEV_1, Forced expired volume in 1 sec; SP-A, surfactant protein A; SFTPA1, gene encoding SP-A1; SFTPA2, gene encoding SP-A2; SFTPB, gene encoding SP-B; SFTPC, gene encoding SP-C; SFTPD, gene encoding SP-D; SNPs, single-nucleotide polymorphism.

Subject Protection Office of the Pennsylvania State University College of Medicine. The clinical data of the study samples are given in **Supplementary Table 1** and summarized below.

Seventy-two pedigrees (family trees) were studied, of which, 43 pedigrees had one case with two parents, 21 pedigrees had one case with a single parent, five pedigrees had 2 cases with 1 or 2 parents, and 3 pedigrees had 1 or 2 cases in 3 generations. There were a total of 205 study samples in the 72 pedigrees and of these 79 were CF cases. Their ethnicity was as follows: 198-White, 7-Hispanic; 196-American, 6-Mexican, and 3- Unknown (**Supplementary Table 1**). A correction for ethnicity and sex was performed in the analysis but no correction was made for age. The lung function was assessed by standard spirometry, and for children, <5 years of age, assessment of disease severity was done by the clinical scoring of CXR by the Wisconsin Scoring System (44, 45). CF disease severity was classified as mild, moderate, and severe by lung function impairment based on percent predicted forced expired volume in 1 sec (FEV_1). FEV_1/FVC: mild = 70–89%; moderate = 40–69%; severe $\leq$ 40% (Cystic Fibrosis Foundation). The number of patients in the present study under this classification is as follows: severe in 4 cases, moderate in 11 cases, and mild in 64 cases.

DNA Isolation

Genomic DNAs were prepared from blood samples using QIAamp Blood kit following the manufacturer's instructions (Qiagen, Valencia, CA, United States).

Selected Genetic Variations for This Study

The target surfactant protein genes, SFTPA1, SFTPA2, SFTPB, SFTPC, and SFTPD, were selected based on gene function and association with lung diseases (especially with CF) from our findings and other published data as described above. A total of 17 genetic SNPs were selected. These SNPs were previously shown to associate with various lung diseases, be important in function or structure, or other: 5 SNPs from SFTPA1, rs1059047, rs1136450, rs1136451, rs1059057, and rs4253527; 4 SNPs from SFTPA2, rs1059046, rs17886395, rs1965707, and 1965708; 4 SNPs from SFTPB, rs7316, rs2077079, rs3024798, and rs1130866; 2 SNPs from SFTPC, rs4715 and rs1124; and 2 SNPs from SFTPD, rs721917 and rs2243639. The SNP ID, other used name, nucleotide change, and association with human disease as well as related references are given in **Table 1**. The genotype frequencies of these SNPs in mild and moderate CF compared to controls are given in **Supplementary Table 2**.

Genotype Analysis

The PCR-based RFLP or cRFLP (135) method was used for genotyping as described in previous publications for SFTPA1, SFTPA2, and SFTPD (136, 137), SFTPB (133, 137), and SFTPC (61). The PCR primer sequences and restriction enzymes used are given in **Table 2**. Briefly, PCRs were performed at 95°C for 2 min, 5 cycles of 95°C for 30 seconds, 50°C for 1 min, and 70°C for 1 min, then 25 cycles of 95°C for 30 s, 55°C for 1 min, and 70°C for 1 min, followed by an extension at 70°C for 4 min. Five microliter of each PCR products were used for appropriate restriction enzyme digestion (**Table 2**). The digested PCR product was separated by 8 or 10% of PAGE gel (based on the length of digested PCR fragments). The genotyping was done blindly. As samples (CF and Controls) were received, each was given a sequential laboratory number with no other identifiers and were genotyped all together without knowledge as to which sample is CF or Control. Therefore we believe that there was no bias in the genotyping. The genotype was scored based on the pattern of the digested PCR products for each sample.

Statistical Analysis

We used the Wang et al.'s (138) approach (provides computer code (written in R) for public use), which is a more efficient approach compared to more traditional methods (139) to test and estimate genetic effects of each pair of the 17 SNPs. This approach integrates the principle of quantitative genetics, enabling the decomposition of the overall genetic effect into different components: the additive (a) and dominant genetic effects (d) of each SNP and additive x additive (aa), additive x dominant (ad), dominant x additive (da), and dominant x dominant epistatic effects (dd) between the two SNPs. By estimating the role of each of these components, this approach can provide a better understanding of inheritance mode by which SNPs impact the disease. By analyzing each SNP pair, we calculated *p*-values for each genetic component. A Bonferroni correction was used to adjust for multiple comparisons.

RESULTS

Association of the Surfactant Protein Genes With CF

Associations of single SNPs or SNP-SNP interactions with CF discussed below are shown in **Tables 3**, **4**. The SNPs studied here are not rare alleles (136). The column "interaction type," in **Table 3** as well as in subsequent relevant tables, is the type of the SNP-SNP interaction (interaction between two SNPs within a given gene - intragenic, or interaction between SNPs of two genes-intergenic). The letter a or d is for additive effect or dominant effect. The number 1 or 2 is for the SNP1 or SNP2. In **Table 3** the d1 stands for a dominant effect for SNP1, and d2 stands for a dominant effect for SNP2. If it is a1d2 (**Table 4**), the interaction type is additive effect for SNP1 and dominant effect for SNP2. For example in **Table 4**, (1) SFTPC rs1124 has a significant dominant effect (d2) ($P = 0.0053$). This means that the heterozygote is beyond the mean of two homozygotes in the degree of severity at this SNP. (2) SFTPA1 rs1059047 × SFTPC rs1124 has a significant additive x dominant epistatic effect (a1d2) ($P = 0.0014$). This means that the combination of the homozygote at the first SNP and the heterozygote at the second SNP is significantly different from other combinations. (3) SFTPA1 rs1059047 × SFTPC rs1124 has a significant dominant x dominant epistatic effect (d1d2) ($P = 0.0021$). This means that the combination of the heterozygote at the first SNP and the heterozygote at the second SNP is significantly different from other combinations. In general, it looks like SFTPB and SFTPC have a dominant effect in most of the interactions, whereas the

TABLE 1 | Genetic variations of surfactant proteins SFTPA1, SFTPA2, SFTPB, SFTPC, and SFTPD association with disease.

Gene	Variation ID	Other used name	Nucleotide	Disease association	References
SFTPA2*	rs1059046	aa9 Asn/Thr	A/C	Respiratory syncytial virus (RSV), Influenza, Asthma, Pneumonia infection	(46–50)
	rs17886395	aa91 Pro/Ala	C/G	RSV, Tuberculosis (TB), Asthma	(46, 48, 51, 52)
	rs1965707	aa140 Ser/Ser	C/T	Asthma	(46)
	rs1965708	aa223 Gln/Lys	C/A	TB, Allergic rhinitis, High altitude pulmonary edema, RSV, recurrent Urinary tract infection (UTI), Meningococcal infection, Influenza	(46, 48, 49, 51–59)
SFTPA1*	rs1059047	aa19 Ala/Val	C/T	Idiopathic pulmonary fibrosis (IPF), Pneumonia infection, Asthma, RSV	(46, 48, 51, 53, 56, 60)
	rs1136450	aa50 Leu/Val	C/G	IPF, Pneumonia infection, Asthma, TB	(46, 48, 61, 62)
	rs1136451	aa62 Pro/Pro	G/A	TB, IPF, Chronic obstructive pulmonary disease (COPD)	(17, 52, 61, 63)
	rs1059057	aa133 Thr/Thr	G/A	Asthma	(46)
	rs4253527	aa219 Arg/Trp	C/T	TB, IPF, Influenza, Asthma, Pneumonia infection	(46, 48, 52, 61–64)
SFTPB*	rs2077079**	CA-18, CA1022	C/A	RSV, Respiratory distress syndrome (RDS), COPD, Asthma	(65–70)
	rs3024798**	CA1013, CA2052	A/C	Invasive pneumococcal disease (IPD), RDS	(69, 71)
	rs1130866†	TC1580, TC2619 aa131 Ile/Thr	T/C	COPD, Influenza, Pneumonia, RSV, Systemic Sclerosis, Acute lung injury	(50, 64, 65, 67–70, 72–84)
	rs7316**	AG9306, AG10345	A/G	Acute lung injury, RDS	(77, 85)
SFTPC‡	rs4715	aa138 Asn/Thr	A/C	RDS, Perinatal respiratory disease (PRD)	(86–89)
	rs1124	aa186 Asn/Ser	A/G	RDS, RSV, Asthma	(86, 88–90)
SFTPD‡	rs721917	aa11 Met/Thr	T/C	TB, Allergic rhinitis (AR), Asthma, COPD, RSV, Coronary artery stenosis, Bronchopulmonary dysplasia (BPD), RDS, Axial spondyloarthritis, Atherosclerosis, Sjogren syndrome, Interstitial lung diseases (ILDs), Type 2 diabetes (T2D), Inflammatory bowel disease (IBD)	(91–123)
	rs2243639	aa160 Thr/Ala	A/G	RSV, Ulcerative colitis (UC), BPD, RDS, COPD, IBD	(16, 54, 73, 77, 93, 94, 99, 101, 102, 106, 109, 111, 124–132)

**Numbering of amino acids in SFTPA2, SFTPA1, and SFTPB, is that of the precursor molecule i.e. includes the signal peptide. ‡Numbering of amino acids in SFTPC and SFTPD is based on the mature protein and does not include the signal peptide.*

*All the SNP changes are located within the exons, except the three SFTPB marked with **. The SFTPB a) rs2077079 is located 10 nt downstream of TATAA box, 5′ regulatory region (133); b) rs3024798 is located in the intron at the splice sequence of intron 2-exon 3 (65); and c) rs7316 is located in the 3′UTR 4 nucleotides upstream of the TAATAA polyadenylation signal (133). The SFTPB rs1130866 marked with † is located within a potential N-linked glycosylation site, which has been shown to be glycosylated (134).*

genes encoding the hydrophilic proteins exhibit primarily an additive effect (**Table 4**). We speculate that the surfactant related functions imparted by SP-B and SP-C variants play a critical differential role in pulmonary CF and that functions imparted by SP-A1/SP-A2 and SP-D variants further enhance the CF disease progression.

Single SNP or Intragenic Interactions

The data in **Table 3** showed that (1) SFTPB SNP rs7316 is associated with CF ($X^2 = 6.9689$, $p = 0.0083$); (2) another two SFTPB SNPs rs2077079 and rs3024798 are associated with CF through an intragenic interaction ($X^2 = 3.2688$, $p = 0.0325$). (3) SFTPC SNP rs1124 is associated with CF ($X^2 = 5.8674$, $p = 0.0154$); (4). Although no single SFTPA1 SNP by itself is associated with CF, the SFTPA1 rs1136451 SNP in an intragenic interaction with either SNP rs1059057 or rs4253527 is shown to associate with CF ($X^2 = 2.7329$, $9 = 0.0469$ or $X^2 = 3.5625$, $p = 0.0238$, respectively) (**Table 3**).

Intergenic Interactions Among the Surfactant Protein Genes

A total of 34 intergenic interactions of different combinations between SNPs of the studied genes were observed to associate with CF after Bonferroni correction. Significant interactions that include each of the studied genes are as follows: 19 interactions for SFTPB (X^2 is 2.045–8.3123, $p = 0.0398$–0.0043); 18 interactions for SFTPC (X^2 is *2.2285–8.4508*, $p = 0.0487$–0.0007); 13 interactions for SFTPA1 (X^2 is 2.2285–7.8947, $p = 0.0487$–0.0007), 9 interactions for SFTPA2 (X^2 is 2.4172–6.4974, $p = 0.0485$–0.0038), and 10 interactions for SFTPD (X^2 is 2.2285–8.4508, $p = 0.0487$–0.0007). Below, we present significant interactions where each interaction contains a SNP from a given gene.

Intergenic interactions that contain SFTPB SNPs

All of the 4 studied SFTPB SNPs, rs7316, rs2077679, rs3024798, and rs1130866, are associated with CF through 18 intergenic

TABLE 2 | PCR primers for the SNPs Study.

Gene	Variation ID		Primer sequence 5′ - 3′	Restriction enzyme	References
SFTPA2	rs1059046	F	GCT GTG CCC TCT GGC CCT Ta	Tru 91	(136)
		R	TCC TTT GAC ACC ATC TC		
	rs17886395	F	AGA GCG TGG AGA GAA GGG GcA	Bbv I	
		R	GGG TTT GTC TGA TCC CCA TC		
	rs1965707	F	CAT AAT GAC AGT AGG AGA GAA GGT CTT CTC	Bfa I	
		R	ACC CTC AGT CAG GCC TAC AT		
	rs1965708	F	GGA GCC TGC AGG TCG GGG AAA Atc G	αTaq I	
		R	TCA GAA CTC ACA GAT GGT CA		
SFTPA1	rs1059047	F	ACC TCA TCT TGA TGT CAG CCT CTG GTG CaG	Bbv I	(136)
		R	AGG GCC CAG GTC TCC TCT GA		
	rs1136450	F	ACC TCA TCT TGA TGT CAG CCT CTG GTG CaG	Dde I	
		R	AGG GCC AGG GTC TCC TcT GA		
	rs1136451	F	TTT TCT CTG CAG GCC CCA TGG GTg C	Hha I	
		R	GGG TTT GTC TGA TCC CCA TC		
	rs1059057	F	TCT GCA GGG CTC CAT ATT Gc	Msp I	
		R	CAC ACA CTG CTC TTT TCC tC		
	rs4253527	F	TCT GCA GGG CTC CAT ATT Gc	αTaq I	
		R	CAC ACA CTG CTC TTT TCC tC		(133)
SFTPB	rs2077079	F	GTC CAG CTA TAA GGG GCC GTG	ApaL I	
		R	GTG AGT GGT GGA GCT GCC TA		
	rs3024798	F	ACT CTT GTG TCC TCC ACC TTG	Nla III	
		R	GGC ATA GGT CAT CCT GGG CA		
	rs1130866	F	CTC GAA TTC ACT CGT GAA CTC CAG CAC CC	Dde I	
		R	GTG AGC TTG CAG CCC TCT CA		
	rs7316	F	CTG TGT AAT ACA ATG TCT GCA CTA	Bfa I	
		R	CTC GAA TTC TGC TGG GAT TGC AGG TGT GA		
SFTPC	rs4715	F	GCT GAT CGC CTA CAA GCC CAG	Spe I	(61)
		R	CTG GAA GTT GTG GAC TTT aCT A		
	rs1124	F	GAT GGA ATG CTC TCT GCA GG	Sac I	
		R	GCA CCT CGC CAC ACA GGG aG		
SFTPD	rs721917	F	CTC CTC TCT GCA CTG GTC AT	Fsp I	(136)
		R	ACC AGG GTG CAA GCA CTG cG		
	rs2243639	F	AGC GTG GAG TCC CTG GAA gC	Hha I	
		R	AGA TTC TCT CCA TGT TCC CAG		

Low case letters: mismatch to DNA sequence.

TABLE 3 | Genetic association of surfactant protein genes SFTPA1, SFTPB, and SFTPC with CF.

	Gene	SNP #1 ID	SNP #2 ID	Interaction type	x^2	*p*-value
Genetic association of STFPB and SFTPC with CF by a single SNP						
1	SFTPB	rs7316		d	6.9689	0.0083
2	SFTPC	rs1124		d	5.8674	0.0154
Genetic association of SFTPB and SFTPA1 with CF by intragenic SNP interaction						
3	SFTPB	rs2077079	rs3024798	d1	3.2688	0.0325
4	SFTPA1	rs1136451	rs1059057	d2	2.7329	0.0469
5	SFTPA1	rs1136451	rs4253527	d2	3.5625	0.0238

Interaction type: d - dominant, in single SNPs.
Number 1 and 2 in interaction type column; represent SNP1 and SNP2.
The d1 stands for a dominant effect for SNP1, and d2 stands for a dominant effect for SNP2.

TABLE 4 | Genetic association of surfactant protein genes SFTPA1, SFTPA2, SFTPB, SFTPC, and SFTPD with CF by intergenic interactions.

Interaction #	SNP #1		SNP #2		Interaction type	x^2	*p*-value
	Gene name	SNP ID	Gene name	SNP ID			
1	SFTPA1	rs1136450	SFTPA2	rs1059046	a1d2	3.1699	0.0485
2	SFTPA1	rs4253527	SFTPA2	rs1059046	a1	5.1800	0.0233
3	SFTPA1	rs1136450	SFTPB	rs7316	d1d2	2.7135	0.0213
4	SFTPA1	rs1059057	SFTPB	rs7316	d2	3.1499	0.0332
5	SFTPA1	rs4253527	SFTPB	rs7316	d2	3.2619	0.0303
6	SFTPA1	rs1059047	SFTPC	rs1124	d2	5.6874	0.0053
					a1d2	7.8947	0.0014
					d1d2	4.6019	0.0021
7	SFTPA1	rs1136451	SFTPC	rs1124	d2	6.1400	0.0007
					a1d2	6.5633	0.0449
					d1d2	3.4875	0.0027
8	SFTPA1	rs1059057	SFTPC	rs1124	d2	6.1715	0.0007
					d1	4.4217	0.0104
					a1d2	8.4508	0.0146
					d1d2	5.3013	0.0293
9	SFTPA1	rs1059047	SFTPC	rs4715	a1d2	3.1655	0.0487
10	SFTPA1	rs1136450	SFTPC	rs4715	a1d2	3.5583	0.0182
11	SFTPA1	rs1136450	SFTPC	rs1124	a1d2	4.1079	0.0187
12	SFTPA1	rs1136451	SFTPC	rs4715	d2	3.2576	0.0328
					a1d2	4.8166	0.0236
					d1d2	2.6958	0.0218
13	SFTPA1	rs4253527	SFTPC	rs1124	d2	2.2285	0.0404
14	SFTPA2	rs1059046	SFTPB	rs1130866	a1d2	3.4707	0.0390
15	SFTPA2	rs1965707	SFTPB	rs2077079	d1d2	4.1099	0.0043
16	SFTPA2	rs1965708	SFTPB	rs2077079	d1d2	2.4405	0.0262
17	SFTPA2	rs1965708	SFTPB	rs7316	d2	2.4172	0.0331
18	SFTPA2	rs17886395	SFTPC	rs1124	a1d2	6.4974	0.0038
					d2	3.6608	0.0257
19	SFTPA2	rs1059046	SFTPC	rs4715	a1d2	4.1992	0.0227
20	SFTPA2	rs1059046	SFTPC	rs1124	d2	2.9051	0.0471
					a1d2	4.1161	0.0221
21	SFTPB	rs2077079	SFTPC	rs1124	a1d2	3.5371	0.0344
22	SFTPB	rs1130866	SFTPC	rs4715	d1a2	4.6271	0.0121
23	SFTPB	rs1130866	SFTPC	rs1124	d2	3.9303	0.0207
24	SFTPB	rs7316	SFTPC	rs1124	d2	2.4947	0.0303
					a1d2	2.4947	0.0392
25	SFTPB	rs2077079	SFTPD	rs2243639	a1a2	8.3123	0.0058
26	SFTPB	rs3024798	SFTPD	rs2243639	a1a2	7.0808	0.0058
					a2	3.5108	0.0311
27	SFTPB	rs7316	SFTPD	rs2243639	d1d2	2.6436	0.0094
					d2	2.0495	0.0494
28	SFTPB	rs2077079	SFTPD	rs721917	a1a2	5.4000	0.0108
					d1d2	2.6197	0.0306
29	SFTPB	rs3024798	SFTPD	rs721917	a1a2	4.4454	0.0398
					d1d2	2.5095	0.0242
					d1a2	4.0265	0.0151
30	SFTPB	rs1130866	SFTPD	rs721917	d1a2	3.4263	0.0193
31	SFTPB	rs1130866	SFTPD	rs2243639	d2	3.1616	0.0382
					d1a2	3.0764	0.0347

(Continued)

TABLE 4 | Continued

Interaction #	SNP #1		SNP #2		Interaction type	x^2	*p*-value
	Gene name	SNP ID	Gene name	SNP ID			
32	SFTPC	rs4715	SFTPD	rs721917	d1a2	5.8333	0.0049
33	SFTPC	rs1124	SFTPD	rs721917	d1	5.0904	0.0075
					d1a2	4.5151	0.0099
34	SFTPC	rs1124	SFTPD	rs2243639	d1	4.4393	0.0247

A total of 34 interactions of the 5 surfactant protein genes are associated with CF. Interaction type: a - additive, d - dominant, ad - additive x dominant, da - dominant x additive, and dd - dominant x dominant between the two SNPs.
Number 1 and 2 in interaction type column; represent SNP1 and SNP2.
The a1 stands for a additive effect for SNP1 and a2 stands for additive effect for SNP2.
The d1 stands for a dominant effect for SNP1, and d2 stands for a dominant effect for SNP2.
The a1d2 stands for the interaction type is additive effect for SNP1 and dominant effect for SNP2.
The d1a2 stands for the interaction type is dominant effect for SNP1 and additive effect for SNP2.

SNP-SNP interactions with 3 SNPs in SFTPA1, 4 SNPs in SFTPA2, 4 SNPs in SFTPC, and 7 SNPs in SFTPD (X^2 is 2.045–8.3123, $p = 0.0398$–0.0043) (**Table 4**). Of the 18 intergenic SNP-SNP interactions that included SFTPB SNPs, only 4 contain SNPs from SFTPC encoding the other hydrophobic surfactant protein, whereas 14 interactions are with genes encoding the hydrophilic surfactant proteins, seven are with SFTPA (3 for SFTPA1 and 4 for SFTPA2) (**Figure 1A**) and seven with SFTPD (**Figure 1B**).

SFTPB SNP rs7316 is associated with CF by itself as noted above (**Table 3**), and by intergenic interactions with 3 SNPs in SFTPA1 ($n = 3$), one SNP in SFTPA2, one SNP in SFTPC, and one SNP in SFTPD. SFTPB SNP rs2077079 is associated with CF by intragenic interaction with rs3024798, and by intergenic interaction with SNPs in SFTPA2 ($n = 2$), SFTPC ($n = 1$), and SFTPD ($n = 2$). SFTPB SNP rs3024798 is associated with CF, in addition to the intragenic interaction with rs2077079 (noted above), by intergenic interactions with SFTPD ($n = 2$). SFTPB SNP rs1130866 is associated with CF by intergenic interaction with SFTPA2 ($n = 1$; **Figure 1A**), SFTPC ($n = 2$), and SFTPD ($n = 2$; **Figure 1B**).

Intergenic interactions that contain SFTPC SNPs

Both of the SFTPC SNPs studied, rs4715 and rs1124, are associated with CF through 18 intergenic SNP-SNP interactions with SNPs in SFTPA1, SFTPA2, SFTPC, and SFTPD (X^2 is 2.2285–8.4508, $p = 0.0487$–0.0007) (**Table 4**). Of the 18 intergenic SNP-SNP interactions associated with CF, eight are with SFTPA1, three are with SFTPA2, four are with SFTPB (**Figure 1A**), and three are with SFTPD (**Figure 1B**).

Of the 18 intergenic SFTPC SNP-SNP interactions, only 4 are with SFTPB the gene that encodes the other hydrophobic surfactant protein, whereas 14 interactions are with genes encoding the hydrophilic surfactant proteins (8 for SFTPA1, 3 for SFTPA2, and 3 for SFTPD). SNP rs1124 as noted above (**Table 3**) is associated with CF by itself, and by 11 intergenic SNP-SNP interactions of the surfactant protein genes, SFTPA1, SFTPA2, SFTPB (**Figure 1A**), and SFTPD (**Figure 1B**). SNP rs4715 is associated with CF by 7 intergenic SNP-SNP interactions with SFTPA1, SFTPA2, SFTPB (**Figure 1A**), and SFTPD (**Figure 1B**).

Intergenic interactions that contain SFTPA1 SNPs

All of the 5 studied SFTPA1 SNPs are associated with CF through 13 intergenic SNP-SNP interactions with SNPs in SFTPA2 ($n = 2$), SFTPB ($n = 3$), and SFTPC ($n = 8$) (X^2 is 2.2285–7.8947, $p = 0.0487$–0.0007) (**Table 4**, **Figure 1A**). Of interest, no SNP-SNP interaction was observed with SFTPD. Each SFTPA1 SNP is shown to have 1–3 intergenic SNP interactions with the other surfactant protein genes. 1) SNP rs1136451 exhibits a significant association with CF through interactions with another two SFTPA1 SNPs (rs1059057 and rs4253527), as well as with both SFTPC SNPs (rs1124 and rs4715). 2) SNPs rs1136450 and rs4253527 are associated with CF through interaction with SNP rs1059046 of the SFTPA2.

Of the 13 intergenic SFTPA1 SNP-SNP interactions, 11 are with SFTPB and SFTPC encoding the hydrophobic surfactant proteins, and only two interactions are with SFTPA2 that encodes the hydrophilic surfactant protein A2 (**Figure 1A**), whereas no interactions are observed with SFTPD.

Intergenic interactions that contain SFTPA2 SNPs

Each SFTPA2 SNP is shown to have 1–3 intergenic SNP interactions with other surfactant protein genes. **Table 4** shows that the SFTPA2 gene is associated with CF through 9 intergenic SNP-SNP interactions with SFTPA1 ($n = 2$), SFTPB ($n = 4$), and SFTPC ($n = 3$) (X^2 is 2.4172–6.4974, $p = 0.0485$–0.0038, **Figure 1A**). Similarly to SFTPA1, no interaction of SFTPA2 with SFTPD was found to be associated with CF. SFTPA2 SNP rs1059046 appears to stand out from the other SFTPA2 SNPs studied, as this SNP (1) is associated with CF via five of the total nine interactions observed with the other SP genes, (2) is the only SNP that shows interactions with two SFTPA1 SNPs, and (3) shows interactions with both hydrophobic surfactant proteins SFTPB and SFTPC (**Figure 1A**). Of the 9 intergenic interactions, 7 are with the SFTPB and SFTPC hydrophobic surfactant proteins genes, and only two interactions are with the hydrophilic surfactant protein gene, SFTPA1, and no interactions were observed with SFTPD.

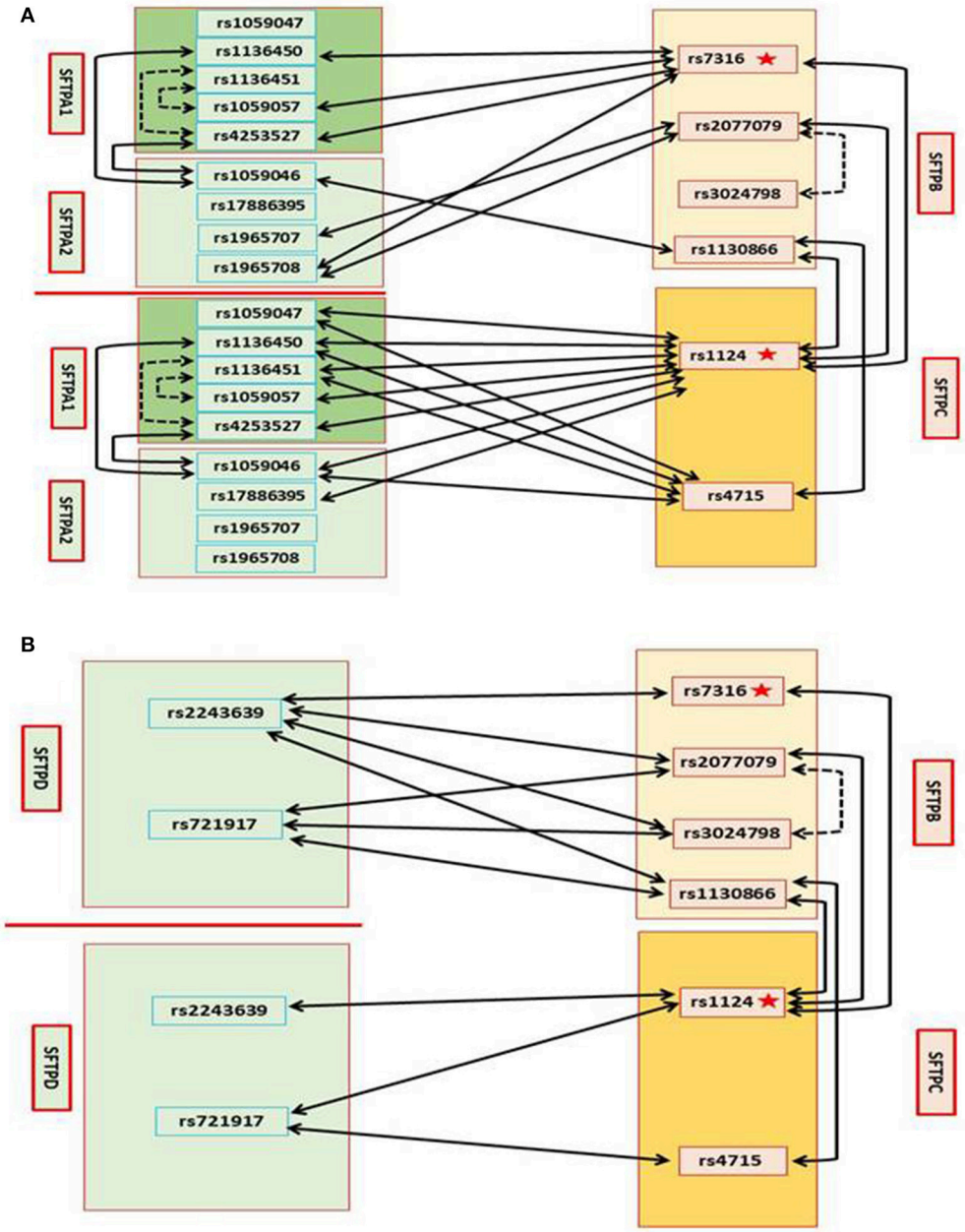

FIGURE 1 | Genetic interactions between SP genes and associations with CF **(A)**. Genetic association of SFTPB and SFTPC with CF by single SNP, and intragenic and intergenic SNP-SNP interactions between SFTPB and SFTPC, and with SFTPA1 and SFTPA2. On the left SNPs of the surfactant genes SFTPA1 and SFTPA2 encoding the hydrophilic surfactant proteins, SP-A1 and SP-A2 and on the right SNPs of the surfactant genes SFTPB and SFTPC, encoding the hydrophobic proteins, SP-B and SP-C, are shown **(B)**. Genetic association of SFTPB and SFTPC with CF by single SNP, and intragenic and intergenic SNP-SNP interactions between SFTPB and SFTPC, and with SFTPD. On the left SNPs of SFTPD and on the right SNPs of SFTPB and SFTPC are shown: In Figure, the star depicts a single SNP association with CF, the black dash line depicts intragenic interactions associated with CF, and the black solid line depicts intergenic interactions associated with CF.

Intergenic interactions that contain SFTPD SNPs

Table 4 shows that SFTPD is associated with CF through 10 intergenic SNP-SNP interactions with SNPs in SFTPB and SFTPC, but as noted above no interactions were observed with SFTPA1 or SFTPA2. Of the 10 intergenic SFTPD interactions associated with CF, seven of these are with SFTPB and three with SFTPC (X^2 is 2.2285–8.4508, $p = 0.0487$–0.0007) (**Figure 1B**). SFTPD SNP rs721917 is associated with CF through 5 intergenic interactions with SFTPB ($n = 3$) and SFTPC ($n = 2$); rs2243639 is associated with CF also through 5 intergenic interactions but four of these are with SFTPB and only one with SFTPC (**Figure 1B**).

In summary, when we studied the entire CF cohort, we observed a) Two SNPs (one from SFTPB and the other from SFTPC) to be individually associated with CF; b) Three intragenic interactions (2 of SFTPA1 and one of SFTPB) to associate with CF; c) A total of 34 intergenic interactions of different combinations between the various genes studied, except between SFTPD and SFTPA1 or SFTPA2, to associate with CF; A summary of all the significant intragenic and intergenic interactions is shown in **Supplementary Table 3**, and **Figure 2**. Moreover, our results have a potential clinical impact. For example, since SFTPA1 rs1059047 x SFTPC rs1124 has a significant additive x dominant epistatic effect (a1d2) ($P = 0.0014$), the combination of the homozygote at the first SNP and the heterozygote at the second SNP is significantly different from other combinations. Thus, we can make a prediction of patients' severity based on their genotypes at these two SNPs.

Association of the Surfactant Protein Genes With CF Disease Severity Subgroups

To gain insight into the contribution of the SP genes to CF disease severity, we separated the CF cohort into two subgroups, mild ($n = 64$) and moderate/severe ($n = 15$). The data showed that after Bonferroni correction a single SFTPB SNP (rs7316) to be associated with mild CF and no other SNPs were found to associate with either CF subgroup. However, there are a number of intergenic SNP interactions ($p < 0.01$ prior to Bonferroni correction) that associated with each CF subgroups (**Supplementary Table 4**).

Given the smaller number of subjects in each CF subgroup, and as we wished to gain further insight into the interactions observed, we focused our attention on significant associations ($p < 0.01$) observed in each subgroup that were also significant after Bonferroni correction in the entire CF group. These are shown in **Table 5** and **Figure 3**. Eight intergenic interactions were observed for the mild subgroup and only one for the moderate/severe subgroup. In the mild group, SNPs of the SFTPB exhibited the same number of interactions with SFTPD ($n = 4$) as they did with SFTPA1+SFTPA2 ($n = 4$). More interactions were observed between SFTPB and SFTPA1 ($n = 3$) than SFTPA2 ($n = 1$) in the mild subgroup. No significant associations with SFTPC were observed with either disease severity group. In addition similar to the entire CF group, no associations were found between SFTPD and SFTPA1 or SFTPA2 in either subgroup.

DISCUSSION

In this study, we investigated the genetic contribution of the surfactant protein genes, SFTPA1, SFTPA2, SFTPB, SFTPC, and SFTPD to CF and disease severity subgroups by genetic association analysis of single SNP and intragenic and intergenic SNP-SNP interactions. (a) For the entire CF group, we observed that all 5 surfactant protein genes are associated with CF by single

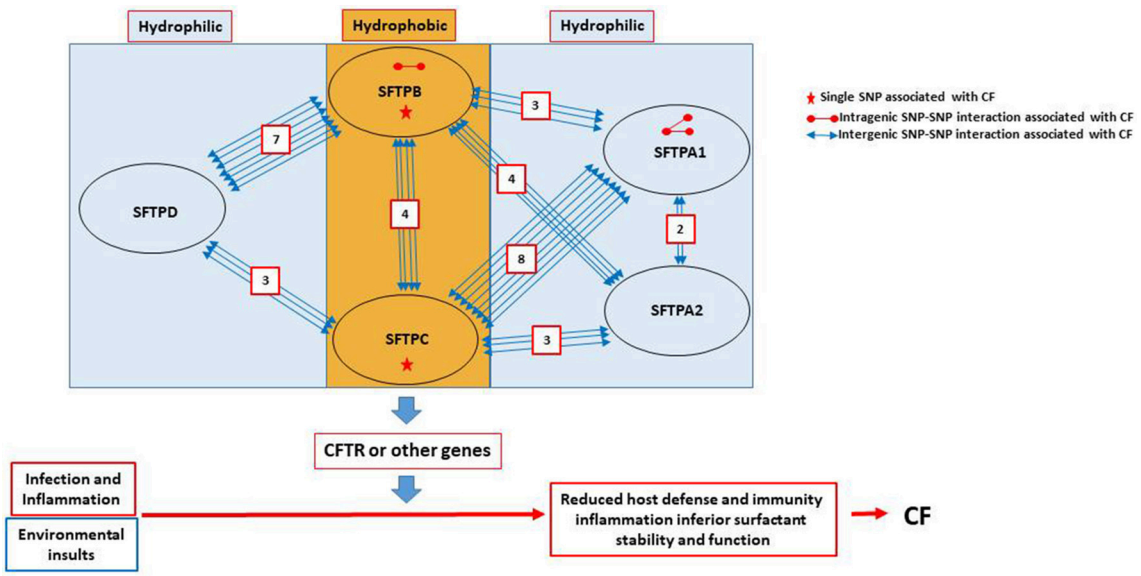

FIGURE 2 | Summary of SNP interactions between genes encoding the surfactant proteins. The cartoon in this figure depicts the observed associations and reveals the following: (a) No association between SFTPD and SFTPA1 or SFTPA2. (b) Out of the 34 intergenic interactions, 28 are between genes encoding the hydrophobic and the hydrophilic surfactant proteins. Only four are between genes (SFTPB and SFTPC) encoding the hydrophobic surfactant proteins and two are between genes (SFTPA1 and SFTPA2) encoding the hydrophilic SP-A1 and SP-A2. (c) SFTPC has the highest number of interactions with SFTPA1 ($n = 8$), while SFTPB has the highest number of interactions with SFTPD ($n = 7$). (d) SFTPB has a total of 14 intergenic interactions with genes encoding hydrophilic proteins, seven with SFTPD, four with SFTPA2, and three with SFTPA1. SFTPC also has 14 intergenic interactions, eight with SFTPA1, three with SFTPA2 and only 3 with SFTPD. (e) SFTPA1 has two intergenic interactions with SFTPA2, as well as intragenic interactions. (f) SFTPB is the only other gene (other than SFTPA1) that has an intragenic interaction. (g) Only SFTPB and SFTPC have each a single SNP association with CF.

TABLE 5 | Interactions in mild and moderate/severe CF subgroups with $p < 0.01$.

Interaction #	SNP #1		SNP #2		Interaction type	x^2	*p*-value
1	SFTPB	rs7316	SFTPA2	rs1965708	d1	3.66565180	0.00820001
2	SFTPB	rs7316	SFTPA1	rs1136450	d1d2	3.81926684	0.00607927
3	SFTPB	rs7316	SFTPA1	rs1059057	d1	4.77551020	0.00931902
4	SFTPB	rs7316	SFTPA1	rs4253527	d1	5.55638114	0.00510446
5	SFTPB	rs3024798	SFTPD	rs721917	d1d2	5.47559633	0.00077503
6	SFTPB	rs1130866	SFTPD	rs721917	d1a2	6.90124062	0.00057516
7	SFTPB	rs1130866	SFTPD	rs2243639	d1a2	5.83841692	0.00299812
8	SFTPB	rs7316	SFTPD	rs2243639	d1d2	3.49498711	0.00210045
9*	SFTPA2	rs1059046	SFTPA1	rs1136450	a1	2.29978355	0.00205943

These were significant after Bonferroni correction in the entire CF group.
*Interactions in mild subgroup (1–8); *Interaction in moderate/severe subgroup.*
Interaction type: a-additive, d- dominant, da - dominant x additive, and dd - dominant x dominant between the two SNPs.
Number 1 and 2 in interaction type column; represent SNP #1 and SNP #2.
The a1 stands for a additive effect for SNP1 and a2 stands for additive effect for SNP2.
The d1 stands for a dominant effect for SNP1, and d2 stands for a dominant effect for SNP2.
The d1a2 stands for the interaction type is dominant effect for SNP1 and additive effect for SNP2.

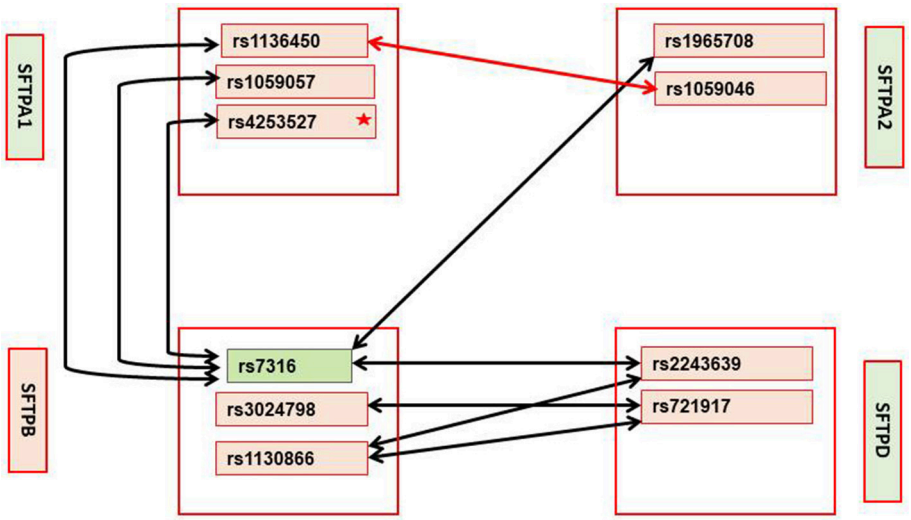

FIGURE 3 | Interactions in mild and moderate/severe CF subgroups with p-value < 0.01; these interactions were significant in the entire CF group after Bonferroni correction. *Mild CF:* Significant interactions between SFTPA1, SFTPA2, SFTPB, and SFTPD are shown with black arrows. Green box indicates the only SNP that remained significant after Bonferroni correction. Star (*) indicates that this SNP is significant at $p < 0.03$ by itself. Moderate/severe CF: Red arrow shows the only significant interaction at $p < 0.01$ that is also significant in the entire CF groups after Bonferroni correction. No significant interactions that include SNPs of the SFTPC are observed in either severity group.

SNP association, intragenic (**Table 3**), and/or intergenic SNP-SNP interactions (**Table 4**).(b) For the CF severity subgroups, we observed after Bonferroni correction a single SFTPB SNP to be associated with mild CF and several interactions ($p < 0.01$) to associate with mild or moderate/severe CF subgroups (**Supplementary Table 4** and **Table 5**).

Human diseases are complex and determined by environmental factors and genes. Single genetic mutations or multiple mutations in a single gene, constitute a part or a small part of disease mechanisms. To study the full spectrum of gene(s) contributing to a disease either by being the primary cause or by modifying disease expression, an integrated genetic approach is needed to understand genetic control and clinical therapy. By integrating quantitative genetic principles (138) a statistical method was developed to test associations of pairwise SNPs and disease in a case-control setting. This method can decompose the overall genetic effect into its underlying components and test the significance of each component, gaining insight into the mechanisms of how SNPs affect disease. It has been used in our previous studies in human inflammatory bowel diseases (IBD) that included both case-control and case-trios studies, and targeting SNPs in one gene and in multiple genes of a metabolic pathway (140, 141). Because this method is powerful and helps understand genetic contribution to a disease

via interactions of genes in a metabolic pathway or gene network, we used it in the present study.

Association of the Surfactant Protein Genes With the Entire CF Group

Association of the Hydrophobic Surfactant Protein Genes, SFTPB and SFTPC, With CF

Surfactant proteins SP-B and SP-C are hydrophobic membrane proteins that increase the rate that surfactant spreads over the alveolar surface, and are required for proper biophysical function of surfactant and lung function. SP-B is also important for SP-C processing, as indicated in SP-B deficient states where an aberrant SP-C was observed (7, 142, 143).

All four of the SFTPB SNPs studied showed significant interactions with SNPs of one or more SP genes. The rs7316 is located in the 3′-UTR and could affect regulation of polyadenylation (133) and has previously been associated with acute lung injury (77). This SFTPB SNP is not only significant by itself but interacts with SNPs of all 4 SP genes. The rs2077079 interacts with SNPs of all SP genes, except SFTPA1. It is located at 11 nt downstream of the TATA box and could affect gene transcription. The rs1130866, which also interacts with SNPs of SP genes, except SFTPA1, is a missense mutation that changes the encoded amino acid (Ile/Thr) and an N-linked glycosylation site of the protein, shown previously to be indeed glycosylated in the Thr-containing variant (1580_C) (134). This is a significant change and may be an important contributing factor in various diseases and/or in response to environmental oxidative stress. Moreover, the SFTPB 1580_C (rs1130866) genetic variant has been observed to be a risk factor in several lung disease, such as idiopathic pulmonary fibrosis (IPF) (61), chronic obstructive pulmonary disease (COPD) (17), acute respiratory distress syndrome (ARDS) (137), septic shock and those with risk of respiratory failure after community acquired pneumonia (144), as well as increases mortality, apoptosis, and lung injury in mice carrying the human SP-B 1580_C variant compared to those with the 1580-T variant (145). On the other hand, the SP-B1580-T/T (rs1130866) is associated with protection against interstitial lung disease (ILD) with systemic sclerosis (64). The rs3024798 is located within the splicing sequence of intron 2–exon 3, and although its effect on splicing is unknown (65) it has previously been associated with invasive pneumococcal disease (IPD) (71). This SNP, in addition to an intragenic interaction, is the only SNP that interacts with a single SP gene, the SFTPD. Together these SNP variations in SFTPB could affect SP-B function by altering N-linked glycosylation and/or affect regulation at several levels including transcription and splicing.

SP-C is a hydrophobic surfactant protein and plays an important role in surfactant function. Mutations in SP-C have also been shown to associate with a number of pulmonary diseases (15), such as ILD and pulmonary alveolar proteinosis (PAP). Both SFTPC variants are missense, where amino acids 186 and 138 are changed, Ser/Asn in rs1124, and Thr/Asn in rs4715, respectively. While both SNPs associate with CF through numerous intergenic interactions with the other SPs, the rs1124 is also associated with CF by itself. The potential mechanisms via which these may affect function are not known. The two SP-C variants (rs1124, Ser/Asn and rs4715, Thr/Asn) have previously been associated with RDS (86, 88, 89), and children infected with respiratory syncytial virus (RSV) (90).

In summary, the observations made indicate that the hydrophobic proteins, shown previously to be key in surfactant function and homeostasis and consequently in lung function may play a central role in CF. The only two individual SNPs to associate with CF by themselves were SNPs of SFTPB rs7316 ($p = 0.0083$) and SFTPC rs1124 ($p = 0.0154$) (indicated by star in **Figure 1A**). Moreover, of the 37 interactions shown to associate with CF, SFTPB or SFTPC was part of the 35 interactions. Given the importance of SP-B and SP-C in surfactant function and lung function, and the fact that lung function deterioration is a major issue in CF, it is likely that the SFTPB and SFTPC genes are modifier genes for CF lung function, by modulating surfactant structural organization and stability.

Association of Hydrophilic Surfactant Protein Genes SFTPA1/A2 and SFTPD With CF

The SP-A1, SP-A2, and SP-D mediate innate immunity in the lung and via interactions with the alveolar macrophage the sentinel cell of innate lung host defense, promote, among others, bacterial and viral phagocytosis, and cytokine production, as well as affect lung inflammatory processes. The mechanisms implicated in these processes may differ among these molecules (19). Of interest in the present study, there were no significant interactions between SNPs of SFTPD and SFTPA1 or SFTPA2 and only two significant intergenic interactions were observed between SFTPA1 and SFTPA2 (**Figure 1A**). A single SNP in SFTPA2 (rs1059046) interacted with two different SNPs in SFTPA1 (rs1136450, aa 50 Leu/Val and rs4253527, aa 219 Arg/Trp). The SFTPA2 SNP (rs1059046) changes the amino acid (Thr/Asn) at codon 9 of the precursor molecule which is part of the signal peptide, having the potential to affect processing of the SP-A2. This SNP was previously shown to associate with increased risk in RSV (47). The two SFTPA1 SNPs (rs1136450, rs4253527) that interact with this SFTPA2 SNP are located in the collagen-like domain and in the carbohydrate recognition domain (CRD), respectively, of the SP-A2 and change the encoded amino acid (rs1136450, aa 50 Leu/Val, rs4253527, aa 219 Arg/Trp). Moreover, higher- or lower-order of oligomerization of SP-A and SP-D is known to affect their functional capabilities (146–149), and has been observed that naturally occurring SP-A and SP-D oligomers have functional relevance in patients with chronic lung diseases such as CF (32, 35). Thus, each of the surfactant protein variants may differentially affect innate immune functions and in CF may each differentially modify lung host defense.

Multiple interactions between the hydrophobic and the hydrophilic protein genes were observed indicating that these two groups of proteins may co-operatively or synergistically contribute to the expression of pulmonary CF. As depicted in **Figure 2**, SFTPD SNPs are primarily found in interaction with SNPs of SFTPB ($n = 7$), whereas SNPs of SFTPA1 are primarily found in interactions with SNPs of SFTPC ($n = 8$). The latter is of interest because SP-A1 has been shown to

affect more efficiently (compared to SP-A2) the structural organization of surfactant (10), indicating that SP-A1 and SP-C may cooperatively affect surfactant structure, which in turn may affect surfactant function and lung function. Moreover, the large number of SNP interactions between SFTPD and SFTPB is puzzling and not intuitively understood as far as surfactant structure or function is concerned. This is because, although SP-D is generally found in the bronchoalveolar lavage fluid and significantly less in alveolar epithelia, and grouped with SP-A1/A2 based on its structural similarity and function with these proteins (5, 6), it is not found in the surfactant lipoprotein complex.

II. Association of the Surfactant Protein Genes With CF Subgroups

When we studied disease severity subgroups (mild and moderate/severe), we found after Bonferroni correction a single SFTPB SNP (rs7316) to associate with mild CF. This SNP has also been shown to associate with acute lung injury (77). Lack of SP-B is not compatible with life, and SP-B deficiency affects SP-C processing (7, 142, 143). This SFTPB SNP is located within the 3′UTR and may affect regulation of polyadenylation (133). Thus, this SFTPB SNP may contribute to CF either by affecting its regulation (133) and/or by affecting SP-C processing (7, 142, 143). In the CF subgroups of the eight significant intergenic interactions ($p < 0.01$) that were also significant in the entire CF group after Bonferroni correction, seven were for the mild group and one for the moderate/severe subgroup. The ones for the mild group all were between SFTPB SNPs and SNPs of the genes encoding the hydrophilic surfactant proteins.

The SFTPB SNP (rs7316) that is significant by itself in mild CF after Bonferroni correction was the only SFTPB SNP that interacted with SNPs of SFTPA1 or SFTPA2, whereas the SNP-SNP intergenic interactions between SFTPB and SFTPD include three of the four SFTPB SNPs studied. These indicate the importance of SFTPB in mild CF which may provide protection in the sense of enabling a milder form of pulmonary CF through its surfactant-associated function or perhaps other currently unknown function. Based on the differences of SNP-SNP interactions; it is likely that the mechanisms via which the hydrophilic proteins contribute to mild CF may differ. The SFTPA1 SNP (rs4253527) was also significant by itself ($p < 0.03$) (**Supplementary Table 4**) in the mild CF group. SP-A and SP-D bind via their carbohydrate recognition domains (CRD) to the carbohydrate motifs on bacteria, viruses, fungi, etc. (150–152). Thus, SNPs in CRD may differentially affect binding to various ligands to trigger the host's innate immune response. The SFTPA1 SNP (rs4253527) is located in the CRD and changes the encoded amino acid (Arg/Trp) holding the potential to differentially affect innate immunity under various conditions including oxidative stress, since Trp is more sensitive to oxidation than Arg (33). In fact SP-A1 variants that differ in CRD at rs4253527 have been shown to differ in their ability to enhance phagocytosis (153) and cytokine production (154). Moreover, SP-A1 has been shown to more efficiently affect surfactant reorganization (than SP-A2) in the alveolar space (10). Whether this SNP provides protection in CF via its role in surfactant function or innate immunity or both remains to be determined. Recently, SP-A1 and SP-A2 have been shown to differentially affect lung mechanics (12) indicating another role of the SP-As beyond innate immunity.

For the moderate/severe group the only significant interaction is between the SNP rs1136450, (aa 50 Leu/Val) of SFTPA1 and SNP rs1059046 (aa 9 Thr/Asn) of SFTPA2. This interaction may be unique to moderate/severe disease group because it was not identified in the mild group even in interactions with $p < 0.05$ (**Supplementary Table 4**). Similarly, interactions 1, 3, 4, 7, and 8 in the mild group (**Table 5**) were not identified in the moderate/severe disease group even in interactions with $p < 0.05$ (**Supplementary Table 4**), indicating that these may be unique to the mild CF group.

In summary, a single SNP of the SFTPB is a marker for mild pulmonary disease in CF. A number of intergenic interactions that all include SNPs of SFTPB as well as a single intragenic SFTPA1 and SFTPA2 interaction are likely to be markers for mild and moderate/severe pulmonary disease in CF, respectively.

Limitations of the study include: (a) The small number of subjects especially after the CF group was divided in the mild and moderate/severe subgroups. This also precluded analysis of the individual components of FEV_1 and FVC; (b) The limited clinical information; the samples were collected at an earlier time using only FEV_1 as a discriminator for the severity subgroups. However, this is still the main biomarker to assess disease severity. (c) The lack of associations with bacterial strain and correction for age. (d) The CFTR mutation is not known although most of the subjects are expected to carry the ΔF508, which is approximately found in 70% of the CF patients.

However, in spite of these limitations the present findings indicate that both groups of surfactant proteins, those involved in innate immunity, and those affecting surfactant functions, associate with CF via complex interactions. These may contribute to pulmonary disease progression in CF, by affecting surfactant structure and function and/or by affecting innate immunity functions. Altered surfactant leads to a compromised lung function, and lung function deterioration is a major setback in CF pulmonary disease. Similarly host defense and inflammatory processes are partially affected in CF and SPs may play a role in these. Thus, based on the collective information with regards to their function and the observations made here, the SP genes are likely to be significant gene modifiers of CF and must be studied further. As gene modifiers, SPs may explain the varied progression of the pulmonary disease in CF in terms of lung function and host defense.

DATA AVAILABILITY

All the data are presented as supplementary files.

ETHICS STATEMENT

All protocols used in this study were evaluated and approved by the institutional review board from the Human Subject

Protection Office of the Pennsylvania State University College of Medicine.

AUTHOR CONTRIBUTIONS

ZL analyzed and synthesized the data, contributed to the manuscript writing. NT analyzed and synthesized data for CF subgroups and contributed to manuscript writing. RW performed statistical analysis and contributed to manuscript writing. SD performed all the genotyping. MY assisted with statistical analysis. NJT attended to human subjects issues, sample collection and contributed to manuscript writing. XL checked genotype data sheets after multiple transfers. TL reviewed literature and made **Table 1**. SW helped with clinical assessment. JF designed the study and provided oversight to the entire project, involved in data analysis, integration, and writing of the manuscript.

FUNDING

This work was supported by NIH HL68947 of JF.

SUPPLEMENTARY MATERIAL

The Supplementary Material for this article can be found online at: https://www.frontiersin.org/articles/10.3389/fimmu.2018.02256/full#supplementary-material

REFERENCES

1. O'Sullivan BP, Freedman SD. Cystic fibrosis. *Lancet* (2009) 373:1891–904. doi: 10.1016/s0140-6736(09)60327-5
2. Buscher R, Eilmes KJ, Grasemann H, Torres B, Knauer N, Sroka K, et al. beta2 adrenoceptor gene polymorphisms in cystic fibrosis lung disease. *Pharmacogenetics* (2002) 12:347–53.
3. Boucher RC, Cotton CU, Gatzy JT, Knowles MR, Yankaskas JR. Evidence for reduced Cl- and increased Na^+ permeability in cystic fibrosis human primary cell cultures. *J Physiol*. (1988) 405:77–103.
4. Ratjen F, Doring G. Cystic fibrosis. *Lancet* (2003) 361:681–9. doi: 10.1016/s0140-6736(03)12567-6
5. Wright JR. Immunoregulatory functions of surfactant proteins. *Nat Rev Immunol*. (2005) 5:58–68. doi: 10.1038/nri1528
6. Kishore U, Greenhough TJ, Waters P, Shrive AK, Ghai R, Kamran MF, et al. Surfactant proteins SP-A and SP-D: structure, function and receptors. *Mol Immunol*. (2006) 43:1293–315. doi: 10.1016/j.molimm.2005.08.004
7. Serrano AG, Perez-Gil J. Protein-lipid interactions and surface activity in the pulmonary surfactant system. *Chem Phys Lipids* (2006) 141:105–18. doi: 10.1016/j.chemphyslip.2006.02.017
8. Phelps DS. Surfactant regulation of host defense function in the lung: a question of balance. *Pediatr Pathol Mol Med*. (2001) 20:269–92. doi: 10.1080/15513810109168822
9. Floros J, Wang G, Mikerov AN. Genetic complexity of the human innate host defense molecules, surfactant protein A1 (SP-A1) and SP-A2–impact on function. *Crit Rev Eukaryot Gene Expr*. (2009) 19:125–37. doi: 10.1615/CritRevEukarGeneExpr.v19.i2.30
10. Lopez-Rodriguez E, Pascual A, Arroyo R, Floros J, Perez-Gil J. Human pulmonary surfactant protein SP-A1 provides maximal efficiency of lung interfacial films. *Biophys J*. (2016) 111:524–36. doi: 10.1016/j.bpj.2016.06.025
11. Wang G, Taneva S, Keough KM, Floros J. Differential effects of human SP-A1 and SP-A2 variants on phospholipid monolayers containing surfactant protein B. *Biochim Biophys Acta* (2007) 1768:2060–9. doi: 10.1016/j.bbamem.2007.06.025
12. Thorenoor N, Zhang X, Umstead TM, Scott Halstead E, Phelps DS, Floros J. Differential effects of innate immune variants of surfactant protein-A1 (SFTPA1) and SP-A2 (SFTPA2) in airway function after Klebsiella pneumoniae infection and sex differences. *Respir Res*. (2018) 19:23. doi: 10.1186/s12931-018-0723-1
13. Sarker M, Jackman D, Booth V. Lung surfactant protein A (SP-A) interactions with model lung surfactant lipids and an SP-B fragment. *Biochemistry* (2011) 50:4867–76. doi: 10.1021/bi200167d
14. Floros J, Hoover RR. Genetics of the hydrophilic surfactant proteins A and D. *Biochim Biophys Acta* (1998) 1408:312–22.
15. Floros J, Thomas N. Genetic variation of surfactant protiens and lung injury, In: Nakos G and Papathanasiou A editors. *Surfactant in Pathogenesis and Treatment of Lung Disease*. India: Research Signpost (2009). pp. 25–48.
16. Silveyra P, Floros J. Genetic variant associations of human SP-A and SP-D with acute and chronic lung injury. *Front Biosci*. (2012) 17:407–29. doi: 10.2741/3935
17. Guo X, Lin HM, Lin Z, Montano M, Sansores R, Wang G, et al. Surfactant protein gene A, B, and D marker alleles in chronic obstructive pulmonary disease of a Mexican population. *Eur Respir J*. (2001) 18:482–90.
18. Sorensen GL. Surfactant protein D in respiratory and non-respiratory diseases. *Front Med*. (2018) 5:18. doi: 10.3389/fmed.2018.00018
19. Nayak A, Dodagatta-Marri E, Tsolaki AG, Kishore U. An Insight into the diverse roles of surfactant proteins, SP-A and SP-D in innate and adaptive immunity. *Front Immunol*. (2012) 3:131. doi: 10.3389/fimmu.2012.00131
20. Carreto-Binaghi LE, Aliouat el M, Taylor ML. Surfactant proteins, SP-A and SP-D, in respiratory fungal infections: their role in the inflammatory response. *Respir Res*. (2016) 17:66. doi: 10.1186/s12931-016-0385-9
21. Nogee LM, Wert SE, Proffit SA, Hull WM, Whitsett JA. Allelic heterogeneity in hereditary surfactant protein B (SP-B) deficiency. *Am J Respir Crit Care Med*. (2000) 161(3 Pt 1):973–981. doi: 10.1164/ajrccm.161.3.9903153
22. Noah TL, Murphy PC, Alink JJ, Leigh MW, Hull WM, Stahlman MT, et al. Bronchoalveolar lavage fluid surfactant protein-A and surfactant protein-D are inversely related to inflammation in early cystic fibrosis. *Am J Respir Crit Care Med*. (2003) 168:685–91. doi: 10.1164/rccm.200301-005OC
23. Hull J, South M, Phelan P, Grimwood K. Surfactant composition in infants and young children with cystic fibrosis. *Am J Respir Crit Care Med*. (1997) 156:161–5. doi: 10.1164/ajrccm.156.1.9609090
24. Griese M, Birrer P, Demirsoy A. Pulmonary surfactant in cystic fibrosis. *Eur Respir J*. (1997) 10:1983–8.
25. Meyer KC, Sharma A, Brown R, Weatherly M, Moya FR, Lewandoski J, et al. Function and composition of pulmonary surfactant and surfactant-derived fatty acid profiles are altered in young adults with cystic fibrosis. *Chest* (2000) 118:164–74. doi: 10.1378/chest.118.1.164
26. Griese M, Essl R, Schmidt R, Rietschel E, Ratjen F, Ballmann M, et al. Pulmonary surfactant, lung function, and endobronchial inflammation in cystic fibrosis. *Am J Respir Crit Care Med*. (2004) 170:1000–5. doi: 10.1164/rccm.200405-575OC
27. Peterson-Carmichael SL, Harris WT, Goel R, Noah TL, Johnson R, Leigh MW, et al. Association of lower airway inflammation with physiologic findings in young children with cystic fibrosis. *Pediatr Pulmonol*. (2009) 44:503–11. doi: 10.1002/ppul.21044
28. Bernhard W, Haagsman HP, Tschernig T, Poets CF, Postle AD, van Eijk ME, et al. Conductive airway surfactant: surface-tension function, biochemical composition, and possible alveolar origin. *Am J Respir Cell Mol Biol*. (1997) 17:41–50. doi: 10.1165/ajrcmb.17.1.2594
29. Postle AD, Mander A, Reid KB, Wang JY, Wright SM, Moustaki M, et al. Deficient hydrophilic lung surfactant proteins A and D with normal surfactant phospholipid molecular species in cystic fibrosis. *Am J Respir Cell Mol Biol*. (1999) 20:90–8. doi: 10.1165/ajrcmb.20.1.3253

30. Griese M, Essl R, Schmidt R, Ballmann M, Paul K, Rietschel E, et al. Sequential analysis of surfactant, lung function and inflammation in cystic fibrosis patients. *Respir Res*. (2005) 6:133. doi: 10.1186/1465-9921-6-133
31. Olesen HV, Holmskov U, Schiotz PO, Sorensen GL. Serum-surfactant SP-D correlates inversely to lung function in cystic fibrosis. *J Cyst Fibros* (2010) 9:257–62. doi: 10.1016/j.jcf.2010.03.011
32. Griese M, Heinrich S, Ratjen F, Kabesch M, Paul K, Ballmann M, et al. Surfactant protein a in cystic fibrosis: supratrimeric structure and pulmonary outcome. *PLoS ONE* (2012) 7:e51050. doi: 10.1371/journal.pone.0051050
33. Wang G, Bates-Kenney SR, Tao JQ, Phelps DS, Floros J. Differences in biochemical properties and in biological function between human SP-A1 and SP-A2 variants, and the impact of ozone-induced oxidation. *Biochemistry* (2004) 43:4227–39. doi: 10.1021/bi036023i
34. Choi EH, Ehrmantraut M, Foster CB, Moss J, Chanock SJ. Association of common haplotypes of surfactant protein A1 and A2 (SFTPA1 and SFTPA2) genes with severity of lung disease in cystic fibrosis. *Pediatr Pulmonol*. (2006) 41:255–62. doi: 10.1002/ppul.20361
35. Kotecha S, Doull I, Davies P, McKenzie Z, Madsen J, Clark HW, et al. Functional heterogeneity of pulmonary surfactant protein-D in cystic fibrosis. *Biochim Biophys Acta* (2013) 1832:2391–400. doi: 10.1016/j.bbadis.2013.10.002
36. Parad RB, Gerard CJ, Zurakowski D, Nichols DP, Pier GB. Pulmonary outcome in cystic fibrosis is influenced primarily by mucoid Pseudomonas aeruginosa infection and immune status and only modestly by genotype. *Infect Immun*. (1999) 67:4744–50.
37. Buscher R, Grasemann H. Disease modifying genes in cystic fibrosis: therapeutic option or one-way road? *Naunyn Schmiedebergs Arch Pharmacol*. (2006) 374:65–77. doi: 10.1007/s00210-006-0101-2
38. Guillot L, Beucher J, Tabary O, Le Rouzic P, Clement A, Corvol H. Lung disease modifier genes in cystic fibrosis. *Int J Biochem Cell Biol*. (2014) 52:83–93. doi: 10.1016/j.biocel.2014.02.011
39. de Lima Marson FA, Bertuzzo CS, Ribeiro JD. Personalized drug therapy in cystic fibrosis: from fiction to reality. *Curr Drug Targets* (2015) 16:1007–17. doi: 10.2174/1389450115666141128121118
40. De Boeck K, Amaral MD. Progress in therapies for cystic fibrosis. *Lancet Respir Med*. (2016) 4:662–74. doi: 10.1016/s2213-2600(16)00023-0
41. Marson FAL. Disease-modifying genetic factors in cystic fibrosis. *Curr Opin Pulm Med*. (2018) 24:296–308. doi: 10.1097/mcp.0000000000000479
42. Floros J, Kala P. Surfactant proteins: molecular genetics of neonatal pulmonary diseases. *Annu Rev Physiol*. (1998) 60:365–84. doi: 10.1146/annurev.physiol.60.1.365
43. Liu W, Bentley CM, Floros J. Study of human SP-A, SP-B and SP-D loci: allele frequencies, linkage disequilibrium and heterozygosity in different races and ethnic groups. *BMC Genet*. (2003) 4:13. doi: 10.1186/1471-2156-4-13
44. Weatherly MR, Palmer CG, Peters ME, Green CG, Fryback D, Langhough R, et al. Wisconsin cystic fibrosis chest radiograph scoring system. *Pediatrics* (1993) 91:488–95.
45. Koscik RE, Kosorok MR, Farrell PM, Collins J, Peters ME, Laxova A, et al. Wisconsin cystic fibrosis chest radiograph scoring system: validation and standardization for application to longitudinal studies. *Pediatr Pulmonol*. (2000) 29:457–67. doi: 10.1002/(SICI)1099-0496(200006)29:6<457::AID-PPUL8>3.0.CO;2-9
46. Pettigrew MM, Gent JF, Zhu Y, Triche EW, Belanger KD, Holford TR, et al. Respiratory symptoms among infants at risk for asthma: association with surfactant protein A haplotypes. *BMC Med Genet*. (2007) 8:15. doi: 10.1186/1471-2350-8-15
47. El Saleeby CM, Li R, Somes GW, Dahmer MK, Quasney MW, DeVincenzo JP. Surfactant protein A2 polymorphisms and disease severity in a respiratory syncytial virus-infected population. *J Pediatr*. (2010) 156:409–14. doi: 10.1016/j.jpeds.2009.09.043
48. Garcia-Laorden MI, Rodriguez de Castro F, Sole-Violan J, Rajas O, Blanquer J, Borderias L, et al. Influence of genetic variability at the surfactant proteins A and D in community-acquired pneumonia: a prospective, observational, genetic study. *Crit Care* (2011) 15:R57. doi: 10.1186/cc10030
49. Herrera-Ramos E, Lopez-Rodriguez M, Ruiz-Hernandez JJ, Horcajada JP, Borderias L, Lerma E, et al. Surfactant protein A genetic variants associate with severe respiratory insufficiency in pandemic influenza A virus infection. *Crit Care* (2014) 18:R127. doi: 10.1186/cc13934
50. Dudina KR, Kutateladze MM, Bokova NO, Znoiko OO, Abramov DD, Kelly EI, et al. [ASSOCIATION OF POLYMORPHISM GENES OF SURFACTANT PROTEINS IN PATIENTS WITH INFLUENZA]. *Zh Mikrobiol Epidemiol Immunobiol* (2015) 6:71–7.
51. Lofgren J, Ramet M, Renko M, Marttila R, Hallman M. Association between surfactant protein A gene locus and severe respiratory syncytial virus infection in infants. *J Infect Dis*. (2002) 185:283–9. doi: 10.1086/338473
52. Malik S, Greenwood CM, Eguale T, Kifle A, Beyene J, Habte A, et al. Variants of the SFTPA1 and SFTPA2 genes and susceptibility to tuberculosis in Ethiopia. *Hum Genet*. (2006) 118:752–9. doi: 10.1007/s00439-005-0092-y
53. Saxena S, Kumar R, Madan T, Gupta V, Muralidhar K, Sarma PU. Association of polymorphisms in pulmonary surfactant protein A1 and A2 genes with high-altitude pulmonary edema. *Chest* (2005) 128:1611–9. doi: 10.1378/chest.128.3.1611
54. Grupe A, Li Y, Rowland C, Nowotny P, Hinrichs AL, Smemo S, et al. A scan of chromosome 10 identifies a novel locus showing strong association with late-onset Alzheimer disease. *Am J Hum Genet*. (2006) 78:78–88. doi: 10.1086/498851
55. Jack DL, Cole J, Naylor SC, Borrow R, Kaczmarski EB, Klein NJ, et al. Genetic polymorphism of the binding domain of surfactant protein-A2 increases susceptibility to meningococcal disease. *Clin Infect Dis*. (2006) 43:1426–33. doi: 10.1086/508775
56. Liu J, Hu F, Liang W, Wang G, Singhal PC, Ding G. Polymorphisms in the surfactant protein a gene are associated with the susceptibility to recurrent urinary tract infection in chinese women. *Tohoku J Exp Med*. (2010) 221:35–42. doi: 10.1620/tjem.221.35
57. Deng Y, Chen S, Chen J, Tao Z, Kong Y, Xu Y, et al. Relationship between surfactant protein A polymorphisms and allergic rhinitis in a Chinese Han population. *Mol Biol Rep*. (2011) 38:1475–82. doi: 10.1007/s11033-010-0254-4
58. Foster MW, Thompson JW, Ledford JG, Dubois LG, Hollingsworth JW, Francisco D, et al. Identification and quantitation of coding variants and isoforms of pulmonary surfactant protein a. *J Proteome Res*. (2014) 13:3722–32. doi: 10.1021/pr500307f
59. Wu AL, Xiong YS, Li ZQ, Liu YG, Quan Q, Wu LJ. Correlation between single nucleotide polymorphisms in hypoxia-related genes and susceptibility to acute high-altitude pulmonary edema. *Genet Mol Res*. (2015) 14:11562–72. doi: 10.4238/2015.September.28.8
60. Pettigrew MM, Gent JF, Zhu Y, Triche EW, Belanger KD, Holford TR, et al. Association of surfactant protein A polymorphisms with otitis media in infants at risk for asthma. *BMC Med Genet*. (2006) 7:68. doi: 10.1186/1471-2350-7-68
61. Selman M, Lin HM, Montano M, Jenkins AL, Estrada A, Lin Z, et al. Surfactant protein A and B genetic variants predispose to idiopathic pulmonary fibrosis. *Hum Genet*. (2003) 113:542–50. doi: 10.1007/s00439-003-1015-4
62. Cooper DN, Kehrer-Sawatzki H. Exploring the potential relevance of human-specific genes to complex disease. *Hum Genomics* (2011) 5:99–107. doi: 10.1186/1479-7364-5-2-99
63. Guan J, Liu X, Xie J, Xu X, Luo S, Wang R, et al. Surfactant protein a polymorphism is associated with susceptibility to chronic obstructive pulmonary disease in Chinese Uighur population. *J Huazhong Univ Sci Technolog Med Sci*. (2012) 32:186–9. doi: 10.1007/s11596-012-0033-7
64. Sumita Y, Sugiura T, Kawaguchi Y, Baba S, Soejima M, Murakawa Y, et al. Genetic polymorphisms in the surfactant proteins in systemic sclerosis in Japanese: T/T genotype at 1580 C/T (Thr131Ile) in the SP-B gene reduces the risk of interstitial lung disease. *Rheumatology (Oxford)* (2008) 47:289–91. doi: 10.1093/rheumatology/kem355
65. Lin Z, deMello DE, Wallot M, Floros, J. An SP-B gene mutation responsible for SP-B deficiency in fatal congenital alveolar proteinosis: evidence for a mutation hotspot in exon 4. *Mol Genet Metab*. (1998) 64:25–35. doi: 10.1006/mgme.1998.2702
66. Floros J, Fan R, Diangelo S, Guo X, Wert J, Luo J. Surfactant protein (SP) B associations and interactions with SP-A in white and black subjects with respiratory distress syndrome. *Pediatr Int*. (2001) 43:567–76. doi: 10.1046/j.1442-200X.2001.01474.x

67. Puthothu B, Forster J, Heinze J, Heinzmann A, Krueger M. Surfactant protein B polymorphisms are associated with severe respiratory syncytial virus infection, but not with asthma. *BMC Pulm Med*. (2007) 7:6. doi: 10.1186/1471-2466-7-6
68. Foreman MG, DeMeo DL, Hersh CP, Carey VJ, Fan VS, Reilly JJ, et al. Polymorphic variation in surfactant protein B is associated with COPD exacerbations. *Eur Respir J*. (2008) 32:938–44. doi: 10.1183/09031936.00040208
69. Hamvas A, Heins HB, Guttentag SH, Wegner DJ, Trusgnich MA, Bennet KW, et al. Developmental and genetic regulation of human surfactant protein B in vivo. *Neonatology* (2009) 95:117–24. doi: 10.1159/000153095
70. Baekvad-Hansen M, Nordestgaard BG, Dahl M. Surfactant protein B polymorphisms, pulmonary function and COPD in 10,231 individuals. *Eur Respir J*. (2011) 37:791–9. doi: 10.1183/09031936.00026410
71. Lingappa JR, Dumitrescu L, Zimmer SM, Lynfield R, McNicholl JM, Messonnier NE, et al. Identifying host genetic risk factors in the context of public health surveillance for invasive pneumococcal disease. *PLoS ONE* (2011) 6:e23413. doi: 10.1371/journal.pone.0023413
72. Lin Z, Wang G, Demello DE, Floros J. An alternatively spliced surfactant protein B mRNA in normal human lung: disease implication. *Biochem J*. (1999) 343(Pt 1):145–149.
73. Hersh CP, Demeo DL, Lange C, Litonjua AA, Reilly JJ, Kwiatkowski D, et al. Attempted replication of reported chronic obstructive pulmonary disease candidate gene associations. *Am J Respir Cell Mol Biol*. (2005) 33:71–8. doi: 10.1165/rcmb.2005-0073OC
74. Wood AM, Stockley RA. The genetics of chronic obstructive pulmonary disease. *Respir Res*. (2006) 7:130. doi: 10.1186/1465-9921-7-130
75. Raleigh SM, Davies BM, Cleal D, Ribbans WJ. No association between coding polymorphism within Exon 4 of the human surfactant protein B gene and pulmonary function in healthy men. *J Physiol Sci*. (2007) 57:199–202. doi: 10.2170/physiolsci.SC002607
76. Wood AM, Tan SL, Stockley RA. Chronic obstructive pulmonary disease: towards pharmacogenetics. *Genome Med*. (2009) 1:112. doi: 10.1186/gm112
77. Dahmer MK, O'Cain P, Patwari PP, Simpson P, Li SH, Halligan N, et al. The influence of genetic variation in surfactant protein B on severe lung injury in African American children. *Crit Care Med*. (2011) 39:1138–44. doi: 10.1097/CCM.0b013e31820a9416
78. Christie JD, Wurfel MM, Feng R, O'Keefe GE, Bradfield J, Ware LB, et al. Genome wide association identifies PPFIA1 as a candidate gene for acute lung injury risk following major trauma. *PLoS ONE* (2012) 7:e28268. doi: 10.1371/journal.pone.0028268
79. Guo Y, Gong Y, Pan C, Qian Y, Shi G, Cheng Q, et al. Association of genetic polymorphisms with chronic obstructive pulmonary disease in the Chinese Han population: a case-control study. *BMC Med Genomics* (2012) 5:64. doi: 10.1186/1755-8794-5-64
80. O'Mahony DS, Glavan BJ, Holden TD, Fong C, Black RA, Rona G, et al. Inflammation and immune-related candidate gene associations with acute lung injury susceptibility and severity: a validation study. *PLoS ONE* (2012) 7:e51104. doi: 10.1371/journal.pone.0051104
81. To KKW, Zhou J, Song YQ, Hung IFN, Ip WCT, Cheng ZS, et al. Surfactant protein B gene polymorphism is associated with severe influenza. *Chest* (2014) 145:1237–43. doi: 10.1378/chest.13-1651
82. Yang J, Wang B, Zhou HX, Liang BM, Chen H, Ma CL, et al. Association of surfactant protein B gene with chronic obstructive pulmonary disease susceptibility. *Int J Tuberc Lung Dis*. (2014) 18:1378–84. doi: 10.5588/ijtld.13.0569
83. Tochimoto A, Kawaguchi Y, Yamanaka H. Genetic susceptibility to interstitial lung disease associated with systemic sclerosis. *Clin Med Insights Circ Respir Pulm Med*. (2015) 9(Suppl. 1):135–140. doi: 10.4137/ccrpm.S23312
84. Ge L, Liu X, Chen R, Xu Y, Zuo YY, Cooney RN, et al. Differential susceptibility of transgenic mice expressing human surfactant protein B genetic variants to *Pseudomonas aeruginosa* induced pneumonia. *Biochem Biophys Res Commun*. (2016) 469:171–5. doi: 10.1016/j.bbrc.2015.11.089
85. Fatahi N, Niknafs N, Kalani M, Dalili H, Shariat M, Amini E, et al. Association of SP-B gene 9306 A/G polymorphism (rs7316) and risk of RDS. *J Matern Fetal Neonatal Med*. 31:2965–70. doi: 10.1080/14767058.2017.1359829
86. Lahti M, Marttila R, Hallman M. Surfactant protein C gene variation in the Finnish population - association with perinatal respiratory disease. *Eur J Hum Genet*. (2004) 12:312–20. doi: 10.1038/sj.ejhg.5201137
87. Salminen A, Paananen R, Karjalainen MK, Tuohimaa A, Luukkonen A, Ojaniemi M, et al. Genetic association of SP-C with duration of preterm premature rupture of fetal membranes and expression in gestational tissues. *Ann Med*. (2009) 41:629–42. doi: 10.1080/07853890903186176
88. Wambach JA, Yang P, Wegner DJ, An P, Hackett BP, Cole FS, et al. Surfactant protein-C promoter variants associated with neonatal respiratory distress syndrome reduce transcription. *Pediatr Res*. (2010) 68:216–20. doi: 10.1203/00006450-201011001-00421
89. Fatahi N, Dalili H, Kalani M, Niknafs N, Shariat M, Tavakkoly-Bazzaz J, et al. Association of SP-C gene codon 186 polymorphism (rs1124) and risk of RDS. *J Matern Fetal Neonatal Med*. (2017) 30:2585–9. doi: 10.1080/14767058.2016.1256994
90. Puthothu B, Krueger M, Heinze J, Forster J, Heinzmann A. Haplotypes of surfactant protein C are associated with common paediatric lung diseases. *Pediatr Allergy Immunol*. (2006) 17:572–7. doi: 10.1111/j.1399-3038.2006.00467.x
91. Floros J, Lin HM, Garcia A, Salazar MA, Guo X, DiAngelo S, et al. Surfactant protein genetic marker alleles identify a subgroup of tuberculosis in a Mexican population. *J Infect Dis*. (2000) 182:1473–8. doi: 10.1086/315866
92. Lahti M, Lofgren J, Marttila R, Renko M, Klaavuniemi T, Haataja R, et al. Surfactant protein D gene polymorphism associated with severe respiratory syncytial virus infection. *Pediatr Res*. (2002) 51:696–9. doi: 10.1203/00006450-200206000-00006
93. Pavlovic J, Papagaroufalis C, Xanthou M, Liu W, Fan R, Thomas NJ, et al. Genetic variants of surfactant proteins A, B, C, and D in bronchopulmonary dysplasia. *Dis Markers* (2006) 22:277–91. doi: 10.1155/2006/817805
94. Thomas NJ, Fan R, Diangelo S, Hess JC, Floros J. Haplotypes of the surfactant protein genes A and D as susceptibility factors for the development of respiratory distress syndrome. *Acta Paediatr*. (2007) 96:985–9. doi: 10.1111/j.1651-2227.2007.00319.x
95. Brandt EB, Mingler MK, Stevenson MD, Wang N, Khurana Hershey GK, Whitsett JA, et al. Surfactant protein D alters allergic lung responses in mice and human subjects. *J Allergy Clin Immunol*. (2008) 121:1140–7.e1142. doi: 10.1016/j.jaci.2008.02.011
96. Berg KK, Madsen HO, Garred P, Wiseth R, Gunnes S, Videm V. The additive contribution from inflammatory genetic markers on the severity of cardiovascular disease. *Scand J Immunol*. (2009) 69:36–42. doi: 10.1111/j.1365-3083.2008.02187.x
97. Deng YQ, Tao ZZ, Kong YG, Xiao BK, Chen SM, Xu Y, et al. Association between single nucleotide polymorphisms of surfactant protein D and allergic rhinitis in Chinese patients. *Tissue Antigens* (2009) 73:546–52. doi: 10.1111/j.1399-0039.2009.01232.x
98. Hilgendorff A, Heidinger K, Bohnert A, Kleinsteiber A, Konig IR, Ziegler A, et al. Association of polymorphisms in the human surfactant protein-D (SFTPD) gene and postnatal pulmonary adaptation in the preterm infant. *Acta Paediatr*. (2009) 98:112–7. doi: 10.1111/j.1651-2227.2008.01014.x
99. Thomas NJ, DiAngelo S, Hess JC, Fan R, Ball MW, Geskey JM, et al. Transmission of surfactant protein variants and haplotypes in children hospitalized with respiratory syncytial virus. *Pediatr Res*. (2009) 66:70–3. doi: 10.1203/PDR.0b013e3181a1d768
100. van Diemen CC, Postma DS, Aulchenko YS, Snijders PJ, Oostra BA, van Duijn CM, et al. Novel strategy to identify genetic risk factors for COPD severity: a genetic isolate. *Eur Respir J*. (2010) 35:768–75. doi: 10.1183/09031936.00054408
101. Foreman MG, Kong X, DeMeo DL, Pillai SG, Hersh CP, Bakke P, et al. Polymorphisms in surfactant protein-D are associated with chronic obstructive pulmonary disease. *Am J Respir Cell Mol Biol*. (2011) 44:316–22. doi: 10.1165/rcmb.2009-0360OC
102. Lin Z, John G, Hegarty JP, Berg A, Yu W, Wang Y, et al. Genetic variants and monoallelic expression of surfactant protein-D in inflammatory bowel disease. *Ann Hum Genet*. (2011) 75:559–68. doi: 10.1111/j.1469-1809.2011.00662.x

103. Ishii T, Hagiwara K, Ikeda S, Arai T, Mieno MN, Kumasaka T, et al. Association between genetic variations in surfactant protein d and emphysema, interstitial pneumonia, and lung cancer in a Japanese population. *Copd* (2012) 9:409–16. doi: 10.3109/15412555.2012.676110
104. Ishii T, Hagiwara K, Kamio K, Ikeda S, Arai T, Mieno MN, et al. Involvement of surfactant protein D in emphysema revealed by genetic association study. *Eur J Hum Genet*. (2012) 20:230–5. doi: 10.1038/ejhg.2011.183
105. Kim DK, Cho MH, Hersh CP, Lomas DA, Miller BE, Kong X, et al. Genome-wide association analysis of blood biomarkers in chronic obstructive pulmonary disease. *Am J Respir Crit Care Med*. (2012) 186:1238–47. doi: 10.1164/rccm.201206-1013OC
106. Shakoori TA, Sin DD, Bokhari SN, Ghafoor F, Shakoori AR. SP-D polymorphisms and the risk of COPD. *Dis Markers* (2012) 33:91–100. doi: 10.3233/dma-2012-0909
107. Pueyo N, Ortega FJ, Mercader JM, Moreno-Navarrete JM, Sabater M, Bonas S, et al. Common genetic variants of surfactant protein-D (SP-D) are associated with type 2 diabetes. *PLoS ONE* (2013) 8:e60468. doi: 10.1371/journal.pone.0060468
108. Horimasu Y, Hattori N, Ishikawa N, Tanaka S, Bonella F, Ohshimo S, et al. Differences in serum SP-D levels between German and Japanese subjects are associated with SFTPD gene polymorphisms. *BMC Med Genet*. (2014) 15:4. doi: 10.1186/1471-2350-15-4
109. Issac MS, Ashur W, Mousa H. Genetic polymorphisms of surfactant protein D rs2243639, Interleukin (IL)-1beta rs16944 and IL-1RN rs2234663 in chronic obstructive pulmonary disease, healthy smokers, and non-smokers. *Mol Diagn Ther*. (2014) 18:343–54. doi: 10.1007/s40291-014-0084-5
110. Johansson SL, Tan Q, Holst R, Christiansen L, Hansen NC, Hojland AT, et al. Surfactant protein D is a candidate biomarker for subclinical tobacco smoke-induced lung damage. *Am J Physiol Lung Cell Mol Physiol*. (2014) 306:L887–895. doi: 10.1152/ajplung.00340.2013
111. Sorensen GL, Dahl M, Tan Q, Bendixen C, Holmskov U, Husby S. Surfactant protein-D-encoding gene variant polymorphisms are linked to respiratory outcome in premature infants. *J Pediatr*. (2014) 165:683–9. doi: 10.1016/j.jpeds.2014.05.042
112. Ou CY, Chen CZ, Hsiue TR, Lin SH, Wang JY. Genetic variants of pulmonary SP-D predict disease outcome of COPD in a Chinese population. *Respirology* (2015) 20:296–303. doi: 10.1111/resp.12427
113. Soto-Cardenas MJ, Gandia M, Brito-Zeron P, Arias MT, Armiger N, Bove A, et al. Etiopathogenic role of surfactant protein d in the clinical and immunological expression of primary Sjogren syndrome. *J Rheumatol*. (2015) 42:111–8. doi: 10.3899/jrheum.140394
114. Chang HY, Li F, Li FS, Zheng CZ, Lei YZ, Wang J. Genetic polymorphisms of SP-A, SP-B, and SP-D and risk of respiratory distress syndrome in preterm neonates. *Med Sci Monit*. (2016) 22:5091–100. doi: 10.12659/MSM.898553
115. Perez-Rubio G, Silva-Zolezzi I, Fernandez-Lopez JC, Camarena A, Velazquez-Uncal M, Morales-Mandujano F, et al. Genetic variants in IL6R and ADAM19 are associated with COPD severity in a mexican mestizo population. *Copd* (2016) 13:610–5. doi: 10.3109/15412555.2016.1161017
116. Shakoori TA, Sin DD. SNP rs3088308 is a risk factor for poor lung function in healthy smokers. *J Pak Med Assoc*. (2016) 66:1137–41.
117. Sorensen GL, Bladbjerg EM, Steffensen R, Tan Q, Madsen J, Drivsholm T, et al. Association between the surfactant protein D (SFTPD) gene and subclinical carotid artery atherosclerosis. *Atherosclerosis* (2016) 246:7–12. doi: 10.1016/j.atherosclerosis.2015.12.037
118. Wu CW, Zhang XF, Liu W, Wang HL, Hao XH, Guo ZY, et al. [Association of surfactant protein D gene polymorphisms at rs3088308 and rs721917 with susceptibility to silicosis]. *Nan Fang Yi Ke Da Xue Xue Bao* (2016) 36:1004–7.
119. Obeidat M, Li X, Burgess S, Zhou G, Fishbane N, Hansel NN, et al. Surfactant protein D is a causal risk factor for COPD: results of Mendelian randomisation. *Eur Respir J*. (2017) 50:1700657. doi: 10.1183/13993003.00657-2017
120. Choi Y, Lee DH, Tu THK, Ban GY, Park H, Shin YS, et al. Surfactant protein D alleviates eosinophil-mediated airway inflammation and remodeling in patients with aspirin-exacerbated respiratory disease. *Allergy* (2018). doi: 10.1111/all.13458. [Epub ahead of print].
121. Fakih D, Akiki Z, Junker K, Medlej-Hashim M, Waked M, Salameh P, et al. Surfactant protein D multimerization and gene polymorphism in COPD and asthma. *Respirology* (2018) 23:298–305. doi: 10.1111/resp.13193
122. Hsieh MH, Ou CY, Hsieh WY, Kao HF, Lee SW, Wang JY, et al. Functional analysis of genetic variations in surfactant protein d in mycobacterial infection and their association with tuberculosis. *Front Immunol*. (2018) 9:1543. doi: 10.3389/fimmu.2018.01543
123. Munk HL, FakihD, Christiansen L, Tan Q, Christensen AF, Ejstrup L, et al. Surfactant protein-D, a potential mediator of inflammation in axial spondyloarthritis. *Rheumatology* (2018) doi: 10.1093/rheumatology/key187. [Epub ahead of print].
124. Hoffjan S, Nicolae D, Ostrovnaya I, Roberg K, Evans M, Mirel DB, et al. Gene-environment interaction effects on the development of immune responses in the 1st year of life. *Am J Hum Genet*. (2005) 76:696–704. doi: 10.1086/429418
125. Constantin JM, Mira JP, Guerin R, Cayot-Constantin S, Lesens O, Gourdon F, et al. Lemierre's syndrome and genetic polymorphisms: a case report. *BMC Infect Dis*. (2006) 6:115. doi: 10.1186/1471-2334-6-115
126. Tanaka M, Arimura Y, Goto A, Hosokawa M, Nagaishi K, Yamashita K, et al. Genetic variants in surfactant, pulmonary-associated protein D (SFTPD) and Japanese susceptibility to ulcerative colitis. *Inflamm Bowel Dis*. (2009) 15:918–25. doi: 10.1002/ibd.20936
127. Byers HM, Dagle JM, Klein JM, Ryckman KK, McDonald EL, Murray JC, et al. Variations in CRHR1 are associated with persistent pulmonary hypertension of the newborn. *Pediatr Res*. (2012) 71:162–7. doi: 10.1038/pr.2011.24
128. Ryckman KK, Dagle JM, Kelsey K, Momany AM, Murray JC. Genetic associations of surfactant protein D and angiotensin-converting enzyme with lung disease in preterm neonates. *J Perinatol*. (2012) 32:349–55. doi: 10.1038/jp.2011.104
129. Xie ZK, Huang QP, Huang J, Xie ZF. Association between the IL1B, IL1RN polymorphisms and COPD risk: a meta-analysis. *Sci Rep*. (2014) 4:6202. doi: 10.1038/srep06202
130. Valverde G, Zhou H, Lippold S, de Filippo C, Tang K, Lopez Herraez D, et al. A novel candidate region for genetic adaptation to high altitude in Andean populations. *PLoS ONE* (2015) 10:e0125444. doi: 10.1371/journal.pone.0125444
131. Liu Y, Yan S, Poh K, Liu S, Iyioriobhe E, Sterling DA. Impact of air quality guidelines on COPD sufferers. *Int J Chron Obstruct Pulmon Dis*. (2016) 11:839–72. doi: 10.2147/copd.S49378
132. Rivera L, Siddaiah R, Oji-Mmuo C, Silveyra GR, Silveyra P. Biomarkers for *Bronchopulmonary Dysplasia* in the preterm infant. *Front Pediatr*. (2016) 4:33. doi: 10.3389/fped.2016.00033
133. Lin Z, deMello DE, Batanian JR, Khammash HM, DiAngelo S, Luo J, et al. Aberrant SP-B mRNA in lung tissue of patients with congenital alveolar proteinosis (CAP). *Clin Genet*. (2000) 57:359–369. doi: 10.1034/j.1399-0004.2000.570506.x
134. Wang G, Christensen ND, Wigdahl B, Guttentag SH, Floros J. Differences in N-linked glycosylation between human surfactant protein-B variants of the C or T allele at the single-nucleotide polymorphism at position 1580: implications for disease. *Biochem J*. (2003) 369(Pt 1):179–184. doi: 10.1042/bj20021376
135. Lin Z, Cui X, Li H. Multiplex genotype determination at a large number of gene loci. *Proc Natl Acad Sci USA*. (1996) 93:2582–7.
136. DiAngelo S, Lin Z, Wang G, Phillips S, Ramet M, Luo J, et al. Novel, non-radioactive, simple and multiplex PCR-cRFLP methods for genotyping human SP-A and SP-D marker alleles. *Dis Markers* (1999) 15:269–81.
137. Lin Z, Pearson C, Chinchilli V, Pietschmann SM, Luo J, Pison U, et al. Polymorphisms of human SP-A, SP-B, and SP-D genes: association of SP-B Thr131Ile with ARDS. *Clin Genet*. (2000) 58:181–91. doi: 10.1034/j.1399-0004.2000.580305.x
138. Wang Z, Liu T, Lin Z, Hegarty J, Koltun WA, Wu R. A general model for multilocus epistatic interactions in case-control studies. *PLoS ONE* (2010) 5:e11384. doi: 10.1371/journal.pone.0011384
139. Liu T, Thalamuthu A, Liu JJ, Chen C, Wang Z, Wu R. Asymptotic distribution for epistatic tests in case-control studies. *Genomics* (2011) 98:145–51. doi: 10.1016/j.ygeno.2011.05.001
140. Lin Z, Hao H, Hegarty JP, Lin TR, Wang Y, Harris LR, et al. Association of the haem oxygenase-1 gene with inflammatory bowel disease. *Swiss Med Wkly*. (2017) 147:w14456. doi: 10.4414/smw.2017.14456

141. Lin Z, Wang Z, Hegarty JP, Lin TR, Wang Y, Deiling S, et al. Genetic association and epistatic interaction of the interleukin-10 signaling pathway in pediatric inflammatory bowel disease. *World J Gastroenterol*. (2017) 23:4897–909. doi: 10.3748/wjg.v23.i27.4897
142. Vorbroker DK, Profitt SA, Nogee LM, Whitsett JA. Aberrant processing of surfactant protein C in hereditary SP-B deficiency. *Am J Physiol* (1995) 268(4 Pt 1):L647–656. doi: 10.1152/ajplung.1995.268.4.L647
143. Akinbi HT, Breslin JS, Ikegami M, Iwamoto HS, Clark JC, Whitsett JA, et al. Rescue of SP-B knockout mice with a truncated SP-B proprotein. *Function of the C-terminal propeptide J Biol Chem*. (1997) 272:9640–7.
144. Quasney MW, Waterer GW, Dahmer MK, Kron GK, Zhang Q, Kessler LA, et al. Association between surfactant protein B + 1580 polymorphism and the risk of respiratory failure in adults with community-acquired pneumonia. *Crit Care Med*. (2004) 32:1115–9. doi: 10.1097/01.CCM.0000124872.55243.5A
145. Xu Y, Ge L, Abdel-Razek O, Jain S, Liu Z, Hong Y, et al. Differential susceptiblity of human SP-B genetic variation on lung injury caused by bacterial pneumonia and the effect of a chemically mdified curcumin. *Shock* (2016) 45:375–84. doi: 10.1097/shk.0000000000000535
146. Crouch EC. Collectins and pulmonary host defense. *Am J Respir Cell Mol Biol*. (1998) 19:177–201. doi: 10.1165/ajrcmb.19.2.140
147. Hickling TP, Malhotra R, Sim RB. Human lung surfactant protein A exists in several different oligomeric states: oligomer size distribution varies between patient groups. *Mol Med*. (1998) 4:266–75.
148. Griese M, Maderlechner N, Ahrens P, Kitz R. Surfactant proteins A and D in children with pulmonary disease due to gastroesophageal reflux. *Am J Respir Crit Care Med*. (2002) 165:1546–50. doi: 10.1164/rccm.2107147
149. Sanchez-Barbero F, Rivas G, Steinhilber W, Casals C. Structural and functional differences among human surfactant proteins SP-A1, SP-A2 and co-expressed SP-A1/SP-A2: role of supratrimeric oligomerization. *Biochem J*. (2007) 406:479–89. doi: 10.1042/bj20070275
150. Sano H, Kuronuma K, Kudo K, Mitsuzawa H, Sato M, Murakami S, et al. Regulation of inflammation and bacterial clearance by lung collectins. *Respirology* (2006) 11(Suppl.):S46–50. doi: 10.1111/j.1440-1843.2006.00808.x
151. Brummer E, Stevens DA. Collectins and fungal pathogens: roles of surfactant proteins and mannose binding lectin in host resistance. *Med Mycol*. (2010) 48:16–28. doi: 10.3109/13693780903117473
152. Silveyra P, Floros J. Air pollution and epigenetics: effects on SP-A and innate host defence in the lung. *Swiss Med Wkly*. (2012) 142:w13579. doi: 10.4414/smw.2012.13579
153. Mikerov AN, Wang G, Umstead TM, Zacharatos M, Thomas NJ, Phelps DS, et al. Surfactant protein A2 (SP-A2) variants expressed in CHO cells stimulate phagocytosis of *Pseudomonas aeruginosa* more than do SP-A1 variants. *Infect Immun*. (2007) 75:1403–12. doi: 10.1128/iai.01341-06
154. Wang G, Umstead TM, Phelps DS, Al-Mondhiry H, Floros J. The effect of ozone exposure on the ability of human surfactant protein a variants to stimulate cytokine production. *Environ Health Perspect*. (2002) 110:79–84. doi: 10.1289/ehp.0211079

Conflict of Interest Statement: The authors declare that the research was conducted in the absence of any commercial or financial relationships that could be construed as a potential conflict of interest.

The reviewer AT and handling Editor declared their shared affiliation.

frontiers in Immunology

ORIGINAL RESEARCH
published: 02 July 2018
doi: 10.3389/fimmu.2018.01543

Functional Analysis of Genetic Variations in Surfactant Protein D in Mycobacterial Infection and Their Association With Tuberculosis

Miao-Hsi Hsieh[1], Chih-Ying Ou[2], Wen-Yu Hsieh[3], Hui-Fang Kao[4], Shih-Wei Lee[5], Jiu-Yao Wang[1,3,6] and Lawrence S. H. Wu[4,7]**

[1] Institute of Basic Medical Science, College of Medicine, National Cheng Kung University, Tainan, Taiwan, [2] Institute of Clinical Medicine, College of Medicine, National Cheng Kung University, Tainan, Taiwan, [3] Institute of Biochemistry and Molecular Biology, College of Medicine, National Cheng Kung University, Tainan, Taiwan, [4] Allergy and Clinical Immunology Research (ACIR) Center, College of Medicine, National Cheng Kung University, Tainan, Taiwan, [5] Chest Medicine, General Taoyuan Hospital, Taoyuan, Taiwan, [6] Institute of Respiratory Research, The First Affiliated Hospital of Guangzhou Medical University, Guangzhou, China, [7] Graduate Institute of Biomedical Sciences, China Medical University, Taichung, Taiwan

OPEN ACCESS

Edited by:
Taruna Madan, National Institute for Research in Reproductive Health (ICMR), India

Reviewed by:
Anthony George Tsolaki, Brunel University London, United Kingdom
Kenneth Reid, University of Oxford, United Kingdom

***Correspondence:**
Jiu-Yao Wang
a122@mail.ncku.edu.tw;
Lawrence S. H. Wu
lshwu@hotmail.com

Specialty section:
This article was submitted to Molecular Innate Immunity, a section of the journal Frontiers in Immunology

Received: *28 February 2018*
Accepted: *21 June 2018*
Published: *02 July 2018*

Citation:
Hsieh M-H, Ou C-Y, Hsieh W-Y, Kao H-F, Lee S-W, Wang J-Y and Wu LSH (2018) Functional Analysis of Genetic Variations in Surfactant Protein D in Mycobacterial Infection and Their Association With Tuberculosis. Front. Immunol. 9:1543. doi: 10.3389/fimmu.2018.01543

Surfactant proteins (SPs)-A and -D are C-type lectins of the collectin family and function in the clearance of infectious particles in the lungs. Some polymorphisms of SPs that give rise to amino acid changes have been found to affect their function. Several SP-A gene polymorphisms have been reported to be associated with respiratory infection diseases, such as tuberculosis (TB). However, the relationship between surfactant proteins D (SP-D) polymorphisms and TB is still unclear. To study the associations between SP-D polymorphisms and TB, the correlations of SP-D polymorphisms with TB were examined in a case–control study, which included 364 patients with TB and 177 control subjects. In addition, we cloned two major SP-D exonic polymorphism C92T (rs721917) and A538G (rs2243639) constructs and used these for *in vitro* assays. The effects of SP-D polymorphisms on agglutination and other interactions with *Mycobacterium bovis* bacillus Calmette–Guérin (*M. bovis* BCG) were evaluated. In comparison with SP-D 92C (amino acid residue 16, Threonine), our results showed that SP-D 92T (amino acid residue 16, Methionine) had a lower binding ability to *M. bovis* BCG, a lower capacity to inhibit phagocytosis, lesser aggregation, poorer survival of bacillus Calmette–Guérin (BCG)-infected MH-S cells, and less inhibition of intracellular growth of *M. bovis* BCG. The case–control association study showed that the 92T homozygous genotype was a risk factor for TB. However, a lesser effect was seen for polymorphism A538G. In conclusion, the results of functional and genetic analyses of SP-D variants consistently showed that the SP-D 92T variant increased susceptibility to TB, which further confirmed the role of SP-D in pulmonary innate immunity against mycobacterial infection.

Keywords: infection, *Mycobacterium*, single-nucleotide polymorphisms, surfactant protein D, tuberculosis

Abbreviations: CRD, carbohydrate recognition domain; HMW, high molecular weight; LMW, low molecular weight; LAM, lipoarabinomannan; *MTB*, *Mycobacterium tuberculosis*; MOI, multiplicity of infection; rSP-D, recombinant SP-D; SNPs, single-nucleotide polymorphisms; SP-D, surfactant proteins D; TB, tuberculosis; *M. bovis* BCG, *Mycobacterium bovis* bacillus Calmette–Guérin.

INTRODUCTION

Pulmonary tuberculosis (TB), caused by *Mycobacterium tuberculosis* (*MTB*), is a global public health issue, as it is the leading cause of death among infectious diseases in many countries. Though TB has diminished over a long period of time, it has reappeared and has become a serious concern once again in many regions. The resurgence of TB is also accompanied by increasing numbers of cases of multidrug-resistant TB due to the development of extensively drug-resistant bacterial strains (1, 2). A study estimated that more than 30% of the world's population has been infected with *MTB*, and the infection kills approximately two million people annually (3). In Taiwan, there were more than 12,000 cases (55/100,000 population) of TB in 2011 alone, and at least 600 deaths (2.8/100,000 population) were caused by TB (4). The development of and susceptibility to TB involves complicated host environment–pathogen interactions, and genetic components have been suggested to be involved in the process. Recently, more evidence has been uncovered to indicate that individuals with certain genetic chrematistics are particularly vulnerable to TB. In addition, data accumulated from different types of studies, such as twin studies (5, 6), genome-wide linkage analyses (7–10), and genome-wide association studies (11–13), have demonstrated that individuals with particular genetic variations are at high risk of TB (14). In fact, among people infected with TB, only 10% develop active pulmonary TB, implying that polymorphisms of genes associated with host immune responses may be key to the development of pulmonary TB (15).

C-type lectins, collagen-like calcium-dependent pulmonary collectins, are some of the molecules correlated with innate host immune responses. These include lung surfactant proteins (SP)-A and -D and pattern recognition molecule–mannose-binding lectin/protein (MBL or MBP) (16). These molecules play important roles in the host cellular response against mycobacterial infections (17). During the course of *MTB* infection, SP-A mediates the adherence of *MTB* to human alveolar macrophages and induces mannose receptor activity, which further increases their phagocytic uptake of *MTB* (18). Surfactant proteins D (SP-D), however, directly interacts with *MTB*, resulting in reduction of *MTB* phagocytosis (19), and the inhibition effect on *MTB* uptake by macrophages is not associated with the bacterial agglutination process (20). Incubation of *MTB* with SP-D results in reduced uptake of the bacteria by macrophages (19) and limits *MTB* growth inside cells by facilitating the fusion of *MTB* phagosomes with lysosomes of cells (21). Allelic variations of SP-A and SP-D genes have been reported to be target candidates in several infectious diseases, including TB, as they are directly involved in the process of lung pathogen clearance (22). A study of patients of a Mexican population showed that several SP flanking marker alleles are associated with an increased risk of susceptibility to TB (23). Intronic single-nucleotide polymorphisms (SNPs) in the collagen region of SP-A2 and intragenic SNPs in SP-A1 and SP-A2 have also been demonstrated to contribute to the risk of susceptibility to TB (24, 25). Thus, based on the aforementioned research and other previous studies, it has been proposed that surfactant polymorphisms may alter splicing regulation and impact on mRNA maturation (25). However, many of the underlying mechanisms are still unclear. Recently, Yang et al. (26) reported that SNPs in SP-A, particularly at alleles of amino acids 91 (G) and 140 (T), are associated with TB in the Han population in China. Studies of protein constitution in bronchoalveolar lavage and surfactant gene polymorphisms have suggested that SP-D is directly linked to several pulmonary inflammatory diseases (16, 27). SP-D polymorphisms have also been found to be connected to severe respiratory syncytial virus infection, with the rs721917 SP-D allele coding for methionine (28). Our previous study also showed that genetic variants of pulmonary SP-D could determine serum levels of SP-D and predict the outcome of chronic obstructive pulmonary disease in a Chinese population (29). To the best of our knowledge, only one study of a Mexican population has identified an association between SP-D polymorphisms and susceptibility to TB (23). However, this research only investigated selective loci, without whole SP-D gene analysis, and lacked functional study of the correlations between SP-D polymorphisms and *MTB* infection. In fact, little comprehensive work has been carried out to analyze the relationships between genetic variants of SP-D proteins and host immunity against *MTB* infection.

In this study, the effects of functional (in exon, non-synonymous) polymorphisms of SP-D on the interaction between SP-D and *Mycobacterium bovis* bacillus Calmette–Guérin (*M. bovis* BCG) were investigated. Furthermore, the associations between SP-D functional polymorphisms and susceptibility to TB were also investigated. This work provides evidence that utilizing functional DNA variants of SP-D in clinical association studies, instead of markers of SNPs, advances our understanding of surfactant genetic susceptibility and innate defense mechanisms to pulmonary TB and other lung diseases.

MATERIALS AND METHODS

Clinical Sample Collection

A total of 364 patients who were treated for active TB at the General Taoyuan Hospital (Taoyuan, Taiwan) and National Cheng Kung University Hospital (Tainan, Taiwan) between 2010 and 2012 were surveyed consecutively. The inclusion criteria were: adult patients newly diagnosed with active TB, evident lesions of TB on simple X-ray and computed tomography images, and positive results of sputum smears and cultures for mycobacteria. Patients with HIV infection were excluded from this study. The control group comprised 177 volunteer subjects without active TB or a history of TB. Written informed consent was obtained from each patient and volunteer enrolled in this study. The study protocol conformed to the ethical guidelines of the 1975 Declaration of Helsinki and was approved by the Ethics Committees of Taoyuan General Hospital and National Cheng Kung University Hospital.

DNA Extraction and SNP Genotyping

Genomic DNA was extracted from oral swabs collected from the enrolled TB patients and non-TB subjects using a QIAamp DNA Mini Kit (QIAGEN, Valencia, CA, USA) according to the manufacturer's instructions. The extracted genomic DNA was analyzed

using agarose gel electrophoresis, quantitatively determined by spectrophotometry, and stored at −80°C until use. Genotyping was performed on the two major non-synonymous SNPs of SP-D, rs721917 (C92T) and rs2243639 (A538G), for genetic association analysis. The SNPs were genotyped using the high-throughput, 384-microtiter plate MassARRAY System, SEQUENOM, according to the manufacturer's protocol. In brief, DNA containing the SNP site of interest was amplified, followed by performance of the homogenous MassEXTEND assay, in which label-free primer extension chemistry was used to generate allele-specific diagnostic products. The allele-specific diagnostic products have a unique molecular weight, and this can be distinguished through the application of matrix-assisted laser desorption ionization time-of-flight mass spectrometry.

Chemicals and Plasmids

QIAprep Miniprep and QIAGEN plasmid Midi Kit for plasmid preparation were obtained from QIAGEN. Restriction enzymes including *Hind* III and *Sac* II were obtained from TaKaRa Bio. *Dpn* I for site mutagenesis was obtained from New England Biolabs. The vector pcDNA3.1/myc-His B was purchased from Invitrogen.

Site-Directed Mutagenesis of Human SP-D

The cDNA fragment encoding human SP-D was amplified by PCR using primers (forward: 5′-CCCAAGCTTGCCATGCTG CTCTTCCTCCTCTCTG-3′ containing a 5′ HindIII adaptor; reverse: 5′-GCTCTAGATCAGAACTCGCAGACCACAAG-3′ containing a 5′ SacII adaptor) and cloned into HindIII and SacII sites, leading to the formation of recombinant plasmid pcDNA3.1/myc-His B-SP-D (92T/538G). Site-directed mutagenesis was performed using mutagenic primers of SP-D 92T (forward: 5′-GA CCTACTCCCACAGAACAACGCCCAGTGCTTG-3′; reverse: 5′-CAAGCACTGGGCGTTGTTCTGTGGGAGTAGGTC-3′ and SP-D538G forward: 5′-GTGGAGTCCCTGGAAACACAGG GGCAGC-3′; reverse: 5′-CAAGCACTGGGCGTTGTTCTGTG GGAGTAGGTC-3′). The recombinant plasmids were then transformed into *Escherichia coli* XL-1 Blue competent cells (Invitrogen) by the heat shock method, and grown in LB broth at 37°C. Colonies of transformed cells were selected for further gel electrophoresis.

Construction and Expression of Recombinant SP-D (rSP-D) Site-Directed Mutants

The construction of recombinant plasmid pcDNA3.1/myc-His B-SP-D (92T/538G) is illustrated in **Figure 1A**. Site-directed mutagenesis of pcDNA3.1/myc-His B-SP-D (92T/538G) resulted in four variants (**Figure 1B**). SNPs in residues 92 and 538 resulted in changes in amino acids (**Figure 1C**). Gel electrophoresis of the four mutagenic DNA products after transformation with *Hind* II and *Sac* II diagnosis digestion is demonstrated in **Figure 2A**. The results of DNA sequencing of the four variants of SP-D are illustrated in **Figure 2B**. Expression and quantification of the four rSP-D site-directed mutants were confirmed by western blot (**Figure 2C**) and SP-D ELISA analysis (data not shown).

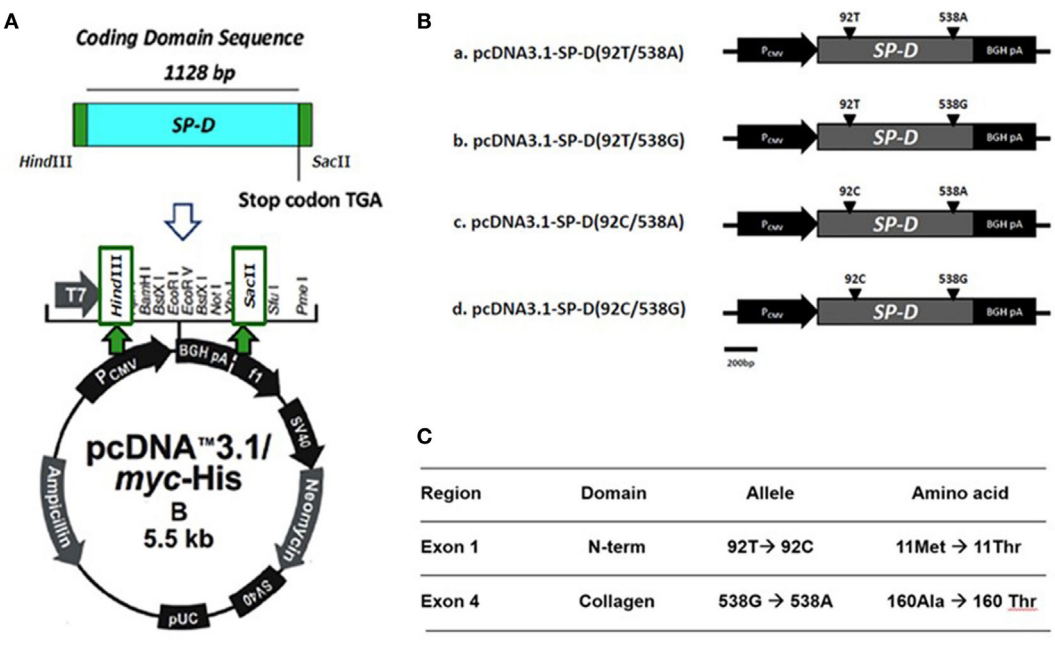

Region	Domain	Allele	Amino acid
Exon 1	N-term	92T→ 92C	11Met → 11Thr
Exon 4	Collagen	538G → 538A	160Ala → 160 Thr

FIGURE 1 | **(A)** Illustration of the construction of recombinant full-length human surfactant proteins D (SP-D) plasmid into which the SP-D gene was inserted at the multiple cloning site of a pcDNA 3.1/myc-His B vector between *Hind* III and *Sac* II. **(B)** Four recombinant SP-D (rSP-D) plasmids that carried two major single-nucleotide polymorphisms under four different combinations (92T/538A, 92T/538G, 92C/538A, and 92C/538G) were created using gene cloning and site-directed mutagenesis. **(C)** Corresponding sites of nucleotides and amino acids in different polymorphisms of SP-D variants.

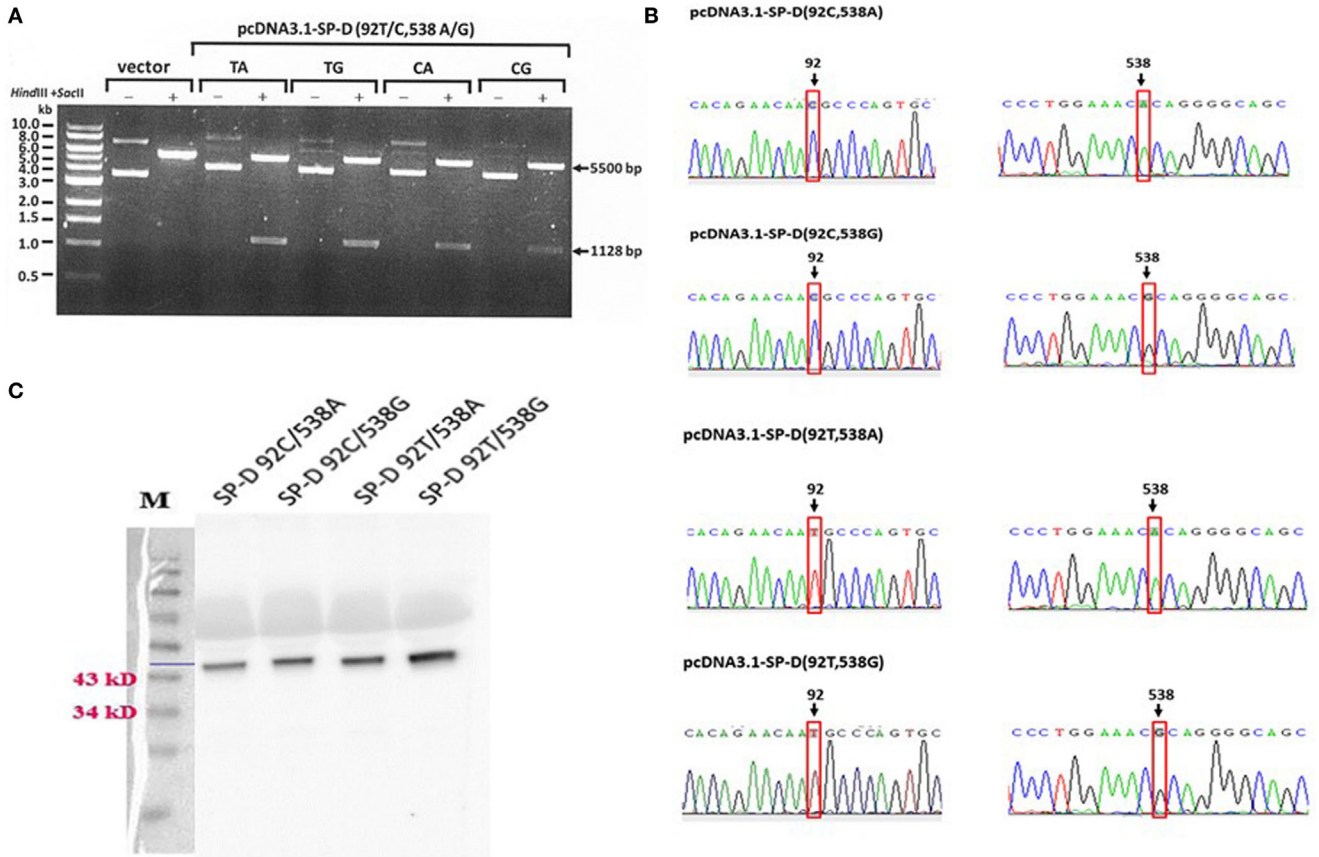

FIGURE 2 | **(A)** Double digestion of the vector and four surfactant proteins D (SP-D) gene variant plasmids using the restriction enzymes *Hind* III and *Sac* II for diagnostic digestion (TA: 92T/538A, TG:92T/538G, CA: 92C/538A, and CG: 92C/538G). **(B)** Sequencing chromatograms of the pcDNA3.1-SPD variant constructs confirmed the generation of four recombinant SP-D (rSP-D) genes using site-directed mutagenesis. **(C)** Western blots of the four rSP-D proteins from transfected HEK 293 cells showing the correct sizes of the proteins.

Expression and Quantification of Four Variants of rSP-D

Four variants of the rSP-D gene were transfected into human embryonic kidney 293 (HEK 293) cells (ATCC No. CRL-1573) using Lipofectamine LYX™ Reagent (Invitrogen). Culture medium (serum-free Dulbecco's Modified Eagle Medium) from transfected HEK 293 cells was collected for further western blot analysis. An SP-D ELISA kit (Hycult) was used for final quantification of the four rSP-D variants.

Cell and Bacterial Culture

The alveolar macrophage cell line derived from BALB/c mice (MH-S cells; American Type Culture Collection, Rockville, MD, USA) used in the study was a continuous cell line of murine alveolar macrophages established after transformation of cells obtained by bronchoalveolar lavage from BALB/c mice with simian virus 40. The cells were cultured in RPMI 1640 medium (Gibco BRL, Gaithersburg, MD, USA) supplemented with 10% fetal bovine serum, 50 U/ml penicillin, 0.05 mg/ml streptomycin, 20 mM L-glutamine, 10 mM HEPES, 10 mM sodium pyruvate, 1% glucose, and 50 μM 2-mercaptoethanol at 37°C in 5% CO_2/95% air.

M. bovis BCG was cultured on Middlebrook 7H11 agar (BD) at 37°C in an incubator. Bacteria were harvested, and pellets were suspended in PBS plus 10% glycerol. Aliquots (~5×10^8/vial) were stored at −80°C. Before infection, the bacteria supplemented with glycerol were replaced with a final concentration of 0.05% v/v Tween 80 and 2 mM $CaCl_2$ PBS to reduce bacillus Calmette–Guérin (BCG) clumping and for subsequent preparation for SP-D binding. To avoid effects on the viability of *M. bovis* BCG, penicillin and streptomycin were not added to the culture medium of the MH-S cells (Sigma-Aldrich, St. Louis, MO, USA) that were prepared for infection.

M. bovis BCG Infection

A multiplicity of infection (MOI) of 1 (1 bacterium per MH-S cell) was used for all the experiments, with the exception of the phagocytosis assay, in which an MOI of 5 was used. Quantitative bacteria in different cell culture plates (6-well: 10^5, 12-well: 5×10^4, 24-well: 2.5×10^4, and 96-well: 5×10^3) were supplemented with 100 mM glucose or 100 mM maltose, with or without 10 mM EDTA, and with one of the four variants of SP-D (0.5 or 1 μg/ml). One hour after infection, un-infected MH-S cells were washed

twice with PBS, and the same conditional medium was used for subsequent analysis.

Solid-Phase Bacterial ELISA

Lipoarabinomannan (LAM) from *M. bovis* BCG, which belongs to the class of LAMs capped with mannosyl residues, has a similar structure and immune-regulatory function to *MTB* (19). LAM also serves as a major binding molecule for SP-D (30). Based on this, we examined the roles of the four variants of rSP-D in the binding to *M. bovis* BCG. In experiments designed to determine the saturable binding activity of the four SP-D variants to *M. bovis* BCG, bacterial suspensions (10^6 bacteria in 100 µl TBS) were first dried at 37°C in an incubator for 7 h, and then exposed to ultraviolet light for 2 h to kill any viable bacteria. After blocking with 3% BSA overnight at 4°C, 1 and 10 µg/ml of the four variants of SP-D in PBS with 2 mM $CaCl_2$ were added with or without 10 mM EDTA, and with 100 mM maltose or 100 mM glucose. The results from 1 and 10 µg/ml of the four variants of SP-D were similar, then 1 µg/ml was used to further experiments. After incubation for 1 h at room temperature, the bacterial suspensions were washed and then incubated with a 1:5,000 dilution of anti-SP-D antibody for 2 h at room temperature. After incubation, the suspensions were washed again and then incubated with a 1:3,000 dilution of goat anti-mouse IgG conjugated to HRP for 2 h at room temperature. Finally, TMB substrate was added after washing. Substrate development was stopped after 12 min by 2N H_2SO_4, and the absorbance of individual wells was determined at O.D. 450 nm using a SpectraMax M2 ELISA reader (Molecular Devices, Sunnyvale, CA, USA).

Phagocytosis of *M. bovis* BCG by MH-S Cells

A Vybrant Phagocytosis Assay Kit (V6694; Invitrogen™, Thermal Fisher Scientific) was used to measure the phagocytosis of mycobacteria by MH-S cells. Briefly, bacteria (10^9/ml) were labeled by incubation with FITC (Sigma-Aldrich) at 1 µg/ml in PBS for 2 h at 37°C. Thereafter, FITC-labeled bacteria were washed twice with PBS, then opsonized, and used for infection as described above. Macrophages infected by FITC-labeled *M. bovis* BCG were analyzed and gated using flow cytometry to assess the effects of the four rSP-D variants on the phagocytosis of MH-S cells. Briefly, MH-S cells (10^5) were incubated with FITC-labeled *M. bovis* BCG (5×10^5 CFU) in a 6-well cell culture plate (BD, Franklin Lakes, NJ, USA) in the absence or presence of the four SP-D variants at concentrations ranging from 0.5 to 1 µg/ml. After incubation for 1 h, MH-S cells were scraped out after fixation with 4% formaldehyde PBS (pH 7.2) and examined using a flow cytometer (FACSCalibur; BD, San Jose, CA, USA) equipped with an argon laser that emits at 488 nm. At least 1×10^4 of cells with FITC-labeled bacteria were counted in the FACS analysis.

Agglutination and Cell Migration of *M. bovis* BCG-Infected MH-S Cells

To further characterize the effects of the four SP-D variants on the agglutination of MH-S cells after mycobacterial infection as described above, micrographs were taken 2 days after infection using an Olympus IX-71 inverted microscope. The area of the agglutinates was measured using ImageJ 1.39g software (National Institutes of Health, Bethesda, MD, USA). The diameter was estimated from the area based on the circular form of the aggregates according to the formula Area $= (R \times D^2)/4$, where R = ratio of a circle's circumference to its diameter and D = diameter. To determine the effects of the four variants of SP-D on macrophage cell migration, 2.5×10^4 MH-S cells were seeded in a 24-well cell culture plate and infected with *M. bovis* BCG as described above. The culture medium was harvested 2 days after infection and added into a new 24-well cell culture plate equipped with Millicell Hanging Cell Culture Inserts (3 µm pore size, Millipore). Each insert was seeded with 5×10^4 MH-S cells. After 1 day of culture, the inserts were removed and observed using an Olympus IX-71 inverted microscope to count the cells migrated through the membrane. The chemoattractive MH-S cells were quantified using ImageJ 1.39g software.

M. bovis BCG-Infected MH-S Cells Survival Assay

Quantitative bacteria in a 96-well cell culture plate (5×10^3 MH-S/100 µl medium) were infected with *M. bovis* BCG as described above. Two days after infection, surviving MH-S cells were evaluated using a Cell Counting Kit-8 (CCK-8) (Dojindo Laboratories, Kumamoto, Japan) with a SpectraMax M2 ELISA reader (Molecular Devices).

M. bovis BCG Intracellular Growth Assay

To determine the effects of the four SP-D variants on the intracellular viability of bacteria after phagocytosis by macrophages, 100 µl RIPA buffer (10×, Millipore) were added to the culture plate 2 days after MH-S cells had been infected (5×10^4 in a 12-well cell culture plate). Aliquots of MH-S cell lysate were then plated onto 7H11 agar (BD) to quantify the intracellular growth of viable *M. bovis* BCG. Colony-forming units were counted after 28 days of bacteria culture.

Statistical Analysis

Results are given as means ± SEs. ANOVA was used to compare the rSP-Ds. All P values less than 0.05 were considered significant. Statistical analysis was carried out using Prism, version 5 (GraphPad Software, San Diego, CA, USA). In the genetic association study, the quality of the genotype data was evaluated by Hardy–Weinberg equilibrium proportion tests. χ^2 tests were used for association analyses. Odds ratios and 95% confidence intervals were calculated from contingency tables. SNPs showing significant associations (P value ≤ 0.05) in the tests were further evaluated using logistic regressions adjusted for age and gender in odds ratio analysis. Statistical analyses for the association study were performed using SPSS 17.0 software (SPSS Inc., Chicago, IL, USA).

RESULTS

Subject Characterization

Surfactant proteins D genetic polymorphisms are most often associated with pulmonary diseases, and our hypostatized genetic variants of SP-D may have different levels of contribution to the

pathogenesis of TB. Therefore, we analyzed the genotype and allele frequencies of SP-D in TB- and non-TB-infected patients. 364 case subjects with diagnosed TB and 177 control subjects without a history of TB infection were enrolled. The mean age of the cases and controls was 55.22 and 57.75 years, respectively (**Table 1**). Cases were more likely to be male ($P < 0.0001$). There was no significant difference between the groups regarding age ($P > 0.05$).

Variants of SP-D Associated With TB

The genotype and allele frequencies of C92T (SNP ID: rs721917) and A538G (SNP ID: rs2243639) could not be derived from the Hardy–Weinberg principle. The association between TB and rs721917 genotypes was marginally significant ($P = 0.050$), and this significance was reduced after adjusting for age and gender (**Table 2**). However, odds ratio analysis showed that subjects with TT homozygous rs721917 alleles had an increased risk of susceptibility to TB (OR = 1.95, $P = 0.045$; **Table 2**), as the homozygous methionine amino acid at SP-D polypeptide position 11 was more frequent in TB patients than in non-TB subjects. The statistically significant association between rs2243639 and TB was increased when the results were adjusted for age and gender (from 0.061 to 0.033; **Table 2**). The homozygous AA (amino acid 160 threonine) genotype of rs2243639 was protective against TB.

Binding Activities of Four Variants of rSP-D to *M. bovis* BCG

To confirm that SP-D 11Thr/160Thr (amino acid residues 11 and 160, both threonine) confer greater protection against TB infection as per the genetic analysis, as well as to further investigate the protective effects of four genetic variants of rSP-D in the progression of TB infection to TB disease, we constructed four genetic variants of SP-D, and then, respectively, measured their protective ability against *M. bovis* BCG *in vitro* (SP-D binds to the surface of pathogens as a first line of defense to prevent pathogens binding before TB infection). We analyzed the binding activities of the four genetic variants of rSP-D with *M. bovis* BCG and found that all four genetic variants of rSP-D bound to *M. bovis* BCG in a dose-dependent and specific manner that could be inhibited by 10 mM EDTA or 100 mM maltose, but not by 100 mM glucose (**Figures 3A,B**). At particular concentrations (1 μg/ml) of these four SP-D mutants, a change in the amino acid at residue 11 [from Met to Thr, i.e., rSP-D (92C/538A) and rSP-D (92C/538G)] led to higher binding activities with *M. bovis* BCG when compared with the other variants of rSP-D [rSP-D (92T/538A) and rSP-D (92T/538G)] (**Figure 3B**). Double reciprocal plot analyses revealed that the dissociation constant of rSP-D (92C/538A) binding to *M. bovis* was approximately sevenfold less than that for rSP-D (92T/538A) [4.5×10^9 M for rSP-D (C/A), 3.1×10^8 M for rSP-D (92T/538A)], indicating that the avidity of SP-D binding to *M. bovis* is affected by the change in amino acid at residue 11. By contrast, the change in amino acid residue 160 (from Thr to Ala) did not lead to a significant difference in binding ability to *M. bovis* BCG.

TABLE 1 | Demographic data of the study subjects.

	Tuberculosis (TB)	Non-TB	
Age (years, mean ± SD)	55.22 ± 20.09	57.75 ± 11.08	$P = 0.060$ ($t = 1.884$)
Gender			
Male	256	108	$P < 0.0001$ ($\chi^2 = 30.600$)
Female	81	96	

Effects of the Four rSP-D Variants on Phagocytosis of MH-S Cells

All rSP-D variants inhibited phagocytosis by alveolar macro_phages following *M. bovis* BCG infection, but with different potencies. As the results presented in **Figure 4A** show, the change in amino acid at residue 11 (from Met to Thr, i.e., 92T→92C) led to significant inhibition of phagocytosis. The SP-D variant 11M/160A (92T/538G) showed a weaker inhibition effect than the other variants (**Figure 4A**). The inhibitory effect of rSP-D could be attenuated by adding maltose as a competitor for bacterial binding.

Determination of Aggregation and Chemotaxis of Infected MH-S Cells to Nearby Responsive Cells

Aggregation of infected MH-S cells, an event in which a collection of macrophages is formed during mycobacterial infection, was also evaluated. The rSP-D variant 11Thr/160Thr (92C/538A) inhibited the aggregation of infected MH-S cells more obviously than the other variants (**Figure 4B**). The protein with Thr at residue 11 [rSP-D (92C/538A) and (92C/538G)] showed a significantly

TABLE 2 | Genotyping results and odds ratio analysis of the associations between surfactant proteins D single-nucleotide polymorphisms (SNPs) and tuberculosis (TB).

SNP/genotype	TB	Non-TB	*P*	Adj. *P*	Adj. OR (95% confidence interval)	*P*
rs721917 (C92T)						
CC (ref.)	134 (36.8%)	80 (45.2%)	0.050	0.104		
CT	176 (48.6%)	82 (46.3%)	$\chi^2 = 5.996$	$\chi^2 = 4.519$	1.27 (0.85, 1.86)	0.240
TT	54 (14.8%)	15 (9%)			1.95 (1.01, 3.75)	0.045
rs2243639 (A538G)						
GG (ref.)	263 (72.2%)	129 (72.9%)	0.061	0.033		
AG	96 (26.4)	40 (22.6%)	$\chi^2 = 5.587$	$\chi^2 = 6.853$	1.15 (0.74, 1.78)	0.545
AA	5 (1.4%)	8 (1.4%)			0.23 (0.07, 0.75)	0.015

Adj., adjusted by age and gender using logistic regression; ref., reference genotype.

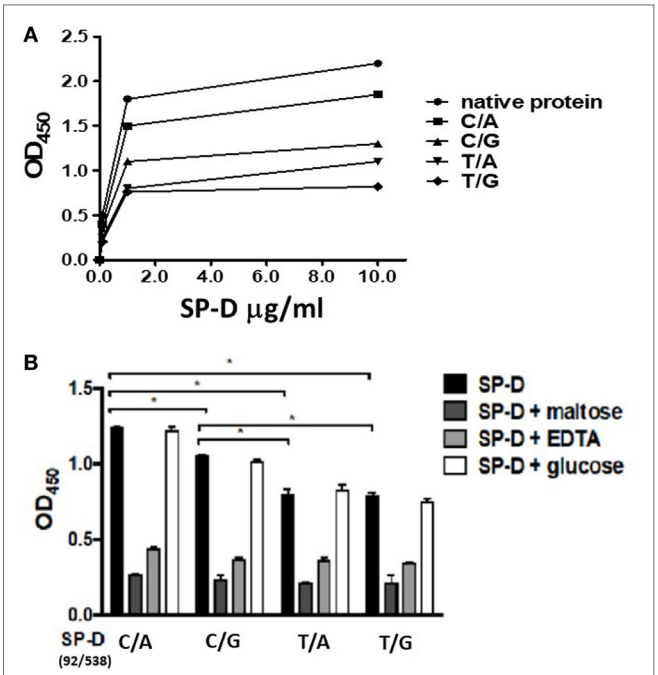

FIGURE 3 | **(A)** Dose-binding curves of native and four genetic variants of recombinant SP-D (rSP-D) proteins to *Mycobacterium bovis* bacillus Calmette–Guérin (*M. bovis* BCG). rSP-D protein (1 and 10 μg/ml) were added to wells coated with ultraviolet-killed *M. bovis* BCG (10^6 bacteria), then quantitated using solid-phase bacterial ELISA. **(B)** Inhibition effects of maltose and EDTA on the binding activity of four variants of rSP-D to *M. bovis* BCG. Surfactant proteins D (SP-D) protein (1 μg/ml) in PBS with 2 mM $CaCl_2$ was added into *M. bovis* BCG-coated wells alone, or with 10 mM EDTA, or 100 mM maltose, or 100 mM glucose. The binding activity to *M. bovis* BCG of rSP-D with residue 11Thr [(92C/538A) and (92C/538G)] was significantly higher than that of rSP-D with residue 11Met [(92T/538A) and (92T/538G)] (*$P < 0.05$). C/A: 11Thr/160Thr; C/G: 11Thr/160Ala; T/A: 11Met/Thr; T/G: 11Met/160Ala.

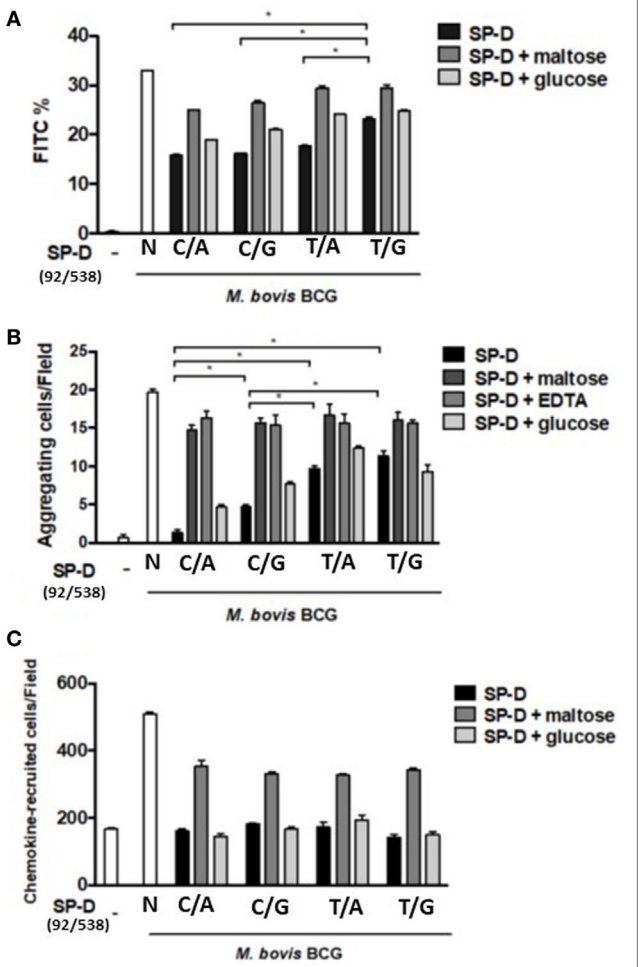

FIGURE 4 | **(A)** Inhibition of alveolar macrophage phagocytosis of *Mycobacterium bovis* bacillus Calmette–Guérin (*M. bovis* BCG) by native and four genetic variants of recombinant SP-D (rSP-D) protein. Macrophages infected with FITC-labeled *M. bovis* BCG were analyzed using flow cytometry to assess the effects of the four rSP-D variants on the phagocytosis of MH-S cells. rSP-D with residue 11Thr [(92C/538A) and (92C/538G)] inhibited phagocytosis of *M. bovis* BCG by MH-S cells to a significantly greater extent than rSP-D with residue 11Met [(92T/538A) and (92T/538G)] (*$P < 0.05$). **(B)** Inhibition of agglutination of *M. bovis* BCG-infected MH-S cells by native and four genetic variants of rSP-D proteins. The method of assessment of agglutination of MH-S cells after mycobacterial infection is described in Section "Materials and Methods." rSP-D with residue 11Thr [(92C/538A) and (92C/538G)] inhibited the aggregation of MH-S cells to a significantly greater extent than rSP-D with residue 11Met [(92T/538A) and (92T/538G)] (*$P < 0.05$). **(C)** Inhibition of cell migration of *M. bovis* BCG-infected MH-S cells by native and four genetic variants of rSP-D proteins. All four rSP-D variants inhibited cell migration of infected MH-S cells to nearby responsive cells in a concentration-dependent manner, but no significant difference was found between the four variants of rSP-D proteins. C/A: 11Thr/160Thr; C/G: 11Thr/160Ala; T/A: 11Met/Thr; T/G: 11Met/160Ala.

stronger inhibitive effect than that with Met at residue 11 [rSP-D (92T/538A) and (92T/538G)]. The protein with Thr at residue 160 showed stronger inhibition than Ala 160 only when residue 11 was Thr and under the following conditions: 1 μg/ml SP-D or 1 μg/ml SP-D + 100 mM glucose.

We further analyzed the associations between aggregation of MH-S cells and various rSP-D mutants through a chemotaxis assay. However, the recruitment of nearby MH-S cells after mycobacterium infection did not differ between the four rSP-D variants (**Figure 4C**).

The Associations Between the Four Variants of rSP-D and Viability of Infected MH-S Cells

When immune cells first encounter a pathogen in the host, macrophages are one of the major cell types to confront the bacterial invasion, and the response of the cells is crucial, as it controls the outcome of infection. To further elucidate the effect of rSP-D on MH-S cells infected by *M. bovis* BCG, a cell survival assay was performed using CCK-8. All variants of rSP-D improved the survival of infected MH-S cells in a concentration-dependent manner (**Figure 5A**). 1 μg/ml rSP-D with residue 11Thr [(92C/538A) and (92C/538G)] demonstrated the most significant protection of infected MH-S cells from cell death. In the rSP-D variants supplemented with 100 mM maltose, a protective effect was not found, and no change to cell survival was observed with treatment supplemented with 100 mM glucose.

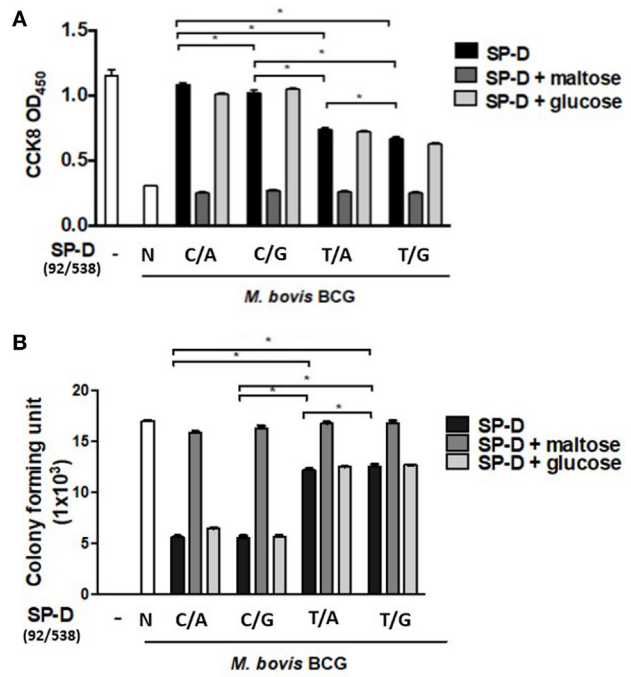

FIGURE 5 | **(A)** Cell survival of *Mycobacterium bovis* bacillus Calmette–Guérin (*M. bovis* BCG)-infected MH-S cells by native and four genetic variant recombinant SP-D (rSP-D) proteins measured using a Cell Counting Kit-8 assay. rSP-D with residue 11Thr [(92C/538A) and (92C/538G)] exhibited significantly better survival of infected MH-S cells than rSP-D with residue 11Met [(92T/538A) and (92T/538G)] (*$P < 0.05$). **(B)** Intracellular variability of *M. bovis* BCG after phagocytosis by alveolar macrophages treated with native and four genetic variants of rSP-D proteins. rSP-D with residue 11Thr [(92C/538A) and (92C/538G)] inhibited *M. bovis* BCG intracellular growth significantly more than rSP-D with residue 11Met [(92T/538A) and (92T/538G)] (*$P < 0.05$). TT: 11T/160T; TA: 11T/160A; MT: 11M/160A; MA: 11M/160A.

The Effects of rSP-D Variants on Intracellular *M. bovis* BCG Growth

The TB survival rate within macrophages is a hallmark of persistent (TB) pathogenesis. Aliquots of infected MH-S cell lysate were plated onto 7H11 agar to evaluate the effects of the four rSP-D variants on intracellular bacteria growth. Our results showed that all four variants of rSP-D inhibited intracellular *M. bovis* BCG growth (**Figure 5B**). The addition of 100 mM maltose reversed the inhibition, while no effect was observed with the addition of 100 mM glucose. Compared with residue 11Met [(92T/538A) and (92T/538G)], rSP-D variants with residue 11Thr [(92C/538A) and (92C/538G)] significantly inhibited the intracellular growth of *M. bovis* BCG (**Figure 5B**). There was no difference in growth whether residue 160 was bearing Ala or Thr.

DISCUSSION

In this study, we used *M. bovis* BCG, a good surrogate representing *MTB*, to study the role of SP-D polymorphism in mycobacterial infection and the connection with TB. Our results showed that *M. bovis* BCG interacted with the different rSP-D variants at various levels; these effects were abolished following the addition of maltose or EDTA, which causes a competitive effect with the lectin domain of SP-D or depletion of calcium. At first glance, it appeared that interaction of SP-D with *MTB* was dependent on its carbohydrate recognition domain (CRD). However, a closer look at the comparison of innate immunity against TB infection of genetic variants in the N-terminal and collagenous regions of rSP-D showed different degrees of activity. We found that SP-D residue 11 polymorphism, Thr (92C) and Met (92T), affected the binding activity of SP-D to *M. bovis* BCG, phagocytosis of infected MH-S cells, aggregation of infected MH-S cells, cell death of infected MH-S cells, and intracellular growth of *M. bovis* BCG. By contrast, the effects of SP-D 160 polymorphism, Ala (538G) and Thr (538A), were weaker than those of residue 11 polymorphism, and did not appear distinctly. From the results of SP-D variant functional and genetic analysis, residue 11 Met (92T) appeared likely to cause susceptibility to TB, which was validated in our TB-infected patients.

The SP-D gene contains a total of eight exons, seven of which are coding. Coding and non-coding SNPs (rs721917, rs6413520, rs2243639, rs3088308, rs1051246, rs1923537, rs2245121, rs911887, rs2255601, and rs7078012) are also found within the SP-D gene (31, 32); most of these have been found to be associated with a number of diseases (23, 33, 34). Among the known SP-D SNPs, two major polymorphisms, C92T (rs721917) and A538G (rs2243639), were chosen for analysis in this study. The rs721917 SFTPD SNP, known as C92T and SP-D A11, located on exon 1 and a short non-collagen-like N-terminal section, is associated with serum levels of SP-D (35), and explains 39% of the phenotypic variation (36), the Met11 (92T) allelic variant being associated at the highest level (37). Consistent with genetic determination of SP-D levels, the constitutive distribution of multimerized (high molecular weight, HMW) and non-multimerized (low molecular weight, LMW) SP-D in human body fluids is also genetically determined, with individuals homozygous for the Met11 allele having a relative predominance of HMW SP-D, and Thr11 (92C) allele homozygotes having more LMW SP-D (37). This change in the multimerization of SP-D may also affect its biological functions *in vitro* and *in vivo* (36). In fact, several studies have linked rs721917 with diseases (38), indicating involvement of SP-D level and/or size variation in disease pathogenesis. Study has shown that amino acid position 343 of SP-D has a critical role in the selective binding of glycolipids from *MTB* (39); however, no polymorphism exists in this genetic position.

Another coding single-nucleotide variation is located on exon 4, and the collagen-like region in the mature protein is rs2243639, known as A538G and SPD A160. As with other genetic alleles, the two-marker SP-D/SP-A haplotype, DA160_A/SP-A2 1A, is protective against the development of neonatal respiratory distress syndrome (40). SP-A2/SP-D haplotypes were also found to protect against bronchopulmonary dysplasia: 1A2-Ala160 (rs2243639) and 1A2-Thr11 (rs721917)-Ala160 (rs2243639) (41). It has been suggested that the protective effect of SP-D Ala160 in bronchopulmonary dysplasia is likely due to interactions with other gene(s). In our study of the interaction with *M. bovis* BCG, residue 160 Ala (92C/538G) showed a lesser binding

activity than 160 Thr (92C/538A) when residue 11 was Thr, but not when it was Met. The SP-D variant 11M/160A (92T/538G) showed weaker inhibition of phagocytosis than the other variants at an SP-D concentration of 1 μg/ml. Our results implied that polymorphism A539G (160 residue Ala/Thr) has less impact than C92T (11 residue Thr/Met) and may exhibit an effect only under specific conditions or through interaction with other genetic factors. The protective effect of homozygous 538A (160 residue Thr) against TB was consistent with the results of functional studies mentioned above.

Surfactant proteins D binds to the bacterial surface and reduces the uptake of bacteria by alveolar macrophages (19). Also, SP-D polymorphisms have been demonstrated to be associated with the risk of TB (23, 42). A genetic study of a Mexican population identified that SP-D A11C (amino acid residue 11, risk allele threonine) was associated with subgroups of patients with TB by comparing a TB group and a tuberculin–skin test-positive group (symptom-free and normal chest radiographs). The association was not found when the TB group was compared with a control group (23). Our association study revealed that homozygous residue 11 Met was a risk genotype for TB, but this is not in agreement with the conclusions of the above study.

In this study, we demonstrated that the genetic variants of rSP-D in the N terminal and collagenous region confer different degrees of innate immunity against TB infection *in vitro*. Therefore, it is likely that SP-D polymorphisms C92T and A538G affect susceptibility to TB, which is in agreement with our findings in an association study of clinical TB patients. There were some limitations to our study. First, we were not able to differentiate whether or not these genetic variants of rSP-D undergo multimerization (HMW vs LMW) under our experimental conditions. HMW SP-D multimers are only partly dependent on disulfide crosslinking of the N terminal region, and some SP-D subunits are non-covalently associated depending on the protein concentration in the solution (36). Several studies have shown some discrepancies in binding characteristics and activities between HMW and LMW SP-D (36, 37, 43). Second, we were not able to demonstrate *in vivo* effects of the genetic variants of rSP-D in a TB-infected animal model due to a small yield of recombinant full-length human SP-D from HEK 293 cells. Third, although high antigenic and structural similarities exist between *MTB* and *M. bovis* BCG, use of *M. bovis* might not wholly represent the infectious nature of *MTB* in hosts. *MTB* could not be utilized in this study due to a lack of availability of the necessary safety equipment in our laboratory.

However, to evaluate the influences of SP-D polymorphisms *in vivo* and in lung diseases, wild-type and transgenic *Sftpd*$^{-/-}$ mice expressing either the human SP-D Met11 or Thr11 allelic variants were generated (44–46). In an acute model of allergic asthma, transgenic mice were sensitized and challenged with ovalbumin, and the results showed that murine expression of human polymorphic SP-D variants in the N-terminal region does not significantly influence the severity of allergic airway inflammation (46). Other studies also showed that low transgene expression levels and differences in the distribution of human rSP-D in the lung made comparison of phenotypes between wild-type and transgenic mice difficult (44, 45). In fact, a 60-kDa recombinant trimeric fragment of SP-D, without the N-terminus but maintaining part of the collagen region, appeared to have comparable effects to native SP-D in *in vivo* and *in vitro* studies, which implies that the homeostatic and anti-microbial effects of SP-D are primarily mediated by its CRD region (47, 48).

In conclusion, our results demonstrated the role of SP-D in innate immunity against TB infection. Although this mostly depends on the binding of CRD with *MTB*, this study elucidates that it is also influenced by the genetic variants in the N-terminal and collagenous domains of SP-D. The two major SP-D polymorphisms C92T and A538G, and especially C92T, appeared to affect susceptibility to TB. Our association study of the susceptibility to TB infection in patients also supported this hypothesis.

ETHICS STATEMENT

The study protocol conformed to the ethical guidelines of the 1975 Declaration of Helsinki and was approved by the Ethics Committees of Taoyuan General Hospital and National Cheng Kung University Hospital.

AUTHOR CONTRIBUTIONS

M-HH, C-YO, W-YH, J-YW, and LW contributed to the conception and design of the study; M-HH and W-YH performed experiments; C-YO and H-FK analyzed the data; C-YO and S-WL collected TB patients and performed genetic analysis; LW and J-YW wrote the first draft of the manuscript; and all authors contributed to manuscript revision, and read and approved the submitted version.

FUNDING

This project was supported by Ministry of Science and Technology (MOST) and Academia Sinica (AS) grants: MOST 107-2321-B-006-008; MOST 104-2321-B-006-008; MOST 103-2321-B-006-030; AS-106-TP-B09.

REFERENCES

1. Maher D, Raviglione M. Global epidemiology of tuberculosis. *Clin Chest Med* (2005) 26:167–82. doi:10.1016/j.ccm.2005.02.009
2. WHO. *Multidrug and Extensively Drug-Resistant TB (M/XDRTB):2010 Global Report on Surveillance and Response*. Geneva, Switzerland: World Health Organization (2010).
3. WHO. *Global Tuberculosis Report 2014*. Geneva, Switzerland: World Health Organization (2014).
4. CDCs Taiwan. *Taiwan Tuberculosis Control Report*. Taiwan, Republic of China: Centers for Disease Control, Department of Health (2012).
5. Comstock GW. Tuberculosis in twins: a re-analysis of the Prophit survey. *Am Rev Respir Dis* (1978) 117:621–4.
6. van der Eijk EA, van de Vosse E, Vandenbroucke JP, van Dissel JT. Heredity versus environment in tuberculosis in twins: the 1950s United Kingdom Prophit Survey Simonds and Comstock revisited. *Am J Respir Crit Care Med* (2007) 176:1281–8. doi:10.1164/rccm.200703-435OC
7. Bellamy R, Beyers N, McAdam KP, Ruwende C, Gie R, Samaai P, et al. Genetic susceptibility to tuberculosis in Africans: a genome-wide scan. *Proc Natl Acad Sci U S A* (2000) 97:8005–9. doi:10.1073/pnas.140201897
8. Cooke GS, Campbell SJ, Bennett S, Lienhardt C, McAdam KP, Sirugo G, et al. Mapping of a novel susceptibility locus suggests a role for MC3R and

CTSZ in human tuberculosis. *Am J Respir Crit Care Med* (2008) 178:203–7. doi:10.1164/rccm.200710-1554OC
9. Mahasirimongkol S, Yanai H, Nishida N, Ridruechai C, Matsushita I, Ohashi J, et al. Genome-wide SNP-based linkage analysis of tuberculosis in Thais. *Genes Immun* (2009) 10:77–83. doi:10.1038/gene.2008.81
10. Miller EN, Jamieson SE, Joberty C, Fakiola M, Hudson D, Peacock CS, et al. Genome-wide scans for leprosy and tuberculosis susceptibility genes in Brazilians. *Genes Immun* (2004) 5:63–7. doi:10.1038/sj.gene.6364031
11. Farhat MR, Shapiro BJ, Kieser KJ, Sultana R, Jacobson KR, Victor TC, et al. Genomic analysis identifies targets of convergent positive selection in drug-resistant *Mycobacterium tuberculosis*. *Nat Genet* (2013) 45:1183–9. doi:10.1038/ng.2747
12. Mahasirimongkol S, Yanai H, Mushiroda T, Promphittayarat W, Wattanapokayakit S, Phromjai J, et al. Genome-wide association studies of tuberculosis in Asians identify distinct at-risk locus for young tuberculosis. *J Hum Genet* (2012) 57:363–7. doi:10.1038/jhg.2012.35
13. Thye T, Vannberg FO, Wong SH, Owusu-Dabo E, Osei I, Gyapong J, et al. Genome-wide association analyses identifies a susceptibility locus for tuberculosis on chromosome 18q11.2. *Nat Genet* (2010) 42:739–41. doi:10.1038/ng.639
14. Moller M, Hoal EG. Current findings, challenges and novel approaches in human genetic susceptibility to tuberculosis. *Tuberculosis (Edinb)* (2010) 90:71–83. doi:10.1016/j.tube.2010.02.002
15. Azad AK, Sadee W, Schlesinger LS. Innate immune gene polymorphisms in tuberculosis. *Infect Immun* (2012) 80:3343–59. doi:10.1128/IAI.00443-12
16. Wang JY, Reid KB. The immunoregulatory roles of lung surfactant collectins SP-A, and SP-D, in allergen-induced airway inflammation. *Immunobiology* (2007) 212:417–25. doi:10.1016/j.imbio.2007.01.002
17. Torrelles JB, Azad AK, Henning LN, Carlson TK, Schlesinger LS. Role of C-type lectins in mycobacterial infections. *Curr Drug Targets* (2008) 9:102–12. doi:10.2174/138945008783502467
18. Gaynor CD, McCormack FX, Voelker DR, McGowan SE, Schlesinger LS. Pulmonary surfactant protein A mediates enhanced phagocytosis of *Mycobacterium tuberculosis* by a direct interaction with human macrophages. *J Immunol* (1995) 155:5343–51.
19. Ferguson JS, Voelker DR, McCormack FX, Schlesinger LS. Surfactant protein D binds to *Mycobacterium tuberculosis* bacilli and lipoarabinomannan via carbohydrate-lectin interactions resulting in reduced phagocytosis of the bacteria by macrophages. *J Immunol* (1999) 163:312–21.
20. Ferguson JS, Voelker DR, Ufnar JA, Dawson AJ, Schlesinger LS. Surfactant protein D inhibition of human macrophage uptake of *Mycobacterium tuberculosis* is independent of bacterial agglutination. *J Immunol* (2002) 168:1309–14. doi:10.4049/jimmunol.168.3.1309
21. Ferguson JS, Martin JL, Azad AK, McCarthy TR, Kang PB, Voelker DR, et al. Surfactant protein D increases fusion of *Mycobacterium tuberculosis*-containing phagosomes with lysosomes in human macrophages. *Infect Immun* (2006) 74:7005–9. doi:10.1128/IAI.01402-06
22. Haataja R, Hallman M. Surfactant proteins as genetic determinants of multifactorial pulmonary diseases. *Ann Med* (2002) 34:324–33. doi:10.1080/07853890232077208 9
23. Floros J, Lin HM, Garcia A, Salazar MA, Guo X, DiAngelo S, et al. Surfactant protein genetic marker alleles identify a subgroup of tuberculosis in a Mexican population. *J Infect Dis* (2000) 182:1473–8. doi:10.1086/315866
24. Madan T, Saxena S, Murthy KJ, Muralidhar K, Sarma PU. Association of polymorphisms in the collagen region of human SP-A1 and SP-A2 genes with pulmonary tuberculosis in Indian population. *Clin Chem Lab Med* (2002) 40:1002–8. doi:10.1515/CCLM.2002.174
25. Malik S, Greenwood CM, Eguale T, Kifle A, Beyene J, Habte A, et al. Variants of the SFTPA1 and SFTPA2 genes and susceptibility to tuberculosis in Ethiopia. *Hum Genet* (2006) 118:752–9. doi:10.1007/s00439-005-0092-y
26. Yang HY, Li H, Wang YG, Xu CY, Zhao YL, Ma XG, et al. Correlation analysis between single nucleotide polymorphisms of pulmonary surfactant protein A gene and pulmonary tuberculosis in the Han population in China. *Int J Infect Dis* (2014) 26:31–6. doi:10.1016/j.ijid.2014.03.1395
27. Sorensen GL, Husby S, Holmskov U. Surfactant protein A and surfactant protein D variation in pulmonary disease. *Immunobiology* (2007) 212:381–416. doi:10.1016/j.imbio.2007.01.003
28. Lahti M, Lofgren J, Marttila R, Renko M, Klaavuniemi T, Haataja R, et al. Surfactant protein D gene polymorphism associated with severe respiratory syncytial virus infection. *Pediatr Res* (2002) 51:696–9. doi:10.1203/00006450-200206000-00006
29. Ou CY, Chen CZ, Hsiue TR, Lin SH, Wang JY. Genetic variants of pulmonary SP-D predict disease outcome of COPD in a Chinese population. *Respirology* (2015) 20:296–303. doi:10.1111/resp.12427
30. Venisse A, Berjeaud JM, Chaurand P, Gilleron M, Puzo G. Structural features of lipoarabinomannan from *Mycobacterium bovis* BCG. Determination of molecular mass by laser desorption mass spectrometry. *J Biol Chem* (1993) 268:12401–11.
31. Lu J, Willis AC, Reid KB. Purification, characterization and cDNA cloning of human lung surfactant protein D. *Biochem J* (1992) 284:795–802. doi:10.1042/bj2840795
32. Crouch E, Persson A, Chang D, Heuser J. Molecular structure of pulmonary surfactant protein D (SP-D). *J Biol Chem* (1994) 269:17311–9.
33. Foreman MG, Kong X, DeMeo DL, Pillai SG, Hersh CP, Bakke P, et al. Polymorphisms in surfactant protein-D are associated with chronic obstructive pulmonary disease. *Am J Respir Cell Mol Biol* (2011) 44:316–22. doi:10.1165/rcmb.2009-0360OC
34. Hilgendorff A, Heidinger K, Bohnert A, Kleinsteiber A, Konig IR, Ziegler A, et al. Association of polymorphisms in the human surfactant protein-D (SFTPD) gene and postnatal pulmonary adaptation in the preterm infant. *Acta Paediatr* (2009) 98:112–7. doi:10.1111/j.1651-2227.2008.01014.x
35. Heidinger K, Konig IR, Bohnert A, Kleinsteiber A, Hilgendorff A, Gortner L, et al. Polymorphisms in the human surfactant protein-D (SFTPD) gene: strong evidence that serum levels of surfactant protein-D (SP-D) are genetically influenced. *Immunogenetics* (2005) 57:1–7. doi:10.1007/s00251-005-0775-5
36. Sorensen GL, Hoegh SV, Leth-Larsen R, Thomsen TH, Floridon C, Smith K, et al. Multimeric and trimeric subunit SP-D are interconvertible structures with distinct ligand interaction. *Mol Immunol* (2009) 46:3060–9. doi:10.1016/j.molimm.2009.06.005
37. Leth-Larsen R, Garred P, Jensenius H, Meschi J, Hartshorn K, Madsen J, et al. A common polymorphism in the SFTPD gene influences assembly, function, and concentration of surfactant protein D. *J Immunol* (2005) 174:1532–8. doi:10.4049/jimmunol.174.3.1532
38. Sorensen GL. Surfactant protein D in respiratory and non-respiratory diseases. *Front Med* (2018) 5:18. doi:10.3389/fmed.2018.00018
39. Carlson TK, Torrelles JB, Smith K, Horlacher T, Castelli R, Seeberger PH, et al. Critical role of amino acid position 343 of surfactant protein-D in the selective binding of glycolipids from *Mycobacterium tuberculosis*. *Glycobiology* (2009) 19:1473–84. doi:10.1093/glycob/cwp122
40. Thomas NJ, Fan R, Diangelo S, Hess JC, Floros J. Haplotypes of the surfactant protein genes A and D as susceptibility factors for the development of respiratory distress syndrome. *Acta Paediatr* (2007) 96:985–9. doi:10.1111/j.1651-2227.2007.00319.x
41. Pavlovic J, Papagaroufalis C, Xanthou M, Liu W, Fan R, Thomas NJ, et al. Genetic variants of surfactant proteins A, B, C, and D in bronchopulmonary dysplasia. *Dis Markers* (2006) 22:277–91. doi:10.1155/2006/817805
42. Vaid M, Kaur S, Taruna M, Singh H, Gupta V, Murthy K, et al. Association of SP-D, MBL and I-NOS genetic variants with pulmonary tuberculosis. *Indian J Human Genet* (2006) 12:105–10. doi:10.4103/0971-6866.29851
43. Fakih D, Akiki Z, Junker K, Medlej-Hashim M, Waked M, Salameh P, et al. Surfactant protein D (SP-D) levels, polymorphisms and multimerization in COPD and asthma. *Respirology* (2018) 23(3):298–305. doi:10.1111/resp.13193
44. Knudsen L, Ochs K, Boxler L, Tornoe I, Lykke-Sorensen G, Mackay RM, et al. Surfactant protein D (SP-D) deficiency is attenuated in humanised mice expressing the Met(11)Thr short nucleotide polymorphism of SP-D: implications for surfactant metabolism in the lung. *J Anat* (2013) 223:581–92. doi:10.1111/joa.12120
45. Kingma PS, Zhang L, Ikegami M, Hartshorn K, McCormack FX, Whitsett JA. Correction of pulmonary abnormalities in Sftpd$^{-/-}$ mice requires the collagenous domain of surfactant protein D. *J Biol Chem* (2006) 281:24496–505. doi:10.1074/jbc.M600651200

46. Winkler C, Bahlmann O, Viereck J, Knudsen L, Wedekind D, Hoymann HG, et al. Impact of a Met(11)Thr single nucleotide polymorphism of surfactant protein D on allergic airway inflammation in a murine asthma model. *Exp Lung Res* (2014) 40:154–63. doi:10.3109/01902148.2014.891062
47. Kishore U, Wang JY, Hoppe HJ, Reid KB. The alpha-helical neck region of human lung surfactant protein D is essential for the binding of the carbohydrate recognition domains to lipopolysaccharides and phospholipids. *Biochem J* (1996) 318:505–11. doi:10.1042/bj3180505
48. Madan T. Recombinant fragment of human surfactant protein D: a hierarchical regulator of pulmonary hypersensitivity. *Am J Respir Crit Care Med* (2017) 196:1495–6. doi:10.1164/rccm.201709-1934ED

Conflict of Interest Statement: The authors declare that the research was conducted in the absence of any commercial or financial relationships that could be construed as a potential conflict of interest.

frontiers in Immunology

REVIEW
published: 13 June 2018
doi: 10.3389/fimmu.2018.01368

The Role and Molecular Mechanism of Action of Surfactant Protein D in Innate Host Defense Against Influenza A Virus

*I-Ni Hsieh, Xavier De Luna, Mitchell R. White and Kevan L. Hartshorn**

Boston University School of Medicine, Boston, MA, United States

Influenza A viruses (IAVs) continue to pose major risks of morbidity and mortality during yearly epidemics and periodic pandemics. The genomic instability of IAV allows it to evade adaptive immune responses developed during prior infection. Of particular concern are pandemics which result from wholesale incorporation of viral genome sections from animal sources. These pandemic strains are radically different from circulating human strains and pose great risk for the human population. For these reasons, innate immunity plays a strong role in the initial containment of IAV infection. Soluble inhibitors present in respiratory lining fluids and blood provide a level of early protection against IAV. In general, these inhibitors act by binding to the viral hemagglutinin (HA). Surfactant protein D (SP-D) and mannose-binding lectin (MBL) attach to mannosylated glycans on the HA in a calcium dependent manner. In contrast, surfactant protein A, ficolins, and other inhibitors present sialic acid rich ligands to which the HA can bind. Among these inhibitors, SP-D seems to be the most potent due to its specific mode of binding to viral carbohydrates and its ability to strongly aggregate viral particles. We have studied specific properties of the N-terminal and collagen domain of SP-D that enable formation of highly multimerized molecules and cooperative binding among the multiple trimeric lectin domains in the protein. In addition, we have studied in depth the lectin activity of SP-D through expression of isolated lectin domains and targeted mutations of the SP-D lectin binding site. Through modifying specific residues around the saccharide binding pocket, antiviral activity of isolated lectin domains of SP-D can be markedly increased for seasonal strains of IAV. Wild-type SP-D causes little inhibition of pandemic IAV, but mutated versions of SP-D were able to inhibit pandemic IAV through enhanced binding to the reduced number of mannosylated glycans present on the HA of these strains. Through collaborative studies involving crystallography of isolated lectin domains of SP-D, glycomics analysis of the HA, and molecular modeling, the mechanism of binding of wild type and mutant forms of SP-D have been determined. These studies could guide investigation of the interactions of SP-D with other pathogens.

Keywords: surfactant protein D, influenza A virus, collectin, carbohydrate recognition domain, glycomics

OPEN ACCESS

Edited by:
Uday Kishore, Brunel University London, United Kingdom

Reviewed by:
Taruna Madan, National Institute for Research in Reproductive Health (ICMR), India
Jiu-Yao Wang, National Cheng Kung University, Taiwan
Lubna Kouser, Imperial College London, United Kingdom

***Correspondence:**
Kevan L. Hartshorn
khartsho@bu.edu

Specialty section:
This article was submitted to Molecular Innate Immunity, a section of the journal Frontiers in Immunology

Received: *02 March 2018*
Accepted: *01 June 2018*
Published: *13 June 2018*

Citation:
Hsieh I-N, De Luna X, White MR and Hartshorn KL (2018) The Role and Molecular Mechanism of Action of Surfactant Protein D in Innate Host Defense Against Influenza A Virus. Front. Immunol. 9:1368. doi: 10.3389/fimmu.2018.01368

INTRODUCTION

Innate immunity plays a key, and surprising complex, role in host defense against influenza A virus (IAV) infection (1). The innate response is especially important in the first days after viral infection with a new strain of IAV. The response includes both soluble and cellular factors, some of which are constitutively present in the respiratory tract and others of which are elicited

in response to infection. The main target cells for IAV infection are respiratory tract lining cells. Soluble innate factors intrinsically present in respiratory lining fluids have the ability to limit attachment of the virus to respiratory epithelium and thus, reduce the infectious process at the outset. Once the virus infects epithelial cells, Type 1 interferons are elicited, and these can potently limit viral infection in a non-inflammatory manner. Of interest, the virus has encoded the NS1 protein which counteracts type 1 interferon at multiple levels, and viruses lacking this protein have marked loss of fitness and infectivity (2–5). If these responses fail to adequately contain the virus, then a sometimes profound pro-inflammatory response occur consisting of cytokines and recruitment of innate immune cells including neutrophils, monocytes, and other cells. This level of response can be protective but may also lead to inflammatory injury in some instances.

Influenza A virus mainly occurs in epidemics and pandemics, either of which can cause substantial morbidity and mortality (6, 7). The current influenza season (2017–2018) has shown a sharp increase in incidence and hospitalization due to influenza, in part due to an overall vaccine effectiveness of 36% (8). Pandemics are of great concern since they reflect more marked shift in viral antigenicity and an even greater challenge for the innate immune system. Since the majority of people recover from IAV uneventfully, it is very important to identify why some develop much more severe disease. It is likely that variations in innate immunity will turn out to explain the particular susceptibility of some subjects to severe outcomes like viral pneumonia, bacterial superinfection, or cardiovascular events. Comorbid illnesses like various lung diseases, diabetes mellitus, and immune deficiencies constitute one subset of patients susceptible to severe IAV. Young children and older adults also show increased susceptibility to severe IAV, but this can vary depending on the viral strain. As an example, older adults were relatively protected from mortality during the 1918 and 2009 pandemics due to immunity acquired to remote prior exposure to similar strains (9, 10). Pandemics have been of particular concern with regard to causing mortality in young, otherwise healthy individuals (11), although the 2017–2018 seasonal epidemic already caused 63 confirmed deaths in children by early February (8).

This review will focus on the soluble factors in respiratory lining fluids that contribute to initial viral containment. The respiratory tract is the principle battle field during influenza, and it is remarkable that a virus which remains confined to the respiratory tract is able to cause such substantial morbidity and mortality. In fact, the majority of deaths caused by influenza are not the result of viral pneumonia *per se* but rather bacterial superinfection due to virus mediated blunting of antibacterial immunity (12). When IAV causes profound systemic inflammation, this may account for cardiovascular deaths during epidemics (13). For the infected host, the optimal outcome of the initial innate response includes limiting viral replication while also blunting potential excess inflammation. Several innate inhibitors, prominently including surfactant protein D (SP-D) and SP-A, mediate both of these desired activities.

THE ROLE OF SOLUBLE INHIBITORS IN AIRWAY LINING FLUID IN THE INITIAL DEFENSE AGAINST IAV

We and others have characterized a variety of IAV inhibitors present in respiratory lining fluid, including SP-D, surfactant protein A (SP-A), mannose-binding lectin (MBL), H-ficolin, LL-37, and other anti-microbial peptides (14). SP-D, SP-A, and H-ficolin are constitutively present in bronchoalveolar lavage fluid (BALF). In mice, SP-D levels were shown to increase in response to IAV infection, whereas SP-A did not (15, 16). LL-37 is mainly expressed in the lung during infection or inflammation (17, 18). Whether levels of H-ficolin increase post-IAV infection has not been studied, but it is present at sufficient quantities human resting human BALF to partially reduce IAV infectivity (19). The soluble inhibitors bind to IAV and limit infectivity by different mechanisms. SP-D and MBL have been shown to bind to high mannose oligosaccharides on the viral hemagglutinin (HA) and reduce viral uptake into epithelial cells (20–23). This mechanism has been referred to as β-inhibition of IAV. A variety of other inhibitors, including SP-A, H-ficolin, pentraxins, gp-340, and mucins contain sialic acid rich attachments on their surface to which the viral HA can bind limiting the ability of the virus to reach and attach to cellular sialic acid receptors (19, 23–28). This mechanism has been termed γ-inhibition. In general, the activity of γ-inhibitors is limited somewhat by the ability of the viral neuraminidase to free the virus from attachment to them. This is evidenced by potentiation of γ-inhibitor activity by the neuraminidase inhibitor oseltamivir (25, 29, 30). This effect of most dramatic for mucins since the virus rapidly escapes attachment to these, but also evident to a lesser extent with SP-A and H-ficolin. LL-37 has a different mechanism of action from either SP-D or SP-A, which does not involve inhibition of viral HA attachment to cell (31). LL-37-treated virus is still taken up by epithelial cells but replication is limited in the early stages of the intracellular life cycle of the virus. The collectins and H-ficolin strongly induce viral aggregation, which appears to be one important of their antiviral activity. This is especially true for SP-D. LL-37, in contrast, does not induce viral aggregation.

The key role of SP-D and SP-A in limiting IAV replication and associated inflammation has been confirmed in many *in vivo* studies in mice (15, 16, 22, 32–34). Human BALF from healthy donors has strong inhibitory activity for seasonal strains and removal of SP-D significantly reduces this activity (23, 35). H-ficolin is closely related to the MBL in structure and like MBL can fix complement directly. Ficolins are abundant in blood as well but H-ficolin is present in BALF of healthy volunteer donors and removal of H-ficolin from human BALF or serum reduces antiviral activity for IAV (19). The IAV neutralizing activity of SP-D greatly exceeds that of SP-A or Ficolins (e.g., for SP-D 50% inhibition occurs at ≈10 ng/ml vs ≈10 μg/ml for SP-A or ficolins) suggesting that the mechanism of action of SP-D is more effective. This is in agreement with murine studies in which absence of SP-D has a greater impact on viral replication and inflammation than absence of SP-A (15, 16, 33, 34).

An important limitation of the action of human or rodent SP-D vs IAV is that it depends on presence high mannose oligosaccharides relatively near the sialic acid binding site of the

HA. This appears to account for the relative inability of SP-D or MBL to inhibit pandemic strains IAV strains from 1918 (H1N1), 1957 (H2N2), 1968 (H3N2) and 2009 (H1N1), and avian strains like H5N1 (36). These strains have a relative lack of glycosylation their HA, especially in the region close to the sialic acid binding site (32, 37–39). H1 and H3 that cause seasonal epidemics have evolved over time within the human populations to express more glycans on the binding head of their HA and as a result are more strongly inhibited by SP-D or MBL (32, 37, 40). It has been shown that such glycans protect this critical region of the HA from recognition by antiviral antibodies. Apparently this evolutionary pressure is not as strong in avian or porcine hosts. There are actually 16 different HA subtypes most of which occur in animal reservoirs (especially birds). Most of these are resistant to inhibition by SP-D (41). Apart from the H1, H2, and H3 subtypes none of the other subtypes have established themselves in a sustained way in the human population. The H5, H7, and H9 subtypes have infected humans with relatively high mortality rates. These are, therefore, of particular concern, but fortunately they have not established sustained transmission from human to human thus far. Overall, it seems likely that the resistance of human pandemic and avian strains to SP-D may be one factor in their pathogenicity for humans, although it is clear that other properties of the HA or other genes are involved in pathogenicity as well (41).

Factors which counteract the action of SP-D, like elevated glucose in diabetes mellitus, could account for increased susceptibility to IAV as demonstrated in mice (42). Glucose, like mannose, is a competitive inhibitor of SP-D binding, although polymers of these saccharides are more potent as inhibitors. Some subjects of known susceptibility to IAV including tobacco smokers, and individuals with COPD or cystic fibrosis have reduced levels of SP-D and SP-A (43–45). In many inflammatory states, multimerization and function of SP-D are altered. Furthermore, there are polymorphic forms of SP-D and SP-A, some of which have reduced activity against IAV *in vitro* and are associated with respiratory infections (46–48). A recent study showed that some SP-A gene variants were associated with severe respiratory insufficiency in humans after infection with the 2009 pandemic H1N1 infection (49). Similar studies are needed with respect to SP-D gene variants. Reduced MBL levels due to specific polymorphisms of the MBL gene appear to increase risk for severe IAV infection as well (50).

DETERMINING THE MOLECULAR MECHANISMS OF ANTIVIRAL ACTIVITY OF SP-D FOR INFLUENZA

Based on these various findings summarized above which indicate the importance of SP-D in host defense against IAV, we have sought to determine the molecular basis of binding of SP-D to the IAV HA and if possible to increase activity through targeted mutations of the SP-D molecule (14). We have studied extensively two main molecular features of SP-D that determine its increased antiviral potency compared to other soluble inhibitors. These features are: (a) its multimerization property which increases its binding affinity and allows it to cause massive aggregation of viruses, bacteria, and other pathogens and (b) its lectin property which allows high affinity binding to mannosylated glycans found on many viruses and other pathogens. A variety of recombinant forms of SP-D were used in our studies as listed in **Table 1**.

TABLE 1 | Modifications of SP-D found to increase or broaden antiviral activity for IAV.

SP-D preparation	Modification	Effect on antiviral activity
Full length recombinant human SP-D	Isolation of high molecular weight multimers	Increased activity compared to trimers or dodecamers (57, 70)
Full length chimeric protein	Rat SP-D and conglutinin (NCRD) chimera	Increased activity compared with rat SP-D (69)
Full length chimeric protein	Human SP-D and mannose-binding lectin (NCRD) chimera	Increased activity compared with similarly multimerized human SP-D (68)
NCRD trimer of human SP-D	D325A or D325S mutation	Slight increase in activity compared to wild-type NCRD (76)
NCRD trimer of human SP-D	R343V mutation	Strong increased activity compared with wild-type NCRD (75)
NCRD trimer of human SP-D	D325A(or S) combined with R343V mutation	Increased activity compared to R343V or D325A alone; significant activity vs pandemic H1N1 and H3N2 (77)

IAV, influenza A virus; SP-D, surfactant protein D; NCRD, neck and carbohydrate recognition domain.

Marked Viral and Bacterial Aggregating Activity Conferred by the N-Terminal and Collagen Domains of SP-D

The multimerization property of SP-D is determined by its N-terminal and collagen domains, which allow for assembly into molecules with from 4 to approximately 32 trimeric arms (51). The extended nature of the collagen domain allows also for very wide separation of the trimeric heads as illustrated in **Figure 1A**.

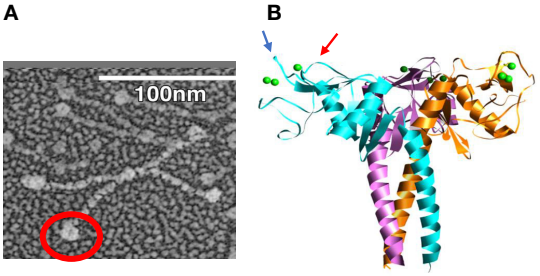

FIGURE 1 | Electron micrograph of dodecameric, intact surfactant protein D (SP-D) molecule **(A)**, electron micrograph of full length dodecameric SP-D **(B)** and structure of H3N2 influenza A viruses hemagglutinin with glycan attachments. The red circle in panel **(A)** is included to highlight the globular NCRD component of the molecule. In panel **(B)**, the blue and red arrows indicate ridges surrounding the lectin binding site of the NCRD. The ridge indicated by the blue arrow is formed by the D325 residue and that shown by the red arrow is formed by R343 [this figure was adapted from Ref. (14)].

This structure allows for extensive cross-linking and aggregation of bacteria or viral particles which exceeds that of SP-A or MBL which have more compact structures (52, 53). The ability of SP-D to aggregate IAV is related not only to its antiviral activity but also to its ability to promote uptake of the virus or bacteria by phagocytes (52–55). The collagen domain *per se* was not found to be critical for increasing viral uptake by neutrophils or monocytes as long as the molecule can form multimers (56, 57). The neck and carbohydrate recognition domains (NCRDs) of collectins can be expressed as small separate trimers as illustrated in **Figure 1B**. A striking finding was that the NCRD of rodent or human SP-D nearly completely lack antiviral activity (58, 59). This finding strongly indicates the importance of cooperativity between binding heads of SP-D in effective viral binding and aggregation. This was further confirmed by showing that antibodies or other treatments which can crosslink NCRD heads without blocking the lectin binding site restore antiviral, aggregating, and opsonizing activity (58, 60, 61). A common polymorphic variant of SP-D (the Thr/Thr11 form) assembles predominantly as trimers and has greatly reduced antiviral activity *in vitro* (62). It is tempting to speculate that individuals with this polymorphism will have less ability to limit IAV infection *in vivo*.

Distinctive Properties of NCRDs of Serum Collectins as Compared to SP-D

We found that NCRDs of MBL and a variety of serum collectins found in bovines including conglutinin, CL-43, and CL-46 have some distinctive properties which give them intrinsically greater antiviral activity (63–66). Given the strong viral aggregating properties of the N-terminal and collagen domains of SP-D, we speculated that combining this with the NCRDs of serum collectins would result in significantly potentiated antiviral activity. This was confirmed by creating chimeric molecules with the SP-D N-terminal and collagen domains and NCRDs or either conglutinin or MBL (67–69). These molecules had increased antiviral, viral aggregating, and viral opsonizing activity than either SP-D, MBL, or conglutinin. One challenge in these comparisons is that there is a great deal of variation in the extent of multimerization that occurs with molecules containing the N-terminal and collagen domains of SP-D. The very high molecular weight multimers of human SP-D occur both naturally and in recombinant preparations and have increased antiviral activity compared to dodecamer forms that are composed of four trimeric arms (53, 70). Similar high molecular weight forms are observed with porcine SP-D (71).

Engineering the NCRD of SP-D to Resemble Those of Serum Collectins

When comparing SP-D and serum collectins, key differences are evident in residues adjacent to the lectin binding site calcium. We speculated that these differences could account for increased viral binding ability of serum collectin NCRDs. CL-43 has a three amino acid insertion of Arg-Ala-Lys (RAK) adjacent to the conserved EPN sequence, which is at the base of the saccharide binding pocket. Addition of this insertion into the NCRD of SP-D conferred increased affinity for mannan and increased ability to inhibit IAV as well (60, 61, 65, 66, 72). Further insights were obtained from study of the crystal structure of the SP-D NCRD (73, 74). Two residues, aspartic acid 325 (D325) and arginine 343 (R343) of SP-D, account for ridges on either side of the lectin binding site as illustrated in **Figure 1B**. R343 is replaced by highly hydrophobic residues (valine or isoleucine) in the serum collectins. Simple substitution of one of these residues (or to a lesser extent alanine) for R343 caused a marked shift in preference of binding to specific oligosaccharides and also marked increase in viral binding and inhibition (75). In contrast, an R343K substitution did not alter antiviral of glycan binding activity.

The D325 residue also differed in some serum collectins (e.g., there is a serine in there in conglutinin), and replacement of D325 with an alanine or serine caused modest increase in antiviral activity (much less than the R343V change) (76, 77). Even the slight D325N alteration (to mimic rat or mouse SP-D) led to a slight shift in saccharide and viral binding (78). More importantly the combined change of D325A(or S) along with R343V in the NCRD of human SP-D enabled greater antiviral activity than either substitution alone (76, 79). The D325A + R343V NCRD had neutralizing activity comparable to full length SP-D dodecamers for seasonal IAV strains and also caused marked viral aggregation despite absence of the N-terminal and collagen domains (77, 80). In addition, administration of D325A + R343V to mice along with an SP-D sensitive (but pathogenic) viral strain significantly reduced viral loads and mortality, whereas the wild-type SP-D NCRD did not (77). A striking additional finding was that the D325A + R343V NCRDs or the related molecule D325S + R343V were able to inhibit pandemic H1N1 of 2009 or 1918 *in vitro* (76). Neither of these strains are inhibited by full length SP-D nor wild-type NCRD. In addition, these double mutant molecules had greater ability to inhibit the 1968 H3N2 pandemic strain than full length SP-D. The D325S + R343V NCRD also reduced viral loads and mortality in mice infected with this pandemic H3N2 strain while with type NCRD did not (76).

Molecular Basis of Increased Neutralization and Viral Aggregation by Double Mutant NCRDs

X-ray crystallographic studies by Drs. Barbara Seaton and Michael Rynkiewicz (Boston University School of Medicine, Physiology and Biophysics) have shown how man9 (an extended mannose chain comparable to those found on viral high mannose glycans) binds to wild-type human SP-D NCRD and the D325A + R343V mutant NCRD (79). They were able to show that mannose chains assume a different orientation with respect to the NCRD surface on the mutant form. This was accounted for by the fact that in the mutant NCRD the penultimate mannose in the chain binds in the lectin site. This contrasts with the wild-type NCRD in which the terminal mannose binds. This finding correlated with increased binding affinity of the mutant NCRD to extended mannose chains as assessed by glycan array studies and increased binding to the Phillipines 82 H3N2 (Phil82) seasonal viral HA by surface plasmon resonance studies (79). Prior seminal studies by Patrick Reading and Margot Anders had shown the importance of the glycan at position 165 for binding of

SP-D or MBL (20–22). Dr. Joseph Zaia (Boston University School of Medicine, Biochemistry) and colleagues were able to confirm that this glycan is of the high mannose type. Based on these findings and those of Drs. Seaton and Rynkiewicz, Drs. Boon Guh, and Klaus Schulten (University of Illinois, Urbana-Champaign, Physics) were able use molecular dynamics to show that the mode of binding of the mutant NCRD to the Phil82 H3N2 HA, using a high mannose glycan at position 165 as the binding site (79). These studies revealed two important insights. Given the different mode of binding of the mutant NCRD to the glycan (i.e., to the penultimate mannose in the chain) it was: (1) able to more fully cover-up the sialic acid binding site of the HA as compared to the wild-type NCRD and (2) able to bind in such a way that the other two lectin sites on the trimer remains exposed to such that they could attach to other HA molecules (see **Figure 2**). The latter observation provides a potential explanation for viral aggregation mediated by the mutant NCRD (in contrast to wild-type NCRD).

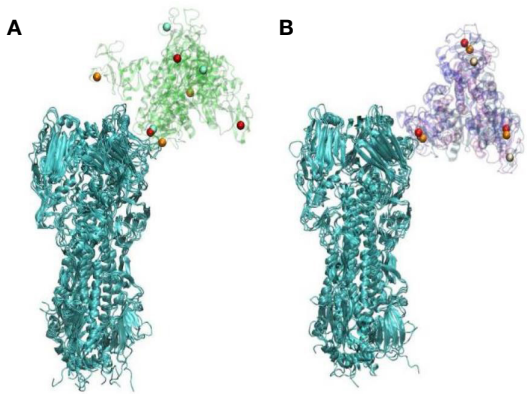

FIGURE 2 | Differences in orientation in hemagglutinin (HA) complexes with WT **(A)** or D325A + R343V **(B)**—this figure represents the endpoints of three repeated simulations. Calcium ions are represented in orange, red, and white; WT and D325A + R343V are in transparent cartoon representation in green and purple, respectively; HA is shown in cartoon representation in cyan [this figure was reprinted with permission from Goh et al. (79)].

Drs. Kshitij Khatri and Joseph Zaia have further expanded on these studies by use of integrated omics and computational biology to determine the true site occupancy and actual glycoforms present on the seasonal Phil82 HA and its bovine serum resistant variant, Phil82/BS. Of interest, not all potential glycan attachment sites on the parental predicted from the protein sequence of the parental Phil82 strain were in fact glycosylated. This supports the importance of actual determination of the location and type of glycan attachments on viral envelope proteins as opposed to basing observations only on attachments predicted by the protein sequence. The structure of the glycosylated HA trimer is shown in **Figure 3A**. Furthermore, the Phil82/BS strain was shown to lack two high mannose glycans on the exposed tip of the HA (those at position 165 and 246).

Using molecular dynamic studies Drs. Khatri and Zaia found that the distance between SP-D NCRD trimeric heads is compatible with binding of all three heads to a single HA molecule (also trimeric) through various potential interactions with glycans at 165 and 246. An interaction of this kind is shown if **Figure 3B**. This provides additional explanation for the ability of SP-D to strongly inhibit certain seasonal H3N2 strains. Note that the pandemic H3N2 strain of 1968 had the glycan at 165 but lacked several other potential glycan attachment sites on its HA. This may account for the reduced ability of wild-type SP-D to inhibit this strain as compared to more recent H3N2 strains including Phil82. Presumably, a similar result may obtain with seasonal vs pandemic H1N1 strains. Note that the 1918 and 2009 H1N1

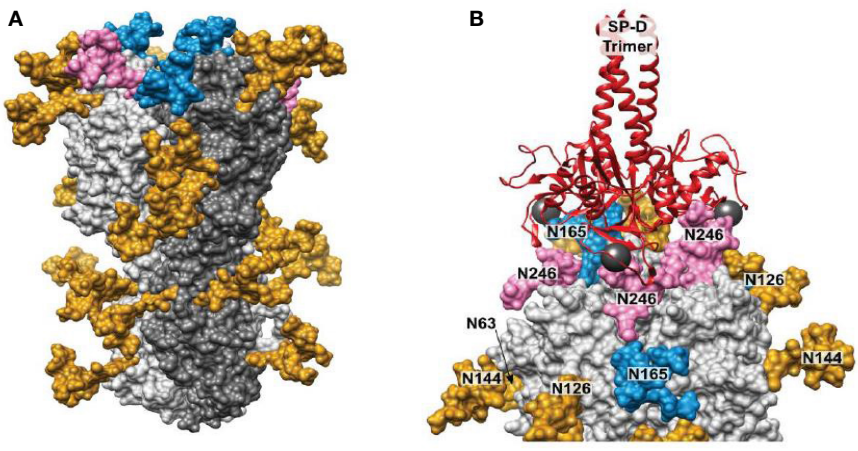

FIGURE 3 | Structure modeling of influenza A virus (IAV) hemagglutinin (HA) and molecular dynamics result showing binding of surfactant protein A (SP-D) neck and carbohydrate recognition domain trimer to the HA. **(A)** 3D model of glycosylated Phil82 hemagglutinin trimer (HA0). One HA monomer is shown in dark gray. Glycans at Asn165 and Asn246 are shown in blue and pink, respectively. **(B)** A model of trimeric SP-D (red ribbons) bound to three N-glycans on the H3 head domain (light gray surface). The 3D structure of the glycosylated H3 was taken from the MD simulation. In this snapshot, Manα residues at sites Asn 246, Asn 165, and Asn 246 on different protomers were approximately 45 Å apart, such that SP-D could bind each residue simultaneously. The calcium atoms found in each SP-D Manα binding site are shown (dark gray spheres) [this figure adapted from Khatri et al. (81) through free usage *via* Creative Commons CC-BY license].

pandemic strains both have a glycan attachment site at position 104. This attachment site has also been predicted to be important for attachment of collectins (20). If this attachment is high mannose as expected, why then are the pandemic H1N1 strains not inhibited by collectins? It is likely that other high mannose glycans (or one other glycan) must be present on seasonal H1N1 strains that developed between 1977 and 2009 during human circulation provide a second important attachment site for collectin. Future studies will hopefully answer this question.

Another very important line of investigation carried out by Drs. Martin van Eijk and Henk Haagsman (University of Utrecht, Netherlands) has shown that porcine SP-D has increased ability to inhibit seasonal IAV strains but also a number of pandemic and avian strains (82, 83). The importance of studying porcine SP-D is that pigs are a source through which pandemic strains can be ultimately transmitted to humans and in the case of the 2009 H1N1. Pigs appear to provide a vessel through which human, porcine, and avian strains can become reassorted to generate new strains potentially adaptable to human transmission. How then does this relate to the increased antiviral activity of porcine SP-D? One speculation is that pigs have partial protection through conferred by innate inhibitors like SP-D allowing them to be infected with multiple IAV strains without strong manifestations of illness. In any case, study of porcine SP-D has revealed important insights into mechanism of collectin inhibition of IAV. Of great interest, porcine SP-D is the only known form of the molecule that has an N-linked glycosylation site on its NCRD. This site has been shown to be highly sialated and to contribute to the enhanced antiviral activity of porcine SP-D (82–86). The presence of the N-linked sugar gives porcine SP-D a dual mechanism of action in which it can bind to viral glycans while also presenting a decoy sialic acid rich ligand to which the viral HA binds. Initial studies by Dr. van Eijk also showed that key residues on the binding surface of the porcine SP-D carbohydrate recognition domain (CRD) differ compared to human or rodent SP-D (71). As in the case of serum collectins, these changes allow the porcine NCRD (even without the N-linked glycan) to inhibit IAV to a much greater extent than wild-type human or rat SP-D NCRDs (87). Further studies of porcine SP-D are important especially given its ability to inhibit pandemic and avian IAV strains.

FUTURE DIRECTIONS

There are other potential impacts of HA glycans including their ability to shield regions of the HA from antibody recognition (9, 88, 89), alteration of the binding properties of the HA (90), and effects on interactions with other host defense lectins like the macrophage mannose receptor, DC-SIGN, or galectins all of which play roles in host defense against IAV (37, 91, 92). It should be noted that such lectin interactions may not always lead to viral inhibition, but can also provide an alternate route for viral entry into and infection of cells (91, 93). Future studies to determine molecular mechanisms of binding to these other host defense lectins will be important.

An important question that is not fully resolved is how SP-D (or SP-A) blunts inflammatory reactions during IAV infection. This immunomodulatory effect is likely to be an important aspect of their protective effect *in vivo*. One hypothesis is that SP-D reduces inflammation simply by reducing viral replication. Alternatively, SP-D could independently act on inflammatory cells to limit their activity. We recently found that SP-D inhibits replication of seasonal IAV in human monocytes and reduces monocyte tumor necrosis factor (TNF) responses to the virus (56). In that study, reduction of the TNF response could be demonstrated even when viral replication was not reduced. Further studies are warranted to determine potential independent effects of SP-D or SP-A on IAV induced lung inflammation. It should be noted that elevated serum levels of SP-D have been associated with worse outcome of severe H1N1 IAV infection (94). Serum levels of SP-D are elevated in a number of conditions in which there is severe lung inflammation and may reflect breakdown in alveolar capillary barriers (43, 95), rather than some adverse effect of SP-D *per se*.

Finally, therapeutics based on SP-A and SP-D can considered with respect to IAV or other respiratory viruses. Potential challenges include selection of patients for such treatment and how to administer protein-based treatments into the airway. Another option is trying to increase endogenous SP-D production as a therapeutic maneuver. It is possible that steroid treatment which is beneficial in some lung infections (e.g., *Pneumocystis carinii*) acts in part through this mechanism. GM-CSF increases surfactant protein production and contributes to host defense against IAV in mice (96, 97). We collaborated with Dr. Frank McCormack of University of Cincinnati School of Medicine to see if keratinocyte growth factor (KGF) would improve outcome of IAV infection in mice based on its known ability to increase pulmonary collectins. However, KGF treatment unexpectedly increased viral replication and mortality in IAV infected mice through a mechanism involving the ability to KGF to increase alveolar epithelial cell proliferation (98). In any case, further research on the role of SP-D in human IAV infection and efforts to harness its antiviral activity for therapeutic purposes remain priorities given the major, ongoing health impacts of IAV and limited options for treatment.

CONCLUSION

Surfactant protein D appears to play an important role in limiting IAV replication and blunting inflammatory responses to the virus. In this review, we detail findings which demonstrate the molecular mechanism of binding to the viral HA to inhibit infectivity and also the mechanism through which SP-D can induce viral aggregation. Aggregation of viruses and other pathogens may be a major mechanism through which SP-D contributes to first line host defense in the airway. We also review, how small changes in the SP-D NCRD are able to increase binding to high mannose glycans and inhibition of IAV. The relative paucity of glycans on the HA of pandemic and avian IAV strains accounts for failure of SP-D to inhibit these strains and this in turn may be one factor in the high level of pathogenicity of these strains. To some extent, modification of the NCRD of SP-D enables it to inhibit some pandemic IAV strains, and this may have therapeutic relevance. Study of molecular interactions of SP-D with IAV has provided a very detailed look at how a lectin-based innate immune protein can mediate binding and defense against a pathogen. Similar studies could be carried out with other pathogens or host defense lectins.

AUTHOR CONTRIBUTIONS

KH supervised much of the work summarized in this review as well doing writing and review of the manuscript. I-NH, XL, and MW carried out experiments described in the review but also wrote and edited parts of the manuscript. All authors approved the final version of the manuscript.

ACKNOWLEDGMENTS

Our laboratory's work was supported by NIH grants AI-83222 and HL-069031. We also gratefully acknowledge many collaborators mentioned throughout this paper who made major contributions to work presented in this paper, with special emphasis on our long-term collaboration with Erika Crouch, the discoverer of SP-D.

REFERENCES

1. Tripathi S, White MR, Hartshorn KL. The amazing innate immune response to influenza A virus infection. *Innate Immun* (2013) 21(1):73–98. doi:10.1177/1753425913508992
2. Ruckle A, Haasbach E, Julkunen I, Planz O, Ehrhardt C, Ludwig S. The NS1 protein of influenza A virus blocks RIG-I-mediated activation of the non-canonical NF-kappaB pathway and p52/RelB-dependent gene expression in lung epithelial cells. *J Virol* (2012) 86:10211–7. doi:10.1128/JVI.00323-12
3. Mangeat B, Cavagliotti L, Lehmann M, Gers-Huber G, Kaur I, Thomas Y, et al. Influenza virus partially counteracts restriction imposed by tetherin/BST-2. *J Biol Chem* (2012) 287:22015–29. doi:10.1074/jbc.M111.319996
4. Lin L, Li Y, Pyo HM, Lu X, Raman SN, Liu Q, et al. Identification of RNA helicase A as a cellular factor that interacts with influenza A virus NS1 protein and its role in the virus life cycle. *J Virol* (2012) 86:1942–54. doi:10.1128/JVI.06362-11
5. Hale BG, Randall RE, Ortin J, Jackson D. The multifunctional NS1 protein of influenza A viruses. *J Gen Virol* (2008) 89:2359–76. doi:10.1099/vir.0.2008/004606-0
6. Novel Swine-Origin Influenza A (H1N1) Virus Investigation Team, Dawood FS, Jain S, Finelli L, Shaw MW, Lindstrom S, et al. Emergence of a novel swine-origin influenza A (H1N1) virus in humans. *N Engl J Med* (2009) 360:2605–15. doi:10.1056/NEJMoa0903810
7. Morens D. Influenza-related mortality: considerations for practice and public health. *JAMA* (2003) 289:227–9. doi:10.1001/jama.289.2.227
8. Budd AP, Wentworth DE, Blanton L, Elal AIA, Alabi N, Barnes J, et al. Update: influenza activity – United States, October 1, 2017–February 3, 2018. *MMWR Morb Mortal Wkly Rep* (2018) 67:169–79. doi:10.15585/mmwr.mm6706a1
9. Wei CJ, Boyington JC, Dai K, Houser KV, Pearce MB, Kong WP, et al. Cross-neutralization of 1918 and 2009 influenza viruses: role of glycans in viral evolution and vaccine design. *Sci Transl Med* (2010) 2:24ra21. doi:10.1126/scitranslmed.3000799
10. McCullers JA, Van De Velde LA, Allison KJ, Branum KC, Webby RJ, Flynn PM. Recipients of vaccine against the 1976 "swine flu" have enhanced neutralization responses to the 2009 novel H1N1 influenza virus. *Clin Infect Dis* (2010) 50:1487–92. doi:10.1086/652441
11. Hartshorn KL. Why does pandemic influenza virus kill? *Am J Pathol* (2013) 183:1125–7. doi:10.1016/j.ajpath.2013.06.020
12. Rynda-Apple A, Robinson KM, Alcorn JF. Influenza and bacterial superinfection: illuminating the immunologic mechanisms of disease. *Infect Immun* (2015) 83:3764–70. doi:10.1128/IAI.00298-15
13. Nguyen JL, Yang W, Ito K, Matte TD, Shaman J, Kinney PL. Seasonal influenza infections and cardiovascular disease mortality. *JAMA Cardiol* (2016) 1:274–81. doi:10.1001/jamacardio.2016.0433
14. Hartshorn KL. In: Wiederschain G, editor. *Glycobiology and Human Diseases*. Boca Raton, FL: CRC Press (2016). p. 97–108.
15. LeVine AM, Hartshorn K, Elliott J, Whitsett J, Korfhagen T. Absence of SP-A modulates innate and adaptive defense responses to pulmonary influenza infection. *Am J Physiol Lung Cell Mol Physiol* (2002) 282:L563–72. doi:10.1152/ajplung.00280.2001
16. LeVine AM, Whitsett JA, Hartshorn KL, Crouch EC, Korfhagen TR. Surfactant protein D enhances clearance of influenza A virus from the lung in vivo. *J Immunol* (2001) 167:5868–73. doi:10.4049/jimmunol.167.10.5868
17. Barlow PG, Svoboda P, Mackellar A, Nash AA, York IA, Pohl J, et al. Antiviral activity and increased host defense against influenza infection elicited by the human cathelicidin LL-37. *PLoS One* (2011) 6:e25333. doi:10.1371/journal.pone.0025333
18. Gaudreault E, Gosselin J. Leukotriene B4 induces release of antimicrobial peptides in lungs of virally infected mice. *J Immunol* (2008) 180:6211–21. doi:10.4049/jimmunol.180.9.6211
19. Verma A, White M, Vathipadiekal V, Tripathi S, Mbianda J, Ieong M, et al. Human H-ficolin inhibits replication of seasonal and pandemic influenza A viruses. *J Immunol* (2012) 189:2478–87. doi:10.4049/jimmunol.1103786
20. Hartley CA, Jackson DC, Anders EM. Two distinct serum mannose-binding lectins function as beta inhibitors of influenza virus: identification of bovine serum beta inhibitor as conglutinin. *J Virol* (1992) 66:4358–63.
21. Anders EM, Hartley CA, Jackson DC. Bovine and mouse serum beta inhibitors of influenza A viruses are mannose-binding lectins. *Proc Natl Acad Sci U S A* (1990) 87:4485–9. doi:10.1073/pnas.87.12.4485
22. Reading PC, Morey LS, Crouch EC, Anders EM. Collectin-mediated antiviral host defense of the lung: evidence from influenza virus infection of mice. *J Virol* (1997) 71:8204–12.
23. Hartshorn KL, Crouch EC, White MR, Eggleton P, Tauber AI, Chang D, et al. Evidence for a protective role of pulmonary surfactant protein D (SP-D) against influenza A viruses. *J Clin Invest* (1994) 94:311–9. doi:10.1172/JCI117323
24. Iwaarden JFV, Benne CA, Strijp JAGV, Verhoef J, Golde LMGV, Kraaijeveld CA. Surfactant protein A (SP-A) prevents infection of cells by influenza A virus. *Am Rev Resp Dis* (1993) 148:A146.
25. Hartshorn KL, Ligtenberg A, White MR, Van Eijk M, Hartshorn M, Pemberton L, et al. Salivary agglutinin and lung scavenger receptor cysteine-rich glycoprotein 340 have broad anti-influenza activities and interactions with surfactant protein D that vary according to donor source and sialylation. *Biochem J* (2006) 393:545–53. doi:10.1042/BJ20050695
26. Hartshorn KL, White MR, Mogues T, Ligtenberg T, Crouch E, Holmskov U. Lung and salivary scavenger receptor glycoprotein-340 contribute to the host defense against influenza A viruses. *Am J Physiol Lung Cell Mol Physiol* (2003) 285:L1066–76. doi:10.1152/ajplung.00057.2003
27. Job ER, Bottazzi B, Gilbertson B, Edenborough KM, Brown LE, Mantovani A, et al. Serum amyloid P is a sialylated glycoprotein inhibitor of influenza A viruses. *PLoS One* (2013) 8:e59623. doi:10.1371/journal.pone.0059623
28. Reading PC, Bozza S, Gilbertson B, Tate M, Moretti S, Job ER, et al. Antiviral activity of the long chain pentraxin PTX3 against influenza viruses. *J Immunol* (2008) 180:3391–8. doi:10.4049/jimmunol.180.5.3391
29. White MR, Crouch E, van Eijk M, Hartshorn M, Pemberton L, Tornoe I, et al. Cooperative anti-influenza activities of respiratory innate immune proteins and neuraminidase inhibitor. *Am J Physiol Lung Cell Mol Physiol* (2005) 288:L831–40. doi:10.1152/ajplung.00365.2004
30. White MR, Helmerhorst EJ, Ligtenberg A, Karpel M, Tecle T, Siqueira WL, et al. Multiple components contribute to ability of saliva to inhibit influenza viruses. *Oral Microbiol Immunol* (2009) 24:18–24. doi:10.1111/j.1399-302X.2008.00468.x
31. Tripathi S, Tecle T, Verma A, Crouch E, White M, Hartshorn KL. The human cathelicidin LL-37 inhibits influenza A viruses through a mechanism distinct from that of surfactant protein D or defensins. *J Gen Virol* (2013) 94:40–9. doi:10.1099/vir.0.045013-0
32. Vigerust DJ, Ulett KB, Boyd KL, Madsen J, Hawgood S, McCullers JA. N-linked glycosylation attenuates H3N2 influenza viruses. *J Virol* (2007) 81:8593–600. doi:10.1128/JVI.00769-07
33. Hawgood S, Brown C, Edmondson J, Stumbaugh A, Allen L, Goerke J, et al. Pulmonary collectins modulate strain-specific influenza a virus infection and host responses. *J Virol* (2004) 78:8565–72. doi:10.1128/JVI.78.16.8565-8572.2004
34. Li G, Siddiqui J, Hendry M, Akiyama J, Edmondson J, Brown C, et al. Surfactant protein-A – deficient mice display an exaggerated early inflammatory response

to a beta-resistant strain of influenza A virus. *Am J Respir Cell Mol Biol* (2002) 26:277–82. doi:10.1165/ajrcmb.26.3.4584
35. White MR, Tecle T, Crouch EC, Hartshorn KL. Impact of neutrophils on antiviral activity of human bronchoalveolar lavage fluid. *Am J Physiol Lung Cell Mol Physiol* (2007) 293:L1293–9. doi:10.1152/ajplung.00266.2007
36. Qi L, Kash JC, Dugan VG, Jagger BW, Lau YF, Sheng ZM, et al. The ability of pandemic influenza virus hemagglutinins to induce lower respiratory pathology is associated with decreased surfactant protein D binding. *Virology* (2011) 412:426–34. doi:10.1016/j.virol.2011.01.029
37. Tate MD, Job ER, Brooks AG, Reading PC. Glycosylation of the hemagglutinin modulates the sensitivity of H3N2 influenza viruses to innate proteins in airway secretions and virulence in mice. *Virology* (2011) 413:84–92. doi:10.1016/j.virol.2011.01.036
38. Job ER, Deng YM, Tate MD, Bottazzi B, Crouch EC, Dean MM, et al. Pandemic H1N1 influenza A viruses are resistant to the antiviral activities of innate immune proteins of the collectin and pentraxin superfamilies. *J Immunol* (2010) 185:4284–91. doi:10.4049/jimmunol.1001613
39. Hartshorn KL, Webby R, White MR, Tecle T, Pan C, Boucher S, et al. Role of viral hemagglutinin glycosylation in anti-influenza activities of recombinant surfactant protein D. *Respir Res* (2008) 9:65. doi:10.1186/1465-9921-9-65
40. Hartshorn KL, Sastry K, White MR, Anders EM, Super M, Ezekowitz RA, et al. Human mannose-binding protein functions as an opsonin for influenza A viruses. *J Clin Invest* (1993) 91:1414–20. doi:10.1172/JCI116345
41. Qi L, Pujanauski LM, Davis AS, Schwartzman LM, Chertow DS, Baxter D, et al. Contemporary avian influenza a virus subtype h1, h6, h7, h10, and h15 hemagglutinin genes encode a mammalian virulence factor similar to the 1918 pandemic virus h1 hemagglutinin. *MBio* (2014) 5(6):e02116. doi:10.1128/mBio.02116-14
42. Reading P, Allison J, Crouch E, Anders E. Increased susceptibility of diabetic mice to influenza virus infection: compromise of collectin-mediated host defense of the lung by glucose. *J Virol* (1998) 72:6884–7.
43. Lomas DA, Silverman EK, Edwards LD, Locantore NW, Miller BE, Horstman DH, et al. Serum surfactant protein D is steroid sensitive and associated with exacerbations of COPD. *Eur Respir J* (2009) 34(1):95–102. doi:10.1183/09031936.00156508
44. Sims MW, Tal-Singer RM, Kierstein S, Musani AI, Beers MF, Panettieri RA, et al. Chronic obstructive pulmonary disease and inhaled steroids alter surfactant protein D (SP-D) levels: a cross-sectional study. *Respir Res* (2008) 9:13. doi:10.1186/1465-9921-9-13
45. Honda Y, Takahashi H, Kuroki Y, Akino T, Abe S. Decreased contents of surfactant proteins A and D in BAL fluids of healthy smokers. *Chest* (1996) 109:1006–9. doi:10.1378/chest.109.4.1006
46. Leth-Larsen R, Garred P, Jensenius H, Meschi J, Hartshorn K, Madsen J, et al. A common polymorphism in the SFTPD gene influences assembly, function, and concentration of surfactant protein D. *J Immunol* (2005) 174:1532–8. doi:10.4049/jimmunol.174.3.1532
47. Thomas NJ, Diangelo S, Hess JC, Fan R, Ball MW, Geskey JM, et al. Transmission of surfactant protein variants and haplotypes in children hospitalized with respiratory syncytial virus. *Pediatr Res* (2009) 66(1):70–3. doi:10.1203/PDR.0b013e3181a1d768
48. Mikerov AN, White M, Hartshorn K, Wang G, Floros J. Inhibition of hemagglutination activity of influenza A viruses by SP-A1 and SP-A2 variants expressed in CHO cells. *Med Microbiol Immunol* (2008) 197:9–12. doi:10.1007/s00430-007-0051-4
49. Herrera-Ramos E, Lopez-Rodriguez M, Ruiz-Hernandez JJ, Horcajada JP, Borderias L, Lerma E, et al. Surfactant protein A genetic variants associate with severe respiratory insufficiency in pandemic influenza A virus infection. *Crit Care* (2014) 18:R127. doi:10.1186/cc13934
50. Gao L, Shang S, Zhang C, Tong M, Chen Y. Lower mannose-binding lectin contributes to deleterious H1N1 2009 infection in children. *APMIS* (2013) 122(2):136–9. doi:10.1111/apm.12111
51. Crouch E, Chang D, Rust K, Persson A, Heuser J. Recombinant pulmonary surfactant protein D. *J Biol Chem* (1994) 269:15808–13.
52. Brown-Augsburger P, Hartshorn K, Chang D, Rust K, Fliszar C, Welgus H, et al. Site directed mutagenesis of Cys15 and Cys20 of pulmonary surfactant protein D: expression of a trimeric protein with altered anti-viral properties. *J Biol Chem* (1996) 271:13724–30. doi:10.1074/jbc.271.23.13724
53. Hartshorn K, Chang D, Rust K, White M, Heuser J, Crouch E. Interactions of recombinant human pulmonary surfactant protein D and SP-D multimers with influenza A. *Am J Physiol* (1996) 271:L753–62.
54. Hartshorn K, Crouch E, White M, Colamussi M, Kakkanatt A, Tauber B, et al. Pulmonary surfactant proteins A and D enhance neutrophil uptake of bacteria. *Am J Physiol* (1998) 274:L958–69.
55. Hartshorn KL, White MR, Crouch EC. Contributions of the N- and C-terminal domains of surfactant protein d to the binding, aggregation, and phagocytic uptake of bacteria. *Infect Immun* (2002) 70:6129–39. doi:10.1128/IAI.70.11.6129-6139.2002
56. White MR, Tripathi S, Verma A, Kingma P, Takahashi K, Jensenius J, et al. Collectins, H-ficolin and LL-37 reduce influence viral replication in human monocytes and modulate virus-induced cytokine production. *Innate Immun* (2017) 23:77–88. doi:10.1177/1753425916678470
57. White M, Kingma P, Tecle T, Kacak N, Linders B, Heuser J, et al. Multimerization of surfactant protein D, but not its collagen domain, is required for antiviral and opsonic activities related to influenza virus. *J Immunol* (2008) 181:7936–43. doi:10.4049/jimmunol.181.11.7936
58. Tecle T, White MR, Sorensen G, Gantz D, Kacak N, Holmskov U, et al. Critical role for cross-linking of trimeric lectin domains of surfactant protein D in antiviral activity against influenza A virus. *Biochem J* (2008) 412:323–9. doi:10.1042/BJ20071663
59. Kingma PS, Zhang L, Ikegami M, Hartshorn K, McCormack FX, Whitsett JA. Correction of pulmonary abnormalities in Sftpd-/- mice requires the collagenous domain of surfactant protein D. *J Biol Chem* (2006) 281:24496–505. doi:10.1074/jbc.M600651200
60. White MR, Boland P, Tecle T, Gantz D, Sorenson G, Tornoe I, et al. Enhancement of antiviral activity of collectin trimers through cross-linking and mutagenesis of the carbohydrate recognition domain. *J Innate Immun* (2010) 2:267–79. doi:10.1159/000272313
61. Hartshorn KL, White MR, Smith K, Sorensen G, Kuroki Y, Holmskov U, et al. Increasing antiviral activity of surfactant protein d trimers by introducing residues from bovine serum collectins: dissociation of mannan-binding and antiviral activity. *Scand J Immunol* (2010) 72:22–30. doi:10.1111/j.1365-3083.2010.02409.x
62. Hartshorn KL, White MR, Tecle T, Tornoe I, Sorensen GL, Crouch EC, et al. Reduced influenza viral neutralizing activity of natural human trimers of surfactant protein D. *Respir Res* (2007) 8:9. doi:10.1186/1465-9921-8-9
63. Hansen S, Holm D, Moeller V, Vitved L, Bendixen C, Reid KBM, et al. CL-46, a novel collectin highly expressed in bovine thymus and liver. *J Immunol* (2002) 169:5726–34. doi:10.4049/jimmunol.169.10.5726
64. Rothmann AB, Mortensen HD, Holmskov U, Hojrup P. Structural characterization of bovine collectin-43. *Eur J Biochem* (1997) 243:630–5. doi:10.1111/j.1432-1033.1997.t01-1-00630.x
65. Crouch E, Tu Y, Briner D, McDonald B, Smith K, Holmskov U, et al. Ligand specificity of human surfactant protein D: expression of a mutant trimeric collectin that shows enhanced interactions with influenza A virus. *J Biol Chem* (2005) 280:17046–56. doi:10.1074/jbc.M413932200
66. Hartshorn KL, Holmskov U, Hansen S, Zhang P, Meschi J, Mogues T, et al. Distinctive anti-influenza properties of recombinant collectin 43. *Biochem J* (2002) 366:87–96. doi:10.1042/bj20011868
67. Zhang L, Hartshorn KL, Crouch EC, Ikegami M, Whitsett JA. Complementation of pulmonary abnormalities in SP-D(-/-) mice with an SP-D/conglutinin fusion protein. *J Biol Chem* (2002) 277:22453–9. doi:10.1074/jbc.M201632200
68. White MR, Crouch E, Chang D, Sastry K, Guo N, Engelich G, et al. Enhanced antiviral and opsonic activity of a human mannose-binding lectin and surfactant protein D chimera. *J Immunol* (2000) 165:2108–15. doi:10.4049/jimmunol.165.4.2108
69. Hartshorn KL, Sastry KN, Chang D, White MR, Crouch EC. Enhanced anti-influenza activity of a surfactant protein D and serum conglutinin fusion protein. *Am J Physiol Lung Cell Mol Physiol* (2000) 278:L90–8. doi:10.1152/ajplung.2000.278.1.L90
70. White MR, Crouch E, Chang D, Hartshorn KL. Increased antiviral and opsonic activity of a highly multimerized collectin chimera. *Biochem Biophys Res Commun* (2001) 286:206–13. doi:10.1006/bbrc.2001.5373
71. van Eijk M, van de Lest CH, Batenburg JJ, Vaandrager AB, Meschi J, Hartshorn KL, et al. Porcine surfactant protein D is N-glycosylated in its carbohydrate recognition domain and is assembled into differently charged

oligomers. *Am J Respir Cell Mol Biol* (2002) 26:739–47. doi:10.1165/ajrcmb.26.6.4520

72. Holmskov U, Teisner B, Willis AC, Reid KBM, Jensenius JC. Purification and characterization of a bovine serum lectin (CL-43) with structural homology to conglutinin and SP-D and carbohydrate specificity similar to mannan-binding protein. *J Biol Chem* (1993) 268:1012010125.
73. Shrive AK, Tharia HA, Strong P, Kishore U, Burns I, Rizkallah PJ, et al. High-resolution structural insights into ligand binding and immune cell recognition by human lung surfactant protein D. *J Mol Biol* (2003) 331:509–23. doi:10.1016/S0022-2836(03)00761-7
74. Hakansson K, Lim N, Hoppe H, Reid K. Crystal structure of the trimeric alpha helical coiled-coil and the three lectin domains of human lung surfactant protein D. *Structure* (1999) 24:255–64. doi:10.1016/S0969-2126(99)80036-7
75. Crouch E, Hartshorn K, Horlacher T, McDonald B, Smith K, Cafarella T, et al. Recognition of mannosylated ligands and influenza A virus by human surfactant protein D: contributions of an extended site and residue 343. *Biochemistry* (2009) 48:3335–45. doi:10.1021/bi8022703
76. Nikolaidis NM, White MR, Allen K, Tripathi S, Qi L, McDonald B, et al. Mutations flanking the carbohydrate binding site of surfactant protein D confer antiviral activity for pandemic influenza A viruses. *Am J Physiol Lung Cell Mol Physiol* (2014) 306:L1036–44. doi:10.1152/ajplung.00035.2014
77. Crouch E, Nikolaidis N, McCormack FX, McDonald B, Allen K, Rynkiewicz MJ, et al. Mutagenesis of surfactant protein D informed by evolution and X-ray crystallography enhances defenses against influenza A virus in vivo. *J Biol Chem* (2011) 286:40681–92. doi:10.1074/jbc.M111.300673
78. Crouch EC, Smith K, McDonald B, Briner D, Linders B, McDonald J, et al. Species differences in the carbohydrate binding preferences of surfactant protein D. *Am J Respir Cell Mol Biol* (2006) 35:84–94. doi:10.1165/rcmb.2005-0462OC
79. Goh BC, Rynkiewicz MJ, Cafarella TR, White MR, Hartshorn KL, Allen K, et al. Molecular mechanisms of inhibition of influenza by surfactant protein D revealed by large-scale molecular dynamics simulation. *Biochemistry* (2013) 52(47):8527–38. doi:10.1021/bi4010683
80. Hartshorn KL, White MR, Tecle T, Sorensen GL, Holmskov U, Crouch EC. Viral aggregating and opsonizing activity in collectin trimers. *Am J Physiol Lung Cell Mol Physiol* (2010) 298:L79–88. doi:10.1152/ajplung.00223.2009
81. Khatri K, Klein JA, White MR, Grant OC, Leymarie N, Woods RJ, et al. Integrated omics and computational glycobiology reveal structural basis for influenza A virus glycan microheterogeneity and host interactions. *Mol Cell Proteomics* (2016) 15:1895–912. doi:10.1074/mcp.M116.058016
82. Hillaire ML, van Eijk M, Nieuwkoop NJ, Vogelzang-van Trierum SE, Fouchier RA, Osterhaus AD, et al. The number and position of N-linked glycosylation sites in the hemagglutinin determine differential recognition of seasonal and 2009 pandemic H1N1 influenza virus by porcine surfactant protein D. *Virus Res* (2012) 169:301–5. doi:10.1016/j.virusres.2012.08.003
83. van Eijk M, White MR, Crouch EC, Batenburg JJ, Vaandrager AB, Van Golde LM, et al. Porcine pulmonary collectins show distinct interactions with influenza A viruses: role of the N-linked oligosaccharides in the carbohydrate recognition domain. *J Immunol* (2003) 171:1431–40. doi:10.4049/jimmunol.171.3.1431
84. Hillaire ML, van Eijk M, Vogelzang-van Trierum SE, Nieuwkoop NJ, van Riel D, Fouchier RA, et al. Assessment of the antiviral properties of recombinant surfactant protein D against influenza B virus in vitro. *Virus Res* (2015) 195:43–6. doi:10.1016/j.virusres.2014.08.019
85. van Eijk M, Bruinsma L, Hartshorn KL, White MR, Rynkiewicz MJ, Seaton BA, et al. Introduction of N-linked glycans in the lectin domain of surfactant protein D: impact on interactions with influenza A viruses. *J Biol Chem* (2011) 286:20137–51. doi:10.1074/jbc.M111.224469
86. van Eijk M, White MR, Batenburg JJ, Vaandrager AB, van Golde LM, Haagsman HP, et al. Interactions of influenza A virus with sialic acids present on porcine surfactant protein D. *Am J Respir Cell Mol Biol* (2004) 30:871–9. doi:10.1165/rcmb.2003-0355OC
87. van Eijk M, Rynkiewicz MJ, White MR, Hartshorn KL, Zou X, Schulten K, et al. A unique sugar-binding site mediates the distinct anti-influenza activity of pig surfactant protein D. *J Biol Chem* (2012) 287:26666–77. doi:10.1074/jbc.M112.368571
88. Job ER, Deng YM, Barfod KK, Tate MD, Caldwell N, Reddiex S, et al. Addition of glycosylation to influenza A virus hemagglutinin modulates antibody-mediated recognition of H1N1 2009 pandemic viruses. *J Immunol* (2013) 190:2169–77. doi:10.4049/jimmunol.1202433
89. Wanzeck K, Boyd KL, McCullers JA. Glycan shielding of the influenza virus hemagglutinin contributes to immunopathology in mice. *Am J Respir Crit Care Med* (2011) 183(6):767–73. doi:10.1164/rccm.201007-1184OC
90. Tsuchiya E, Sugawara K, Hongo S, Matsuzaki Y, Muraki Y, Li ZN, et al. Effect of addition of new oligosaccharide chains to the globular head of influenza A/H2N2 virus haemagglutinin on the intracellular transport and biological activities of the molecule. *J Gen Virol* (2002) 83:1137–46. doi:10.1099/0022-1317-83-12-3067
91. Londrigan SL, Turville SG, Tate MD, Deng YM, Brooks AG, Reading PC. N-linked glycosylation facilitates sialic acid-independent attachment and entry of influenza A viruses into cells expressing DC-SIGN or L-SIGN. *J Virol* (2011) 85:2990–3000. doi:10.1128/JVI.01705-10
92. Yang ML, Chen YH, Wang SW, Huang YJ, Leu CH, Yeh NC, et al. Galectin-1 binds to influenza virus and ameliorates influenza virus pathogenesis. *J Virol* (2011) 85:10010–20. doi:10.1128/JVI.00301-11
93. Spear GT, Zariffard MR, Xin J, Saifuddin M. Inhibition of DC-SIGN-mediated trans infection of T cells by mannose-binding lectin. *Immunology* (2003) 110:80–5. doi:10.1046/j.1365-2567.2003.01707.x
94. Delgado C, Krotzsch E, Jimenez-Alvarez LA, Ramirez-Martinez G, Marquez-Garcia JE, Cruz-Lagunas A, et al. Serum surfactant protein D (SP-D) is a prognostic marker of poor outcome in patients with A/H1N1 virus infection. *Lung* (2015) 193:25–30. doi:10.1007/s00408-014-9669-3
95. Wang SX, Liu P, Wei MT, Chen L, Guo Y, Wang RY, et al. Roles of serum clara cell protein 16 and surfactant protein-D in the early diagnosis and progression of silicosis. *J Occup Environ Med* (2007) 49:834–9. doi:10.1097/JOM.0b013e318124a927
96. Sever-Chroneos Z, Murthy A, Davis J, Florence JM, Kurdowska A, Krupa A, et al. GM-CSF modulates pulmonary resistance to influenza A infection. *Antiviral Res* (2011) 92:319–28. doi:10.1016/j.antiviral.2011.08.022
97. Huang FF, Barnes PF, Feng Y, Donis R, Chroneos ZC, Idell S, et al. GM-CSF in the lung protects against lethal influenza infection. *Am J Respir Crit Care Med* (2011) 184:259–68. doi:10.1164/rccm.201012-2036OC
98. Nikolaidis NM, Noel JG, Pitstick LB, Gardner JC, Uehara Y, Wu H, et al. Mitogenic stimulation accelerates influenza-induced mortality by increasing susceptibility of alveolar type II cells to infection. *Proc Natl Acad Sci U S A* (2017) 114:E6613–22. doi:10.1073/pnas.1621172114

Conflict of Interest Statement: The authors declare that the research was conducted in the absence of any commercial or financial relationships that could be construed as a potential conflict of interest.

frontiers in Immunology

ORIGINAL RESEARCH
published: 30 July 2018
doi: 10.3389/fimmu.2018.01586

Entry Inhibition and Modulation of Pro-Inflammatory Immune Response Against Influenza A Virus by a Recombinant Truncated Surfactant Protein D

Mohammed N. Al-Ahdal[1], Valarmathy Murugaiah[2], Praveen M. Varghese[2], Suhair M. Abozaid[1], Iram Saba[1], Ahmed Ali Al-Qahtani[1], Ansar A. Pathan[2], Lubna Kouser[2,3], Béatrice Nal[2] and Uday Kishore[2]*

[1] Department of Infection and Immunity, King Faisal Specialist Hospital and Research Centre, Riyadh, Saudi Arabia, [2] Biosciences, College of Health and Life Sciences, Brunel University London, Uxbridge, United Kingdom, [3] Allergy & Clinical Immunology Inflammation, Repair and Development, Imperial College London, London, United Kingdom

OPEN ACCESS

Edited by:
Francesca Granucci, Università degli studi di Milano Bicocca, Italy

Reviewed by:
Luisa Martinez-Pomares, University of Nottingham, United Kingdom
Junji Xing, Houston Methodist Research Institute, United States

***Correspondence:**
Mohammed N. Al-Ahdal
ahdal@kfshrc.edu.sa

Specialty section:
This article was submitted to Molecular Innate Immunity, a section of the journal Frontiers in Immunology

Received: *13 February 2018*
Accepted: *26 June 2018*
Published: *30 July 2018*

Citation:
Al-Ahdal MN, Murugaiah V, Varghese PM, Abozaid SM, Saba I, Al-Qahtani AA, Pathan AA, Kouser L, Nal B and Kishore U (2018) Entry Inhibition and Modulation of Pro-Inflammatory Immune Response Against Influenza A Virus by a Recombinant Truncated Surfactant Protein D. Front. Immunol. 9:1586. doi: 10.3389/fimmu.2018.01586

Surfactant protein D (SP-D) is expressed in the mucosal secretion of the lung and contributes to the innate host defense against a variety of pathogens, including influenza A virus (IAV). SP-D can inhibit hemagglutination and infectivity of IAV, in addition to reducing neuraminidase (NA) activity via its carbohydrate recognition domain (CRD) binding to carbohydrate patterns (N-linked mannosylated) on NA and hemagglutinin (HA) of IAV. Here, we demonstrate that a recombinant fragment of human SP-D (rfhSP-D), containing homotrimeric neck and CRD regions, acts as an entry inhibitor of IAV and downregulates M1 expression considerably in A549 cells challenged with IAV of H1N1 and H3N2 subtypes at 2 h treatment. In addition, rfhSP-D downregulated mRNA levels of TNF-α, IFN-α, IFN-β, IL-6, and RANTES, particularly during the initial stage of IAV infection of A549 cell line. rfhSP-D also interfered with IAV infection of Madin Darby canine kidney (MDCK) cells through HA binding. Furthermore, rfhSP-D was found to reduce luciferase reporter activity in MDCK cells transduced with H1+N1 pseudotyped lentiviral particles, where 50% of reduction was observed with 10 µg/ml rfhSP-D, suggestive of a critical role of rfhSP-D as an entry inhibitor against IAV infectivity. Multiplex cytokine array revealed that rfhSP-D treatment of IAV challenged A549 cells led to a dramatic suppression of key pro-inflammatory cytokines and chemokines. In the case of pH1N1, TNF-α, IFN-α, IL-10, IL-12 (p40), VEGF, GM-CSF, and eotaxin were considerably suppressed by rfhSP-D treatment at 24 h. However, these suppressive effects on IL-10, VEGF, eotaxin and IL-12 (p40) were not so evident in the case of H3N2 subtype, with the exception of TNF-α, IFN-α, and GM-CSF. These data seem to suggest that the extent of immunomodulatory effect of SP-D on host cells can vary considerably in a IAV subtype-specific manner. Thus, rfhSP-D treatment can downregulate pro-inflammatory milieu encouraged by IAV that otherwise causes aberrant inflammatory cell recruitment leading to cell death and lung damage.

Keywords: innate immunity, influenza A virus, surfactant protein D, pseudotyped lentiviral particles, inflammation

INTRODUCTION

The innate immune system is composed of both cellular and humoral players to encounter invading pathogens. It is also an important component in the initiation and modulation of the adaptive immunity. To distinguish self from non-self, the innate immune system has evolved to recognize pathogen-associated molecular patterns through a number of pattern recognition receptors, including toll like receptors and C-type lectin receptors. Collectins are collagenous lectins, representing a crucial group of calcium-dependent pattern recognition molecules present in pulmonary secretions and mammalian serum (1). They play a crucial role in the first line of defense against a diverse range of pathogens by interacting with specific glycoconjugates and lipid moieties present on the surface of microorganisms. A significant number of *in vitro and in vivo* studies have focused on the immunomodulatory functions of a lung collectin, human surfactant protein D (SP-D). SP-D is primarily organized into four regions: a cysteine-linked N-terminal region involved in multimerization, a triple-helical collagen region composed of Gly-X-Y repeats, an α-helical, coiled-coil trimerizing neck region, and the C-terminal carbohydrate recognition domains (CRDs) or C-type lectin domain (2). Human SP-D is primarily synthesized by alveolar type II and Clara cells, in addition to being present in several extra-pulmonary tissues. SP-D triggers a range of anti-microbial defense mechanisms, including agglutination/aggregation, phagocytosis, and direct growth inhibition (1). SP-D is also capable of controlling pulmonary inflammation including allergy and asthma, and thus, linking innate with adaptive immunity *via* modulation of dendritic cell maturation, and polarization of helper T cells (1).

The direct nature of interaction between SP-D and Influenza A Virus (IAV) has been reported (3, 4), which often results in virus neutralization and enhanced phagocytosis (5, 6). Anti-viral roles of SP-D during IAV infection have been well-documented, principally by Hartshorn group. IAV is an enveloped RNA virus and a member of Orthomyxoviridae family that possesses eight single-stranded RNA segments with negative orientation. These RNA segments can encode up to 13 viral proteins, including two surface glycoproteins, an ion channel protein, nucleocapsid protein, structural scaffolding protein, a tripartite polymerase complex, two non-structural proteins, and three non-essential proteins (7). IAV is subtyped based on their surface glycoproteins, such as hemagglutinin (HA) and neuraminidase (NA); to date, there are 19 HA and 9 NA protein subtypes that have been well established. Both HA and NA play an important role in the host range, viral replication, and pathogenicity (8). Among the three genera of influenza viruses reported, infection by IAV is the most common and severe in humans, swine, and avian species. It is also known to cause pandemic infections, being diverse in host specificity. IAV is considered as a major human respiratory pathogen following 1918 H1N1 influenza pandemic (Spanish Flu) (9), which is believed to have resulted in the zoonotic transmission of an avian virus to a human host and has rapidly dispersed (10).

Binding of IAV to target cells is mediated *via* the globular head of HA to sialic acid (SA) receptors present on the host cell surface (11, 12). IAV subtypes have adapted to human preferentially *via* binding with α (2–6) linkage of SA receptors (13). Following IAV–SA receptor interaction, virus particles are internalized *via* clathrin, resulting in clathrin-mediated endocytosis, or *via* caveolin/clathrin-independent mechanism (14, 15). Thus, acidic environment triggers M2 ion channel and transfers protons and potassium into the interior portion of the virion to dissociate M1 protein from the ribonucleoprotein (RNP) (16). Acidification also initiates HA-mediated conformational changes, which leads to viral fusion and RNPs release into the cytoplasm, resulting in viral transcription and replication. It is, therefore, suggested that SA and its linkage are crucial for the initiation of IAV infection of both epithelial and immune cells. Thus, inhibition of SA receptor binding or enzymatic switching of SA-mediated linkages can confer cell resistance, and/or alter susceptibility to IAV infection. Hence, cell surface SA is considered as an important primary receptor and determinant of IAV tropism, contributing to induction of immune responses as well as to viral pathogenesis.

It is crucial to understand the molecular mechanisms of host defense against IAV in order to design novel anti-IAV strategies. SP-D binding to HA leads to a direct inhibition of cellular infection by preventing HA–SA receptor interaction (4). SP-D has been shown to bind HA-mediated glycosylation sites, identified as β-type inhibitor of IAV. This interaction is calcium dependent, and binding of SP-D to NA inhibits the release of progeny virions from infected cells (17, 18). It has been reported that recombinant full-length porcine SP-D has a potent antiviral activity against a wide range of IAV by similar mechanisms, more than human SP-D due to structural differences, such as an additional loop in its CRD, an additional glycosylation site, and an additional cysteine in the collagen domain (19). In this study, we have used a well-characterized recombinant homotrimeric fragment of human SP-D comprising neck and CRD region (rfhSP-D), and examined its ability to act as an entry inhibitor of IAV and pseudotyped viral particles, and modulate subsequent immunological response *in vitro*.

MATERIALS AND METHODS

Reagents

Viruses and Reagents

The A/England/2009 (pH1N1) and the A/HK/99 (H3N2) strains were gifted by Wendy Barclay from the Imperial College, London and Leo Poon from the University of Hong Kong, respectively. The plasmids used to produce the H1+N1 pseudotyped lentiviral particles were obtained from Addgene. The pHIV-Luciferase plasmid was a gift from Bryan Welm (Addgene plasmid # 21375); psPAX2 was a gift from Didier Trono (Addgene plasmid # 12260); and Vesicular Stomatitis Virus (VSV-G) was offered by Bob Weinberg (Addgene plasmid #8454). Monoclonal Anti-Influenza Virus H1 HA, A/California/04/2009 (H1N1)pdm09, Clone 5C12 (produced *in vitro*), NR-42019 and Polyclonal Anti-Influenza Virus H3 HA, A/Hong Kong/1/1968 (H3N2) (antiserum, Goat), NR-3118 were obtained from BEI Resources, NIAID, NIH, USA.

Cell Culture

Adenocarcinomic human alveolar basal epithelial cells (A549), Madin Darby Canine Kidney (MDCK), and human embryonic kidney (HEK) 293T cell lines were cultured in Dulbecco's Modified

Eagle's Medium (DMEM) (Sigma-Aldrich), supplemented with 10% v/v fetal bovine serum (FBS), 2 mM L-glutamine, 100 U/ml penicillin (Sigma-Aldrich), 100 µg/ml streptomycin (Sigma-Aldrich) and 1 mM sodium pyruvate (Sigma-Aldrich), and left to grow at 37°C in the presence of 5% v/v CO_2 for approximately 3 days before passaging. Since these cells were adherent, they were detached using 2× Trypsin-EDTA (0.5%) (Fisher Scientific) for 10 min at 37°C. Cells were then centrifuged at 1,200 rpm for 5 min, followed by re-suspension in complete DMEM with FBS, penicillin, and streptomycin, as described above. To determine the cell count and viability, an equal volume of the cell suspension and Trypan Blue (0.4% w/v) (Fisher Scientific) solution were vortexed, followed by cell count using a hemocytometer with Neubauer rulings (Sigma-Aldrich). Cells were then re-suspended in complete DMEM for further use.

Purification of IAV Subtypes

MDCK cells at 80–90% confluency were washed with sterile PBS twice before infection. Diluted pH1N1 (2×10^4) or H3N2 (3.3×10^4) (600 µl/flask) was transferred to the flask containing 20 ml of complete DMEM, and incubated at 37°C for 1 h. Unbound viruses were removed by washing three times with sterile PBS. 25 ml of infection medium [DMEM with 1% penicillin/streptomycin, 0.3% bovine serum albumin (BSA), and 1 µg/ml of L-1-Tosylamide-2-phenylethyl chloromethyl ketone (TPCK)—Trypsin] (Sigma-Aldrich) were added to the flasks, and incubated at 37°C for 3 days. The virus particles were then harvested *via* centrifugation of the infection medium at 3,000 × *g* at 4°C for 15 min. The supernatant obtained was centrifuged at 10,000 × *g* for 30 min at 4°C. 26 ml of supernatant was added slowly to new ultra-clear centrifuge tubes containing 30% w/v sucrose (8 ml/tube) (Sigma-Aldrich), and centrifuged at 25,000 × *g* at 4°C for 90 min. The upper phase of the medium and the sucrose phase were carefully removed; IAV particles at the bottom were re-suspended in 100 µl of sterile PBS. Virus suspension (15 µl) was subsequently analyzed by SDS-PAGE and ELISA.

Tissue Culture Infectious Dose 50% ($TCID_{50}$) Assay

Purified pH1N1 or H3N2 virus stocks were prepared with a starting dilution of 10^{-2} in DMEM and 146 µl of the diluted virus was added to all wells; uninfected MDCK cells were used as a control. 46 µl of pH1N1 or H3N2 was then serially diluted ($1/2\log_{10}$ up to 10^{-7}) and incubated at 37°C for 1 h in a microtiter plate. 1×10^5 MDCK cells, earlier trypsinised and re-suspended in 2× infection medium, were added to each well and incubated for 3 days at 37°C under 5% v/v CO_2 until cytopathic effect (CPE) was observed. After 5 days, each well was observed under microscope, and the number of wells that were positive and negative for CPE at each dilution was recorded.

Expression and Purification of a Recombinant Fragment of Human SP-D Containing Neck and CRD Regions

A recombinant fragment of human SP-D (rfhSP-D) was expressed under bacteriophage T7 promoter in *Escherichia coli* BL21 (λDE3) pLysS (Invitrogen), transformed with plasmid pUK-D1 containing cDNA sequences for the 8 Gly-X-Y repeats, neck and CRD regions of human SP-D, as described previously (20). Briefly, a primary inoculum of 25 ml bacterial culture was inoculated into 500 ml of LB containing 100 µg/ml ampicillin and 34 µg/ml chloramphenicol (Sigma-Aldrich), grown to OD_{600} of 0.6, and then induced with 0.5 mM isopropyl β-D-1-thiogalactopyranoside (IPTG) (Sigma-Aldrich) for 3 h. The bacterial cell pellet was re-suspended in lysis buffer (50 mM Tris–HCl pH7.5, 200 mM NaCl, 5 mM EDTA pH 8, 0.1% v/v Triton X-100, 0.1 mM phenyl-methyl-sulfonyl fluoride, 50 µg/ml lysozyme) and sonicated (five cycles, 30 s each). The sonicate was harvested at 12,000 × *g* for 30 min, followed by solubilization of inclusion bodies in refolding buffer (50 mM Tris–HCl pH 7.5, 100 mM NaCl, 10 mM 2-Mercaptoethanol) containing 8 M urea. The solubilized fraction was then dialyzed stepwise against refolding buffer containing 4 M, 2 M, 1 M, and no urea. The clear dialysate was loaded onto a maltose agarose column (5 ml; Sigma-Aldrich) and the bound rfhSP-D was eluted using 50 mM Tris–HCl, pH 7.5, 100 mM NaCl, and 10 mM EDTA. The eluted fractions were then passed through PierceTM High Capacity Endotoxin Removal Resin (Qiagen) to remove endotoxin. The endotoxin levels were measured *via* QCL-1000 Limulus amebocyte lysate system (Lonza), and found to be <5 pg/µg of rfhSP-D.

Direct Binding ELISA

Maxisorp 96-well microtiter plates were coated with rfhSP-D (5, 2.5, 1.25, and 0.625 µg/well) in carbonate-bicarbonate buffer (CBC), pH 9.6, and incubated overnight at 4°C. After removing the CBC buffer, microtiter wells were washed with PBS three times, blocked with 2% w/v BSA in PBS for 2 h at 37°C, and then washed three times with PBST (PBS + 0.05% Tween 20). 20 µl of concentrated pH1N1, H3N2 virus (1.36×10^6 pfu/ml), or purified recombinant HA (2.5 µg/ml) was diluted in 200 µl of PBS, 10 µl of diluted virus was added to each well, and incubated at room temperature (RT) for 2 h in buffer containing 5 mM $CaCl_2$. VSV-G pseudotyped lentivirus was used as a negative control. The microtiter wells were washed with PBST three times and the binding was probed with primary antibody: monoclonal anti-influenza virus H1 (BEI-Resources) and polyclonal anti-influenza virus H3 (BEI-Resources) antibody (1:5,000 dilution in PBS) for 1 h at 37°C. The wells were washed again with PBST and incubated with anti-mouse IgG-Horseradish peroxidase (HRP)-conjugate (1:5,000) (Fisher Scientific) and Protein A-HRP-conjugate (Fisher Scientific) in PBS (100 µl/well), respectively, for 1 h at 37°C. Color was developed using 3,3′, 5,5′-Tetramethylbenzidine (TMB) substrate (Sigma-Aldrich). The reaction was stopped using 2 N H_2SO_4 and the absorbance was read at 450 nm using iMark™ microplate absorbance reader (Bio-Rad).

Far Western Blotting

rfhSP-D (5 µg) or 10 µl of concentrated pH1N1/H3N2 (1.36×10^6 pfu/ml) were run separately on a 12% (w/v) SDS-PAGE, and then electrophoretically transferred onto a nitrocellulose membrane (320 mA for 2 h) in 1× transfer buffer (25 mM Tris–HCl pH 7.5, 190 mM glycine, and 20% methanol), followed

by blocking overnight in 5% w/v dried milk powder in PBS (Sigma-Aldrich) at 4°C on a rotatory shaker. The membrane was then washed with PBST three times, 10 min each. For far western blotting, the nitrocellulose membrane was incubated with 5 μg/ml of rfhSP-D in PBS containing 5 mM $CaCl_2$ for 1 h at RT and 1 h at 4°C. Following PBST wash, the membrane was incubated with primary antibodies, polyclonal rabbit anti-human SP-D, monoclonal anti-influenza virus H1 (BEI-Resources), or polyclonal anti-influenza virus H3 (BEI-Resources) in PBS (1:1,000) for 1 h at RT. Following washing, the membrane was probed with secondary antibodies: protein-A-HRP-conjugate, or rabbit anti-mouse IgG HRP conjugate (1:1,000) (Fisher Scientific) in PBS (100 μl/well) for 1 h at RT. After PBST wash, the blot was developed either using 3,3′-diaminobenzidine (DAB) or enhanced chemiluminescence substrate. For M1 detection, following 6 h incubation, both untreated (cells + virus) and treated samples (cells + virus + 10 μg/ml rfhSP-D) were run on the 12% (w/v) SDS-PAGE, and transferred onto a nitrocellulose membrane, as described above. The M1 expression was detected using anti-M1 monoclonal antibody (BEI-Resources).

Cell-Binding Assay

A549 cells were seeded in microtiter wells using complete DMEM (1×10^5 cells/well) and incubated overnight at 37°C. The wells were washed with PBS three times, and then rfhSP-D (10, 5, 2.5, and 1.25 μg/ml) was pre-incubated with pH1N1 or H3N2 virus (1.36×10^6 pfu/ml) diluted in 200 μl of PBS + 5 mM $CaCl_2$; 10 μl of diluted virus was added to the corresponding wells, and incubated at RT for 2 h. Maltose-binding protein (MBP) was used as a negative control. The microtiter wells were then washed with PBS three times, and fixed with 4% paraformaldehyde (Fisher Scientific) for 10 min at RT. The wells were washed again with PBS three times, and blocked with 2% w/v BSA in PBS for 2 h at 37°C. Monoclonal anti-influenza virus H1 (BEI-Resources) and polyclonal anti-influenza virus H3 (BEI-Resources) in PBS (1:5,000) were added to each well and incubated for 1 h at 37°C. After washing with PBST three times, the corresponding wells were probed with goat anti-mouse IgG-HRP-conjugate (Thermo-Fisher), or Protein A-HRP conjugate (1:5,000) in PBS for 1 h at 37°C. The wells were washed again with PBST three times and the color was developed using TMB substrate. The reaction was stopped using 2 M H_2SO_4, followed by absorbance reading at 450 nm.

Titration Assay

Maxisorp 96-well plates were coated with 0.01% collagen (Sigma-Aldrich) and incubated at RT for 3 h. After removing the excess collagen, the wells were washed with PBS twice. 75,000 A549 cells were seeded and grown overnight at 37°C in the presence of 5% v/v CO_2, until 75–80% confluency. Cells were washed with 1× PBS twice, pH1N1 or H3N2 virus (MOI of 1) diluted in pure DMEM with 10 μg/ml rfhSP-D was added to cells, respectively. The plates were incubated at 37°C for 1 h. The wells were then washed with PBS twice and 200 μl of infection medium was added to the cells, and incubated for 24 h at 37°C with 5% v/v CO_2. The media of the infected cells in the presence or absence of rfhSP-D was collected and virus titer was estimated by $TCID_{50}$.

Infection Assay Using pH1N1 and H3N2

A549 cells were cultured in complete DMEM with usual supplements at 37°C in CO_2 incubator until about 70–80% confluence. Cells, washed with PBS twice, trypsinised, and adjusted to 5×10^5 cells in 12-well plates (Fisher Scientific), were left to adhere overnight at 37°C in serum-free complete DMEM. Cells were washed in PBS before the addition of rfhSP-D (10 μg/well) in pure DMEM containing 5 mM $CaCl_2$ with MOI 1 of pH1N1 or H3N2 virus (1 h at RT and 1 h at 4°C). The pre-incubated virus and protein mix was then added onto the cells in a circular motion and incubated at 37°C for 1 h in DMEM only. Medium containing unabsorbed virus and rfhSP-D protein was removed, cells were washed with PBS twice, infection medium was added, and then left to incubate 2 and 6 h. The infected cells were detached by scrapping with a sterile cell scrapper, centrifuged at $1{,}500 \times g$ for 3 min, and frozen at −80°C until further analysis *via* qPCR.

Real-Time Quantitative PCR Analysis

The infected A549 cells were lysed using a lysis solution (50 mM Tris–HCl pH 7.5, 200 mM NaCl, 5 mM EDTA pH 8, 0.1% v/v Triton X-100). Total RNA was extracted using RNase Mini Kit (Qiagen). Contaminating DNA was removed by DNase I treatment, followed by heat-inactivation at 70°C of DNase I and RNase. A260 nm was used to quantify the amount of RNA using NanoDrop 2000/2000c (Sigma-Aldrich), and the RNA purity was assessed using A260/A280 ratio between 1.8 and 2.1. The isolated RNA was then converted into cDNA using SuperScript II Reverse Transcriptase (Thermo-Fisher Scientific). Oligo-dT primers were added to initiate cDNA synthesis and to avoid labeling of the rRNA and tRNA. cDNA was synthesized using high capacity RNA to cDNA Kit (Thermo-Fisher Scientific) using 1–2 μg of total RNA. Primer sequences were designed for specificity using the Primer-BLAST software (Basic Local Alignment Search Tool) (http://blast.ncbi.nlm.nih.gov/Blast.cgi) (**Table 1**). The qRT-PCR was performed using the Light Cycler system (Applied Biosciences). The amplification program used was at 95°C for 5 min, followed by 45 cycles of 95°C for 10 s, 60°C for 10 s, and 72°C for 10 s. The specificity of the assay was established by melting-curve analysis.

Multiplex Cytokine Array Analysis

Supernatant from A549 cells, incubated with IAV with or without rfhSP-D for 24 h were collected for measuring secreted cytokines [TNF-α, IL-6, IL-10, IL-1α, interferon (IFN)-α, and IL-12p40], chemokine (eotaxin) and growth factors (GM-CSF and VEGF). The analytes were measured using MagPixMilliplex kit (EMD Millipore). 25 μl of assay buffer was added to each well of a 96-well plate, followed by addition of 25 μl of standard, control, or supernatant from A549 cells infected with pH1N1 or H3N2 (with or without rfhSP-D). 25 μl of magnetic beads, coupled to analytes, were added to each well, and incubated for 18 h at 4°C. The plate was washed with the assay buffer and 25 μl of detection antibodies were incubated with the beads for 1 h at RT. 25 μl of Streptavidin–Phycoerythrin was then added to each well and incubated for 30 min at RT. Following a washing step, 150 μl

TABLE 1 | Target genes, forward primers, and reverse primers used for qPCR.

Target	Forward primer	Reverse primer
18S	5′-ATGGCCGTTC TTAGTTGGTG-3′	5′-CGCTGAGCCA GTCAGTGTAG-3′
IL-6	5′-GAAAGCAGCA AAGAGGCACT-3′	5′-TTTCACCAGG CAAGTCTCCT-3′
IL-12	5′-AACTTGCAGC TGAAGCCATT-3′	5′-GACCTGAACG CAGAATGTCA-3′
TNF-α	5′-AGCCCATGTT GTAGCAAACC-3′	5′-TGAGGTACAG GCCCTCTGAT-3′
M1	5′AAACATATGTCTGATAAC GAAGGAGAACAGTTCTT-3′	5′GCTGAATTCTACCT CATGGTCTTCTTGA-3′
RANTES	5′-GCGGGTACCAT GAAGATCTCTG-3′	5′-GGGTCAGAATC AAGAAACCCTC-3′
IFN-α	5′-TTT CTC CTG CC T GAA GGA CAG-3′	5′-GCT CAT GAT TTC TGC TCT GAC A-3′
IFN-β	5′-AAA GAA GCA G CA ATT TTC AGC-3′	5′-CCT TGG CCT TCA GGT AAT GCA-3′

of sheath fluid was added to each well and the plate was read using the Luminex Magpix instrument. Assays were conducted in duplicate.

Production of H1+N1 Pseudotyped Lentiviral Particles

HEK293T cells were co-transfected with 20 μg of pcDNA3.1-swineH1-flag (H1 from swine H1N1 A/California/04/09) (Invitrogen), pcDNA3.1-swine N1-flag (N1 from swine H1N1 A/California/04/09) (Invitrogen), pHIV-Luciferase backbone (Addgene), which carries a modified proviral HIV-1 genome with *env* deleted and designed to express the firefly luciferase reporter, and psPAX2 (Addgene). psPAX2 is a second-generation lentiviral packaging plasmid and can be used with second or third generation lentiviral vectors and envelope expressing plasmid. VSV-G lentivirus was produced in a similar way as described above, without H1+N1 plasmids. Supernatant containing the released H1+N1 pseudotyped and VSV-G lentiviral particles were harvested at 24 and 48 h and centrifuged at 5,000 × *g* for 10 min to remove any debris, and concentrated *via* ultra-centrifugation. The transfected HEK293T cells were lysed using lysis buffer (50 mM Tris–HCl pH 7.5, 200 mM NaCl, 5 mM EDTA, 0.1% v/v Triton X-100). The filtered supernatant and the cell lysate were analyzed *via* western blotting and luciferase reporter activity assay.

Luciferase Reporter Activity Assay

MDCK cells were cultured in supplemented DMEM as described earlier, until about 70–80% confluency. The harvested H1+N1 pseudotyped particles at 24 and 48 h were used to perform luciferase reporter activity using luciferase one-step assay kit (Thermo Scientific). rfhSP-D (5 and 10 μg/ml) was used to determine its effect on the luciferase reporter activity; cells only, and cells + H1+N1 particles were used as controls. Readings were measured using a GloMax 96 Microplate Luminometer (Promega).

Statistical Analysis

Graphs were generated using GraphPad Prism 6.0 software and the statistical analysis was performed using a two-way ANOVA test. Significant values were considered based on $^{*}p < 0.1$, $^{**}p < 0.05$, $^{***}p < 0.01$, and $^{****}p < 0.001$ between treated and untreated conditions. Error bars show the SD or SEM, as indicated in the figure legends.

RESULTS

rfhSP-D Binds Directly to IAV Subtypes

Escherichia coli BL21 (λDE3) pLysS containing pUK-D1 construct (20) expressed a ~20 kDa protein following IPTG induction, compared to the un-induced bacterial cells (**Figure 1A**). The overexpressed insoluble rfhSP-D as inclusion bodies was refolded *via* denaturation and renaturation cycle. The soluble rfhSP-D fractions were affinity purified using maltose–agarose column, which appeared as a single band on 12% SDS-PAGE (v/v) under reducing condition (**Figure 1B**). The immunoreactivity of purified rfhSP-D was confirmed *via* western blotting using rabbit polyclonal anti-human SP-D antibody that was raised against native human SP-D purified from lung lavage of alveolar proteinosis patients (**Figure 1C**). The ability of pH1N1 and H3N2 subtypes to bind microtiter-coated rfhSP-D was examined *via* ELISA. As shown in **Figure 2**, rfhSP-D bound both IAV subtypes in a dose- and calcium-dependent manner. VSV-G pseudotyped lentivirus was used as a negative control RNA virus, where no significant binding was seen with all rfhSP-D concentrations tested. For cell-binding assay, A549 cells were challenged with purified pH1N1 or H3N2 pre-incubated with a range of rfhSP-D concentrations (**Figure 3**). The maximum inhibition (50%) of cell binding was seen at 10 μg/ml. MBP was used as a negative control protein.

rfhSP-D Binds to HA and Restricts Replication of IAV in A549 Cells

Previous studies have shown that SP-D binds to the glycosylation site of HA1 domain on IAV (18). Far western blotting revealed that rfhSP-D bound to HA (70 kDa) and M1 (27 kDa) of pH1N1 (**Figure 4A**) and H3N2 (**Figure 4B**) subtypes. As shown in **Figure 4C**, rfhSP-D was able to bind purified recombinant HA protein in a concentration-dependent manner. The binding of rfhSP-D may inhibit cellular viral infection by restricting the interaction of HA with SA containing receptors, and HA-mediated fusion in endosomes. The interaction between rfhSP-D and HA appears to offer another dimension at which rfhSP-D may suppress target cell infection and intracellular replication. The mechanism of direct inhibition of IAV by rfhSP-D was thus investigated *via* infection assay. A549 cells infected with pH1N1 and H3N2 revealed an upregulation of M1 expression at 2 and 6 h time points (**Figure 5**). However, A549 cells, pre-treated with rfhSP-D showed downregulation of viral M1 expression when compared to untreated cells challenged with virus (**Figure 5**). The downregulation of M1 expression due to rfhSP-D pre-incubation was more effective in the case of pH1N1 compared to H3N2, where −8 $\log_{10}$ fold downregulation was seen at 2 h (**Figure 5A**). This was validated *via* western blotting, where a low M1 expression was detected

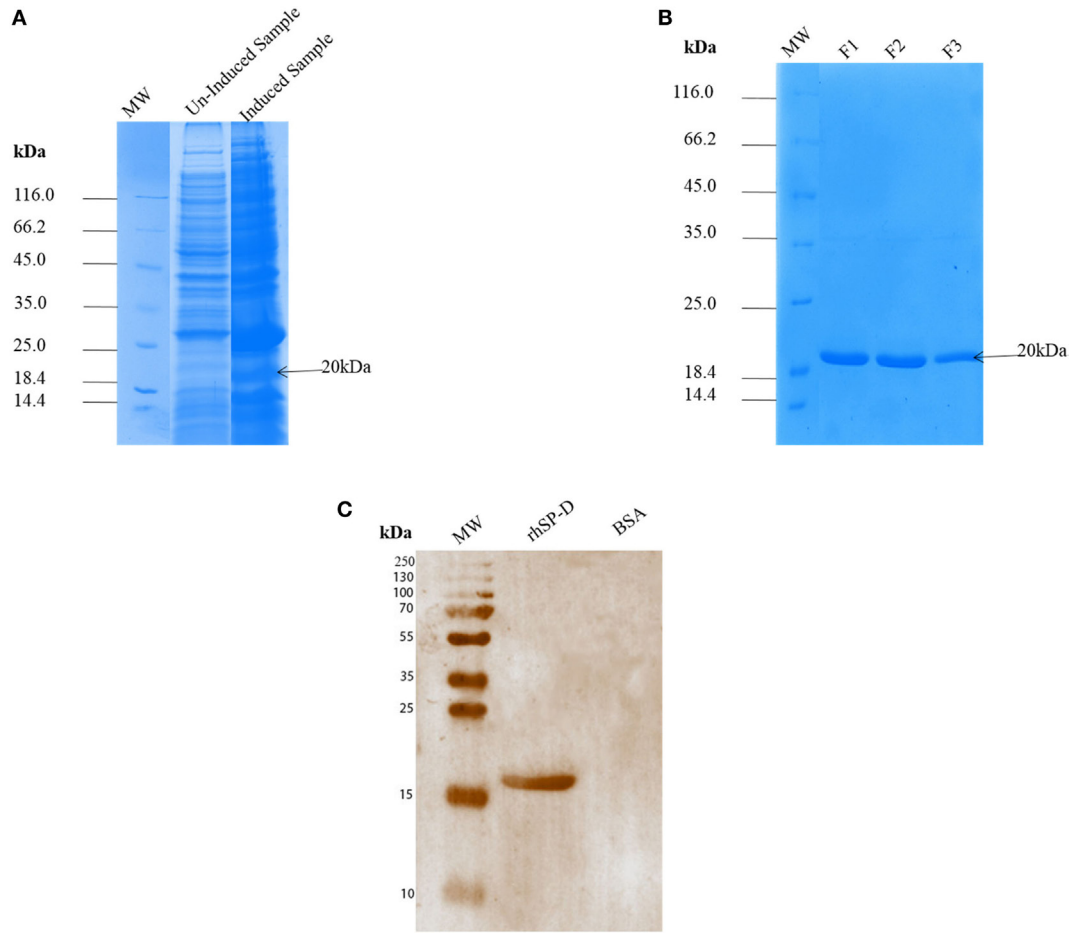

FIGURE 1 | SDS-PAGE (12% v/v) under reducing conditions showing expression and purification of a recombinant surfactant protein D (rfhSP-D). The neck and carbohydrate recognition domain regions were expressed in *Escherichia coli* BL21 (λDE3) pLysS. **(A)** Following induction with 0.5 mM IPTG, a ~20 kDa band appeared being overexpressed compared to uninduced sample. Following denaturation–renaturation cycle, the rfhSP-D was purified on an affinity column to homogeneity after elution with EDTA as fractions F1, F2 and F3 **(B)**. A rabbit polyclonal antibody raised against full-length SP-D purified from human bronchoalveolar lavage **(C)** recognized the purified rfhSP-D, but not BSA that was used as a negative control protein.

in rfhSP-D (10 μg/ml) treated sample following 6 h incubation, when compared to untreated samples (cells + virus) (**Figure 5C**). Furthermore, anti-IAV activity of rfhSP-D was confirmed *via* virus titration assay (**Figures 5D,E**). Approximately 40% titer reduction was seen in 10 μg rhfSP-D treated cells compared to untreated samples, suggesting the ability of rfhSP-D to act as an entry inhibitor. Differential inhibitory effects of rfhSP-D on IAV subtypes may reflect on the glycosylation of the HA protein of IAV, suggesting a correlation between HA-glycan attachment and susceptibility of IAV strains to inhibition by rfhSP-D that involves specific interaction sites on HA.

rfhSP-D Modulates Pro-Inflammatory Cytokine/Chemokine Immune Responses Following Virus Challenge to A549 Cells

The qPCR analysis revealed that there was an upregulation of pro-inflammatory cytokines TNF-α and IL-6 by H3N2 strain, which were brought down slightly by rfhSP-D at 2 h (**Figure 6A**). However, both TNF-α and IL-6 in the case of pH1N1 were found to be downregulated considerably by rfhSP-D at 2 h, which gradually recovered by 6 h (**Figure 6B**). IL-6, which is crucial for the resolution of IAV infection, acts by inducing neutrophil mediated viral clearance. An elevated level of IL-6 in lung and serum has been reported in patients infected with pH1N1 (21). TNF-α and IL-6 are the key contributors to IAV-mediated respiratory diseases and acute lung injury. By contrast, there was a broad level of downregulation of IL-12 in the case of both IAV subtypes incubated with rfhSP-D, suggesting a likely reduction of Th1 response and suppression of IFN-γ production by $CD4^+$ T cells. Suppressed transcript level of RANTES (1 $\log_{10}$ fold) by rfhSP-D was observed at 2 h treatment in the case of pH1N1. However, in the case of H3N2 strain, RANTES was downregulated by 0.5-fold ($\log_{10}$) (**Figure 6B**) at 2 h following treatment with rfhSP-D compared to untreated A549 cells. Furthermore, suppression of IFN-α and IFN-β were also seen with rfhSP-D treatment at both 2 and 6 h time points (**Figure 6C**). Both of these type I IFN cytokines play a crucial anti-viral role against IAV, and

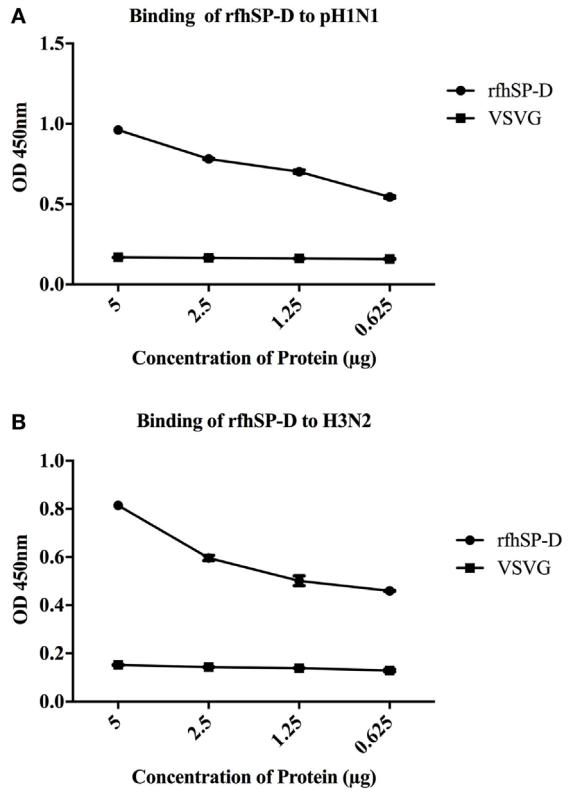

FIGURE 2 | ELISA to show binding of rfhSP-D to **(A)** pH1N1 and **(B)** H3N2: microtiter wells were coated with different concentrations of rfhSP-D (5, 2.5, 1.25, and 0.625 µg/ml). 20 µl of concentrated pH1N1 or H3N2 virus (1.36×10^6 pfu/ml) was diluted in 200 µl of PBS + 5 mM $CaCl_2$ and 10 µl of diluted virus was added to all the wells, and probed with either monoclonal anti-influenza virus H1 or polyclonal anti-influenza virus H3 antibody. VSV-G pseudotyped lentivirus was used as a negative RNA virus control. The data were expressed as mean of three independent experiments done in triplicates ± SEM.

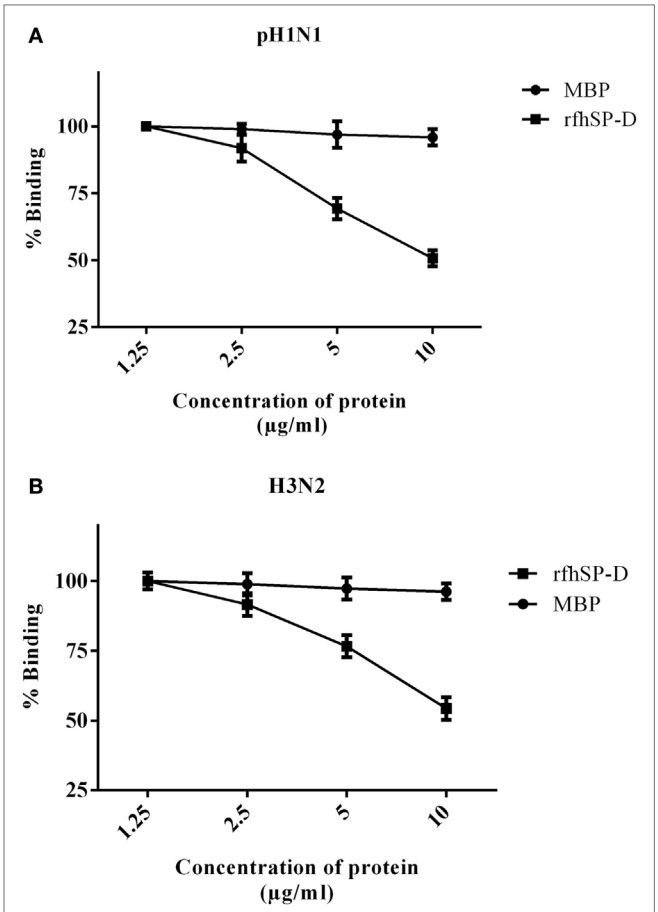

FIGURE 3 | Cell-binding assay to show binding of **(A)** pH1N1 and **(B)** H3N2 pre-incubated with rfhSP-D to A549 cells. Microtiter wells were coated with A549 cells (1×10^5 cells/ml) and incubated overnight at 37°C. Varied concentrations of pre-incubated rfhSP-D (10, 5, 2.5, and 1.25 µg/ml) with pH1N1 and H3N2 virus were added to the corresponding wells, followed by incubation at room temperature for 1–2 h. After fixing the cells with 4% paraformaldehyde solution, monoclonal anti-influenza virus H1, or polyclonal anti-influenza virus H3 were added to corresponding well. Maltose-binding protein (MBP) was used as a negative control protein. The data were expressed as mean of three independent experiments done in triplicates ± SEM.

determine the rate of viral replication in the initial stages of infection. Suppression of type I IFN levels suggests the ability of rfhSP-D to reduce the rate of viral replication, thereby reducing the levels of INF produced by the innate immune system.

Multiplex Cytokine Array Analysis Reveals a Differential Ability of rfhSP-D to Downregulate Pro-Inflammatory Cytokines and Chemokines

To assess secretion of cytokines, chemokines, and growth factors over a period of 24 h post rfhSP-D treatment, a multiplex cytokine array was performed using supernatants of the IAV challenged and rfhSP-D treated A549 cells. rfhSP-D induced a dramatic suppression of some of the key pro-inflammatory cytokines and chemokines in the virus infected A549 cells. In the case of pH1N1, TNF-α, IFN-α, IL-10, IL-12 (p40), VEGF, GM-CSF, and eotaxin were considerably suppressed by rfhSP-D treatment at 24 h (**Figure 7A**). However, these suppressive effects on IL-10, VEGF, eotaxin, and IL-12 (p40) were not so evident in the case of H3N2 subtype, with the exception of TNF-α, IFN-α, and GM-CSF (**Figure 7**). These data seem to suggest that the extent of immunomodulatory effect of rfhSP-D on host cells can vary considerably in a IAV subtype-specific manner.

rfhSP-D Binds to H1+N1 Pseudotyped Lentivirus and Reduces Luciferase Reporter Activity

H1+N1 pseudotyped lentiviral particles were produced as a safe strategy to study the differential or combinatorial involvement of HA or NA viral glycoproteins in the recognition and neutralization of IAV by rfhSP-D. The production of lentiviral particles pseudotyped with envelope proteins H1+N1 was carried out by co-transfecting HEK293T cells with plasmid containing the coding sequence of the indicated H1+N1, pHIV-Luciferase backbone, and psPAX2. Purified H1+N1 pseudotyped particles

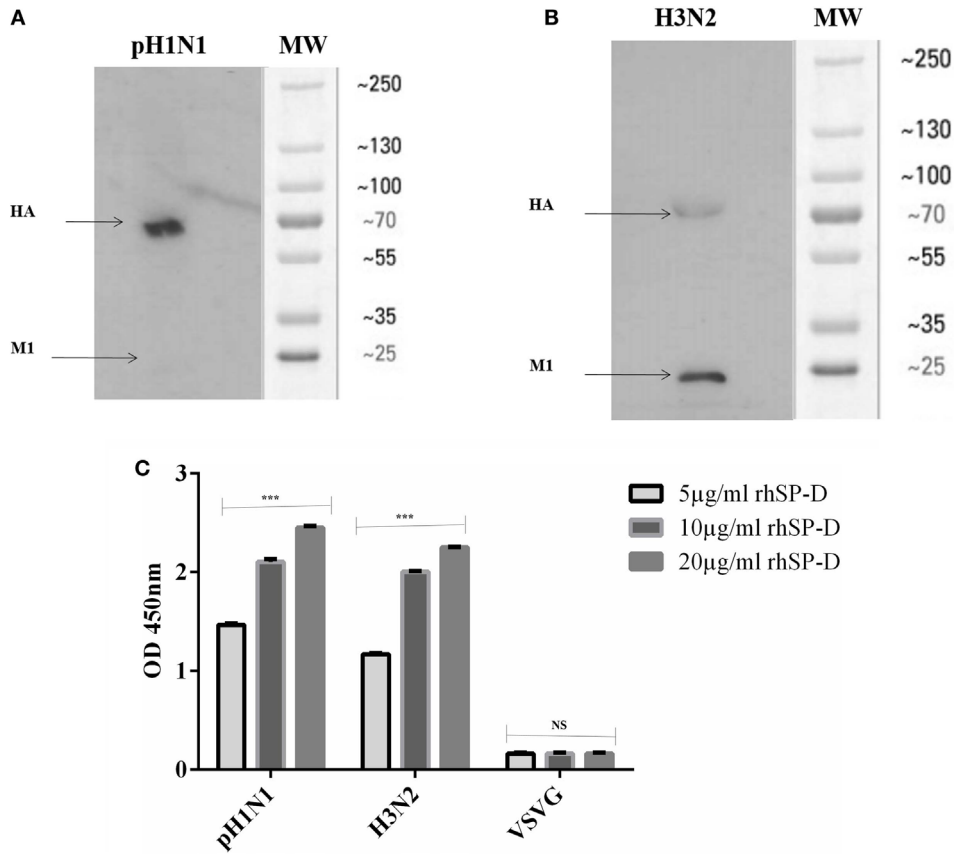

FIGURE 4 | Far western blot analysis to show rfhSP-D binding to purified **(A)** pH1N1 and **(B)** H3N2: 10 µl of concentrated virus (1.36×10^6 pfu/ml) was first run on the SDS-PAGE under reducing conditions, and then transferred onto a nitrocellulose membrane and incubated with 5 µg of rfhSP-D. The membrane was probed with anti-rabbit SP-D polyclonal antibodies. rfhSP-D bound to HA (70 kDa) and M1 (27 kDa) in the case of both pH1N1 and H3N2 subtypes. **(C)** ELISA to show the binding of rfhSP-D to purified recombinant hemagglutinin (HA) (µg/ml). VSV-G was used as a negative control. The data were expressed as mean of three independent experiments carried out in triplicates ± SEM. Significance was determined using the unpaired one-way ANOVA test (***$p < 0.0001$) ($n = 3$).

and cell lysate harvested at 24 and 48 h were analyzed *via* western blotting, and the expression level of HA was determined using anti-H1 monoclonal antibody (**Figure 8A**); HA was evident at 70 kDa. Far western blotting revealed binding of rfhSP-D to HA at 70 kDa (**Figure 8B**), suggesting that the binding of rfhSP-D to HA is crucial for the inhibition of viral infectivity. Purified H1+N1 pseudotyped particles harvested at 24 and 48 h were used to transduce MDCK cells to measure the luciferase reporter activity assay. Higher levels of luciferase reporter activity were observed at 24 h when compared to 48 h post-transfection (**Figure 8C**). Thus, pseudotyped particles harvested at 24 h were used to transduce MDCK cells with or without rfhSP-D (5 and 10 µg/ml) (**Figure 8D**). Nearly 50% reduction in the luciferase reporter activity was observed with 10 µg/ml of rfhSP-D compared to cells challenged with H1+N1 pseudotyped particles. This suggested an entry inhibitory role of rfhSP-D against IAV.

DISCUSSION

Respiratory tract infection caused by IAV is associated with up to half a million mortality rates worldwide and five million cases of morbidity per year. A new swine-origin H1N1 IAV, identified in April 2009, spread worldwide, and was officially declared pandemic in June 2009. There are concerns that H1N1 or H3N2 viruses reassort with existing H5N1 virus using bird or pig as intermediate hosts, giving rise to more pathogenic IAV. Thus, it is important to understand molecular mechanisms of host's first line of defense against IAV in order to design and develop novel and effective anti-IAV strategies. SP-D expressed at the mucosal sites including lungs plays an important role during IAV infection (22). SP-D has been shown to have a wide range of innate immune roles including neutralization, agglutination, opsonization and clearance of viruses including IAV. The binding ability of rfhSP-D to HIV-1 gp120 was reported, primarily in a dose- and calcium-dependent manner (23). Human SP-D has also been shown to bind IAV-HA and NA, resulting in the inhibition of viral attachment and entry into the host cells (24). However, the mechanism of direct inhibition of IAV and pseudotyped viral particles by SP-D and subsequent immune response is not fully explored.

Using two different IAV subtypes (pH1N1 and H3N2), we have shown that the entry inhibitory capability of rfhSP-D is not limited

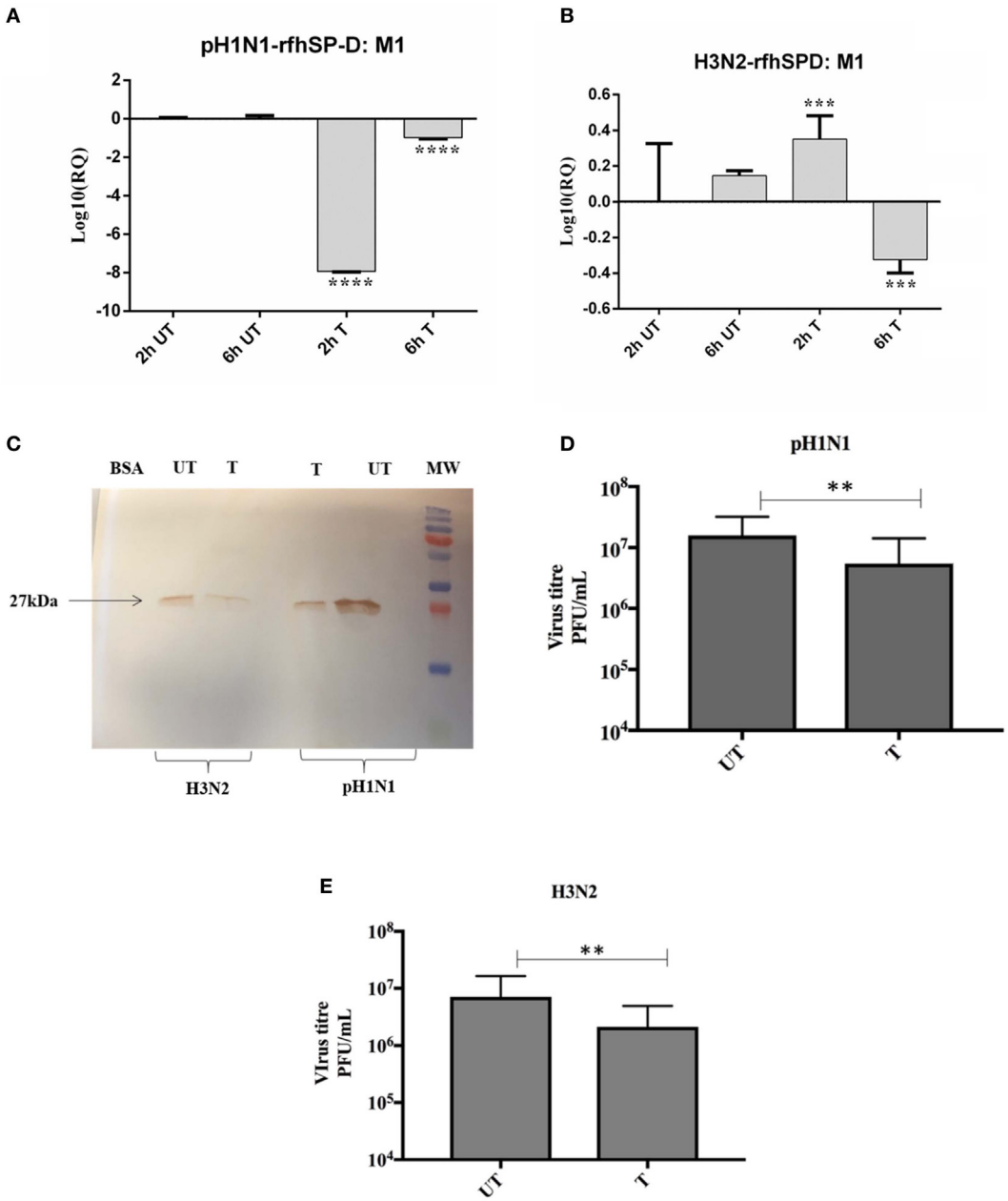

FIGURE 5 | rfhSP-D restricts replication of **(A)** pH1N1 and **(B)** H3N2 in target human A549 cells. M1 expression of both pH1N1 and H3N2 influenza A virus (IAV) (MOI 1) after infection of A549 cells at differential time points at 2 and 6 h. A549 cells were incubated either with pre-incubated pH1N1 and H3N2 with (10 μg) or without purified rfhSP-D. Cell pellets were harvested at 2 and 6 h to analyze the M1 expression of IAV. Cells were lysed, and purified RNA extracted was converted into cDNA. Infection was measured *via* qRT-PCR using M1 primers and 18S was used as an endogenous control. Results shown are normalized to M1 levels at 2 h untreated. Significance was determined using the unpaired one-way ANOVA test (**$p < 0.01$, ***$p < 0.001$, and ****$p < 0.0001$) ($n = 3$). **(C)** Western blotting to shown M1 expression in both untreated (cells + virus) and treated (cells + virus + 10 μg/ml rfhSP-D) following 6 h incubation. Titration assay to show the anti-IAV activity of rfhSP-D (10 μg/ml), using both pH1N1 **(D)** and H3N2 **(E)** subtypes. A549 cells were infected with pH1N1/H3N2 (MOI 1) for 24 h. Then, the supernatants were collected and virus titers measured using a TCID50 assay. Treatment with rfhSP-D reduced viral titers by approximately 40%, suggesting that rfhSP-D acts as an entry inhibitor.

to a particular IAV subtype. To identify the interaction of rfhSP-D with IAV viral proteins, protein–protein interaction studies were carried out *via* ELISA, cell-binding assay, and far western blot. The ELISA (**Figure 2**) and cell-binding assay (**Figure 3**) revealed the maximal binding of rfhSP-D to both pH1N1 and H3N2 IAV subtypes at 5 μg/ml, and the maximum inhibition of cell binding was seen at 10 μg/ml of rfhSP-D. Furthermore, rfhSP-D bound purified recombinant HA protein in a concentration- and calcium-dependent manner (**Figure 4C**). rfhSP-D bound HA (70 kDa) and M1 (25 kDa) (**Figure 4**). N-linked oligosaccharides

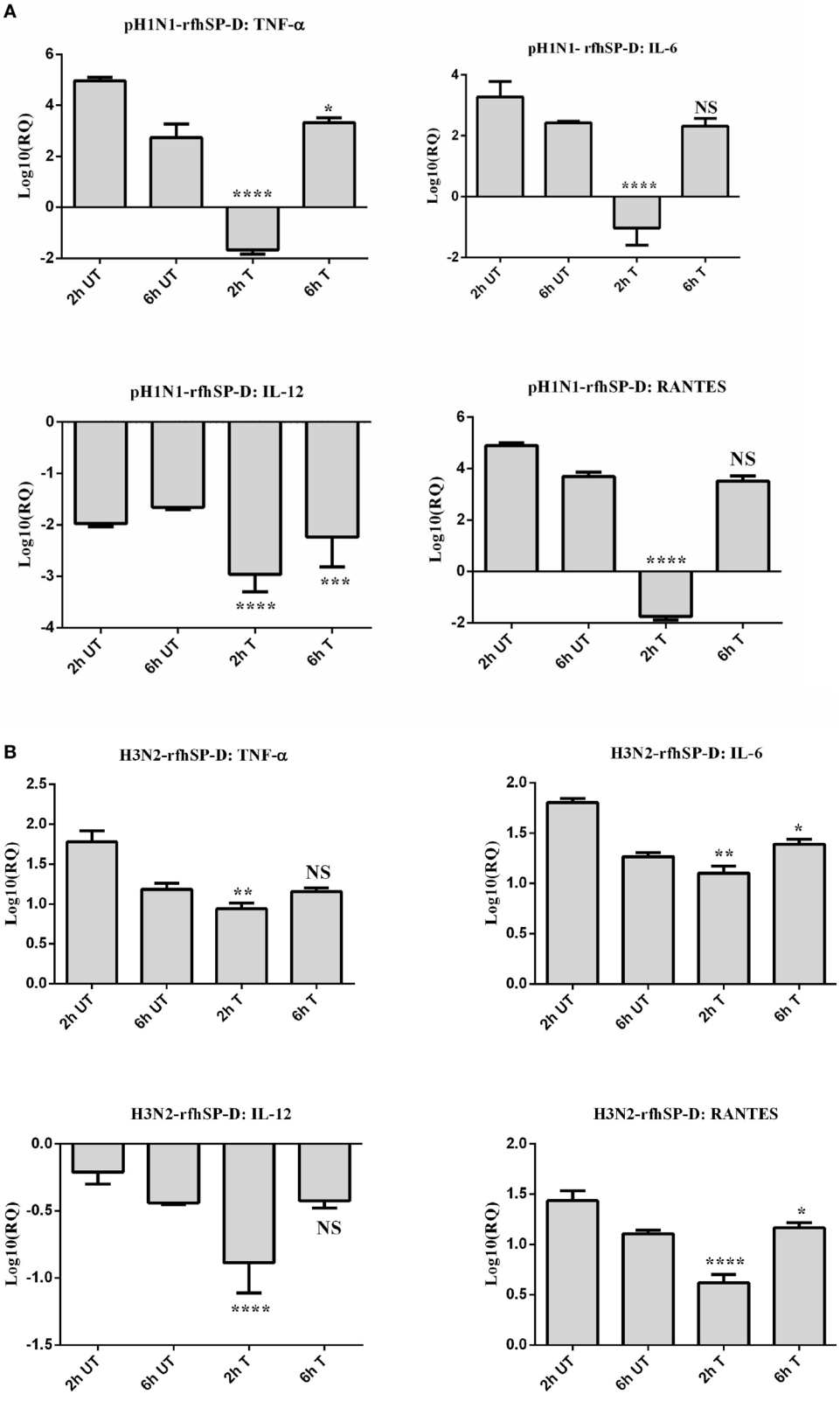

FIGURE 6 | Continued

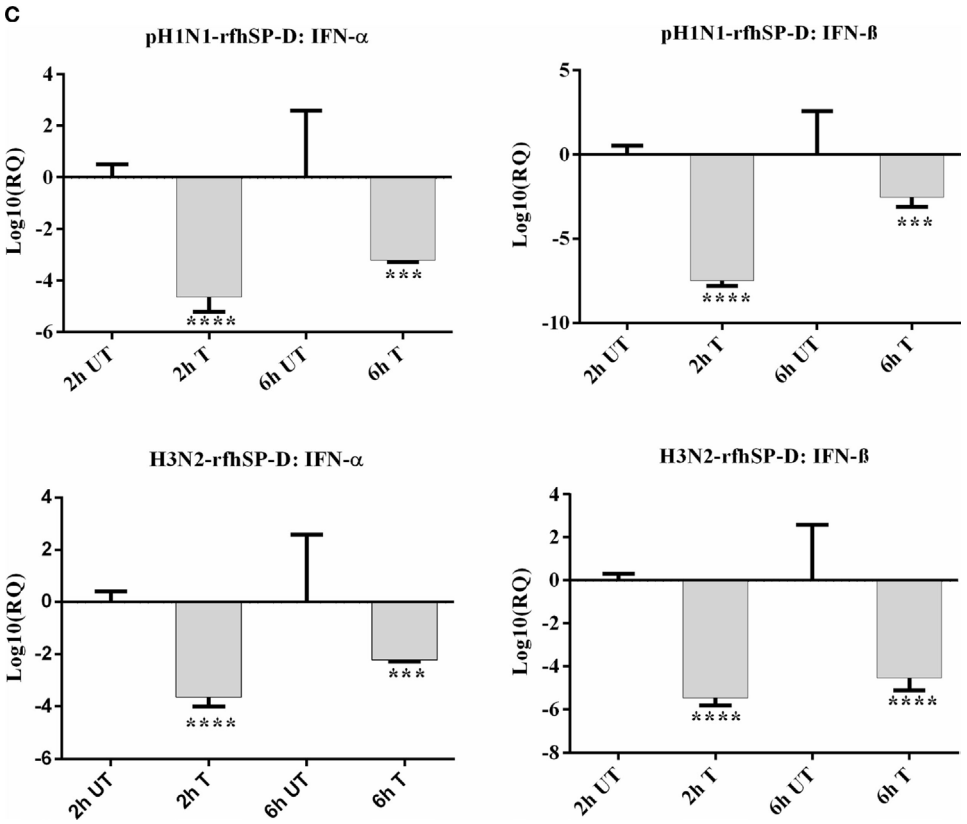

FIGURE 6 | Differential mRNA expression profile of A549 cells challenged with pre-incubated **(A)** pH1N1, **(B)** H3N2 with rfhSP-D, and **(C)** expression levels of type I interferon (IFN) subtypes in both untreated and treated samples. The expression levels of cytokines and chemokine were measured using qRT-PCR and the data were normalized *via* 18S rRNA expression as a control. The relative expression (RQ) was calculated by using cells only time point as the calibrator. The RQ value was calculated using the formula: $RQ = 2^{-\Delta\Delta Ct}$. Assays were conducted in triplicates and error bars represents ± SEM. Significance was determined using the unpaired one-way ANOVA test (*$p < 0.05$, **$p < 0.01$, ***$p < 0.001$, and ****$p < 0.0001$) ($n = 3$).

found on the IAV envelope glycoproteins (HA and NA) are known to be recognized by the CRD region of SP-D. Thus, HA-exposed glycans differing in location and numbers between IAV subtypes may be responsible for this interaction. rfhSP-D is likely to inhibit IAV infection by preventing the HA interaction with SA containing receptors. A reverse genetic approach has been used to analyze the role of N-glycosylation sites on the head of H1 in modulating sensitivity to SP-D *in vitro* and *in vivo* (25). It was found that HA Asn-144 was a critical factor in sensitivity to SP-D (25).

We also examined the immune response of A549 lung epithelial cells following IAV challenge in the presence or absence of rfhSP-D, which can impact upon cellular infection and viral replication. Therefore, the ability of rfhSP-D to modulate viral replication as well as inflammatory immune response following IAV challenge was examined *via* infection assay, qPCR, and multiplex cytokine array. The key aspect of host–pathogen interaction arising out of this study is the ability of rfhSP-D-bound pH1N1 and H3N2 to undergo suppressed replication, as evident by the expression of M1 gene. M1 is a matrix protein of IAV that lies beneath the lipid layer and is the most abundant protein, which is essential for viral stability and integrity. Thus, it plays a critical role in the recruitment and assembly of viral sites, nuclear export of viral RNPs, and thus, establishing the host components for viral budding (26). rfhSP-D suppressed the expression of M1 in pH1N1 (**Figure 5A**) at 2 h, while downregulating at 6 h in the case of H3N2 (**Figure 5B**). In addition, a lowered M1 expression was detected *via* western blot in the rfhSP-D treated sample compared to untreated sample following 6 h incubation (**Figure 5C**). Viral replication was also reduced in the presence of rfhSP-D as evident in **Figures 5D,E**. This suggests that rfhSP-D could act as an entry inhibitor against the subtypes tested (pH1N1 and H3N2). It is known that HA undergoes N-linked glycosylation, leading to modulation of antigenicity, fusion activity, receptor-binding specificity, and immune evasion of IAV. Therefore, SP-D can play an important role in innate defense against IAV as entry inhibitor by interfering with glycosylation sites and binding to glycans on the viral HA. It has been reported that the combinatorial substitutions of D325A/S+R343V in a trimeric neck and CRD fragment of human SP-D markedly increased anti-viral activity against pandemic IAV. This is because of the increased ability of the mutant to block the SA binding sites, aggregate the virus and reduce viral uptake (27).

Our qPCR data demonstrated an increased expression level of TNF-α and IL-6 in the case of H3N2 subtype (**Figure 6B**)

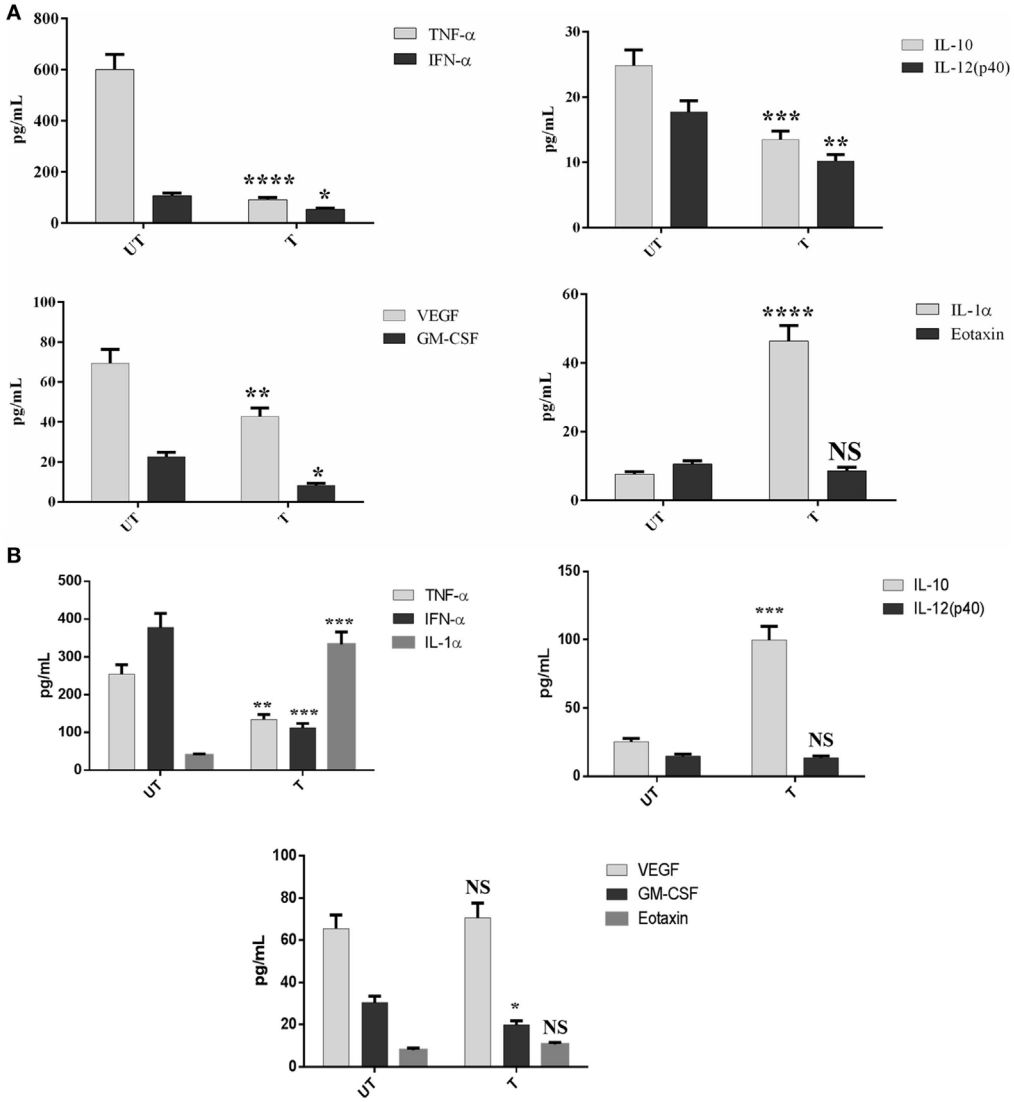

FIGURE 7 | Multiplex cytokine array analysis of supernatants that were collected at 24 h time point. A549 cells were infected with pH1N1 **(A)** and H3N2 **(B)**, treated with 10 μg/ml of rfhSP-D. Cytokines (TNF-α, IL-6, IL-10, IL-1α, IFN-α, and IL-12p40), chemokine (eotaxin), and growth factors (GM-CSF and VEGF) were measured using a commercially available MagPix Milliplex kit (EMD Millipore). Assays were conducted in triplicates and error bars represent ± SEM ($n = 3$); significance was determined using unpaired one-way ANOVA test (*$p < 0.05$, **$p < 0.01$, ***$p < 0.001$ and ****$p < 0.0001$).

compared to pH1N1. However, when pH1N1 was treated with rfhSP-D, TNF-α and IL-6 were suppressed at 2 h (**Figure 6A**), which recovered later (6 h). Elevated TNF-α and IL-6 levels can contribute to virus-mediated respiratory diseases or acute lung injury. IL-12 was considerably downregulated by rfhSP-D in the case of both IAV subtypes, suggesting the likely suppression of Th1 immune response. mRNA expression of RANTES was 10-fold ($log_{10}1$ fold) downregulated in the presence of rfhSP-D at 2 h time point in pH1N1 compared to A549 cells challenged with IAV. However, cells, challenged with H3N2 and treated with rfhSP-D, were seen to have log_{10} one-fold downregulation of RANTES expression. In this study, we also report the ability of rfhSP-D (10 μg/ml) to downregulate both IFN-α and IFN-β expression (**Figure 6C**) at 2 and 6 h. Higher expression levels of IFN-α and IFN-β were detected in the untreated (cells + virus) sample, which was threefold (log10 fold) downregulated in the presence of rfhSP-D at 6 h. This suggests that when cells were incubated with pH1N1/H3N3 (MOI 1), higher levels of both IFN-α and IFN-β were produced by A549 cells to clear the virions. Since addition of rfhSP-D caused inhibition of viral replication, lower levels of INF were detected. Recently, the E3 ubiquitin ligase, TRIM29, has been shown to be a negative regulator of type I IFN responses in the lungs post-IAV challenge *in vivo*. TRIM29 acts by inhibiting IFN-regulatory factors and signaling *via* NF-κB, leading to degradation of NF-κB essential modulator (28). Whether rfhSP-D works *via* similar mechanisms is worth further investigation using SP-D gene-deficient mice (29). In addition, cytokine array analysis using supernatants that were collected at

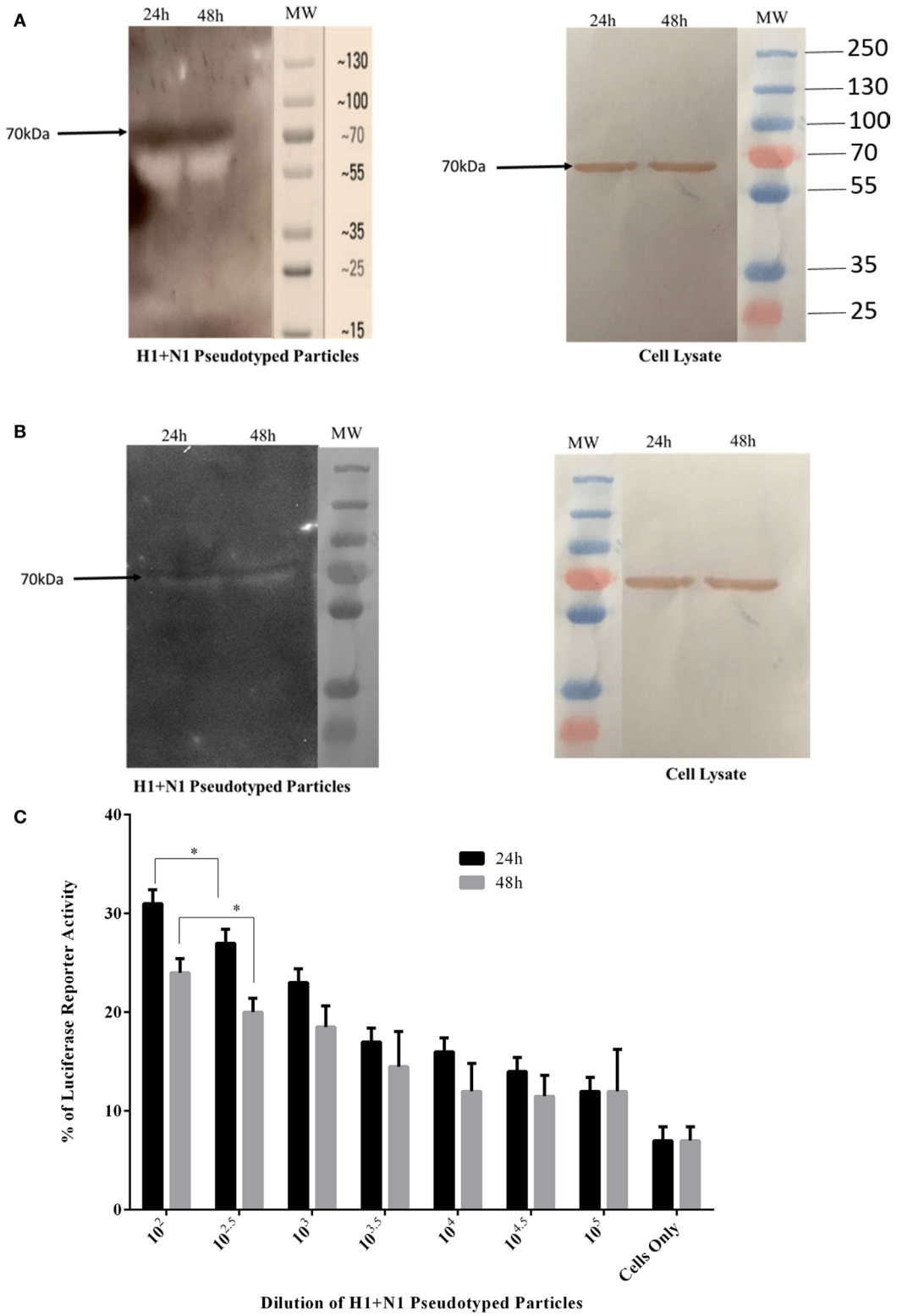

FIGURE 8 | Continued

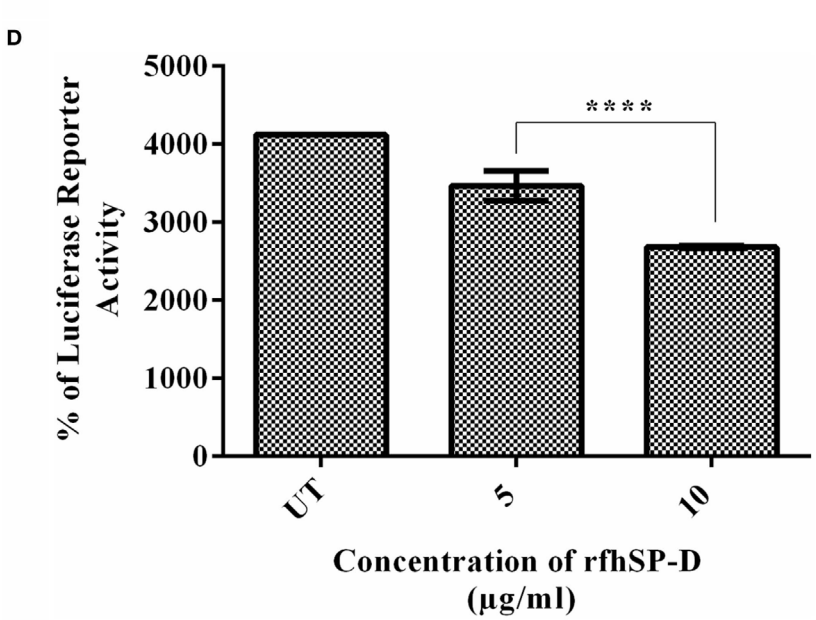

FIGURE 8 | **(A)** Western blotting to show the expression of influenza A virus-hemagglutinin (HA) protein in purified H1+N1 pseudotyped lentiviral particles and cell lysate at 24 and 48 h. The presence of HA was identified at 70 kDa. **(B)** Far western blotting to show rfhSP-D binding in both purified H1+N1 pseudotyped lentiviral particles and cell lysate at 24 and 48 h. HA was evident at 70 kDa when probed with rfhSP-D. **(C)** Luciferase reporter activity of purified H1+N1 pseudotyped lentiviral particles at 24 and 48 h, and **(D)** Luciferase reporter activity of rfhSP-D treated MDCK cells transduced with these lentiviral particles. Significance was determined using the unpaired one-way ANOVA test (*$p < 0.05$ and ****$p < 0.0001$) ($n = 3$).

24 h showed considerable downregulation of some of the key pro-inflammatory cytokines, chemokines, and other soluble factors in the presence of rfhSP-D. The downregulation of various humoral factors by rfhSP-D treatment could also facilitate the prevention of life-threatening secondary bacterial infections that may be caused by aberrant virus-mediated immune modulation.

In this study, we have produced the second-generation lentiviral vectors pseudotyped for H1+N1 of IAV. This system contains a single packaging plasmid (psPAX2) encoding genes including Gag, Pol, and Tat. pHIV-Luciferase was used as a lentiviral transfer plasmid, which is flanked with long terminal repeat (LTR) sequences, and designed to express the firefly luciferase reporter. Thus, pHIV-Luciferase is "replication incompetent" which contains an additional sequence deletion in the 3′ LTR leading to viral "self-inactivation" post-integration. This was selected as a safe alternative method to mimic the structure and surfaces of IAV, and to prove rfhSP-D as an entry inhibitor in cells transduced with pseudotyped IAV particles that are restricted to only one replicative cycle. The lentiviral particles pseudotyped with H1+N1 were analyzed *via* SDS-PAGE and western blotting. Expression of HA in purified H1+N1 pseudotyped lentiviral particles from transfected HEK293T cells was assessed by western blotting using anti-H1 monoclonal antibody (**Figure 8A**). H1+N1 pseudotyped lentiviral particles, purified *via* ultra-centrifugation, were used to investigate the combinatorial or differential involvement of viral envelope glycoproteins in the recognition and neutralization of HA by rfhSP-D. Incubation of rfhSP-D with these H1+N1 pseudotyped lentiviral particles was found to facilitate its binding to HA that appeared at 70 kDA in the far western blot (**Figure 8B**). To validate the effectiveness of rfhSP-D as an entry inhibitor of IAV, luciferase reporter activity assay was performed. Nearly 50% luminescent signal was seen with 10 µg/ml of rfhSP-D when compared to MDCK cells challenged with H1+N1 pseudotyped lentiviral particles alone. This, therefore, suggested the ability of rfhSP-D to inhibit viral infectivity through binding to cell surface bound HA found on the infected MDCK cells.

In summary, suppression of M1 expression, pro-inflammatory cytokine response, as well as luciferase reporter activity in target A549 cells by rfhSP-D highlight its potential as a therapeutic molecule in an entry inhibitory role against IAV.

AUTHOR CONTRIBUTIONS

MA-A, BN, and UK led the project; VM, PV, LK, and AP carried out crucial experiments; SA, IS, and AA-Q provided important reagents. VM, UK, and MA-A wrote the manuscript.

ACKNOWLEDGMENTS

This work is part of a project funded by the Biotechnology program of the King Abdulaziz City for Science and Technology (14-MED258-20) and approved by the Research Advisory Council of the King Faisal Specialist Hospital and Research Centre, Riyadh (2150031). We thank Maureene Delos Reyes and Hanan Shaarawi for secretarial and logistic assistance.

REFERENCES

1. Nayak A, Dodagatta-Marri E, Tsolaki AG, Kishore U. An insight into the diverse roles of surfactant proteins, SP-A and SP-D in innate and adaptive immunity. *Front Immunol* (2012) 3:131. doi:10.3389/fimmu.2012.00131
2. Kishore U, Greenhough TJ, Waters P, Shrive AK, Ghai R, Kamran MF, et al. Surfactant proteins SP-A and SP-D: structure, function and receptors. *Mol Immunol* (2006) 43(9):1293–315.
3. Crouch E, Hartshorn K, Horlacher T, McDonald B, Smith K, Cafarella T, et al. Recognition of mannosylated ligands and influenza A virus by human surfactant protein D: contributions of an extended site and residue 343. *Biochemistry* (2009) 48:3335–45. doi:10.1021/bi8022703
4. Hartshorn KL, Webby R, White MR, Tecle T, Pan C, Boucher S, et al. Role of viral hemagglutinin glycosylation in anti-influenza activities of recombinant surfactant protein D. *Respir Res* (2008) 9:65–9921–9–65. doi:10.1186/1465-9921-9-65
5. Hartshorn KL, Crouch EC, White MR, Eggleton P, Tauber AI, Chang D, et al. Evidence for a protective role of pulmonary surfactant protein D (SP-D) against influenza A viruses. *J Clin Invest* (1994) 94:311–9. doi:10.1172/JCI117323
6. Hartshorn KL, Sastry K, White MR, Anders EM, Super M, Ezekowitz RA, et al. Human mannose-binding protein functions as an opsonin for influenza A viruses. *J Clin Invest* (1993) 91:1414–20. doi:10.1172/JCI116345
7. Roberts KL, Manicassamy B, Lamb RA. Influenza A virus uses intercellular connections to spread to neighboring cells. *J Virol* (2015) 89:1537–49. doi:10.1128/JVI.03306-14
8. Mitnaul LJ, Matrosovich MN, Castrucci MR, Tuzikov AB, Bovin NV, Kobasa D, et al. Balanced hemagglutinin and neuraminidase activities are critical for efficient replication of influenza A virus. *J Virol* (2000) 74:6015–20. doi:10.1128/JVI.74.13.6015-6020.2000
9. Morens DM, Taubenberger JK, Harvey HA, Memoli MJ. The 1918 influenza pandemic: lessons for 2009 and the future. *Crit Care Med* (2010) 38:e10–20. doi:10.1097/CCM.0b013e3181ceb25b
10. Taubenberger JK, Morens DM. 1918 influenza: the mother of all pandemics. *Emerg Infect Dis* (2006) 12:15–22. doi:10.3201/eid1209.05-0979
11. Skehel JJ, Wiley DC. Receptor binding and membrane fusion in virus entry: the influenza hemagglutinin. *Annu Rev Biochem* (2000) 69:531–69. doi:10.1146/annurev.biochem.69.1.531
12. Wilson IA, Cox NJ. Structural basis of immune recognition of influenza virus hemagglutinin. *Annu Rev Immunol* (1990) 8:737–71. doi:10.1146/annurev.iy.08.040190.003513
13. Glaser L, Stevens J, Zamarin D, Wilson IA, Garcia-Sastre A, Tumpey TM, et al. A single amino acid substitution in 1918 influenza virus hemagglutinin changes receptor binding specificity. *J Virol* (2005) 79:11533–6. doi:10.1128/JVI.79.17.11533-11536.2005
14. Lakadamyali M, Rust MJ, Zhuang X. Ligands for clathrin-mediated endocytosis are differentially sorted into distinct populations of early endosomes. *Cell* (2006) 124:997–1009. doi:10.1016/j.cell.2005.12.038
15. de Vries E, Tscherne DM, Wienholts MJ, Cobos-Jimenez V, Scholte F, Garcia-Sastre A, et al. Dissection of the influenza A virus endocytic routes reveals macropinocytosis as an alternative entry pathway. *PLoS Pathog* (2011) 7:e1001329. doi:10.1371/journal.ppat.1001329
16. Stauffer S, Feng Y, Nebioglu F, Heilig R, Picotti P, Helenius A. Stepwise priming by acidic pH and a high K^+ concentration is required for efficient uncoating of influenza A virus cores after penetration. *J Virol* (2014) 88:13029–46. doi:10.1128/JVI.01430-14
17. Tecle T, White MR, Crouch EC, Hartshorn KL. Inhibition of influenza viral neuraminidase activity by collectins. *Arch Virol* (2007) 152:1731–42. doi:10.1007/s00705-007-0983-4
18. Hartshorn KL, White MR, Voelker DR, Coburn J, Zaner K, Crouch EC. Mechanism of binding of surfactant protein D to influenza A viruses: importance of binding to haemagglutinin to antiviral activity. *Biochem J* (2000) 351(Pt 2):449–58. doi:10.1042/bj3510449
19. Hillaire ML, van Eijk M, Vogelzang-van Trierum SE, Fouchier RA, Osterhaus AD, Haagsman HP, et al. Recombinant porcine surfactant protein D inhibits influenza A virus replication ex vivo. *Virus Res* (2014) 181:22–6. doi:10.1016/j.virusres.2013.12.032
20. Singh M, Madan T, Waters P, Parida SK, Sarma PU, Kishore U. Protective effects of a recombinant fragment of human surfactant protein D in a murine model of pulmonary hypersensitivity induced by dust mite allergens. *Immunol Lett* (2003) 86:299–307. doi:10.1016/S0165-2478(03)00033-6
21. Paquette SG, Banner D, Zhao Z, Fang Y, Huang SS, Leomicronn AJ, et al. Interleukin-6 is a potential biomarker for severe pandemic H1N1 influenza A infection. *PLoS One* (2012) 7:e38214. doi:10.1371/journal.pone.0038214
22. Ng WC, Tate MD, Brooks AG, Reading PC. Soluble host defense lectins in innate immunity to influenza virus. *J Biomed Biotechnol* (2012) 2012:732191. doi:10.1155/2012/732191
23. Dodagatta-Marri E, Mitchell DA, Pandit H, Sonawani A, Murugaiah V, Idicula-Thomas S, et al. Protein-protein interaction between surfactant protein D and DC-SIGN via C-type lectin domain can suppress HIV-1 transfer. *Front Immunol* (2017) 8:834. doi:10.3389/fimmu.2017.00834
24. Yang J, Li M, Shen X, Liu S. Influenza A virus entry inhibitors targeting the hemagglutinin. *Viruses* (2013) 5:352–73. doi:10.3390/v5010352
25. Tate MD, Brooks AG, Reading PC. Specific sites of N-linked glycosylation on the hemagglutinin of H1N1 subtype influenza A virus determine sensitivity to inhibitors of the innate immune system and virulence in mice. *J Immunol* (2011) 187:1884–94. doi:10.4049/jimmunol.1100295
26. Rossman JS, Lamb RA. Influenza virus assembly and budding. *Virology* (2011) 411:229–36. doi:10.1016/j.virol.2010.12.003
27. Nikolaidis NM, White MR, Allen K, Tripathi S, Qi L, McDonald B, et al. Mutations flanking the carbohydrate binding site of surfactant protein D confer antiviral activity for pandemic influenza A viruses. *Am J Physiol Lung Cell Mol Physiol* (2014) 306:L1036–44. doi:10.1152/ajplung.00035.2014
28. Xing J, Weng L, Yuan B, Wang Z, Jia L, Jin R, et al. Identification of a role for TRIM29 in the control of innate immunity in the respiratory tract. *Nat Immunol* (2016) 17(12):1373–80. doi:10.1038/ni.3580
29. Madan T, Reid KB, Singh M, Sarma PU, Kishore U. Susceptibility of mice genetically deficient in the surfactant protein (SP)-A or SP-D gene to pulmonary hypersensitivity induced by antigens and allergens of *Aspergillus fumigatus*. *J Immunol* (2005) 174(11):6943–54. doi:10.4049/jimmunol.174.11.6943

Conflict of Interest Statement: The authors declare that the research was conducted in the absence of any commercial or financial relationships that could be construed as a potential conflict of interest.

frontiers in Immunology

ORIGINAL RESEARCH
published: 31 July 2017
doi: 10.3389/fimmu.2017.00834

Protein–Protein Interaction between Surfactant Protein D and DC-SIGN *via* C-Type Lectin Domain Can Suppress HIV-1 Transfer

*Eswari Dodagatta-Marri[1], Daniel A. Mitchell[2], Hrishikesh Pandit[3], Archana Sonawani[3], Valarmathy Murugaiah[1], Susan Idicula-Thomas[3], Béatrice Nal[1,4], Maha M. Al-Mozaini[5], Anuvinder Kaur[1], Taruna Madan[3] and Uday Kishore[1]**

[1] Department of Life Sciences, College of Health and Life Sciences, Brunel University London, Uxbridge, United Kingdom, [2] Clinical Sciences Research Laboratories, Warwick Medical School, University Hospital Coventry and Warwickshire Campus, Coventry, United Kingdom, [3] Department of Innate Immunity, National Institute for Research in Reproductive Health, Indian Council of Medical Research, Mumbai, India, [4] Institute of Environment, Health and Societies, Brunel University London, Uxbridge, United Kingdom, [5] Department of Infection and Immunity, King Faisal Specialist Hospital and Research Centre, Riyadh, Saudi Arabia

Surfactant protein D (SP-D) is a soluble C-type lectin, belonging to the collectin (collagen-containing calcium-dependent lectin) family, which acts as an innate immune pattern recognition molecule in the lungs at other mucosal surfaces. Immune regulation and surfactant homeostasis are salient functions of SP-D. SP-D can bind to a range of viral, bacterial, and fungal pathogens and trigger clearance mechanisms. SP-D binds to gp120, the envelope protein expressed on HIV-1, through its C-type lectin or carbohydrate recognition domain. This is of importance since SP-D is secreted by human mucosal epithelial cells and is present in the female reproductive tract, including vagina. Another C-type lectin, dendritic cell (DC)-specific intercellular adhesion molecule-3-grabbing non-integrin (DC-SIGN), present on the surface of the DCs, also binds to HIV-1 gp120 and facilitates viral transfer to the lymphoid tissues. DCs are also present at the site of HIV-1 entry, embedded in vaginal or rectal mucosa. In the present study, we report a direct protein–protein interaction between recombinant forms of SP-D (rfhSP-D) and DC-SIGN *via* their C-type lectin domains. Both SP-D and DC-SIGN competed for binding to immobilized HIV-1 gp120. Pre-incubation of human embryonic kidney cells expressing surface DC-SIGN with rfhSP-D significantly inhibited the HIV-1 transfer to activated peripheral blood mononuclear cells. *In silico* analysis revealed that SP-D and gp120 may occupy same sites on DC-SIGN, which may explain the reduced transfer of HIV-1. In summary, we demonstrate, for the first time, that DC-SIGN is a novel binding partner of SP-D, and this interaction can modulate HIV-1 capture and transfer to $CD4^+$ T cells. In addition, the present study also reveals a novel and distinct mechanism of host defense by SP-D against HIV-1.

Keywords: surfactant protein D, DC-SIGN, HIV-1 infection, protein–protein interactions, gp120

OPEN ACCESS

Edited by:
Jagadeesh Bayry, Institut national de la santé et de la recherche médicale, France

Reviewed by:
Kenneth Reid, Green Templeton College University of Oxford, United Kingdom
Jiu-Yao Wang, National Cheng Kung University, Taiwan
Kevan Hartshorn, Boston University School of Medicine, United States

****Correspondence:***
Uday Kishore
uday.kishore@brunel.ac.uk, ukishore@hotmail.com

Specialty section:
This article was submitted to Molecular Innate Immunity, a section of the journal Frontiers in Immunology

Received: *22 December 2016*
Accepted: *03 July 2017*
Published: *31 July 2017*

Citation:
Dodagatta-Marri E, Mitchell DA, Pandit H, Sonawani A, Murugaiah V, Idicula-Thomas S, Nal B, Al-Mozaini MM, Kaur A, Madan T and Kishore U (2017) Protein–Protein Interaction between Surfactant Protein D and DC-SIGN via C-Type Lectin Domain Can Suppress HIV-1 Transfer. Front. Immunol. 8:834. doi: 10.3389/fimmu.2017.00834

INTRODUCTION

Surfactant protein D (SP-D) is a collagen-containing C-type lectin, belonging to the collectin family (1). The primary structure of human SP-D is composed of three subunits of polypeptide chains; each subunit consists of a short N-terminal region, a triple-helical collagen-like region, an α-helical coiled-coil neck region, and a calcium-dependent highly conserved C-type lectin or carbohydrate recognition domain (CRD) at the C-terminus (2, 3). The primary structure can get cross-linked *via* the cysteine-containing N-terminal region to give rise to a cruciform structure, which can undergo further multimerization to yield a fuzzy ball, where the CRD regions are facing toward the exterior. SP-D, *via* its homotrimeric CRD region, is known to interact with a wide range of viral, bacterial, and fungal pathogens and bring about clearance mechanisms that involve aggregation or agglutination, opsonization, enhanced phagocytosis, and super-oxidative burst (3, 4). Primarily found in the lungs as a part of pulmonary surfactant, SP-D has been localized at a range of extrapulmonary sites as a part of mucosal defense system (5).

SP-D is present throughout the female genital tract, with likely involvement in the prevention of uterine infections (6). Epithelial linings of vagina, cervix, uterus, fallopian tubes, and ovaries are positively immunostained for SP-D (7). SP-D has been shown to bind to different strains of HIV-1 (BaL and IIIB) at pH 7.4 (physiological) and 5.0 similar to the pH found in the female urogenital tract (8). Glycoprotein gp120, a highly conserved mannosylated oligosaccharide present on the envelope of HIV-1 virion, plays an important role in the viral entry and facilitates viral replication by activating the NF-κB pathway. SP-D has been shown to bind gp120 of various strains of HIV-1 and prevent HIV-1 interaction with CD4 receptor on T cells, thereby inhibiting viral entry and replication (9, 10).

Another pattern recognition immune regulatory molecule, DC-SIGN/CD209, a type-II transmembrane protein of 44 kDa present on dendritic cell (DC) surface (11), plays a major role in mediating DC adhesion, migration, inflammation, and activation of T cell. DC-SIGN can serve as a route of immune escape for pathogens and tumors (12) and is a known receptor for many viruses, including HIV-1 and HIV-2. DC-SIGN is expressed by both mature and immature DCs in lymphoid tissues (11, 13), but not on follicular DCs, plasmacytoid DCs or $CD1a^+$ Langerhans cells (14), monocytes, T cells, B cells, thymocytes, and $CD34^+$ bone marrow cells. It is also expressed by polarized (M2) macrophages that infiltrate tumors (15), and on antigen-presenting cells such as macrophages, and in chorionic villi of placenta (16). Cells expressing DC-SIGN are located in T cell area of lymph nodes, tonsils, and spleen and dermal DCs in skin ($CD14^+$ macrophages) (17). DC-SIGN expressing cells are seen in mucosal tissue of rectum (18) (with high antigen-presenting capacities), cervix, and uterus, in hepatic sinusoid and lymphatic sinus (19, 20).

HIV-1 virus, when exposed to genital and anal mucosal tissues, binds to DC-SIGN on tissue embedded DCs (21, 22) and gets transmitted to $CD4^+$ T cells, activating adaptive immune response (23, 24). DC-SIGN facilitates HIV-1 transmission in both *cis* and *trans* fashion (25). Expression of DC-SIGN is regulated by IL-4 during monocyte–DC differentiation pathway, along with GM-CSF (26). TGF-β and IFNs are known to be inhibitors of DC-SIGN expression, and, thus, indirectly regulate HIV-1 transmission (26).

The interaction between HIV-1 and DC-SIGN takes place in the mucosal tract where SP-D is present. Since both SP-D and DC-SIGN can bind gp120, we set out to examine if interplay between these proteins can modulate DC-SIGN-mediated viral transfer of HIV-1. This view was further substantiated by observations that SP-D levels are increased in the broncho-alveolar fluid of HIV-1 patients (27); and recombinant forms of SP-D (rfhSP-D) can bind to gp120 of HIV-1, acting as a potent inhibitor of viral infection *in vitro via* inhibition of the interaction between CD4 and gp120 (10). In this study, we show, using recombinant forms of tetrameric and monomeric forms of DC-SIGN and its homolog, DC-SIGNR, that there is a protein–protein interaction between the two C-type lectins *via* CRD regions. They compete for binding to HIV-1 gp120, and thus, SP-D suppresses DC-SIGN mediated transfer of HIV-1 to $CD4^+$ cells.

MATERIALS AND METHODS

Recombinant Expression and Purification of Soluble Forms of Tetrameric and Monomeric DC-SIGN and DC-SIGNR

E. coli strain BL21 (λDE3) (Invitrogen, UK) was transformed with pT5T plasmid encoding DC-SIGN and DC-SIGNR sequences (inserted at the BamHI restriction site into plasmid construct) with and without multimerizing neck region. In the presence of neck region, the bacterial cells expressed tetrameric DC-SIGN and DC-SIGNR; without the neck region, the corresponding constructs produced monomeric forms of DC-SIGN and DC-SIGNR (28). *E. coli* strain BL21 (λDE3) cells containing ampicillin (50 μg/ml) (Sigma-Aldrich) resistant plasmids [except in the case of DC-SIGNR monomer expressing construct that was kanamycin (50 μg/ml) (Sigma-Aldrich) resistant] were subcultured overnight at 37°C. One liter LB medium containing ampicillin or kanamycin was inoculated with 10 ml of overnight bacterial culture and grown at 37°C until the OD_{600} reached 0.7, and then induced with 0.5 mM isopropyl β-D-1-thiogalactopyranoside (IPTG). After 3 h, the bacterial cells were centrifuged at 13,800 × *g* for 15 min to collect the bacterial pellet. Protein expression was analyzed *via* 12% SDS-PAGE.

The cell pellet was treated with 22 ml of lysis buffer, containing 100 mM Tris, pH 7.5, 0.5 M NaCl, lysozyme (50 μg/ml), 2.5 mM EDTA, pH 8.0, and 0.5 mM phenylmethylsulfonyl fluoride (PMSF), and left to stir for 1 h at 4°C. Cells were then sonicated for 10 cycles, each cycle of 30 sec with 2 min interval. The sonicated cell suspension was spun at 10,000 × *g* for 15 min at 4°C. The inclusion bodies, present in the pellet, were solubilized in 20 ml of 6 M urea, 10 mM Tris–HCl, pH 7.0, and 0.01% β-mercaptoethanol (β-ME) by rotating on a shaker for 1 h at 4°C. The mixture was then centrifuged at 13,000 × *g* for 30 min at 4°C and the supernatant was drop-wise diluted fivefold with loading buffer containing 25 mM Tris–HCl, pH 7.8, 1 M NaCl, and 2.5 mM $CaCl_2$ with gentle stirring. This was then dialyzed against 2 l of loading buffer with three buffer changes every 3 h. Following further centrifugation

at 13,000 × *g* for 15 min at 4°C, the supernatant was loaded onto a Mannan agarose column (5 ml; Sigma) pre-equilibrated with the loading buffer. The column was washed with five bed volumes of the loading buffer and the bound protein was eluted in 1 ml fractions using the elution buffer containing 25 mM Tris–HCl, pH 7.8, 1 M NaCl, and 2.5 mM EDTA. The absorbance was read at 280 nm and the peak fractions were frozen at −20. Purity of protein was analyzed by 15% w/v SDS-PAGE.

Expression and Purification of rfhSP-D

E. coli BL21 (λDE3) pLysS containing plasmid pUK-D1 (containing cDNA sequences for 8 Gly–X–Y repeats, neck, and CRD region of human SP-D) was cultured in ampicillin (100 μg/ml) (Sigma-Aldrich) and chloramphenicol (50 μg/ml) (Sigma-Aldrich) at 37°C overnight. Expression and purification was carried out as described earlier (29, 30). Bacterial cells were grown until the OD_{600} reached 0.6 to 0.8, then induced with 0.4 mM IPTG and allowed to grow for an additional three hours. Cells were then pelleted *via* centrifugation and was re-suspended in 50 ml of lysis buffer (50 mM Tris–HCl, pH 7.5, 200 mM NaCl, 5 mM EDTA with freshly added 0.1 mM PMSF, and 100 μg/ml lysozyme) at 4°C for 1 h. The cell lysate was then sonicated at 4 kHz for 30 s with 2 min interval for 15 cycles. The sonicate was centrifuged at 13,800 × *g* for 15 min at 4°C to collect the rfhSP-D-rich pellet containing inclusion bodies. 25 ml of solubilization buffer (50 mM Tris–HCl, pH 7.5, 100 mM NaCl, 5 mM EDTA, 6 M urea) was used to re-suspend the pellet, and incubated at 4°C for 1 h. The dialysate was then centrifuged at 13,800 × *g*, at 4°C for 15 min, and the supernatant was dialyzed against solubilization buffer containing 4 M urea and 10 mM β-ME for 2 h at 4°C. The dialysis buffer was serially changed to solubilization buffer containing 2, 1, and 0 M urea at 4°C, 2 h each. Final dialysis was done in solubilization buffer containing 5 mM $CaCl_2$ for 3 h to completely remove any traces of urea. The dialysate was centrifuged at 13,800 × g, 4°C for 15 min and the clear supernatant containing rfhSP-D was affinity-purified using maltosyl-agarose column (Sigma-Aldrich). The bound protein was eluted with solubilization buffer containing 10 mM EDTA, pH 7.5. Endotoxin levels were removed by passing the purified protein fractions through Polymyxin B column (Detoxi-Gel, Peirce & Warriner, UK) and the levels were measured using the Limulus Amebocyte Lysate Assay (BioWhitaker, UK). The endotoxin level was found to be <5 pg/μg rfhSP-D.

SDS-PAGE and Far Western Blot Analysis

DC-SIGN and DC-SIGNR proteins were separated on a 12% (w/v) SDS-PAGE under reducing conditions. After electrophoresis, the polyacrylamide gels were stained with Coomassie Brilliant Blue. For the far western blotting, proteins were electrotransferred onto polyvinylidene difluoride (PVDF) membrane (Sigma) and blocked with 5% w/v milk in PBS. The membrane bound proteins were probed with rfhSP-D (5 μg/ml) for 2 h, followed by addition of anti-SP-D (1:1,000) (Medical Research Council Immunochemistry Unit, Oxford) polyclonal antibodies. The blot was then probed with Protein A-HRP Conjugate (1:1,000) (Sigma), followed by color development with diaminobenzidine as a substrate (Sigma-Aldrich, UK).

ELISA

Microtitre wells were coated with DC-SIGN and DC-SIGNR proteins in carbonate/bicarbonate buffer, pH 9.6 in decreasing double dilutions (5–0.625 μg/well) in duplicates and left overnight at 4°C. The microtiter wells were blocked with 2% w/v BSA in PBS for 2 h at 37°C. The wells were then washed three times with PBS + 0.05% v/v Tween 20 and incubated with a constant concentration (2.5 μg) of rfhSP-D in 20 mM Tris–HCl, pH 7.5, 100 mM NaCl, 5 mM $CaCl_2$ or 5 mM EDTA at 37°C for 1 h, followed by 1 h at 4°C. Following PBS + Tween 20 wash, the bound rfhSP-D was detected using anti-SP-D (1:5,000) polyclonal antibody and Protein A-HRP conjugate (1:5,000). Color was developed using *o*-Phenylenediamine (OPD) as a substrate and absorbance was measured at 490 nm.

Competitive ELISA

The ability of rfhSP-D to compete with and DC-SIGN for binding to HIV-1 gp120 (Abcam; ab167715) gp120 was analyzed by competitive ELISA. Gp120 was coated at 250 ng/well in duplicates and left overnight at 4°C. Wells were blocked with 2% BSA in PBS for 2 h at 37°C. The wells were washed three times with PBS + 0.05% v/v Tween 20. A constant concentration of DC-SIGN tetramer (5 μg/ml) and decreasing concentrations of rfhSP-D (5 − 0.625 μg/well) in calcium buffer were added to the wells, which were subsequently probed with anti-DC-SIGN (1:5000) polyclonal antibodies. Following washes, the wells were incubated with Protein HRP conjugate (1:1,000). Color was developed using OPD as a substrate.

Fluorescence Microscopy

Human embryonic kidney cells 293 (HEK 293), transfected with DC-SIGN construct (DC–HEK) (31), were grown and maintained in DMEM (Life technologies, UK) containing 10% v/v fetal calf serum, 2 mM L-glutamine, penicillin (100 U/ml)/streptomycin (100 μg/ml) (Thermo Fisher), and blasticidin (5 μg/ml) (Gibco). HEK 293 cells were grown and maintained in DMEM (Life technologies) containing 10% FBS. Both cell lines were grown under standard conditions (37°C, 5% v/v CO_2) until 80–90% confluency was reached. HEK 293 and DC–HEK cells (0.5×10^5) were grown on the coverslips in a 24-well plate (Nunc) overnight to perform three different sets of immunofluorescence experiments; DC-SIGN expression (primary antibody: rabbit anti-DC-SIGN, 1:500 and secondary antibody: anti-rabbit/CY3, 1:500, Thermo Fisher), rfhSP-D (10 μg/ml) binding to DC-SIGN (primary antibody: monoclonal anti-SP-D, 1:500 and secondary antibody: anti-mouse conjugated/CY5, 1:500, Abcam) and co-localization of DC-SIGN and rfhSP-D (primary antibodies: anti-DC-SIGN polyclonal and anti-SP-D monoclonal, 1:500 and secondary antibodies: anti-rabbit/CY3 and anti-mouse/FITC, 1:500) on the cell surface of DC–HEK cells. HEK 293 cells were used as a control for all experiments and DC–HEK cells were incubated with secondary antibody alone as an additional control. Hoechst (1:10,000, Thermo Fisher) was used to stain the nucleus for all the staining experiments. The cells were incubated for 1 h with primary antibody followed by 1 h incubation with secondary antibodies as described earlier with three times

phosphate-buffered saline (PBS, Thermo Fisher) washes between each step. For rfhSP-D binding with DC-SIGN analysis, the rfhSP-D was incubated with the cells for 1 h at 4°C. The cells were fixed with 4% paraformaldehyde (Sigma) before mounting on the coverslips to visualize under a HF14 Leica DM4000 microscope.

Viral Transfer Assay

Pooled human peripheral blood mononuclear cells (PBMCs) (HiMedia Laboratories, India) were stimulated in RPMI 1640 medium (Sigma-Aldrich) containing 10% v/v FBS, 1% Penicillin–Streptomycin and 5 µg/ml phytohemaglutinin (PHA) and 10 U/ml of rhIL-2 (Gibco) for 24 h. PHA/IL-2 was washed off and activated PBMCs were cultured further in complete RPMI medium. For the experiment, DC–HEK cells were grown in a 12-well tissue culture plate until 80% confluence in complete DMEM/F12 (Sigma-Aldrich, USA) containing 10% FBS (Gibco) and blasticidin. Indicated concentrations of rfhSP-D containing 5 mM $CaCl_2$ was added to each well and incubated for 2 h to allow binding to DC-SIGN. The wells without rfhSP-D were used as controls. Excess protein was removed, and cells were challenged for 1 h with 5 ng/ml p24 of HIV-1 SF-162 strain (kindly provided by Dr. Jay Levy, AIDS Program, National Institutes of Health, USA). 5 mM EDTA was added along with the virus in EDTA controls. Unbound virus was washed off and DC–HEK cells were cocultured with PHA/IL-2 activated PBMCs for 24 h to facilitate transfer. PBMCs along with the medium were then

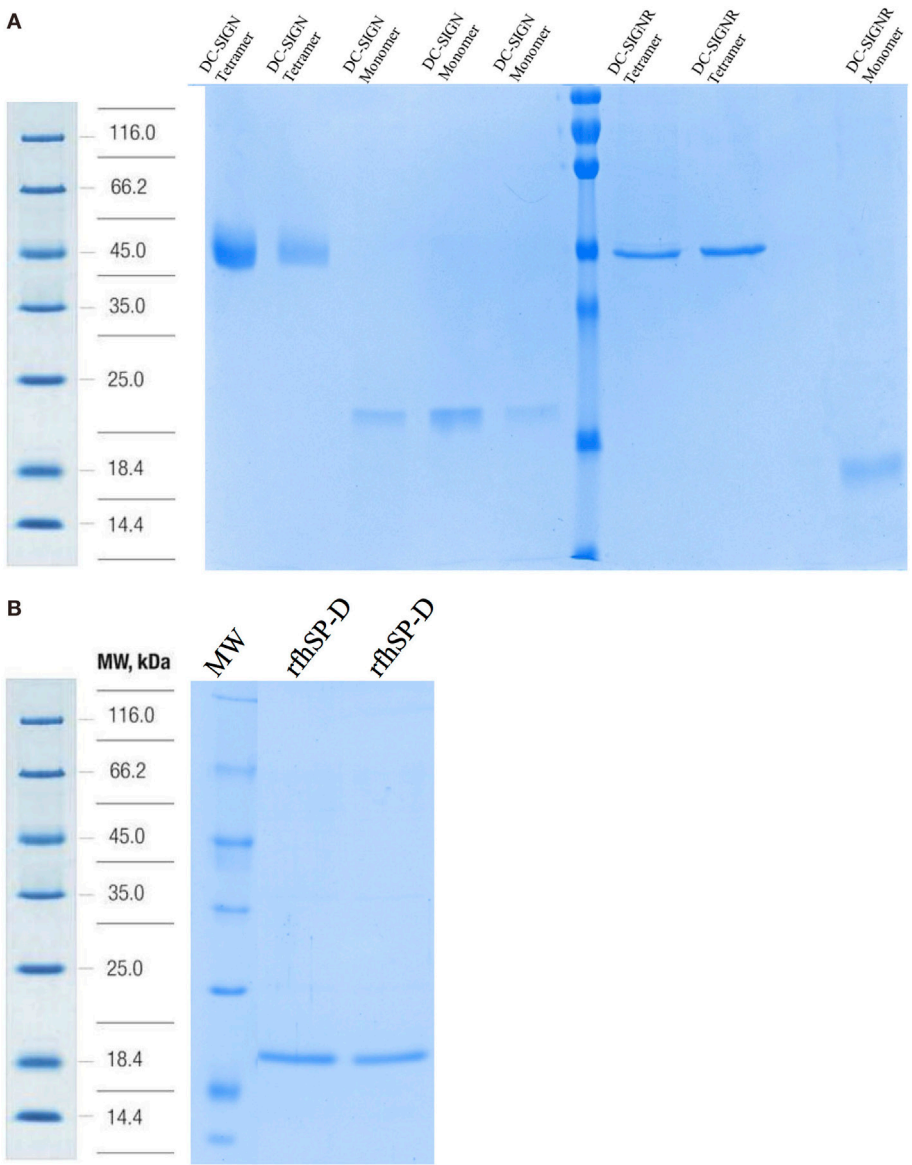

FIGURE 1 | SDS-PAGE analysis of purified recombinant forms of DC-SIGN, DC-SIGNR, and recombinant forms of SP-D (rfhSP-D). **(A)** 12% SDS-PAGE of affinity-purified tetrameric and monomeric forms of DC-SIGN and DC-SIGNR under reduced conditions. **(B)** 12% v/v SDS-PAGE of affinity-purified rfhSP-D.

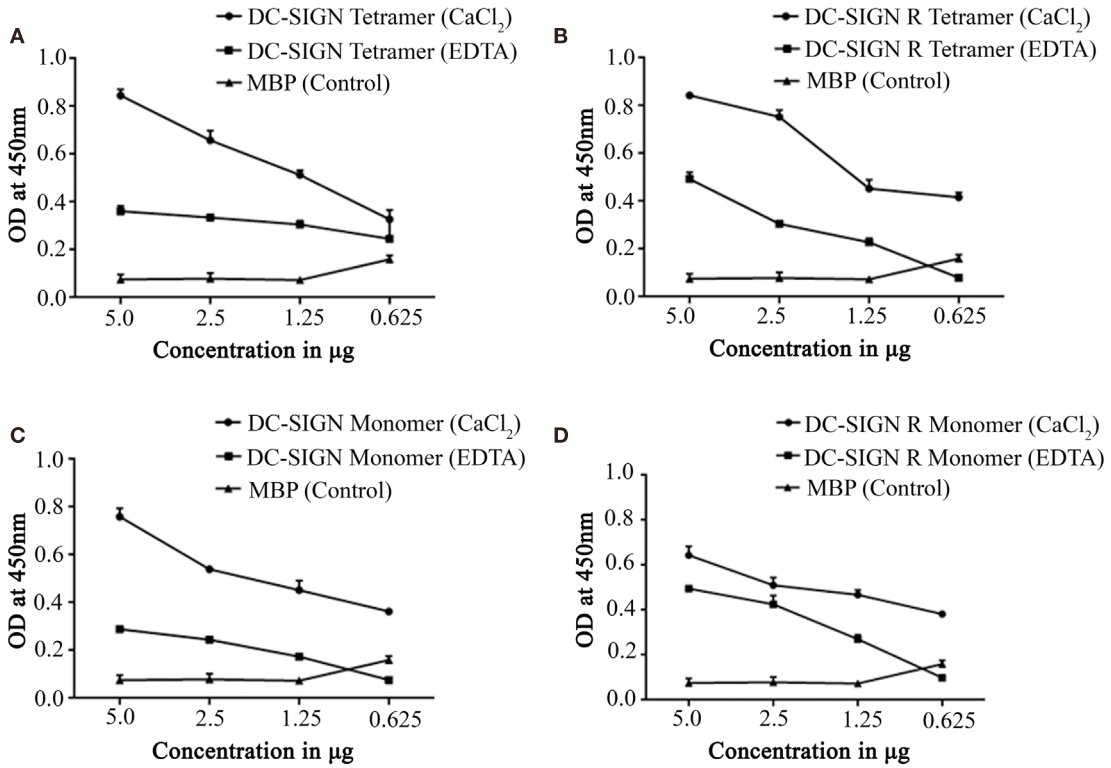

FIGURE 2 | Direct binding ELISA showing interaction between recombinant forms of SP-D (rfhSP-D) and DC-SIGN/DC-SIGNR. DC-SIGN tetramer **(A)**, DC-SIGNR tetramer **(B)**, DC-SIGN monomer **(C)**, and DC-SIGNR monomer **(D)** were coated at decreasing double dilutions from 5 to 0.625 µg/well and then probed with 2.5 µg of rfhSP-D in either in calcium or EDTA buffer. The binding was detected using anti-human surfactant protein D polyclonal antibodies (1:5,000 dilutions). The data represent mean and SD values of at least five experiments.

separated (siphoned off) from the DC–HEK monolayer and were transferred to fresh plates. They were cultured further in RPMI 1640 medium containing 10% FBS for 7 days, and viral titers were determined in supernatants on day 4 and 7 using HIV-1 p24 antigen ELISA kit (XpressBio Life Science Products, Frederick, MD, USA).

Molecular Modeling and Bioinformatics

The crystal structures of trimeric human lung SP-D (PDB ID: 1PW9), CD4 bound to HIV-1 envelope glycoprotein gp120 (PDB ID:1GC1) and homo 10-mer DC-SIGN complexed with sugars (PDB ID:1K9I) were retrieved from Protein Data Bank. The tetrameric form of non-glycosylated DC-SIGN was used for docking studies as this structure was found to bind to rfhSP-D *in vitro* experiments. DC-SIGN tetramer was docked to CD4 already bound to HIV-1 envelope glycoprotein gp120 (PDB ID: 1GC1) using Patch Dock server with default parameters.

The CRD-mediated protein–protein interaction between trimeric SP-D and tetrameric DC-SIGN, as observed in this study was further examined by docking these two molecules using ZDOCK algorithm of Discovery Studio (Accelrys Inc.). The best pose of these two molecules was subsequently docked into gp120 using Patch Dock server. The shortlisted poses from PatchDock and ZDOCK were further refined using Fire Dock and RDOCK, respectively.

RESULTS

rfhSP-D and DC-SIGN Can Interact with Each Other *via* Their C-Type Lectin Domains

Structurally, DC-SIGN is composed of an extracellular domain (ECD) which exists as a tetramer, stabilized by an N-terminal α-helical neck region, followed by a CRD. DC-SIGN and DC-SIGNR comprising of the entire ECD (tetramer) (**Figure 1A**) and the CRD region alone (monomer) (**Figure 1A**) were expressed in *E. coli* and affinity-purified on Mannose-agarose (28). The CRD regions of DC-SIGN and SIGNR bound mannose weakly as majority of the proteins appeared in the flow through. The ECD domains of both DC-SIGN and DC-SIGNR bound to mannose with much greater affinity in the presence of Ca^{2+} and eluted with EDTA. A recombinant form of human SP-D, containing 8 Gly–X–Y repeats of the collagen, neck, and CRD regions were expressed and purified as homotrimeric molecules, as described earlier (29, 30) (**Figure 1B**). Tetrameric and monomeric forms of DC-SIGN and DC-SIGNR were checked for their respective interactions with rfhSP-D *via* ELISA (**Figure 2**), which showed a calcium- and dose-dependent interaction between the two lectins; tetrameric forms bound rfhSP-D better than the monomers. This was confirmed by a far western blot (**Figure 3A**), which revealed that rfhSP-D was able to bind to DC-SIGN and DC-SIGNR

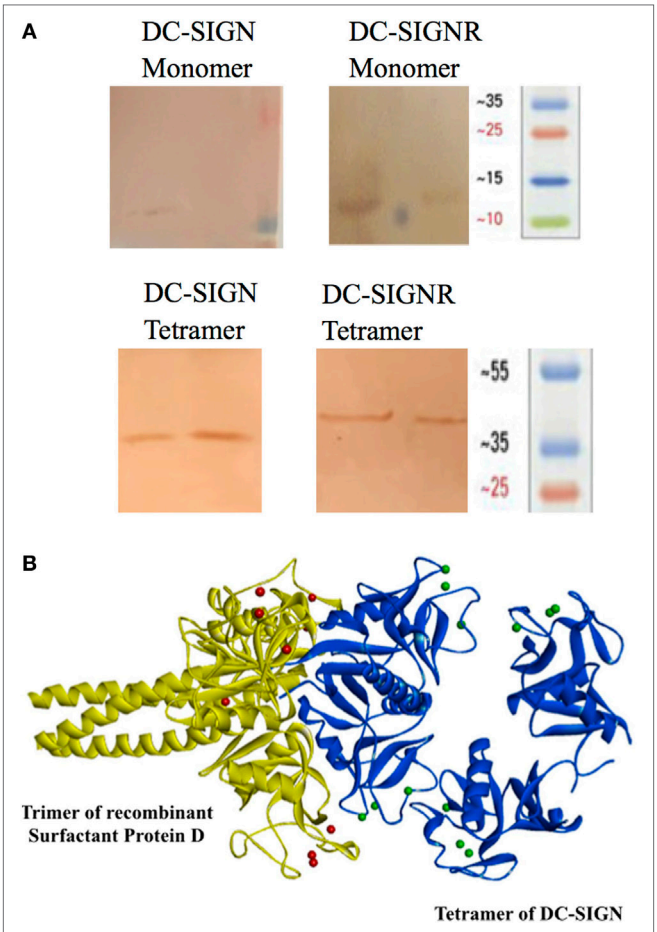

FIGURE 3 | Far western blot to detect binding of recombinant forms of SP-D (rfhSP-D) to PVDF bound DC-SIGN and DC-SIGNR. **(A)** Tetrameric and monomeric variants of DC-SIGN and DC-SIGNR were run on a SDS-PAGE and were transferred to a PVDF membrane followed by incubation with 5 μg/ml rfhSP-D and then probed with anti-SP-D polyclonal antibody. **(B)** Docked structure of trimeric surfactant protein D (SP-D) (yellow cartoon) and tetrameric DC-SIGN (blue cartoon). The two molecules interact *via* their carbohydrate recognition domains.

proteins immobilized on PVDF membrane. The CRD-mediated protein–protein interaction between trimeric SP-D and tetrameric DC-SIGN was further studied by docking these two molecules. The docked pose showed that the two molecules likely interact *via* their CRD regions (**Figure 3B**).

rfhSP-D:DC-SIGN Interaction Leads to Competition for Binding to HIV-1 gp120

To examine if rfhSP-D can inhibit the binding of DC-SIGN to gp120, we carried out a competitive ELISA. As expected, both rfhSP-D and DC-SIGN tetramer bound gp120 in a dose- and calcium-dependent manner (data not shown) (32). In order to assess a likely interference by rfhSP-D in DC-SIGN: gp120 interaction, a constant concentration of DC-SIGN tetramer was used against different concentrations of rfhSP-D and added to solid-phase gp120 (**Figure 4**). With increasing concentration, rfhSP-D was able to inhibit DC-SIGN-gp120 interaction, suggesting that

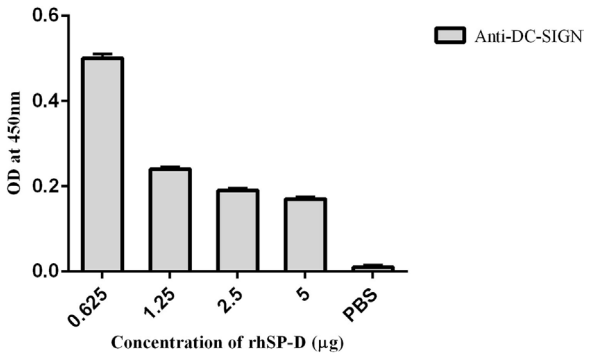

FIGURE 4 | Competitive inhibition ELISA to show that recombinant form of SP-D (rfhSP-D) inhibits DC-SIGN binding to immobilized HIV-1 gp120. HIV-1 gp120 trimer (250 ng per well) was first coated to which 5–0.625 μg/well of rfhSP-D and a constant concentration (5 μg/well) of DC-SIGN tetramer were added. Bound DC-SIGN tetramer was detected by anti-DC-SIGN polyclonal antibodies. Protein A-HRP conjugate (1:1,000) was used to detect the antibodies bound and color was developed using *o*-Phenylenediamine. 0 in the graph represents the control where only PBS was used instead of gp120, and the experiments were repeated three times.

the binding sites on these two C-type lectins for gp120 may be overlapping.

rfhSP-D Co-Localizes with DC-SIGN on the Surface of Transfected HEK 293 Cells

Human embryonic kidney cells transfected with DC-SIGN construct (DC–HEK cells) were shown to express DC-SIGN *via* immunofluorescence microscopy. The DC-SIGN expression seen on the cell surface on DC–HEK cells was evenly distributed, as compared to HEK 293 cells, which were used as a control, using anti-DC-SIGN polyclonal antibody (**Figure 5A**). DC–HEK cells, incubated with secondary antibody alone, did not show any expression (**Figure 5A**). rfhSP-D binding was visible on the cell surface of DC–HEK cells, whereas rfhSP-D binding could not be detected in either HEK 293 cells or DC–HEK cells incubated with secondary antibody alone as controls (**Figure 5B**). rfhSP-D and DC-SIGN co-localized on the HEK cell surface transfected with DC-SIGN construct (**Figure 5C**).

rfhSP-D Inhibits DC-SIGN-Mediated Viral Transfer to PBMCs in a Dose-Dependent Manner

To understand whether interaction between rfhSP-D and DC-SIGN impacted upon DC-SIGN-mediated HIV-1 transfer to T cells, we performed a coculture assay using DC–HEK cells and mitogen-activated PBMCs. Presence of rfhSP-D led to a significantly ($p < 0.005$) reduced HIV-1 p24 levels in day 4 and day 7 PBMC culture supernatants in a dose-dependent manner (**Figure 6**). This suggested that, in presence of rfhSP-D, the viral uptake by DC–HEK was significantly inhibited resulting in reduced transfer and replication of HIV-1 in PBMC cultures. It is likely that rfhSP-D may have occupied sites on both DC-SIGN as well as HIV-1 gp120 that resulted in reduced

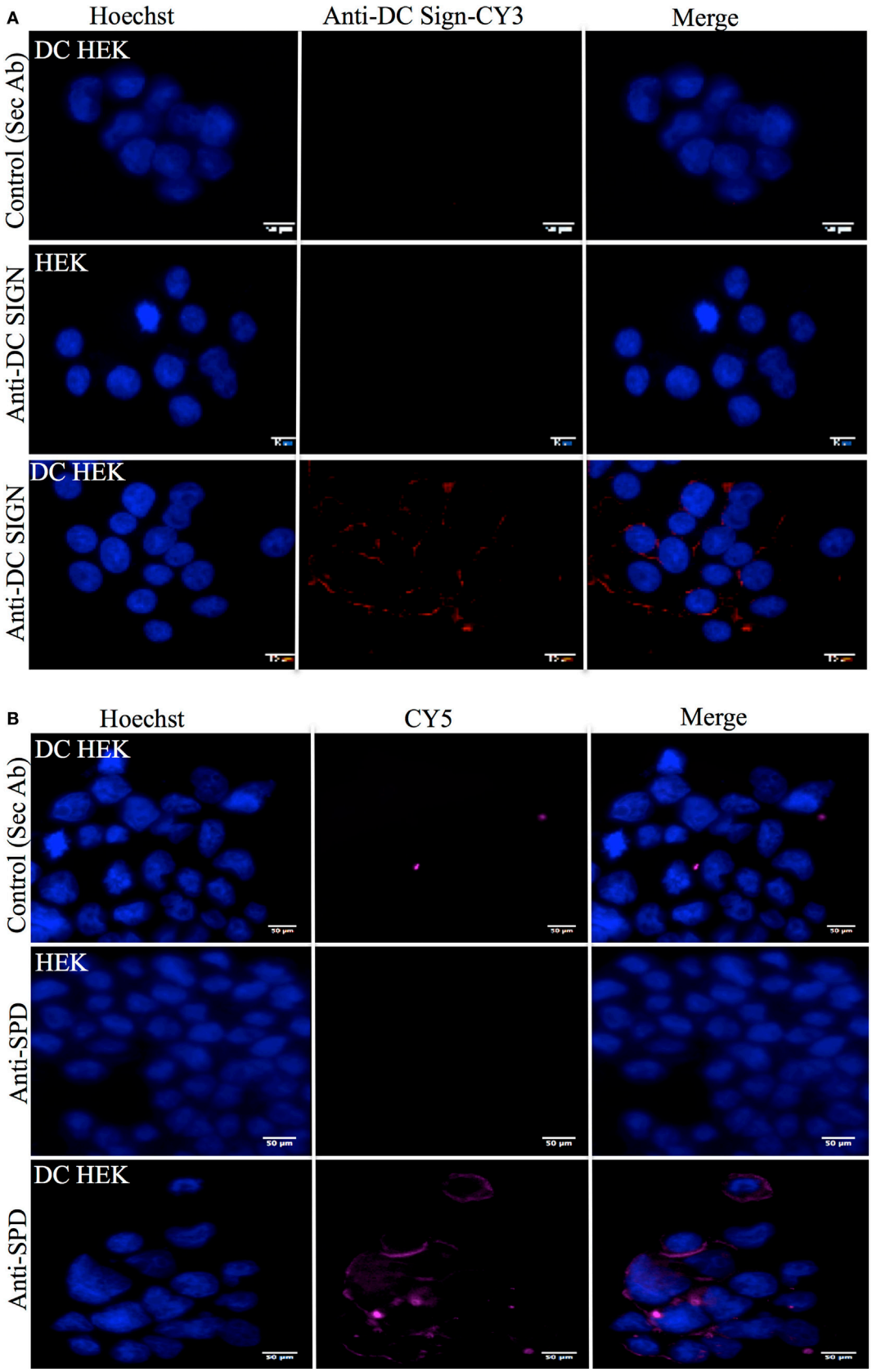

FIGURE 5 | Continued

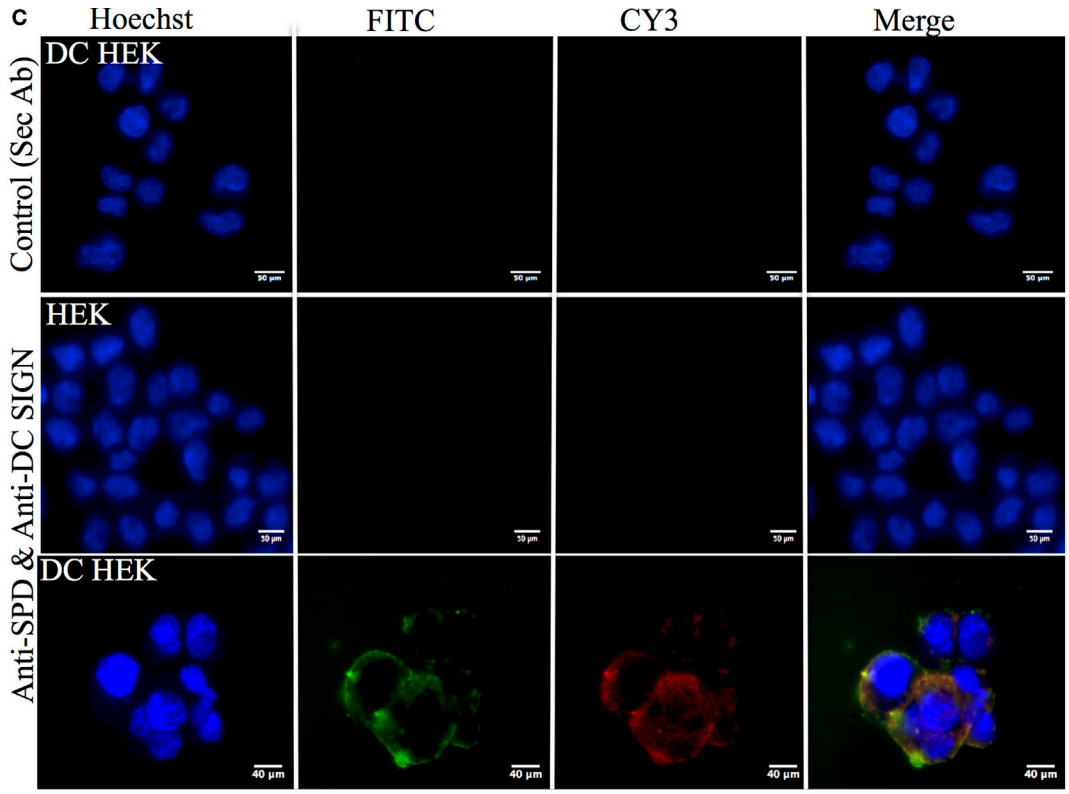

FIGURE 5 | Immunofluorescence microscopy to show recombinant forms of SP-D (rfhSP-D) binding to DC-SIGN on the surface of the human embryonic kidney (HEK) cells transfected with DC-SIGN construct (DC–HEK cells). **(A)** DC–HEK cells incubated with anti-rabbit/CY3 did not show DC-SIGN expression (control). DC–HEK and HEK cells incubated with anti-DC-SIGN followed by anti-rabbit conjugated with CY3 showed the DC-SIGN expression in DC–HEK cells only and not HEK cells. Hoechst was used to stain the nucleus. **(B)** Analysis of rfhSP-D binding to DC-SIGN on the DC–HEK cells *via* immunofluorescence. DC–HEK cells incubated with anti-SP-D for 1 h and then probed with anti-mouse/CY5 did not show binding. DC–HEK cells incubated with rfhSP-D (5 µg/ml) for 1 h, followed by anti-SP-D for 1 h and then anti-mouse/CY5 showed the binding on the cell surface. **(C)** DC-SIGN expression and rfhSP-D binding co-localization analysis *via* immunofluorescence microscopy. DC–HEK cells incubated with secondary antibodies only (anti-mouse/FITC and anti-rabbit/FITC) for 1 h did not show immunofluorescence. DC–HEK and HEK cells incubated with rfhSP-D for 1 h prior to incubation anti-SP-D monoclonal and anti-DC-SIGN polyclonal for 1 h followed by anti-mouse/FITC and anti-rabbit/CY3 for 1 h showed co-localization for rfhSP-D binding and DC–HEK expression.

DC-SIGN interaction with HIV-1 gp120. EDTA significantly inhibited DC–HEK-mediated viral transfer, as reported previously (33).

Bioinformatics Analysis Revealed That HIV-1 gp120 and rfhSP-D May Occupy the Same Site on the CRDs of DC-SIGN

To support our hypothesis that DC-SIGN once bound to rfhSP-D may not interact with gp120, we performed *in silico* analyses. The best-docked pose of rfhSP-D and DC-SIGN was subsequently docked to gp120 using Patch Dock server. The shortlisted poses from Patch Dock and ZDOCK were further refined using Fire Dock and RDOCK, respectively. Two poses appear to suggest that HIV-1 gp120 and rfhSP-D possibly occupy the same site on the CRD of DC-SIGN (**Figure 7**). Thus, in the presence of rfhSP-D, it is likely that interaction of DC-SIGN with gp120 could be inhibited. To validate our bioinformatics strategy, we evaluated the known interaction of gp120 with DC-SIGN followed by docking with CD4. DC-SIGN binds to gp120 at a site distant from its CD4 binding site, and hence, DC-SIGN-bound HIV-1 possibly interacts with CD4 for viral transmission (**Figure 8**). The global energy of these docked complexes has also been presented (**Table 1**).

DISCUSSION

In this study, we report, for the first time, an interaction of DC-SIGN and SP-D, two C-type lectins and pattern recognition receptors; both proteins are known to bind to HIV-1 gp120. We demonstrate that this interaction involves their CRD domains, which is relevant in inhibiting DC-SIGN-mediated HIV-1 trans-infection of $CD4^+$ T cells. Interaction of HIV-1 gp120 with DC-SIGN not only increases the affinity of gp120 for CD4 (34) but also leads to a productive infection *via* reactivation of provirus involving NF-κB pathway (35, 36). This interaction also results in downregulation of Nef-induced release of IL-6 (37) and leads to Ask-1-dependent activation leading to induction of apoptosis of human DCs (38). Simultaneous binding of rfhSP-D to both

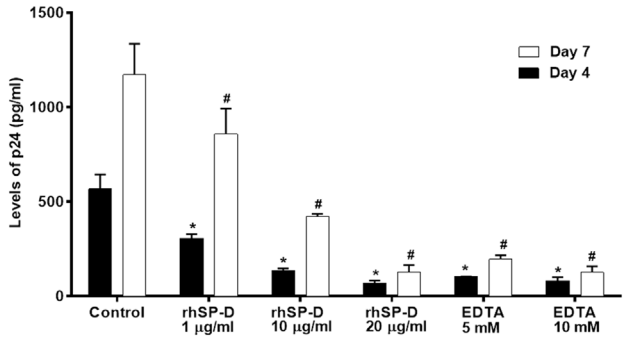

FIGURE 6 | DC-SIGN-mediated HIV-1 transfer assay. DC–HEK cells were grown in a 12-well plate until 80% confluence. 20, 10, and 1 μg/ml of recombinant forms of SP-D (rfhSP-D) concentrations were added to the cells and incubated for 2 h for binding. Unbound protein was removed and cells were challenged with 2.5 ng/ml p24 of HIV-1 (SF-162 strain) for 1 h (to bind to DC-SIGN). After 1 h, unbound virus was washed off and cells were cocultured with phytohemaglutinin-activated peripheral blood mononuclear cells (PBMCs) for 24 h. This allows the DC-SIGN captured virus to be transferred to $CD4^+$ cells, where virus will multiply. PBMCs were separated from the monolayer and cultured separately for 4 days to determine viral titer.

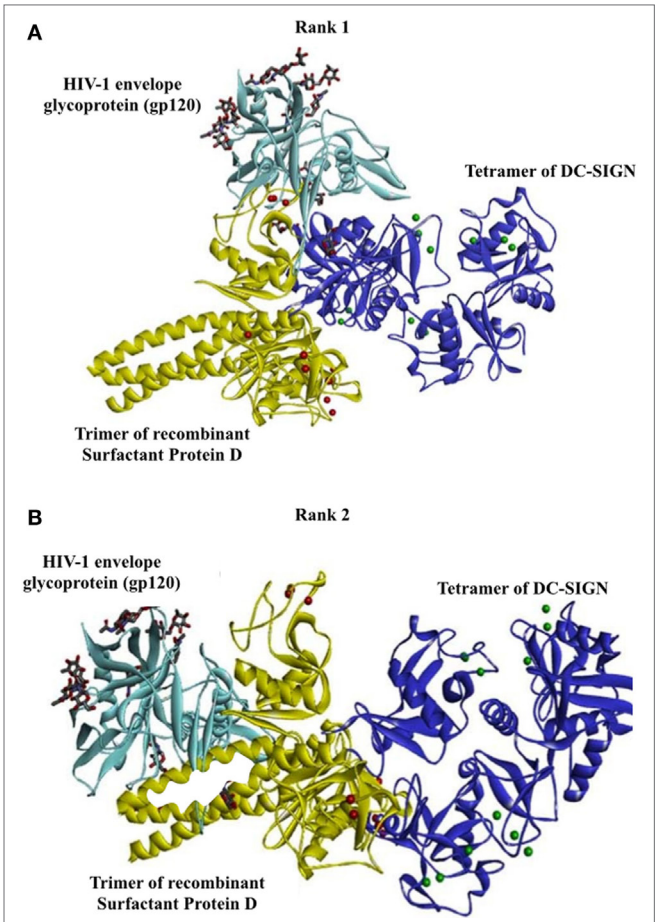

FIGURE 7 | Two poses suggesting that HIV-1 gp120 and recombinant forms of SP-D possibly occupy the same site on carbohydrate recognition domain of DC-SIGN. Docked structures of surfactant protein D trimer (yellow cartoon and calcium ions as red spheres) complexed with DC-SIGN tetramer (blue cartoon and calcium ions as green spheres) and HIV-1 envelope glycoprotein, gp120 (cyan cartoon). The sugars present in gp120 are shown as sticks. The calcium ions of DC-SIGN are represented as green spheres. **(A)** Rank no. 1. **(B)** Rank no. 2.

gp120 and DC-SIGN, thus, may result in blockade of DC-SIGN-mediated viral transmission and inhibition of replication.

Structure–function studies have revealed that the CRD region of DC-SIGN is the specific ligand-binding site that is reliant on the neck region within the extracellular domain (ECD) (39). This notion was validated in our binding ELISA type assays when we used the tetrameric forms of DC-SIGN and DC-SIGNR (comprising of the ECD and CRD region) as well as the monomeric forms, which only consist of the CRD region. The binding studies involving rfhSP-D highlighted that multimeric forms of DC-SIGN and DC-SIGNR bind better, not surprisingly, due to multivalent nature of interactions. Since DC-SIGN promotes HIV-1 infection, we examined if rfhSP-D by virtue to its ability to bind gp120 as well as DC-SIGN can potentially interfere with HIV-1 (40–42). We also included DC-SIGNR (DC-SIGN-Related), a homolog of DC-SIGN, in our study. DC-SIGNR, expressed on endothelium including liver sinusoidal, lymph node sinuses, and placental capillary, can also bind gp120 to facilitate HIV-1 viral infection (43).

The current study provides the first evidence that DC-SIGN is a novel immune receptor or adaptor for the CRD region of SP-D, modulating the HIV-1 infection. Interaction of gp120 and rfhSP-D is calcium dependent as reported earlier (8–10). Tetrameric DC-SIGN also efficiently binds gp120 in a dose-dependent manner, which is not significantly inhibited in presence of sugars similar to previous reports (28, 44). The recombinant rfhSP-D has been shown to inhibit the gp120-CD4 interaction (10) while, DC-SIGN-bound trimeric gp140 interacts with CD4 more avidly (34). *In vitro* competitive assays and the bioinformatics analysis confirmed that rfhSP-D and DC-SIGN compete for gp120. The reduced p24 levels confirmed that rfhSP-D significantly inhibits the DC-SIGN mediated viral transfer.

The rfhSP-D molecule (a recombinant fragment of human SP-D comprising homotrimeric C-type lectins), with part of collagen region, α-helical coiled-coil neck, and CRD region, has been extensively studied *via in vitro*, *in vivo*, and *ex vivo* experiments. In a number of studies, rfhSP-D has worked at par with full-length SP-D, as evident from its ability to be therapeutic in murine models of allergic bronchopulmonary aspergillosis (45, 46), invasive pulmonary aspergillosis (45), and dust mite allergy (47). It can also induce apoptosis in activated eosinophils (29, 48) and PBMCs (49). Thus, rfhSP-D is an excellent well-tested therapeutically active molecule.

Mannose-binding lectin, another serum collectin, is also known to inhibit DC-SIGN-mediated trans-infection of HIV-1 T cells (50) whereas SP-A and SP-D facilitate this transfer (8, 51). Madsen et al. incubated SP-D-HIV-1 complexes with immature monocyte-derived DCs and demonstrated increased viral uptake and transfer from DCs to PM-1 cells. However, the assay system employed in the two studies (Madsen and ours) significantly differed, thus the observed variation in the results. Further studies in appropriate animal models will

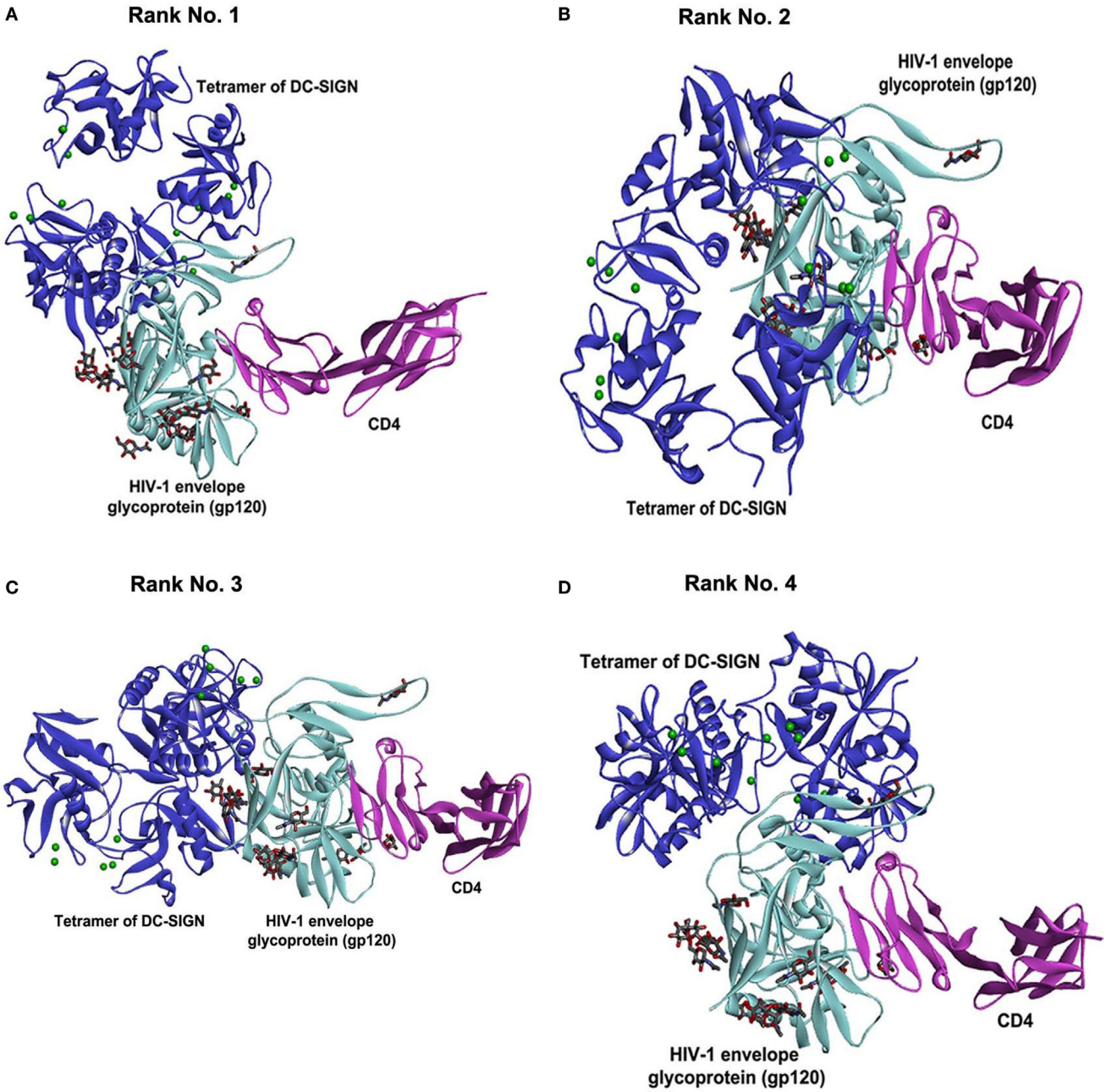

FIGURE 8 | Known interaction of gp120 with DC-SIGN followed by docking with CD4. Selected docked poses of tetrameric DC-SIGN (blue cartoon) and HIV-1 envelope glycoprotein gp120 (cyan cartoon) bound to CD4 (pink cartoon). The sugars present in gp120 are shown as sticks. **(A)** Rank no. 1. **(B)** Rank no. 2. **(C)** Rank no. 3. **(D)** Rank no. 4.

TABLE 1 | Energy for docked complexes of DC-SIGN and gp120 bound to CD4 refined using FireDock.

Rank no.	Global energy (kcal/mol)
1	−27.01
2	−21.83
3	−11.99
4	−10.94

help to determine the overall effects of SP-D and DC-SIGN binding during virus infections. Our findings have revealed a new phenomenon in SP-D-mediated viral transfer through DCs as rfhSP-D occupies similar sites as gp120 on DC-SIGN. Hence, pre-incubation of rfhSP-D may have occupied gp120-binding site on DC-SIGN (displacement of gp120 *via* ELISA and *in silico* analysis), resulting in poor uptake. This must

have resulted in reduced transfer of viral particles to activated PBMCs, adding another aspect to rfhSP-D-mediated anti-HIV activity.

To summarize, rfhSP-D has the ability to directly inhibit the viral entry by interacting with gp120 and to significantly inhibit the DC-SIGN-mediated viral transfer. Importantly, these molecular interactions inhibit the immunomodulation mediated by gp120 and DC-SIGN further disfavoring the HIV-1 pathogenesis. DC-SIGN binding to SP-D could be one of the ligand–receptor interactions that in turn could play a major role in the inhibition of viral entry. Further, *in vivo* assays and clinical trials can elucidate the physiological conditions for therapeutic purposes against the infection.

ACKNOWLEDGMENTS

We are extremely grateful to Dr. Peter Kwong and Marie Pancerea, Structural Biology Section, NIAIDS, NIH for providing PDB coordinates of HIV-1 gp120 modelled with glycans.

AUTHOR CONTRIBUTIONS

ED-M, DM, HP, and AK carried out crucial set of experiments; supporting experiments were done by AS, VM, ST, BN, and MA-M; TM supervised critical infection assays; UK led the project and wrote the manuscript with due help from ED-M, HP, and TM.

REFERENCES

1. Holmskov U, Thiel S, Jensenius JC. Collections and ficolins: humoral lectins of the innate immune defense. *Annu Rev Immunol* (2003) 21:547–78. doi:10.1146/annurev.immunol.21.120601.140954
2. Kishore U, Reid KB. Structures and functions of mammalian collectins. *Results Probl Cell Differ* (2001) 33:225–48. doi:10.1007/978-3-540-46410-5_12
3. Kishore U, Greenhough TJ, Waters P, Shrive AK, Ghai R, Kamran MF, et al. Surfactant proteins SP-A and SP-D: structure, function and receptors. *Mol Immunol* (2006) 43:1293–315. doi:10.1016/j.molimm.2005.08.004
4. Tino MJ, Wright JR. Surfactant protein A stimulates phagocytosis of specific pulmonary pathogens by alveolar macrophages. *Am J Physiol* (1996) 270:L677–88.
5. Nayak A, Dodagatta-Marri E, Tsolaki AG, Kishore U. An insight into the diverse roles of surfactant proteins, SP-A and SP-D in innate and adaptive immunity. *Front Immunol* (2012) 3:131. doi:10.3389/fimmu.2012.00131
6. Madhukaran SP, Alhamlan FS, Kale K, Vatish M, Madan T, Kishore U. Role of collectins and complement protein C1q in pregnancy and parturition. *Immunobiology* (2016) 221:1273–88. doi:10.1016/j.imbio.2016.06.002
7. Leth-Larsen R, Floridon C, Nielsen O, Holmskov U. Surfactant protein D in the female genital tract. *Mol Hum Reprod* (2004) 10:149–54. doi:10.1093/molehr/gah022
8. Madsen J, Gaiha GD, Palaniyar N, Dong T, Mitchell DA, Clark HW. Surfactant Protein D modulates HIV infection of both T-cells and dendritic cells. *PLoS One* (2013) 8:e59047. doi:10.1371/journal.pone.0059047
9. Meschi J, Crouch EC, Skolnik P, Yahya K, Holmskov U, Leth-Larsen R, et al. Surfactant protein D binds to human immunodeficiency virus (HIV) envelope protein gp120 and inhibits HIV replication. *J Gen Virol* (2005) 86:3097–107. doi:10.1099/vir.0.80764-0
10. Pandit H, Gopal S, Sonawani A, Yadav AK, Qaseem AS, Warke H, et al. Surfactant protein D inhibits HIV-1 infection of target cells via interference with gp120-CD4 interaction and modulates pro-inflammatory cytokine production. *PLoS One* (2014) 9:e102395. doi:10.1371/journal.pone.0102395
11. Geijtenbeek TB, Krooshoop DJ, Bleijs DA, van Vliet SJ, van Duijnhoven GC, Grabovsky V, et al. DC-SIGN-ICAM-2 interaction mediates dendritic cell trafficking. *Nat Immunol* (2000) 1:353–7. doi:10.1038/79815
12. van Kooyk Y, Geijtenbeek TB. DC-SIGN: escape mechanism for pathogens. *Nat Rev Immunol* (2003) 3:697–709. doi:10.1038/nri1182
13. Bleijs DA, Geijtenbeek TB, Figdor CG, van Kooyk Y. DC-SIGN and LFA-1: a battle for ligand. *Trends Immunol* (2001) 22:457–63. doi:10.1016/S1471-4906(01)01974-3
14. Engering A, Geijtenbeek TB, van Vliet SJ, Wijers M, van Liempt E, Demaurex N, et al. The dendritic cell-specific adhesion receptor DC-SIGN internalizes antigen for presentation to T cells. *J Immunol* (2002) 168:2118–26. doi:10.4049/jimmunol.168.5.2118
15. Dominguez-Soto A, Sierra-Filardi E, Puig-Kroger A, Perez-Maceda B, Gomez-Aguado F, Corcuera MT, et al. Dendritic cell-specific ICAM-3-grabbing non-integrin expression on M2-polarized and tumor-associated macrophages is macrophage-CSF dependent and enhanced by tumor-derived IL-6 and IL-10. *J Immunol* (2011) 186:2192–200. doi:10.4049/jimmunol.1000475
16. Soilleux EJ, Morris LS, Lee B, Pohlmann S, Trowsdale J, Doms RW, et al. Placental expression of DC-SIGN may mediate intrauterine vertical transmission of HIV. *J Pathol* (2001) 195:586–92. doi:10.1002/path.1026
17. Ochoa MT, Loncaric A, Krutzik SR, Becker TC, Modlin RL. "Dermal dendritic cells" comprise two distinct populations: CD1+ dendritic cells and CD209+ macrophages. *J Invest Dermatol* (2008) 128:2225–31. doi:10.1038/jid.2008.56
18. Kamada N, Hisamatsu T, Honda H, Kobayashi T, Chinen H, Kitazume MT, et al. Human CD14+ macrophages in intestinal lamina propria exhibit potent antigen-presenting ability. *J Immunol* (2009) 183:1724–31. doi:10.4049/jimmunol.0804369
19. Jameson B, Baribaud F, Pohlmann S, Ghavimi D, Mortari F, Doms RW, et al. Expression of DC-SIGN by dendritic cells of intestinal and genital mucosae in humans and rhesus macaques. *J Virol* (2002) 76:1866–75. doi:10.1128/JVI.76.4.1866-1875.2002
20. Zhou T, Chen Y, Hao L, Zhang Y. DC-SIGN and immunoregulation. *Cell Mol Immunol* (2006) 3:279–83.
21. Royce RA, Sena A, Cates W Jr, Cohen MS. Sexual transmission of HIV. *N Engl J Med* (1997) 336:1072–8. doi:10.1056/NEJM199704103361507
22. Masurier C, Salomon B, Guettari N, Pioche C, Lachapelle F, Guigon M, et al. Dendritic cells route human immunodeficiency virus to lymph nodes after vaginal or intravenous administration to mice. *J Virol* (1998) 72:7822–9.
23. Banchereau J, Briere F, Caux C, Davoust J, Lebecque S, Liu YJ, et al. Immunobiology of dendritic cells. *Annu Rev Immunol* (2000) 18:767–811. doi:10.1146/annurev.immunol.18.1.767
24. Banchereau J, Steinman RM. Dendritic cells and the control of immunity. *Nature* (1998) 392:245–52. doi:10.1038/32588
25. Soilleux EJ, Coleman N. Expression of DC-SIGN in human foreskin may facilitate sexual transmission of HIV. *J Clin Pathol* (2004) 57:77–8. doi:10.1136/jcp.57.1.77
26. Relloso M, Puig-Kroger A, Pello OM, Rodriguez-Fernandez JL, de la Rosa G, Longo N, et al. DC-SIGN (CD209) expression is IL-4 dependent and is negatively regulated by IFN, TGF-beta, and anti-inflammatory agents. *J Immunol* (2002) 168:2634–43. doi:10.4049/jimmunol.168.6.2634
27. Jambo KC, French N, Zijlstra E, Gordon SB. AIDS patients have increased surfactant protein D but normal mannose binding lectin levels in lung fluid. *Respir Res* (2007) 8:42. doi:10.1186/1465-9921-8-42
28. Mitchell DA, Fadden AJ, Drickamer K. A novel mechanism of carbohydrate recognition by the C-type lectins DC-SIGN and DC-SIGNR. Subunit organization and binding to multivalent ligands. *J Biol Chem* (2001) 276:28939–45. doi:10.1074/jbc.M104565200
29. Mahajan L, Madan T, Kamal N, Singh VK, Sim RB, Telang SD, et al. Recombinant surfactant protein-D selectively increases apoptosis in eosinophils of allergic asthmatics and enhances uptake of apoptotic eosinophils by macrophages. *Int Immunol* (2008) 20:993–1007. doi:10.1093/intimm/dxn058

30. Dodagatta-Marri E, Qaseem AS, Karbani N, Tsolaki AG, Waters P, Madan T, et al. Purification of surfactant protein D (SP-D) from pooled amniotic fluid and bronchoalveolar lavage. *Methods Mol Biol* (2014) 1100:273–90. doi:10.1007/978-1-62703-724-2_22
31. Lang SM, Bynoe MO, Karki R, Tartell MA, Means RE. Kaposi's sarcoma-associated herpesvirus K3 and K5 proteins down regulate both DC-SIGN and DC-SIGNR. *PLoS One* (2013) 8:e58056. doi:10.1371/journal.pone.0058056
32. Hong PW, Nguyen S, Young S, Su SV, Lee B. Identification of the optimal DC-SIGN binding site on human immunodeficiency virus type 1 gp120. *J Virol* (2007) 81:8325–36. doi:10.1128/JVI.01765-06
33. Pohlmann S, Leslie GJ, Edwards TG, Macfarlan T, Reeves JD, Hiebenthal-Millow K, et al. DC-SIGN interactions with human immunodeficiency virus: virus binding and transfer are dissociable functions. *J Virol* (2001) 75:10523–6. doi:10.1128/JVI.75.21.10523-10526.2001
34. Hijazi K, Wang Y, Scala C, Jeffs S, Longstaff C, Stieh D, et al. DC-SIGN increases the affinity of HIV-1 envelope glycoprotein interaction with CD4. *PLoS One* (2011) 6:e28307. doi:10.1371/journal.pone.0028307
35. Gringhuis SI, Geijtenbeek TB. Carbohydrate signaling by C-type lectin DC-SIGN affects NF-kappaB activity. *Methods Enzymol* (2010) 480:151–64. doi:10.1016/S0076-6879(10)80008-4
36. van der Sluis RM, Jeeninga RE, Berkhout B. Establishment and molecular mechanisms of HIV-1 latency in T cells. *Curr Opin Virol* (2013) 3:700–6. doi:10.1016/j.coviro.2013.07.006
37. Sarkar R, Mitra D, Chakrabarti S. HIV-1 gp120 protein downregulates Nef induced IL-6 release in immature dendritic cells through interplay of DC-SIGN. *PLoS One* (2013) 8:e59073. doi:10.1371/journal.pone.0059073
38. Chen Y, Hwang SL, Chan VS, Chung NP, Wang SR, Li Z, et al. Binding of HIV-1 gp120 to DC-SIGN promotes ASK-1-dependent activation-induced apoptosis of human dendritic cells. *PLoS Pathog* (2013) 9:e1003100. doi:10.1371/journal.ppat.1003100
39. Lozach PY, Lortat-Jacob H, de Lacroix de Lavalette A, Staropoli I, Foung S, Amara A, et al. DC-SIGN and L-SIGN are high affinity binding receptors for hepatitis C virus glycoprotein E2. *J Biol Chem* (2003) 278:20358–66. doi:10.1074/jbc.M301284200
40. Balzarini J, Van Damme L. Microbicide drug candidates to prevent HIV infection. *Lancet* (2007) 369:787–97. doi:10.1016/S0140-6736(07)60202-5
41. Balzarini J, Van Laethem K, Daelemans D, Hatse S, Bugatti A, Rusnati M, et al. Pradimicin A, a carbohydrate-binding nonpeptidic lead compound for treatment of infections with viruses with highly glycosylated envelopes, such as human immunodeficiency virus. *J Virol* (2007) 81:362–73. doi:10.1128/JVI.01404-06
42. Hoorelbeke B, Xue J, LiWang PJ, Balzarini J. Role of the carbohydrate-binding sites of griffithsin in the prevention of DC-SIGN-mediated capture and transmission of HIV-1. *PLoS One* (2013) 8:e64132. doi:10.1371/journal.pone.0064132
43. Bashirova AA, Geijtenbeek TB, van Duijnhoven GC, van Vliet SJ, Eilering JB, Martin MP, et al. A dendritic cell-specific intercellular adhesion molecule 3-grabbing nonintegrin (DC-SIGN)-related protein is highly expressed on human liver sinusoidal endothelial cells and promotes HIV-1 infection. *J Exp Med* (2001) 193:671–8. doi:10.1084/jem.193.6.671
44. Geijtenbeek TB, van Kooyk Y. DC-SIGN: a novel HIV receptor on DCs that mediates HIV-1 transmission. *Curr Top Microbiol Immunol* (2003) 276:31–54.
45. Madan T, Kishore U, Singh M, Strong P, Clark H, Hussain EM, et al. Surfactant proteins A and D protect mice against pulmonary hypersensitivity induced by *Aspergillus fumigatus* antigens and allergens. *J Clin Invest* (2001) 107:467–75. doi:10.1172/JCI10124
46. Madan T, Kaur S, Saxena S, Singh M, Kishore U, Thiel S, et al. Role of collectins in innate immunity against aspergillosis. *Med Mycol* (2005) 43(Suppl 1): S155–63. doi:10.1080/13693780500088408
47. Singh M, Madan T, Waters P, Parida SK, Sarma PU, Kishore U. Protective effects of a recombinant fragment of human surfactant protein D in a murine model of pulmonary hypersensitivity induced by dust mite allergens. *Immunol Lett* (2003) 86:299–307. doi:10.1016/S0165-2478(03)00033-6
48. Mahajan L, Gautam P, Dodagatta-Marri E, Madan T, Kishore U. Surfactant protein SP-D modulates activity of immune cells: proteomic profiling of its interaction with eosinophilic cells. *Expert Rev Proteomics* (2014) 11:355–69. doi:10.1586/14789450.2014.897612
49. Pandit H, Thakur G, Koippallil Gopalakrishnan AR, Dodagatta-Marri E, Patil A, Kishore U, et al. Surfactant protein D induces immune quiescence and apoptosis of mitogen-activated peripheral blood mononuclear cells. *Immunobiology* (2016) 221:310–22. doi:10.1016/j.imbio.2015.10.004
50. Spear GT, Zariffard MR, Xin J, Saifuddin M. Inhibition of DC-SIGN-mediated trans infection of T cells by mannose-binding lectin. *Immunology* (2003) 110:80–5. doi:10.1046/j.1365-2567.2003.01707.x
51. Gaiha GD, Dong T, Palaniyar N, Mitchell DA, Reid KB, Clark HW. Surfactant protein A binds to HIV and inhibits direct infection of CD4+ cells, but enhances dendritic cell-mediated viral transfer. *J Immunol* (2008) 181:601–9. doi:10.4049/jimmunol.181.1.601

Conflict of Interest Statement: The authors declare that the research was conducted in the absence of any commercial or financial relationships that could be construed as a potential conflict of interest.

frontiers in Immunology

ORIGINAL RESEARCH
published: 28 March 2019
doi: 10.3389/fimmu.2019.00264

Surfactant Protein D Reverses the Gene Signature of Transepithelial HIV-1 Passage and Restricts the Viral Transfer Across the Vaginal Barrier

Hrishikesh Pandit[1,2], Kavita Kale[1], Hidemi Yamamoto[2], Gargi Thakur[1], Sushama Rokade[1], Payal Chakraborty[3], Madavan Vasudevan[3], Uday Kishore[4], Taruna Madan[1] and Raina Nakova Fichorova[2]**

[1] Department of Innate Immunity, ICMR National Institute for Research in Reproductive Health, Mumbai, India, [2] Laboratory of Genital Tract Biology, Harvard Medical School and Brigham and Women's Hospital, Boston, MA, United States, [3] Genome Informatics Research Group, Bionivid Technology Pvt. Ltd., Bengaluru, India, [4] Biosciences, College of Health and Life Sciences, Brunel University London, Uxbridge, United Kingdom

OPEN ACCESS

Edited by:
Robert Braidwood Sim,
University of Oxford, United Kingdom

Reviewed by:
Kenneth Reid,
University of Oxford, United Kingdom
Vishukumar Aimanianda,
Institut Pasteur, France

***Correspondence:**
Taruna Madan
taruna_m@hotmail.com
Raina Nakova Fichorova
rfichorova@rics.bwh.harvard.edu

Specialty section:
This article was submitted to Molecular Innate Immunity, a section of the journal Frontiers in Immunology

Received: 13 November 2018
Accepted: 31 January 2019
Published: 28 March 2019

Citation:
Pandit H, Kale K, Yamamoto H, Thakur G, Rokade S, Chakraborty P, Vasudevan M, Kishore U, Madan T and Fichorova RN (2019) Surfactant Protein D Reverses the Gene Signature of Transepithelial HIV-1 Passage and Restricts the Viral Transfer Across the Vaginal Barrier. Front. Immunol. 10:264. doi: 10.3389/fimmu.2019.00264

Effective prophylactic strategy against the current epidemic of sexually transmitted HIV-1 infection requires understanding of the innate gatekeeping mechanisms at the genital mucosa. Surfactant protein D (SP-D), a member of the collectin family of proteins naturally present in the vaginal tract, is a potential HIV-1 entry inhibitor at the cellular level. Human EpiVaginal tissues compartmentalized in culture inserts were apically exposed to HIV-1 and/or a recombinant fragment of human SP-D (rfhSP-D) and viral passage was assessed in the basal chamber containing mononuclear leukocytes. To map the gene signature facilitating or resisting the transepithelial viral transfer, microarray analysis of the HIV-1 challenged EpiVaginal tissues was performed in the absence or presence of rfhSP-D. Mucosal biocompatibility of rfhSP-D was assessed *ex vivo* and in the standard rabbit vaginal irritation model. The passage of virus through the EpiVaginal tissues toward the underlying target cells was associated with a global epithelial gene signature including differential regulation of genes primarily involved in inflammation, tight junctions and cytoskeletal framework. RfhSP-D significantly inhibited HIV-1 transfer across the vaginal tissues and was associated with a significant reversal of virus induced epithelial gene signature. Pro-inflammatory NF-κB and mTOR transcripts were significantly downregulated, while expression of the tight junctions and cytoskeletal genes was upheld. In the absence of virus, rfhSP-D directly interacted with the EpiVaginal tissues and upregulated expression of genes related to structural stability of the cell and epithelial integrity. There was no increment in the viral acquisition by the PBMCs present in basal chambers wherein, the EpiVaginal tissues in apical chambers were treated with rfhSP-D. The effective concentrations of rfhSP-D had no effect on *lactobacilli,* epithelial barrier integrity and were safe on repeated applications onto the rabbit vaginal mucosa. This pre-clinical safety data, coupled with its efficacy of restricting viral passage via reversal of virus-induced gene expression of the vaginal barrier, make a strong argument for clinical trials of rfhSP-D as a topical anti-HIV microbicide.

Keywords: surfactant protein D, HIV-1, vaginal, microarray, chemokines, microbicide

INTRODUCTION

A clear majority of the HIV-1 infections are due to heterosexual contact; more than 50% of HIV-1 infected individuals are women and most children living with HIV-1 today are infected via mother-to-child transmission (1). Thus, an effective vaginal microbicide for the prevention of sexual transmission of HIV-1 to women will have a huge impact on limiting the HIV epidemic and its devastating consequences for both adults and children. Despite this well-perceived need of intervention and the efforts made to date in understanding the vaginal mucosal barrier (2–4), the development of a safe and effective topical vaginal microbicide has several technical challenges (5–7). Clinical trials involving most of the promising candidates showed reduced efficacy as they adversely affected the vaginal milieu (7). Evaluation of microbicides *in vivo* using SIV-macaque and humanized mouse models comes at a high cost and the findings may only be an extrapolation to HIV-1 transmission in humans (7). A serious limitation is lack of an appropriate *ex vivo* model for the evaluation of efficacy of potential compounds on the viral passage across the vaginal barrier to the target immune cells (8–11). The *ex vivo* model should also assess compatibility of the candidate molecules with the mucosal integrity and barrier function including the colonization with healthy vaginal microbiome.

Of special interest for pharmaceutical development are candidate microbicides that would regulate vaginal innate immune responses with minimal adverse effects on the physiology (12, 13). Collectins are a group of secreted, anti-microbial pattern recognition proteins in the female reproductive tract (14–17). Surfactant Protein D (SP-D) is one such collectin expressed by the epithelium, lining the vaginal tract (18). Previously, we have demonstrated that a recombinant fragment of human SP-D (rfhSP-D) containing homotrimeric neck and C-type lectin domains binds to HIV-1 envelope glycoprotein gp120, and inhibits viral entry and replication in target immune cells (19). Beyond its pattern recognition capability, SP-D interacts with various immune cells, maintains Th1/Th2 balance in the lungs and induces immune quiescence (20, 21). By virtue of its natural presence in the vaginal tract, broad anti-microbial activity and immune-regulatory functions, SP-D is a unique microbicide candidate. Importantly, anti-HIV-1 activity of rfhSP-D was intact in physiological fluids like vaginal lavage and seminal plasma which comprise of diverse enzymes, pH and inhibitors (19).

In this study, we assessed the effect of rfhSP-D on the interactions of vaginal epithelial tissues and HIV-1 using a rational scheme for *ex vivo* microbicide testing. The scheme is designed to resemble sexual transmission of the virus and comprises of bioengineered vaginal tissues, immune cells and clinical isolates of *Lactobacillus*. In our model, HIV-1 traverses through the intact, multi-layered vaginal epithelium toward the underlying mononuclear leukocytes. We report, for the first time, a "gatekeeping" gene signature of bioengineered human tissues induced upon HIV-1 exposure. In this model, rfhSP-D showed no adverse effects on the vaginal barrier, concomitant with a significant impediment of viral movement to the activated PBMCs in the basal compartment. Epithelial transcriptome revealed reversal of HIV-1 induced differential expression of genes associated with the cytoskeleton, inflammation and barrier integrity. A range of preclinical assays confirmed safety of rfhSP-D for vaginal application at the similar concentrations it restricted viral transfer *ex vivo*, and thus, establishing it as a promising anti-HIV-1 vaginal microbicide.

MATERIALS AND METHODS

Human Cell Lines

Well-characterized and immortalized human vaginal (Vk2/E6E7, ATCC® CRL-2616™), endocervical (End1/E6E7, ATCC® CRL-2615™), and ectocervical (Ect1/E6E7, ATCC® CRL-2614™) cell lines developed by Dr. Raina Fichorova (22), were cultured in antibiotic-free keratinocyte serum-free medium (KSFM), supplemented with 50 μg/ml bovine pituitary extract, 0.1 ng/ml epidermal growth factor (Gibco, Invitrogen, USA), and 0.4 mM $CaCl_2$ (Fisher Scientific, USA). These cell lines are known to retain their physiological characteristics and are useful models for various female reproductive tract infections, including HIV-1 (22–26).

Vaginal Bioengineered Tissue (EpiVaginal Tissue)

Twenty four EpiVaginal™ (VEC-100™) tissues and medium were purchased from MatTek (Ashland, MA, USA). These tissues are derived from primary human ectocervical/vaginal epithelial cells, and possess characteristics comparable to that of the normal tissues of origin (26, 27).

Clinical *Lactobacillus* Isolates

Lactobacillus crispatus isolates were obtained from vaginal swab samples of healthy women participating in a vaginal microflora research study at the Brigham and Women's Hospital (Boston, MA, USA) (6). *Lactobacillus fermentum spps mucosae* (TRF#36), *Lactobacillus gasseri* (TRF#8), and *Lactobacillus salivarius* (TRF#30) were a kind gift from Prof. GP Talwar, the Talwar Research Foundation (New Delhi, India) (28).

Preparation of rfhSP-D

A recombinant fragment of human SP-D (rfhSP-D), composed of trimeric neck and lectin domains along with 8 Gly-X-Y repeats, was expressed in *E. coli*, purified and characterized, as described previously (19, 29, 30). The endotoxin level in the rfhSP-D preparations was determined using the QCL-1000 *Limulus amebocyte* lysate system (BioWhittaker Inc., USA). The endotoxin concentration in the various preparations ranged between 2.8 and 5.1 pg/μg of rfhSP-D. Controls of various experiments were spiked by adding equivalent amounts of LPS (Sigma-Aldrich, USA).

Assessment of the Expression of SP-D in Human Vaginal Cells (VK2/E6E7) and Cervicovaginal Lavage (CVL)

To assess the presence of SP-D in CVL, total protein was precipitated using chilled acetone; 25 μg total protein was loaded per well and subjected to 12% SDS-PAGE under

reducing conditions and then electrophoretically transferred to a nitrocellulose membrane for immuno-blotting. Mouse monoclonal anti-human SP-D antibody (Abcam, UK) was used at a dilution of 1:500, whereas, rabbit polyclonal anti-mouse secondary antibody conjugated to horseradish peroxidase (HRP) was used at a dilution of 1:1,000 (Dako). Detection was done using chemiluminescent detection kit (Amersham Biosciences, Piscataway, NJ). For immunostaining, Vk2/E6E7 cells were grown on cover slips, probed with the mouse monoclonal anti-human SP-D antibody (Abcam) and further detected with anti-mouse Phycoerythrin-conjugates (Molecular Probes). Nuclei were counterstained with 4′,6-Diamidine-2′-phenylindole dihydrochloride (DAPI) (Sigma-Aldrich), the coverslips were mounted in Vectashield (Vector Laboratories) and visualized under a confocal microscope (Zeiss, Germany). To determine transcript levels of SP-D, total RNA was extracted using Trizol (Invitrogen) from Vk2/E6E7 cells; 3 μg of total RNA was reverse transcribed into cDNA using Superscript III first strand synthesis kit (Invitrogen) and subjected to PCR (Veriti Machine, Applied Biosystems). Primers for SP-D, SP-A2, and 18S were designed using NCBI Primer BLAST Software (**Supplementary Table 1**). The resultant PCR products were electrophoresed on a 2% agarose gel at 100V on electrophoresis. The bands were detected via ethidium bromide under UV light.

Ex vivo Model of Vaginal HIV-1 Transmission

In order to mimic vaginal transmission of HIV-1, a novel *ex vivo* model was developed using EpiVaginal tissues (**Figure 1A**). Upon delivery, EpiVaginal tissues were acclimatized in the medium overnight. Blood (from non-autologous donors) was subjected to Ficoll separation and PBMCs were isolated. PBMCs were activated for 48 h using rhIL-2 (100 U/ml) (Sigma-Aldrich) and PHA (5 μg/ml) in the RPMI 1640 medium (Fisher Scientific) containing 10% FBS and 0.5% antibiotic solution (Gibco, Invitrogen). Activated PBMCs (10^5) were seeded in a 12-well plate as target cells for further replication of migrated virions. In a fresh tissue culture plate, inserts containing EpiVaginal tissues were placed in each well. In our previous study, we have reported the anti-HIV activity of purified native human SP-D, rfhSP-D and another variant of recombinant fragment of SP-D, lacking eight triplets of collagen repeats (delta-rfhSP-D) (19). Although delta-rfhSP-D showed anti-HIV activity in the TZMbl reporter assays (IC_{50} 43.282 ± 10.76 μg/ml), it was 3-fold less potent than the native human SP-D and rfhSP-D (IC_{50} of rfhSP-D with various viral isolates and target cell types ranged between 6.726 ± 0.63 and 13.676 ± 3.37 μg/ml) (19). In another assay (as described in the section "Viability MTT assay"), we evaluated the effect of various concentrations of rfhSP-D (1.562–100 μg/ml) on the viability of vaginal epithelial cells and used the maximal tolerated dose of rfhSP-D (100 μg/ml) in the *ex vivo* model. The physiological concentration of free SP-D in various body fluids ranges from 0.5 to ∼3 μg/ml (31, 32). In view of the ability of SP-D to bind several molecules, such as immunoglobulins, fatty acids and nucleic acids, its total physiological concentration is expected to be much higher (33–35). Apical tissues were treated with rfhSP-D (100 μg/ml) or a synthetic analog of *Mycoplasma fermentans* lipopeptide macrophage activating lipopeptide 2 (MALP-2) (Alexis Biochemicals, USA) (25 nM) for 20 min before inoculation with 100 $TCID_{50}$ R5 tropic HIV-1_{JR-CSF}. After 24 h incubation, apical and basal supernatants were collected for determining levels of immune mediators. Basal supernatants were used to determine HIV-1 p24 Ag by ELISA, as per manufacturer's instructions (R&D Systems).

Microarray Gene Expression Analysis

The microarray data, described in this study, has been deposited in the NCBI Gene Expression Omnibus (GEO) under the GEO series accession number GSE107478.

RNA Isolation

Total RNA was extracted using TRIZOLVR Reagent (Invitrogen); RNA quantity and quality were determined using NanodropVR spectrophotometer (NanoDrop Technologies, Wilmington, DE). Targets were prepared using the Illumina RNA amplification kit (Ambion, Austin, TX). cRNA was synthesized from 200 ng of the total RNA followed by amplification and labeling steps. Amplified biotin-labeled cRNA was hybridized to the Illumina Human HT12 V6 bead chip. Illumina Bead Studio was used to extract the raw data from the bead chip. Raw data was Quantile normalized and baseline transformation was carried out to obtain median of all samples using GeneSpring GX 12.5 software (Agilent Technologies Inc, Santa Clara, USA).

Statistical Analysis and Differentially Expressed Genes

Differentially expressed probe sets (genes) in the treated cells in comparison to the untreated cells were identified by applying Volcano Plot using a fold-change threshold (absolute fold-change >1.5). A statistically significant "*t*-test" "*P*-value" threshold was adjusted for false discovery rate of <0.001. Statistically significantly enriched transcripts with a "*P*-value" adjusted for false discovery rate of <0.05, based on the hyper-geometric distribution test corresponding to differentially expressed genes, were determined using the Student's "*t*-test" along with Benjamini Hocheberg FDR test. Unsupervised hierarchical clustering of the differentially expressed genes following treatment in comparison to the untreated cells was performed using Euclidian algorithm with Centroid linkage rule to identify gene clusters whose expression levels were significantly reproduced across the replicates.

Biological Pathways and Gene Ontology Enrichment Analysis

Differentially expressed gene list was subjected to a biological significance analysis by GOElite tool. A total of 21,887 protein coding genes were used as the background and the differentially expressed gene list was used as query. Database of GeneOntology categories, Wikipathways, KEGG Pathways, Pathway Commons, Pheno Ontology, Diseases, Protein Domains, Transcription factor targets, and tissue expression were configured for significance analysis. Each query list was subjected to the "Over-representation Analysis" against each of the above databases.

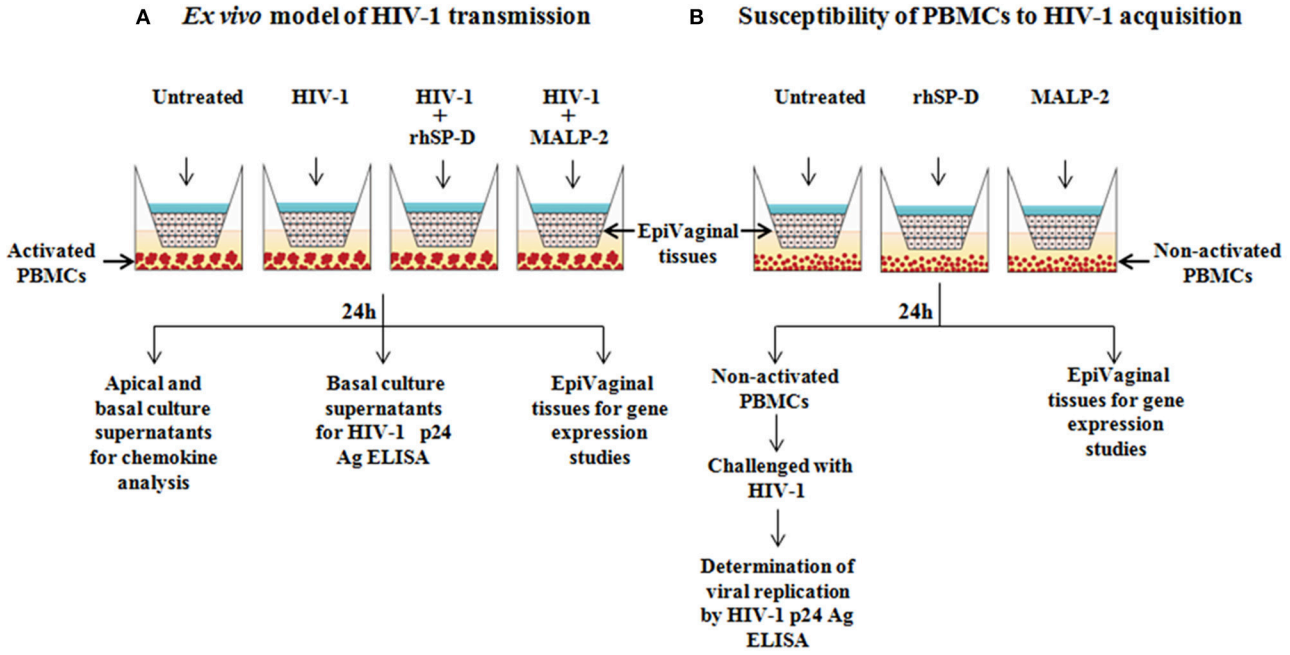

FIGURE 1 | Experimental designs. **(A)** *Ex vivo* model for vaginal transmission of HIV-1. Reconstructed, multi-layered EpiVaginal tissues placed in the cell culture inserts were challenged with HIV-1 in the apical chamber for 24 h. The activated PBMCs placed in the basal chamber served as HIV-1 targets when HIV-1 traversed through the EpiVaginal tissues. Twenty minutes prior to the HIV-1 challenge, the EpiVaginal tissues were either treated with rfhSP-D (HIV-1 entry inhibitor) or MALP-2 (inflammatory TLR agonist). **(B)** *Ex vivo* model to predict susceptibility of basal PBMCs to HIV-1 acquisition. Reconstructed, multi-layered EpiVaginal tissues placed in the cell culture inserts were either treated with rfhSP-D (HIV-1 entry inhibitor) or MALP-2 (inflammatory TLR agonist). The non-activated PBMCs were placed in the basal chamber to determine if the rfhSP-D and MALP-2 treatment of the vaginal tissue may lead to secretion of certain mediators resulting in the activation of PBMCs. These treated PBMCs from the basal chamber were subsequently challenged with HIV-1 to evaluate their susceptibility to virus acquisition.

Z score and permutation or Fisher's Exact Test *p*-value were calculated to assess over-representation of the enriched biological categories.

Biological Analysis Network Modeling of Differential Regulome

Enriched biological categories, along with the differentially expressed genes, were used as input for BridgeIsland Software (Bionivid, Bangalore, India) for identifying the key edges that connect genes with biological categories. Statistical scores from differential expression and biological analysis were used as attributes to visualize the network. Output of BridgeIsland Software was used as input to CytoScape V 2.8. Circular layout and yFiles algorithm were used to visualize the network that encompasses biological categories. Further to this core network, all the differentially expressed genes were colored based on their fold change to reflect the rfhSP-D treatment induced differential regulome.

Validation by Real Time RT-PCR

Since, EpiVaginal tissues (of ectocervical origin) used in the assays were sufficient enough for microarray analysis, we carried out the validation of microarray data using an ectocervical cell line (Ect1/E6E7) under conditions similar to the *ex vivo* model of HIV-1 transmission (same MOI). Cells were seeded in a 96-well plate, grown up to confluence and then treated with rfhSP-D (100 μg/ml) for 20 min, before inoculation with 100 $TCID_{50}$ R5 tropic HIV-1_{JR-CSF} at 37°C for 24 h. Total RNA was isolated using Trizol (Invitrogen) and the quality of RNA was assessed by nano-spectrophotometry and the nucleotide: protein ratio (260:280) was determined. 1–3 μg of RNA was reverse transcribed into cDNA using Superscript III first strand synthesis kit (Invitrogen). The resulting cDNA was used for real time PCR via the Bio-Rad CFX96 TouchTM real-time PCR detection system using the iQTM SYBR Green Supermix (Bio-Rad, USA). 18s RNA was used as the housekeeping control. Primers were designed using NCBI Primer BLAST Software. Primer sequences and conditions are provided in the **Supplementary Table 1**.

mRNA Levels of Tight Junction Proteins in EpiVaginal Tissues After HIV-1 Challenge

In order to determine the status of the vaginal barrier after the viral challenge, transcripts from EpiVaginal tissues for the tight junction proteins viz. Claudin 2, 3, 4, 5, and occludin were quantified using real time qPCR. Owing to the limited EpiVaginal tissue, the qPCR analysis was not extended to quantitation of protein levels. Primers sequences were synthesized (Sigma-Aldrich) as reported previously (36). Primer sequences and conditions are provided in the **Supplementary Table 1**.

Susceptibility of PBMCs to HIV-1 Acquisition

HIV-1 is known to replicate faster in the activated human PBMCs (37). We have shown previously that rfhSP-D rfhSP-D does not alter the activation alter the activation of PBMCs and leads to induction of quiescence in the activated PBMCs (21). The present assay was designed to specifically determine the impact of supernatants from rfhSP-D treated EpiVaginal tissues on the activation status and viral acquisition of PBMCs. Non-activated PBMCs (10^5) were seeded in a 12-well plate and apical regions of the culture inserts containing EpiVaginal tissues were treated with rfhSP-D (100 μg/ml), MALP-2 (25 nM), or left untreated for 24 h. Following incubation, basal PBMCs were collected and challenged with 100 $TCID_{50}$ HIV-1_{JR-CSF} for 4 h to assess the rate of HIV-1 acquisition (**Figure 1B**). PBMCs were washed and cultured further in RPMI 1640 medium containing 10% FBS and 1% antibiotic solution for 7 days, and HIV-1 p24 levels in culture supernatants were measured. Viability of PBMCs was evaluated at the end of the assay (data not shown).

MTT Viability Assay

To assess the likely effect of rfhSP-D on cell viability, MTT assay was performed on Vk2/E6E7 and Ect1/E6E7 cell monolayers. Cells were seeded in a 96-well plate, grown up to confluence and then treated with a range of rfhSP-D concentrations at 37°C for 24 h. Culture supernatants were then collected for measuring immune mediators. Cells were treated with 1 × MTT containing KSFM and incubated overnight; 0.04 N acidified isopropanol was added to the cells to dissolve the formazan crystals. This color intensity, read at OD_{570}, is directly proportional to the number of viable cells, as measured by a Victor2 counter with Wallac 2.01 software (PerkinElmer Life Sciences, USA) using a reference wavelength at 630 nm. The OD of untreated (medium alone) control cells was considered as 100%; percent viability of rfhSP-D treated cells was calculated as compared to untreated control.

NF-κB Luciferase Assay

End1/E6E7 immortalized epithelial cells were transfected with pHTS–NF-κB firefly luciferase reporter vector (Biomyx Technology, USA) using a gene-juice transfection protocol (38). Cells were seeded in a 96-well plate, grown until confluent monolayers and treated with indicated concentrations of rfhSP-D for 24 h at 37°C. A synthetic analog of viral double-stranded RNA, Poly (I:C) (10 μg/ml) (InvivoGen, USA), a TLR3 agonist, and MALP-2 (25 nM), a TLR2/6 agonist, were used as positive controls. After incubation, the supernatant was removed, cells were lysed in GloLysis buffer, and activation of luciferase was determined using a Bright-Glo luciferase assay system (Promega, USA). Luminescence signal was quantified via a Victor2 1420 multi-label microplate counter with Wallac 2.01 software (PerkinElmer Life Sciences).

Assay for Toxicity to *Lactobacillus*

Direct toxicity assay on vaginal lactobacilli was performed using a colorimetric assay as described previously (39). TRF#8, TRF#30, TRF#36, and *Lactobacillus crispatus* LC223 were grown in the *Lactobacillus* MRS Broth (HiMedia™ Laboratories). Bacterial density was adjusted to an OD_{670} of 0.06, corresponding to a 0.5 McFarlands turbidity standard or ca. 10^8 CFU/ml. RfhSP-D was plated at the appropriate concentrations into a 96-well round bottom plates in a volume of 100 μl, and the diluted *Lactobacillus spps* were added in a volume of 100 μl. Commercially available penicillin-streptomycin solution (Gibco, Invitrogen) at a maximal test concentration of 1.25 U/ml and 1.25 μg/ml respectively) was used as a positive control for toxicity. Plates were incubated in an orbital shaker at 35°C under anaerobic conditions using AnaeroPack system (PML Microbiologicals, Wilsonville, OR) for 24 h. Bacterial growth was determined by measurement of the OD_{490} using a Victor2 counter with Wallac 2.01 software (PerkinElmer Life Sciences) (40).

Lactobacilli-Epithelial Colonization Assay

Colonization of epithelial cells by lactobacilli in presence of rfhSP-D was assayed as described earlier (6). Briefly, the *Lactobacillus crispatus* isolate, suspended in antibiotic-free KSFM (2.2×10^6 CFU/cm^2), was added to confluent epithelial surfaces Vk2/E6E7 and End1/NF-κB cells (10:1 ratio) and allowed to adhere on the epithelial monolayer; unbound bacteria were washed off by two washes of sterile Dulbecco's phosphate-buffered saline (PBS) (Invitrogen). To the bacteria-epithelial cell co-culture, indicated concentrations of rfhSP-D, Poly (I:C) or MALP-2 was added to each well. Supernatants were collected after 24 h to measure immune mediators. Vk2/E6E7 epithelial cells were washed twice with sterile PBS and examined for viability by MTT (data not shown) and colony forming unit (CFU) assays. End1/NF-κB co-culture plate was used to evaluate NF-κB activation.

Colony Forming Units (CFU) Counts

Viable bacteria associated with Vk2/E6E7 monolayers were measured by CFU counts after 24 h of epithelial colonization followed by 24 h exposure to rfhSP-D (6). To enumerate cell-associated bacteria, epithelial cells were washed with cold PBS and hypotonically lysed in ice-cold HyPure water for 15 min, followed by adjustment of osmolality with PBS (2X) (Fisher Scientific). Bacteria collected were plated on Brucella anaerobic agar with 5% sheep blood (Becton, Dickinson and Company, USA) as per the standardized protocol, and incubated in an anaerobic chamber (Coy Laboratory Products, USA) (10% hydrogen, 10% carbon dioxide, and 80% nitrogen) at 35°C for up to 72 h (until colonies were formed), followed by visual counting of CFU.

Quantitation of Immune Mediators

Culture supernatants from the EpiVaginal tissues (apical), PBMCs (basal) and Vk2/E6E7 (with or without bacterial co-culture) were collected separately from various experiments. A custom designed 3-plex assay for GRO-α (CXCL1), MIP-3α (CCL20), and RANTES (CCL5) was used via Multiplex Electro-chemiluminescence (Meso Scale Discovery, USA) as per manufacturer's instructions.

Rabbit Vaginal Irritation (RVI) Model

Treatment

Young adult reproductive age nulliparous Belgium white rabbits (5–8 months old, body weight 2.2 kg ± 20%) ($n = 5$ per group)

were divided into rfhSP-D, placebo and SDS (positive control) groups. The aqueous gel formulation was prepared by dissolving methyl paraben 0.18% (w/v) and propyl paraben 0.02% (w/v) in heated glycerin 8.6% (v/v). Hydroxyethyl cellulose 2.5% (w/v) was added and dispersed to form an organic phase. Citric acid 1.0% (w/v) was dissolved in purified water alone or aqueous solutions of rfhSP-D (100 μg/ml) or 1% SDS. The pH was adjusted to 4.4, and the solution was clarified by passage through a 0.22 μm filter. Aqueous and organic phases were mixed and stirred well before use. Various gel formulations (1 ml) were administered intra-vaginally to their respective groups using an insulin syringe (without a needle) daily for 10 consecutive days. Necropsy was done on day 11 following euthanasia. The vaginal tissues were collected in formalin and processed for making paraffin blocks. 5μ ribbon of paraffin bearing sections were made using a microtome and collected on poly-L-lysine-coated glass slides.

RVI Scoring

RVI scoring of hematoxylin-eosin stained tissue slides was blinded. Briefly, the tissues were scored from 0 to 4 for epithelial damage (0 = normal, 1 = flattening, 2 = metaplasia, 3 = erosion, and 4 = ulceration) and leukocyte infiltration, edema and congestion (0 = absent, 1 = minimal, 3 = moderate, 4 = marked). At least three sections of vaginal tissues (both proximal and distal) of each animal were assessed for each of the above four parameters. Total score of each animal was calculated and was averaged with number of sections analyzed. Standard RVI method suggests that a total score from 1 to 4 is to be considered as minimal irritation, 5–8 as mild irritation, 9–11 as moderate irritation and 12–13 as marked irritation (41).

Statistical Analysis

Student *t*-test, One-way analysis of variance (ANOVA; Bonferroni or Dunnett's multiple-comparison analyses) was performed using GraphPad Prism version 6.00 for Windows (GraphPad Software, San Diego, CA). *p*-value of <0.05 was considered significant.

RESULTS

Global Gene Signature of HIV-1 Challenged EpiVaginal Tissues: Clues to Early Events During Vaginal Transmission

Figure 1 depicts the experimental design used in the study to map the transcriptome of EpiVaginal tissues under different conditions. We report here, for the first time, a compendium of genes that were differentially expressed in EpiVaginal tissues when challenged with HIV-1 alone (355), HIV-1 in presence of rfhSP-D (518), or rfhSP-D alone (185) (**Supplementary Figures S1, S2, S4**). For the identification of differentially expressed genes, data was subjected to unsupervised hierarchical clustering using Pearson Uncentered algorithm with average linkage rule using Cluster 3.0 software. The resultant cluster was visualized using Tree View software. It revealed distinct patterns of upregulated and downregulated genes following treatments and indicated significant reproducibility within the replicates (**Supplementary Figures S1, S2, S4**). The microarray data was validated by evaluation of transcript expression by real time RT-PCR for six randomly selected, differentially expressed genes by HIV-1 and rfhSP-D to represent the three functional categories (**Figures 2B**, **4D**). Gene regulatory network analysis of the three interactions revealed involvement of several biological processes and pathways. Differentially expressed genes, along with the pathways, were subjected to regulatory network modeling, that resulting in the identification of key genes that act as bridges (involved in more than one process) and islands (which are specific to a process) (**Figures 2A, 4B,C, 6B**; **Supplementary Figure S3**). We have focused on three important processes involved in HIV-1 transmission, which are cell-cell interaction and barrier integrity, innate immune response, and cell survival. The networks were refined further to comprise the most relevant genes (**Figures 4B,C, 6B**).

The gene signature of EpiVaginal tissues post 24 h HIV-1 exposure showed 187 upregulated and 168 downregulated genes (**Supplementary Figure S1**), associated with biological processes, such as cell integrity, inflammation and innate immune response, pyroptosis, cell survival, cell signaling and cytoskeleton (**Figure 2A**). Microarray results were validated by real time RT-PCR for PYCARD, CD44, XRCC2, SERPINE1, STX3, and CREB1 (**Figure 2B**). PYCARD, CD44, and SERPINE1 were among the prominent genes downregulated by HIV-1 but upregulated by rfhSP-D and XRCC2; STX3 and CREB1 were among the prominent genes upregulated by HIV-1 but downregulated by rfhSP-D.

HIV-1 induces a cytokine/chemokine storm at the mucosal sites (42) that facilitates the viral entry and transmission. HIV-1 challenged EpiVaginal tissues showed an upregulation of transcripts of cytokines and chemokines, such as IL-32, CCL20, and CXCL9. Transcripts of other pro-inflammatory genes, such as MYD88, ADAM17, TNFSF14, IL-1R2, HLA-F, CD58, PKN2, and STX3 were also upregulated. A significant upregulation of PSMB10, executioner caspases CASP7 and CASP1 of the inflammasome is suggestive of pyroptosis. However, a few inflammation-related genes MMP9, MUC-1, SERPINE1, TGF-α, TMEM173 were downregulated.

Interestingly, a group of interferon-inducible guanylate-binding proteins (GBP1, GBP2, and GBP5) were upregulated, suggesting that the vaginal epithelium attempts to mount an anti-viral response. TRIM21, another interferon-inducible gene, was also found to be upregulated along with the interferon-inducible transcription factors, such as IRF1, ATF3, BATF2, and CREB1.

A likely breach in the vaginal barrier after HIV-1 exposure is evident by alterations in several genes encoding for proteins of plasma membrane, cytoskeletal framework and gap junction. Actin cytoskeleton rearrangement (CNN3), integral plasma membrane proteins (CAV-1, STX6), microtubules and cytoplasmic dynactin binding (DCTN1), extracellular matrix glycoprotein (LAMB1), cell-cell recognition and signaling molecules (MSN, CD44) were all downregulated. Gap junction proteins, GJA1 and GJB6, were also downregulated. TFF2, which protects the mucosa from injury or insults, stabilizes the mucus layer and aids healing of the epithelium, was

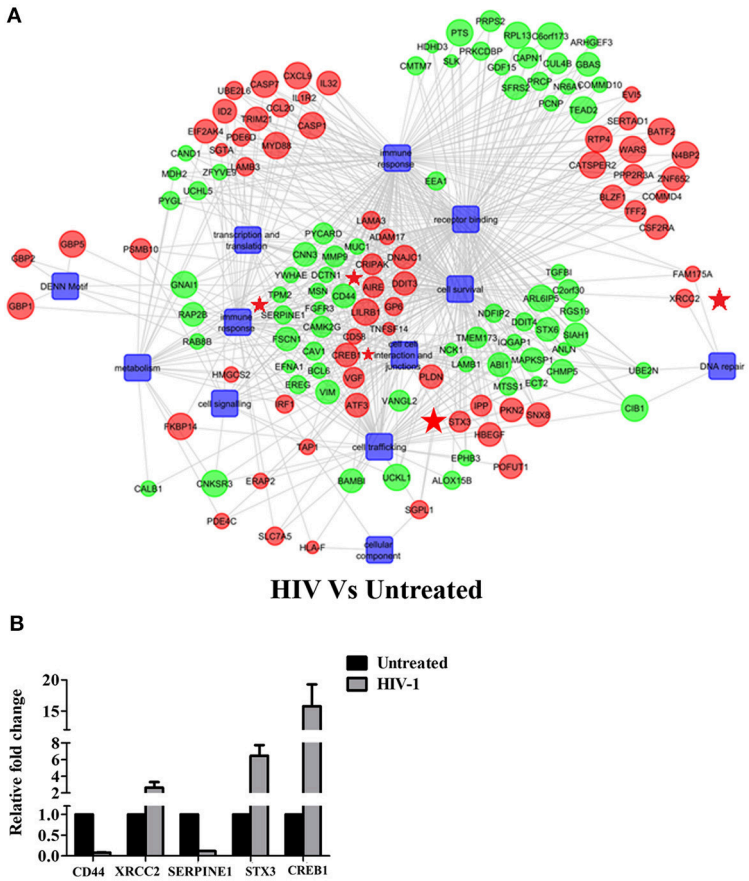

FIGURE 2 | HIV-1 induced global gene signature of EpiVaginal tissues: **(A)** Gene regulatory network of differentially expressed genes and pathways by the EpiVaginal tissues treated with HIV-1 vs. Untreated EpiVaginal Control tissues. Biological processes are blue colored blocks downregulated genes are green colored, and upregulated are in red. Circles are sized according to their *p*-value. Genes that were used for validation (CD44, XRCC2, SERPINE1, STX3, CREB1) have been highlighted with a red star in their vicinity. **(B)** Validation of microarray data by real time qPCR. Ect/E6E7 cells were subjected to identical conditions and treatments as for EpiVaginal tissues. RNA was isolated and cDNA was subjected to real time qPCR. Data represents mean ± S. D of three independent experiments. Fold change in expression of the 5 genes for validation were statistically significant ($p < 0.05$) relative to untreated Ect/E6E7 cells.

upregulated, suggesting a plausible feedback in response to the damaged epithelium.

To corroborate the HIV-1 induced inflammation in the *ex vivo* model, we evaluated the levels of chemokines, such as RANTES, MIP-3α, and GRO-α in the apical (EpiVaginal) and basal (PBMCs) supernatants. A significant rise in RANTES and GRO-α but not in MIP-3α levels was observed in the supernatants of basal chambers of the EpiVaginal tissues upon HIV-1 challenge. MALP-2, a TLR2/6 agonist, induced all the three chemokines, indicating excessive inflammation (**Figure 3**), which is reminiscent of enhanced HIV-1 acquisition during RTI/STIs.

HIV-1 Traverses Through EpiVaginal Tissue and rfhSP-D Impedes This Movement

The *ex vivo* model (**Figure 1A**). Mimics several aspects of vaginal transmission of HIV-1. The reconstructed, multi-layered EpiVaginal explants in the upper chamber serve as the first line of protection. The activated PBMCs present in the lower chamber serve as targets for the viral particles that traversed through the EpiVaginal tissues. In this model, along with HIV-1, rfhSP-D or both, we also used MALP-2 as a positive control for inflammation.

At 24 h, HIV-1 p24 Ag was detected in the supernatants of basal chambers. A higher level of p24 Ag detected in the supernatants, when the vaginal tissues were challenged with HIV-1 in presence of MALP-2 (>1.6-fold higher than control; [Medium alone]), suggested that more virions migrated to the basal chamber (though could not attain statistical significance). RfhSP-D significantly reduced the viral transfer and only one-fifth (20 ± 2.6%) of the HIV-1 p24 Ag level was detected in the basal PBMCs supernatants, as compared to the HIV-1 alone (100%) (**Figure 4A**).

RfhSP-D Reverses the HIV-1-Induced Gene Signature: Decoding the Protective Response

To recognize the gene signature that illustrates inhibition of vaginal transfer of HIV-1, we analyzed transcriptome of rfhSP-D treated HIV-1 challenged EpiVaginal tissues in the

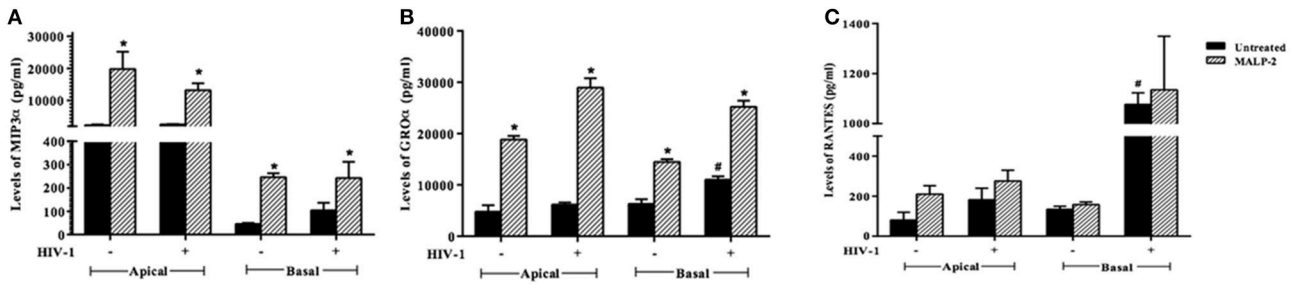

FIGURE 3 | Chemokine response of EpiVaginal tissues upon HIV-1 challenge: Levels of **(A)** MIP-3α, **(B)** GRO-α, and **(C)** RANTES in the culture supernatant of EpiVaginal tissues (apical) and PBMCs (basal) with or without HIV-1 challenge. Each bar represents the mean ± S.D in pg/ml and of triplicates. *indicates statistical significance ($p < 0.05$) relative to control (untreated) whereas # indicates statistical significance ($p < 0.05$) relative to HIV-1 challenge EpiVaginal tissues.

apical chamber (**Supplementary Figure S2**). We observed a remarkable reversal of gene expression associated with gap junction proteins, plasma membrane and cytoskeletal framework of the cell. Several genes including GJA1, GJB6, CAV1, CAV2, LAMB1, ACTN1, DBN1, and DCTN1 were upregulated upon rfhSP-D treatment, which were otherwise downregulated by HIV-1 (**Supplementary Table S2**; **Figures 4B,C**). Maintenance of vaginal barrier integrity by rfhSP-D was evident from upregulation of NECTIN1 and CD44 along with gap junction genes. Interestingly, DBN1, ACTN1, NECTIN1, and CD44 have been shown to act as anti-viral or entry inhibitors (**Table 1**). Inflammation is the primary reason for epithelium breakage and compromised vaginal barrier. RfhSP-D reversed HIV-1 induced inflammatory genes, such as ADAM17, MYD88, SMAD3, SMAD6, CD58, CCL20, TRIM21, and SMARC1. NF-κB and mTOR, the two master regulators of inflammation, were also downregulated, suggesting induction of a state of quiescence within the EpiVaginal tissues. A few anti-inflammatory genes were upregulated; IL-20, BCL-3, NME1, NME2, CHEK1, and CDKN1C. SOCS2 and SOCS3 were selectively upregulated, suggesting rfhSP-D mediated dampening of pro-inflammatory cytokine production. TGF-β pathway seems to be relevant in vaginal transfer of virus since several genes (SMAD3, SMAD6, TSC1, EID2, TGF-β-1L1, TGF-βR, and TGFA) of this pathway were altered by HIV-1 and reversed by rfhSP-D (**Table 1**; **Figures 4C,D**).

We identified some pro-inflammatory genes that were upregulated in rfhSP-D treated HIV-challenged EpiVaginal tissues, such as CD40, ILK, ESR1, EGF, FGFR2, HIPK2, SOD1, MAP3K1, IFI16, NOD2, IL-1B, HTRA1, EDNRA. Interestingly, there was a downregulation of the intrinsic SP-D gene expression that suggested a mitigation of inflammatory response of vaginal tissues in presence of rfhSP-D (**Figures 4C,D**). HIV-1 challenged EpiVaginal tissues showed an upregulation of SFTPD (gene encoding SP-D protein) transcript (**Figure 4C**) whereas, rfhSP-D pre-treatment followed by HIV-1 challenge reverted the HIV-1 induced upregulation of rfhSP-D (**Figure 4D**). rfhSP-D treatment alone did not alter the expression of native SP-D transcript (**Figure 6B**).

HIV-1 Induced Downregulation of Tight Junction Gene Expression Is Rescued by RfhSP-D

HIV-1 is known to downregulate tight junction proteins in order to traverse through the weakened vaginal barrier (36). We assessed the status of claudins and occludin in the EpiVaginal tissues. HIV-1 challenge led to a significant decrease in the transcript levels of tight junction proteins that were further downregulated when simultaneously treated with MALP-2 (**Figures 5A–E**). RfhSP-D countered the HIV-1 induced downregulation of transcripts of claudin 2, 3, 5 and occludin, except claudin 4, suggesting a reduced damage to the vaginal integrity (**Figures 5A–E**).

RfhSP-D Does Not Enhance the Susceptibility of Target Cells to HIV-1 Acquisition

Another experimental setup was designed to interrogate whether rfhSP-D, on its own, caused inflammation within EpiVaginal tissues (in the absence of HIV-1 challenge), which in turn increased susceptibility of target cells (**Figure 1B**). PBMCs in the basal chamber of rfhSP-D treated tissues showed no significant increase in the acquisition of HIV-1 while the inflammatory MALP-2 treated tissues showed increased p24 levels on day 6 (**Figure 6A**).

RfhSP-D Treatment Strengthened Vaginal Barrier: SP-D a Natural Vaginal Host Defense Molecule

Alterations in the transcripts of EpiVaginal tissues induced by rfhSP-D were also identified by microarray analysis. Of the total 185 genes differentially regulated, 103 were upregulated and 82 were downregulated (**Supplementary Figure S4**). Upregulation of CAV1 and CAV2, along with Laminins (LAMA3, LAMB1, LAMC1, and LAMC2), which are essential for formation and function of the basement membrane, was suggestive of a strengthened mucosal barrier. Collagen transcripts (COL4A5, COL5A1, COL5A2 and COL7A1, COL17A1), important structural components of basement membranes, were also upregulated. With an integral role in adhesion of the epithelium

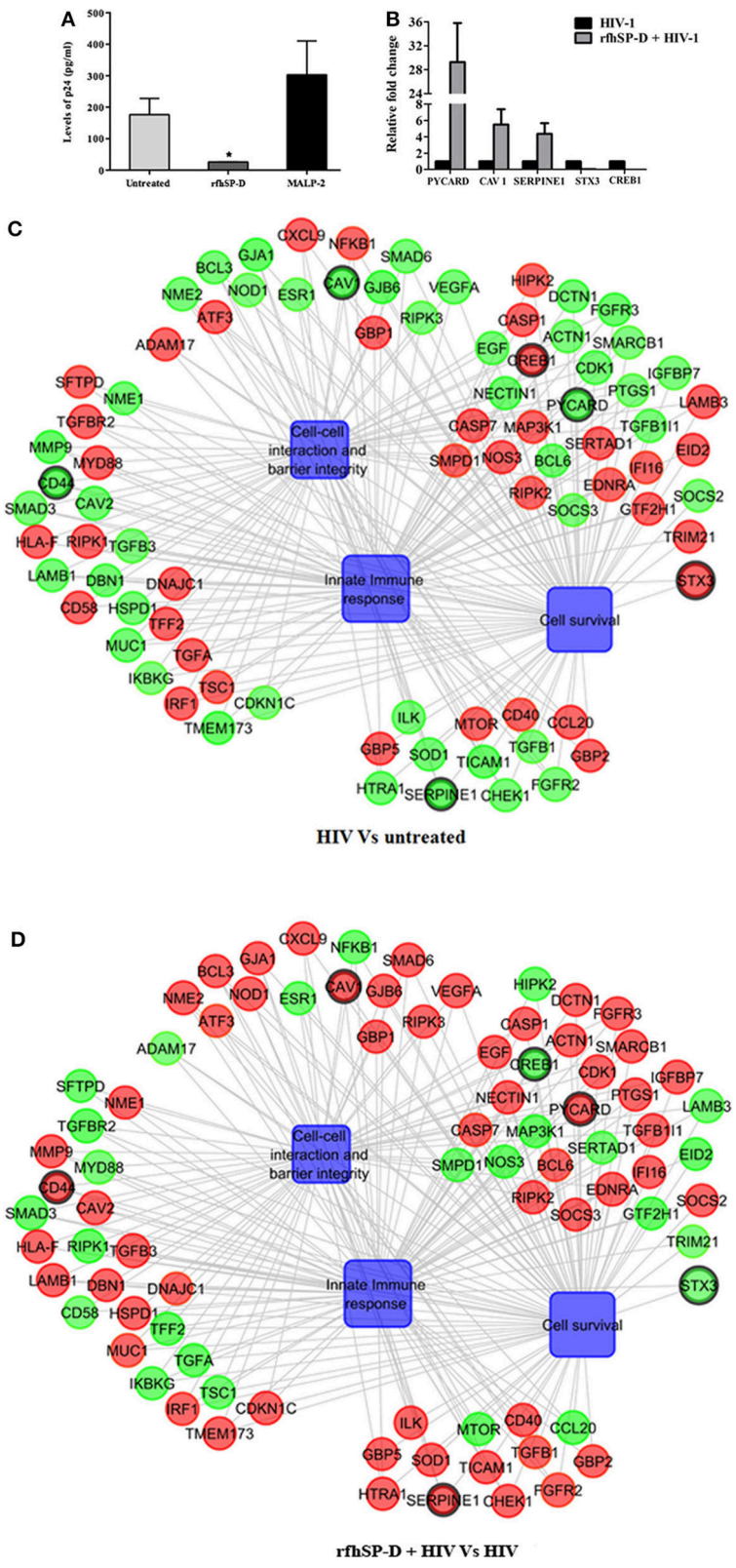

FIGURE 4 | rfhSP-D impedes viral movement across the EpiVaginal tissue barrier and reverses HIV-1 induced gene signature: **(A)** Determination of HIV-1 p24 Ag by ELISA in supernatants from basal chambers at 24 h. Data represents mean ± S. D of three sets. *indicates statistical significance *$p < 0.05$ relative to medium alone.

(Continued)

FIGURE 4 | Gene regulatory network for EpiVaginal tissues treated with HIV-1 Vs untreated **(C)** and EpiVaginal tissues treated with rfhSP-D + HIV-1 vs. HIV-1 **(D)**. Biological processes are blue colored blocks and > 1.5-fold downregulated genes are green colored, > 1.5-fold upregulated genes are red, and <1.5-fold upregulated genes are orange. Circles are sized according to their *p*-value. **(B)** Validation of microarray data by real time RT-PCR. Ect/E6E7 cells were subjected to identical conditions and treatments as for EpiVaginal tissues. RNA was isolated and cDNA was subjected to real time RT-PCR. Data represents mean ± S. D of three independent experiments. Fold change in expression of the 5 genes for validation were statistically significant ($p < 0.05$) relative to untreated Ect/E6E7 cells.

to extracellular matrix, integrins α_3, α_6, and β_4, were upregulated by rfhSP-D (**Figure 6B**; **Supplementary Figure S5**). Specific upregulation of genes related to structural stability of the cell and epithelial integrity suggested that rfhSP-D strengthened the local tissue architecture. Consistent with its established anti-inflammatory role, rfhSP-D downregulated genes that promote inflammatory signals, such as GBP2, IRF1, ATF3, CREB1, IGFBP2, and IGFBP7.

SP-D is synthesized by the human vaginal epithelial cells and its uterine expression is hormone regulated (17). We detected SP-D in the vaginal lavage of normal cycling women (**Supplementary Figure S5A**). Vaginal epithelial cells (Vk2/E6E7) also showed transcripts of SP-D (**Supplementary Figure S5B**). In addition, confocal microscopy revealed that SP-D protein was being produced by Vk2/E6E7 and could be localized in the cytoplasm (**Supplementary Figure S5C**). With its natural presence in the vaginal tract, its role as a pattern recognition protein and in strengthening of the vaginal barrier as evident from gene expression studies, SP-D seems to be vital as the first line of defense at the vaginal surfaces.

rfhSP-D Has No Adverse Effect on Cell Viability and NF-κB Translocation

In addition to the *ex vivo* efficacy of rfhSP-D as an inhibitor of the vaginal transmission of HIV-1, it was pertinent to evaluate the safety of rfhSP-D application on the vaginal surface. As a first step, we assessed its effect on the viability and inflammation of vaginal and ectocervical cells. Within the concentration range of 1.562–100 μg/ml and a duration of 24 h treatment, the viability of vaginal and ectocervical cells was unaltered (**Figure 7A**). NF-κB activation is a prerequisite for inflammation and breach of vaginal barrier providing access to HIV-1 entry. Hence, to determine the effect of rfhSP-D on the NF-κB activation, we used an endocervical cell line (End1/E6E7) transfected with pHTS–NF-κB firefly luciferase reporter. None of the indicated rfhSP-D concentrations induced NF-κB activation, whereas MALP-2 and poly I:C, agonists of TLR-2/6 and TLR3 respectively, led to a significant activation (**Figure 7B**). Furthermore, rfhSP-D did not cause any alteration in the levels of anti-inflammatory immune mediators, such as interleukin-1 receptor antagonist (IL-1RA), secretory leukocyte protease inhibitor (SLPI) and elafin, which are known to maintain vaginal homeostasis (data not shown).

RfhSP-D Does Not Adversely Affect Vaginal *Lactobacilli*

Lactobacilli, as vaginal commensals, are integral to the female reproductive tract. A direct toxicity assay revealed that rfhSP-D did not adversely affect viability of the clinical isolates of *Lactobacilli* (TRF #8, TRF #30, TRF#36 and *Lactobacillus crispatus* LC223) (**Figure 8A**). Lactic acid produced by *Lactobacilli* contributes to vaginal defense and any alteration in its production would enhance susceptibility to pathogens including HIV-1 (43). The pH of the supernatant from cultures treated with rfhSP-D was acidic like untreated controls. As expected, Pen-Strep reduced the viability of *Lactobacilli* and the supernatant showed a significantly higher pH (toward neutral) (**Figure 8B**).

rfhSP-D Does Not Interfere With Vaginal Epithelium-*Lactobacilli* Interaction

Since the vaginal microflora tightly controls the epithelial immune functions in a species- and strain-specific manner, any interference from topically applied microbicides or potential anti-HIV-1 agents may prove detrimental. Thus, we employed vaginal *Lactobacilli* colonization model that mimics *in vivo* conditions (6). In the co-culture conditions, rfhSP-D treatment did not lead to any reduction in CFU counts (**Figure 8C**).

Epithelial interaction with commensals leads to enhanced inflammation in a regulated manner; when exacerbated, it enhances susceptibility to HIV-1 and when calmed, it compromises immunity. Hence, we assessed the effect of rfhSP-D on NF-κB induction in this co-culture model. Importantly, NF-κB levels were not affected across all the tested concentrations of rfhSP-D (**Figure 8D**). Poly I:C and MALP-2 did show an exaggerated NF-κB activity. Further, rfhSP-D did not significantly alter the levels of chemokines, such as RANTES, GRO-α, MIP-3α, corroborating no adverse effect on vaginal immune physiology (**Figures 9A–C**).

Repeated Application of rfhSP-D on Rabbit Vaginal Surface Does Not Induce Inflammation

Rabbits with repeated vaginal application of 1% SDS (positive controls) showed rupturing of the epithelial barrier and hemorrhage, whereas, rfhSP-D and placebo groups showed no signs of inflammation (**Figures 10A–C**). As per the RVI scoring, vaginal sections of rfhSP-D and placebo groups showed none or minimal irritation. The total sum of RVI scoring was 2.98 ± 0.6 for the rfhSP-D group and was not significantly different from the RVI score of 2.54 ± 0.3 for the placebo group, whereas, 1% SDS showed a moderate inflammation score of 9.7 ± 1.01, indicating gross toxicity (**Figure 10D**).

DISCUSSION

Inflammation and breach of mucosal barrier are the two major events that render the "gatekeeping mechanisms" ineffective

TABLE 1 | rfhSP-D-mediated reversal of HIV-1 induced alteration of gene expressions in EpiVaginal tissues.

Gene name	HIV-1 (FC)	rfhSP-D + HIV-1 (FC)	Functions	Ref.	Role in HIV	Ref.
INFLAMMATION						
ADAM17	Up (1.51)	Down (−1.16)	A protease critical in cleavage of TNF-α and other inflammatory proteins to active form. Important in diverse cellular processes such proliferation, migration, cell adhesion	PMID: 20184396	Nef activates and shuttles activated ADAM17 into exosomes Exosomal Nef and ADAM17 activates quiescent CD4+ T Lymphocytes via TNF-α	PMID: 23317503 PMC4178784
MMP9	Down (−3.69)	Up (3.75)	Proteolytic enzyme, degrades extracellular matrix.	PMID: 12540195	Induced by Tat in astrocytes Upregulated by gp120 in vaginal epithelial cell line	PMC2679334 PMC3222676
MYD88	Up (1.82)	Down (−1.26)	universal adapter protein downstram of TLRs (except TLR 3) to activate the transcription factor NF-κB	PMID 18064347	HIV-1 Tat Activates both the MyD88 and TRIF Pathways To Induce TNF-α and IL-10 in Monocytes	PMID: 27053552
RIPK1	Up (1.29)	Down (−1.95)	Serine/threonine kinase that regulate a variety of cellular processes such as cell death and innate immune responses to viral and bacterial infection, induces necroptosis	PMID: 19524512 PMID: 24129419 PMID: 26086143	Cleaved by HIV proteases and modulate cellular response	PMC4546280
CD58	Up (1.64)	Down (−1.25)	Interaction between CD2 and its counterreceptor, CD58 (LFA-3) aids in T cell-APC cell cell contact	PMID: 10380930	Engagement of CD58 enhances HIV-1 replication in monocytic cells	PMID: 8656013
TFF2	Up (1.99)	Down (−2.11)	Secreted into the mucus layer where it stabilizes the mucin gel layer and stimulates migration of epithelial cells. Upgregulated in chronic inflammation	PMID: 19064997	–	–
SERPINE1	Down (−2.04)	Up (2.92)	An inhibitor of fibrinolysis, high concentrations of the gene product are associated with thrombophilia	PMID: 24669362	Monocytes from asymptomatic viremic HIV(+) individuals show increased PAI-1 (SERPINE1)	PMID: 22815948
CCL20	Up (2.94)	Down (−2.61)	Responsible for the chemo-attraction of iDCs, effector/memory B cells and T cells. High specificity for CCR6	PMID: 27617163	Attracting key immune cells, including Th17 cells and dendritic cells, to sites of infection and propagating the virus to other sites of the body	PMID: 28005525
TRIM21	Up (3.29)	No change (1.08)	Intracellular antibody effector in the intracellular antibody-mediated proteolysis pathway. Directs the virions to the proteasome.	PMID: 21045130	Chimeric restriction factor TRIM21-CypA provides highly potent protection against HIV-1 without loss of normal innate immune TRIM activity	PMID: 22909012
SOCS2	Down (−1.2)	Up (1.63)	Down-regulation of cytokine signaling	PMID: 12208853	Tat impaired the IFN γ - receptor signaling pathway at the level of STAT1 activation, via Tat-dependent induction of suppressor of cytokine signaling-2 (SOCS-2) activity	PMID: 19279332

(Continued)

TABLE 1 | Continued

Gene name	HIV-1 (FC)	rfhSP-D + HIV-1 (FC)	Functions	Ref.	Role in HIV	Ref.
SOCS3	No change (1.09)	Up (1.9)	Down-regulation of cytokine signaling	PMID: 9202125 PMID: 9430658 PMID: 9857039	Protein levels were lower in CD4 (+) T cells of HIV-infected patients than in healthy controls, Suppressed Th17 levels correlate with elevated SOCS3 expression in CD4 T cells during acute simian immunodeficiency virus infection	PMID: 21337543 PMID: 23596301
NOS3	Up (1.16)	Down (−1.14)	Major determinant of vascular tone and blood pressure	PMID: 7514568	Nitric oxide inhibits HIV tat-induced NF-κB activation	PMID: 10393859
PYCARD	Down (−1.64)	Up (2.47)	Involved in NLRP3 induced inflammasome. Responsible for cleavage of pro-caspase 1	PMID: 20303873	Involved caspase-1 dependent pyroptosis of HIV infected CD4 T cells	PMC4047036
SMARCD1	Down (−1.95)	Up (2.45)	Part of SWI/SNF complexes that regulate gene activity of chromatin remodeling, may act as tumor suppressor	PMCID: PMC5406539	Role in HIV-1 assembly, interaction between Nef and INI1/SMARCB1 augments replicability of HIV-1 in resting PBMCs facilitate Tat-mediated HIV-1 transcription	PMID: 27558426 PMID: 25559666 PMID: 16889668
CREB1	Up (1.69)	Down (−2.04)	CREB family of transcription factors consists of cAMP-responsive activators including CREB, cAMP response element modulator, and activating transcription factor	PMID: 10872467	Tat utilizes CREB to promote IL-10 production, although the significance of this regarding HIV pathogenesis is not entirely clear, IL-10 can inhibit HIV-1 replication in monocytes and macrophages	PMID: 7527449
RIPK3	Down (−1.28)	Up (1.64)	Serine/threonine kinases that regulate a cellular processes such as cell death and innate immune responses to viral and bacterial infection, induces necroptosis	PMID: 19524512 PMID: 24129419 PMID: 26086143	Not cleaved by HIV proteases and modulate cellular response	PMC4546280
SOD1	Down (−1.30)	Up (1.23)	Enzyme attaches (binds) to molecules of copper and zinc to break down toxic, charged oxygen molecules called superoxide radicals.	PMID: 7901908	SOD1 prevented gp120 and Tat elicited reactive oxygen species (ROS) and rescued neuron apoptosis	PMID: 17336361
TGFBR2	Up (1.21)	Down (−1.7)	TGF-β mediates its actions through heteromeric kinase receptor complex consisting of TGF receptors of type 1 and 2	PMID: 1333888	Increased expression upon Tat treatment of epithelial cells	PMID: 15857508
TGFA	Up (1.15)	Down (−1.46)	Exerts several effects on target cells, such as neovascularization promotion and mitogenic signaling.	PMID: 9242560	Significant rise in chronic HIV type 1 infection	PMID: 27268396
SMAD6	Down (−1.37)	Up (1.59)	Smad6 inhibits signaling by the TGF-beta superfamily	PMID: 9335505	Down-regulated after Tat treatment of U937 macrophages	PMID: 16282533
STX3	Up (2.01)	Down (−2.04)	Potentially involved in secretion of IL-6 from dendritic cells following activation of TLRs	PMID: 25674084	Depletion of STX3 reduced HCMV production	PMID: 25583387

(Continued)

TABLE 1 | Continued

Gene name	HIV-1 (FC)	rfhSP-D + HIV-1 (FC)	Functions	Ref.	Role in HIV	Ref.
XRCC2	Up (2.33)	Down (−2.38)	DNA repair protein binding to double stranded breaks	PMID: 10227297	Suppression of retroviral infection by XRCC2	PMID: 15297876
CYTOSKELETON AND CELL-CELL INTERACTION AND INTEGRITY						
GJA1	Down (−3.07)	Up (3.39)	Involved in intercellular communication (GJIC) between cells to regulate cell death, proliferation, and differentiation. Involved in inflammation	PMID: 25110696 PMID: 25560303	–	–
CD44	Down (−2.42)	Up (5.25)	Cell-surface glycoprotein involved in cell–cell interactions, cell adhesion and migration	PMID: 28546458	Blocking of HIV entry through CD44–hyaluronic acid interactions.	PMID: 25155464 PMID: 25320329
CAV1	Down (−1.89)	Up (2.53)	Cav-1 is enriched in caveolae, involved in endocytosis, signal transduction. Role in innate immune defense, and it regulates macrophage cytokine production and signaling	PMID: 16982844	Cav-1Tat induced alterations of tight junction protein. Cav-1 mediated uptake via langerin restricts HIV-1 infectivity	PMID: 18667611 PMID: 25551286
CAV2	Down (−1.22)	Up (2.48)	Similar to Cav-1 and also inhibits cell proliferation, migration and invasion	PMID: 23454155	–	–
DBN1	Down (−1.86)	Up (1.74)	DBN1 suppresses dynamin-mediated endocytosis via interaction with cortactin. DBN1 restricts the entry of viruses into host cells and more broadly to function as a crucial negative regulator of diverse dynamin-dependent endocytic pathways	PMID: 28416666	Drebrin is a negative regulator of HIV entry and HIV-mediated cell fusion. Down-regulation of drebrin expression promotes HIV-1 entry, decreases F-actin polymerization, and enhances profilin local accumulation in response to HIV-1	PMID: 23926103
NECTIN1	No change (1.04)	Up (2.94)	Nectin cell adhesion molecule, plays role in organization of adheren junctions and tight junction	PMID: 28392352	HIV-Induced Exposure of Nectin-1 Facilitates HSV-1 Infection	PMID: 24586397
IGFBP3	No change (−1.05)	Up (2.11)	Binds IGF-I and IGF-II with relatively low affinity, and belongs to a subfamily of low-affinity IGFBPs. It also stimulates prostacyclin production and cell adhesion.	PMID: 21835307	Inhibit the replication of HIV-1 in cultured cord blood mononuclear cells and chronically HIV-infected U937 cells	PMID: 7576911
ACTN1	No change (−1.01)	Up (1.34)	Major actin cross-linking proteins found in virtually all cell types as a cytoskeleton.	PMID: 26312134	α-Actinin regulates the immune synapse formation and is required for efficient T cell activation. silencing of either EWI-2 or α-actinin-4 increased cell infectivity. Regulation of the actin cytoskeleton at T cell immune and virological synapses	PMID: 22689882
GJB6	Down (−1.95)	Up (2.87)	Gap junctions allow the transport of ions and metabolites between the cytoplasm of adjacent cells	PMID: 19944606	Gap junction channels shutdown under inflammatory conditions, including viral diseases.	PMC4774036

FC-Fold Change.

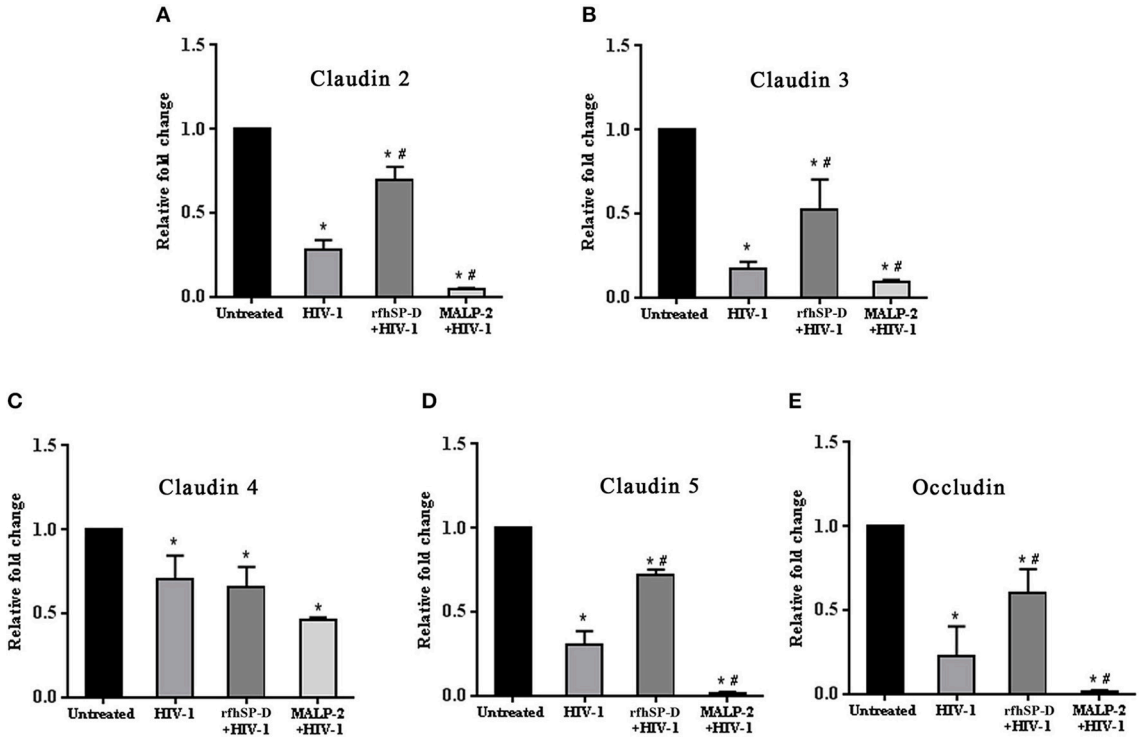

FIGURE 5 | HIV-1 mediated downregulation of transcripts of tight junction genes while rfhSP-D maintained integrity. Relative expression of transcripts of **(A)** Claudin 2, **(B)** Claudin 3, **(C)** Claudin 4, **(D)** Claudin 5, **(E)** Occludin were determined in EpiVaginal tissues by real time qPCR. When compared with HIV-1 challenged tissues, rfhSP-D treatment led to significant upregulation of Claudin 2, 3, 5, and occludin. Data is represented as mean ± S. D. *, # indicate statistical significance of $p < 0.05$ in comparison to untreated and HIV-1 treated EpiVaginal tissues, respectively.

leading to HIV-1 transmission. The present study establishes a recombinant fragment of human SP-D (rfhSP-D) as a candidate microbicide, which remarkably inhibited HIV-1 transfer in an *ex vivo* model comprising of multi-layered vaginal mucosal tissue. We also report the gene expression profile of HIV-1 challenged EpiVaginal tissues. RfhSP-D specifically reversed the infection-promoting gene signature induced by the virus, thereby, maintaining the integrity of vaginal epithelium and suppressing the pro-inflammatory milieu. Furthermore, *in vitro* and *in vivo* safety studies implied that the rfhSP-D is safe for mucosal application at the concentrations that to restrict viral passage.

Transcriptome snapshot of the EpiVaginal tissues upon HIV-1 challenge revealed an inflammatory response comprising of chemokines, cytokines and components of inflammasome. Upregulation of these genes would act in sync, contributing to a generalized local inflammation in the vaginal epithelium. Fanibunda et al. (44) reported global gene expression in a monolayer of vaginal epithelial cell line (Vk2/E6E7) challenged with HIV-1 recombinant gp120 protein with a predominant induction of immunomodulatory processes and proteases. Following HIV-1 exposure, primary genital epithelial cell cultures showed enhanced proinflammatory cytokines (e.g., TNF-α and IL-6) and disruption of tight junctions, such as claudins, occluding, and ZO-1, leading to a compromised barrier (36, 45). Barouch et al. demonstrated that 24 h post-vaginal SIV challenge, the host lacked expression of the antiviral restriction factors and the response comprised of NLRX1 and TGF-α which incapacitated a strong anti-viral response (46). Consistent with the previous reports, the *ex vivo* model of human vaginal tissues showed pro-inflammatory response on viral challenge. Alongwith, it showed upregulation of host restriction factors, such as guanylate-binding proteins (GBP1, GBP2, GBP5), TRIM21 and other IFN-inducible genes. GBP5 has been recently reported as a host restriction factor in virus-challenged macrophages (47). Although, not proven in the context of HIV-1, TRIM21 is known to obstruct the incoming antibody-opsonized non-enveloped virions and efficiently mediate post-entry neutralization and innate immune signaling (48, 49). Being effective intracellularly, it is possible to hypothesize that these restriction factors may prevent further movement of the transcytosed virions (50). HIV-1 can also pass freely through the intercellular gaps in the vaginal epithelium. We observed a dramatic downregulation of several genes of the plasma membrane and cytoskeleton framework along with downregulation of tight junction proteins (claudins and occludin) induced by the virus. Although the EpiVaginal tissue attempts to mount an interferon response, the excessive inflammation and a disturbance in cellular functions weaken the epithelial barrier and provide a gateway to the underlying

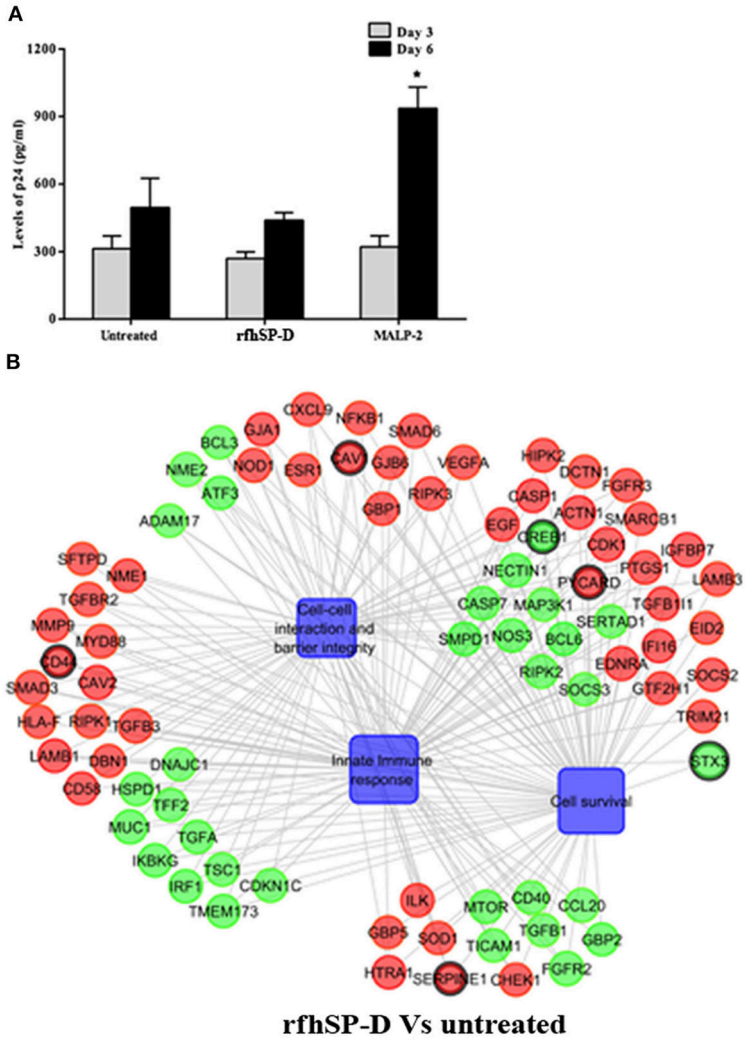

FIGURE 6 | Susceptibility of PBMCs to HIV-1 acquisition: **(A)** Day 3 and 6 HIV-1 p24 Ag levels as determined by ELISA. RfhSP-D did not enhance susceptibility to HIV acquisition whereas MALP-2 treatment enhanced it on day 6. Data is representative of three biological replicates and is represented as mean ± S. D. *indicate statistical significance of $p < 0.05$ in comparison to day 6 untreated (control). **(B)** Gene regulatory network for EpiVaginal tissues treated with rfhSP-D vs. untreated. Biological processes are blue colored blocks, downregulated genes are green colored, upregulated are red, unaltered are in orange. Circles are sized according to their *p*-value.

target cells (**Figure 11A**). There are several compelling evidence of interaction of HIV-1 with the vaginal epithelial cells via TLR2 and TLR4 (46), gp340 (51), syndecans (52), and human mannose receptor (53). These receptors, when engaged with PAMPs, initiate an inflammatory cascade. In our model, MALP-2 that activated the TLR2/6 inflammatory axis, synergizes with HIV-1 to further reduce the expression of tight junction proteins and enhances chemokine secretion, reiterating their crucial role in HIV transmission.

The gene signature of EpiVaginal tissues, induced by HIV-1, reflected key mechanisms for viral movement across the multilayered epithelium resulting in its acquisition by the underlying PBMCs. RfhSP-D showed a remarkable ability to restrict viral movement (though not a complete blockade in the experimental conditions). Previously, we and others have shown that rfhSP-D (as well as native SP-D) potently binds to HIV-1 gp120, leading to agglutination and inhibition of infectivity of target cells (19, 54). It can, therefore, be considered that interaction of trimeric rfhSP-D with HIV-1 plausibly results in large complexes that are unable to travel through the tight vaginal barrier. Moreover, since HIV-1 envelope protein gp120 primarily makes the first contact with the epithelium, restriction of this interaction by rfhSP-D may also contribute to a shift from HIV-1 induced gene signature. The presence of a fraction of the virions in the basal chamber of rfhSP-D treated EpiVaginal tissues indicated interaction of the HIV-1 with the EpiVaginal tissues (although it was significantly reduced). In addition, evident from the differential gene expression of the rfhSP-D treated EpiVaginal tissues, rfhSP-D directly interacted with the vaginal epithelial cells and thus strengthened

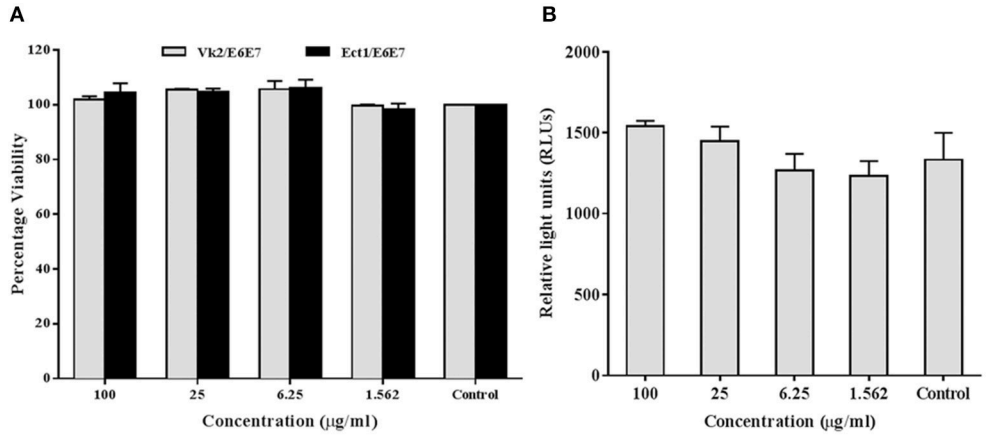

FIGURE 7 | rfhSP-D does not affect viability or NF-κB activation: **(A)** MTT assay showing no significant alteration in cellular viability of vaginal (Vk2/E6E7) and ectocervical (Ect1/E6E7) cells 24 h after rfhSP-D treatment. **(B)** NF-κB activity measured by firefly luciferase reporter assay at 24 h of stimulation of endocervical epithelial (End1/NF-κB) cells with rfhSP-D (up to 100 μg/ml). Values represent mean ± SD.

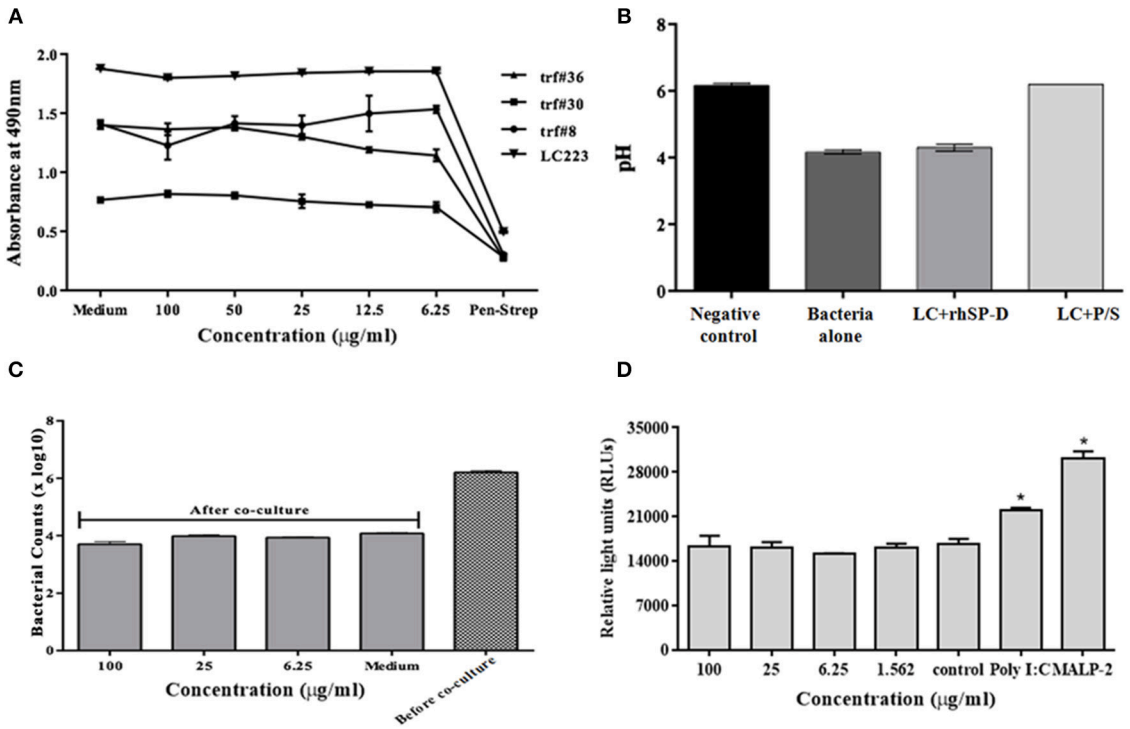

FIGURE 8 | No adverse effects of rfhSP-D on vaginal lactobacilli and epithelium-commensal interaction: **(A)** Bacterial growth was assessed at 490 nm. At 24 h, none of the indicated rfhSP-D concentrations led to any alteration in growth of lactobacilli (*Lactobacillus fermentum spps mucosae* (TRF#36), *Lactobacillus gasseri* (TRF#8), *Lactobacillus salivarius* (TRF#30) and *Lactobacillus crispatus* (LC223) whereas penicillin-streptomycin (P/S) significantly inhibited its growth. **(B)** pH of the spent medium is a measure of lactic acid production. LC-Lactobacillus crispatus (LC223). Values represent means ± SD of three experiments. **(C)** CFU counts before and after epithelial (Vk2/E6E7)-bacterial (*Lactobacillus crispatus*) co-cultures were treated with rfhSP-D. **(D)** Co-cultures of epithelial cells (End1/NF-κB)-bacteria (*Lactobacillus crispatus*) were assayed for luciferase activity. No apparent rise in luciferase activity was observed following treatment with rfhSP-D whereas Poly I:C and MALP-2 showed a significant increase in NF-κB activity. Values represent mean ± SD. *$p < 0.05$ in comparison to untreated.

the barrier with upregulated expression of cytoskeleton-related genes. Taken together, these observations suggest that rfhSP-D was able to contain the HIV-1 induced changes in gene expression of the EpiVaginal tissues. Significant upregulation of transcripts for several tight junction proteins in the HIV-1 challenged EpiVaginal tissues in presence of rfhSP-D validated this hypothesis. The two key pro-inflammatory players, NF-κB and mTOR (55, 56), were significantly downregulated, suggesting

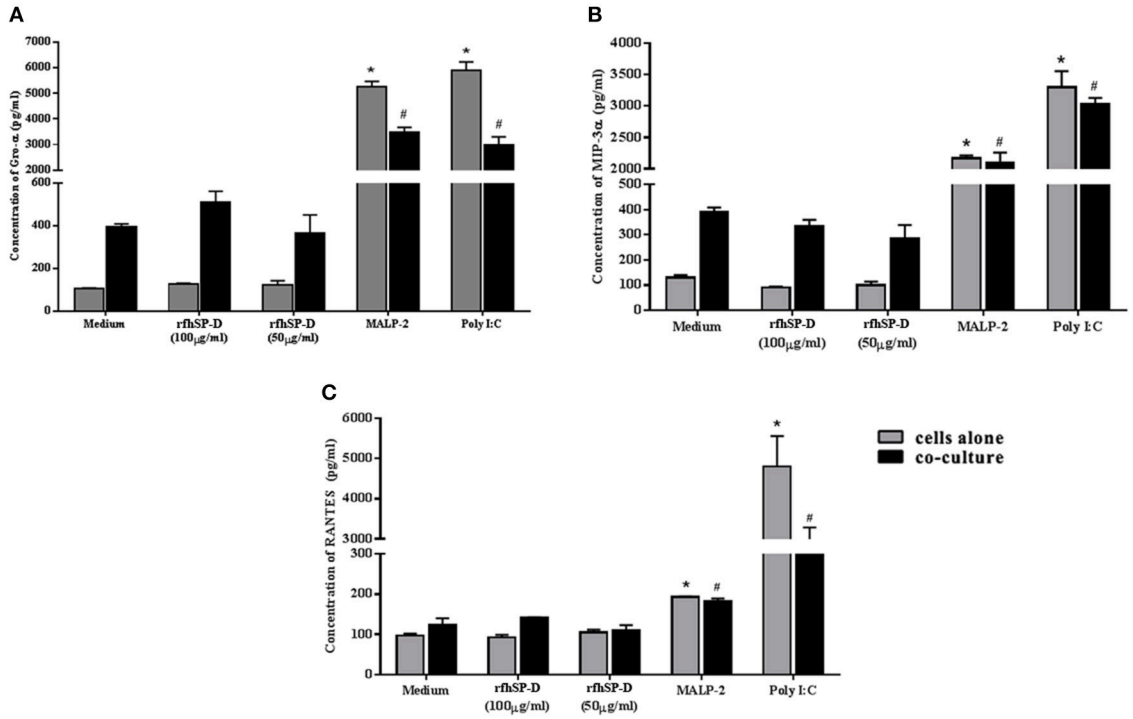

FIGURE 9 | rfhSP-D does not alter basal levels of chemokines: **(A)** GRO-α, **(B)** MIP-3α, and **(C)** RANTES Levels were determined using MSD assay in the epithelial cells (Vk2/E6E7)—bacterial (*Lactobacillus crispatus*, LC223) co-culture. Data is representative as mean ± S. D. $^*p < 0.05$ was considered statistically significant.

likely inhibition of the sequential steps of HIV-1 transmission. Notably, the Guanylate binding proteins (GBPs) were either upregulated or unaltered, suggesting that rfhSP-D facilitated the protective response mounted by the EpiVaginal tissue against HIV-1 (**Figure 11B**). We have recently reported DC-SIGN as a novel receptor of SP-D (using rfhSP-D). A tripartite engagement between DC-SIGN, rfhSP-D and gp120 significantly inhibited transfer of HIV-1 from DC-SIGN to the PBMCs (57). This finding may hold immense importance in vaginal transmission of HIV-1, since DC-SIGN on dendritic cells acts as "Trojan horse" that captures HIV-1 in the mucosa and facilitates its transport to secondary lymphoid organs rich in $CD4^+$ T cells followed by trans-infection (58).

SP-D has been shown to potently inhibit the infectivity of other enveloped viruses, such as Influenza A Virus (IAV) (59) and Respiratory Syncytial Virus (RSV) (60), concomitant with induction of an anti-inflammatory environment by interacting with mucosal epithelial and immune cells. This unique property has made rfhSP-D a viable therapeutic option for cystic fibrosis, neonatal lung disease and smoking-induced emphysema (61). RfhSP-D seems to have a similar role against HIV-1 at the vaginal interface. While rfhSP-D limits viral access, it also induces a state of immune quiescence in the vaginal tissues. There is a direct correlation of immune quiescence at the mucosal sites, with resistance to HIV-1 acquisition in serodiscordant women (62). It would be worth exploring the clinical significance of the candidate genes associated with restricted transmission identified in the present study in the highly exposed seronegative women.

An anti-HIV molecule can be effective as a microbicide only if it retains its anti-viral activity without inducing immune activation. Several candidates have failed in the clinical trials due to inflammation caused to the epithelial and target cells, leading to enhanced susceptibility to the virus. Our model revealed that treatment with rfhSP-D did not induce any aberrant inflammatory response by EpiVaginal tissues and did not lead to activation of PBMCs (target cells), and thus, minimized the likelihood of viral transfer and acquisition. In contrast, MALP-2 showed increased activation and susceptibility of PBMCs to the virus, confirming the appropriateness of the model for the evaluation microbicides (63).

To save time and resources, an extensive characterization of candidate prophylactics is warranted before testing their efficacy *in vivo*. Therefore, we subjected rfhSP-D to a series of safety evaluations. RfhSP-D was well-tolerated by human vaginal and ectocervical cells; even at the highest concentration (100 μg/ml), no apparent alterations in the viability of vaginal epithelial cells or inflammation were observed. Similarly, rfhSP-D did not adversely affect the growth of lactobacilli or acid production. However, in the vagina, the epithelial cells and microflora together determine the vaginal health. Vaginal microflora is critical in regulating the epithelial innate immune response. To accurately replicate the *in vivo* condition, we tested safety of rfhSP-D in an epithelial-bacterial colonization model (6). As is the case for a successful microbicide candidate, rfhSP-D did not affect lactobacilli counts, NF-kB activation and chemokine levels in the co-culture. Although SP-D potently

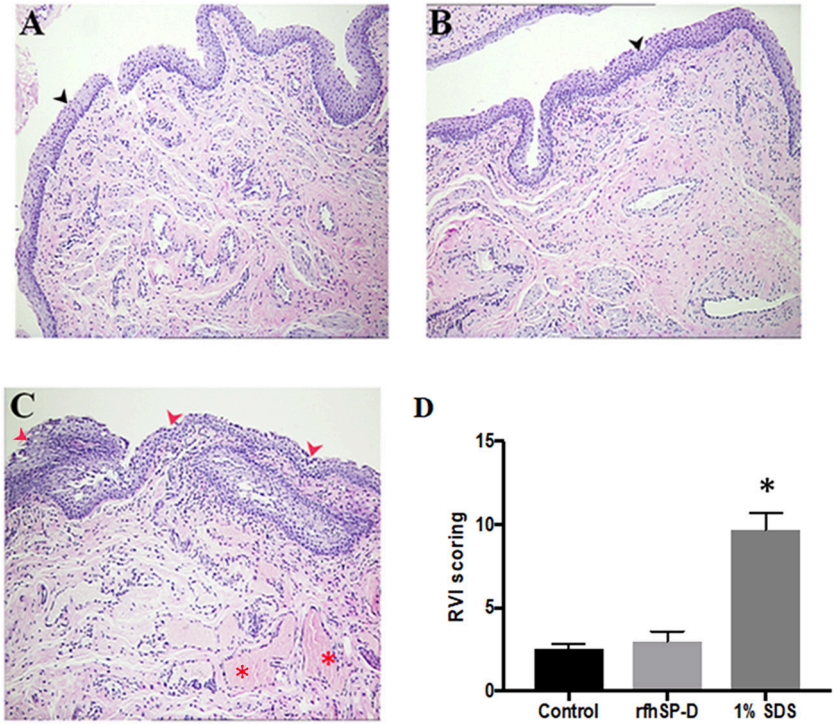

FIGURE 10 | Rabbit Vaginal Irritation (RVI) model demonstrates intact integrity of mucosal barrier on repeated application of rfhSP-D gel: H&E staining of vaginal sections of rabbits ($n = 5$/group) treated with **(A)** placebo gel **(B)** rfhSP-D (100 μg/ml) gel and **(C)** 1% SDS gel (positive control) daily for 10 consecutive days. Sections from 1% SDS gel treated rabbits showed inflamed epithelial barrier with significant infiltration of polymorphonuclear cells (PMNs) (depicted by "red arrows") and hemorrhage (depicted by the "red asterisk"). Black arrow heads depict epithelial membrane with minimal infiltration of PMNs in the "placebo gel" and "rfhSP-D (100 μg/mL) gel" in **(A,B)**. Magnification 10×. **(D)** RVI score of the rfhSP-D treated group was not significantly different from the placebo group. At least three sections of vaginal tissues (both proximal and distal) of each animal (blinded) were scored from 0 to 4 for epithelial damage (0 = normal, 1 = flattening, 2 = metaplasia, 3 = erosion, and 4 = ulceration) and leukocyte infiltration, edema and congestion (0 = absent, 1 = minimal, 3 = moderate, 4 = marked). Total score of each animal was calculated and was averaged with number of sections analyzed. A total score from 1 to 4 is to be considered as minimal irritation, 5–8 as mild irritation, 9–11 as moderate irritation, and 12–13 as marked irritation. *$p < 0.05$ was considered statistically significant.

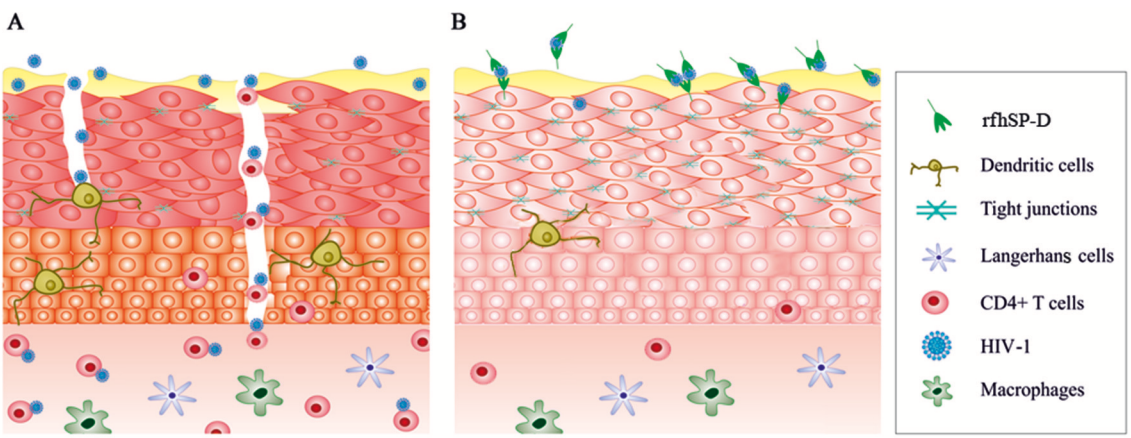

FIGURE 11 | A schematic model illustrating effects of HIV-1 and rfhSP-D on EpiVaginal tissues. **(A)** The intact epithelium seems to be breached after HIV-1 exposure. Alterations in the genes encoding tight junction proteins, cytoskeleton and those contributing to inflammation are plausibly the critical events in HIV-1 transmission through the multi-layered tissue. **(B)** rfhSP-D potently binds to HIV-1 and interacts with EpiVaginal tissues, reverses HIV-1 induced gene signature, and inhibits HIV-1 transmission.

inhibits reproductive tract pathogens, such as Chlamydia (64) and Candida (65), we report the SP-D-commensal interaction for the first time. Further investigations may ascertain molecular determinants that define the ability of SP-D to differentiate between vaginal pathogens and commensals. One plausible reason could be evolution of tolerance of the vaginal microflora in the presence of SP-D and other anti-microbial proteins and peptides naturally secreted in the vagina (66). SP-D is naturally expressed and secreted by the human vaginal epithelial cells. Therefore, it was expected that repeated application of rfhSP-D may not harm the vaginal surface. There were no evident histological signs of mucosal toxicity in the rabbit vagina, suggesting that rfhSP-D is well-tolerated *in vivo*.

In summary, we demonstrate the transcriptional gene expression signatures of EpiVaginal tissues in response to HIV-1. An *ex vivo* model of vaginal transmission of HIV-1 was developed that revealed novel genes and features of HIV-1 transmission, and offers a highly reproducible, cost-effective, non-animal model to study efficacy of candidate microbicides. Importantly, rfhSP-D emerges as a potent anti-HIV-1 microbicide candidate, and the results provide a strong argument for its further evaluation in non-human primate models.

ETHICS STATEMENT

Cervicovaginal lavage (CVL) was collected from the normal cycling females with an approval from the Institutional Ethics Committee for Clinical Studies, ICMR-NIRRH (Project No. 148/2008). Blood ($n = 5$) was collected from healthy donors (as determined by clinical examination) at the Department of Pathology, Brigham and Women's Hospital, Boston, MA, under the Partners Healthcare IRB approval (2003P002150). Written informed consent was obtained from each participant. The rabbit vaginal irritation study was approved by the "Institutional Animal Ethics Committee (IAEC)," ICMR-NIRRH, Mumbai (Project No. 08/2012). The IAEC has been recognized by the central organization "Committee for the Purpose of Control & Supervision of Experiments on Animals (CPCSEA)." We strictly adhered to the CPCSEA protocols and guidelines for animal care during the animal experimentation.

AUTHOR CONTRIBUTIONS

HP conceived the study, designed, performed and analyzed the experiments, and wrote the paper. KK carried out the RVI model study. KK, GT, and SR carried out the primer designing and Real-time RT-PCR validation of the gene expression. HY conducted the cell viability assessment, recruitment of study participants, and data analysis. PC and MV carried out the microarray analysis, pathway analysis, and presentation. UK provided rfhSP-D for the study and critical suggestions for the manuscript. TM conceived and co-ordinated the study, procured the intra-mural grant and ICMR-Medical Innovation Fund support, mediated the clinical collaboration, defended the protocol for IEC approval, analyzed the data, and edited the paper. RF conceived and co-ordinated the study, facilitated HP's experimentation at BWH, analyzed the data, and edited the paper. All authors reviewed the results and approved the final version of the manuscript.

ACKNOWLEDGMENTS

The authors thank HIV Research Trust, UK for providing scholarship to Hrishikesh Pandit to work at the Fichorova's Laboratory. This study was partly supported by Medical Innovation Fund (Project no. 2011-16850) of Indian Council of Medical Research (ICMR), New Delhi, India. We are grateful to Director, NIRRH for providing financial support via the Institutional Grant and the Institutional facilities (Accession no. 618). The funders had no role in study design, data collection and analysis, decision to publish, and preparation of the manuscript. Mr. Vaibhav Shinde is gratefully acknowledged for his help with improving figure resolution and art work. Authors acknowledge veterinary support from Dr. Uddhav K. Chaudhari, ICMR-NIRRH for the RVI model. We thank Eswari Dodagatta-Marri, Anuvinder Kaur and Valarmathy Murugaiah for supplying rfhSP-D as and when required.

SUPPLEMENTARY MATERIAL

The Supplementary Material for this article can be found online at: https://www.frontiersin.org/articles/10.3389/fimmu.2019.00264/full#supplementary-material

REFERENCES

1. UNAIDS, WHO. *AIDS Epidemic Update 2009*. Geneva, Switzerland: UNAIDS/World Health Organization (2010). Available online at: http://www.unaids.org/en/KnowledgeCentre/HIVData/EpiUpdate/EpiUpdArchive/2007/ (accessed September 10, 2010).
2. Wira CR, Fahey JV, Ghosh M, Patel MV, Hickey DK, Ochiel DO. Sex hormone regulation of innate immunity in the female reproductive tract: the role of epithelial cells in balancing reproductive potential with protection against sexually transmitted pathogens. *Am J Reprod Immunol.* (2010) 63:544–65. doi: 10.1111/j.1600-0897.2010.00842.x
3. Lee SK, Kim CJ, Kim DJ, Kang J. Immune cells in the female reproductive tract. *Immune Netw.* (2015) 15:16–26. doi: 10.4110/in.2015.15.1.16
4. Vitali D, Wessels JM, Kaushic C. Role of sex hormones and the vaginal microbiome in susceptibility and mucosal immunity to HIV-1 in the female genital tract. *AIDS Res Ther.* (2017) 14:39. doi: 10.1186/s12981-017-0169-4
5. Fichorova RN. Guiding the vaginal microbicide trials with biomarkers of inflammation. *J Acquir Immune Defic Syndr.* (2004) 37:S184–93.
6. Fichorova RN, Yamamoto HS, Delaney ML, Onderdonk AB, Doncel GF. Novel vaginal microflora colonization model providing new insight into microbicide mechanism of action. *MBio.* (2011) 25:e00168-11. doi: 10.1128/mBio.00168-11
7. Alexandre KB, Mufhandu HT, London GM, Chakauya E, Khati M. Progress and perspectives on HIV-1 microbicide development. *Virology.* (2016) 497:69–80. doi: 10.1016/j.virol.2016.07.004
8. McElrath MJ, Ballweber L, Terker A, Kreger A, Sakchalathorn P, Robinson B, et al. *Ex vivo* comparison of microbicide efficacies for preventing HIV-1 genomic integration in intraepithelial vaginal cells. *Antimicrob Agents Chemother.* (2010) 54:763–72. doi: 10.1128/AAC.00891-09

9. Lin X, Paskaleva EE, Chang W, Shekhtman A, Canki M. Inhibition of HIV-1 infection in *ex vivo* cervical tissue model of human vagina by palmitic acid; implications for a microbicide development. *PLoS ONE*. (2011) 6:e24803. doi: 10.1371/journal.pone0024803
10. Carias AM, McCoombe S, McRaven M, Anderson M, Galloway N, Vandergrift N, et al. Defining the interaction of HIV-1 with the mucosal barriers of the female reproductive tract. *J Virol.* (2013) 87:11388–400. doi: 10.1128/JVI.01377-13
11. Merbah M, Introini A, Fitzgerald W, Grivel JC, Lisco A, Vanpouille C, et al. Cervico-vaginal tissue *ex vivo* as a model to study early events in HIV-1 infection. *Am J Reprod Immunol.* (2011) 65:268–78. doi: 10.1111/j.1600-0897.2010.00967.x
12. Iqbal SM, Ball TB, Levinson P, Maranan L, Jaoko W, Wachihi C, et al. Elevated elafin/ trappin-2 in the female genital tract is associated with protection against HIV acquisition. *AIDS*. (2009) 23:1669–77. doi: 10.1097/QAD.0b013e32832ea643
13. Burgener A, Rahman S, Ahmad R, Lajoie J, Ramdahin S, Mesa C, et al. Comprehensive proteomic study identifies serpin and cystatin antiproteases as novel correlates of HIV-1 resistance in the cervicovaginal mucosa of female sex workers. *J Proteome Res.* (2014) 10:5139–49. doi: 10.1021/pr200596r
14. Kay S, Metkari SM, Madan T. Ovarian hormones regulate SP-D expression in the mouse uterus during estrous cycle and early pregnancy. *Am J Reprod Immunol.* (2015) 74:77–88. doi: 10.1111/aji.12369
15. Macneill C, de Guzman G, Sousa GE, Umstead TM, Phelps DS, Floros J, et al. Cyclic changes in the level of the innate immune molecule, surfactant protein-A, and cytokines in vaginal fluid. *Am J Reprod Immunol.* (2012) 68:244–50. doi: 10.1111/j.1600-0897.2012.01155.x
16. Bulla R, De Seta F, Radillo O, Agostinis C, Durigutto P, Pellis V, et al. Mannose-binding lectin is produced by vaginal epithelial cells and its level in the vaginal fluid is influenced by progesterone. *Mol Immunol.* (2010) 48:281–6. doi: 10.1016/j.molimm.2010.07.016
17. Oberley RE, Goss KL, Hoffmann DS, Ault KA, Neff TL, Ramsey KH, et al. Regulation of surfactant protein D in the mouse female reproductive tract *in vivo*. *Mol Hum Reprod.* (2007) 13:863–8. doi: 10.1093/molehr/gam074
18. Leth-Larsen R, Floridon C, Nielsen O, Holmskov U. Surfactant protein D in the female genital tract. *Mol Hum Reprod.* (2004) 10:149–54. doi: 10.1093/molehr/gah022
19. Pandit H, Gopal S, Sonawani A, Yadav AK, Qaseem AS, Warke H, et al. Surfactant protein D inhibits HIV-1 infection of target cells via interference with gp120-CD4 interaction and modulates pro-inflammatory cytokine production. *PLoS ONE*. (2014) 18:e102395. doi: 10.1371/journal.pone.0102395
20. Madan T, Reid KB, Singh M, Sarma PU, Kishore U. Susceptibility of mice genetically deficient in the surfactant protein (SP)-A or SP-D gene to pulmonary hypersensitivity induced by antigens and allergens of *Aspergillus fumigatus*. *J Immunol.* (2005) 174:6943–54.
21. Pandit H, Thakur G, Koippallil Gopalakrishnan AR, Dodagatta-Marri E, Patil A, Kishore U, et al. Surfactant protein D induces immune quiescence and apoptosis of mitogen-activated peripheral blood mononuclear cells. *Immunobiology*. (2016) 221:310–22. doi: 10.1016/j.imbio.2015.10.004
22. Fichorova RN, Rheinwald JG, Anderson DJ. Generation of papillomavirus-immortalized cell lines from normal human ectocervical, endocervical, and vaginal epithelium that maintain expression of tissue-specific differentiation proteins. *Biol Reprod.* (1997) 57:847–55.
23. Fichorova RN, Bajpai M, Chandra N, Hsiu JG, Spangler M, Ratnam V, et al. Interleukin (IL)-1, IL-6, and IL-8 predict mucosal toxicity of vaginal microbicidal contraceptives. *Biol Reprod.* (2004) 71:761–9. doi: 10.1095/biolreprod.104.029603
24. Fichorova RN, Cronin AO, Lien E, Anderson DJ, Ingalls RR. Response to *Neisseria gonorrhoeae* by cervicovaginal epithelial cells occurs in the absence of toll-like receptor 4-mediated signaling. *J Immunol.* (2002) 168:2424–32. doi: 10.4049/jimmunol.168.5.2424
25. Fichorova RN, Tucker LD, Anderson DJ. The molecular basis of nonoxynol-9-induced vaginal inflammation and its possible relevance to human immunodeficiency virus type 1 transmission. *J Infect Dis.* (2001) 184:418–28. doi: 10.1086/322047
26. Canny GO, Trifonova RT, Kindelberger DW, Colgan SP, Fichorova RN. Expression and function of bactericidal/permeability-increasing protein in human genital tract epithelial cells. *J Infect Dis.* (2006) 194:498–502. doi: 10.1086/505712
27. Trifonova RT, Pasicznyk JM, Fichorova RN. Biocompatibility of solid-dosage forms of anti-human immunodeficiency virus type 1 microbicides with the human cervicovaginal mucosa modeled *ex vivo*. *Antimicrob Agents Chemother.* (2006) 50:4005–10. doi: 10.1128/AAC.00588-06
28. Talwar GP, Garg K, Atrey N, Singh P, Gaur J, et al. A safe wide spectrum polyherbal microbicide and three meritorious strains of probiotics for regressing infections and restoration of vaginal health (regression of vaginosis with BASANT and probiotics). *J Womens Health Care*. (2015) 4:256. doi: 10.4172/2167-0420.1000256
29. Mahajan L, Madan T, Kamal N, Singh VK, Sim RB, Telang SD, et al. Recombinant surfactant protein-D selectively increases apoptosis in eosinophils of allergic asthmatics and enhances uptake of apoptotic eosinophils by macrophages. *Int Immunol.* (2008) 20:993–1007. doi: 10.1093/intimm/dxn058
30. Shrive AK, Tharia HA, Strong P, Kishore U, Burns I, Rizkallah PJ, et al. High-resolution structural insights into ligand binding and immune cell recognition by human lung surfactant protein D. *J Mol Biol.* (2003) 331:509–23. doi: 10.1016/S0022-2836(03)00761-7
31. Miyamura K, Malhotra R, Hoppe HJ, Reid KB, Phizackerley PJ, Macpherson P, et al. Surfactant proteins A (SP-A) and D (SP-D): levels in human amniotic fluid and localization in the fetal membranes. *Biochim Biophys Acta*. (1994) 1210:303–7.
32. Postle AD, Mander A, Reid KB, Wang JY, Wright SM, Moustaki M, et al. Deficient hydrophilic lung surfactant proteins A and D with normal surfactant phospholipid molecular species in cystic fibrosis. *Am J Respir Cell Mol Biol.* (1999) 20:90–8. doi: 10.1165/ajrcmb.20.1.3253
33. Nadesalingam J, Reid KB, Palaniyar N. Collectin surfactant protein D binds antibodies and interlinks innate and adaptive immune systems. *FEBS Lett.* (2005) 579:4449–53. doi: 10.1016/j.febslet.2005.07.012
34. DeSilva NS, Ofek I, Crouch EC. Interactions of surfactant protein D with fatty acids. *Am J Respir Cell Mol Biol.* (2003) 29:757–70. doi: 10.1165/rcmb.2003-0186OC
35. Palaniyar N1, Nadesalingam J, Reid KB. Innate immune collectins bind nucleic acids and enhance DNA clearance *in vitro*. *Ann N Y Acad Sci.* (2003) 1010:467–70. doi: 10.1196/annals.1299.084
36. Nazli A, Chan O, Dobson-Belaire WN, Ouellet M, Tremblay MJ. Exposure to HIV-1 directly impairs mucosal epithelial barrier integrity allowing microbial translocation. *PLoS Pathog.* (2010) 6:e1000852. doi: 10.1371/journal.ppat.1000852
37. Card CM, Rutherford WJ, Ramdahin S, Yao X, Kimani M, Wachihi C, et al. Reduced cellular susceptibility to *in vitro* HIV infection is associated with $CD4^+$ T cell quiescence. *PLoS ONE*. (2012) 7:e45911. doi: 10.1371/journal.pone.0045911
38. Fichorova RN, Trifonova RT, Gilbert RO, Costello CE, Hayes GR, Lucas JJ, et al. Trichomonas vaginalis lipophosphoglycan triggers a selective upregulation of cytokines by human female reproductive tract epithelial cells. *Infect Immun.* (2006) 74:5773–9. doi: 10.1128/IAI.00631-06
39. Lackman-Smith C, Osterling C, Luckenbaugh K, Mankowski M, Snyder B, Lewis G, et al. Development of a comprehensive human immunodeficiency virus type 1 screening algorithm for discovery and preclinical testing of topical microbicides. *Antimicrob Agents Chemother.* (2008) 52:1768–81. doi: 10.1128/AAC.01328-07
40. Jorgenson JH, Turnidge JD, Washington JA. Antibacterial susceptibility tests: dilution and disk diffusion methods. In: Murray PR, Baron EJ, Pfaller MA, Tenover FC, Yolken RH, editors. *Manual of Clinical Microbiology*, 7th ed. (1999) Washington, DC: ASM Press. p. 1526–43.
41. Fichorova RN, Mendonca K, Yamamoto HS, Murray R, Chandra N, Doncel GF. A quantitative multiplex nuclease protection assay reveals immunotoxicity gene expression profiles in the rabbit model for vaginal drug safety evaluation. *Toxicol Appl Pharmacol.* (2015) 285:198–206. doi: 10.1016/j.taap.2015.02.017
42. Stacey AR, Norris PJ, Qin L, Haygreen EA, Taylor E, Heitman J, et al. Induction of a striking systemic cytokine cascade prior to peak viremia in acute human immunodeficiency virus type 1 infection, in contrast to more modest and delayed responses in acute hepatitis B and C virus infections. *J Virol.* (2009) 83:3719–33. doi: 10.1128/JVI.01844-08

43. Wira CR, Ghosh M, Smith JM, Shen L, Connor RI, Sundstrom P, et al. Epithelial cell secretions from the human female reproductive tract inhibit sexually transmitted pathogens and *Candida albicans* but notH *Lactobacillus*. *Mucosal Immunol.* (2011) 4:335–42. doi: 10.1038/mi.2010.72
44. Fanibunda SE, Modi DN, Bandivdekar AH. HIV gp120 induced gene expression signatures in vaginal epithelial cells. *Microbes Infect.* (2013) 15:806–15. doi: 10.1016 j.micinf.2013.07.003
45. Nazli A, Kafka JK, Ferreira VH, Anipindi V, Mueller K, Osborne BJ, et al. HIV-1 gp120 induces TLR2- and TLR4-mediated innate immune activation in human female genital epithelium. *J Immunol.* (2013) 191:4246–58. doi: 10.4049/jimmunol.1301482
46. Barouch DH, Ghneim K, Bosche WJ, Li Y, Berkemeier B, Hull M, et al. Rapid inflammasome activation following mucosal SIV infection of rhesus monkeys. *Cell*. (2016) 165:656–67. doi: 10.1016/j.cell.2016.03.021
47. Krapp C, Hotter D, Gawanbacht A, McLaren PJ, Kluge SF, Stürzel CM, et al. Guanylate binding protein (GBP) 5 is an interferon-inducible inhibitor of HIV-1 infectivity. *Cell Host Microbe*. (2016) 19:504–14. doi: 10.1016/j.chom.2016.02.019
48. McEwan WA, Tam JC, Watkinson RE, Bidgood SR, Mallery DL, James LC. Intracellular antibody-bound pathogens stimulate immune signaling via the Fc receptor TRIM21. *Nat Immunol.* (2013) 14:327–36. doi: 10.1038/ni.2548
49. McEwan WA, Hauler F, Williams CR, Bidgood SR, Mallery DL, Crowther RA, et al. Regulation of virus neutralization and the persistent fraction by TRIM21. *J Virol.* (2012) 86:8482–91. doi: 10.1128/JVI.00728-12
50. Kinlock BL, Wang Y, Turner TM, Wang C, Liu B. Transcytosis of HIV-1 through vaginal epithelial cells is dependent on trafficking to the endocytic recycling pathway. *PLoS ONE*. (2014) 9:e96760. doi: 10.1371/journal.pone.0096760
51. Stoddard E, Cannon G, Ni H, Karikó K, Capodici J, Malamud D, et al. gp340 expressed on human genital epithelia binds HIV-1 envelope protein and facilitates viral transmission. *J Immunol.* (2007) 179:3126–32.
52. Bobardt MD, Saphire AC, Hung HC, Yu X, Van der Schueren B, Zhang Z, et al. (2003) Syndecan captures, protects, and transmits HIV to T lymphocytes. *Immunity*. (2003) 18:27–39.
53. Fanibunda SE, Modi DN, Gokral JS, Bandivdekar AH. HIV gp120 binds to mannose receptor on vaginal epithelial cells and induces production of matrix metalloproteinases. *PLoS ONE*. (2011) 6:e28014. doi: 10.1371/journal.pone.0028014
54. Madsen J, Gaiha GD, Palaniyar N, Dong T, Mitchell DA, Clark HW. Surfactant protein D modulates HIV infection of both T-cells and dendritic cells. *PLoS ONE*. (2013) 8:e59047. doi: 10.1371/journal.pone.0059047
55. Lawrence T. The nuclear factor NF-kappaB pathway in inflammation. *Cold Spring Harb Perspect Biol.* (2009) 1:a001651. doi: 10.1101/cshperspect.a001651
56. Weichhart T, Hengstschläger M, Linke M. Regulation of innate immune cell function by mTOR. *Nat Rev Immunol.* (2015) 15:599–614. doi: 10.1038/nri3901
57. Dodagatta-Marri E, Mitchell DA, Pandit H, Sonawani A, Murugaiah V, Idicula-Thomas S, et al. Protein-proteininteraction between surfactant protein D and DC-SIGN via C-type lectin domain can suppress HIV-1 transfer. *Front Immunol.* (2017) 8:834. doi: 10.3389/fimmu.2017.00834
58. Geijtenbeek TB, Kwon DS, Torensma R, van Vliet SJ, van Duijnhoven GC, Middel J, et al. DC-SIGN, a dendritic cell-specific HIV-1-binding protein that enhances trans-infection of T cells. *Cell.* (2000) 100:587–97.
59. Tecle T, White MR, Sorensen G, Gantz D, Kacak N, Holmskov U, et al. Critical role for cross-linking of trimeric lectin domains of surfactant protein D in antiviral activity against influenza A virus. *Biochem J.* (2008) 412:323–9. doi: 10.1042/BJ20071663
60. Hickling TP, Bright H, Wing K, Gower D, Martin SL, Sim RB, et al. A recombinant trimeric surfactant protein D carbohydrate recognition domain inhibits respiratory syncytial virus infection *in vitro* and *in vivo*. *Eur J Immunol.* (1999) 29:3478–84. doi: 10.1002/(SICI)1521-4141(199911)29:11<3478::AID-IMMU3478>3.0.CO;2-W
61. Hartl D, Griese M. Surfactant protein D in human lung diseases. *Eur J Clin Invest.* (2006) 36:423–35. doi: 10.1111/j.1365-2362.2006.01648.x
62. Card CM, Ball TB, Fowke KR. Immune quiescence: a model of protection against HIV infection. *Retrovirology*. (2013) 10:141. doi: 10.1186/1742-4690-10-141
63. Morris GC, Lacey CJ. Microbicides and HIV prevention: lessons from the past, looking to the future. *Curr Opin Infect Dis.* (2010) 23:57–63. doi: 10.1097/QCO.0b013e328334de6d
64. Oberley R, Goss K, Ault K, Crouch E, Snyder J. Surfactant protein D is present in the human female reproductive tract and inhibits *Chlamydia trachomatis* infection. *Mol Hum Reprod.* (2004) 10:861–70. doi: 10.1093/molehr/gah117
65. van Rozendaal BA, van Spriel AB, van De Winkel JG, Haagsman HP. Role of pulmonary surfactant protein D in innate defense against *Candida albicans*. *J Infect Dis.* (2000) 182:917–22. doi: 10.1086/315799
66. Eade CR, Cole AL, Diaz C, Rohan LC, Parniak MA, Marx P, et al. The anti-HIV microbicide candidate RC-101 inhibits pathogenic vaginal bacteria without harming endogenous flora or mucosa. *Am J Reprod Immunol.* (2013) 69:150–8. doi: 10.1111/aji.12036

Conflict of Interest Statement: The authors declare that the research was conducted in the absence of any commercial or financial relationships that could be construed as a potential conflict of interest.

The handling Editor declared a past co-authorship with the authors UK and TM.

frontiers in Immunology

ORIGINAL RESEARCH
published: 04 June 2018
doi: 10.3389/fimmu.2018.01126

A Recombinant Fragment of Human Surfactant Protein D induces Apoptosis in Pancreatic Cancer Cell Lines *via* Fas-Mediated Pathway

*Anuvinder Kaur[1], Muhammad Suleman Riaz[1], Valarmathy Murugaiah[1], Praveen Mathews Varghese[1], Shiv K. Singh[2] and Uday Kishore[1]**

[1] Biosciences, College of Health and Life Sciences, Brunel University London, Uxbridge, United Kingdom,
[2] Department of Gastroenterology and Gastrointestinal Oncology, University Medical Center, Goettingen, Germany

OPEN ACCESS

Edited by:
Janos G. Filep, Université de Montréal, Canada

Reviewed by:
Taruna Madan, National Institute for Research in Reproductive Health (ICMR), India
Soren Werner Karlskov Hansen, University of Southern Denmark Odense, Denmark
Kenneth Reid, University of Oxford, United Kingdom

***Correspondence:**
Uday Kishore
uday.kishore@brunel.ac.uk, ukishore@hotmail.com

Specialty section:
This article was submitted to Molecular Innate Immunity, a section of the journal Frontiers in Immunology

Received: *13 October 2017*
Accepted: *03 May 2018*
Published: *04 June 2018*

Citation:
Kaur A, Riaz MS, Murugaiah V, Varghese PM, Singh SK and Kishore U (2018) A Recombinant Fragment of Human Surfactant Protein D induces Apoptosis in Pancreatic Cancer Cell Lines via Fas-Mediated Pathway. Front. Immunol. 9:1126. doi: 10.3389/fimmu.2018.01126

Human surfactant protein D (SP-D) is a potent innate immune molecule, which is emerging as a key molecule in the recognition and clearance of altered and non-self targets. Previous studies have shown that a recombinant fragment of human SP-D (rfhSP-D) induced apoptosis *via* p53-mediated apoptosis pathway in an eosinophilic leukemic cell line, AML14.3D10. Here, we report the ability of rfhSP-D to induce apoptosis *via* TNF-α/Fas-mediated pathway regardless of the p53 status in human pancreatic adenocarcinoma using Panc-1 ($p53^{mt}$), MiaPaCa-2 ($p53^{mt}$), and Capan-2 ($p53^{wt}$) cell lines. Treatment of these cell lines with rfhSP-D for 24 h caused growth arrest in G1 cell cycle phase and triggered transcriptional upregulation of pro-apoptotic factors such as TNF-α and NF-κB. Translocation of NF-κB from the cytoplasm into the nucleus of pancreatic cancer cell lines was observed *via* immunofluorescence microscopy following treatment with rfhSP-D as compared to the untreated cells. The rfhSP-D treatment caused upregulation of pro-apoptotic marker Fas, as analyzed *via* qPCR and western blot, which then triggered caspase cascade, as evident from cleavage of caspase 8 and 3 analyzed *via* western blot at 48 h. The cell number following the rfhSP-D treatment was reduced in the order of Panc-1 (~67%) > MiaPaCa-2 (~60%) > Capan-2 (~35%). This study appears to suggest that rfhSP-D can potentially be used to therapeutically target pancreatic cancer cells irrespective of their p53 phenotype.

Keywords: pancreatic cancer, innate immunity, surfactant protein D, apoptosis, immune surveillance

INTRODUCTION

Human surfactant protein D (SP-D), a member of soluble C-type lectin family called Collectins, plays a vital role in linking the innate and adaptive immunity to protect against infection, allergy, and inflammation (1). Although its homeostatic role in lungs has been widely studied, its specific functions at extra-pulmonary tissues such as kidney, human trachea, brain, testis, heart, prostate, kidneys, and pancreas are poorly understood (1–3). SP-D deficiency in animal models has been shown to be associated with considerable pathophysiological consequences (4–6). SP-D gene knockout mice showed chronic inflammation and fibrosis due to accumulation of surfactant phospholipids in the lungs, monocytes infiltration, and activation of pro-inflammatory alveolar macrophages (5, 6). The absence of SP-D in children makes them more susceptible to frequent pneumonia as compared to

SP-D sufficient children (7). *SFTPD* (SP-D gene) polymorphisms increase the susceptibility to chronic and infectious lung diseases (8), pneumococcal lung disease (9), emphysema (10), tuberculosis (11, 12), Crohn's disease, and ulcerative colitis (12).

SP-D has been shown to be a potent innate immune molecule at pulmonary as well as extra-pulmonary mucosal surfaces by virtue of its ability to control inflammatory response and helper T cell polarization (3). The first clue came *via* a murine model of allergic hypersensitivity, when therapeutic treatment with a recombinant fragment of human SP-D (rfhSP-D) lowered peripheral and pulmonary eosinophilia, in addition to specific IgE levels and Th2 cytokines in the spleen (13, 14). It turned out that rfhSP-D selectively induced apoptosis in sensitized eosinophils derived from allergic patients (15). Using an eosinophilic cell line, AML14.3D10 (a model cell line for leukemia), it was established, *via* proteomics analysis, that apoptosis induction by rfhSP-D involved upregulation of p53 (16, 17). Another crucial study by Pandit et al. (18) revealed that rfhSP-D was able to induce apoptosis in activated human PBMCs, but not in resting, non-activated PBMCs. These studies, for the first time, raised the possibility that SP-D can have a function of immune surveillance against activated self and perhaps altered self. Recently, human lung adenocarcinoma cells (A549 cell line), when exogenously treated with SP-D, showed suppressed epidermal growth factor (EGF) signaling by reducing the EGF binding to EGFR, which subsequently reduced the cell proliferation, invasion, and migration of cancer cells (19).

Here, we set out to examine a possible pro-apoptotic role of SP-D in pancreatic cancer. Pancreatic cancer is the fourth leading cause of cancer-related mortality in the western world (20, 21) and its 5-year survival rate is ~5% (22). The poor prognosis has been attributed to the silent nature of the tumor in early stages, aggressive phenotype, surgical complications, and lack of targeted efficacious therapies (23). In this study, we show that rfhSP-D, composed of 8 Gly-X-Y repeats, homotrimeric neck and carbohydrate recognition domains (CRDs) (1), induces cell growth arrest in G1 phase and subsequent apoptosis in human pancreatic adenocarcinoma cells using Panc-1, MiaPaCa-2, and Capan-2 cell lines. The apoptosis induction appears to involve TNF-α, NF-κB, and Fas axis, revealing a p53 independent route of apoptosis induction in the p53 mutated Panc-1 and MiaPaCa-2 cell lines and p53-dependent apoptosis in p53 wild type Capan-2 cell line by rfhSP-D.

MATERIALS AND METHODS

Cell Culture and Treatments

Human pancreatic cancer cells lines, Panc-1 (CRL-1469), MiaPaCa-2 (CRL-1420), and Capan-2 (HTB-80), were obtained from ATCC and used as an *in vitro* model in this study. All cell lines were cultured at 37°C under 5% v/v CO_2 using DMEM-F12 media (Thermo Fisher) containing 10% v/v fetal calf serum with 2 mM L-glutamine, and penicillin (100 U/ml)/streptomycin (100 μg/ml) (Thermo Fisher) until 80–90% confluency was reached.

Expression and Purification of rfhSP-D

Plasmid pUK-D1 (containing cDNA sequences for 8 Gly-X-Y repeats, neck, and CRD region of human SP-D), transformed into *Escherichia coli* BL21 (λDE3) pLysS (Invitrogen), was used to express rfhSP-D, as described earlier (15, 16). The expression cassette included a short stretch of eight N-terminal Gly–X–Y triplets with substitution of S for P in position 2 (residue 180), followed by the α-helical coiled-coil neck region (residues 203–235) and the globular CRD region (residues 236–355). Endotoxin levels were determined using the QCL-1000 Limulus amebocyte lysate system (Lonza) and the assay was found to be linear over a range of 0.1–1.0 EU/ml (10 EU = 1 ng of endotoxin). The amount of endotoxin levels were <4 pg/μg of the rfhSP-D. Full length native SP-D (FL-SP-D) was purified form lung washings of alveolar proteinosis patients using methods previously described by Strong et al. (24).

Fluorescence Microscopy

All cell lines used in this study (Panc-1, MiaPaCa-2, and Capan-2) were grown on coverslips using 0.5×10^5 cells overnight. Next day, cells were washed three times with PBS before being incubated with rfhSP-D (20 μg/ml) in a serum-free DMEM-F12 medium. For rfhSP-D and FL-SP-D binding analysis, the coverslips were incubated for 1 h with mouse anti-human SP-D (rfhSP-D) and rabbit anti-human SP-D (FL-SP-D) (MRC Immunochemistry Unit, Oxford; 1:200), followed by goat anti-mouse IgG H&L (Cy5) and Goat anti-Rabbit IgG H&L Alexa Fluor 488 (1:500; Abcam), respectively, and Hoechst (1:10,000; Thermo Fisher) for fluorescence microscopy analysis. For apoptosis analysis *via* fluorescence microscopy using an FITC annexin V apoptosis detection kit with propidium iodide (PI) (BioLegend), the cells were incubated with rfhSP-D (20 μg/ml) for 48 h. After 48 h, the cells were incubated with annexin V binding buffer containing FITC annexin V (1:200), PI (1:200), and Hoechst (1:10,000) for 15 min, and washed twice with PBS before mounting on the slides to visualize under a HF14 Leica DM4000 microscope.

Flow Cytometry

Cell lines were plated in a 6-well plate (0.1×10^7) and incubated with rfhSP-D (20 μg/ml), FL-SP-D (10 and 20 μg/ml), and an

TABLE 1 | Target genes and terminal primers used in the qPCR analysis.

Target gene	Forward primer	Reverse primer
18S	5′-ATGGCCGTTCT TAGTTGGTG-3′	5′-CGCTGAGCCAG TCAGTGTAG-3′
Fas	5′-ACACTCACCAG CAACACCAA-3′	5′-TGCCACTGTTTC AGGATTTAA-3′
mTOR	5′-TGCCAACTATCT TCGGAACC-3′	5′-GCTCGCTTCACC TCAAATTC-3′
TNF-α	5′-GTATCGCCAGG AATTGTTGC-3′	5′-AGCCCATGTTGT AGCAAACC-3′
NF-κB	5′-TGAGGTACAGGC CCTCTGAT-3′	5′-GTATTTCAACCAC AGATGGCACT-3′
P53	5′-AGCACTGTCCAA CAACACCA-3′	5′-CTTCAGGTGGCT GGAGTGAG-3′

untreated control, for 24 and 48 h, followed by cell detachment using 5 mM EDTA, pH 8, and centrifugation at 1,200 × *g* for 5 min. For cell cycle analysis, the cells were fixed in 70% v/v ethanol for 30 min at 4°C, followed by PBS wash twice at 850 × *g*. The cells were then treated with ribonuclease (100 µg/ml) to ensure DNA staining without RNA contamination before staining with PI (50 µg/ml). 10,000 cells were then acquired for both treated and untreated samples and the PI histograms were plotted using the set markers within the analysis program of Novocyte Flow Cytometer. For apoptosis analysis *via* FACS, FITC annexin V apoptosis detection kit with PI (BioLegend) was used, as per manufacturer's instructions. Compensation parameters were acquired using unstained, untreated FITC stained, and untreated PI stained cells.

MTT Assay

MTT (3-[4,5-dimethylthiazol-2-yl]-2,5-diphenyltetrazolium bromide) (Thermo Fisher) assay was performed by incubating pancreatic cancer cells (0.1×10^5) in a 96-well microtiter plate with rfhSP-D, FL-SP-D (10 and 20 µg/ml), and an untreated control in serum-free DMEM-F12 medium for 48 h, followed by incubation with 50 µg/µl MTT (5 mg/ml stock) per well for 4 h at 37°C. Majority of the media was removed leaving behind 25 µl per well, which was mixed thoroughly with 50 µl of dimethyl

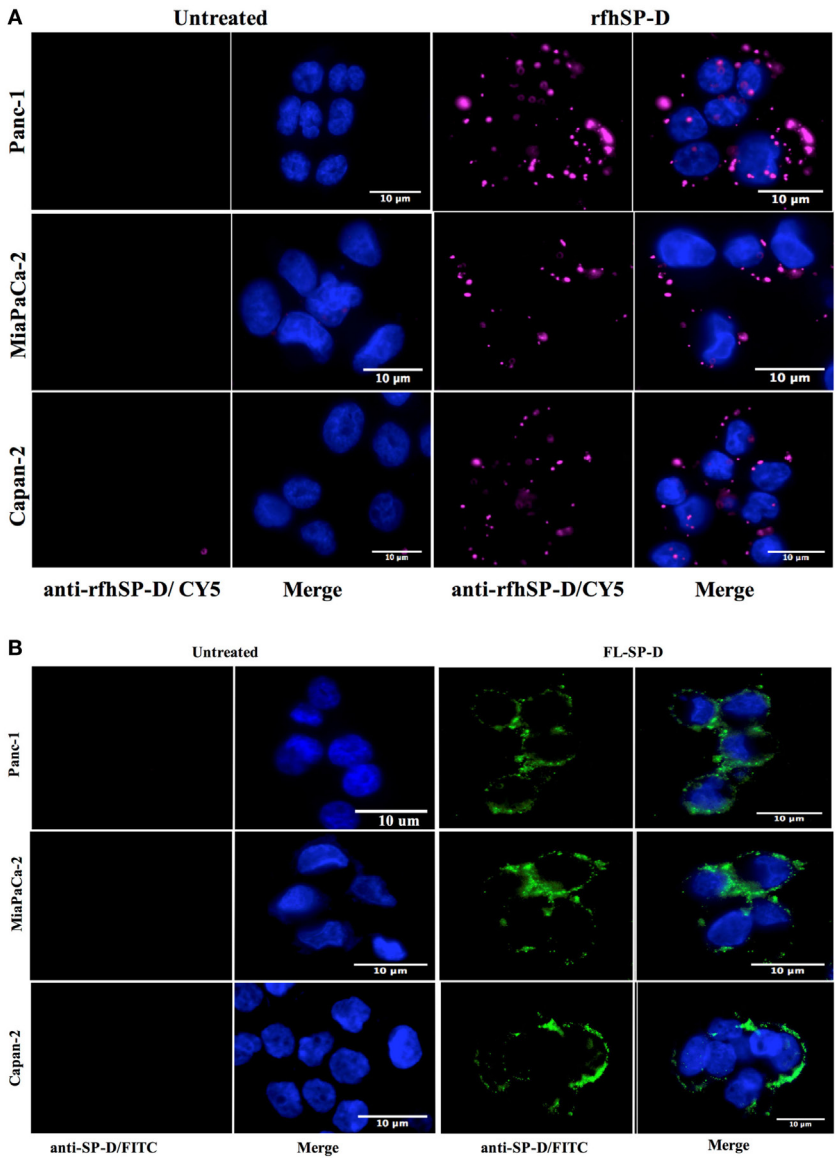

FIGURE 1 | **(A)** Fluorescence microscopy showing binding of rfhSP-D and **(B)** FL-SP-D (10 µg/ml; 1 h incubation) to Panc-1, MiaPaCa-2, and Capan-2 cells. The nucleus of the cells was stained with Hoechst. Cells were probed with mouse anti-human SP-D/CY5 (rfhSP-D) and rabbit anti-human/FITC (FL-SP-D); the bound proteins are visible on the cell membrane in the treated cells. No CY5 or FITC fluorescence was detected in the untreated control cells.

sulfoxide and incubated for another 10 min at 37°C. The absorbance was read at 570 nm using a plate reader.

Western Blot

Cell lines (0.1×10^7 cells) were seeded in a 6-well plate (Nunc) and incubated with rfhSP-D (20 µg/ml), together with an untreated control, in a serum-free DMEM-F12 medium. The cells were lysed within the wells using treatment buffer (50 mM Tris-HCl pH 6.8, 2% v/v β-mercaptoethanol, 2% v/v SDS, 0.1% w/v bromophenol blue, and 10% v/v glycerol) and transferred to pre-cooled microcentrifuge tubes followed by sonication for 15 s. The samples were heated at 100°C for 10 min and subjected to SDS-PAGE (12% w/v) for 90 min at 120 V. The SDS-PAGE separated proteins were then electrophoretically transferred onto a nitrocellulose membrane (Thermo Fisher) using an iBLOT (Thermo Fisher). The membrane was then blocked using 5% w/v dried milk powder (Sigma) in 100 ml PBS for 2 h on a rotatory shaker at room temperature. The membrane was incubated with rabbit anti-human caspase primary antibodies (anti-cleaved caspase 3; anti-cleaved caspase 8; Cell Signaling) at 4°C overnight, followed by incubation with secondary Goat anti-rabbit IgG HRP-conjugate (1:1,000; Promega) for 1 h at room temperature. The membrane was washed with PBST (PBS + 0.05% Tween 20) three times, 10 min each time. The color was developed using 3,3′-diaminobenzidine substrate kit (Thermo Fisher).

Quantitative RT-PCR

Panc-1, MiaPaCa-2, and Capan-2 cells were incubated with and without rfhSP-D (20 µg/ml) for various time points. The cell pellet

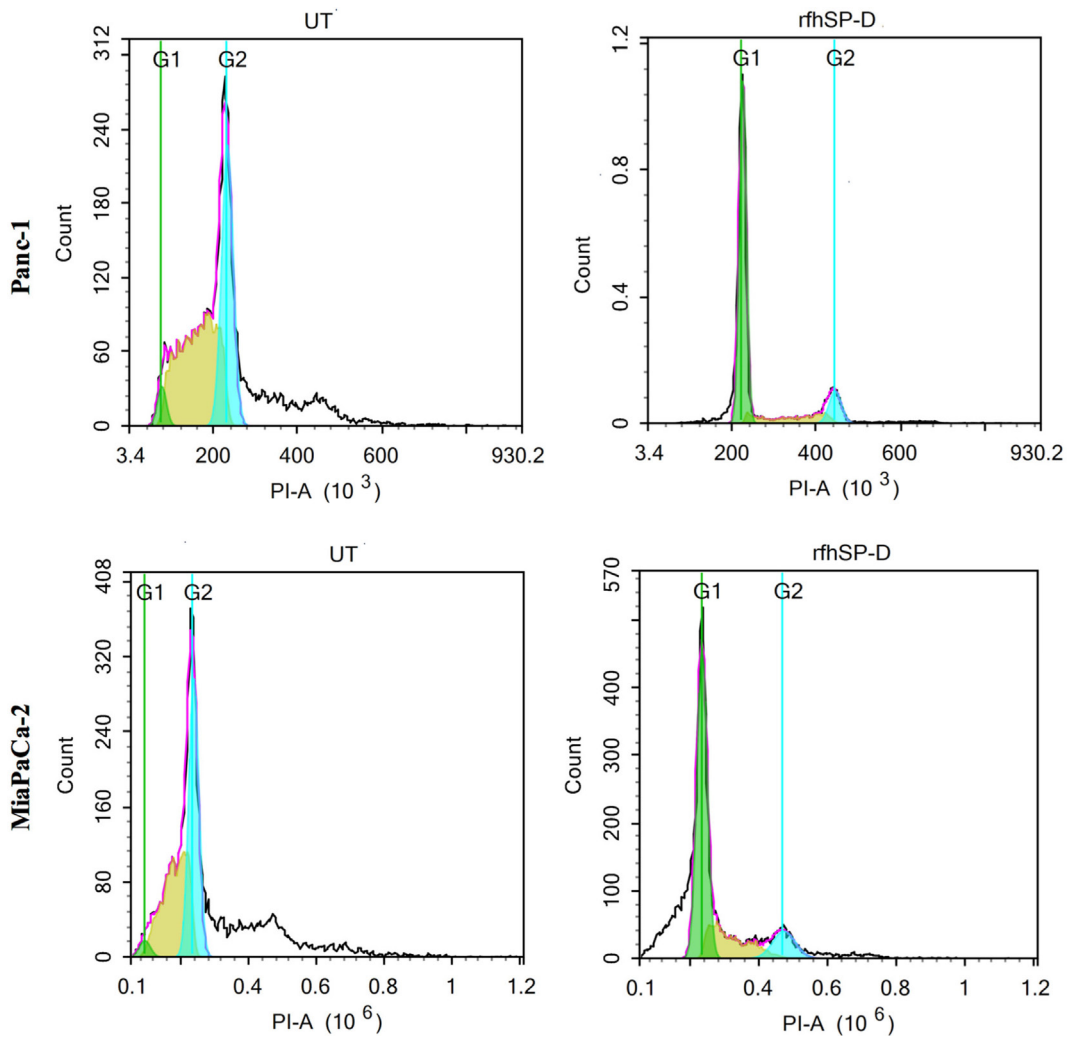

FIGURE 2 | Cell cycle analysis following 24 h treatment of pancreatic cancer cell lines with rfhSP-D. Propidium iodide (PI) was used to stain DNA. PI histograms were plotted using set markers within the analysis program of Novocyte Flow cytometer. The rfhSP-D treated pancreatic cancer cells show arrest in G1 phase in the case of Panc-1 (G1 phase: 68%; S phase: 13%; G2 phase: 11%) and MiaPaCa-2 (G1 phase: ~50%; S phase: 17%; G2 phase: 10%) cell line at 24 h, whereas untreated Panc-1 cells (G1 phase: 3%; S phase: 42%; G2 phase: 32%) and MiaPaCa-2 cells (G1 phase: 2%; S phase: 32%; G2 phase: 33%) progressed to the next cell cycle phases.

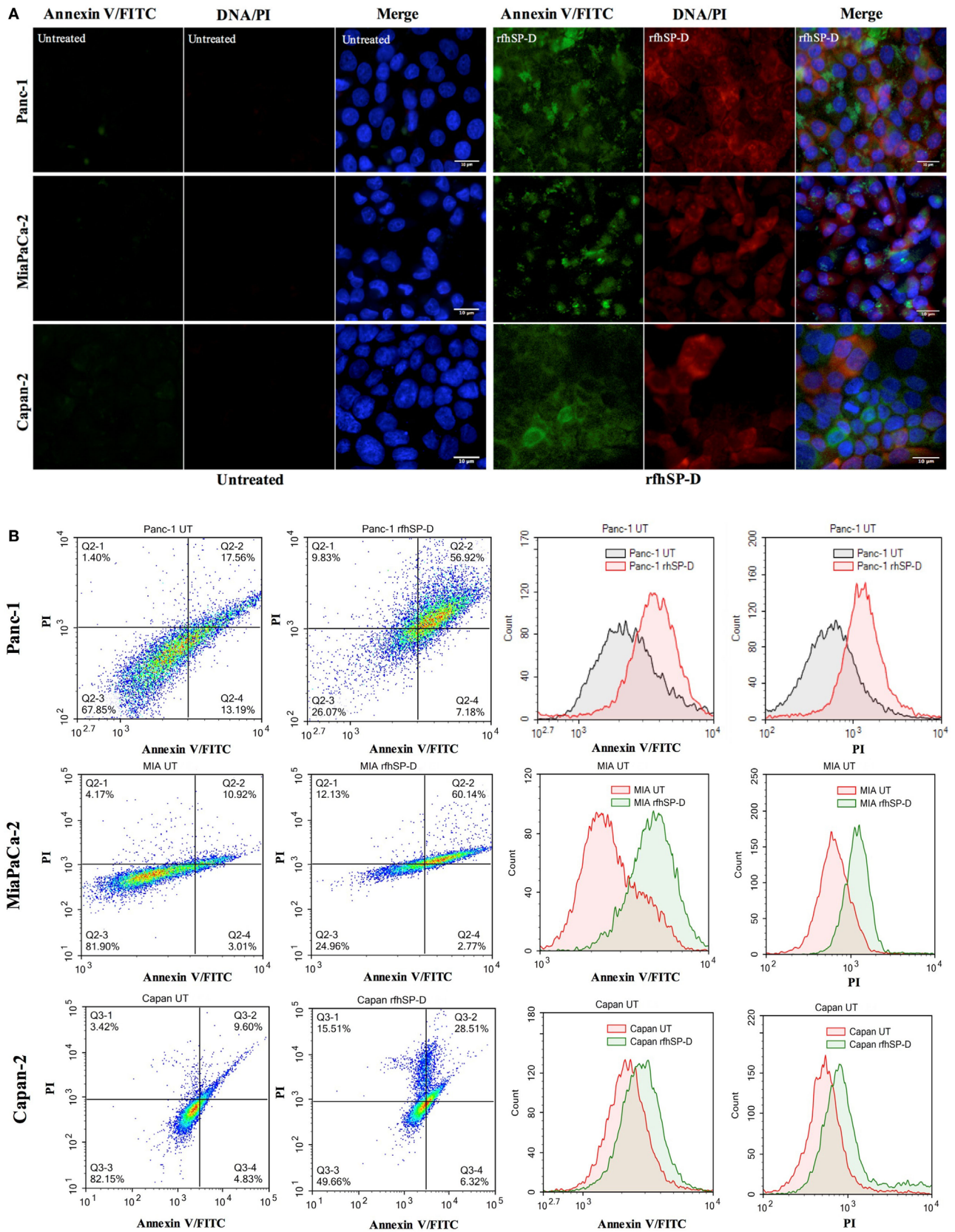

FIGURE 3 | Continued

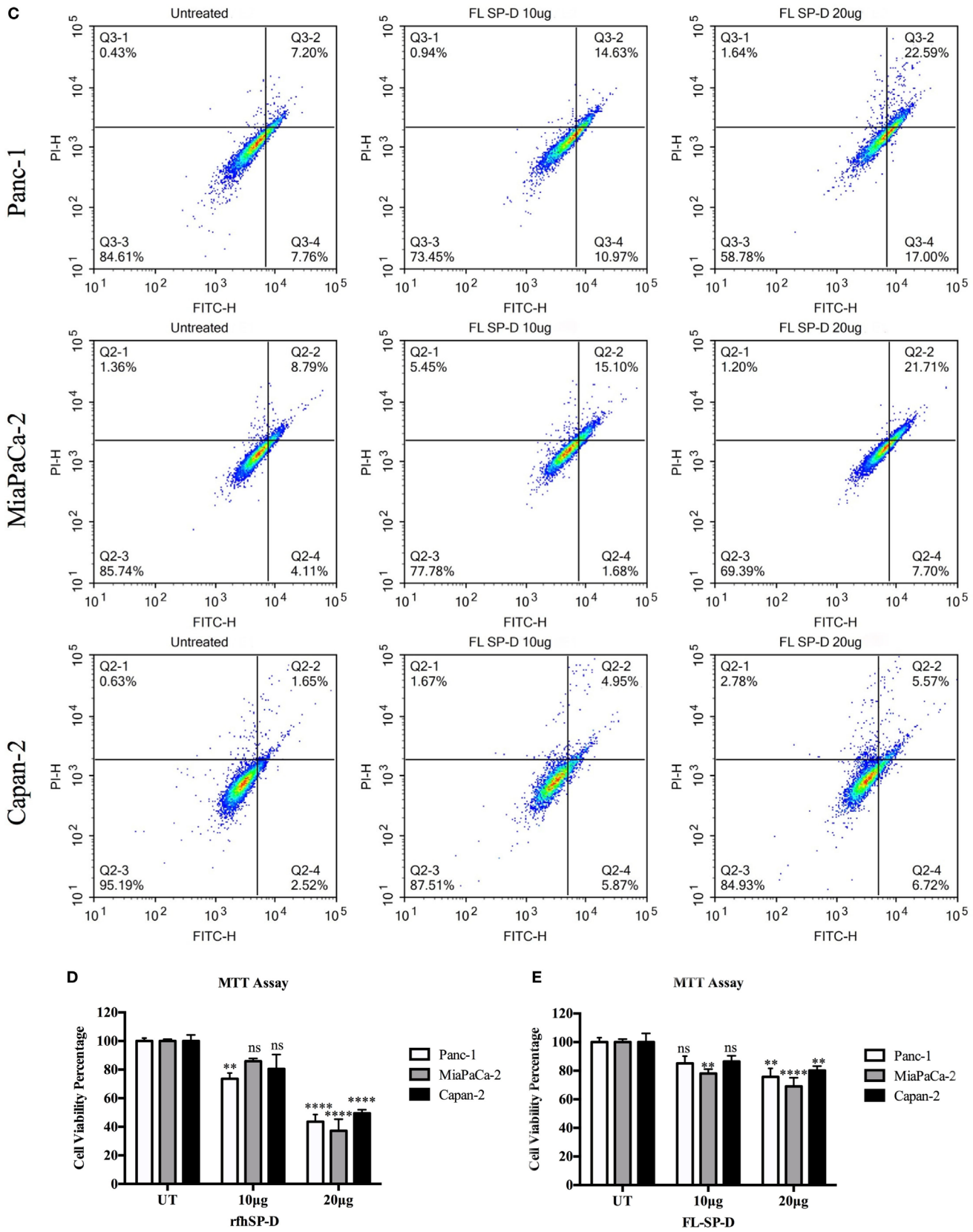

FIGURE 3 | Continued

FIGURE 3 | **(A)** Fluorescence microscopy to analyze apoptosis in pancreatic cancer cell lines following treatment with rfhSP-D. Cells were treated with rfhSP-D for 48 h and apoptosis was analyzed using an annexin V/propidium iodide (PI) staining kit. The cell membrane was positively stained for annexin V and the DNA staining is visible in the treated cells indicating that the cells underwent apoptosis turning the membrane inside out, thus making phosphatidylserine available for annexin V binding; due to the porous membrane, PI was taken in which stained the DNA of apoptotic cells. No such staining was seen in the untreated cells. The nucleus was stained with Hoechst for both treated and untreated cells. **(B,C)** Quantitative analysis of apoptosis using Flow Cytometer. Cells were treated with rfhSP-D or FL-SP-D for 48 h and apoptosis was analyzed using annexin V with PI kit. 10,000 cells were acquired and plotted for both annexin V/FITC and DNA/PI staining, which showed a shift in the fluorescence intensity of both FITC and PI between treated and untreated cells. Approximately 67% of Panc-1 cells, ~60% MiaPaCa-2 cells, and ~35% Capan-2 cells underwent apoptosis following rfhSP-D treatment and ~25% Panc-1 and MiaPaCa-2 cells following FL-SP-D treatment as compared to untreated cells. No significant difference was seen in Capan-2 cells following FL-SP-D treatment. **(D,E)** MTT assay to assess cell viability following treatment with rfhSP-D and FL-SP-D (10 and 20 μg/ml) and untreated for 48 h (±SEM, of three independent experiments). Cell numbers were reduced by approximately 70% in the rfhSP-D-treated Panc-1, 60% in MiaPaCa-2, and 45% in Capan-2 cells, as compared to untreated cells. Cell numbers were reduced by approximately 25% in the Panc-1 and MiaPaCa-2 and less than 10% in Capan-2 cells treated with FL-SP-D as compared to untreated cells. Significance was established using the unpaired two-way ANOVA test (**$p < 0.01$, ****$p < 0.0001$, ns: non-significant) ($n = 3$).

for each time-point was centrifuged and stored at −80°C. RNA was extracted using GenElute Mammalian Total RNA Purification Kit (Sigma-Aldrich, UK), as per manufacturer's instructions, followed by treatment with DNase I (Sigma-Aldrich, UK). The absorbance at 260 and 260:280 nm ratio was used to determine the concentration and purity of total RNA, respectively, using NanoDrop 2000/2000c (Thermo-Fisher Scientific). Total RNA (2 μg) was used for cDNA synthesis using High Capacity RNA to cDNA Kit (Applied Biosystems). The forward and reverse primers used in this study were designed using the web based Basic Local Alignment Search Tool and Primer-BLAST (http://blast.ncbi.nlm.nih.gov/Blast.cgi) are given in **Table 1**.

Relative mRNA expression was determined by qPCR reactions performed in triplicates consisting of 10 μl final volume per well [5 μl Power SYBR Green MasterMix (Applied Biosystems), 75 nM of forward and reverse primers, and 500 ng cDNA], using the 7900HT Fast Real-Time PCR System (Applied Biosystems). Samples were initially incubated at 50°C (2 min) and 95°C (10 min), followed by 40 cycles (each cycle for 15 s at 95°C and 1 min at 60°C) for amplification of the template. Human 18S rRNA, an endogenous control, was used to normalize the gene expression. Relative quantification (RQ) value and formula: $RQ = 2^{-\Delta\Delta Ct}$ was used to calculate the relative expression of each target.

Statistical Analysis

Graphs were made and statistically analyzed using Graphpad Prism 6.0 by applying an unpaired two-way ANOVA test. Significance of values is based on *$p < 0.05$, **$p < 0.01$, ***$p < 0.001$, ****$p < 0.0001$ between treated and untreated samples. Error bars represent the SD or SEM, as indicated in the figure legends.

RESULTS

rfhSP-D Binds to a Range of Pancreatic Cell Lines

The fluorescence microscopy analysis of rfhSP-D and FL-SP-D binding to Panc-1, MiaPaCa-2, and Capan-2 cells revealed its membrane localization following 1 h incubation at 4°C (**Figure 1**). The rfhSP-D probed with mouse anti-human SP-D-CY5 antibody and FL-SP-D probed with rabbit anti-human SP-D-FITC appeared evenly bound in clusters on the cell membrane, along with nucleus stained positively with Hoechst. All cell lines showed a similar rfhSP-D and FL-SP-D binding pattern. No CY5 or FITC fluorescence was detected in the untreated controls, probed with primary and secondary antibodies, for each cell line, suggesting the rfhSP-D and FL-SP-D binding observed in the treated cell lines was protein-specific.

rfhSP-D Induces Cell Cycle Arrest in G1 Phase in Panc-1 and MiaPaCa-2

Panc-1, MiaPaCa-2, and Capan-2 cell lines were individually treated with rfhSP-D for 24 h to assess whether rfhSP-D induced growth arrest. DNA binding dye, PI, was used to analyze the cell cycle for both treated and untreated cells *via* DNA quantitation. rfhSP-D induced inhibition of DNA synthesis in treated Panc-1 (68%) and MiaPaCa-2 (50%) in comparison to untreated Panc-1 (3%) and MiaPaCa-2 (2%) cells, respectively, as the cells were arrested in G1 phase (**Figure 2**). DNA synthesis was unaffected in the untreated cells for both cell lines since Panc-1 (43%) and MiaPaCa-2 (31%) were seen in S phase and Panc-1 (32%) and MiaPaCa-2 (33%) in the G2 phase of cell cycle. The growth arrest was, however, not seen in Capan-2 cell line following the rfhSP-D treatment (data not shown). Growth arrest at 24 h following rfhSP-D treatment prompted the determination of cell fate at a later time point; therefore, all cell lines were analyzed for likely apoptosis at 48 h.

rfhSP-D Induces Apoptosis Induction in Pancreatic Cancer Cells by 48 h

The qualitative apoptosis analysis of Panc-1, MiaPaCa-2, and Capan-2 treated with FL-SP-D or rfhSP-D for 48 h using immunofluorescence microscopy (**Figure 3A**) showed that the cell membrane was disoriented and the PI bound to DNA in the treated cells as compared to untreated cells, where no florescence was detected, indicating that cells were undergoing apoptosis at 48 h.

The flow cytometry analysis to quantify apoptosis showed significant reduction in the viable cell percentage of Panc-1, MiaPaCa-2, and Capan-2. The rfhSP-D induced apoptosis in ~67% of Panc-1 cells at 48 h, out of which, ~57% Panc-1 cells were both FITC and PI positive and ~7% were FITC alone positive, suggesting annexin V/FITC binding to phosphatidylserine, a cell membrane phospholipid, which is externalized during early apoptotic stage and the passage of PI, a DNA stain, through the porous cell membrane into the nucleus in order to intercalate the DNA. Approximately, 10% cells were PI alone positive, which

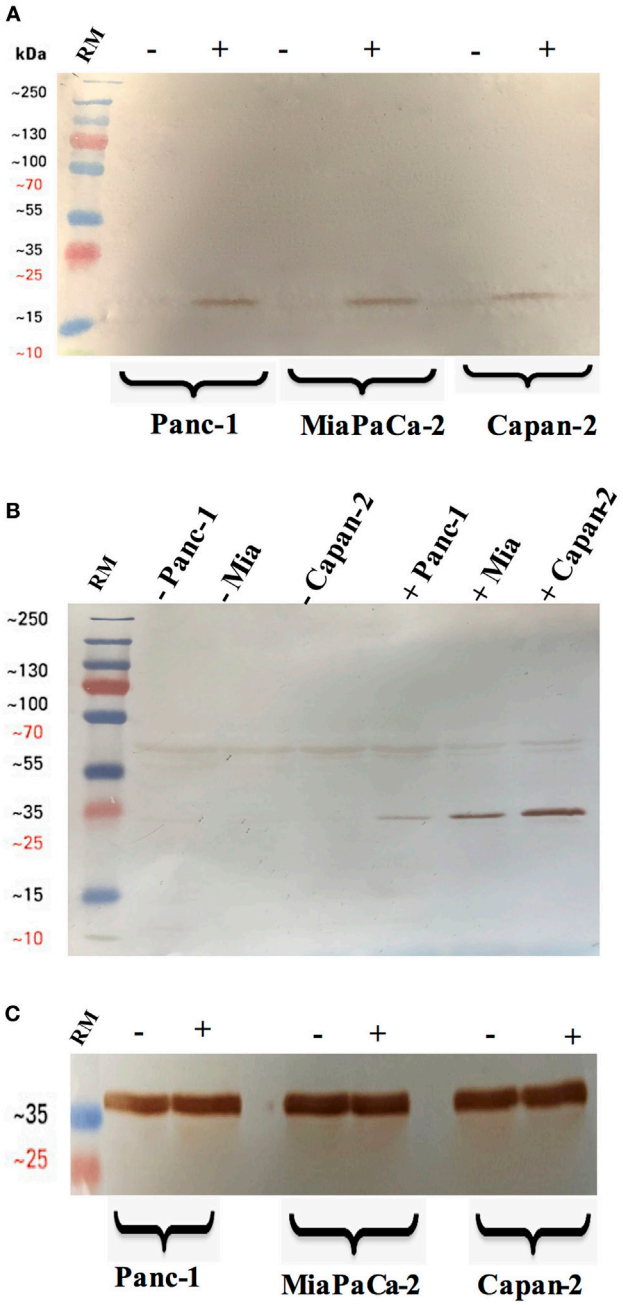

FIGURE 4 | Cleavage of caspase 3 **(A)** and 8 **(B)** in pancreatic cancer cell lines following rfhSP-D treatment. Pancreatic cancer cell lines were analyzed for caspase 8 and 3 activation *via* western blot using anti-rabbit cleaved caspase 3 and 8 (1:1,000) at 4°C overnight, followed by incubation with secondary anti-rabbit IgG HRP-conjugate (1:1,000) for 1 h at room temperature. The membrane was washed with PBST (PBS + 0.05% Tween 20) three times, 10 min each between each step. The bands were developed using 3,3′-diaminobenzidine substrate kit. The cleaved caspase 3 and 8 were detected only in the rfhSP-D treated samples of all cell lines, whereas no bands appeared in the untreated cell samples. Full-length caspase 8 bands are visible around 43 kDa. **(C)** Anti-GAPDH was used as a loading control.

suggested that these cells were either dead or in late apoptotic stage. The percentage of viable cells, i.e., unstained, in the untreated sample was significantly higher (70%) as compared to treated (26%) (**Figure 3B**). The rfhSP-D induced apoptosis in MiaPaCa-2 was ~60%. However, rfhSP-D induced apoptosis in Capan-2 (~35%) cell line, which was not as much as in Panc-1 and MiaPaCa-2 cell lines (**Figure 3B**). The treatment with FL-SP-D (20 μg/ml) for 48 h induced apoptosis in approximately 25% of Panc-1 and MiaPaCa-2 cell lines, and less than 10% in Capan-2 cell line. No significant difference was seen with FL-SP-D (10 μg/ml)

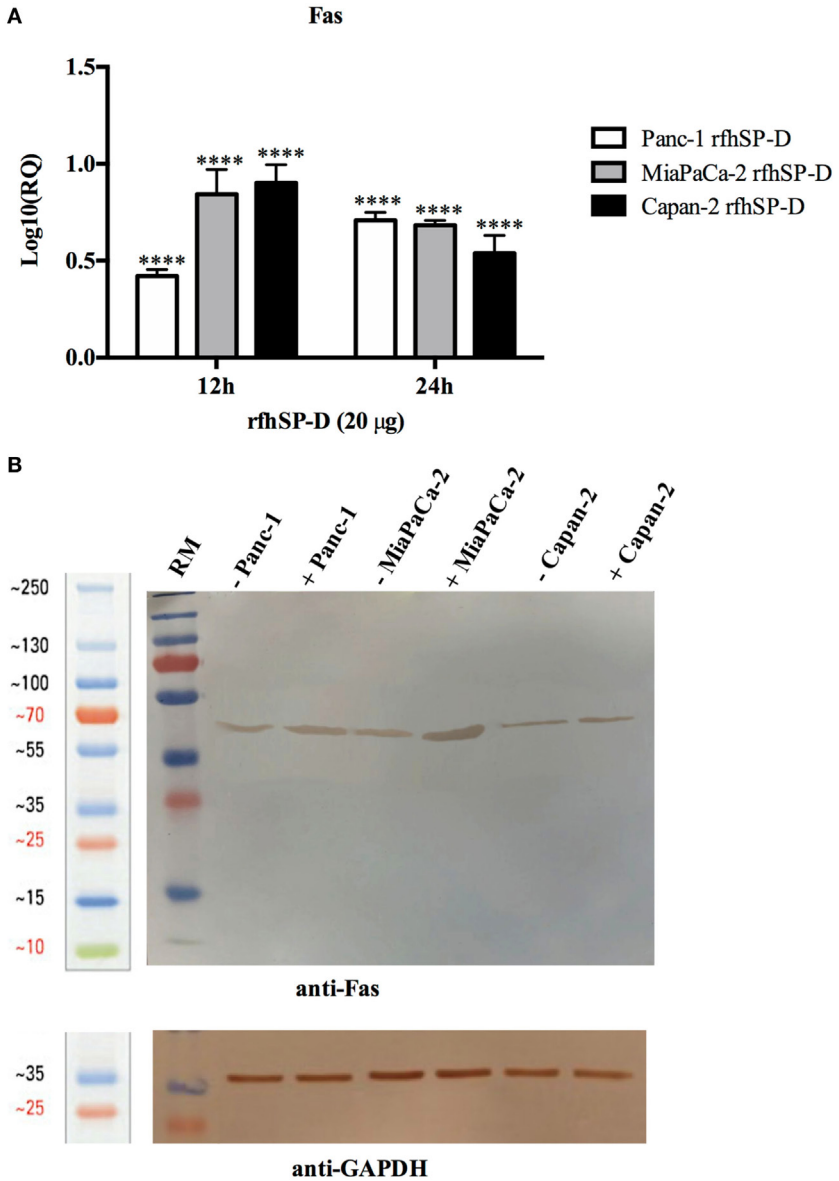

FIGURE 5 | Relative quantification (RQ) of Fas mRNA expression in Panc-1, MiaPaCa-2, and Capan-2 cell lines treated with rfhSP-D (20 μg/ml) for 12 and 24 h. **(A)** Fas expression was upregulated in the treated samples at 12 and 24 h as compared to untreated cells. Significance was determined using the unpaired two-way ANOVA test (****$p < 0.0001$) ($n = 3$). **(B)** Fas expression *via* western blot analysis in pancreatic cell lines treated with rfhSP-D for 24 h using rabbit anti-human Fas (1:1,000) at 4°C overnight, followed by incubation with secondary anti-rabbit IgG HRP-conjugate (1:1,000) for 1 h at room temperature. The bands were developed using diaminobenzidine substrate kit. Fas expression at ~50 kDa was upregulated in the treated samples at 24 h for all cells as compared to untreated. Anti-GAPDH used as a loading control.

treatment for 48 h in all the cell lines investigated in this study (**Figure 3C**).

The cell viability analysis *via* MTT assay following rfhSP-D treatment showed ~60% decrease in the cell viability of Panc-1 and MiaPaCa-2 and 45% in Capan-2 as compared to untreated (**Figure 3D**) and BSA (10 and 20 μg/ml; data not shown) controls. The cell viability analysis *via* MTT assay following FL-SP-D treatment also showed consistent reduction as seen in flow cytometer analysis (**Figure 3E**). Apoptosis was further confirmed by analyzing the activation of caspase to determine the pathway involved.

rfhSP-D Activates Cleavage of Caspase 8 and 3

Western blot analysis revealed that caspase 8 and 3 were cleaved in all the cell lines following treatment with rfhSP-D for 48 h (**Figure 4**). The cleavage of caspase 3, however, was not seen in the untreated cells and faint bands appeared for caspase 8 in

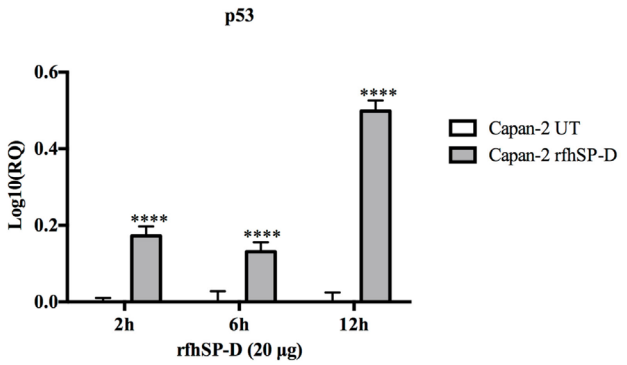

FIGURE 6 | Relative quantification (RQ) of p53 mRNA expression in Capan-2 cell line treated with rfhSP-D (20 µg/ml) for 2, 6, and 12 h. p53 expression was significantly upregulated in the rfhSP-D-treated samples at 2, 6, and 12 h as compared to the untreated. Significance was determined using the unpaired two-way ANOVA test (****$p < 0.0001$) ($n = 3$).

the untreated cells (**Figure 4**), which further confirmed that cell death occurred *via* apoptosis. Interestingly, although Capan-2 cell line appeared unaffected in terms of cell cycle arrest at 24 h; yet, the cleaved bands for caspase 8 and 3 were seen in Capan-2 treated cells too, which suggested that rfhSP-D can affect the cancer cells *via* multiple pathways. Caspase 9 was tested as a marker for intrinsic apoptosis pathway; however, no difference was noted between treated and untreated cells (data not shown). Therefore, gene expressions were assessed for pro-apoptotic genes such as Bax, an intrinsic pathway marker, and Fas, an extrinsic pathway marker, to further determine the apoptotic pathway.

rfhSP-D Upregulates the Expression of Pro-Apoptotic Marker, Fas

Human pancreatic cancer cells often escape apoptosis by down-regulating apoptosis stimulators such as FasL/FasR (25), or pro-apoptotic proteins such as Bax (26). These pro-apoptotic genes, Bax and Fas, for time-points ranging from 2 to 24 h in all the cell lines, were analyzed. Bax was unaffected following the treatment with rfhSP-D in Panc-1 and MiaPaCa-2 cell lines at all time-points (data not shown), which, in addition to unaffected caspase 9, suggested that intrinsic pathway may not have been involved in causing the cell death in these cell lines. Fas expression was unaffected at earlier time-points up to 6 h (data not shown); however, it was upregulated at 12 and 24 h in Panc-1 ($\log_{10}$ ~0.5), MiaPaCa-2 ($\log_{10}$ ~1), and Capan-2 ($\log_{10}$ ~1) cell lines (**Figure 5A**), which indicated that apoptosis induction by rfhSP-D is likely to take place *via* the extrinsic pathway. Western blot analysis also showed upregulation of Fas at the protein level in rfhSP-D treated cells as compared to untreated cells (**Figure 5B**). Since TNF-α and NF-κB are crucial factors in the apoptotic pathway and they can regulate Fas expression (27), the effect of rfhSP-D on the gene expression of TNF-α and NF-κB as well as translocation of NF-κB from the cytoplasm to nucleus was investigated.

rfhSP-D Upregulates p53 Expression in Capan-2 Cell Line

The p53 transcript levels were measured by qPCR following the treatment with rfhSP-D at 2, 6, and 12 h in Capan-2 cells and compared with the p53 levels in untreated cells for each time-point. Interestingly, the levels of p53 were upregulated, most significantly at 12 h, which suggested that p53 may also have contributed to the apoptosis in Capan-2 cells (**Figure 6**).

rfhSP-D Upregulates the Expression of TNF-α and Causes Nuclear Translocation of NF-κB

Following treatment with rfhSP-D, the analysis of TNF-α mRNA expression levels showed a significant upregulation in Panc-1 ($\log_{10}$ ~0.5), MiaPaCa-2 ($\log_{10}$ ~1), and Capan-2 ($\log_{10}$ ~1) at 12 and 24 h; however, no difference was observed at earlier time-points. Similar transcriptional upregulation was noted for NF-κB for Panc-1 ($\log_{10}$ ~0.4), MiaPaCa-2 ($\log_{10}$ ~0.8), and Capan-2 ($\log_{10}$ ~0.6) at 12 and 24 h (**Figure 7A**). Immunofluorescence microscopy of Panc-1, MiaPaCa-2, and Capan-2 cell lines showed that NF-κB was translocated to the nucleus at 24 h, which was not seen in the untreated cells (**Figure 7B**). This further confirmed that NF-κB could play a key role in deciding the apoptotic fate of the pancreatic cancer cells following the rfhSP-D treatment.

rfhSP-D Downregulates the Survival Pathway, mTOR

The mTOR is often deregulated in the pancreatic cancer (28) and its activation is associated with poor prognosis (29). Upon treatment with rfhSP-D, mRNA expression of mTOR was downregulated in Panc-1 and MiaPaCa-2 cell line at 12 h (**Figure 8A**), however, no difference was seen in Capan-2 (data not shown). In addition, immunofluorescence analysis revealed that in comparison to the untreated cells, a significant decrease in the cytoplasmic levels and an increased accumulation of mTOR in the nucleus of MiaPaCa-2 cells was evident (**Figure 8B**), where it has been shown to be present in its inactive form (30).

DISCUSSION

In this study, we show that a recombinant fragment of human surfactant protein D (rfhSP-D) induces apoptosis in a range of pancreatic cancer cell lines. We show that rfhSP-D induces apoptosis regardless of p53 status using two p53 mutated, aggressive cell lines, Panc-1 (derived from head of the pancreas), MiaPaCa-2 (derived from the body and tail of the pancreas), and a p53 wild type, non-aggressive cell line, Capan-2 (derived from head of the pancreas) (31).

Following the treatment with rfhSP-D, Panc-1 and MiaPaCa-2 cells were arrested in G1 phase at 24 h, whereas untreated cells progressed to S and G2 phase. In addition, upregulation of Fas, an apoptosis stimulator, and pro-apoptotic TNF-α (and associated transcription factor, NF-κB) at 24 h was consistent with the cleavage of caspase 8 and 3 at 48 h. These findings indicated that cell death is likely to occur *via* TNF-α/

Fas-mediated apoptosis pathway (32–34). The cell viability after 48 h of rfhSP-D treatment was reduced in the order of Panc-1 > MiaPaCa-2 > Capan-2, which coincided with the approximate growth arrested percentage of Panc-1 and MiaPaCa-2 at 24 h. Although Capan-2 cells were not arrested in the cell cycle, yet they underwent apoptosis at 48 h, which may be attributed to their increased sensitivity to Fas-mediated apoptosis as compared to other two cell lines (25) and upregulation of p53 transcripts following the treatment with rfhSP-D, as reported previously (16). Treatment with FL-SP-D induced apoptosis in approximately 25% of Panc-1 and MiaPaCa-2, compared to Panc-1 (~67%) > MiaPaCa-2 (~60%) > Capan-2 (~35) by rfhSP-D. This quantitative difference is likely to be due to difference in the molar ration of the two proteins at the same concentration.

Fas is a type I membrane protein that belongs to TNF superfamily (35, 36) that undergoes trimerization upon binding to its physiological ligand, FasL, to form a Fas-associated death domain protein (FADD) *via* its cytoplasmic domain (37, 38). It then activates downstream caspase cascade, which subsequently causes cleavage of caspase 3 as the terminal molecular event during apoptosis (39, 40). When the Panc-1, MiaPaCa-2, and Capan-2 cell lines were treated with rfhSP-D, Fas remained unaffected up to 12 h. Upregulation of Fas transcripts as well as protein was seen at 24 h, indicating that TNF-α (41) and NF-κB (33) might also be affected since they are well known to tightly regulate the Fas-mediated apoptosis pathway. TNF-α, another member of TNF superfamily, acts *via* TNFR2 to increase the susceptibility of the target cells to Fas-mediated death; in addition, it stimulates the downstream NF-κB signaling (42) by recruitment and activation

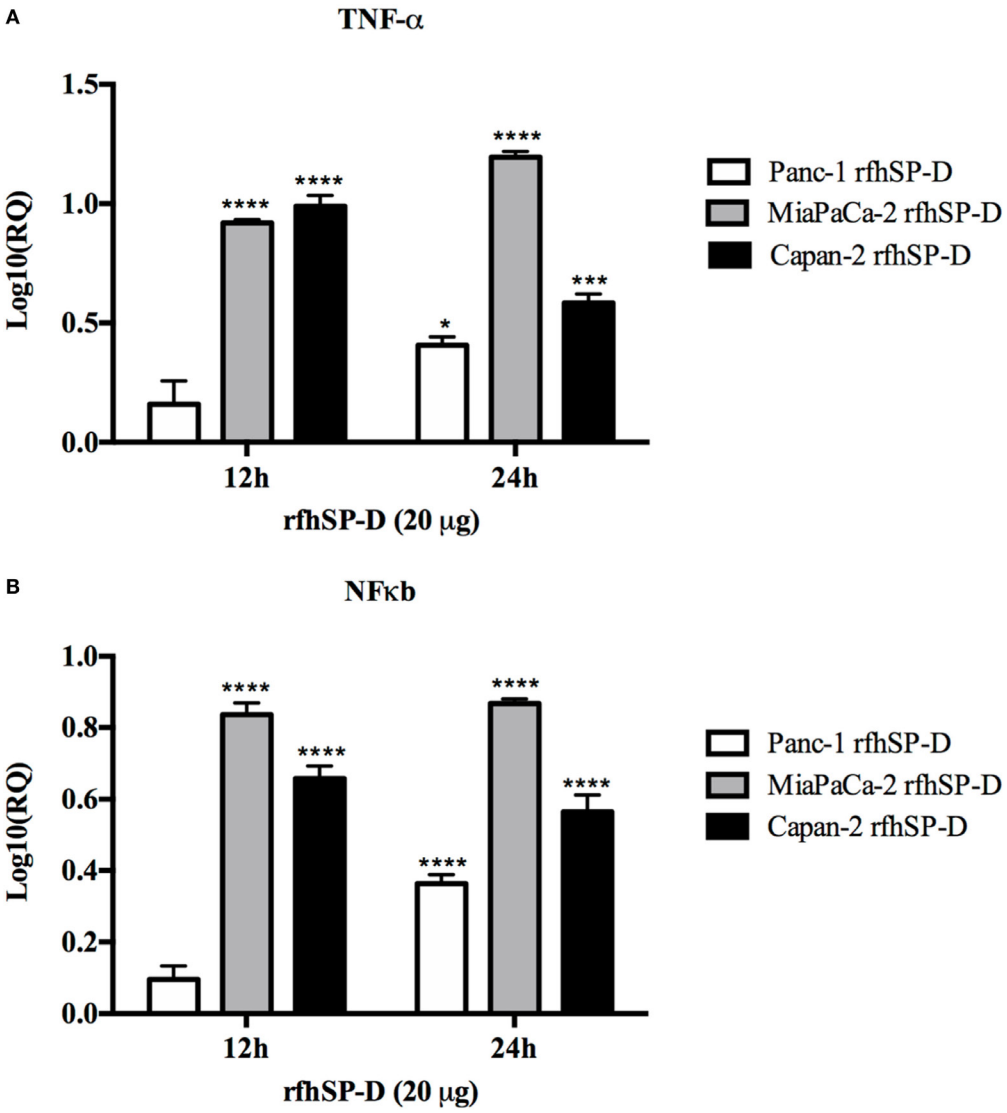

FIGURE 7 | Continued

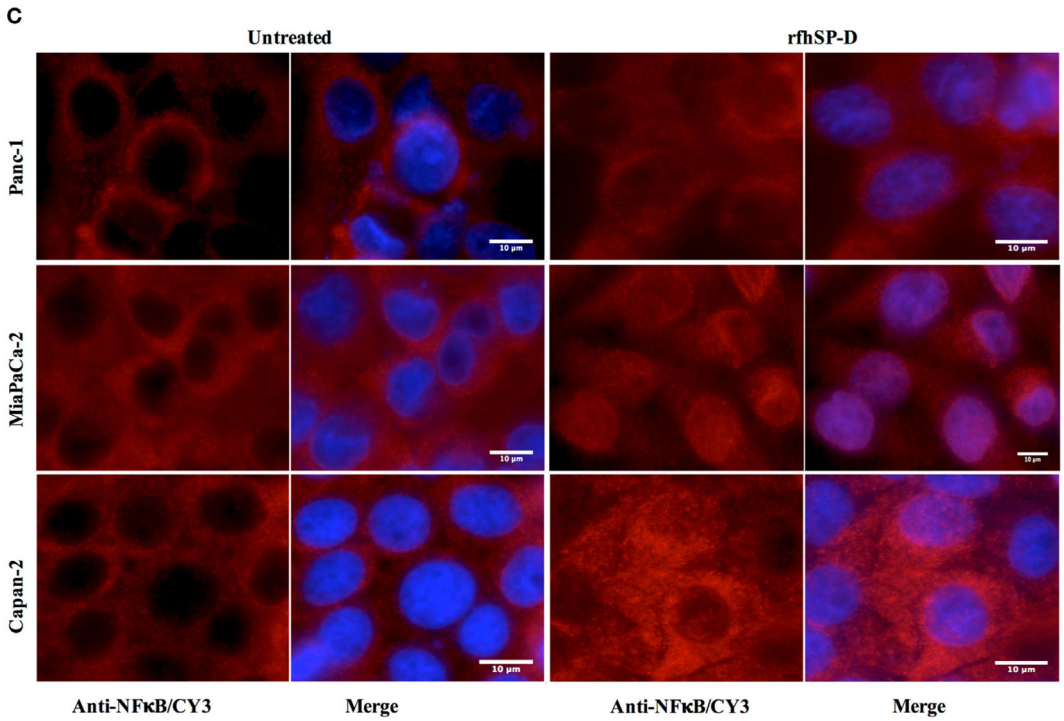

FIGURE 7 | Relative quantification (RQ) comparisons of TNF-α **(A)** and NF-κB **(B)** mRNA expression in Panc-1, MiaPaCa-2, and Capan-2 cell lines treated with rfhSP-D (20 µg/ml) for 12 and 24 h. The transcriptional expressions of both TNF-α and NF-κB were upregulated in the treated samples at 12 and 24 h as compared to untreated. Significance was determined using the unpaired two-way ANOVA test (*$p < 0.05$, ***$p < 0.001$, ****$p < 0.0001$) ($n = 3$). **(C)** Immunofluorescence microscopy to determine the translocation of NF-κB into nucleus following rfhSP-D treatment. Anti-NF-κB stained positively in the nucleus of treated cells as compared to untreated in all cell lines at 24 h.

of inhibitor of IκB kinases (IKK), which in turn enables its translocation to the nucleus where transcription of NF-κB-dependent genes such as Fas occurs (33, 43).

In this study, transcriptional levels of both NF-κB and TNF-α were upregulated at the same time-point as Fas, which was largely anticipated (33). In addition, the immunofluorescence microscopy revealed NF-κB translocation to nucleus at 24 h in the rfhSP-D-treated cells as compared to the untreated counterpart, which suggested that TNF-α induced canonical NF-κB pathway (44). NF-κB can regulate both pro- as well as anti-apoptotic genes, depending upon its canonical or non-canonical signaling (43, 44). Interestingly, canonical NF-κB has been shown to bind directly to the Fas promoter to facilitate cell death *via* Fas-mediated pathway (33). NF-κB plays an important role in deciding the cell fate as its canonical activation acts a transcription factor of Fas, which upon stimulation induces apoptosis signaling (32, 33). However, SP-D has been shown to regulate steady-state NF-κB activation in alveolar macrophages of SP-D deficient mice (45). Interestingly, SP-D has also been shown to trigger TNF-α production in human $CCR2^+$ inflammatory monocytes (46). These studies present an interesting central role of SP-D and their interdependent regulation, which could be important in deciding the cell viability/apoptosis. Moreover, cleaved caspase 8 and 3 were seen at 48 h, whereas intrinsic apoptosis markers such as caspase 9 and Bax remained unaffected (27), in all rfhSP-D-treated pancreatic cancer cell lines as compared to untreated cells, which further confirmed the cell death *via* Fas-mediated pathway alone. In addition, mTOR pathway was downregulated following the treatment with rfhSP-D, which is crucial for cell survival and proliferation, and thus, to protect the cancer cells from apoptosis (47). These findings are also supported by studies such as targeting mTOR pathway using rapamycin (48), or its regulating component RICTOR knockdown (49), significantly reduces the pancreatic cancer cell growth. Interestingly, immunofluorescence microscopy showed that rfhSP-D causes nuclear accumulation of mTOR in the treated cells, which may have a transcriptional role. However, the nuclear versions do not form an intact mTORC1 required for regulatory signaling pathways (30).

rfhSP-D bound all the pancreatic cell lines tested in this study: Panc-1, MiaPaCa-2, and Capan-2 (**Figure 1A**). However, the putative SP-D receptor or the ligand on the pancreatic cancer cell surface is not yet known. Recently, an interaction between the CRD region of human SP-D and N-glycans of EGFR has been reported which led to downregulated EGF signaling in human lung adenocarcinoma, A549 cell line cells (19).

In conclusion, rfhSP-D upregulates pro-apoptotic factors such as TNF-α, NF-κB, and Fas to activate caspase cascade to induce apoptosis in pancreatic cancer cell lines, which needs further exploration in orthotropic murine models. Majority of the conventional anti-cancer therapies only target the rapidly proliferating cancer cells, therefore, new strategies involving immune molecules such as rfhSP-D that target the signaling pathways to reduce the cell growth merit further investigation as these would

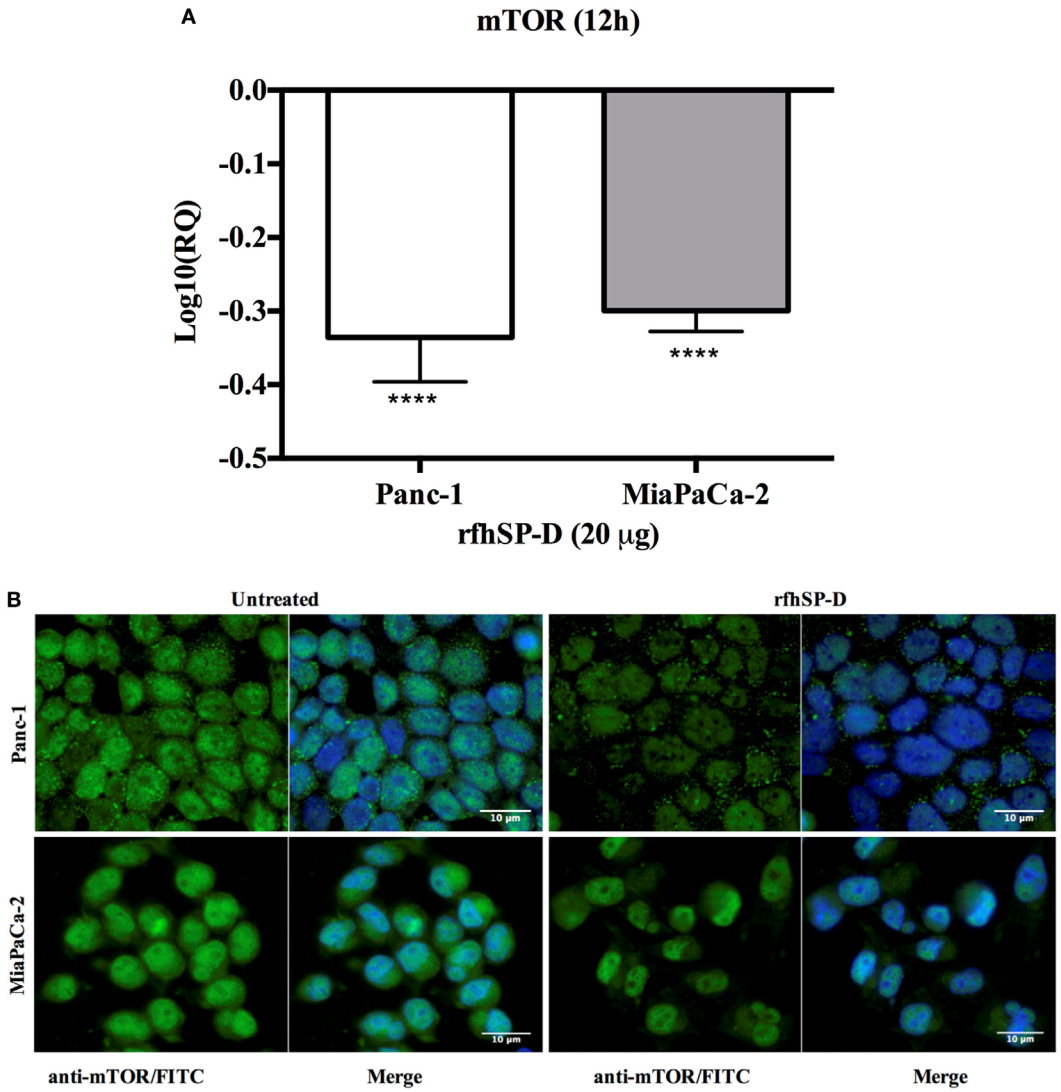

FIGURE 8 | rfhSP-D downregulated the survival pathway, mTOR. **(A)** rfhSP-D treatment of Panc-1 and MiaPaCa-2 cells downregulated the mRNA expression of mTOR (****$p < 0.0001$). **(B)** Immunofluorescence microscopy showed reduced cytoplasmic levels of mTOR following treatment as compared to the untreated. Nuclear accumulation is clearly visible in the rfhSP-D treated cells.

not only help eliminate the tumor but could also influence recurrence or migratory capacity of the tumor cells.

AUTHOR CONTRIBUTIONS

AK carried out most crucial experiments and was supported by MR, VM, and PV. SS provided ideas for crucial experiments and offered important reagents. AK wrote the first draft. UK led the study and helped with the manuscript preparation.

FUNDING

SS is supported by a Max-Elder Research Grant.

REFERENCES

1. Kishore U, Greenhough TJ, Waters P, Shrive AK, Ghai R, Kamran MF, et al. Surfactant proteins SP-A and SP-D: structure, function and receptors. *Mol Immunol* (2006) 43:1293–315. doi:10.1016/j.molimm.2005.08.004
2. Ujma S, Horsnell WG, Katz AA, Clark HW, Schafer G. Non-pulmonary immune functions of surfactant proteins A and D. *J Innate Immun* (2017) 9:3–11. doi:10.1159/000451026
3. Nayak A, Dodagatta-Marri E, Tsolaki AG, Kishore U. An insight into the diverse roles of surfactant proteins, SP-A and SP-D in innate and adaptive immunity. *Front Immunol* (2012) 3:131. doi:10.3389/fimmu.2012.00131
4. Schaub B, Westlake RM, He H, Arestides R, Haley KJ, Campo M, et al. Surfactant protein D deficiency influences allergic immune responses. *Clin Exp Allergy* (2004) 34:1819–26. doi:10.1111/j.1365-2222.2004.02068.x
5. Wert SE, Yoshida M, LeVine AM, Ikegami M, Jones T, Ross GF, et al. Increased metalloproteinase activity, oxidant production, and emphysema in surfactant

protein D gene-inactivated mice. *Proc Natl Acad Sci U S A* (2000) 97:5972–7. doi:10.1073/pnas.100448997
6. Ikegami M, Na CL, Korfhagen TR, Whitsett JA. Surfactant protein D influences surfactant ultrastructure and uptake by alveolar type II cells. *Am J Physiol Lung Cell Mol Physiol* (2005) 288:L552–61. doi:10.1152/ajplung.00142.2004
7. Griese M, Steinecker M, Schumacher S, Braun A, Lohse P, Heinrich S. Children with absent surfactant protein D in bronchoalveolar lavage have more frequently pneumonia. *Pediatr Allergy Immunol* (2008) 19:639–47. doi:10.1111/j.1399-3038.2007.00695.x
8. Foreman MG, Kong X, DeMeo DL, Pillai SG, Hersh CP, Bakke P, et al. Polymorphisms in surfactant protein-D are associated with chronic obstructive pulmonary disease. *Am J Respir Cell Mol Biol* (2011) 44:316–22. doi:10.1165/rcmb.2009-0360OC
9. Lingappa JR, Dumitrescu L, Zimmer SM, Lynfield R, McNicholl JM, Messonnier NE, et al. Identifying host genetic risk factors in the context of public health surveillance for invasive pneumococcal disease. *PLoS One* (2011) 6:e23413. doi:10.1371/journal.pone.0023413
10. Ishii T, Hagiwara K, Ikeda S, Arai T, Mieno MN, Kumasaka T, et al. Association between genetic variations in surfactant protein D and emphysema, interstitial pneumonia, and lung cancer in a Japanese population. *COPD* (2012) 9:409–16. doi:10.3109/15412555.2012.676110
11. Silveyra P, Floros J. Genetic variant associations of human SP-A and SP-D with acute and chronic lung injury. *Front Biosci (Landmark Ed)* (2012) 17:407–29. doi:10.2741/3935
12. Tanaka M, Arimura Y, Goto A, Hosokawa M, Nagaishi K, Yamashita K, et al. Genetic variants in surfactant pulmonary-associated protein D (SFTPD) and Japanese susceptibility to ulcerative colitis. *Inflamm Bowel Dis* (2009) 15:918–25. doi:10.1002/ibd.20936
13. Madan T, Kishore U, Singh M, Strong P, Clark H, Hussain EM, et al. Surfactant proteins A and D protect mice against pulmonary hypersensitivity induced by *Aspergillus fumigatus* antigens and allergens. *J Clin Invest* (2001) 107:467–75. doi:10.1172/JCI10124
14. Singh M, Madan T, Waters P, Parida SK, Sarma PU, Kishore U. Protective effects of a recombinant fragment of human surfactant protein D in a murine model of pulmonary hypersensitivity induced by dust mite allergens. *Immunol Lett* (2003) 86:299–307. doi:10.1016/S0165-2478(03)00033-6
15. Mahajan L, Madan T, Kamal N, Singh VK, Sim RB, Telang SD, et al. Recombinant surfactant protein-D selectively increases apoptosis in eosinophils of allergic asthmatics and enhances uptake of apoptotic eosinophils by macrophages. *Int Immunol* (2008) 20:993–1007. doi:10.1093/intimm/dxn058
16. Mahajan L, Pandit H, Madan T, Gautam P, Yadav AK, Warke H, et al. Human surfactant protein D alters oxidative stress and HMGA1 expression to induce p53 apoptotic pathway in eosinophil leukemic cell line. *PLoS One* (2013) 8:e85046. doi:10.1371/journal.pone.0085046
17. Mahajan L, Gautam P, Dodagatta-Marri E, Madan T, Kishore U. Surfactant protein SP-D modulates activity of immune cells: proteomic profiling of its interaction with eosinophilic cells. *Expert Rev Proteomics* (2014) 11:355–69. doi:10.1586/14789450.2014.897612
18. Pandit H, Thakur G, Koippallil Gopalakrishnan AR, Dodagatta-Marri E, Patil A, Kishore U, et al. Surfactant protein D induces immune quiescence and apoptosis of mitogen-activated peripheral blood mononuclear cells. *Immunobiology* (2016) 221(2):310–22. doi:10.1016/j.imbio.2015.10.004
19. Hasegawa Y, Takahashi M, Ariki S, Asakawa D, Tajiri M, Wada Y, et al. Surfactant protein D suppresses lung cancer progression by downregulation of epidermal growth factor signaling. *Oncogene* (2015) 34:4285–6. doi:10.1038/onc.2014.20
20. Malvezzi M, Bertuccio P, Rosso T, Rota M, Levi F, La Vecchia C, et al. European cancer mortality predictions for the year 2015: does lung cancer have the highest death rate in EU women? *Ann Oncol* (2015) 26:779–86. doi:10.1093/annonc/mdv001
21. Siegel RL, Miller KD, Jemal A. Cancer statistics, 2016. *CA Cancer J Clin* (2016) 66:7–30. doi:10.3322/caac.21332
22. Wolfgang CL, Herman JM, Laheru DA, Klein AP, Erdek MA, Fishman EK, et al. Recent progress in pancreatic cancer. *CA Cancer J Clin* (2013) 63:318–48. doi:10.3322/caac.21190
23. Ansari D, Tingstedt B, Andersson B, Holmquist F, Sturesson C, Williamsson C, et al. Pancreatic cancer: yesterday, today and tomorrow. *Future Oncol* (2016) 12:1929–46. doi:10.2217/fon-2016-0010
24. Strong P, Kishore U, Morgan C, Lopez Bernal A, Singh M, Reid KB. A novel method of purifying lung surfactant proteins A and D from the lung lavage of alveolar proteinosis patients and from pooled amniotic fluid. *J Immunol Methods* (1998) 220:139–49. doi:10.1016/S0022-1759(98)00160-4
25. von Bernstorff W, Spanjaard RA, Chan AK, Lockhart DC, Sadanaga N, Wood I, et al. Pancreatic cancer cells can evade immune surveillance via nonfunctional Fas (APO-1/CD95) receptors and aberrant expression of functional Fas ligand. *Surgery* (1999) 125:73–84. doi:10.1016/S0039-6060(99)70291-6
26. Friess H, Lu Z, Graber HU, Zimmermann A, Adler G, Korc M, et al. Bax, but not Bcl-2, influences the prognosis of human pancreatic cancer. *Gut* (1998) 43:414–21. doi:10.1136/gut.43.3.414
27. Fulda S, Debatin KM. Extrinsic versus intrinsic apoptosis pathways in anti-cancer chemotherapy. *Oncogene* (2006) 25:4798–811. doi:10.1038/sj.onc.1209608
28. Semba S, Moriya T, Kimura W, Yamakawa M. Phosphorylated Akt/PKB controls cell growth and apoptosis in intraductal papillary-mucinous tumor and invasive ductal adenocarcinoma of the pancreas. *Pancreas* (2003) 26:250–7. doi:10.1097/00006676-200304000-00008
29. Kennedy AL, Morton JP, Manoharan I, Nelson DM, Jamieson NB, Pawlikowski JS, et al. Activation of the PIK3CA/AKT pathway suppresses senescence induced by an activated RAS oncogene to promote tumorigenesis. *Mol Cell* (2011) 42:36–49. doi:10.1016/j.molcel.2011.02.020
30. Betz C, Hall MN. Where is mTOR and what is it doing there? *J Cell Biol* (2013) 203:563–74. doi:10.1083/jcb.201306041
31. Deer EL, Gonzalez-Hernandez J, Coursen JD, Shea JE, Ngatia J, Scaife CL, et al. Phenotype and genotype of pancreatic cancer cell lines. *Pancreas* (2010) 39:425–35. doi:10.1097/MPA.0b013e3181c15963
32. Kaur A, Sultan SH, Murugaiah V, Pathan AA, Alhamlan FS, Karteris E, et al. Human C1q induces apoptosis in an ovarian cancer cell line via tumor necrosis factor pathway. *Front Immunol* (2016) 7:599. doi:10.3389/fimmu.2016.00599
33. Liu F, Bardhan K, Yang D, Thangaraju M, Ganapathy V, Waller JL, et al. NF-κB directly regulates Fas transcription to modulate Fas-mediated apoptosis and tumor suppression. *J Biol Chem* (2012) 287:25530–40. doi:10.1074/jbc.M112.356279
34. Ashkenazi A, Dixit VM. Death receptors: signaling and modulation. *Science* (1998) 281:1305–8. doi:10.1126/science.281.5381.1305
35. Armitage RJ. Tumor necrosis factor receptor superfamily members and their ligands. *Curr Opin Immunol* (1994) 6:407–13. doi:10.1016/0952-7915(94)90119-8
36. Schulze-Osthoff K, Ferrari D, Los M, Wesselborg S, Peter ME. Apoptosis signaling by death receptors. *Eur J Biochem* (1998) 254:439–59. doi:10.1046/j.1432-1327.1998.2540439.x
37. Boldin MP, Varfolomeev EE, Pancer Z, Mett IL, Camonis JH, Wallach D. A novel protein that interacts with the death domain of Fas/APO1 contains a sequence motif related to the death domain. *J Biol Chem* (1995) 270:7795–8. doi:10.1074/jbc.270.14.7795
38. Chinnaiyan AM, O'Rourke K, Tewari M, Dixit VM. FADD, a novel death domain-containing protein, interacts with the death domain of Fas and initiates apoptosis. *Cell* (1995) 81:505–12. doi:10.1016/0092-8674(95)90071-3
39. Janicke RU, Sprengart ML, Wati MR, Porter AG. Caspase-3 is required for DNA fragmentation and morphological changes associated with apoptosis. *J Biol Chem* (1998) 273:9357–60. doi:10.1074/jbc.273.16.9357
40. Zheng TS, Schlosser SF, Dao T, Hingorani R, Crispe IN, Boyer JL, et al. Caspase-3 controls both cytoplasmic and nuclear events associated with Fas-mediated apoptosis in vivo. *Proc Natl Acad Sci U S A* (1998) 95:13618–23. doi:10.1073/pnas.95.23.13618
41. Elzey BD, Griffith TS, Herndon JM, Barreiro R, Tschopp J, Ferguson TA. Regulation of Fas ligand-induced apoptosis by TNF. *J Immunol* (2001) 167:3049–56. doi:10.4049/jimmunol.167.6.3049
42. Micheau O, Tschopp J. Induction of TNF receptor I-mediated apoptosis via two sequential signaling complexes. *Cell* (2003) 114:181–90. doi:10.1016/S0092-8674(03)00521-X

43. Oeckinghaus A, Ghosh S. The NF-kappaB family of transcription factors and its regulation. *Cold Spring Harb Perspect Biol* (2009) 1:a000034. doi:10.1101/cshperspect.a000034
44. Perkins ND. Integrating cell-signalling pathways with NF-κB and IKK function. *Nat Rev Mol Cell Biol* (2007) 8:49–62. doi:10.1038/nrm2083
45. Yoshida M, Korfhagen TR, Whitsett JA. Surfactant protein D regulates NF-κB and matrix metalloproteinase production in alveolar macrophages via oxidant-sensitive pathways. *J Immunol* (2001) 166:7514–9. doi:10.4049/jimmunol.166.12.7514
46. Barrow AD, Palarasah Y, Bugatti M, Holehouse AS, Byers DE, Holtzman MJ, et al. OSCAR is a receptor for surfactant protein D that activates TNF-alpha release from human CCR2$^+$ inflammatory monocytes. *J Immunol* (2015) 194:3317–26. doi:10.4049/jimmunol.1402289
47. Laplante M, Sabatini DM. mTOR signaling at a glance. *J Cell Sci* (2009) 122:3589–94. doi:10.1242/jcs.051011
48. Matsubara S, Ding Q, Miyazaki Y, Kuwahata T, Tsukasa K, Takao S. mTOR plays critical roles in pancreatic cancer stem cells through specific and stemness-related functions. *Sci Rep* (2013) 3:3230. doi:10.1038/srep03230
49. Schmidt KM, Hellerbrand C, Ruemmele P, Michalski CW, Kong B, Kroemer A, et al. Inhibition of mTORC2 component RICTOR impairs tumor growth in pancreatic cancer models. *Oncotarget* (2017) 8:24491–505. doi:10.18632/oncotarget.15524

Conflict of Interest Statement: The authors declare that the research was conducted in the absence of any commercial or financial relationships that could be construed as a potential conflict of interest.

frontiers in Immunology

ORIGINAL RESEARCH
published: 15 August 2018
doi: 10.3389/fimmu.2018.01844

Human Surfactant Protein D Suppresses Epithelial-to-Mesenchymal Transition in Pancreatic Cancer Cells by Downregulating TGF-β

*Anuvinder Kaur[1], Muhammad Suleman Riaz[1], Shiv K. Singh[2] and Uday Kishore[1]**

[1] Biosciences Division, College of Health and Life Sciences, Brunel University London, Uxbridge, United Kingdom,
[2] Department of Gastroenterology and Gastrointestinal Oncology, University Medical Center, Gottingen, Germany

Human surfactant protein-D (SP-D), an innate immune pattern recognition soluble factor, is known to modulate a range of cytokines and chemokines, such as TNF-α and TGF-β at mucosal surfaces during infection, allergy, and inflammation. A recent study has shown that treatment with a recombinant fragment of human SP-D (rfhSP-D) for 48 h induces apoptosis in pancreatic cancer cells. Our hypothesis is that at earlier time points, SP-D can also influence key cytokines as a part of its putative role in the immune surveillance against pancreatic cancer, where the inflammatory tumor microenvironment contributes to the epithelial-to-mesenchymal transition (EMT), invasion, and metastasis. Here, we provide the first evidence that rfhSP-D can suppress the invasive-mesenchymal properties of highly aggressive pancreatic cancer cells. Mechanistically, rfhSP-D inhibited TGF-β expression in a range of pancreatic cancer cell lines, Panc-1, MiaPaCa-2, and Capan-2, thereby reducing their invasive potential. Smad2/3 expression diminished in the cytoplasm of rfhSP-D-treated cells as compared to the untreated control, suggesting that an interrupted signal transduction negatively affected the transcription of key mesenchymal genes. Thus, expressions of Vimentin, Zeb1, and Snail were found to be downregulated upon rfhSP-D treatment in the pancreatic cancer cell lines. Furthermore, blocking TGF-β with neutralizing antibody showed similar downregulation of mesenchymal markers as seen with rfhSP-D treatment. This study highlights yet another novel innate immune surveillance role of SP-D where it interferes with EMT induction by attenuating TGF-β pathway in pancreatic cancer.

Keywords: surfactant protein, surfactant protein-D, pancreatic cancer, epithelial-to-mesenchymal transition, metastasis, transformation growth factor

OPEN ACCESS

Edited by:
Joao P. B. Viola, Instituto Nacional de Câncer (INCA), Brazil

Reviewed by:
Kenneth Reid, University of Oxford, United Kingdom
Kushagra Bansal, Harvard Medical School, United States

****Correspondence:***
Uday Kishore
uday.kishore@brunel.ac.uk, ukishore@hotmail.com

Specialty section:
This article was submitted to Molecular Innate Immunity, a section of the journal Frontiers in Immunology

Received: *23 May 2018*
Accepted: *26 July 2018*
Published: *15 August 2018*

Citation:
Kaur A, Riaz MS, Singh SK and Kishore U (2018) Human Surfactant Protein D Suppresses Epithelial-to-Mesenchymal Transition in Pancreatic Cancer Cells by Downregulating TGF-β. Front. Immunol. 9:1844. doi: 10.3389/fimmu.2018.01844

INTRODUCTION

Pancreatic ductal adenocarcinoma (PDA) is one of the most lethal of all human malignancies with a dismal 5-year survival rate of below 7%; it is estimated to become the third leading cause of cancer-related death by 2030 (1). PDA is associated with a high rate of mortality due to metastasis, resistance to conventional chemotherapy, and high tumor recurrence rate after surgery (2). Metastasis requires epithelial-to-mesenchymal transition (EMT), which is considered a principal cause of tumor recurrence and resistance to conventional therapies (3–6). EMT is a complex and

hierarchical process during tumor progression; it enables the tumor cells to acquire increased motility, leading to invasion of adjoining tissue and infiltration to systemic circulation and subsequent penetration into the adjacent tissues, resulting in macroscopic secondary tumors (7, 8). A number of EMT markers appear to regulate the invasion-metastasis process in the pancreatic tumor cells. Aberrant activation of EMT has been attributed to over-expression of mesenchymal markers, such as Zeb1 (zinc finger E-box binding homeobox 1) (9), Snail (10), and Vimentin (10), as well as repression of E-cadherin, an epithelial marker (6) in the pancreatic cancer cells. During the EMT process, E-cadherin expression is lost whereas mesenchymal markers, including fibronectin and Vimentin, are over-expressed (11). Markers, such as Snail, Slug, Zeb1, Zeb2, and Twist, to name a few, have been shown to suppress E-cadherin. E-cadherin gene-deficient mice do not survive past implantation (12). The Snail-expressing metastatic tumors are associated with poor prognosis, and drug and immune resistance, offering limited opportunity for therapeutic intervention (12).

Recent studies have shown that an inflammatory tumor microenvironment influences early tumor dissemination, EMT, and metastasis in pancreatic cancer (5, 6, 13). Pro-tumorigenic cytokines, including TGF-β, have also been linked to EMT, invasion, metastasis, and drug-resistance in many types of cancer (14, 15). In PDA, elevated TGF-β expression has been associated with a highly invasive (metastatic) phenotype, acquired through SMAD signaling. Importantly, TGF-β signaling regulates EMT-gene signatures, thereby promoting cell motility and invasiveness in the pancreatic cancer cells (8, 16–19).

Human surfactant protein-D (SP-D), a soluble collagen containing C-type lectin (collectin), is a potent innate immune molecule, found at the pulmonary and extra-pulmonary mucosal surfaces. While acting as a link between innate and adaptive immunity, SP-D is known for its role in immune surveillance and immunomodulation in infection and allergy (20). SP-D has been considered for quite some time as a modulator of inflammatory response. However, recent studies have shown its anti-proliferative properties against cancer cells (21, 22). In addition, SP-D deficiency in animal models has been shown to trigger serious adverse pathological consequences as in emphysema (23), chronic and infectious lung diseases (24–26), Crohn's disease, and ulcerative colitis (27). A new dimension to the defense mechanism attributable to SP-D became evident when a recombinant fragment of human SP-D (rfhSP-D) comprising homotrimeric neck region and carbohydrate recognition domain (rfhSP-D) was found to selectively induce apoptosis in the sensitized eosinophils derived from allergic patients, whereas eosinophils derived from healthy individuals were unaffected (28). Proteomics analysis of an eosinophil-like leukemic cell line (AML14.3D10), treated with rfhSP-D, showed that it caused cell cycle arrest *via* activation of G2/M checkpoints, and subsequently induced apoptosis *via* p53 pathway (21). Treatment of human lung adenocarcinoma A549 cell line with SP-D has been shown to suppress the epidermal growth factor (EGF) signaling by interrupting the EGF–EGFR interaction, thus reducing cell proliferation, invasion, and migration (22). Recently, Kaur et al. have shown that treatment with rfhSP-D for 48 h differentially induced apoptosis in pancreatic cancer cell lines, such as Panc-1, MiaPaCa-2, and Capan-2 *via* Fas-mediated pathway, involving cleavage of caspase 8 and 3 (29).

In this study, we demonstrate, for the first time, an early anti-tumorigenic role of rfhSP-D, where it suppresses the EMT and invasive-mesenchymal phenotype in pancreatic cancer cell lines. We show that rfhSP-D inhibits the invasive functions of TGF-β/SMAD expressing pancreatic cancer cells. Mechanistically, rfhSP-D downregulates the EMT-related gene signatures (Vimentin, Zeb1, and Snail), and hence, pancreatic cancer cells invasion, mainly by attenuating TGF-β signaling pathway.

MATERIALS AND METHODS

Cell Culture

Human pancreatic cancer cell lines, such as Panc-1 (CRL-1469), MiaPaCa-2 (CRL-1420), and Capan-2 (HTB-80), were obtained from ATCC, and used as an *in vitro* model in this study. All cell lines were cultured in DMEM-F12 media supplemented with 2 mM L-glutamine, 10% v/v fetal calf serum (FCS), and penicillin (100 units/ml)/streptomycin (100 µg/ml) (Thermo Fisher). All cell lines were grown at 37°C under 5% v/v CO_2 until 80–90% confluency was attained.

Expression and Purification of rfhSP-D

Expression and purification of a recombinant form of human SP-D was carried out as reported previously (28). Plasmid pUK-D1 (containing cDNA sequences for 8 Gly-X-Y repeats, neck and CRD region of human SP-D) was transformed into *Escherichia coli* BL21 (λDE3) pLysS strain (Invitrogen). A single colony was inoculated in 25 ml of Luria–Bertani (LB) medium containing ampicillin (100 µg/ml) and chloramphenicol (34 µg/ml) (Sigma-Aldrich) at 37°C on a shaker overnight. The overnight inoculum was grown in a 1 l LB medium (containing ampicillin and chloramphenicol) until the OD_{600} reached 0.6, induced with 0.4 mM isopropyl β-D-thiogalactoside (IPTG) (Sigma-Aldrich, UK) for 3 h at 37°C on an orbital shaker, and then centrifuged (5,000 × *g*, 4°C, 15 min). The bacterial cell pellet was lysed using 50 ml of lysis buffer (50 mM Tris–HCl, pH 7.5, 200 mM NaCl, 5 mM EDTA, pH 7.5) containing lysozyme (100 µg/ml; Sigma-Aldrich) and 0.1 mM phenylmethylsulfonyl fluoride (PMSF; Sigma-Aldrich, UK) at 4°C for 1 h. The bacterial cell suspension was sonicated at 60 Hz for 30 s with an interval of 2 min each (15 cycles) and centrifuged at 13,800 × *g* for 15 min at 4°C. The pellet containing insoluble rfhSP-D as inclusion bodies was suspended in 25 ml of solubilization buffer (50 mM Tris–HCl, pH 7.5, 100 mM NaCl, 5 mM EDTA, pH 7.5) containing 6 M urea at 4°C for 1 h and then centrifuged at 13,800 × *g* at 4°C for 15 min. The supernatant was serially dialyzed against solubilization buffer containing 4, 2, 1, and 0 M urea and 10 mM β-mercaptoethanol for 2 h at 4°C, followed by final dialysis in solubilization buffer containing 5 mM $CaCl_2$ (Affinity buffer) for 3 h and centrifuged at 13,800 × *g*, 4°C for 15 min. The supernatant containing soluble rfhSP-D was passed through a 5 ml Maltose-Agarose column (Sigma-Aldrich). The

affinity-column was washed extensively using affinity buffer containing 1 M NaCl (20 ml) before eluting the bound rfhSP-D protein with solubilization buffer containing 10 mM EDTA, pH 7.5. The concentration of the eluted protein was determined *via* OD_{280}. The peak fractions were passed through Pierce™ High Capacity Endotoxin Removal Resin (Qiagen) to remove lipopolysaccharide (LPS). Endotoxin levels were determined using the QCL-1000 Limulus amebocyte lysate system (Lonza); the assay was linear over a range of 0.1–1.0 EU/ml (10 EU = 1 ng of endotoxin). The amount of endotoxin levels was found to be <4 pg/μg of the rfhSP-D protein.

Cell Morphological Studies

Morphological alterations were examined in order to determine the optimal dose of rfhSP-D for the treatment of pancreatic cell lines. Panc-1 cells were seeded at a low density (0.1×10^4) and grown overnight in DMEM-F12 containing 10% FCS in a 12-well plate (Nunc). The cells were washed twice with PBS and incubated in serum-free medium with and without rfhSP-D (5, 10, or 20 μg/ml). An area of 5–10 cells was selected for each treatment condition for analysis at 0, 6, and 24 h using phase contrast Axioscope microscope.

Matrigel Invasion Assay

The invasion assay was performed using Corning™ BioCoat™ Matrigel™ Invasion Chamber (BD Matrigel Matrix). Inserts, pre-coated with basement membrane that was extracted from Engelbreth-Holm-Swarm mouse tumor, were reconstituted in serum-free DMEM-F12 at 37°C for 2 h. 35,000 cells, re-suspended in 500 μl serum-free DMEM-F12, were added to the top wells of the inserts with and without rfhSP-D (20 μg/ml), and 500 μl of medium containing serum was added to the bottom of the inserts in a 24-well plate and incubated at 37°C for 22 h. Next, medium containing non-evaded cells were discarded and remaining cells were scraped off from the membrane using a sterile cotton bud, ensuring cells at the bottom of the membrane remained intact for fixing. Fixation was done using 100% methanol for 2 min, followed by 2 min incubation with toluidine blue to stain the evaded cells. The membrane was cut using a sterile scalpel and mounted on the slide to count the evaded cells.

Fluorescence Microscopy

Cells (0.5×10^5) were grown on coverslips overnight at 37°C under 5% v/v CO_2. Next day, cells were washed three times with sterile PBS before being incubated with and without rfhSP-D (5, 10, or 20 μg/ml) in a serum-free DMEM-F12 for 1 h for rfhSP-D binding to the cells, and 12 or 24 h for intracellular staining. The coverslips were washed three times with PBS in between each step. For rfhSP-D binding analysis, the coverslips were incubated for 1 h with mouse anti-human SP-D (a kind gift from Prof. U. Holmskov, Odnese, Denmark; 1:200) followed by goat anti-mouse IgG H&L (Cy5 ®, 1:500; Abcam) and Hoechst (1:10,000; Thermo Fisher) for immunofluorescence analysis. For the intracellular staining (Vimentin, Zeb1, E-Cadherin, SP-D, and TGF-β), the cells were fixed and permeabilized using ice-cold 100% methanol at −20°C for 10 min. This was followed by 1 h incubation with rabbit anti-human IgG antibody (Vimentin, Zeb1, and TGF-β) (1:500; Cell Signaling) and human SP-D (1:500), and another 1 h incubation with Alexa Fluor 488 (1:500; Thermo Fisher) and Hoechst (1:10,000; Thermo Fisher) for immunofluorescence analysis. For human pancreatic tissue, immunofluorescence was performed as described previously (30). Immunostaining was visualized using confocal laser-scanning microscope (Olympus). The human pancreatic tissue was obtained from the Department of Pathology, Philipps-University of Marburg, Germany following ethical considerations as stipulated by the University's ethical guidelines.

Quantitative RT-PCR

Pancreatic cancer cell lines were incubated with either rfhSP-D (20 μg/ml) or anti-TGF-β neutralizing antibody (Thermo Fisher) for various time points and the centrifuged cell pellets were stored at −80°C. Total RNA was extracted using GenElute Mammalian Total RNA Purification Kit (Sigma-Aldrich, UK), followed by DNase I treatment to remove any DNA impurities. The concentration and purity of total RNA were determined by measuring the absorbance at 260 nm and 260:280 nm ratio, respectively, using NanoDrop 2000/2000c (Thermo-Fisher Scientific). Total RNA (2 μg) was used to synthesize cDNA using High Capacity RNA to cDNA Kit (Applied Biosystems). The web-based Basic Local Alignment Search Tool and Primer-BLAST (http://blast.ncbi.nlm.nih.gov/Blast.cgi) were used to design the forward and reverse primer sequences (**Table 1**).

Each qPCR reaction, carried out in triplicates, consisted of 5 μl Power SYBR Green MasterMix (Applied Biosystems), 75 nM of forward and reverse primers, and 500 ng cDNA, making up to a 10 μl final volume per well. Relative mRNA expression was analyzed using 7900HT Fast Real-Time PCR System (Applied Biosystems). Samples were initially incubated at 50°C (2 min) and 95°C (10 min), followed by amplification of the template for 40 cycles (each cycle for 15 s at 95°C and 1 min at 60°C). Human 18S RNA, an endogenous control, was used to normalize the gene expressions. The cycle threshold (Ct) mean value for each target gene was used to calculate the relative expression using the relative quantification (RQ) value and

TABLE 1 | Target genes and terminal primers used in the qPCR analysis.

Gene	Forward primer	Reverse primer
Snail	5′- GAGCTGACCTCCCTGT CAGA-3′	5′-GTTGAAGGCCTTTCGA GCCT-3′
Vimentin	5′-CTCTGGCACGTCTTGA CCTT-3′	5′-TCTTGGCAGCCACAC TTTCA-3′
Zeb1	5′-AAGGGCAAGAAATCCT GGGG-3′	5′-ATGACCACTGGCTTCT GGTG-3′
TGF-β	5′-GTACCTGAACCCGTGT TGCT-3′	5′-GTATCGCCAGGAATTG TTGC-3′
18S	5′-ATGGCCGTTCTTAGTTG GTG-3′	5′-CGCTGAGCCAGTCAG TGTAG-3′

formula: RQ = $2^{-\Delta\Delta Ct}$, which was compared with the relative expression of the untreated cells.

Western Blot

Cells (0.1×10^7) were cultured in a 6-well plate (Nunc) and incubated with and without rfhSP-D (20 μg/ml) in a serum-free DMEM-F12 for various time points. The cells were then mixed with 2× treatment buffer (50 mM Tris–HCL pH 6.8, 2% v/v β-merceptoethanol, 2% v/v SDS, 0.1% w/v bromophenol blue, and 10% v/v glycerol) and sonicated for 30 s before running on a SDS-PAGE (12% w/v) for 90 min at 120 V. The SDS-PAGE separated proteins were electrophoretically transferred onto a nitrocellulose membrane using an iBlot 7-min Blotting System (Thermo Fisher), followed by blocking with 5% w/v non-fat dried milk powder (Sigma) in 100 ml PBS for 2 h on a rotatory shaker at room temperature. The membrane was washed with PBST (PBS + 0.05% Tween 20) three times, each time for 10 min. The membrane was then incubated with primary anti-human TGF-β antibody, (1:1,000; R&D systems) at 4°C overnight on a rotatory shaker, followed by secondary anti-rabbit IgG horseradish peroxidase-conjugate (1:1,000; Promega) for 1 h at room temperature. The positive bands were visualized using 3,3′-diaminobenzidine (DAB) substrate kit (Thermo Fisher).

Statistical Analysis

Graphs were made and statistically analyzed using an unpaired one-way or two-way ANOVA tests in Graphpad Prism 6.0. Significant values were considered based on $^*p < 0.05$, $^{**}p < 0.01$, $^{***}p < 0.001$, and $^{****}p < 0.0001$ between treated and untreated samples. Error bars show the SEM, as indicated in the figure legends.

RESULTS

Presence of SP-D Can be Detected in Human Pancreatic Cancer Tissues

Immunofluorescence studies of human pancreatic cancer tissues probed with anti-human SP-D monoclonal antibody showed positive staining, confirming the presence of SP-D in the tissues (**Figure 1**). Additionally, the tissues were probed with anti-Vimentin, which also showed positive staining. However, we could not detect or purify SP-D from the culture supernatants of all three pancreatic cancer cell lines (data not shown). It is possible that the SP-D staining pertains to the tumor micro-environment. Thus, we proceeded to test the effect of exogenous rfhSP-D (**Figure 2**) on cultured pancreatic cancer cell lines.

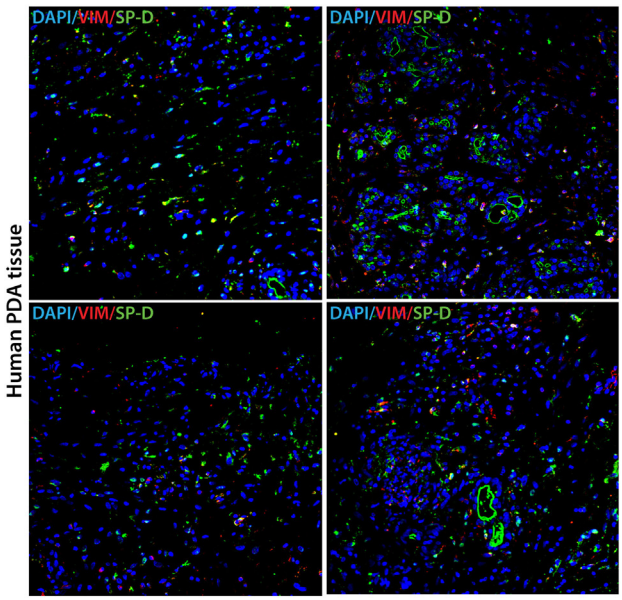

FIGURE 1 | Human pancreatic cancer tissue expressing SP-D and Vimentin. Double immunofluorescence staining of SP-D (green), Vimentin (red), and DAPI (blue) in four different areas of representative human pancreatic cancer tissue. Scale bars, 50 μm.

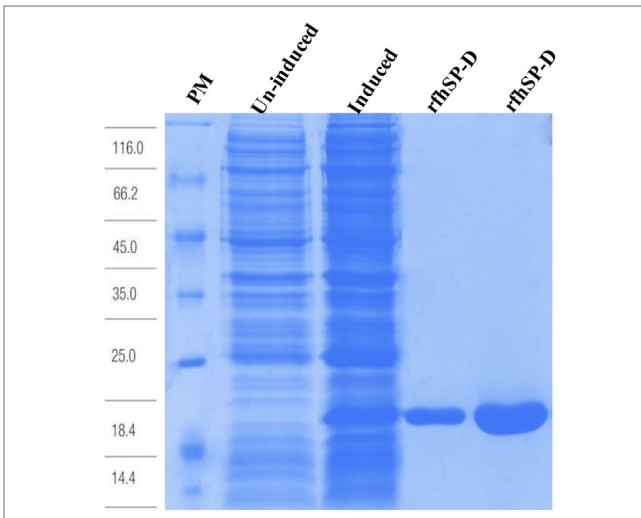

FIGURE 2 | Recombinant fragment of human SP-D (rfhSP-D) expression and purification. *Escherichia coli* BL21 (λDE3) pLysS containing pUK-D1 was induced with IPTG. The expressed bacterial cells show rfhSP-D over-expression at ~20 kDa as compared to un-induced cells. The insoluble inclusion bodies were refolded and affinity purified on maltose-agarose. The peak fractions shown here appeared homogenous on a 12% SDS-PAGE.

rfhSP-D Induces Morphological Alterations in the Pancreatic Cancer Cell Line, Panc-1

To determine the optimal dose of rfhSP-D, Panc-1 cells were incubated with 5, 10, and 20 μg/ml for up to 24 h. The colonies of 10–15 cells were selected for each protein dose to observe the effect of rfhSP-D on cell morphology and cell division. The images of the selected cell colonies were taken at 0, 6, and 24 h (**Figure 3**). Untreated Panc-1 cells, as well as those treated with rfhSP-D (5 μg/ml), acquired spindle-type cell morphology, reduced cell–cell contact, and continued to divide in a time-dependent manner. However, Panc-1 cells, treated with 10 and 20 μg/ml concentration of rfhSP-D, did not acquire spindle shape and appeared to be static. However, cell morphology at 10 μg/ml appeared to be regaining the spindle shape and reduced cell–cell

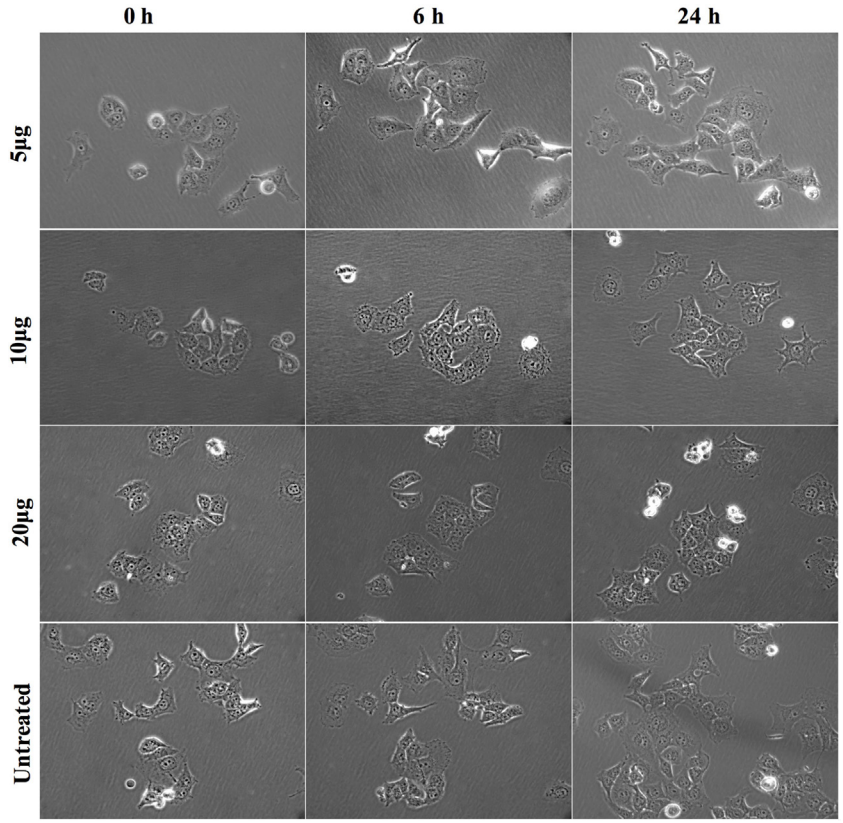

FIGURE 3 | Morphological changes in Panc-1 cells following rfhSP-D treatment. Panc-1 cells (0.1×10^4) were grown overnight in a 12-well plate tissue culture and colonies of 5–10 cells were selected for analysis with and without rfhSP-D (5, 10, and 20 µg/ml) at 0, 6, and 24 h. The cells treated with 5 µg/ml and untreated appeared to undergo epithelial-to-mesenchymal transition as they acquired spindle shape and showed reduced cell–cell contact, whereas cells treated with 10 and 20 µg/ml appeared static and did not acquire spindle shape.

contact, with some evidence of cell division by 24 h. At 20 µg/ml, the non-spindle effect continued up to 24 h. Although some cell division was noted, cells remained in close contact with each other and static. Therefore, 20 µg/ml dose of rfhSP-D was selected to investigate its possible effect on EMT and invasion involving Panc-1, MiaPaCa-2, and Capan-2 cells.

rfhSP-D Suppresses the Invasive Capacity of the Pancreatic Cancer Cell Lines

The matrigel invasive chambers, pre-coated with extracellular matrix proteins, were used to incubate the pancreatic cancer cells (3.5×10^4) in the presence and absence of rfhSP-D (20 µg/ml) in the upper surface of the chamber; serum containing DMEM-F12 was used as a chemo-attractant in the bottom surface for 22 h. Both Panc-1 and MiaPaCa-2 cell lines, treated with rfhSP-D, showed significantly reduced invasion in the matrigel (**Figure 4A**); however, almost no invasion occurred in Capan-2 whether rfhSP-D treated or untreated. This was anticipated since Capan-2 is a low-grade cancer cell line. MiaPaCa-2 was most affected as the invasion was reduced by 65%, followed by Panc-1 cell line, which was approximately 50% less than the untreated cells (**Figure 4B**). Since pancreatic cancer cells are well known to overexpress TGF-β, which has a prominent-role in inducing EMT, the expression of TGF-β in the pancreatic cell lines was investigated following the treatment with rfhSP-D (20 µg/ml).

rfhSP-D Downregulates TGF-β Gene Expression in Pancreatic Cancer Cells

The transcriptional expression of TGF-β was significantly downregulated in Panc-1 (~$\log_{10}$ 0.5-fold) and MiaPaCa-2 (~$\log_{10}$ 0.3-fold) at 12 h (**Figure 5A**), whereas Capan-2 showed no difference following rfhSP-D treatment. This suggested that reduced TGF-β transcripts were being made following the rfhSP-D treatment. Thus, the total cell extracts for all cell lines were analyzed by Western blot using anti-human TGF-β monoclonal antibody, which revealed a reduction in the amount of TGF-β (~60 kDa band) in the rfhSP-D-treated Panc-1 and MiaPaCa-2 samples, as compared to the untreated cells; the amount of TGF-β in Capan-2 was unaffected (**Figure 5B**). The qualitative analysis by immunofluorescence microscopy showed that TGF-β expression at 24 h diminished considerably within the cytoplasm of Panc-1 and MiaPaCa-2 cell lines following rfhSP-D treatment (**Figure 5C**); however, this was not evident in the case of Capan-2 cells (result not shown). During TGF-β induced EMT pathway, Smad2/3 are phosphorylated in the cytoplasm, followed by translocation into nucleus; however, Smad2/3 staining appeared very weak in the

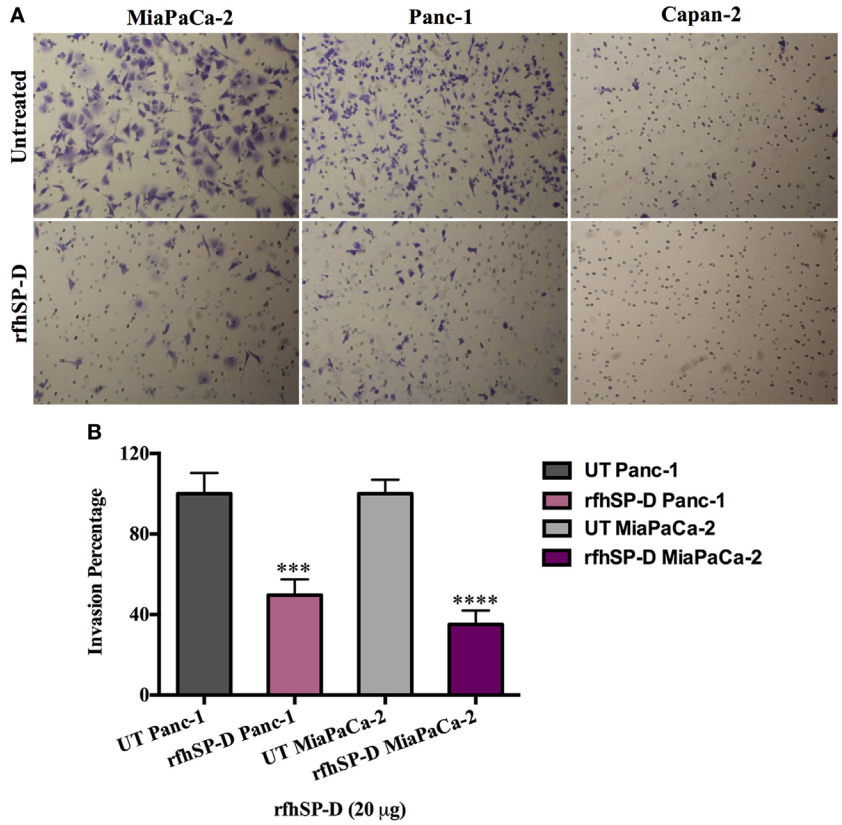

FIGURE 4 | Recombinant fragment of human SP-D (rfhSP-D) supresses invasiveness in pancreatic cancer cell lines. **(A)** The cell invasion was analyzed by incubating 35,000 cells with and without rfhSP-D (20 μg/ml) in the BioCoat™ Matrigel™ Invasion Chambers at 37°C for 22 h. The invasive cells were fixed and stained before mounting the membrane on the slide for cell counting. The images show the difference between treated and untreated. **(B)** Treatment with rfhSP-D significantly reduced the cell invasion as for Panc-1 (~50%) and MiaPaCa-2 (~65%). However, as anticipated, no invasion was detected in Capan-2 cell line, neither in treated nor untreated samples. Significant values were considered based on $^{***}p < 0.001$ and $^{****}p < 0.0001$ between treated and untreated samples.

cytoplasm of the rfhSP-D-treated Panc-1 and MiaPaCa-2 cell lines (**Figure 5D**). No difference was seen in Capan-2-treated and untreated cells (data not shown). Next, key regulators of EMT were examined.

rfhSP-D Reduces the Expression of EMT Markers

To determine whether exogenous rfhSP-D was affecting the key regulators of EMT, we examined the gene expression of Vimentin, Zeb1, and Snail at various time points. All of these markers were differentially downregulated in all the cell lines. Vimentin was significantly downregulated in Panc-1, ~$\log_{10}$ one-fold at 1 h, and ~$\log_{10}$ 0.5-fold at 6 h (**Figure 6A**). MiaPaCa-2 showed ~$\log_{10}$ 0.5-fold downregulation at 1 h that remained constant at 6 h (**Figure 6A**). Vimentin downregulation occurred at a later time-point (6 h) in Capan-2 cell line (~$\log_{10}$ 0.5-fold) (**Figure 6A**). All cell lines showed a similar pattern of decrease in the transcript levels of Vimentin at 12 h compared to earlier time-points following rfhSP-D.

Snail was significantly downregulated in Panc-1 (~$\log_{10}$ one-fold), MiaPaCa-2 (~$\log_{10}$ 0.5-fold), and Capan-2 (~$\log_{10}$ one-fold) at 1 h and remained downregulated at 6 and 12 h (**Figure 6A**). Zeb1 transcript level was significantly reduced in Panc-1 (~$\log_{10}$ 0.5-fold) at 1 and 6 h and MiaPaCa-2 (~$\log_{10}$ two-fold) at 12 h (**Figure 6A**). No difference in Zeb1 gene expression was seen in Capan-2. Since TGF-β regulates these EMT markers and rfhSP-D downregulates TGF-β, rfhSP-D mediated downregulation of EMT markers (Vimentin, Snail, and Zeb1) was logically evident.

Qualitative analysis of Vimentin (**Figure 6B**) and Zeb1 expressions (**Figure 6C**) in Panc-1 and MiaPaCa-2 cell lines *via* immunofluorescence microscopy revealed a significant difference in the cytoplasmic presence of these proteins in the rfhSP-D-treated cells, as compared to untreated cells. These observations were consistent with flow cytometry data that was carried out to further validate quantitatively the downregulation of the Vimentin, Zeb1, and Snail in Panc-1 and MiaPaCa-2 cells (**Figure 6D**) following 24 h treatment with rfhSP-D. The mean fluorescence values for Vimentin, Zeb1, and Snail were approximately 50% less in the rfhSP-D-treated cells as compared to their untreated counterparts and a clear shift was seen in the fluorescence intensity between rfhSP-D-treated and untreated cells (**Figure 6D**).

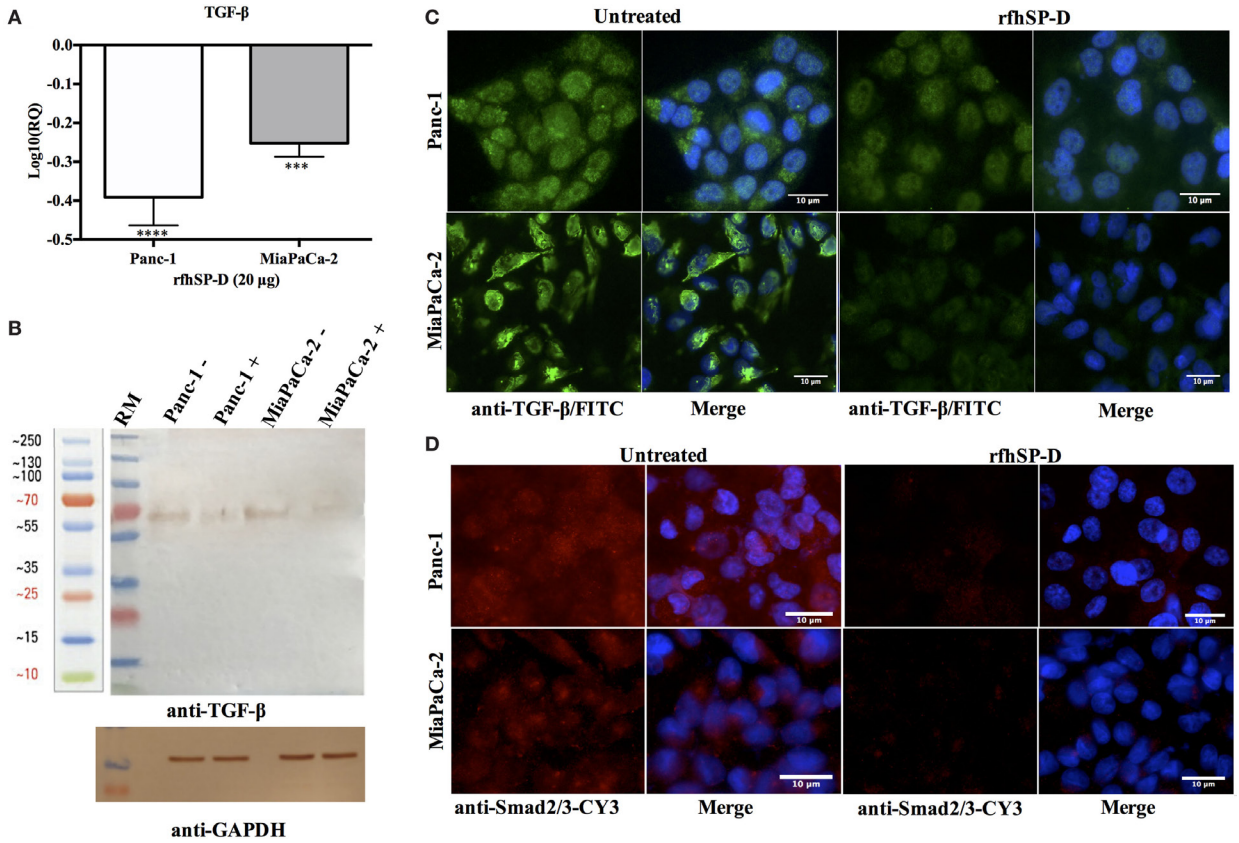

FIGURE 5 | Treatment with rfhSP-D downregulates TGF-β expression. **(A)** TGF-β gene expression, as determined by qPCR, was significantly downregulated at 12 h in both Panc-1 and MiaPaCa-2 cell lines. Significant values were considered based on ***$p < 0.001$ and ****$p < 0.0001$ between treated and untreated samples. **(B)** Western blot analysis revealed a ~60 kDa band that was very faint in the rfhSP-D-treated sample. **(C)** TGF-β intracellular staining for cell lines. 0.5×10^5 cells were incubated with and without rfhSP-D (20 µg/ml) for 24 h followed by probing with rabbit anti-human TGF-β1 antibody (1:500), and then by Alexa Fluor 488 (1:500) and Hoechst (1:10,000). Immunofluorescence analysis showed bright green fluorescence in the cytoplasm of the untreated cells as compared to weak staining in the treated cells. **(D)** Smad 2/3 intracellular staining for Panc-1 and MiaPaCa-2 cell lines with and without rfhSP-D (20 µg/ml) treatment for 24 h using rabbit anti-human Smad2/3 antibody (1:500) and then probed with anti-rabbit CY3 (1:1,000) showed the presence of Smad2/3 in the cytoplasm of untreated cells; however, no CY3 fluorescence was detected in the rfhSP-D-treated cells.

Blocking TGF-β *Via* Neutralizing Antibody Reduces the Expression of EMT Markers in a Way Similar to rfhSP-D

To further establish the TGF-β association, we used neutralizing antibody in order to block TGF-β in all cell lines and assessed the expression of these EMT markers. All cells lines were incubated with TGF-β neutralizing antibody for 6 h and the mRNA expression for EMT markers (Vimentin, Snail, and Zeb1) was measured by qPCR. Interestingly, blocking TGF-β showed similar downregulation trend as seen for the rfhSP-D treatment, which further validated that rfhSP-D treatment caused downregulation of TGF-β, which in turn suppressed EMT regulators (**Figure 7A**). The images were taken for Panc-1 cell line to analyze the cell morphological differences following treatment with rfhSP-D, anti-TGF-β antibody, or rfhSP-D + anti-TGF-β together, to compare with those cells that were untreated at 6 h (**Figure 7B**). Less branches and cell movement were observed in all the treated cells as compared to the untreated control, which suggested that suppressed EMT effects become apparent as early as 6 h following the rfhSP-D treatment. Interestingly, but not surprisingly, the effect was even more pronounced when rfhSP-D (20 µg/ml) and anti-TGF-β were added together (**Figure 7B**).

DISCUSSION

SP-D was originally considered to be a lung-specific hydrophilic surfactant protein that agglutinated a diverse range of pathogens (viruses, bacteria, and fungi). It also acts as an opsonin, enhancing pathogens' phagocytosis and subsequent killing (31). However, its ability to bind allergens (of *Aspergillus fumigatus* and house dust mite) and inhibit allergen IgE interaction and subsequent histamine release from sensitized basophils raised the possibility that SP-D could be involved in dampening pulmonary hypersensitivity (32, 33). In a murine model of allergic hypersensitivity, rfhSP-D treatment lowered specific IgE level, reduced pulmonary and peripheral eosinophilia, and caused Th2 to Th1 polarization (34). Subsequently, it was found that eosinophils derived from

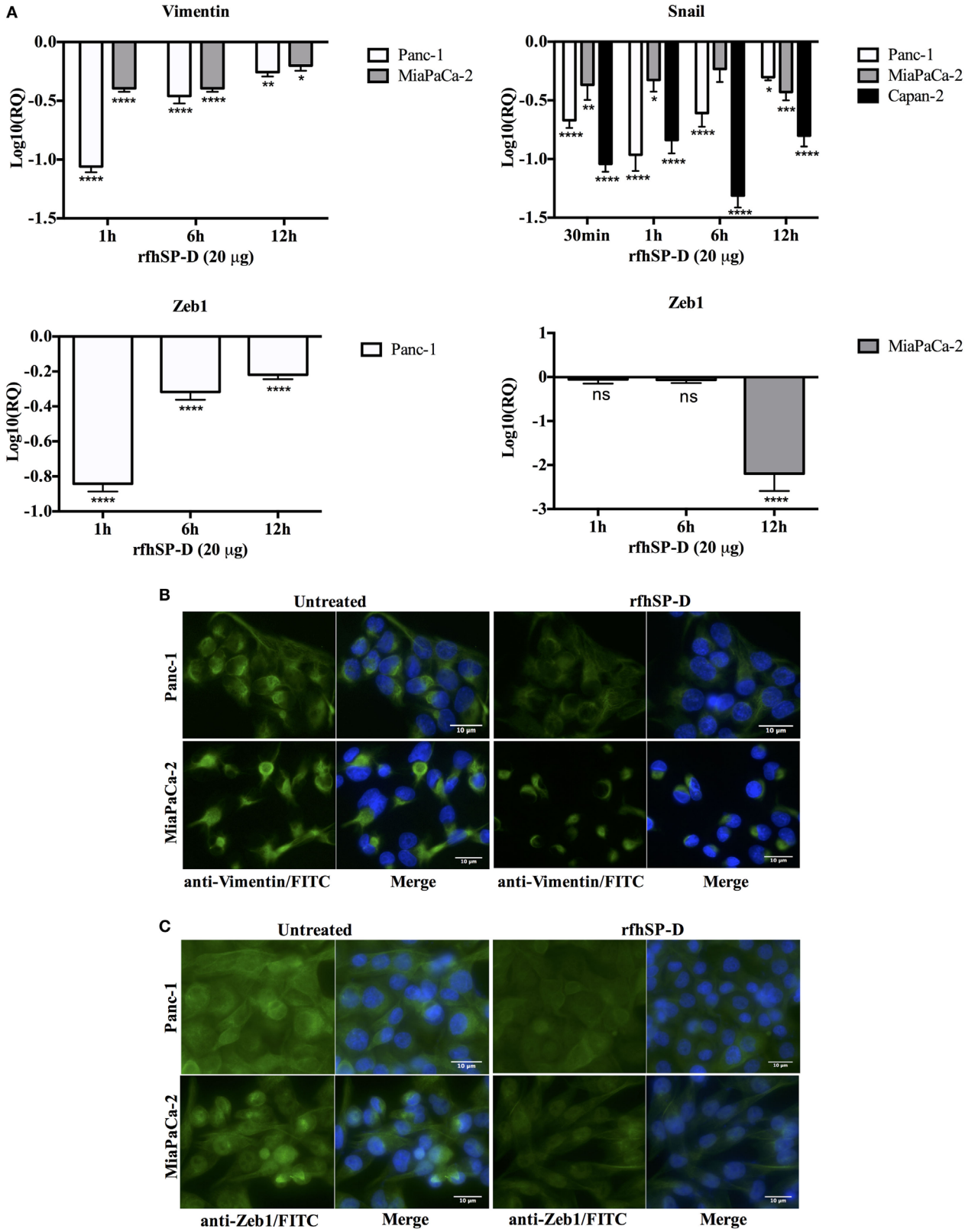

FIGURE 6 | Continued

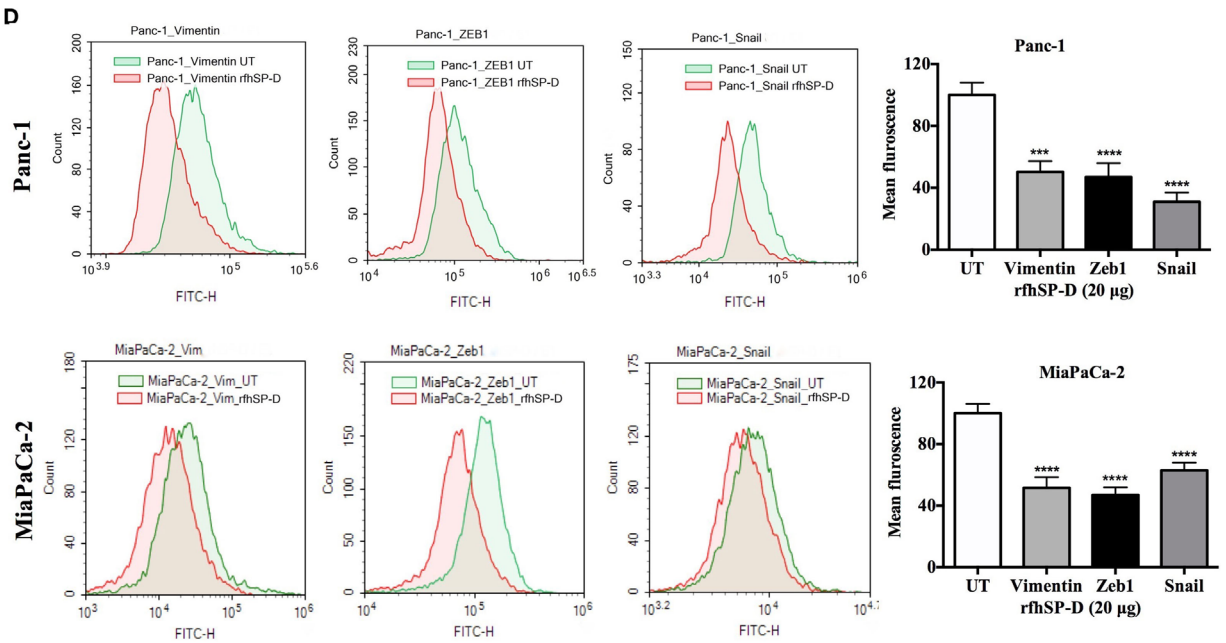

FIGURE 6 | Recombinant fragment of human SP-D (rfhSP-D) downregulates the expression of epithelial-to-mesenchymal transition (EMT) markers (Vimentin, Snail, and Zeb1). **(A)** All cell lines were incubated with and without rfhSP-D (20 µg/ml) for various time points and total RNA was extracted to synthesize cDNA. Each qPCR reaction was carried out in triplicates and human 18S RNA, an endogenous control, was used to normalize the gene expressions. The cycle threshold mean was used to calculate the relative expression to compare treated and untreated. EMT inducers, Vimentin, Snail, and Zeb1, were significantly downregulated across all cell lines. Significant values were considered based on $^{*}p < 0.05$, $^{**}p < 0.01$, $^{***}p < 0.001$, and $^{****}p < 0.0001$ between treated and untreated samples. **(B)** Vimentin intracellular staining for all cell lines using 0.5×10^5 cells incubated with and without rfhSP-D (20 µg/ml) for 24 h followed by probing with rabbit anti-human Vimentin antibody (1:500) and then with Alexa Fluor 488 conjugated with FITC (1:500) and Hoechst (1:10,000) for immunofluorescence analysis showed bright green fluorescence in the cytoplasm of the untreated cells as compared to very weak staining in the rfhSP-D-treated cells. **(C)** Zeb1 intracellular staining for all cell lines using 0.5×10^5 cells incubated with and without rfhSP-D (20 µg/ml) for 24 h followed by probing with rabbit anti-human Zeb1 antibody (1:500) and then with Alexa Fluor 488 (1:500) and Hoechst (1:10,000) for immunofluorescence analysis showed bright green fluorescence in the cytoplasm of the untreated cells of all cell lines as compared to minor staining in the treated cells of Panc-1 and MiaPaCa-2. **(D)** The quantitative analysis of the mean fluorescence of Vimentin, Zeb1, and Snail of Panc-1 and MiaPaCa-2 cell lines showed a significant reduction in the rfhSP-D-treated cells as compared to untreated counterparts. Significant values were considered based on $^{****}p < 0.0001$ between treated and untreated samples.

allergic patients, but not non-sensitized eosinophils derived from healthy subjects, underwent apoptosis when treated with rfhSP-D *in vitro* (28). An eosinophilic leukemic cell line, AML14.3D10, was thus examined to understand the mechanism of apoptosis induction by rfhSP-D (21). It revealed that levels of various apoptotic markers, such as activated p53, cleaved caspase 9, PARP, and G2/M checkpoints were considerably increased following rfhSP-D treatment, in addition to reduced levels of survival factors including HMGA1 (21, 35). Experiments with activated PBMCs also mirrored these observations (36). These studies have lent credence to the idea that SP-D is an innate immune surveillance molecule, especially outside lungs.

Hasegawa et al. have earlier shown that by interfering with EGF–EGFR interaction, SP-D can downregulate EGF signaling in A549 and H441 human lung adenocarcinoma cells (22), thus suppressing proliferation, migration, and invasiveness. Recently, Kaur et al. have shown that rfhSP-D can induce apoptosis in a range of pancreatic cancer cell lines *via* TNF-α/Fas-mediated pathway irrespective of the p53 status of the cells (29). Using Panc-1 ($p53^{mt}$), MiaPaCa-2 ($p53^{mt}$), and Capan-2 ($p53^{wt}$) pancreatic cancer cell lines, we found that rfhSP-D treatment for 24 h caused growth arrest in G1 cell cycle phase and triggered upregulation of pro-apoptotic markers, TNF-α, and Fas, which eventually caused apoptosis by 48 h (29).

In the current study, we wanted to assess the effects of rfhSP-D on PDA cell lines at earlier time points of the rfhSP-D treatment with a view that EMT may potentially be modulated. We have earlier reported that the binding of rfhSP-D to PDA cells is calcium-dependent but not sugar-dependent. Thus, it is likely that CRDs are involved in binding to target ligand on the cancer cell surface *via* protein–protein interaction. As a follow up study (29), we mainly focused on investigating the effects of rfhSP-D on EMT on these cancer cells. We have earlier reported using all necessary controls (including BSA and full length SP-D) and experiments (cell binding and cell viability assays), which established the specificity of rfhSP-D. BSA did not have any effect on PDA cell lines while full-length native SP-D purified from the lung lavage of alveolar proteinosis patients, was as good as rfhSP-D (29). Due to the ease of the production of large amounts of rfhSP-D, compared to full length SP-D, we have carried out these experiments using rfhSP-D, which is well characterized in the literature as a potential therapeutic molecule.

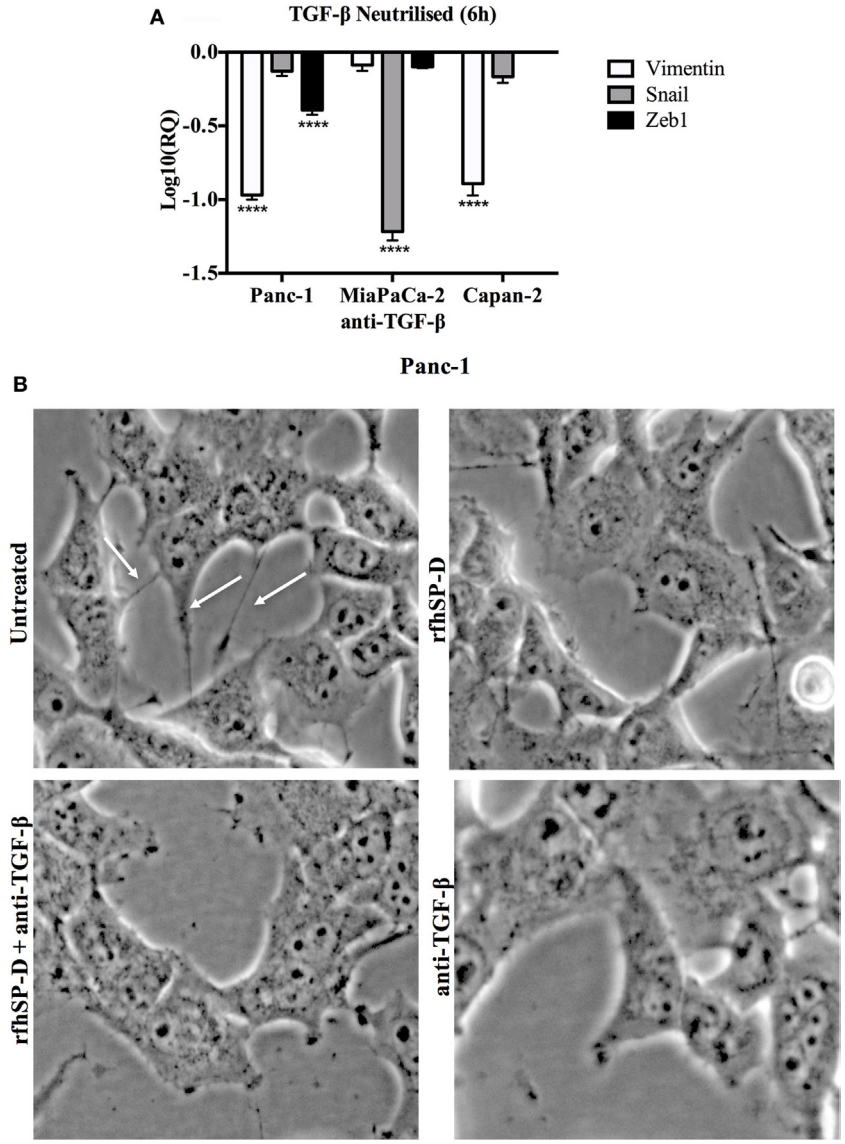

FIGURE 7 | **(A)** TGF-β caused downregulation of epithelial-to-mesenchymal transition (EMT) markers. All cell lines were incubated with TGF-β neutralizing antibody for 6 h to analyze the gene expression of Vimentin, Snail, and Zeb1, which showed that all EMT markers were downregulated in a manner similar to recombinant fragment of human SP-D (rfhSP-D) treatment. Significant values were considered based on $^{****}p < 0.0001$ between treated and untreated samples. **(B)** Analysis of images taken at 6 h following the treatment with rfhSP-D, anti-TGF-β, both rfhSP-D and anti-TGF-β and untreated begins to show less branches (highlighted with white arrows in UT) and decreased cell movement in all the treated samples as compared to untreated control, which translates into significant difference by 24 h as shown in cell invasion assay.

EMT induction is characterized by morphological alterations, enhanced motility, reduced cell–cell contact (17), and upregulation of mesenchymal markers, such as Vimentin (8), Snail (18), and Zeb1 (9). In this study, we report, for the first time, a novel anti-EMT role of human SP-D, which interferes with TGF-β induced EMT by blocking Smad phosphorylation, using pancreatic cancer cell lines, Panc-1, and MiaPaCa-2, and Capan-2. The rfhSP-D treatment of these cell lines for up to 24 h prevented their morphological alterations associated with EMT, reduced tumor cell invasion in the matrigel, downregulated TGF-β production, and downregulated key mesenchymal gene expression, such as Vimentin, Zeb1, and Snail. These hierarchical observations suggested that rfhSP-D can attenuate the TGF-β pathway to suppress EMT.

Overexpression of TGF-β1 in tumor microenvironment suppresses immune surveillance and facilitates the escape, migration, and increased resistance to anti-tumor immune responses (37–39). TGF-β exerts anti-proliferative effects on natural killer cells and cytotoxic T cells (40–43). TGF-β1 has also been shown to upregulate vascular endothelial growth factor (VEGF) production, thus, enhances the liver metastasis of pancreatic cancer by regulating angiogenesis in a mouse model (44). TGF-β binds to heterotetrameric receptor complex

consisting of type I (TβRI/ALK5) and type II receptors (TβRII) to activate downstream SMADs, which act as signal transducers from the receptors to the nucleus (45, 46). TGF-β expression, as revealed by qPCR and Western blot, was downregulated in Panc-1 and MiaPaCa-2 cell lines following rfhSP-D treatment. Capan-2 was unaffected, which may be attributed to its attenuated TGF-β signaling (47), thus, this cell line acted as a negative control in this study. In addition, minimal presence of SMAD 2/3 was detected in the cytoplasm and no translocation to the nucleus was detected in the rfhSP-D-treated cells as compared to untreated Panc-1 and MiaPaCa-2 cell lines. This suggested that the downregulation of TGF-β had prevented the recruitment of SMADs, the signal transduction molecules into the nucleus. Previous studies have shown that TGF-β stimulation causes the phosphorylation of SMAD 2/3, which then accumulate in nucleus to drive transcription of various target genes (46), including key mesenchymal markers, such as Vimentin (10) and Snail (10, 48) in pancreatic cancer, which regulate EMT by either direct or indirect effect on epithelial cell adhesion marker such as E-cadherin (49).

The treatment of Panc-1, MiaPaCa-2, and Capan-2 with rfhSP-D resulted in downregulation of Snail and Zeb1; however, Vimentin downregulation was only observed in Panc-1 and MiaPaCa-2 cells. Capan-2 has previously been shown not to express Vimentin (50). This suggests that due to downregulation of TGF-β, phosphorylation of SMADs is affected, since no Smad2/3 was seen either in the cytoplasm or nucleus, which then further causes the downregulation of EMT inducing genes resulting in a static state and loss of key EMT-associated morphological features. Moreover, when TGF-β was blocked for 6 h by a neutralizing antibody, gene expressions of Vimentin, Snail, and Zeb1 were downregulated similar to rfhSP-D treatment, re-affirming that rfhSP-D suppressed EMT by downregulating TGF-β pathway. These results, thus, explain the significantly reduced invasion of rfhSP-D-treated Panc-1 and MiaPaCa-2 in the matrigel matrix pre-coated with extracellular matrix proteins that promotes invasion, whereas the non-invasive Capan-2 cells remained unaffected.

In a previous study, stable and short hairpin RNA-mediated Zeb1-knockdown in Panc-1 and MiaPaCa-2 cells with overexpressed Zeb1 showed a reduced sphere formation, a hallmark of self-renewal and differentiation (9). In addition, Zeb1 knock-out in orthotopic mouse xenograft models significantly affected the tumor growth and EMT by switching the expression of Vimentin and E-cadherin (9). Similarly, downregulation of Snail in Panc-1 cells has been shown to increase its sensitivity to chemotherapeutics or radiation (51). Therefore, downregulation of mesenchymal markers can be crucial to target the EMT driven by TGF-β signaling pathway, which is a critical event in the progression of pancreatic cancer. In view of this study, rfhSP-D offers potentially a novel therapeutic approach to restore the epithelial phenotype in pancreatic cancer. Interestingly, rfhSP-D was most effective in the invasive cancer cells lines, i.e., Panc-1 and MiaPaCa-2, unlike in the non-invasive Capan-2 cell line, which indicates that it selectively targets the mesenchymal-differentiated cells. This is consistent with previous studies where rfhSP-D did not affect the eosinophils derived from healthy individual whereas it induced apoptosis in the sensitized eosinophils from allergic patients (21, 28). Targeting EMT pathway using rfhSP-D could not only lead to decreased invasiveness but also promote drug sensitivity. As mentioned earlier, Zeb1 knockout Panc-1 clones were more susceptible to chemotherapy and their proliferation was significantly reduced (9). Silencing of Zeb1 in Panc-1 and MiaPaCa-2 cells reversed the E-cadherin expression and a significantly increased apoptotic cell death was observed following gemcitabine, 5-FU, and cisplatin treatment (52). Therefore, it is important to explore the EMT suppressor role of rfhSP-D in combination with conventional chemotherapy as a therapeutic strategy against pre-malignant stages of solid tumor progression such as PDA.

AUTHOR CONTRIBUTIONS

AK carried out most of the crucial experiments with support from MR. SS provided key data, reagents, and ideas. UK led the project and prepared the manuscript together with AK and SS.

ACKNOWLEDGMENTS

SS is supported by a Max-Eder Group Leader Research Grant (Deutsche Krebshilfe). We thank Professor Uffe Holmskov, Odense University, Denmark for kindly providing mouse anti-human SP-D monoclonal antibody, and Valarmathy Murugaiah for help with revised figures and arranging bibliography.

REFERENCES

1. Siegel RL, Miller KD, Jemal A. Cancer statistics, 2016. *CA Cancer J Clin* (2016) 66:7–30. doi:10.3322/caac.21332
2. Ansari D, Tingstedt B, Andersson B, Holmquist F, Sturesson C, Williamsson C, et al. Pancreatic cancer: yesterday, today and tomorrow. *Future Oncol* (2016) 12:1929–46. doi:10.2217/fon-2016-0010
3. Brabletz T, Jung A, Spaderna S, Hlubek F, Kirchner T. Opinion: migrating cancer stem cells – an integrated concept of malignant tumour progression. *Nat Rev Cancer* (2005) 5:744–9. doi:10.1038/nrc1694
4. Brabletz T. EMT and MET in metastasis: where are the cancer stem cells? *Cancer Cell* (2012) 22:699–701. doi:10.1016/j.ccr.2012.11.009
5. Rhim AD, Mirek ET, Aiello NM, Maitra A, Bailey JM, McAllister F, et al. EMT and dissemination precede pancreatic tumor formation. *Cell* (2012) 148:349–61. doi:10.1016/j.cell.2011.11.025
6. Singh SK, Chen NM, Hessmann E, Siveke J, Lahmann M, Singh G, et al. Antithetical NFATc1-Sox2 and p53-miR200 signaling networks govern pancreatic cancer cell plasticity. *EMBO J* (2015) 34:517–30. doi:10.15252/embj.201489574
7. Fidler IJ. The pathogenesis of cancer metastasis: the 'seed and soil' hypothesis revisited. *Nat Rev Cancer* (2003) 3:453–8. doi:10.1038/nrc1098
8. Maier HJ, Wirth T, Beug H. Epithelial-mesenchymal transition in pancreatic carcinoma. *Cancers (Basel)* (2010) 2:2058–83. doi:10.3390/cancers2042058
9. Wellner U, Schubert J, Burk UC, Schmalhofer O, Zhu F, Sonntag A, et al. The EMT-activator ZEB1 promotes tumorigenicity by repressing stemness-inhibiting microRNAs. *Nat Cell Biol* (2009) 11:1487–95. doi:10.1038/ncb1998
10. Nishioka R, Itoh S, Gui T, Gai Z, Oikawa K, Kawai M, et al. SNAIL induces epithelial-to-mesenchymal transition in a human pancreatic cancer cell line (BxPC3) and promotes distant metastasis and invasiveness in vivo. *Exp Mol Pathol* (2010) 89:149–57. doi:10.1016/j.yexmp.2010.05.008

11. Beuran M, Negoi I, Paun S, Ion AD, Bleotu C, Negoi RI, et al. The epithelial to mesenchymal transition in pancreatic cancer: a systematic review. *Pancreatology* (2015) 15:217–25. doi:10.1016/j.pan.2015.02.011
12. Kaufhold S, Bonavida B. Central role of Snail1 in the regulation of EMT and resistance in cancer: a target for therapeutic intervention. *J Exp Clin Cancer Res* (2014) 33:62. doi:10.1186/s13046-014-0062-0
13. Noll EM, Eisen C, Stenzinger A, Espinet E, Muckenhuber A, Klein C, et al. CYP3A5 mediates basal and acquired therapy resistance in different subtypes of pancreatic ductal adenocarcinoma. *Nat Med* (2016) 22:278–87. doi:10.1038/nm.4038
14. Heldin CH, Vanlandewijck M, Moustakas A. Regulation of EMT by TGFbeta in cancer. *FEBS Lett* (2012) 586:1959–70. doi:10.1016/j.febslet.2012.02.037
15. Oshimori N, Oristian D, Fuchs E. TGF-beta promotes heterogeneity and drug resistance in squamous cell carcinoma. *Cell* (2015) 160:963–76. doi:10.1016/j.cell.2015.01.043
16. Friess H, Yamanaka Y, Buchler M, Berger HG, Kobrin MS, Baldwin RL, et al. Enhanced expression of the type II transforming growth factor beta receptor in human pancreatic cancer cells without alteration of type III receptor expression. *Cancer Res* (1993) 53:2704–7.
17. Ellenrieder V, Hendler SF, Ruhland C, Boeck W, Adler G, Gress TM. TGF-beta-induced invasiveness of pancreatic cancer cells is mediated by matrix metalloproteinase-2 and the urokinase plasminogen activator system. *Int J Cancer* (2001) 93:204–11. doi:10.1002/ijc.1330
18. Peinado H, Quintanilla M, Cano A. Transforming growth factor beta-1 induces snail transcription factor in epithelial cell lines: mechanisms for epithelial mesenchymal transitions. *J Biol Chem* (2003) 278:21113–23. doi:10.1074/jbc.M211304200
19. Roshani R, McCarthy F, Hagemann T. Inflammatory cytokines in human pancreatic cancer. *Cancer Lett* (2014) 345:157–63. doi:10.1016/j.canlet.2013.07.014
20. Kishore U, Greenhough TJ, Waters P, Shrive AK, Ghai R, Kamran MF, et al. Surfactant proteins SP-A and SP-D: structure, function and receptors. *Mol Immunol* (2006) 43:1293–315. doi:10.1016/j.molimm.2005.08.004
21. Mahajan L, Pandit H, Madan T, Gautam P, Yadav AK, Warke H, et al. Human surfactant protein D alters oxidative stress and HMGA1 expression to induce p53 apoptotic pathway in eosinophil leukemic cell line. *PLoS One* (2013) 8:e85046. doi:10.1371/journal.pone.0085046
22. Hasegawa Y, Takahashi M, Ariki S, Asakawa D, Tajiri M, Wada Y, et al. Surfactant protein D suppresses lung cancer progression by downregulation of epidermal growth factor signaling. *Oncogene* (2015) 34:4285–6. doi:10.1038/onc.2015.266
23. Ishii T, Hagiwara K, Kamio K, Ikeda S, Arai T, Mieno MN, et al. Involvement of surfactant protein D in emphysema revealed by genetic association study. *Eur J Hum Genet* (2012) 20:230–5. doi:10.1038/ejhg.2011.183
24. Foreman MG, Kong X, DeMeo DL, Pillai SG, Hersh CP, Bakke P, et al. Polymorphisms in surfactant protein-D are associated with chronic obstructive pulmonary disease. *Am J Respir Cell Mol Biol* (2011) 44:316–22. doi:10.1165/rcmb.2009-0360OC
25. Lingappa JR, Dumitrescu L, Zimmer SM, Lynfield R, McNicholl JM, Messonnier NE, et al. Identifying host genetic risk factors in the context of public health surveillance for invasive pneumococcal disease. *PLoS One* (2011) 6:e23413. doi:10.1371/journal.pone.0023413
26. Silveyra P, Floros J. Genetic variant associations of human SP-A and SP-D with acute and chronic lung injury. *Front Biosci (Landmark Ed)* (2012) 17:407–29. doi:10.2741/3935
27. Tanaka M, Arimura Y, Goto A, Hosokawa M, Nagaishi K, Yamashita K, et al. Genetic variants in surfactant, pulmonary-associated protein D (SFTPD) and Japanese susceptibility to ulcerative colitis. *Inflamm Bowel Dis* (2009) 15:918–25. doi:10.1002/ibd.20936
28. Mahajan L, Madan T, Kamal N, Singh VK, Sim RB, Telang SD, et al. Recombinant surfactant protein-D selectively increases apoptosis in eosinophils of allergic asthmatics and enhances uptake of apoptotic eosinophils by macrophages. *Int Immunol* (2008) 20:993–1007. doi:10.1093/intimm/dxn058
29. Kaur A, Riaz MS, Murugaiah V, Varghese PM, Singh SK, Kishore U. A recombinant fragment of human surfactant protein D induces apoptosis in pancreatic cancer cell lines via fas-mediated pathway. *Front Immunol* (2018) 9:1126. doi:10.3389/fimmu.2018.01126
30. Singh SK, Fiorelli R, Kupp R, Rajan S, Szeto E, Lo Cascio C, et al. Post-translational modifications of OLIG2 regulate glioma invasion through the TGF-beta pathway. *Cell Rep* (2016) 16:950–66. doi:10.1016/j.celrep.2016.06.045
31. Kishore U, Bernal AL, Kamran MF, Saxena S, Singh M, Sarma PU, et al. Surfactant proteins SP-A and SP-D in human health and disease. *Arch Immunol Ther Exp (Warsz)* (2005) 53:399–417.
32. Wang JY, Kishore U, Lim BL, Strong P, Reid KB. Interaction of human lung surfactant proteins A and D with mite (*Dermatophagoides pteronyssinus*) allergens. *Clin Exp Immunol* (1996) 106:367–73. doi:10.1046/j.1365-2249.1996.d01-838.x
33. Madan T, Kishore U, Shah A, Eggleton P, Strong P, Wang JY, et al. Lung surfactant proteins A and D can inhibit specific IgE binding to the allergens of *Aspergillus fumigatus* and block allergen-induced histamine release from human basophils. *Clin Exp Immunol* (1997) 110:241–9. doi:10.1111/j.1365-2249.1997.tb08323.x
34. Madan T, Kishore U, Singh M, Strong P, Clark H, Hussain EM, et al. Surfactant proteins A and D protect mice against pulmonary hypersensitivity induced by *Aspergillus fumigatus* antigens and allergens. *J Clin Invest* (2001) 107:467–75. doi:10.1172/JCI10124
35. Mahajan L, Gautam P, Dodagatta-Marri E, Madan T, Kishore U. Surfactant protein SP-D modulates activity of immune cells: proteomic profiling of its interaction with eosinophilic cells. *Expert Rev Proteomics* (2014) 11:355–69. doi:10.1586/14789450.2014.897612
36. Pandit H, Thakur G, Koippallil Gopalakrishnan AR, Dodagatta-Marri E, Patil A, Kishore U, et al. Surfactant protein D induces immune quiescence and apoptosis of mitogen-activated peripheral blood mononuclear cells. *Immunobiology* (2016) 221:310–22. doi:10.1016/j.imbio.2015.10.004
37. Sun L, Wu G, Willson JK, Zborowska E, Yang J, Rajkarunanayake I, et al. Expression of transforming growth factor beta type II receptor leads to reduced malignancy in human breast cancer MCF-7 cells. *J Biol Chem* (1994) 269:26449–55.
38. Beauchamp RD, Lyons RM, Yang EY, Coffey RJ Jr, Moses HL. Expression of and response to growth regulatory peptides by two human pancreatic carcinoma cell lines. *Pancreas* (1990) 5:369–80. doi:10.1097/00006676-199007000-00001
39. Reiss M. TGF-beta and cancer. *Microbes Infect* (1999) 1:1327–47. doi:10.1016/S1286-4579(99)00251-8
40. Kehrl JH, Roberts AB, Wakefield LM, Jakowlew S, Sporn MB, Fauci AS. Transforming growth factor beta is an important immunomodulatory protein for human B lymphocytes. *J Immunol* (1986) 137:3855–60.
41. Rook AH, Kehrl JH, Wakefield LM, Roberts AB, Sporn MB, Burlington DB, et al. Effects of transforming growth factor beta on the functions of natural killer cells: depressed cytolytic activity and blunting of interferon responsiveness. *J Immunol* (1986) 136:3916–20.
42. Wahl SM, McCartney-Francis N, Mergenhagen SE. Inflammatory and immunomodulatory roles of TGF-beta. *Immunol Today* (1989) 10:258–61. doi:10.1016/0167-5699(89)90136-9
43. Kehrl JH, Wakefield LM, Roberts AB, Jakowlew S, Alvarez-Mon M, Derynck R, et al. Pillars article: production of transforming growth factor beta by human T lymphocytes and its potential role in the regulation of T cell growth. *J Immunol* (2014) 192:2939–52.
44. Teraoka H, Sawada T, Yamashita Y, Nakata B, Ohira M, Ishikawa T, et al. TGF-beta1 promotes liver metastasis of pancreatic cancer by modulating the capacity of cellular invasion. *Int J Oncol* (2001) 19:709–15. doi:10.3892/ijo.19.4.709
45. Massague J. How cells read TGF-β signals. *Nat Rev Mol Cell Biol* (2000) 1:169–78. doi:10.1038/35043051
46. Massague J, Wotton D. Transcriptional control by the TGF-β/Smad signaling system. *EMBO J* (2000) 19:1745–54. doi:10.1093/emboj/19.8.1745
47. Subramanian G, Schwarz RE, Higgins L, McEnroe G, Chakravarty S, Dugar S, et al. Targeting endogenous transforming growth factor beta receptor signaling in SMAD4-deficient human pancreatic carcinoma cells inhibits their invasive phenotype1. *Cancer Res* (2004) 64:5200–11. doi:10.1158/0008-5472.CAN-04-0018
48. Horiguchi K, Shirakihara T, Nakano A, Imamura T, Miyazono K, Saitoh M. Role of Ras signaling in the induction of snail by transforming growth factor-beta. *J Biol Chem* (2009) 284:245–53. doi:10.1074/jbc.M804777200
49. Imamichi Y, Konig A, Gress T, Menke A. Collagen type I-induced Smad-interacting protein 1 expression downregulates E-cadherin in pancreatic cancer. *Oncogene* (2007) 26:2381–5. doi:10.1038/sj.onc.1210012

50. Diaferia GR, Balestrieri C, Prosperini E, Nicoli P, Spaggiari P, Zerbi A, et al. Dissection of transcriptional and cis-regulatory control of differentiation in human pancreatic cancer. *EMBO J* (2016) 35:595–617. doi:10.15252/embj.201592404
51. Zhang K, Jiao X, Liu X, Zhang B, Wang J, Wang Q, et al. Knockdown of snail sensitizes pancreatic cancer cells to chemotherapeutic agents and irradiation. *Int J Mol Sci* (2010) 11:4891–2. doi:10.3390/ijms11124891
52. Arumugam T, Ramachandran V, Fournier KF, Wang H, Marquis L, Abbruzzese JL, et al. Epithelial to mesenchymal transition contributes to drug resistance in pancreatic cancer. *Cancer Res* (2009) 69:5820–8. doi:10.1158/0008-5472.CAN-08-2819

Conflict of Interest Statement: The authors declare that the research was conducted in the absence of any commercial or financial relationships that could be construed as a potential conflict of interest.

frontiers in Immunology

ORIGINAL RESEARCH
published: 06 August 2018
doi: 10.3389/fimmu.2018.01748

Pathological Significance and Prognostic Value of Surfactant Protein D in Cancer

Alessandro Mangogna[1†], Beatrice Belmonte[2†], Chiara Agostinis[3†], Giuseppe Ricci[3,4], Alessandro Gulino[2], Ines Ferrara[2], Fabrizio Zanconati[4], Claudio Tripodo[2], Federico Romano[3], Uday Kishore[5] and Roberta Bulla[2]*

[1] Department of Life Sciences, University of Trieste, Trieste, Italy, [2] Tumor Immunology Unit, Department of Health Sciences, Human Pathology Section, University of Palermo, Palermo, Sicily, Italy, [3] Institute for Maternal and Child Health, IRCCS (Istituto di Ricovero e Cura a Carattere Scientifico) Burlo Garofolo, Trieste, Italy, [4] Department of Medical, Surgical and Health Science, University of Trieste, Trieste, Italy, [5] Biosciences, College of Health and Life Sciences, Brunel University London, Uxbridge, United Kingdom

Surfactant protein D (SP-D) is a pattern recognition molecule belonging to the Collectin (collagen-containing C-type lectin) family that has pulmonary as well as extra-pulmonary existence. In the lungs, it is a well-established opsonin that can agglutinate a range of microbes, and enhance their clearance *via* phagocytosis and super-oxidative burst. It can interfere with allergen–IgE interaction and suppress basophil and mast cell activation. However, it is now becoming evident that SP-D is likely to be an innate immune surveillance molecule against tumor development. SP-D has been shown to induce apoptosis in sensitized eosinophils derived from allergic patients and a leukemic cell line *via* p53 pathway. Recently, SP-D has been shown to suppress lung cancer progression *via* interference with the epidermal growth factor signaling. In addition, a truncated form of recombinant human SP-D has been reported to induce apoptosis in pancreatic adenocarcinoma *via* Fas-mediated pathway in a p53-independent manner. To further establish a correlation between SP-D presence/levels and normal and cancer tissues, we performed a bioinformatics analysis, using Oncomine dataset and the survival analysis platforms Kaplan–Meier plotter, to assess if SP-D can serve as a potential prognostic marker for human lung cancer, in addition to human gastric, breast, and ovarian cancers. We also analyzed immunohistochemically the presence of SP-D in normal and tumor human tissues. We conclude that (1) in the lung, gastric, and breast cancers, there is a lower expression of SP-D than normal tissues; (2) in ovarian cancer, there is a higher expression of SP-D than normal tissue; and (3) in lung cancer, the presence of SP-D could be associated with a favorable prognosis. On the contrary, at non-pulmonary sites such as gastric, breast, and ovarian cancers, the presence of SP-D could be associated with unfavorable prognosis. Correlation between the levels of SP-D and overall survival requires further investigation. Our analysis involves a large number of dataset; therefore, any trend observed is reliable. Despite apparent complexity within the results, it is evident that cancer tissues that produce less levels of SP-D compared to their normal tissue counterparts are probably less susceptible to SP-D-mediated immune surveillance mechanisms *via* infiltrating immune cells.

Keywords: innate immunity, surfactant protein D, immune surveillance, bioinformatics analysis, immunohistochemistry, cancers, tumor microenvironment

OPEN ACCESS

Edited by:
Francesca Granucci, Università degli studi di Milano Bicocca, Italy

Reviewed by:
Kenneth Reid, University of Oxford, United Kingdom
Anuvinder Kaur, Independent Researcher, London; Brunel University London, United Kingdom

****Correspondence:***
Chiara Agostinis
chiara.agostinis@burlo.trieste.it

[†]These authors have contributed equally to this work.

Specialty section:
This article was submitted to Molecular Innate Immunity, a section of the journal Frontiers in Immunology

Received: *30 May 2018*
Accepted: *16 July 2018*
Published: *06 August 2018*

Citation:
Mangogna A, Belmonte B, Agostinis C, Ricci G, Gulino A, Ferrara I, Zanconati F, Tripodo C, Romano F, Kishore U and Bulla R (2018) Pathological Significance and Prognostic Value of Surfactant Protein D in Cancer. Front. Immunol. 9:1748. doi: 10.3389/fimmu.2018.01748

INTRODUCTION

Surfactant protein D (SP-D) is a collagenous glycoprotein encoded by *SFTPD* gene belonging to the collectins family (1). Like other members of the collectin family, SP-D has a primary subunit structure that comprises of an N-terminal cysteine-rich region, a triple-helical collagen-like domain, an α-helical coiled neck domain, and a C-terminal C-type lectin domain [also called carbohydrate recognition domain (CRD)] (2). Each subunit of human SP-D comprises three identical polypeptide chains of 43 kDa, which is assembled into a tetrameric structure with four of the homotrimeric subunits linked *via* their N-terminal regions, but trimers, dimers, and monomers also exist. Tetrameric structures can undergo further oligomerization to give SP-D multimers that could contain up to 96 individual chains. SP-D was originally described in association with pulmonary surfactant; in the lung, it is synthesized and secreted by type II alveolar cells and non-ciliated bronchiolar epithelial cells. It has a key role in the maintenance of surfactant homeostasis by reducing surface tension (3). Reduced SP-D expression or genetic variations (single-nucleotide polymorphism) have been associated with an increased risk of respiratory diseases (4, 5).

Extra-pulmonary existence of SP-D has also been reported. SP-D is also expressed by epithelial cells lining various exocrine ducts, the mucosa of the gastrointestinal and genitourinary tracts, the nasal cavity, and in the brain (2). Furthermore, its presence has been demonstrated in healthy lacrimal gland, conjunctiva, cornea, and nasolacrimal duct samples (6). Other studies have shown the presence of SP-D in synovial fluid derived from patients with rheumatoid arthritis (7).

In addition to its role in surfactant homeostasis, SP-D has a critical function as a regulator of inflammation (3). It is involved in the recognition and neutralization of pathogens which promotes aggregation/agglutination and inhibition of microbial growth (8), SP-D has also been implicated in the clearance of necrotic and apoptotic cells (9). Thus, its function in the recognition of non-self and altered self makes it a potent and versatile humoral pattern recognition receptor (10–12). SP-D has also been described as a potent link between innate and adaptive immune mechanisms (13–15). Studies involving *in vivo* and *ex vivo* models of allergic inflammation revealed that SP-D can alleviate pulmonary hypersensitivity *via* suppression of IgE levels, promotion of Th2 to Th1 polarization (16), apoptosis induction in sensitized eosinophils *via* p53-mediated pathway (17), and inhibition of IgE synthesis by B cells (18). These studies highlighted a potential role of SP-D as an immune surveillance molecule. It has recently been shown that SP-D also plays a role in the control of lung cancer progression *via* epidermal growth factor (EGF) signaling (19). Very recently, Kaur et al. have shown that a recombinant fragment of human SP-D, composed of homotrimeric neck and C-type lectin domains, can induce apoptosis in pancreatic adenocarcinoma cell lines, such as Panc-1 ($p53^{mt}$), MiaPaCa-2 ($p53^{mt}$), and Capan-2 ($p53^{wt}$), *via* Fas-mediated pathway (20).

In the current study, we performed a bioinformatics analysis in order to investigate whether SP-D can serve as a potential prognostic marker for human lung cancer. We extended our investigation to several non-pulmonary sites such as human gastric, breast, and ovarian cancer. We used the Oncomine dataset and the survival analysis platforms Kaplan–Meier plotter. Our results appear to suggest a likely pro-tumorigenic role of SP-D in gastric, breast, and ovarian cancers and an anti-tumor effect in lung cancer. Furthermore, we analyzed the presence of SP-D in normal and tumor human tissues *via* immunohistochemistry (IHC). Differential expression of SP-D was also investigated in human cells isolated from normal and tumor ovary tissues by real-time PCR. This *in silico* study, if validated *via* a retrospective study at the protein level, could be a step forward in ascertaining the importance of SP-D as a prognostic biomarker for different cancers.

MATERIALS AND METHODS

Oncomine Database Analysis

The expression level of *SFTPD* gene in various types of cancer was analyzed using Oncomine,[1] a cancer microarray database and web-based data mining platform from genome-wide expression analyses (21, 22). We compared the differences in mRNA level between normal tissue and cancer. The mRNA expression level in neoplastic tissues compared to the healthy tissues was obtained as the parameters of p-value < 0.001, fold change $>$ all, and gene ranking in the top 10%. Information about the datasets used in this study is summarized in **Table 1**.

Kaplan–Meier Plotter Database Analysis

A Kaplan–Meier plotter database can assess the effect of 54,675 genes on survival using 10,461 cancer samples (5,143 breast, 1,816 ovarian, 2,437 lung, and 1,065 gastric cancer patients with a mean follow-up of 69/40/49/33 months) using probe sets on the HGU133 Plus 2.0 array. The prognostic significance of SP-D expression and survival in breast, ovarian, lung, and gastric cancer was analyzed by Kaplan–Meier plotter[2] (23). The hazard ratio with 95% confidence intervals and logrank p-value was also computed.

Patients and Specimens

Eight fresh clinical specimens (four normal ovarian epithelial tissues and four malignant ovarian epithelial tumor tissues) were obtained from the Department of Gynaecology of IRCCS "Burlo Garofolo", in Trieste, Italy between 2016 and 2017. Cancer patients underwent laparoscopy for diagnosis of pelvic mass whereas control patients underwent laparoscopy for other indications. Tissue samples from patients were collected after informed consent following ethical approval by the Institutional Board of IRCCS "Burlo Garofolo", Trieste, Italy.

Immunohistochemical Analysis

For the immunohistochemical analysis, human normal and neoplastic tissues, including lung, breast, ovary, and stomach samples, were selected from the archives of the Department of

[1] www.oncomine.org.
[2] www.kmplot.com.

TABLE 1 | Data characteristics used in the bioinformatics analysis.

Datasets	Study description	Experiment type
Bhattacharjee lung	139 lung adenocarcinoma, 21 squamous cell lung carcinoma, 20 lung carcinoid tumor, 6 small cell lung carcinoma, and 17 normal lung samples were analyzed on Affymetrix U95A microarrays. Sample data includes type, age, M stage, max tumor percentage, N stage, primary/metastatic, recurrence, sex, site of metastasis, smoking rate (packs per year), stage, survival, and T stage	mRNA
Hou lung	91 non-small cell lung carcinoma and 65 adjacent normal lung samples were analyzed. Sample data includes age, sex, cancer sample site, and survival	mRNA
Garber lung	67 lung carcinoma samples of various types and 6 normal lung samples were analyzed on cDNA microarrays. Sample data includes type, grade, TNM stage, and survival	mRNA
Cho gastric	65 gastric adenocarcinoma, 19 paired surrounding normal tissue, and 6 gastrointestinal stromal tumor samples were analyzed. Sample data includes age, grade, stage, TNM stage, sex, and subgroup	mRNA
DErrico gastric	31 paired gastric carcinoma and adjacent normal gastric mucosa and 7 unmatched gastric carcinoma samples were analyzed. Sample data includes microsatellite status, age, sex, and TNM stage	mRNA
Zhao breast	Normal breast ($n = 3$) and breast carcinoma ($n = 61$) samples were analyzed on cDNA microarrays. Sample data includes tumor percentage, age, E-Cadherin status, estrogen receptor status, grade, HER2 status, lymph node metastasis status, and progesterone receptor status	mRNA
TCGA breast	532 invasive breast carcinoma, 61 paired normal breast tissue, and 3 paired metastatic samples were analyzed. Sample data includes age, histology, TNM stage, ER/PR/ERBB2 status, sex, stage, and others. This dataset consists of Level 2 (processed) data from the TCGA data portal	mRNA
Curtis breast	1,992 breast carcinoma samples and 144 paired normal breast samples were analyzed for the METABRIC project. Sample data includes ER/PR/ERBB2 status, overall survival status and follow-up time, stage, grade, and others	mRNA
Yoshihara ovarian	43 ovarian serous adenocarcinomas and 10 normal peritoneum samples were analyzed. Sample data includes cancer sample site, stage, and sex	mRNA
TCGA ovarian	586 ovarian serous cystadenocarcinoma samples and 8 normal ovary samples were analyzed. Sample data includes age, stage, grade, survival, and others. This dataset consists of Level 2 (processed) data from the TCGA data portal	mRNA

Abbreviations: TNM, Tumor-Nodes-Metastasis; HER2, Human Epidermal Growth Factor Receptor 2; ER, Estrogen Receptor; PR, Progesterone Receptor; ERBB, Erb-b2 receptor tyrosine kinase 2.

Pathology, University of Palermo. Immunohistochemistry (IHC) was performed using a polymer detection method. Briefly, tissue samples were fixed in 10% v/v buffered formalin and then paraffin embedded. 4 μm-thick tissue sections were deparaffinized and rehydrated. The antigen unmasking technique was carried out using Novocastra Epitope Retrieval Solutions, pH 9 (Leica Biosystems) in a PT Link pre-treatment module (Dako) at 98°C for 30 min. Sections were then brought to room temperature and washed in PBS. After neutralization of the endogenous peroxidase with 3% v/v H_2O_2 and Fc blocking by a specific protein block (Novocastra, Leica Biosystems), samples were incubated overnight at 4°C with rabbit anti-human SP-D (dilution 1:300) polyclonal antibodies (MRC Immunochemistry Unit, Oxford, UK). Staining was revealed *via* polymer detection kit (Novocastra, Leica Biosystems) and AEC (3-amino-9-ethylcarbazole, Dako, Denmark) substrate-chromogen. Slides were counterstained with Harris Hematoxylin (Novocastra, Leica Biosystems). Sections were analyzed under the Axio Scope A1 optical microscope (Zeiss) and microphotographs were collected through the Axiocam 503 color digital camera (Zeiss) using the Zen2 software.

Cell Isolation and Culture

Ovarian carcinoma cells (OvCa) and normal epithelial ovarian cells (OvEp) were isolated from biopsies derived from ovarian tissue. The tissue was finely minced with a cutter, incubated with a digestion solution composed by 0.5% trypsin (Sigma-Aldrich, Milan, Italy) and 50 μg/ml DNase I (Roche, Milan, Italy) in Hanks' Balanced Salt solution containing 0.5 mM $Ca^{2+}Mg^{2+}$ (Sigma-Aldrich) overnight at 4°C. Next, the enzymatic solution was changed to collagenase type 1 (1.5 mg/ml) (Worthington Biochemical Corporation, DBA) diluted in Medium 199 with Hank's salts (Euroclone Spa, Milan, Italy) for 30 min at 37°C. The digestion was blocked with 10% v/v fetal bovine serum (FBS; GIBCO, Life Technology) and the cell suspension was passed through a 100 μm pore filter (BD Biosciences, Italy). The cells were seeded in a 25 cm^2 flask, coated with bovine gelatine, and cultured using Human Endothelial cells serum-free medium (HESF; Life Technologies), 10% heat-inactivated FBS supplemented with EGF (10 ng/ml), basic FGF (20 ng/ml) and Penicillin–Streptomycin (Sigma-Aldrich). Fresh medium was replaced every 2–3 days. The cells were maintained at 37°C in humidified atmosphere with 5% v/v CO_2 and used at their fifth to eighth passage for *in vitro* experiments.

RNA Isolation, cDNA Synthesis, and Quantitative Real-Time PCR (qPCR)

Total RNA was extracted from cells using EuroGOLD trifast (Euroclone), according to the manufacturer's instructions, and reverse-transcribed as previously described (24). qPCR was carried out using a Rotor-Gene 6000 (Corbett, Qiangen, Ancona, Italy) using iQ SYBR Green Supermix (Applied Biosystems, Milan, Italy). The sequences of the primers used for amplification of TataBox Binding Protein (TBP) housekeeping gene are Forward 5′-GAGCCAAGAGTGAAGAACAGTC-3′; Reverse 5′-GCTCCCCACCATATTCTGAATCT-3′. The sequences of SP-D primers are Forward 5′-AGGCTGCTTTC

CTGAGCATGAC-3′; Reverse 5′-CCATTGGTGAAGATCTCC ACACAG-3′. The melting curve was recorded between 55 and 99°C with a hold every 2 s. The relative amount of gene production in each sample was determined by the Comparative Quantification method supplied as part of the Rotor Gene 1.7 software (Corbett Research) (25). The relative amount of each gene was normalized with TBP and expressed as arbitrary units (AU) considering 1 AU obtained from fully differentiated macrophage used as calibrator.

Statistical Analysis

Survival curves were generated by the Kaplan–Meier plots. All results are displayed with p values from a logrank test. p-values < 0.05 were considered significant. Similarly, with Oncomine, the statistical significance of data (p-values) was provided by the program.

RESULTS

Clinical Significance of SP-D Expression in Lung Cancer

We initially compared the differences in the mRNA level of SP-D between neoplastic and healthy tissues using the Oncomine platform. While analyzing Bhattacharjee's, Hou's, and Garber's datasets, we detected a significantly lower SP-D mRNA expression in lung adenocarcinoma, squamous cell carcinoma, large cell carcinoma, small cell carcinoma, and tumor carcinoid, compared to the normal lung tissue (**Figure 1A**, $p < 0.05$; Figure S1 in Supplementary Material, $p < 0.05$). We subsequently performed a bioinformatic analysis of SP-D mRNA expression using the Kaplan–Meier plotter dataset. As shown in **Figure 1B**, SP-D mRNA expression was positively related to an overall survival rate of the patients with lung cancer, stratified into lung adenocarcinoma and squamous cell carcinoma ($p < 0.05$).

IHC staining for SP-D confirmed a differential expression in healthy and neoplastic pulmonary parenchyma. Moreover, in lung adenocarcinoma and squamous cell lung carcinoma tissues, we observed a lower expression of SP-D within its microenvironment compared to the healthy pulmonary parenchyma (**Figure 2**).

Pathological Significance of SP-D mRNA Expression in Gastric, Breast, and Ovarian Cancers

The bioinformatics analysis on SP-D mRNA expression in gastric cancer *via* Cho's and DErrico's datasets showed its higher expression in healthy gastric mucosa compared to its malignant counterpart, stratified into intestinal, diffuse, and mixed-type

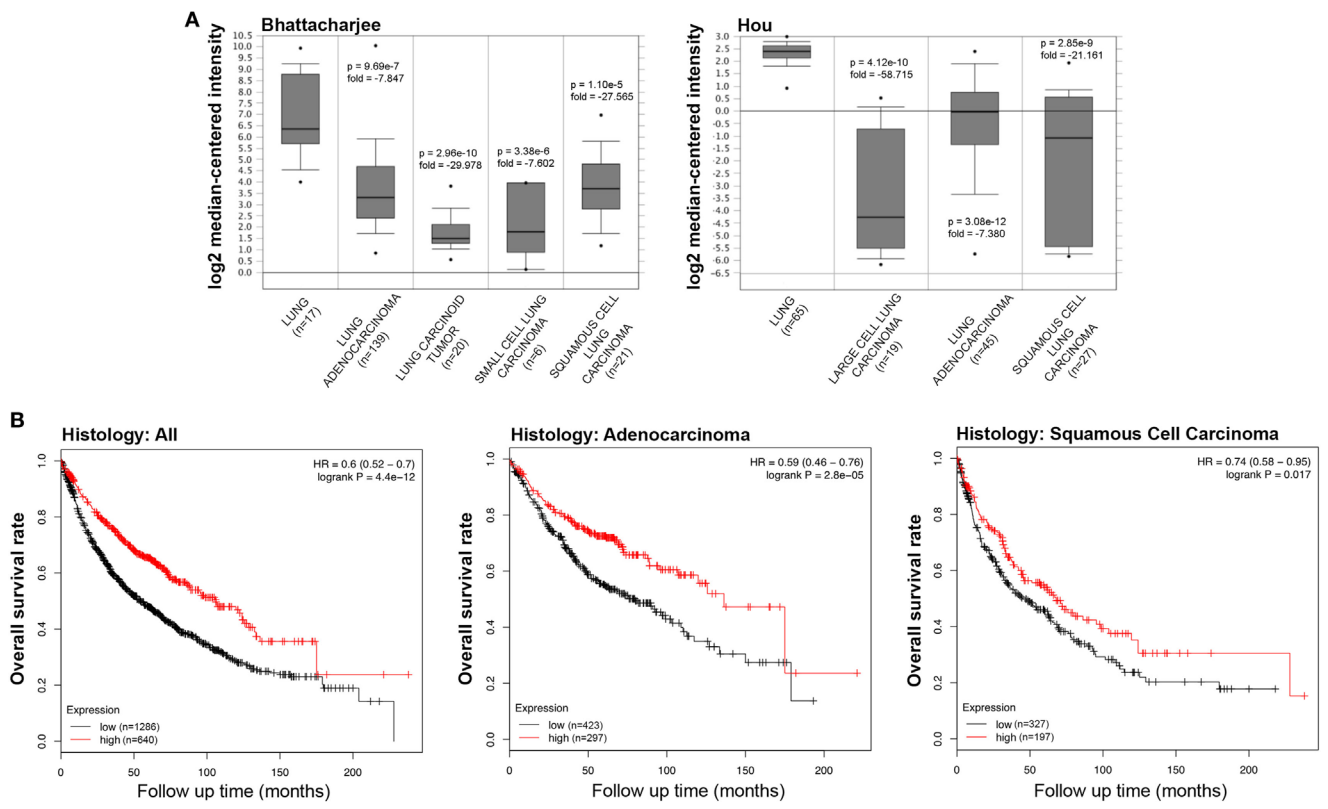

FIGURE 1 | Pathological significance of SP-D expression in lung cancer. Bhattacharjee's and Hou's datasets were used for bioinformatics analysis to explore SP-D mRNA expression in the lung cancer. A lower SP-D mRNA expression was detectable in lung adenocarcinoma, squamous cell carcinoma, large cell carcinoma, small cell carcinoma, and tumor carcinoid than in normal lung tissue [**(A)** $p < 0.05$]. According to the data from Kaplan–Meir plotter, SP-D mRNA expression was positively related to an overall survival rate of the patients with lung cancer, even stratified into lung adenocarcinoma and squamous cell carcinoma [**(B)** $p < 0.05$]. Abbreviations: HR, hazard ratio; SP-D, surfactant protein D.

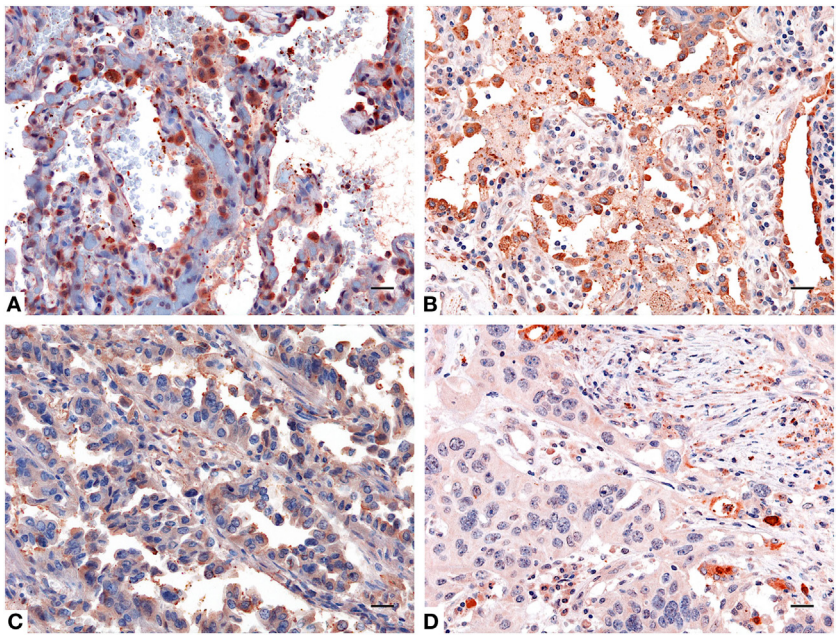

FIGURE 2 | Immunohistochemistry analysis for surfactant protein D (SP-D) in lung. Compared to healthy lung **(A,B)** a decreased expression of SP-D in adenocarcinoma **(C)** and squamous cell carcinoma of the lung **(D)** was observed. Polymer detection system with AEC (red) chromogen was used; scale bars, 50 μm. Polymer detection system with AEC (red) chromogen was used; scale bars, 50 μm.

adenocarcinoma by Lauren's classification (**Figure 3A**, $p < 0.05$; Figure S2 in Supplementary Material, $p < 0.05$). According to the data from Kaplan–Meier plotter, SP-D mRNA expression was negatively related to an overall survival rate of the patients with gastric cancer (**Figure 3B**, $p < 0.05$). If stratified by Lauren's classification, SP-D mRNA expression had a statistically significant association with intestinal-type adenocarcinoma, whereas no association with diffuse- and mixed-type adenocarcinomas was found (**Figure 3C**, $p < 0.05$). A higher expression of SP-D was negatively correlated with an overall survival rate in the patients without distant metastasis, HER2-negative and only intestinal-type adenocarcinoma (**Figure 3D**, $p < 0.05$).

The information regarding the SP-D mRNA expression in breast cancer was obtained from Zhao's, TCGA's, and Curtis's datasets, which showed that *SFTPD* was expressed at a lower level in invasive ductal breast carcinoma, male breast carcinoma, and breast phyllodes tumor, compared to normal breast tissues (**Figure 4A**, $p < 0.05$; Figure S3A in Supplementary Material, $p < 0.05$). According to the data from Kaplan–Meir plotter, *SFTPD* expression was negatively linked to the high overall survival rate in breast cancer patients with Luminal-A grade-1 and grade-2 cancers (**Figure 4B**, $p < 0.05$; Figure S3B in Supplementary Material, $p < 0.05$). No correlation between SP-D mRNA expression and overall survival rate was observed in patients with the other characteristics (Luminal-B, $HER2^+$, Basal, grade-3, mutated p53, wild-type p53).

Using IHC, we observed a variable presence and distribution of SP-D in normal tissues with respect to their cancer counterpart. In fact, IHC performed on either healthy or neoplastic gastric mucosa highlighted a significantly reduced expression of SP-D in the intestinal-type adenocarcinoma compared to gastric control tissue (**Figures 5A,C**). Likewise, a higher expression of SP-D in the normal mammary parenchyma was detected compared to that observed within microenvironment within the invasive ductal breast carcinoma, Luminal-A (**Figures 5B,D**).

We collected the results from Yoshihara's and TCGA's datasets and analyzed *SFTPD* expression in ovarian cancer. We observed a lower expression of *SFTPD* mRNA expression in normal ovary than in serous cystadenocarcinoma (**Figure 6A**, $p < 0.05$). The Kaplan–Meier plotter data, derived from stage-1 and -2 patients, showed a negative ratio between *SFTPD* expression and either overall or progression-free survival rates of patients with serous cystadenocarcinoma (**Figure 6B**, $p < 0.05$). However, no correlation was observed between *SFTPD* expression and these parameters (overall or progression-free survival rates) of patients with stage-3 and -4 ovarian cancer.

SP-D Expression in the Microenvironment of Ovarian Cancer

The mRNA expression of SP-D was also evaluated by real-time PCR in primary cells isolated from four samples each of human ovarian serous cystadenocarcinoma and normal ovarian tissues. As shown in **Figure 7A**, the cells isolated from ovarian serous cystoadenocarcinoma tissues expressed more SP-D compared to the normal tissue, confirming the data obtained with the bioinformatics analysis. IHC analysis also revealed the presence and the distribution of SP-D in the normal ovary where it appeared to be localized in the ovarian epithelium lining and in the serous cystadenocarcinoma. In addition, we detected a differential expression

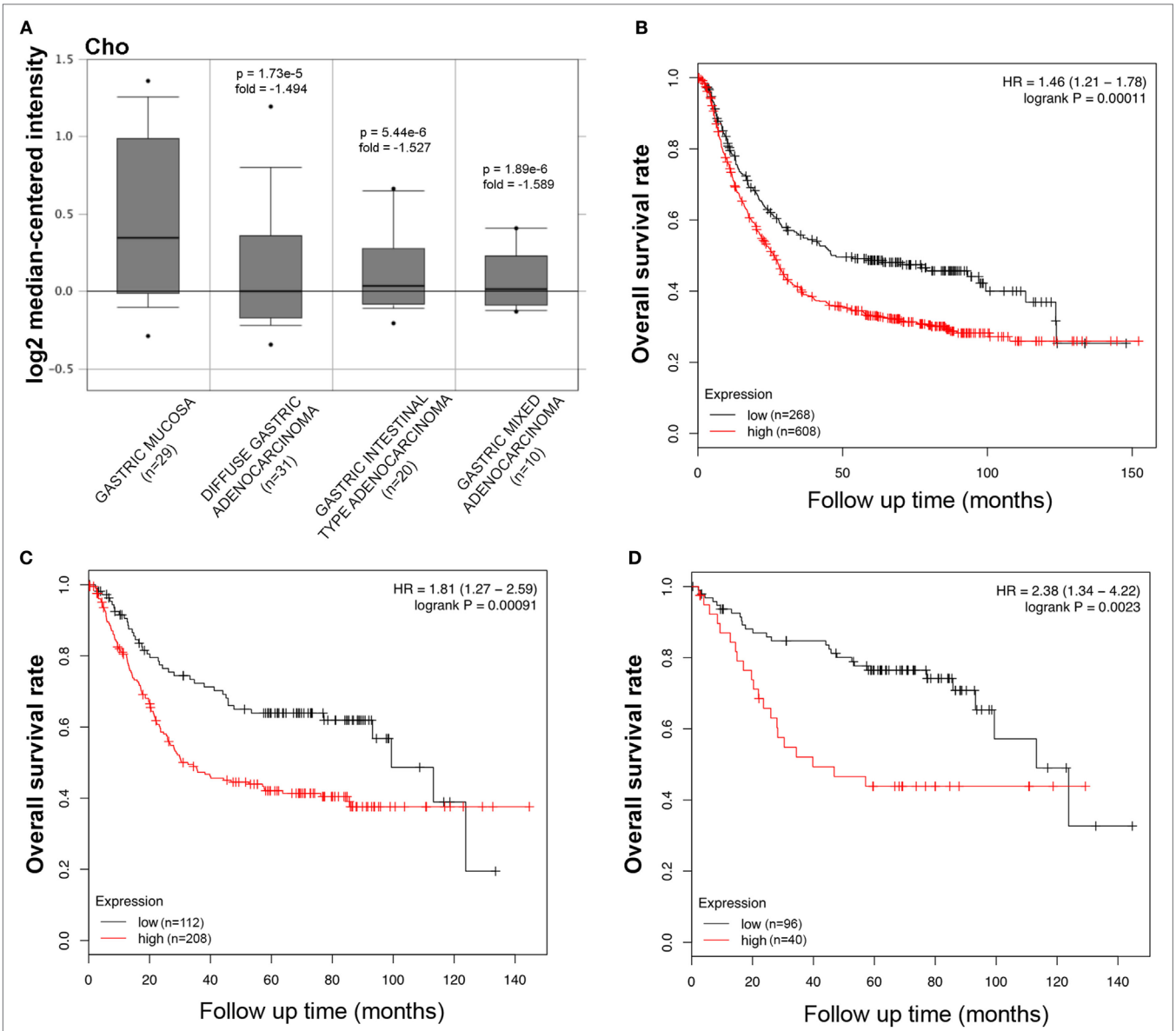

FIGURE 3 | Pathological significance of SP-D expression in gastric cancer. Cho's dataset has explored SP-D mRNA expression in gastric cancer. A lower *SFTPD* expression was detectable in gastric cancer than that in normal mucosa, even stratified into diffuse-, intestinal-, and mixed-type adenocarcinomas by Lauren's classification [**(A)** $p < 0.05$]. According to the data from Kaplan–Meier plotter, SP-D mRNA expression was negatively related to an overall survival rate of the patients with gastric cancer [**(B)** $p < 0.05$]. If stratified by Lauren's classification, SP-D mRNA expression was negatively related to an overall survival rate in the patients with intestinal-type adenocarcinoma [**(C)** $p < 0.05$], without distant metastasis and Her2-negative [**(D)** $p < 0.05$]. Abbreviations: HR, hazard ratio; SP-D, surfactant protein D.

in the normal as well as its malignant histotypes. Moreover, in the ovarian context, it showed an enrichment of SP-D expressing cells within the tumor microenvironment compared to the control tissue (**Figures 7B,C**).

DISCUSSION

The importance of SP-D in the regulation of the inflammation and homeostasis and in the protection against infection and allergens in the lung and at a range of extra-pulmonary mucosal sites is well documented (26, 27). However, there are recent evidences to implicate SP-D as an immune surveillance molecule against cancer (19, 20). In this study, we examined the potential prognostic value of this protein in lung, gastric, breast, and ovarian cancers. We focused our attention on these tumor types because we performed a bioinformatics analysis using the Kaplan–Meier plotter dataset, a manually curated database containing the information of 54,675 genes on 5,143 breast, 1,816 ovarian, 2,437 lung, and 1,065 gastric cancer samples. This is the most updated and reliable dataset available that offers the possibility of stratifying

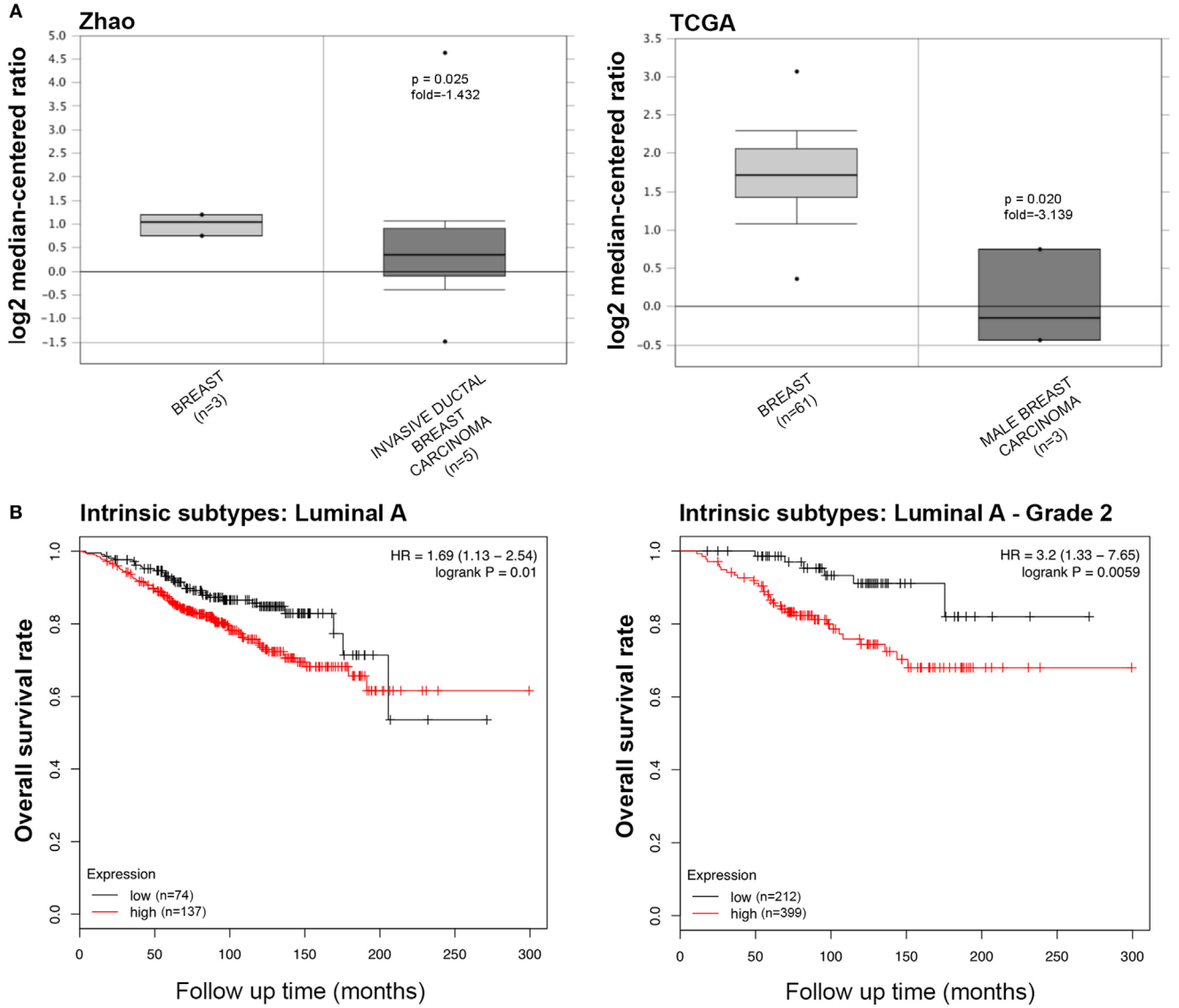

FIGURE 4 | The clinicopathological significances of SP-D expression in breast cancer. Zhao's and TCGA's datasets have revealed a lower SP-D mRNA expression in invasive ductal breast carcinoma and male breast carcinoma than in normal breast tissues [**(A)** $p < 0.05$]. There was a negative association between SP-D mRNA expression and a favorable prognosis in the breast cancer patients with Luminal-A only with grade-1 and -2 cancers, for Kaplan–Meir plotter [**(B)** $p < 0.05$]. Abbreviations: HR, hazard ratio; SP-D, surfactant protein D.

the analysis based on different tumor settings. The bioinformatics analysis highlighted a favorable prognostic effect of SP-D mRNA expression in the lung cancer, both in adenocarcinoma and squamous cell carcinoma; on the contrary, an unfavorable prognostic effect in gastric, ovarian, and breast cancer was revealed. In particular, SP-D mRNA expression showed a negative correlation with the intestinal-type gastric adenocarcinomas, grade-1 and grade-2 breast cancers and with stage-1 and -2 ovarian cancers. No significant correlation was showed within stage-3 and -4 in breast and ovarian cancers.

Sin et al. (28) have suggested that low SP-D levels may be correlated with the development of lung cancer. They observed a reduction of the concentration of SP-D in the bronchoalveolar lavage fluid of heavy smokers that was linked to bronchial dysplasia. More recently, Hasegawa et al. (19) noted the presence of SP-D in lung cancer, and demonstrated that SP-D was able to interfere, *via* its CRD region, with the interaction between EGF and EGF receptor (EGFR), a tyrosine kinase receptor of the ErbB family, causing downregulation of the EGF induced signaling (19). EGFR is commonly altered in epithelial tumors and its dysregulation leads to cell proliferation, angiogenesis, invasion, and metastasis (29). Furthermore, it has been recently demonstrated that SP-D is also able to interact with the mutant form of EGFR, inhibiting its ligand-independent dimerization (29). In addition, Kaur et al.

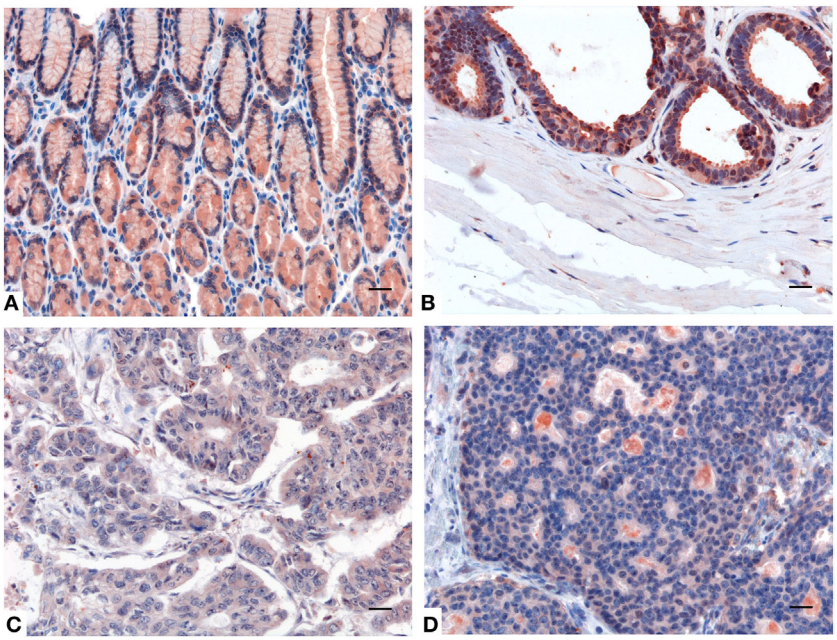

FIGURE 5 | Representative immunohistochemical microphotographs of surfactant protein D (SP-D) expression in the healthy gastric mucosa **(A)**, and ductal mammary epithelium **(B)** and their malignant histotypes intestinal-type gastric adenocarcinoma **(C)** and invasive ductal breast carcinoma, Luminal-A **(D)**. A decreased expression of SP-D in the intestinal-type gastric adenocarcinoma and invasive ductal breast carcinoma, Luminal-A respect to their normal counterparts can be observed. Polymer detection system with AEC (red) chromogen; scale bars, 50 μm.

have reported the ability of a recombinant truncated form of human SP-D to induce apoptosis *via* TNF-α/Fas-mediated pathway in human pancreatic adenocarcinoma using Panc-1 ($p53^{mt}$), MiaPaCa-2 ($p53^{mt}$), and Capan-2 ($p53^{wt}$) cell lines. Treatment of these cell lines with a recombinant form of truncated human SP-D (made up of homotrimeric neck and C-type lectin domains) for 24 h caused growth arrest in G1 cell cycle phase and triggered transcriptional upregulation of pro-apoptotic factors such as TNF-α and NF-κB. Translocation of NF-κB from the cytoplasm into the nucleus of pancreatic cancer cell lines was observed following treatment with SP-D. SP-D treatment caused upregulation of pro-apoptotic marker Fas, which then triggered cleavage of caspase 8 and 3. This study raises the possibility of using recombinant SP-D as a therapeutic molecule against pancreatic cancer irrespective of their p53 phenotype (20).

The EGFR is commonly overexpressed in non-small cell lung cancer (in 89% squamous cell carcinoma; 41% adenocarcinomas) (30), and therefore, it is considered a potential target for cancer therapy (30). The presence of SP-D in these cancers could exert a protective effect *via* downregulation of the EGFR pathway. It has also been shown that serum level of SP-D reflects its levels in the lung and that higher amount of SP-D in the serum correlated with better overall survival in patients with EGFR mutant adenocarcinoma undergoing treatment with gefitinib, a tyrosine kinase inhibitor (29).

Our study appears to highlight a more favorable prognosis for adenocarcinoma with respect to squamous cell carcinoma. A possible explanation of this observation may be that adenocarcinoma originates from peripheral airways progenitor cells that are able to produce SP-D. Moreover, more SP-D production may be indicative of a more differentiated cancer.

SFTPD, together with a number of genes selectively expressed in the respiratory epithelial cells, is under the control of the thyroid transcription factor 1 (TTF-1) (31, 32). A recent meta-analysis showing that TTF-1 overexpression is related to a favorable prognosis for non-small cell lung carcinoma patients (33), appears to strengthen the results being reported here.

Although the overexpression of the *EGFR* gene has also been reported in a variety of other cancers including those of head and neck, ovary, cervix, bladder, esophagus, stomach, brain, breast, endometrium, and colon (24), the above-mentioned mechanisms cannot explain the opposite results obtained *via* the bioinformatics analysis of Kaplan–Mayer dataset for gastric, ovarian, and breast carcinomas, where SP-D showed an unfavorable prognostic effect. We think that the unfavorable prognostic effect of SP-D in other tumor settings can be due to its direct or indirect action on the immune population present in the tumor microenvironment (15). The following mechanisms can explain the role of SP-D in determining a tumor microenvironment favorable to tumor progression. For example, the protective effect of SP-D against breast cancer cells can be negated by the presence of hyaluronic acid, which is abundantly present in the microenvironment of a number of solid tumors (34) (Murugaiah, Bulla, and Kishore, unpublished data).

SP-D is able to reduce the expression of CD11c (15). CD11c is predominantly expressed on dendritic cells, but also on effector

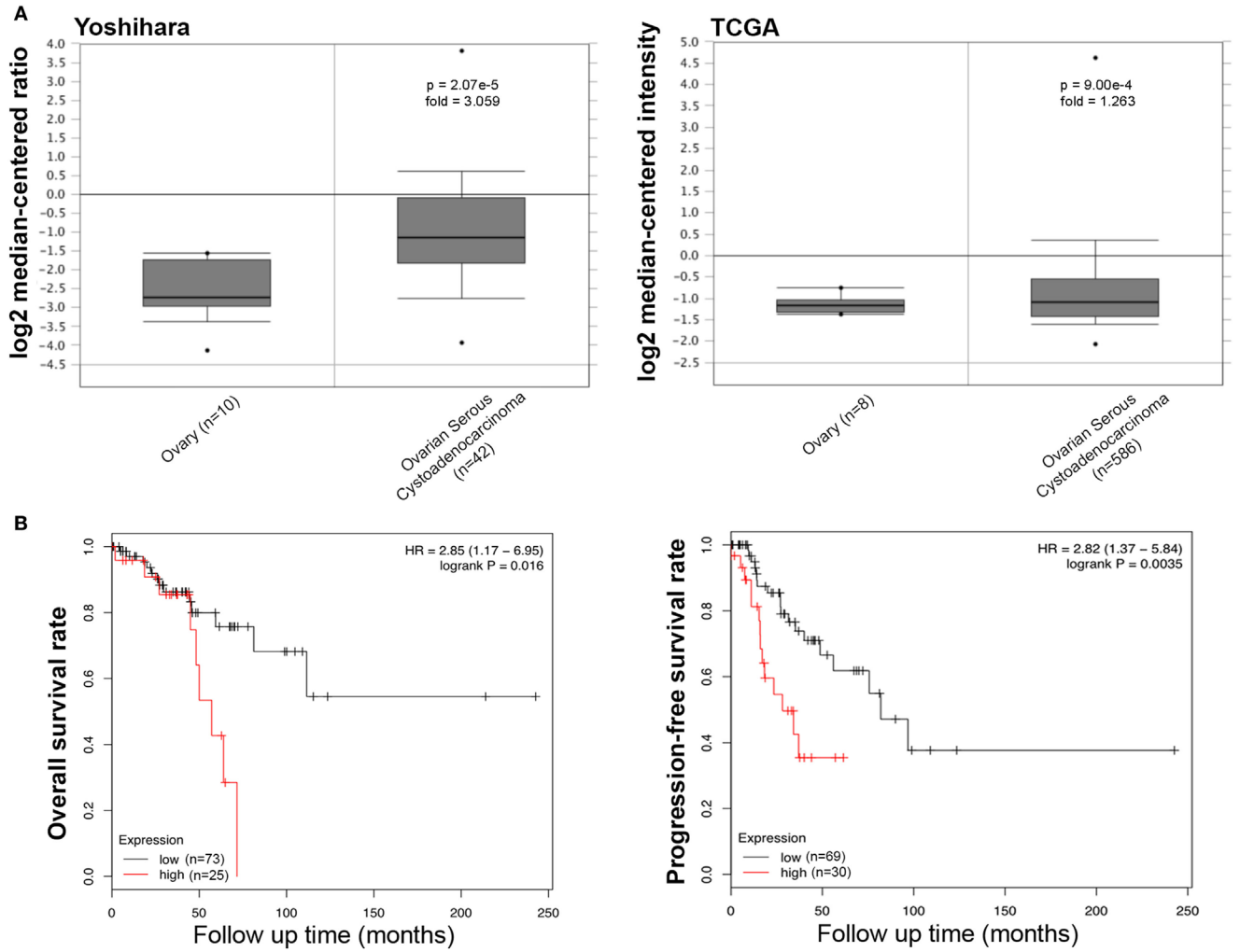

FIGURE 6 | Pathological significance of SP-D expression in ovarian cancer. Yoshihara's and TCGA's datasets explored SP-D mRNA expression in ovarian cancer. A higher SP-D mRNA expression was detectable in serous cystadenocarcinoma than that in normal ovary [**(A)** $p < 0.05$]. According to the data from Kaplan–Meir plotter, SP-D mRNA expression showed a negative relationship both overall or progression-free survival rates of patients with serous cystadenocarcinoma, if stratified by stage-1 and -2 [**(B)** $p < 0.05$]. Abbreviations: HR, hazard ratio; SP-D, surfactant protein D.

cells in the local tumor microenvironment, such as some macrophages, natural killer (NK), and activated T cells (25). It has been shown that low CD11c expression indicates unfavorable prognosis in patients with gastric cancer (35).

SP-D can promote production of TNF-α and IFN-γ (16, 18, 36). The anti-tumor effects of Th1 cells may reflect their known role in enhancing $CD8^+$ T cell responses and activating macrophages, through the secretion of TNF-α and IFN-γ. IFN-γ can increase tumor cell class I MHC expression and sensitivity to lysis by NK cells and cytotoxic T lymphocytes (CTLs). Besides, antigen-presenting cells such as macrophages and dendritic cells can directly activate antigen-specific Th1 or CTLs, which can activate the anti-tumor immune response and are thus associated with favorable prognosis in a diverse range of cancers (37, 38).

It has been demonstrated that SP-D binds to lymphocytes and suppress T cell proliferation (14) *via* apoptosis induction in activated PBMCs. SP-D has been shown to enhance expression of CTLA-4, a negative regulator of T cell activation and proliferation (39). In addition, monocytes expressed CTLA-4, but only the lymphocytes treated with SP-D show a significant overexpression of CTLA-4 (15). There are strong experimental and clinical evidence to suggest that T cell responses to some tumors are inhibited by the involvement of CTLA-4, one of the best-defined inhibitory pathways in T cells (40, 41). In fact, tumor-infiltrating T cells often have a dysfunctional (exhausted) phenotype that is characterized by impaired effector functions and increased expression of CTLA-4 and other inhibitory molecules (40, 41). Blockade of the CTLA-4 pathways is now being widely used in the clinic to reverse the dysfunctional phenotype of tumor-specific T cells and enhance their ability to kill tumor cells (41). Thus, SP-D, by increasing the expression of CTLA-4, may contribute to the inhibition of the anti-tumor immune responses.

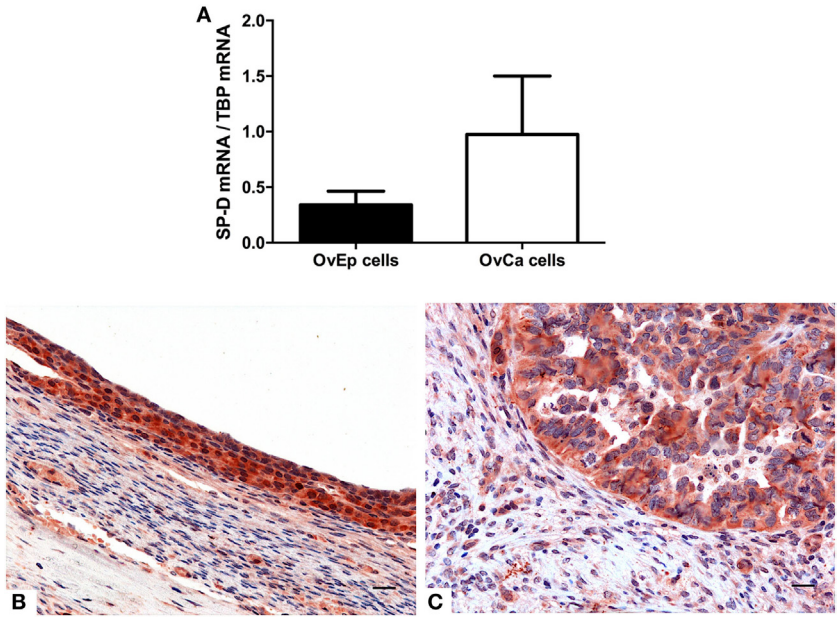

FIGURE 7 | Quantitative real-time PCR analysis of surfactant protein D (SP-D) performed on the normal ovarian epithelium and the epithelial ovarian tumor **(A)**. Representative microphotographs showing an enrichment in SP-D positive cells in the serous cystadenocarcinoma **(B)** compared to the normal ovarian epithelium **(C)**. Polymer detection system with AEC (red) chromogen; scale bars, 50 μm.

SP-D is able to inhibit the IL-12p40 production by macrophages *via* the SIRPα/ROCK/ERK signaling pathway (12). IL-12p40 is a component of IL-12p70 and IL-23, and its regulation is important for both innate and adaptive immunity. IL-12p40 is a marker of M1-like macrophages and data indicate that IL-12p40 may be contributing to inducing Th 1 polarization (42, 43). Macrophages derived from IL-12p40-deficient mice have a bias toward M2-like polarization (42). The production of IL-12p40 by macrophages and dendritic cells is associated with the ability to migrate to the lymph node and initiate T cell responses (44). We think that SP-D repressing the expression of IL-12p40 in macrophages may maintain the steady M2-like polarization and inhibit Th1 polarization.

SP-D has also been shown to interact with the leukocyte-associated Ig-like receptor-1 (LAIR-1) (45), known as CD305. This molecule is a transmembrane glycoprotein and is expressed on almost all immune cells as well as $CD34^+$ hematopoietic progenitor cells. SP-D acts as a ligand for the inhibitory receptor LAIR-1, which inhibits the function of multiple types of immune cells (45), indicating that SP-D present in the tumor microenvironment may exert its immunomodulatory effect and inhibit the anti-tumor immune responses through LAIR-1 activation. Thus, the context of immune infiltration and composition of tumor microenvironment are likely to dictate the consequent effects of SP-D, and hence, tumor progression or resistance.

In summary, our *in silico* analysis, if confirmed with a retrospective study at the protein level, could highlight a possible role of SP-D as a novel marker for tumor prognosis in a range of cancers. The presence of SP-D could be associated with a favorable prognosis in lung cancer where it has been demonstrated to downregulate the EGF signaling, and unfavorable prognosis in non-pulmonary sites such as gastric, breast, and ovarian cancers.

ETHICS STATEMENT

This study was carried out in accordance with the recommendations of governmental guidelines, and approved by the CEUR (Comitato Etico Unico Regionale, FVG, Italy) with written informed consent from all subjects, who gave written informed consent in accordance with the Declaration of Helsinki.

AUTHOR CONTRIBUTIONS

Conception and design: AM and RB. Development of methodology: AG, IF, CA, and FR. Acquisition of data: BB and CA. Analysis and interpretation of data (e.g., statistical analysis, biostatistics, and computational analysis): CT, FZ, AM, BB, and CA. Writing, review, and/or revision of the manuscript: RB, UK, CA, and GR. Study supervision: RB.

ACKNOWLEDGMENTS

We thank Yari Ciani (Bioinformatics and Functional Genomics Unit (BFGU) LNCIB Area Science Park, Trieste, Italy) for the important support to the bioinformatics analysis, and Gabriella Zito (Department of Gynaecology of IRCCS "Burlo Garofolo", Trieste, Italy) and Andrea Romano (Operative Clinical Unit of Anatomy and Pathological Histology, Cattinara Hospital, Trieste, Italy) for the tissue sample collection.

FUNDING

This work was supported by grants from the Institute for Maternal and Child Health, IRCCS "Burlo Garofolo", Trieste, Italy (RC20/16); AIRC to CT; Fondazione Cassa di Risparmio Trieste to RB.

SUPPLEMENTARY MATERIAL

The Supplementary Material for this article can be found online at https://www.frontiersin.org/articles/10.3389/fimmu.2018.01748/full#supplementary-material.

FIGURE S1 | Surfactant protein D (SP-D) expression in lung cancer. Garber's dataset has explored SP-D mRNA expression in the lung cancer. A lower SP-D mRNA expression was detectable in large cell carcinoma, adenocarcinoma, squamous cell carcinoma, and small cell carcinoma than in normal lung tissue ($p < 0.05$).

FIGURE S2 | Surfactant protein D (SP-D) expression in gastric cancer. DErrico's dataset has revealed a lower SP-D mRNA expression in intestinal-type adenocarcinoma than in normal mucosa ($p < 0.05$).

FIGURE S3 | Pathological significance of SP-D expression in breast cancer. Curtis's dataset has revealed a lower SP-D mRNA expression in phyllodes tumor than in normal breast tissue [**(A)** $p < 0.05$]. There was a negative association between SP-D mRNA expression and a favorable prognosis in the breast cancer patients with Luminal-A with grade-1, for Kaplan–Meir plotter [**(B)** $p < 0.05$]. Abbreviations: HR, hazard ratio; SP-D, surfactant protein D.

REFERENCES

1. Lu J, Teh C, Kishore U, Reid KB. Collectins and ficolins: sugar pattern recognition molecules of the mammalian innate immune system. *Biochim Biophys Acta* (2002) 1572(2–3):387–400. doi:10.1016/S0304-4165(02)00320-3
2. Nayak A, Dodagatta-Marri E, Tsolaki AG, Kishore U. An insight into the diverse roles of surfactant proteins, SP-A and SP-D in innate and adaptive immunity. *Front Immunol* (2012) 3:131. doi:10.3389/fimmu.2012.00131
3. Kishore U, Greenhough TJ, Waters P, Shrive AK, Ghai R, Kamran MF, et al. Surfactant proteins SP-A and SP-D: structure, function and receptors. *Mol Immunol* (2006) 43(9):1293–315. doi:10.1016/j.molimm.2005.08.004
4. Ishii T, Hagiwara K, Ikeda S, Arai T, Mieno MN, Kumasaka T, et al. Association between genetic variations in surfactant protein d and emphysema, interstitial pneumonia, and lung cancer in a Japanese population. *COPD* (2012) 9(4):409–16. doi:10.3109/15412555.2012.676110
5. Lin Z, Thomas NJ, Bibikova M, Seifart C, Wang Y, Guo X, et al. DNA methylation markers of surfactant proteins in lung cancer. *Int J Oncol* (2007) 31(1):181–91.
6. Madsen J, Kliem A, Tornoe I, Skjodt K, Koch C, Holmskov U. Localization of lung surfactant protein D on mucosal surfaces in human tissues. *J Immunol* (2000) 164(11):5866–70. doi:10.4049/jimmunol.164.11.5866
7. Christensen AF, Sorensen GL, Junker K, Revald PH, Varnum C, Sorensen FB, et al. Localization of surfactant protein-D in the rheumatoid synovial membrane. *APMIS* (2018) 126(1):9–13. doi:10.1111/apm.12785
8. Tenner AJ, Robinson SL, Borchelt J, Wright JR. Human pulmonary surfactant protein (SP-A), a protein structurally homologous to C1q, can enhance FcR- and CR1-mediated phagocytosis. *J Biol Chem* (1989) 264(23):13923–8.
9. Liu Z, Shi Q, Liu J, Abdel-Razek O, Xu Y, Cooney RN, et al. Innate immune molecule surfactant protein D attenuates sepsis-induced acute pancreatic injury through modulating apoptosis and NF-kappaB-mediated inflammation. *Sci Rep* (2015) 5:17798. doi:10.1038/srep17798
10. Hartshorn K, Chang D, Rust K, White M, Heuser J, Crouch E. Interactions of recombinant human pulmonary surfactant protein D and SP-D multimers with influenza A. *Am J Physiol* (1996) 271(5 Pt 1):L753–62.
11. Ferguson JS, Voelker DR, McCormack FX, Schlesinger LS. Surfactant protein D binds to *Mycobacterium tuberculosis* bacilli and lipoarabinomannan via carbohydrate-lectin interactions resulting in reduced phagocytosis of the bacteria by macrophages. *J Immunol* (1999) 163(1):312–21.
12. Yamaguchi R, Sakamoto A, Yamamoto T, Ishimaru Y, Narahara S, Sugiuchi H, et al. Surfactant protein D inhibits interleukin-12p40 production by macrophages through the SIRPalpha/ROCK/ERK signaling pathway. *Am J Med Sci* (2017) 353(6):559–67. doi:10.1016/j.amjms.2017.03.013
13. Madan T, Eggleton P, Kishore U, Strong P, Aggrawal SS, Sarma PU, et al. Binding of pulmonary surfactant proteins A and D to *Aspergillus fumigatus* conidia enhances phagocytosis and killing by human neutrophils and alveolar macrophages. *Infect Immun* (1997) 65(8):3171–9.
14. Borron PJ, Crouch EC, Lewis JF, Wright JR, Possmayer F, Fraher LJ. Recombinant rat surfactant-associated protein D inhibits human T lymphocyte proliferation and IL-2 production. *J Immunol* (1998) 161(9):4599–603.
15. Pandit H, Thakur G, Koippallil Gopalakrishnan AR, Dodagatta-Marri E, Patil A, Kishore U, et al. Surfactant protein D induces immune quiescence and apoptosis of mitogen-activated peripheral blood mononuclear cells. *Immunobiology* (2016) 221(2):310–22. doi:10.1016/j.imbio.2015.10.004
16. Madan T, Kishore U, Singh M, Strong P, Clark H, Hussain EM, et al. Surfactant proteins A and D protect mice against pulmonary hypersensitivity induced by *Aspergillus fumigatus* antigens and allergens. *J Clin Invest* (2001) 107(4):467–75. doi:10.1172/JCI10124
17. Mahajan L, Pandit H, Madan T, Gautam P, Yadav AK, Warke H, et al. Human surfactant protein D alters oxidative stress and HMGA1 expression to induce p53 apoptotic pathway in eosinophil leukemic cell line. *PLoS One* (2013) 8(12):e85046. doi:10.1371/journal.pone.0085046
18. Qaseem AS, Singh I, Pathan AA, Layhadi JA, Parkin R, Alexandra F, et al. A recombinant fragment of human surfactant protein D suppresses basophil activation and T-helper type 2 and B-cell responses in grass pollen-induced allergic inflammation. *Am J Respir Crit Care Med* (2017) 196(12):1526–34. doi:10.1164/rccm.201701-0225OC
19. Hasegawa Y, Takahashi M, Ariki S, Asakawa D, Tajiri M, Wada Y, et al. Surfactant protein D suppresses lung cancer progression by downregulation of epidermal growth factor signaling. *Oncogene* (2015) 34(7):838–45. doi:10.1038/onc.2014.20
20. Kaur A, Riaz MS, Murugaiah V, Varghese PM, Singh SK, Kishore U. A recombinant fragment of human surfactant protein D induces apoptosis in pancreatic cancer cell lines via fas-mediated pathway. *Front Immunol* (2018) 9:1126. doi:10.3389/fimmu.2018.01126
21. Rhodes DR, Kalyana-Sundaram S, Mahavisno V, Varambally R, Yu J, Briggs BB, et al. Oncomine 3.0: genes, pathways, and networks in a collection of 18,000 cancer gene expression profiles. *Neoplasia* (2007) 9(2):166–80. doi:10.1593/neo.07112
22. Rhodes DR, Yu J, Shanker K, Deshpande N, Varambally R, Ghosh D, et al. ONCOMINE: a cancer microarray database and integrated data-mining platform. *Neoplasia* (2004) 6(1):1–6. doi:10.1016/S1476-5586(04)80047-2
23. Lanczky A, Nagy A, Bottai G, Munkacsy G, Szabo A, Santarpia L, et al. miRpower: a web-tool to validate survival-associated miRNAs utilizing expression data from 2178 breast cancer patients. *Breast Cancer Res Treat* (2016) 160(3):439–46. doi:10.1007/s10549-016-4013-7
24. Sharma SV, Bell DW, Settleman J, Haber DA. Epidermal growth factor receptor mutations in lung cancer. *Nat Rev Cancer* (2007) 7(3):169–81. doi:10.1038/nrc2088
25. Castro FV, Tutt AL, White AL, Teeling JL, James S, French RR, et al. CD11c provides an effective immunotarget for the generation of both CD4 and CD8 T cell responses. *Eur J Immunol* (2008) 38(8):2263–73. doi:10.1002/eji.200838302
26. Ujma S, Horsnell WG, Katz AA, Clark HW, Schafer G. Non-pulmonary immune functions of surfactant proteins A and D. *J Innate Immun* (2017) 9(1):3–11. doi:10.1159/000451026
27. Sorensen GL. Surfactant protein D in respiratory and non-respiratory diseases. *Front Med* (2018) 5:18. doi:10.3389/fmed.2018.00018
28. Sin DD, Man SFP, McWilliams A, Lam S. Surfactant protein D and bronchial dysplasia in smokers at high risk of lung cancer. *Chest* (2008) 134(3):582–8. doi:10.1378/chest.08-0600
29. Umeda Y, Hasegawa Y, Otsuka M, Ariki S, Takamiya R, Saito A, et al. Surfactant protein D inhibits activation of non-small cell lung cancer-associated mutant

EGFR and affects clinical outcomes of patients. *Oncogene* (2017) 36(46): 6432–45. doi:10.1038/onc.2017.253
30. Prabhakar CN. Epidermal growth factor receptor in non-small cell lung cancer. *Transl Lung Cancer Res* (2015) 4(2):110–8. doi:10.3978/j.issn.2218-6751.2015.01.01
31. Dave V, Childs T, Whitsett JA. Nuclear factor of activated T cells regulates transcription of the surfactant protein D gene (Sftpd) via direct interaction with thyroid transcription factor-1 in lung epithelial cells. *J Biol Chem* (2004) 279(33):34578–88. doi:10.1074/jbc.M404296200
32. Whitsett J. A lungful of transcription factors. *Nat Genet* (1998) 20(1):7–8. doi:10.1038/1654
33. Qian HH, Xu TS, Cai XQ, Ji TL, Guo HX. Prognostic value of TTF-1 expression in patients with non-small cell lung cancer: a meta-analysis. *Clin Chim Acta* (2015) 451(Pt B):208–14. doi:10.1016/j.cca.2015.01.023
34. Whatcott CJ, Han H, Posner RG, Hostetter G, Von Hoff DD. Targeting the tumor microenvironment in cancer: why hyaluronidase deserves a second look. *Cancer Discov* (2011) 1(4):291–6. doi:10.1158/2159-8290.CD-11-0136
35. Wang Y, Xu B, Hu WW, Chen LJ, Wu CP, Lu BF, et al. High expression of CD11c indicates favorable prognosis in patients with gastric cancer. *World J Gastroenterol* (2015) 21(31):9403–12. doi:10.3748/wjg.v21.i31.9403
36. Madan T, Reid KB, Singh M, Sarma PU, Kishore U. Susceptibility of mice genetically deficient in the surfactant protein (SP)-A or SP-D gene to pulmonary hypersensitivity induced by antigens and allergens of *Aspergillus fumigatus*. *J Immunol* (2005) 174(11):6943–54. doi:10.4049/jimmunol.174.11.6943
37. Ramanathapuram LV, Hopkin D, Kurago ZB. Dendritic cells (DC) facilitate detachment of squamous carcinoma cells (SCC), while SCC promote an immature CD16(+) DC phenotype and control DC migration. *Cancer Microenviron* (2013) 6(1):41–55. doi:10.1007/s12307-011-0077-4
38. Mahmoud SM, Lee AH, Paish EC, Macmillan RD, Ellis IO, Green AR. Tumour-infiltrating macrophages and clinical outcome in breast cancer. *J Clin Pathol* (2012) 65(2):159–63. doi:10.1136/jclinpath-2011-200355
39. Lin KW, Jen KY, Suarez CJ, Crouch EC, Perkins DL, Finn PW. Surfactant protein D-mediated decrease of allergen-induced inflammation is dependent upon CTLA4. *J Immunol* (2010) 184(11):6343–9. doi:10.4049/jimmunol.0901947
40. Gajewski TF, Schreiber H, Fu YX. Innate and adaptive immune cells in the tumor microenvironment. *Nat Immunol* (2013) 14(10):1014–22. doi:10.1038/ni.2703
41. Buchbinder EI, Desai A. CTLA-4 and PD-1 pathways: similarities, differences, and implications of their inhibition. *Am J Clin Oncol* (2016) 39(1):98–106. doi:10.1097/COC.0000000000000239
42. Bastos KR, Alvarez JM, Marinho CR, Rizzo LV, Lima MR. Macrophages from IL-12p40-deficient mice have a bias toward the M2 activation profile. *J Leukoc Biol* (2002) 71(2):271–8.
43. Lim HX, Hong HJ, Jung MY, Cho D, Kim TS. Principal role of IL-12p40 in the decreased Th1 and Th17 responses driven by dendritic cells of mice lacking IL-12 and IL-18. *Cytokine* (2013) 63(2):179–86. doi:10.1016/j.cyto.2013.04.029
44. Cooper AM, Khader SA. IL-12p40: an inherently agonistic cytokine. *Trends Immunol* (2007) 28(1):33–8. doi:10.1016/j.it.2006.11.002
45. Olde Nordkamp MJ, van Eijk M, Urbanus RT, Bont L, Haagsman HP, Meyaard L. Leukocyte-associated Ig-like receptor-1 is a novel inhibitory receptor for surfactant protein D. *J Leukoc Biol* (2014) 96(1):105–11. doi:10.1189/jlb.3AB0213-092RR

Conflict of Interest Statement: The authors declare that the research was conducted in the absence of any commercial or financial relationships that could be construed as a potential conflict of interest.

The reviewer AK declared a shared affiliation, though no other collaboration, with one of the authors UK to the handling Editor.

frontiers in Immunology

REVIEW
published: 20 September 2019
doi: 10.3389/fimmu.2019.02264

The Dual Role of Surfactant Protein-D in Vascular Inflammation and Development of Cardiovascular Disease

*Kimmie B. Colmorten, Anders Bathum Nexoe and Grith L. Sorensen**

Department of Molecular Medicine, Faculty of Health Sciences, University of Southern Denmark, Odense, Denmark

Cardiovascular disease (CVD) is responsible for 31% of all global deaths. Atherosclerosis is the major cause of cardiovascular disease and is a chronic inflammatory disorder in the arteries. Atherosclerosis is characterized by the accumulation of cholesterol, extracellular matrix, and immune cells in the vascular wall. Recently, the collectin surfactant protein-D (SP-D), an important regulator of the pulmonary immune response, was found to be expressed in the vasculature. Several *in vitro* studies have examined the role of SP-D in the vascular inflammation leading to atherosclerosis. These studies show that SP-D plays a dual role in the development of atherosclerosis. In general, SP-D shows anti-inflammatory properties, and dampens local inflammation in the vessel, as well as systemic inflammation. However, SP-D can also exert a pro-inflammatory role, as it stimulates C-C chemokine receptor 2 inflammatory blood monocytes to secrete tumor necrosis-factor α and increases secretion of interferon-γ from natural killer cells. *In vivo* studies examining the role of SP-D in the development of atherosclerosis agree that SP-D plays a proatherogenic role, with SP-D knockout mice having smaller atherosclerotic plaque areas, which might be caused by a decreased systemic inflammation. Clinical studies examining the association between SP-D and cardiovascular disease have reported a positive association between circulatory SP-D level, carotid intima-media thickness, and coronary artery calcification. Other studies have found that circulatory SP-D is correlated with increased risk of both total and cardiovascular disease mortality. Both *in vitro*, *in vivo*, and *clinical studies* examining the relationship between SP-D and CVDs will be discussed in this review.

Keywords: collectins, SP-D, cardiovascular disease, atherosclerosis, inflammation

OPEN ACCESS

Edited by:
Uday Kishore,
Brunel University London,
United Kingdom

Reviewed by:
Taruna Madan,
National Institute for Research in Reproductive Health (ICMR), India
Barbara Bottazzi,
Milan University, Italy
Anthony George Tsolaki,
Brunel University London,
United Kingdom

****Correspondence:***
Grith L. Sorensen
glsorensen@health.sdu.dk

Specialty section:
This article was submitted to Molecular Innate Immunity, a section of the journal Frontiers in Immunology

Received: *24 June 2019*
Accepted: *09 September 2019*
Published: *20 September 2019*

Citation:
Colmorten KB, Nexoe AB and Sorensen GL (2019) The Dual Role of Surfactant Protein-D in Vascular Inflammation and Development of Cardiovascular Disease. Front. Immunol. 10:2264. doi: 10.3389/fimmu.2019.02264

INTRODUCTION

Cardiovascular disease (CVD) is the most frequent cause of death worldwide, with an estimated 17.9 million deaths every year, accounting for about 31% of all global deaths (1). Atherosclerosis is the major cause of CVD and is caused by both genetic and environmental factors (2, 3). We know that atherosclerosis is a chronic inflammatory disorder of the arteries characterized by the accumulation of cholesterol, extracellular matrix, and immune cells in the subendothelial space. Both the innate and adaptive immune systems are implicated in the development of atherosclerotic plaques (4).

Briefly, circulating lipoprotein particles, such as low-density lipoprotein (LDL), can penetrate the arterial wall and accumulate in the subendothelial space. Atherogenic modification of LDL, such as oxidation (oxLDL), induces an immune response triggering immune cells, including neutrophils, natural killer (NK) cells, and monocytes/macrophages, which are the first responders. Macrophages especially participate in the engulfment and accumulation of intracellular oxLDL, leading to the transition of well-functioning macrophages to lipid-filled foam cells (5, 6). Activation of the innate immune cells leads to the secretion of various pro-inflammatory cytokines, where interleukin (IL)-1 (7–9), interferon (IFN)-γ (10–12), and tumor necrosis factor (TNF-)α (13, 14) have an especially proatherogenic effect (6). IL-6 is also a major contributor to the development of atherosclerosis by playing a dual pathological and protective role (15–17).

Following activation of an innate immune response, an adaptive immune response is triggered and mediated by T- and B-cells. Activation of type 1 T helper (Th1) cells by exogenous or endogenous antigens, including oxLDL, leads to the secretion of IFN-γ and enhancement of monocyte infiltration, foam-cell formation, lipid accumulation, and macrophage activation (4).

Recently, the collectin surfactant protein (SP)-D, an important regulator of the innate immune response in the lung, was shown to be expressed in the vasculature, where it regulates local inflammation (18, 19).

This review gives a comprehensive overview of recent *in vitro*, *in vivo*, and *clinical studies* that have attempted to examine SP-D-mediated inflammation in the vasculature and its function in the pathogenesis of CVD.

THE COLLECTIN FAMILY AND ROLES IN INFLAMMATION

The collectins are members of a superfamily of collagenous, calcium-dependent (C-type) lectins. All members of the collectin family are characterized by the presence of a cysteine-rich N-terminal non-collagenous domain, a collagen-like domain, an α-helical coiled-coil neck domain, and a globular C-type lectin domain (20). These are soluble effector proteins that also possess the property of pattern recognition by recognizing terminal conserved carbohydrate domains on microbes, leading to complement activation (20). The family includes mannose-binding proteins (MBLs), SP-A, SP-D, and three novel human defense collagens; collectin-10, collectin-11, and collectin-12 (21–23). The collectins are known to be an important part of the innate immune defense due to their interaction with a range of microbes. Binding of MBL leads to opsonization of the microorganisms through complement activation via the lectin pathway, whereas SP-A and SP-D have more direct antimicrobial effects (24). SP-D/-A cooperate with alveolar macrophages to facilitate phagocytosis via binding of bacteria, viruses, fungi, and helminthic parasites for clearance through opsonization (24). The collectins do not only exert anti-microbial effects but possess dual biological activity either by suppressing or enhancing the production of pro-inflammatory cytokines (25, 26). Gardai et al. (25) suggested that collectins are capable of differential cellular receptor binding through either their collagen-like domain or their C-type lectin domain, and thereby initiate pro-inflammatory or anti-inflammatory signaling, respectively. Under normal conditions, collectins bind the cellular receptor, signal regulatory protein (SIRP)-α, on innate immune cells via their C-type lectin domain and prevent pro-inflammatory signaling. When pathogens are present, the C-type lectin domain is occupied by its corresponding ligand, and the collectins will then interact with the innate immune cells through a receptor complex of cluster of differentiation (CD)91 and calreticulin. This binding is mediated through the collagen-like domain on the collectin and induces pro-inflammatory signaling (25). Gardai et al. (25) only validated the hypothesis for SP-A, but a study by Fournier et al. validated the binding between SP-D and SIRP-α (27). Moreover, a series of additional cellular receptors have been suggested as mediators of SP-D signaling. Central receptors are mentioned beneath.

THE STRUCTURE OF SP-D

SP-D is a large oligomeric structure, composed of oligomers of 130 kDa subunits (28). The subunits are comprised of three identical polypeptide chains containing an N-linked oligosaccharide structure (**Figure 1**). Following assembly of the triple-helical collagen-like domain, the N-terminal cysteine residues form disulfide bridges between monomers, dictating the degree of multimerization and thus the SP-D isoform (28). Human SP-D has different isoforms; the 520 kDa dodecameric isoform structure is the most commonly found in bronchoalveolar lavage fluid (BALF), but also fuzzy ball, trimeric, dimeric, and monomeric isoforms are present in BALF from healthy subjects (29). To understand the function of SP-D, it is important to keep in mind that a shift in SP-D isoforms can lead to changes in its pro- or anti-inflammatory role. The importance of SP-D isoforms will be discussed in this review.

SP-D SITES OF EXPRESSION AND FUNCTION

For many years, SP-D/-A were referred to as lung-specific; they were discovered in the phospholipid-rich pulmonary surfactant (28, 30). The fact that surfactant-like lubrication is produced and secreted by a number of other organs led to the hypothesis that SP-D/-A are also synthesized in extra-pulmonary tissues.

SP-D/-A are primarily synthesized in the lung, where they are produced and secreted onto the epithelial surface by alveolar type II epithelial cells and unciliated bronchial epithelial cells (31). In the lung, SP-D/-A function as regulators of lipid levels in the pulmonary surfactant, where they also exert their antimicrobial effects (24, 32). Since SP-D/-A were first discovered in the lung, this is also the organ where their function is most extensively examined. Studies on SP-D/-A knockout (KO) mice generally reported increased susceptibility to acute and chronic infections and a general enhanced acute inflammatory response upon pathogen or smoke exposure of the lung (33–36). Taken together,

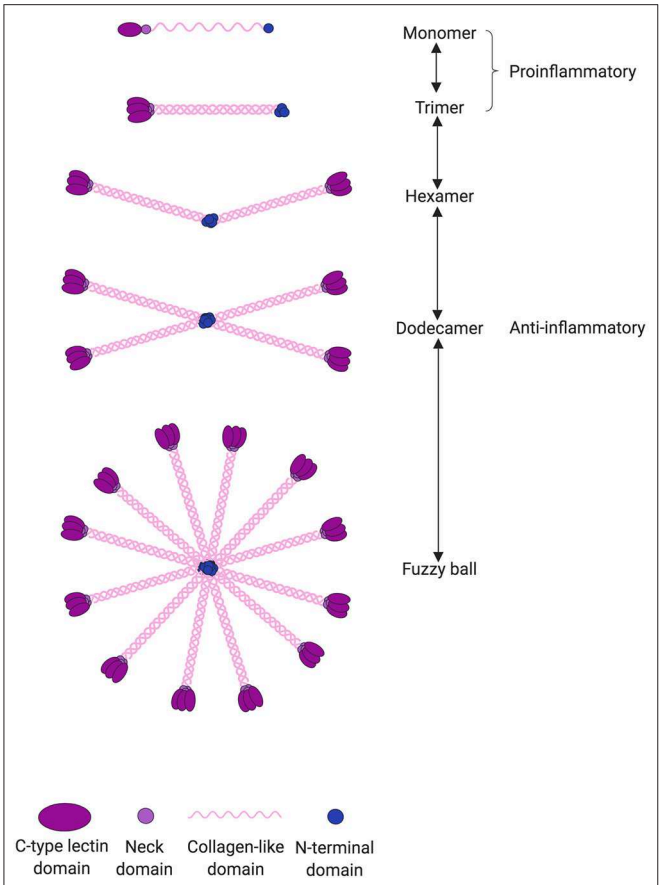

FIGURE 1 | SP-D can undergo several post-translational modifications leading to changes in both structure and function. SP-D is capable of multimerization depending on the local environment. The most common isoform is the dodecameric structure, which is thought to have anti-inflammatory properties through binding via its C-type lectin domain. However, in an inflammatory or more acidic environment, the dodecameric form can change to a trimeric or monomeric isoform. The monomers and trimers are believed to have pro-inflammatory properties through binding via its collagen-like domain. When pathogens are present, the C-type lectin domain is occupied by its corresponding ligand and thus incapable of eliciting its anti-inflammatory signaling.

these studies underline the important roles of SP-D/-A in the pulmonary innate host defense and regulation of surfactant homeostasis (31).

Even though the primary site of SP-D expression is in the lung, it has been localized to a range of non-pulmonary tissues, including the external or luminal surfaces of the gastrointestinal tract (37, 38), glandular system (37, 38), reproductive tract (37–39), urinary tract (37, 38), and in the cardiovascular (CV) system (18, 19). In the CV system, SP-D expression has been localized to endothelial and smooth muscle cells (SMCs), where its suggested function is the modulation of inflammatory signaling (18, 19). The sources of circulating SP-D are not fully clarified. In addition to lung spillover as primary contributor, it is possible that SP-D can be secreted from the arterial wall and affect the total serum concentration. Recent studies by Kati et al. and Gargiulo et al. have shown that circulatory SP-D levels correlate with the presence of pulmonary embolism (40) and with alveolar leakage in heart failure (41), thereby supporting the hypothesis that circulatory SP-D variation is partly a consequence of CVD-mediated lung damage. Based on recent clinical studies pinpointing SP-D as a systemic biomarker of CVD morbidity and mortality (42, 43), it is suggested that SP-D has an important function in the cardiovascular system as a regulator of inflammation, which might have implications for atherosclerosis and CVD.

IN VITRO STUDIES OF SP-D-MEDIATED CELLULAR EFFECTS

Several *in vitro* studies have examined how SP-D modulates the function of a range of cell types (**Table 1**). This section focuses on recently published *in vitro* studies investigating SP-D-mediated cellular effects that might be relevant for the development of CVD.

Vascular Inflammation as an SP-D-Mediated Contributor to the Development of CVD

It is well established that chronic inflammation within the vessel wall is a strong contributor to the development of atherosclerosis. Chronic low levels of inflammation caused by pro-inflammatory molecules, such as lipopolysaccharide (LPS), has previously been implicated in the development of atherosclerosis (both in mice and humans) (57, 58). Although SP-D has been implicated in atherosclerosis, the exact mechanisms are very poorly understood.

It is recognized that SP-D/-A can modify the inflammatory response upon binding to LPS on the bacterial surface (59–61). Snyder et al. (19) examined the expression of SP-D in the human coronary artery SMCs and its ability to modify LPS-induced inflammation within these cells. After treatment of the human coronary artery SMCs with LPS, exogenously added SP-D had the ability to suppress the secretion of the pro-inflammatory cytokine IL-8 (**Figure 2**). Thus, SP-D is shown to have an anti-inflammatory role in SMCs when exposed to LPS and could possibly exert local protection against atherosclerosis in this way. A study by Liu et al. (62) examined the serum levels of the pro-inflammatory and proatherogenic cytokines IL-6 and TNF-α in septic wildtype and SP-D KO mice. This study showed that SP-D KO mice had significantly increased levels of both cytokines in serum. These results show that SP-D regulates not only local tissue inflammation but also systemic inflammation and, thus, possibly the propensity of atherosclerotic plaque formation.

SP-D-Mediated Effects on Immune Cells

Peripheral Blood Mononuclear Cells

The cellular effects of SP-D on inflammatory cytokine levels are multifaceted. Borron et al. (44) investigated the effect of SP-D/-A on peripheral blood mononuclear cell (PBMC) proliferation and found that SP-D/-A directly inhibits T lymphocyte proliferation; both IL-2-dependent and -independent (**Figure 2**). A recent

TABLE 1 | SP-D-mediated effects related to CVD.

Cell type	Experiment	Outcome	References
***IN VITRO* ANALYSIS**			
Human coronary SMCs	LPS-induced inflammation in coronary SMCs	SP-D suppresses the secretion of IL-8 in human coronary SMCs	(19)
PBMCs	PHA- or Con A-stimulated PBMCs treated with recombinant rat SP-D	SP-D inhibits T lymphocyte proliferation; both IL-2-dependent and -independent	(44)
PBMCs	PHA-stimulated PBMCs treated with rhSP-D	SP-D suppresses circulatory IL-6 and TNF-α levels	(45)
Plaque macrophages	Lipid-laden macrophages from atherosclerotic plaques	SP-D binding to OSCAR induced secretion of TNF-α from CCR2+ inflammatory monocytes	(46)
Monocytes and macrophages	Monocytes and macrophages expressing LAIR-1	SP-D binds LAIR-1 on monocytes and macrophages, thereby inhibiting ROS production	(47)
Pulmonary NK cells	Pulmonary NK cells expressing or not expressing NKp46	SP-D binds directly to pulmonary NK cells through the receptor NKp46, thereby inducing IFN-γ secretion	(48)
Mouse model	**Experiment**	**Outcome**	**References**
ANALYSIS OF GENE-DEFICIENT MICE			
SP-D/ApoE DKO mice	SP-D/ApoE DKO mice receiving proatherogenic diet	SP-D/ApoE DKO mice had reduced plaque lesion area, increased plasma cholesterol and weight, decreased plasma IL-6	(31)
SP-D/ApoE DKO mice	SP-D/ApoE DKO mice receiving proatherogenic diet with cholate	SP-D/ApoE DKO mice had reduced plaque lesion area, increased plasma triglycerides and HDL	(18)
SP-D KO mice	SP-D KO mice exposed to cigarette smoke	Control SP-D KO mice showed similar contractility in the coronary artery to that of cigarette smoking WT mice	(49)
SP-D KO mice	SP-D KO mice exposed to cigarette smoke	SP-D KO mice had aggravated airway inflammation and ceramide accumulation	(36)
SP-D KO mice	LPS-challenged SP-D KO mice	SP-D KO mice had increased testicular levels of immunosuppressive molecules, reduced levels of immune cell activation markers and reduced response to LPS in testis	(50)
Patient cat.	**Experiment**	**Outcome**	**References**
CLINICAL PHENOTYPIC-ASSOCIATION STUDIES			
Elderly twin population	689 elderly subjects, 13-year follow-up period.	Increased circulatory SP-D is associated with total mortality	(43)
Patients undergoing coronary angiography	806 patients, angiography happened between 1992 and 1995, follow-up in 2007.	Increased circulatory SP-D is associated with CVD morbidity and mortality	(42)
Patients undergoing maintenance hemodialysis	116 patients, cross-sectional study.	A positive association between circulatory SP-D level and carotid intima-media thickness and coronary artery calcification	(51)
Patients with heart failure	263 patients, 2.2-year follow-up period.	Circulatory SP-D is associated with a higher risk of heart transplantation, death, and worsened heart failure	(52)
PAD patients	364 patients, prospective study.	Circulatory SP-D is associated with more severe PAD and a higher prevalence of diabetes mellitus	(53)
Patients with subclinical carotid artery atherosclerosis	687 patients	No association between plasma SP-D and carotid artery intima-media thickness or subclinical atherosclerotic plaque development	(54)
Patients with chronic heart failure	89 patients and 17 healthy subjects	Circulatory SP-D levels are increased in patients with heart failure	(41)
Patients with non-massive and sub-massive pulmonary embolism	20 patients with non-massive, 20 patients with sub-massive and 20 healthy subjects	Circulatory SP-D correlated with the presence of sub-massive pulmonary embolism	(40)

(Continued)

TABLE 1 | Continued

Patient cat.	Experiment	Outcome	References
CLINICAL GENETIC-ASSOCIATION STUDIES			
206 healthy subjects	SNPs in the SP-D gene SFTPD	The SNP rs721917 (Met11Thr) affects the oligomeric structure of SP-D	(55)
2,711 type 2 diabetic patients or healthy subjects	SNPs in the SP-D gene SFTPD	The SNP rs721917 is associated with diabetes mellitus and insulin resistance	(56)
396 patients with subclinical atherosclerosis	SNPs in the SP-D gene SFTPD	The SNPs rs721917 and rs3088308 are both associated with decreased plasma SP-D; rs721917 is associated with carotid intima-media thickness	(54)

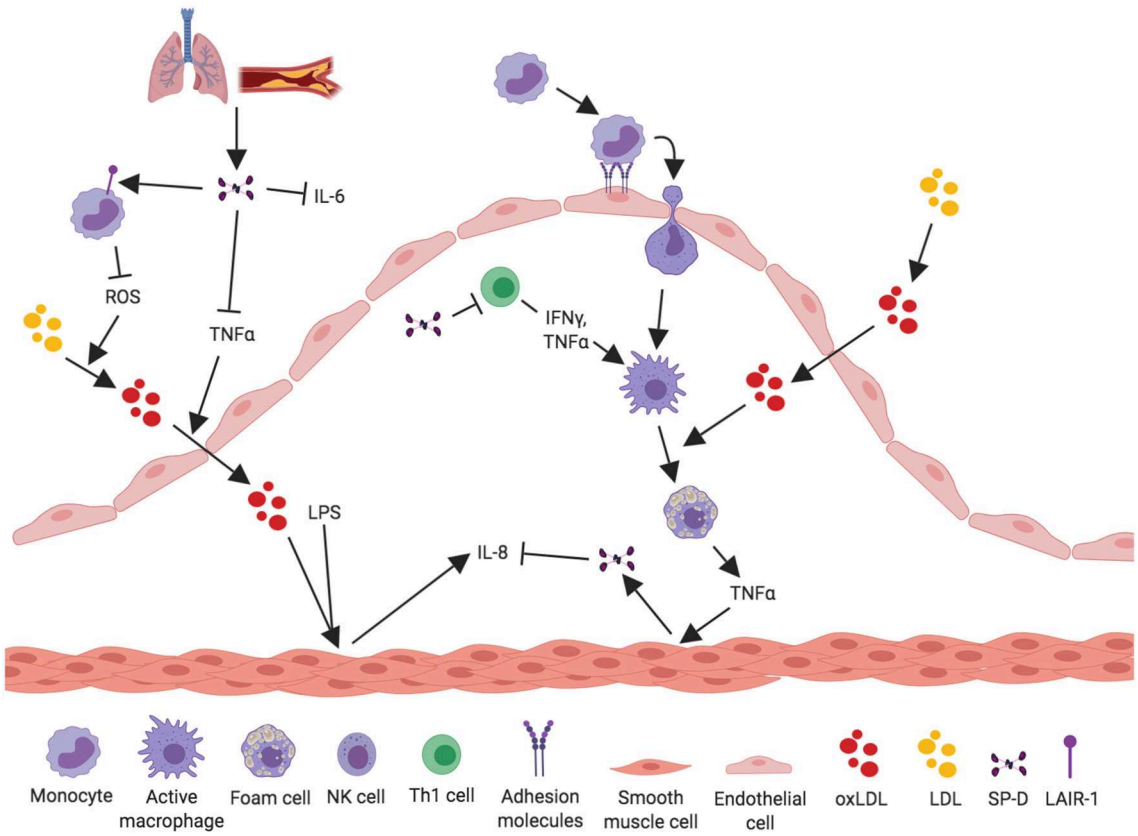

FIGURE 2 | Proposed anti-inflammatory mechanisms for SP-D in the development of atherosclerosis. SP-D plays a dual role in the development of atherosclerosis. This figure aims to depict what we know about the anti-inflammatory properties of SP-D in the development of atherosclerosis. Circulatory SP-D originates from lung-spillover or directly from the atherosclerotic artery. SP-D binds its receptor LAIR-1 on PBMCs, leading to inhibition of ROS and thereby inhibition of the oxidation process of serum LDL. Circulatory SP-D also inhibits circulatory IL-6 and TNF-α and thus the transport of oxidized LDL from the artery lumen to the subendothelial space. SP-D has been shown to inhibit the proliferation of Th1 cells and their secretion of IFN-γ and TNF-α; this ultimately leads to inhibition of activated macrophages and foam cell formation. TNF-α secretion from NK cells and foam cells stimulates vascular smooth muscle cells (VSMC) to produce and secrete SP-D into the subendothelial space, where it again exerts its negative-feedback loop on NK cells. SP-D is able to inhibit IL-8 from LPS-stimulated VSMC, thus decreasing vascular inflammation.

study by Pandit et al. (45) further examined how recombinant human (rh)SP-D affects phytohaemagglutinin (PHA)-stimulated PBMCs (45). The levels of two potent pro-inflammatory and pro-atherosclerotic cytokines, circulatory IL-6 and TNF-α, were significantly downregulated in rhSP-D treated PBMCs (**Figure 2**). Interestingly, this study observed no effect on IL-2 expression by rhSP-D (45). The identification of SP-D as a down-regulator of serum IL-6 and TNF-α is in agreement with the observations in Liu et al. (62).

Pro-atherosclerotic effects of IL-6 include vascular SMC proliferation (63, 64) and activation of endothelial cells (65, 66). However, the atheroprotective effects of IL-6 have also

been reported, as IL-6 lowers plasma LDL by upregulating LDL receptor gene expression (67, 68). Clinical studies have shown that serum IL-6 is elevated in coronary artery calcification in patients with chronic kidney disease and might be a predictive biomarker of mortality risk, coronary artery disease, and inflammation related to CVD (69–71). Similar to the function of IL-6, TNF-α is also a pro-atherosclerotic cytokine and increases the development of atherosclerosis in several ways. Circulating TNF-α is associated with endothelial dysfunction and barrier disruption (72, 73), increased expression of adhesion molecules on endothelial cells (74), and vascular SMC proliferation (75).

Monocytes and Macrophages

Recently, a new receptor for SP-D was found on the cell surface of C-C chemokine receptor 2 (CCR2)+ inflammatory blood monocytes (46). The SP-D receptor osteoclast-associated receptor (OSCAR) was strongly expressed in lipid-laden macrophages localized in the tunica intima and in some of the macrophages in tunica media of clinical atherosclerosis plaques. Binding of SP-D to OSCAR induced secretion of TNF-α from the CCR2+ inflammatory monocytes infiltrating the atherosclerotic plaques (46) (**Figure 3**).

Olde Nordkamp et al. (47) found that SP-D binds the leukocyte-associated immunoglobulin-like receptor 1 (LAIR-1), a receptor expressed on most immune cells, including monocytes, and macrophages (76, 77) (**Figure 2**). SP-D inhibits reactive oxygen species (ROS) production through binding between SP-D collagen domains and LAIR-1 (47). ROS production is strongly associated with the development of atherosclerosis (78–80). A newer study by Yi et al. (81) demonstrated that silencing of LAIR-1 in human Tohoku Hospital Pediatrics (THP)-1 macrophages increases foam cell formation. This could be a possible link between SP-D and development of atherosclerosis, suggesting that binding between SP-D and LAIR-1 leads to a decreased foam cell formation, but this needs further examination.

These studies support a dual role for SP-D in the development of atherosclerosis. Signaling through OSCAR results in TNF-α secretion from monocytes that leads to a pro-inflammatory response, whereas signaling through LAIR-1 inhibits ROS formation but possibly induces foam cell formation.

NK Cells

A study by Ge et al. (48) showed that SP-D binds directly to pulmonary natural killer (NK) cells through the receptor NKp46 and thereby induces secretion of IFN-γ (**Figure 3**). This is the most specific receptor for NK cells and is expressed on the surface of all NK cell subsets (82, 83). It is possible that SP-D can bind and activate NK cells present in the artery, leading to secretion of IFN-γ, and thus stimulating an inflammatory response within the artery.

IN VIVO STUDIES OF SP-D IN CVD

Two *in vivo* studies have been performed to investigate the role of SP-D in atherosclerosis (**Table 1**). A study by Hirano et al. examined the function of SP-D in the development of atherosclerosis in ApoE (KO) mice (31). A similar study was previously performed by Sorensen et al. in SP-D KO mice receiving a proatherogenic diet containing a low percentage of cholate (18).

The function of SP-D has also been examined in relation to tobacco smoking, as tobacco is a major contributor to CVD. Haanes et al. (49), examined the contractile changes in the vasculature after 3-months sidestream smoking in wildtype and SP-D KO mice.

Plaques Size and Composition

Hirano et al. (31) assessed the development of atherosclerosis in ApoE KO and SP-D/ApoE double KO (DKO) mice. Atherosclerotic plaque size was measured in the brachiocephalic arteries and aortic root where plaque formation often is seen. The DKO mice exhibited significantly reduced plaque size in both the brachiocephalic arteries (37% reduction) and aortic root (25% reduction) compared to ApoE KO mice (31). This result is supported by Sorensen et al. who examined the function of SP-D in relation to atherosclerosis in mice fed an atherogenic diet (18). These authors found that SP-D KO mice had significantly smaller lesion areas only consisting of foam cells, whereas WT mice had larger mature atherosclerotic plaques with an extracellular matrix containing lipid and collagen (18).

Furthermore, Hirano et al. revealed that the plaques in SP-D/ApoE DKO mice harbored significantly fewer macrophages in each plaque (46% reduction) and had more SMC coverage of the luminal surface of the plaque compared to ApoE KO mice. SMC coverage of the luminal surface of the plaque is associated with a more stable plaque phenotype in humans (84, 85). Based on these results it seems that SP-D has a function in the attraction of macrophages and thereby initiation of early inflammation, which ultimately leads to the development of more severe atherosclerosis. Furthermore, it seems as if SP-D has a function in changing the stability of the plaque, leading to a more unstable plaque formation and a higher risk of plaque rupture.

Lipoprotein Profile

The smaller plaque areas observed in SP-D KO and SP-D/ApoE DKO mice were hypothesized to be caused by an SP-D-mediated change in the lipoprotein profile, leading to a lower degree of lipids and cholesterol in the blood. Both Hirano et al. and Sorensen et al. detected a significant change in the lipoprotein profile of the SP-D KO and SP-D/ApoE DKO mice (18, 31). Surprisingly, SP-D/ApoE DKO mice had a 39% higher fasting plasma level of cholesterol and significantly higher levels of chylomicron cholesterol, very-low-density lipoprotein cholesterol (VLDL-C), as well as high-density lipoprotein cholesterol (HDL-C) (31). In addition to disturbed blood lipids, SP-D/ApoE DKO mice had elevated body weight and adipose tissue mass, as well as increased fasting plasma insulin, glucose, leptin, and adiponectin compared to ApoE KO mice (31). Sorensen et al. found that SP-D KO mice had significantly higher levels of plasma HDL-C (18%) and triglycerides (27%) but similar levels of LDL and total cholesterol compared to WT mice (18). Sorensen et al. (18) examined the effect of intravenous administration of rhSP-D on plasma lipid concentrations. Administration of rhSP-D to SP-D/ApoE DKO

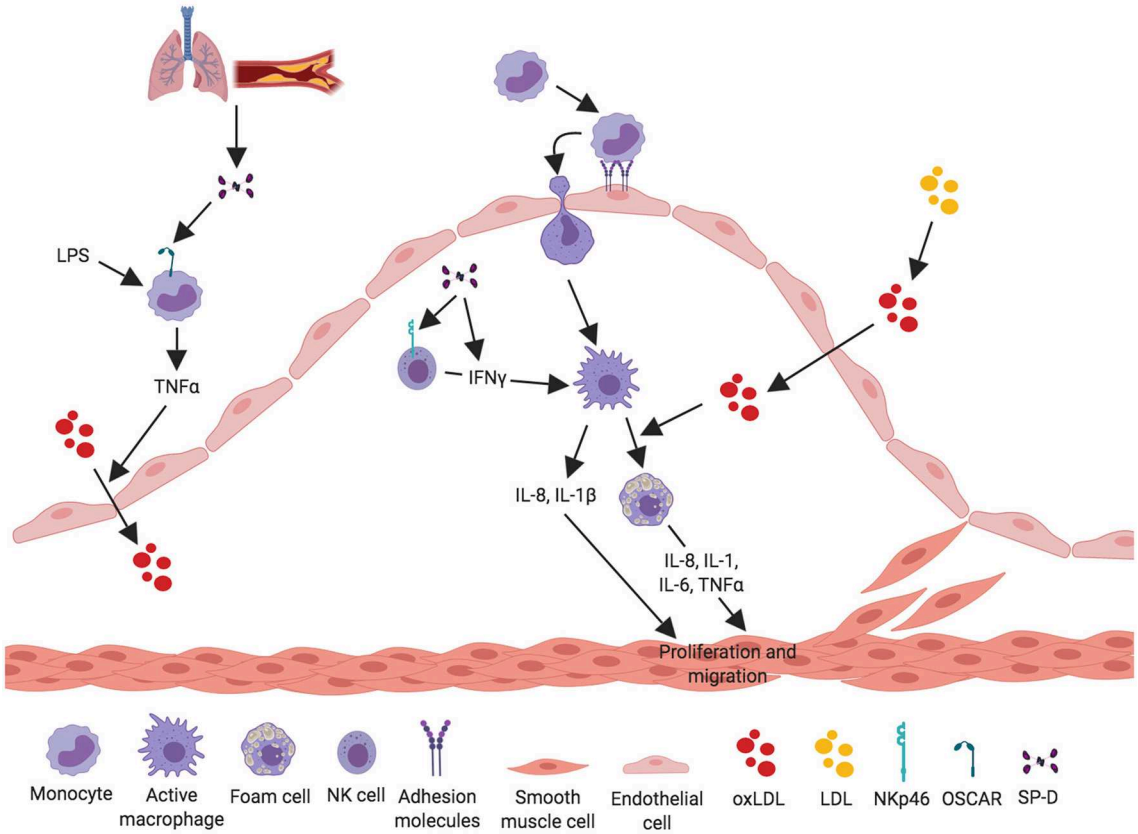

FIGURE 3 | Proposed pro-inflammatory mechanisms for SP-D in the development of atherosclerosis. SP-D plays a dual role in the development of atherosclerosis. The figure aims to depict what we know about the pro-inflammatory properties of SP-D in the development of atherosclerosis. SP-D is actively contributing to the inflammatory process in the artery. SP-D stimulates LPS-induced TNF-α-secretion from CCR2+ inflammatory monocytes through binding via its receptor OSCAR. TNF-α stimulates translocation of oxidized LDL from the artery lumen to the subendothelial space and thus contributes to the atherosclerotic plaque formation. The pro-inflammatory role of SP-D is also mediated through NK cells, where SP-D binds the receptor NKp46 leading to secretion of IFN-γ, which activates macrophages. Activated macrophages secrete the cytokines IL-8 and IL-1 and are able to engulf the oxidized LDL, leading to foam cell formation and production of IL-8, IL-1, IL-6, and TNF-α. These cytokines stimulate and activate VSMC to proliferate and migrate to stabilize the growing atherosclerotic plaque.

mice decreased the serum concentration of HDL-C, LDL-C, and total cholesterol. This SP-D-mediated regulation of multiple lipid fractions indicates that a general factor in lipid metabolism or transport is affected by SP-D.

It is well-known that obesity, insulin resistance, increased fasting glucose, and increased levels of plasma VLDL, LDL, and cholesterol are associated with the development of atherosclerosis and CVD (86–90). However, the SP-D mediated mechanisms modulating these metabolic outcomes and how they are interlinked with CVD remain unknown.

Inflammation *in vivo*

To investigate if the effect of SP-D on plaque size was caused by a change in inflammatory markers, Hirano et al. (31) and Sorensen et al. (18) evaluated the level of cytokines in plasma. Strikingly, SP-D/ApoE DKO mice had significantly lower plasma level of IL-6 compared to ApoE KO mice (31). It has previously been shown that injection of IL-6 in ApoE KO mice increases the levels of pro-inflammatory cytokines and lesion size and that the use of IL-6 lentivirus led to the destabilization of plaques (15, 16). The decreased plasma IL-6 level could, therefore, be partly responsible for the attenuation of atherosclerosis in SP-D/ApoE DKO mice, despite the elevated body weight and plasma lipoproteins, which are known risk factors for the development of CVD (86–90). However, this is not in accordance with an *in vitro* study by Liu et al. (62), who found that serum levels of IL-6 and TNF-α were increased in septic SP-D KO mice compared to wildtype. This discrepancy can be explained by a change in the function of SP-D during sepsis—where it possibly functions as a neutralizer of the sepsis-inducing agent—compared to its function at basal state.

Furthermore, SP-D/ApoE DKO mice had significantly reduced absolute blood monocyte (46% reduction) and neutrophil counts (49% reduction), as well as a 46% reduction in spleen weight (relative to body weight) compared to ApoE KO mice (31). The spleen is a major reservoir of both monocytes and neutrophils, and its reduced weight can explain the decreased monocyte and neutrophil counts. Sorensen et al. found that SP-D KO mice had a significantly lower level of plasma TNF-α (18), which could contribute to the lower atherosclerosis propensity, similar to the IL-6 regulation mentioned above. TNF-α is

associated with an increased risk of CV disease in clinical studies (91), and TNF-α/ApoE DKO mice had reduced lesion areas (50%) with a decreased number of foam cells in the vessel wall (92).

SP-D-Mediated Responses to Smoking

Tobacco smoking is a well-studied cause of CVD (93). A study by Haanes et al. (49), examined the contractile changes in the vasculature after 3-months sidestream smoking in wildtype and SP-D KO mice. Haanes et al. (49) studied the vasocontractile endothelin-1 receptor and the uridine diphosphate receptor P2Y6 in the pulmonary artery left anterior descending coronary artery and the basilar artery. Endothelin-1 sensitivity was not affected by SP-D. When stimulating the P2Y6 receptor in the coronary artery, there was a significantly decreased contraction after cigarette smoking in the wildtype mice compared to control wild-type mice. This significant decrease in contraction was not observed after smoking in the SP-D KO mice compared to control SP-D KO mice. Thus, the control SP-D KO mice had similar UDP-induced contractility in the coronary artery to those of cigarette smoking WT mice.

Although the SP-D mediated mechanisms were not investigated, the observation suggests that the SP-D-deficient artery is more vulnerable to inflammatory stimuli, such as tobacco smoking.

Pilecki et al. (36) recently performed a study combining observations of SP-D immunostaining in resected lung tissue from smoking patients with both *in vitro* and *in vivo* experiments. These authors found an increased expression of SP-D in lungs exposed to cigarette smoke, that SP-D deficiency aggravated airway inflammation and ceramide accumulation in mice exposed to cigarette smoke, and that treatment with rhSP-D ameliorated cigarette smoke-induced inflammation and epithelial apoptosis in both mice and alveolar (A)459 cells. This indicates that SP-D takes part in the regulation of ceramide synthesis, which has also been implicated in atherosclerosis. Ceramides promote the secretion of IL-6 and C-reactive protein (94), increases ROS formation (95), promotes transcytosis of oxLDL across endothelial cells (96), and increases monocyte adhesion (97), thereby promoting inflammation and atherosclerosis (98, 99).

SP-D VARIATION IN CLINICAL STUDIES

It has long been known that chronic lung disease is associated with increased risk of CVD and total mortality. Independent studies have suggested that SP-D might function as a blood biomarker of smoke-induced lung injury and chronic obstructive pulmonary disease (COPD) (**Table 1**) (100–103). COPD is an independent risk factor for coronary artery disease, and COPD patients are at increased risk of death due to CVD (104, 105).

Association Between Circulatory SP-D, Total Mortality, and CVD

A recent elderly twin population study by Wulf-Johansson et al. (43) examined the correlation between circulating SP-D levels with total mortality. The twin with highest-circulating SP-D level had a significantly increased risk of dying before the co-twin during the study follow-up period. Adjusting for smoking did not change this result. This observation is supported by Hill et al. (42), who examined the correlation between circulating SP-D and the risk of cardiovascular morbidity and mortality. The study found that increased serum SP-D was associated with total mortality in patients with documented coronary artery disease also when adjusting for well-established risk factors such as smoking, age, sex, plasma cholesterol, and plasma IL-6 levels. The relationship between SP-D and CVD was further supported by Hu et al. (51), showing a positive association between circulatory SP-D level and carotid intima-media thickness and coronary artery calcification.

A new study by Brankovic et al. (52) examined the potential of SP-D as a biomarker in patients with chronic heart failure. Brankovic et al. (52) reported that SP-D was associated with a worsened clinical outcome (worsened heart failure, heart transplantation, death to CVD) independently of the patient's clinical profile and pharmacological treatment during the follow-up period. However, SP-D did not remain as a significant biomarker after adjustment for time-varying cardiac biomarkers, including N-terminal pro-brain natriuretic peptide and high-sensitivity cardiac troponin T (52). The study mainly based its results on a population with a less severe heart failure (74% was in NYHA class 1 or 2), which might have contributed to the failure to show a robust association between SP-D and heart failure, since lung damage is more pronounced in the more advanced stages of chronic heart failure (41). Another recent study by Otaki et al. (53) examined the association between SP-D and the outcome of peripheral artery disease (PAD) patients. PAD is an occlusive disease in the lower limb arteries and is a well-known risk factor for the development of CVD and death. Patients with a high circulatory SP-D level ($\geq$ 100 ng/mL) had more severe PAD determined using the Fontaine class according to TASC II guidelines (53). Patients with high SP-D also had a higher prevalence of diabetes mellitus and tibial or peroneal artery stenosis/occlusion compared to patients with low SP-D. Furthermore, the study found an association of SP-D levels with endpoints, such as cardiovascular death, heart failure, and leg amputation. The study concluded that circulating SP-D could be a potential therapeutic target and also be useful as a biomarker for tracking atherosclerotic health status in PAD patients.

Single Nucleotide Polymorphisms in the SP-D Gene Related to CVDs

Leth-Larsen et al. (55) and Pueyo et al. (56) examined single nucleotide polymorphisms (SNPs) in the SP-D gene *SFTPD* and their relationships to SP-D oligomerization and development of diseases (55, 56). Leth-Larsen et al. (55) showed that a common SNP, rs721917, resulting in either threonine or methionine at position 11 in the mature protein (Met11Thr), affects the oligomeric structure of the SP-D molecule. Interestingly, this SNP was also found to be associated with type 2 diabetes mellitus and insulin resistance independently of circulatory SP-D levels (56). A recent study by Sorensen et al. (54) examined the relationship between plasma SP-D and subclinical carotid

artery atherosclerosis. The study found no association between plasma SP-D and carotid artery intima-media thickness or subclinical atherosclerotic plaque development. Sorensen et al. (54) further examined two SNPs in the SP-D gene *SFTPD*: rs721917 and rs3088308. Both SNPs were significantly associated with a decreased plasma SP-D level independently of patient smoking status. Moreover, rs721917 was significantly associated with carotid intima-media thickness, whereas rs3088308 was significantly associated with the presence of plaques—both as a smoking-dependent effect of the SNPs (54). Thus, the effects of SP-D are likely caused by an interplay between structural SP-D variations and tobacco smoking.

DISCUSSION

SP-D can undergo several post-translational modifications leading to changes in both structure and function (106, 107). The most common isoform is the dodecameric structure, which is thought to have anti-inflammatory properties (29, 106). However, in an inflammatory environment, the dodecameric form can change to a trimeric or monomeric isoform that is believed to have pro-inflammatory properties (106) (**Figure 1**). This could explain the ambiguous role of SP-D as both an anti- and pro-inflammatory stimulator in the development of CVD and in the absence of microbial binding. Most studies do not examine which SP-D isoform exerts the observed effect, and therefore the relationship between SP-D isoforms and risk of CVD and all-cause mortality is unknown. It is also relevant to examine the correlation between not only total circulatory SP-D and CVD but also between SP-D polymorphisms and CVD; Met11Thr is especially known to affect the function of SP-D. Also, many studies do not report the content of SP-D in BALF or other measurements of lung disease and thus do not consider where the circulatory SP-D originates from. In a recent study by Sarashina-Kida et al. (108), it was shown that SP-D could also originate from the gallbladder, where it had an anti-inflammatory role in a dextran sulfate sodium (DSS)-induced murine colitis. However, Nexoe et al. (109) performed a similar study and could not replicate the anti-inflammatory role of SP-D in the DSS-model. Regardless, the conclusion is that SP-D not only originates from the lung but can be secreted by various sources, such as the arteries and gallbladder. Where the SP-D originates from is important since previous studies have suggested that SP-D might be upregulated in non-pulmonary organs during inflammation. Future studies are needed to explore which tissues and cell types secrete SP-D.

When interpreting results from *in vivo* studies examining SP-D KO mice, it is important to keep in mind that these data can sometimes be misleading. Deficiency of an immunoregulatory protein, such as SP-D, might lead to a compensatory increase in other immunoregulatory proteins. This compensatory mechanism might lead to a different outcome than expected. Rokade et al. (50), examined the function of SP-D in testicular immune privilege and sperm function in LPS-challenged SP-D KO mice. These authors found that endogenous absence of SP-D resulted in significantly increased testicular levels of immunosuppressive molecules and reduced levels of immune cell activation markers. The change in immunoregulative moieties led to a reduced response to LPS in testis and could be a compensatory mechanism to restore the immune dysregulation caused by SP-D KO to preserve fertility. In a similar way, SP-D KO in murine CVD models might promote compensatory mechanisms, resulting in reduced plaque areas and immune cell counts.

Studies examining the function of SP-D have previously been focused on its association with pulmonary diseases, especially COPD. It is important to elucidate the role of SP-D in other pathologies, and its recent association with CVD supports the possibility of SP-D as a potential therapeutic target. The effect of exogenously added SP-D in atherosclerotic mouse models needs further validation but results from basic cardiovascular studies suggest systemic side effects, such as disturbance of lipoprotein levels and body fat distribution. These studies imply that treatment with exogenously added SP-D, when possible, should be locally administered instead of systemically. The conformation-dependent pro- or anti-inflammatory role of SP-D should be further elucidated, as blockage or stimulation of certain isoforms can change the SP-D-mediated treatment effect. Besides being a target for CVD treatment, SP-D has shown promise as a new potential biomarker for the severity and clinical outcome of CVD. Studies have shown significant association between circulatory SP-D levels and development of atherosclerosis and heart failure. Circulatory SP-D might reflect the level of atherosclerosis or the risk of cardiovascular-related death and thus the clinical outcome. It is important to continue examining the association between SP-D and CVD to fully elucidate the potential of SP-D as a treatment target and/or CVD biomarker.

AUTHOR CONTRIBUTIONS

KC was the main author of the manuscript under the guidance of professor GS. AN supported the writing of the manuscript.

FUNDING

The work was supported by the Independent Research Fund Denmark and Novo Nordisk Project Grants in Bioscience and Basic Biomedicine.

REFERENCES

1. WHO. *World Health Organization, Cardiovascular diseases (CVDs)* (2017). Available online at: https://www.who.int/en/news-room/fact-sheets/detail/cardiovascular-diseases-(cvds) (accessed March 06, 2019).
2. Lusis AJ. Atherosclerosis. *Nature*. (2000) 407:233–41. doi: 10.1038/35025203
3. Biros E, Karan M, Golledge J. Genetic variation and atherosclerosis. *Curr Genomics*. (2008) 9:29–42. doi: 10.2174/138920208783884856

4. Miteva K, Madonna R, De Caterina R, Van Linthout S. Innate and adaptive immunity in atherosclerosis. *Vascul Pharmacol*. 107:67–77. (2018). doi: 10.1016/j.vph.2018.04.006
5. Bobryshev YV, Ivanova EA, Chistiakov DA, Nikiforov NG, Orekhov AN. Macrophages and their role in atherosclerosis: pathophysiology and transcriptome analysis. *Biomed Res Int*. (2016) 2016:9582430. doi: 10.1155/2016/9582430
6. Fatkhullina AR, Peshkova IO, Koltsova EK. The role of cytokines in the development of atherosclerosis. *Biochemistry*. (2016) 81:1358–70. doi: 10.1134/S0006297916110134
7. Freigang S, Ampenberger F, Weiss A, Kanneganti TD, Iwakura Y, Hersberger M, et al. Fatty acid-induced mitochondrial uncoupling elicits inflammasome-independent IL-1alpha and sterile vascular inflammation in atherosclerosis. *Nat Immunol*. (2013) 14:1045–53. doi: 10.1038/ni.2704
8. Clarke MC, Talib S, Figg NL, Bennett MR. Vascular smooth muscle cell apoptosis induces interleukin-1-directed inflammation: effects of hyperlipidemia-mediated inhibition of phagocytosis. *Circ Res*. (2010) 106:363–72. doi: 10.1161/CIRCRESAHA.109.208389
9. Kamari Y, Shaish A, Shemesh S, Vax E, Grosskopf I, Dotan S, et al. Reduced atherosclerosis and inflammatory cytokines in apolipoprotein-E-deficient mice lacking bone marrow-derived interleukin-1alpha. *Biochem Biophys Res Commun*. (2011) 405:197–203. doi: 10.1016/j.bbrc.2011.01.008
10. Koltsova EK, Garcia Z, Chodaczek G, Landau M, McArdle S, Scott SR, et al. Dynamic T cell-APC interactions sustain chronic inflammation in atherosclerosis. *J Clin Invest*. (2012) 122:3114–26. doi: 10.1172/JCI61758
11. Ranjbaran H, Sokol SI, Gallo A, Eid RE, Iakimov AO, D'Alessio A, et al. An inflammatory pathway of IFN-gamma production in coronary atherosclerosis. *J Immunol*. (2007) 178:592–604. doi: 10.4049/jimmunol.178.1.592
12. Koga M, Kai H, Yasukawa H, Yamamoto T, Kawai Y, Kato S, et al. Inhibition of progression and stabilization of plaques by postnatal interferon-gamma function blocking in ApoE-knockout mice. *Circ Res*. (2007) 101:348–56. doi: 10.1161/CIRCRESAHA.106.147256
13. Ohta H, Wada H, Niwa T, Kirii H, Iwamoto N, Fujii H, et al. Disruption of tumor necrosis factor-alpha gene diminishes the development of atherosclerosis in ApoE-deficient mice. *Atherosclerosis*. (2005) 180:11–7. doi: 10.1016/j.atherosclerosis.2004.11.016
14. Canault M, Peiretti F, Poggi M, Mueller C, Kopp F, Bonardo B, et al. Progression of atherosclerosis in ApoE-deficient mice that express distinct molecular forms of TNF-alpha. *J Pathol*. (2008) 214:574–83. doi: 10.1002/path.2305
15. Huber SA, Sakkinen P, Conze D, Hardin N, Tracy R. Interleukin-6 exacerbates early atherosclerosis in mice. *Arterioscler Thromb Vasc Biol*. (1999) 19:2364–7. doi: 10.1161/01.ATV.19.10.2364
16. Schieffer B, Selle T, Hilfiker A, Hilfiker-Kleiner D, Grote K, Tietge UJ, et al. Impact of interleukin-6 on plaque development and morphology in experimental atherosclerosis. *Circulation*. (2004) 110:3493–500. doi: 10.1161/01.CIR.0000148135.08582.97
17. Schuett H, Oestreich R, Waetzig GH, Annema W, Luchtefeld M, Hillmer A, et al. Transsignaling of interleukin-6 crucially contributes to atherosclerosis in mice. *Arterioscler Thromb Vasc Biol*. (2012) 32:281–90. doi: 10.1161/ATVBAHA.111.229435
18. Sorensen GL, Madsen J, Kejling K, Tornoe I, Nielsen O, Townsend P, et al. Surfactant protein D is proatherogenic in mice. *Am J Physiol Heart Circ Physiol*. (2006) 290:H2286–94. doi: 10.1152/ajpheart.01105.2005
19. Snyder GD, Oberley-Deegan RE, Goss KL, Romig-Martin SA, Stoll LL, Snyder JM, et al. Surfactant protein D is expressed and modulates inflammatory responses in human coronary artery smooth muscle cells. *Am J Physiol Heart Circ Physiol*. (2008) 294:H2053–9. doi: 10.1152/ajpheart.91529.2007
20. Holmskov U, Thiel S, Jensenius JC. Collections and ficolins: humoral lectins of the innate immune defense. *Annu Rev Immunol*. (2003) 21:547–78. doi: 10.1146/annurev.immunol.21.120601.140954
21. Ohtani K, Suzuki Y, Eda S, Kawai T, Kase T, Yamazaki H, et al. Molecular cloning of a novel human collectin from liver (CL-L1). *J Biol Chem*. (1999) 274:13681–9. doi: 10.1074/jbc.274.19.13681
22. Nakamura K, Funakoshi H, Miyamoto K, Tokunaga F, Nakamura T. Molecular cloning and functional characterization of a human scavenger receptor with C-type lectin (SRCL), a novel member of a scavenger receptor family. *Biochem Biophys Res Commun*. (2001) 280:1028–35. doi: 10.1006/bbrc.2000.4210
23. Keshi H, Sakamoto T, Kawai T, Ohtani K, Katoh T, Jang SJ, et al. Identification and characterization of a novel human collectin CL-K1. *Microbiol Immunol*. (2006) 50:1001–13. doi: 10.1111/j.1348-0421.2006.tb03868.x
24. Bourbon JR, Chailley-Heu B. Surfactant proteins in the digestive tract, mesentery, and other organs: evolutionary significance. *Comp Biochem Physiol A Mol Integr Physiol*. (2001) 129:151–61. doi: 10.1016/S1095-6433(01)00312-9
25. Gardai SJ, Xiao YQ, Dickinson M, Nick JA, Voelker DR, Greene KE, et al. By binding SIRPalpha or calreticulin/CD91, lung collectins act as dual function surveillance molecules to suppress or enhance inflammation. *Cell*. (2003) 115:13–23. doi: 10.1016/S0092-8674(03)00758-X
26. Ohya M, Nishitani C, Sano H, Yamada C, Mitsuzawa H, Shimizu T, et al. Human pulmonary surfactant protein D binds the extracellular domains of Toll-like receptors 2 and 4 through the carbohydrate recognition domain by a mechanism different from its binding to phosphatidylinositol and lipopolysaccharide. *Biochemistry*. (2006) 45:8657–64. doi: 10.1021/bi060176z
27. Fournier B, Andargachew R, Robin AZ, Laur O, Voelker DR, Lee WY, et al. Surfactant protein D (Sp-D) binds to membrane-proximal domain (D3) of signal regulatory protein alpha (SIRPalpha), a site distant from binding domain of CD47, while also binding to analogous region on signal regulatory protein beta (SIRPbeta). *J Biol Chem*. (2012) 287:19386–98. doi: 10.1074/jbc.M111.324533
28. Kishore U, Greenhough TJ, Waters P, Shrive AK, Ghai R, Kamran MF, et al. Surfactant proteins SP-A and SP-D: structure, function and receptors. *Mol Immunol*. (2006) 43:1293–315. doi: 10.1016/j.molimm.2005.08.004
29. Arroyo R, Martin-Gonzalez A, Echaide M, Jain A, Brondyk WH, Rosenbaum J, et al. Supramolecular assembly of human pulmonary surfactant protein SP-D. *J Mol Biol*. (2018) 430:1495–509. doi: 10.1016/j.jmb.2018.03.027
30. Haczku A. Protective role of the lung collectins surfactant protein A and surfactant protein D in airway inflammation. *J Allergy Clin Immunol*. (2008) 122:861–79; quiz : 80–1 doi: 10.1016/j.jaci.2008.10.014
31. Hirano Y, Choi A, Tsuruta M, Jaw JE, Oh Y, Ngan D, et al. Surfactant protein-D deficiency suppresses systemic inflammation and reduces atherosclerosis in ApoE knockout mice. *Cardiovasc Res*. (2017) 113:1208–18. doi: 10.1093/cvr/cvx067
32. Sorensen GL. Surfactant protein D in respiratory and non-respiratory diseases. *Front Med*. (2018) 5:18. doi: 10.3389/fmed.2018.00018
33. Hawgood S, Akiyama J, Brown C, Allen L, Li G, Poulain FR. GM-CSF mediates alveolar macrophage proliferation and type II cell hypertrophy in SP-D gene-targeted mice. *Am J Physiol Lung Cell Mol Physiol*. (2001) 280:L1148–56. doi: 10.1152/ajplung.2001.280.6.L1148
34. LeVine AM, Whitsett JA, Hartshorn KL, Crouch EC, Korfhagen TR. Surfactant protein D enhances clearance of influenza A virus from the lung *in vivo*. *J Immunol*. (2001) 167:5868–73. doi: 10.4049/jimmunol.167.10.5868
35. Li G, Siddiqui J, Hendry M, Akiyama J, Edmondson J, Brown C, et al. Surfactant protein-A–deficient mice display an exaggerated early inflammatory response to a beta-resistant strain of influenza A virus. *Am J Respir Cell Mol Biol*. (2002) 26:277–82. doi: 10.1165/ajrcmb.26.3.4584
36. Pilecki B, Wulf-Johansson H, Stottrup C, Jorgensen PT, Djiadeu P, Nexoe AB, et al. Surfactant protein D deficiency aggravates cigarette smoke-induced lung inflammation by upregulation of ceramide synthesis. *Front Immunol*. (2018) 9:3013. doi: 10.3389/fimmu.2018.03013
37. Madsen J, Kliem A, Tornoe I, Skjodt K, Koch C, Holmskov U. Localization of lung surfactant protein D on mucosal surfaces in human tissues. *J Immunol*. (2000) 164:5866–70. doi: 10.4049/jimmunol.164.11.5866
38. Stahlman MT, Gray ME, Hull WM, Whitsett JA. Immunolocalization of surfactant protein-D (SP-D) in human fetal, newborn, and adult tissues. *J Histochem Cytochem*. (2002) 50:651–60. doi: 10.1177/002215540205000506
39. Leth-Larsen R, Floridon C, Nielsen O, Holmskov U. Surfactant protein D in the female genital tract. *Mol Hum Reprod*. (2004) 10:149–54. doi: 10.1093/molehr/gah022
40. Kati C, Alacam H, Duran L, Guzel A, Akdemir HU, Sisman B, et al. The effectiveness of the serum surfactant protein D (Sp-D) level to indicate lung injury in pulmonary embolism. *Clin Lab*. (2014) 60:1457–64. doi: 10.7754/Clin.Lab.2013.131009

41. Gargiulo P, Banfi C, Ghilardi S, Magri D, Giovannardi M, Bonomi A, et al. Surfactant-derived proteins as markers of alveolar membrane damage in heart failure. *PLoS ONE*. (2014) 9:e115030. doi: 10.1371/journal.pone.0115030
42. Hill J, Heslop C, Man SF, Frohlich J, Connett JE, Anthonisen NR, et al. Circulating surfactant protein-D and the risk of cardiovascular morbidity and mortality. *Eur Heart J*. (2011) 32:1918–25. doi: 10.1093/eurheartj/ehr124
43. Wulf-Johansson H, Thinggaard M, Tan Q, Johansson SL, Schlosser A, Christensen K, et al. Circulating surfactant protein D is associated to mortality in elderly women: a twin study. *Immunobiology*. (2013) 218:712–7. doi: 10.1016/j.imbio.2012.08.272
44. Borron PJ, Mostaghel EA, Doyle C, Walsh ES, McHeyzer-Williams MG, Wright JR. Pulmonary surfactant proteins A and D directly suppress CD3+/CD4+ cell function: evidence for two shared mechanisms. *J Immunol*. (2002) 169:5844–50. doi: 10.4049/jimmunol.169.10.5844
45. Pandit H, Thakur G, Koippallil Gopalakrishnan AR, Dodagatta-Marri E, Patil A, Kishore U, et al. Surfactant protein D induces immune quiescence and apoptosis of mitogen-activated peripheral blood mononuclear cells. *Immunobiology*. (2016) 221:310–22. doi: 10.1016/j.imbio.2015.10.004
46. Barrow AD, Palarasah Y, Bugatti M, Holehouse AS, Byers DE, Holtzman MJ, et al. OSCAR is a receptor for surfactant protein D that activates TNF-alpha release from human CCR2+ inflammatory monocytes. *J Immunol*. (2015) 194:3317–26. doi: 10.4049/jimmunol.1402289
47. Olde Nordkamp MJ, van Eijk M, Urbanus RT, Bont L, Haagsman HP, Meyaard L. Leukocyte-associated Ig-like receptor-1 is a novel inhibitory receptor for surfactant protein D. *J Leukoc Biol*. (2014) 96:105–11. doi: 10.1189/jlb.3AB0213-092RR
48. Ge MQ, Kokalari B, Flayer CH, Killingbeck SS, Redai IG, MacFarlane AWt, et al. Correction: cutting edge: role of NK cells and surfactant protein D in dendritic cell lymph node homing: effects of ozone exposure. *J Immunol*. (2016) 196:3212. doi: 10.4049/jimmunol.1600095
49. Haanes KA, Kruse LS, Wulf-Johansson H, Stottrup CC, Sorensen GL, Edvinsson L. Contractile changes in the vasculature after subchronic smoking: a comparison between wild type and surfactant protein D knock-out mice. *Nicotine Tob Res*. (2016) 18:642–6. doi: 10.1093/ntr/ntv243
50. Rokade S, Kishore U, Madan T. Surfactant protein D regulates murine testicular immune milieu and sperm functions. *Am J Reprod Immunol*. (2017) 77:12620–9. doi: 10.1111/aji.12629
51. Hu F, Zhong Q, Gong J, Qin Y, Cui L, Yuan H. Serum surfactant protein D is associated with atherosclerosis of the carotid artery in patients on maintenance hemodialysis. *Clin Lab*. (2016) 62:97–104. doi: 10.7754/Clin.Lab.2015.150536
52. Brankovic M, Martijn Akkerhuis K, Mouthaan H, Constantinescu A, Caliskan K, van Ramshorst J, et al. Utility of temporal profiles of new cardio-renal and pulmonary candidate biomarkers in chronic heart failure. *Int J Cardiol*. (2019) 276:157–65. doi: 10.1016/j.ijcard.2018.08.001
53. Otaki Y, Watanabe T, Takahashi H, Sugai T, Yokoyama M, Nishiyama S, et al. Circulating surfactant protein-D is associated with clinical outcomes in peripheral artery disease patients following endovascular therapy. *Circ J*. (2018) 82:1926–34. doi: 10.1253/circj.CJ-17-1446
54. Sorensen GL, Bladbjerg EM, Steffensen R, Tan Q, Madsen J, Drivsholm T, et al. Association between the surfactant protein D (SFTPD) gene and subclinical carotid artery atherosclerosis. *Atherosclerosis*. (2016) 246:7–12. doi: 10.1016/j.atherosclerosis.2015.12.037
55. Leth-Larsen R, Garred P, Jensenius H, Meschi J, Hartshorn K, Madsen J, et al. A common polymorphism in the SFTPD gene influences assembly, function, and concentration of surfactant protein D. *J Immunol*. (2005) 174:1532–8. doi: 10.4049/jimmunol.174.3.1532
56. Pueyo N, Ortega FJ, Mercader JM, Moreno-Navarrete JM, Sabater M, Bonas S, et al. Common genetic variants of surfactant protein-D (SP-D) are associated with type 2 diabetes. *PLoS ONE*. (2013) 8:e60468. doi: 10.1371/journal.pone.0060468
57. Hansson GK. Inflammation, atherosclerosis, and coronary artery disease. *N Engl J Med*. (2005) 352:1685–95. doi: 10.1056/NEJMra043430
58. Wiedermann CJ, Kiechl S, Dunzendorfer S, Schratzberger P, Egger G, Oberhollenzer F, et al. Association of endotoxemia with carotid atherosclerosis and cardiovascular disease: prospective results from the Bruneck Study. *J Am Coll Cardiol*. (1999) 34:1975–81. doi: 10.1016/S0735-1097(99)00448-9
59. Zhang L, Meng Q, Yepuri N, Wang G, Xi X, Cooney RN. Surfactant Proteins-A and -D attenuate LPS-Induced Apoptosis in Primary Intestinal Epithelial Cells (IECs). *Shock*. (2018) 49:90–8. doi: 10.1097/SHK.0000000000000919
60. Saka R, Wakimoto T, Nishiumi F, Sasaki T, Nose S, Fukuzawa M, et al. Surfactant protein-D attenuates the lipopolysaccharide-induced inflammation in human intestinal cells overexpressing toll-like receptor 4. *Pediatr Surg Int*. (2016) 32:59–63. doi: 10.1007/s00383-015-3812-y
61. Du X, Meng Q, Sharif A, Abdel-Razek OA, Zhang L, Wang G, et al. Surfactant proteins SP-A and SP-D ameliorate pneumonia severity and intestinal injury in a murine model of staphylococcus aureus pneumonia. *Shock*. (2016) 46:164–72. doi: 10.1097/SHK.0000000000000587
62. Liu Z, Shi Q, Liu J, Abdel-Razek O, Xu Y, Cooney RN, et al. Innate immune molecule surfactant protein D attenuates sepsis-induced acute pancreatic injury through modulating apoptosis and NF-kappaB-mediated inflammation. *Sci Rep*. (2015) 5:17798. doi: 10.1038/srep17798
63. Watanabe S, Mu W, Kahn A, Jing N, Li JH, Lan HY, et al. Role of JAK/STAT pathway in IL-6-induced activation of vascular smooth muscle cells. *Am J Nephrol*. (2004) 24:387–92. doi: 10.1159/000079706
64. Morimoto S, Nabata T, Koh E, Shiraishi T, Fukuo K, Imanaka S, et al. Interleukin-6 stimulates proliferation of cultured vascular smooth muscle cells independently of interleukin-1 beta. *J Cardiovasc Pharmacol*. (1991) 17 (Suppl. 2):S117–8. doi: 10.1097/00005344-199117002-00026
65. Wung BS, Hsu MC, Wu CC, Hsieh CW. Resveratrol suppresses IL-6-induced ICAM-1 gene expression in endothelial cells: effects on the inhibition of STAT3 phosphorylation. *Life Sci*. (2005) 78:389–97. doi: 10.1016/j.lfs.2005.04.052
66. Chen Q, Fisher DT, Clancy KA, Gauguet JM, Wang WC, Unger E, et al. Fever-range thermal stress promotes lymphocyte trafficking across high endothelial venules via an interleukin 6 trans-signaling mechanism. *Nat Immunol*. (2006) 7:1299–308. doi: 10.1038/ni1406
67. Gierens H, Nauck M, Roth M, Schinker R, Schurmann C, Scharnagl H, et al. Interleukin-6 stimulates LDL receptor gene expression via activation of sterol-responsive and Sp1 binding elements. *Arterioscler Thromb Vasc Biol*. (2000) 20:1777–83. doi: 10.1161/01.ATV.20.7.1777
68. Lubrano V, Gabriele M, Puntoni MR, Longo V, Pucci L. Relationship among IL-6, LDL cholesterol and lipid peroxidation. *Cell Mol Biol Lett*. (2015) 20:310–22. doi: 10.1515/cmble-2015-0020
69. Kaminska J, Stopinski M, Mucha K, Jedrzejczak A, Golebiowski M, Niewczas MA, et al. IL 6 but not TNF is linked to coronary artery calcification in patients with chronic kidney disease. *Cytokine*. (2019) 120:9–14. doi: 10.1016/j.cyto.2019.04.002
70. Zakai NA, Katz R, Jenny NS, Psaty BM, Reiner AP, Schwartz SM, et al. Inflammation and hemostasis biomarkers and cardiovascular risk in the elderly: the cardiovascular health study. *J Thromb Haemost*. (2007) 5:1128–35. doi: 10.1111/j.1538-7836.2007.02528.x
71. Wainstein MV, Mossmann M, Araujo GN, Goncalves SC, Gravina GL, Sangalli M, et al. Elevated serum interleukin-6 is predictive of coronary artery disease in intermediate risk overweight patients referred for coronary angiography. *Diabetol Metab Syndr*. (2017) 9:67. doi: 10.1186/s13098-017-0266-5
72. Lee J, Lee S, Zhang H, Hill MA, Zhang C, Park Y. Interaction of IL-6 and TNF-alpha contributes to endothelial dysfunction in type 2 diabetic mouse hearts. *PLoS ONE*. (2017) 12:e0187189. doi: 10.1371/journal.pone.0187189
73. Marcos-Ramiro B, Garcia-Weber D, Millan J. TNF-induced endothelial barrier disruption: beyond actin and Rho. *Thromb Haemost*. (2014) 112:1088–102. doi: 10.1160/th14-04-0299
74. Chandrasekharan UM, Siemionow M, Unsal M, Yang L, Poptic E, Bohn J, et al. Tumor necrosis factor alpha (TNF-alpha) receptor-II is required for TNF-alpha-induced leukocyte-endothelial interaction *in vivo*. *Blood*. (2007) 109:1938–44. doi: 10.1182/blood-2006-05-020875
75. Rastogi S, Rizwani W, Joshi B, Kunigal S, Chellappan SP. TNF-alpha response of vascular endothelial and vascular smooth muscle cells involve differential utilization of ASK1 kinase and p73. *Cell Death Differ*. (2012) 19:274–83. doi: 10.1038/cdd.2011.93

76. Martinez-Esparza M, Ruiz-Alcaraz AJ, Carmona-Martinez V, Fernandez-Fernandez MD, Anton G, Munoz-Tornero M, et al. Expression of LAIR-1 (CD305) on human blood monocytes as a marker of hepatic cirrhosis progression. *J Immunol* Res. (2019) 2019:2974753. doi: 10.1155/2019/2974753
77. Jin J, Wang Y, Ma Q, Wang N, Guo W, Jin B, et al. LAIR-1 activation inhibits inflammatory macrophage phenotype *in vitro*. *Cell Immunol*. (2018) 331:78–84. doi: 10.1016/j.cellimm.2018.05.011
78. Di Marco E, Gray SP, Kennedy K, Szyndralewiez C, Lyle AN, Lassegue B, et al. NOX4-derived reactive oxygen species limit fibrosis and inhibit proliferation of vascular smooth muscle cells in diabetic atherosclerosis. *Free Radic Biol Med*. (2016) 97:556–67. doi: 10.1016/j.freeradbiomed.2016.07.013
79. Schurmann C, Rezende F, Kruse C, Yasar Y, Lowe O, Fork C, et al. The NADPH oxidase Nox4 has anti-atherosclerotic functions. *Eur Heart J*. (2015) 36:3447–56. doi: 10.1093/eurheartj/ehv460
80. Sussan TE, Jun J, Thimmulappa R, Bedja D, Antero M, Gabrielson KL, et al. Disruption of Nrf2, a key inducer of antioxidant defenses, attenuates ApoE-mediated atherosclerosis in mice. *PLoS ONE*. (2008) 3:e3791. doi: 10.1371/journal.pone.0003791
81. Yi X, Zhang J, Zhuang R, Wang S, Cheng S, Zhang D, et al. Silencing LAIR-1 in human THP-1 macrophage increases foam cell formation by modulating PPARgamma and M2 polarization. *Cytokine*. (2018) 111:194–205. doi: 10.1016/j.cyto.2018.08.028
82. Narni-Mancinelli E, Chaix J, Fenis A, Kerdiles YM, Yessaad N, Reynders A, et al. Fate mapping analysis of lymphoid cells expressing the NKp46 cell surface receptor. *Proc Natl Acad Sci USA*. (2011) 108:18324–9. doi: 10.1073/pnas.1112064108
83. Walzer T, Blery M, Chaix J, Fuseri N, Chasson L, Robbins SH, et al. Identification, activation, and selective *in vivo* ablation of mouse NK cells via NKp46. *Proc Natl Acad Sci USA*. (2007) 104:3384–9. doi: 10.1073/pnas.0609692104
84. Lin HL, Xu XS, Lu HX, Zhang L, Li CJ, Tang MX, et al. Pathological mechanisms and dose dependency of erythrocyte-induced vulnerability of atherosclerotic plaques. *J Mol Cell Cardiol*. (2007) 43:272–80. doi: 10.1016/j.yjmcc.2007.05.023
85. Kolodgie FD, Gold HK, Burke AP, Fowler DR, Kruth HS, Weber DK, et al. Intraplaque hemorrhage and progression of coronary atheroma. *N Engl J Med*. (2003) 349:2316–25. doi: 10.1056/NEJMoa035655
86. Gast KB, Tjeerdema N, Stijnen T, Smit JW, Dekkers OM. Insulin resistance and risk of incident cardiovascular events in adults without diabetes: meta-analysis. *PLoS ONE*. (2012) 7:e52036. doi: 10.1371/journal.pone.0052036
87. Prenner SB, Mulvey CK, Ferguson JF, Rickels MR, Bhatt AB, Reilly MP. Very low density lipoprotein cholesterol associates with coronary artery calcification in type 2 diabetes beyond circulating levels of triglycerides. *Atherosclerosis*. (2014) 236:244–50. doi: 10.1016/j.atherosclerosis.2014.07.008
88. Park C, Guallar E, Linton JA, Lee DC, Jang Y, Son DK, et al. Fasting glucose level and the risk of incident atherosclerotic cardiovascular diseases. *Diabetes Care*. (2013) 36:1988–93. doi: 10.2337/dc12-1577
89. Ritchie SA, Connell JM. The link between abdominal obesity, metabolic syndrome and cardiovascular disease. *Nutr Metab Cardiovasc Dis*. (2007) 17:319–26. doi: 10.1016/j.numecd.2006.07.005
90. Van Gaal LF, Mertens IL, De Block CE. Mechanisms linking obesity with cardiovascular disease. *Nature*. (2006) 444:875–80. doi: 10.1038/nature05487
91. Jovinge S, Hamsten A, Tornvall P, Proudler A, Bavenholm P, Ericsson CG, et al. Evidence for a role of tumor necrosis factor alpha in disturbances of triglyceride and glucose metabolism predisposing to coronary heart disease. *Metabolism*. (1998) 47:113–8. doi: 10.1016/S0026-0495(98)90203-7
92. Branen L, Hovgaard L, Nitulescu M, Bengtsson E, Nilsson J, Jovinge S. Inhibition of tumor necrosis factor-alpha reduces atherosclerosis in apolipoprotein E knockout mice. *Arterioscler Thromb Vasc Biol*. (2004) 24:2137–42. doi: 10.1161/01.ATV.0000143933.20616.1b
93. Prasad DS, Kabir Z, Dash AK, Das BC. Smoking and cardiovascular health: a review of the epidemiology, pathogenesis, prevention and control of tobacco. *Indian J Med Sci*. (2009) 63:520–33. doi: 10.4103/0019-5359.58884
94. de Mello VD, Lankinen M, Schwab U, Kolehmainen M, Lehto S, Seppanen-Laakso T, et al. Link between plasma ceramides, inflammation and insulin resistance: association with serum IL-6 concentration in patients with coronary heart disease. *Diabetologia*. (2009) 52:2612–5. doi: 10.1007/s00125-009-1482-9
95. Li H, Junk P, Huwiler A, Burkhardt C, Wallerath T, Pfeilschifter J, et al. Dual effect of ceramide on human endothelial cells: induction of oxidative stress and transcriptional upregulation of endothelial nitric oxide synthase. *Circulation*. (2002) 106:2250–6. doi: 10.1161/01.CIR.0000035650.05921.50
96. Li W, Yang X, Xing S, Bian F, Yao W, Bai X, et al. Endogenous ceramide contributes to the transcytosis of oxLDL across endothelial cells and promotes its subendothelial retention in vascular wall. *Oxid Med Cell Longev*. (2014) 2014:823071. doi: 10.1155/2014/823071
97. Gao D, Pararasa C, Dunston CR, Bailey CJ, Griffiths HR. Palmitate promotes monocyte atherogenicity via de novo ceramide synthesis. *Free Radic Biol Med*. (2012) 53:796–806. doi: 10.1016/j.freeradbiomed.2012.05.026
98. Li Z, Fan Y, Liu J, Li Y, Huan C, Bui HH, et al. Impact of sphingomyelin synthase 1 deficiency on sphingolipid metabolism and atherosclerosis in mice. *Arterioscler Thromb Vasc Biol*. (2012) 32:1577–84. doi: 10.1161/ATVBAHA.112.251538
99. Dong J, Liu J, Lou B, Li Z, Ye X, Wu M, et al. Adenovirus-mediated overexpression of sphingomyelin synthases 1 and 2 increases the atherogenic potential in mice. *J Lipid Res*. (2006) 47:1307–14. doi: 10.1194/jlr.M600040-JLR200
100. Lopez-Cano C, Lecube A, Garcia-Ramirez M, Munoz X, Sanchez E, Seminario A, et al. Serum surfactant protein D as a biomarker for measuring lung involvement in obese patients with type 2 diabetes. *J Clin Endocrinol Metab*. (2017) 102:4109–16. doi: 10.1210/jc.2017-00913
101. Eisner MD, Parsons P, Matthay MA, Ware L, Greene K, Acute Respiratory Distress Syndrome N. Plasma surfactant protein levels and clinical outcomes in patients with acute lung injury. *Thorax*. (2003) 58:983–8. doi: 10.1136/thorax.58.11.983
102. Determann RM, Royakkers AA, Haitsma JJ, Zhang H, Slutsky AS, Ranieri VM, et al. Plasma levels of surfactant protein D and KL-6 for evaluation of lung injury in critically ill mechanically ventilated patients. *BMC Pulm Med*. (2010) 10:6. doi: 10.1186/1471-2466-10-6
103. Lomas DA, Silverman EK, Edwards LD, Locantore NW, Miller BE, Horstman DH, et al. Serum surfactant protein D is steroid sensitive and associated with exacerbations of COPD. *Eur Respir J*. (2009) 34:95–102. doi: 10.1183/09031936.00156508
104. Fisher KA, Stefan MS, Darling C, Lessard D, Goldberg RJ. Impact of COPD on the mortality and treatment of patients hospitalized with acute decompensated heart failure: the Worcester Heart Failure Study. *Chest*. (2015) 147:637–45. doi: 10.1378/chest.14-0607
105. Finkelstein J, Cha E, Scharf SM. Chronic obstructive pulmonary disease as an independent risk factor for cardiovascular morbidity. *Int J Chron Obstruct Pulmon Dis*. (2009) 4:337–49. doi: 10.2147/COPD.S6400
106. Guo CJ, Atochina-Vasserman EN, Abramova E, Foley JP, Zaman A, Crouch E, et al. S-nitrosylation of surfactant protein-D controls inflammatory function. *PLoS Biol*. (2008) 6:e266. doi: 10.1371/journal.pbio.0060266
107. Matalon S, Shrestha K, Kirk M, Waldheuser S, McDonald B, Smith K, et al. Modification of surfactant protein D by reactive oxygen-nitrogen intermediates is accompanied by loss of aggregating activity, *in vitro* and *in vivo*. *FASEB J*. (2009) 23:1415–30. doi: 10.1096/fj.08-120568
108. Sarashina-Kida H, Negishi H, Nishio J, Suda W, Nakajima Y, Yasui-Kato M, et al. Gallbladder-derived surfactant protein D regulates gut commensal bacteria for maintaining intestinal homeostasis. *Proc Natl Acad Sci USA*. (2017) 114:10178–83. doi: 10.1073/pnas.1712837114
109. Nexoe AB, Pilecki B, Von Huth S, Husby S, Pedersen AA, Detlefsen S, et al. Colonic epithelial surfactant protein D expression correlates with inflammation in clinical colonic inflammatory bowel disease. *Inflamm Bowel Dis*. (2019) 25:1349–56. doi: 10.1093/ibd/izz009

Conflict of Interest: The authors declare that the research was conducted in the absence of any commercial or financial relationships that could be construed as a potential conflict of interest.

Advantages of publishing in Frontiers

OPEN ACCESS
Articles are free to read for greatest visibility and readership

FAST PUBLICATION
Around 90 days from submission to decision

HIGH QUALITY PEER-REVIEW
Rigorous, collaborative, and constructive peer-review

TRANSPARENT PEER-REVIEW
Editors and reviewers acknowledged by name on published articles

Frontiers
Avenue du Tribunal-Fédéral 34
1005 Lausanne | Switzerland

Visit us: www.frontiersin.org
Contact us: info@frontiersin.org | +41 21 510 17 00

REPRODUCIBILITY OF RESEARCH
Support open data and methods to enhance research reproducibility

DIGITAL PUBLISHING
Articles designed for optimal readership across devices

FOLLOW US
@frontiersin

IMPACT METRICS
Advanced article metrics track visibility across digital media

EXTENSIVE PROMOTION
Marketing and promotion of impactful research

LOOP RESEARCH NETWORK
Our network increases your article's readership